Novel Approaches Towards Sequence-Definition in Polymer Chemistry Using Multicomponent Reactions

Zur Erlangung des akademischen Grades einer

DOKTORIN DER NATURWISSENSCHAFTEN

(Dr. rer. nat.)

von der KIT-Fakultät für Chemie und Biowissenschaften
des Karlsruher Instituts für Technologie (KIT)

genehmigte
DISSERTATION
von

M.Sc. Katharina Sophia Wetzel

aus Bühl

Dekan: Prof. Dr. Manfred Wilhelm

Referent: Prof. Dr. Michael Meier

Korreferent: Prof. Dr. Joachim Podlech

Tag der mündlichen Prüfung: 14.10.2019

"One of the lessons I have learned in the different stages of my career is

that science is not done alone.

It is through talking with others and sharing that

progress is made."

Carol W. Greider

Molecular biologist and Nobel prize laureate

Acknowledgements

An dieser Stelle möchte ich mich bei den Personen bedanken, die mich während meiner Promotion begleitet und unterstützt haben, und die maßgeblich dazu beigetragen haben, dass die vergangenen drei Jahre zu einer wunderschönen und intensiven Zeit wurden, an die ich mich immer gerne zurückerinnern werde.

Mike, vielen Dank für die Aufnahme in die Arbeitsgruppe, für dein Vertrauen und deine Unterstützung, die du mir während meiner gesamten Promotion entgegengebracht hast. Ich schätze sehr, dass deine Tür für uns alle jederzeit offensteht und dass ich mich mit allen Problemen und Fragen jederzeit an dich wenden konnte. Die freundschaftliche und offene Atmosphäre, nicht nur bei der Arbeit, sondern auch bei zahlreichen Gruppenaktivitäten und Ausflügen, hat mich immer motiviert, mein Bestes zu geben und ich habe die Atmosphäre in unserem AK immer als etwas sehr Besonderes wahrgenommen. Daher bin ich dankbar ein Teil des AK Meiers sein zu dürfen. Danke auch dafür, dass du mir meinen Auslandsaufenthalt in Gent und die zahlreichen interessanten Konferenzen ermöglicht hast!

I would like to thank the whole Meier group as well as the former group members for the enjoyable working atmosphere. You are more than just colleagues and I am grateful for the many friendships that grew during the last years. Thank you for many group activities, BBQs after work, active breaks and many great trips or conferences.

Yasmin, wir haben unser ganzes Studium und die Promotion miteinander verbracht, was eine irre lange Zeit ist. Es war schön, dich als Schreibtisch Nachbarin zu haben und (zumindest zeitweise) ein Labor zu teilen. Auf deine Meinung und Unterstützung kann ich immer zählen. Danke für unsere wunderbare Freundschaft!

Susanne, mit deinem Enthusiasmus hast du den Grundstein für mein Interesse an der Sequenzkontrolle gelegt und deine Vorarbeiten waren für meine gesamte Promotion eine wichtige und hilfreiche Basis, auf der ich aufbauen konnte. Danke für die schöne gemeinsame Zeit im Labor und für die gute Freundschaft, die wir seither weiterhin pflegen. Maxi, danke dir für viele lustige gemeinsame Abende und Ausflüge, zahlreiche Skype Telefonate nach Australien, gemeinsame Sport- und Yoga Sessions, für deine Hilfe mit den ESI Messungen und die schöne Zusammenarbeit in A3. Bohni, vielen Dank für die schöne gemeinsame Zeit auf Kreta und in Gent, und danke auch für die gemeinsamen Foto Ausflüge, wobei ich so viel gelernt habe. Philip, herzlichen Dank für viele lange gute Gespräche und die schönen gemeinsame Tage in Gent und in Lüttich. Es war schön von deinen belgischen Erfahrungen zu profitieren. Pia, dir danke ich für deine Unterrichtsstunden im Nähen und die immer super lustigen Abende, die der perfekte Ausgleich nach einem stressigen Tag waren. Dafni, thank you for the most delicious amatriciana and all the other nice evenings together. Meeting Mizithra is always a highlight of course. Thank you for your support during my PhD, for many helpful discussions and for your corrections. Dani und Ben, meine Laborkollegen, ich danke euch für die schöne Zeit in 410, die ich bei guter Musik und dummen Sprüchen immer sehr genossen habe. Roman

und Michi, unser Dream-Team, ihr macht jeden Arbeitstag ein bisschen angenehmer. Rieke, die Aktivpause mit dir war immer am lustigsten, nicht nur wegen deiner Gesichtsfarbe, sondern auch weil du in deiner Motivation unübertroffen warst. Danke auch für deine Hilfe bei meinen vielen IR Messungen. Thank you Eren, for the coffee breaks together with our favourite cup. Danke Juli, für euren Besuch in Gent; dich am Meer zu sehen war ein absolutes Highlight! Kenny, thanks for teaching me Igbo, that was so much fun. Ein besonderer Dank gilt auch Pinar für die liebe Unterstützung bei allen organisatorischen Fragen und für die Hilfe bei der nicht immer unkomplizierten Organisation meines Auslandsaufenthaltes. Außerdem möchte ich mich herzlich bei Becci bedanken, für deine Unterstützung bei der Synthese aber auch für deinen Einsatz im und außerhalb des Labors, was unsere Gruppe sehr unterstützt. Ein herzlicher Dank gilt auch Bapti, Luca, Kevin, Marcel, Stefan, Barbara, Audrey, Charlotte, Maike, Andi, Patrick, Rebekka, und Gregor. Thank you to all of you because you made my PhD an unforgettable time and after so many years, the AK Meier almost feels a bit like family. Danke auch an alle meine fleißigen Korrekturleser Yasmin, Pia, Dafni, Bohni, Maxi, Waldemar, Roman and Philip. Danke für eure Mühe und eure Korrekturvorschläge.

I would like to thank Filip for giving me the opportunity to come to Ghent and work with the PCR group in a very interesting cooperation project. The whole PCR group offered me a very nice and enjoyable working atmosphere, which I truly appreciate and which made my time in Ghent unforgettable. Thank you Christian, Melissa, Hannes, Lae, Jan, Resat, Steven, Stef, Chiel, Niels, Maarten, Martijn, Yann, Hatice, Marc, Bastiaan and Bernhard for the good time in your group. Josh, thank you for your support during my time in Ghent which did not only result in nice curves and a publication of a successful cooperation, but also in a great friendship, which for sure will continue. Thank you for a beautiful boat trip on the canals in Ghent, funny moments in Crete with an Ananas and many nice evenings in Ghent and Karlsruhe.

Bei meinen Freunden außerhalb des Labors, insbesondere Leonie und Uli, möchte ich mich für die Freundschaft, schon während des Studiums, und für unser wöchentliches Kommilitonenessen bedanken.

Waldemar, bei dir möchte ich mich bedanken für die sehr gute Zusammenarbeit in unserem SFB Projekt A3. Es ist super, wenn man in einer so angenehmen, freundschaftlichen Atmosphäre zusammenarbeiten kann. Danke für die vielen guten Gespräche und die entspannten Kaffeepausen.

Vielen Dank an Roman, Yixuan und Philipp, die ihre Vertieferarbeit unter meiner Betreuung im Labor angefertigt haben und an die Hiwis Lea und Moritz für die Zusammenarbeit. Danke für eure tatkräftige Unterstützung und für alles was ich in der Zusammenarbeit mit euch lernen durfte.

Ein herzlicher Dank geht an die Analytik Abteilung des Instituts für Organische Chemie, insbesondere an Angelika Mösle für die vielen Messungen und an Richard von Budberg für die zahlreichen Reparaturen und netten Gespräche. Insbesondere die Spiel- und Streicheleinheiten mit Kiwi waren immer eine willkommene Abwechslung.

Bei Prof. Barner-Kowollik und dem CBK Masse Team möchte ich mich bedanken für den Zugang zum SEC-ESI-MS Equipment und für die zahlreichen Messungen.

Der Deutschen Forschungsgemeinschaft danke ich für die Finanzierung meiner Doktorarbeit im Rahmen des SFB 1176 „Strukturierung weicher Materie“ (Projekt A3). Ein besonderer Dank gilt hier auch Mike, Prof. Manfred Wilhelm, Dominik Voll, Marc von Czapiewski und Cornelia Weber für die Betreuung und

Organisation des SFB und des Graduiertenkollegs. Außerdem möchte ich dem gesamten „Sequenzkontrolle Team“ des Projekts A3 und meinen Kooperationspartnern Xiaoai und Sebastian für die angenehme und erfolgreiche Zusammenarbeit danken. Bei allen weiteren SFB Kollegen möchte ich mich für die gute Zeit bedanken.

Abschließend gilt mein größter Dank meiner Familie, insbesondere meinen Eltern und meiner Schwester Friederike, sowie meinem Freund Stefan. Ihr seid schon immer mein Anker gewesen. Danke für eure Unterstützung, euren Rückhalt und eure Liebe! Ohne euch wäre diese Arbeit nicht so geworden wie sie ist und ich kann nicht in Worte fassen was für eine Riesenstütze ihr für mich seid.

Die vorliegende Arbeit wurde von Mai 2016 bis September 2019 unter Anleitung von Prof. Dr. Michael A. R. Meier am Institut für Organische Chemie (IOC) des Karlsruher Instituts für Technologie (KIT) angefertigt.

Erklärung

Hiermit versichere ich, dass ich die Arbeit selbstständig angefertigt, nur die angegebenen Quellen und Hilfsmittel benutzt und mich keiner unzulässigen Hilfe Dritter bedient habe. Insbesondere habe ich wörtlich oder sinngemäß aus anderen Werken übernommene Inhalte als solche kenntlich gemacht. Die Satzung des Karlsruher Instituts für Technologie (KIT) zur Sicherung wissenschaftlicher Praxis habe ich beachtet. Des Weiteren erkläre ich, dass ich mich derzeit in keinem laufenden Promotionsverfahren befinde, und auch keine vorausgegangenen Promotionsversuche unternommen habe. Die elektronische Version der Arbeit stimmt mit der schriftlichen Version überein und die Primärdaten sind gemäß Abs. A (6) der Regeln zur Sicherung guter wissenschaftlicher Praxis des KIT beim Institut abgegeben und archiviert.

Karlsruhe, 04.09.2019

Katharina Wetzel

Abstract

The rapidly growing field of sequence-defined polymers is inspired by highly defined biomacromolecules, such as peptides or deoxyribonucleic acid (DNA), which occur in Nature and whose complex and precisely defined primary structure enables their biochemical function. The specific catalytic capabilities of enzymes or the ability of DNA to store and replicate information, and thus the fundamental layout of organisms, explain the fascination behind sequence-defined polymers. However, up to date Nature's precision remains unreached, as polymer chemists worldwide strive to achieve more control over the structure of synthetic macromolecules. This thesis investigates novel approaches towards sequence-defined macromolecules of different structure and architecture using the well-established Passerini three-component reaction in combination with other reactions, such as the 1,2,4-triazoline-3,5-dione (TAD) Diels-Alder click reaction or ring-closing metathesis, in order to exceed the versatility of literature known methods.

Large, defined macrocycles were formed *via* a template-free approach by cyclisation of linear precursors. The precursors were obtained from a two-step iterative bidirectional growth strategy using a specifically designed AB-monomer and allowed for the establishment of structure activity-relationships concerning ring-closing metathesis. In the second part of this thesis, the same iterative cycle utilising a library of nine different monomers was employed, enabling the independent variation of the side chain and the backbone, leading to dual sequence-defined macromolecules obtained by multicomponent reactions. The increased density of characteristic moieties per repeating unit allowed to increase the data storage capacity of these macromolecules and sequential read-out by tandem mass spectrometry techniques confirmed this. Finally, the Passerini three-component reaction was combined with orthogonal TAD Diels-Alder click reactions to give rise to a protecting group-free synthetic pathway. The powerful combination of the two highly efficient reactions led to an ideal situation for iterative growth, enabling a fast build-up of long sequences. By transferring the approach to the solid phase, a comprehensive comparative study of solid and solution phase synthesis was conducted, highlighting the advantages and disadvantages of both strategies.

This work aims to extend the literature known pathways towards sequence-defined structures using the Passerini three-component reaction, while at the same time increasing the degree of control over sequence as well as achievable architectures, thus allowing to improve the applicability of such macromolecules.

Kurzzusammenfassung

Das sich rasch weiterentwickelnde Gebiet der sequenz-definierten Polymere ist durch hochdefinierte, in der Natur vorkommende Biomakromoleküle wie DNA oder Peptide inspiriert, deren definierte Primärstruktur komplizierte biochemische Prozesse ermöglichen. Sowohl die einzigartigen katalytischen Eigenschaften von Enzymen, als auch die Fähigkeit von DNA, die fundamentalen Informationen eines Organismus zu speichern und replizieren, erklären die Faszination, die Sequenzdefinition in der Polymerchemie birgt. Während Polymerchemiker weltweit nach mehr Kontrolle in der Polymerstruktur streben, ist die Präzision der Natur weiterhin unerreichbar. In dieser Arbeit wurden neue Ansätze untersucht, die die etablierte Passerini Dreikomponentenreaktion nutzen und mit anderen leistungsfähigen Reaktionen, wie der 1,2,4-Triazolin-3,5-dion (TAD) Diels-Alder Klick Reaktion oder der Ringschlussmetathese kombiniert, um die Vielseitigkeit bereits bekannter Ansätze noch zu übertreffen.

Große, definierte Makrozyklen wurden über einen templat-freien Ansatz durch Zyklisierung linearer Vorstufen gebildet. Die Vorstufen wurden in einem zweistufigen iterativen Reaktionszyklus basierend auf bidirektionalem Wachstum mit einem dafür geeigneten AB-Monomer erhalten und für Untersuchungen von Struktur-Aktivitäts-Zusammenhängen in der Ringschlussmetathese verwendet. Ein zweiter Ansatz greift auf den gleichen zweistufigen iterativen Ansatz zurück und verwendet dabei erstmals neun verschiedene Monomere. Durch das unabhängige Variieren von Seitenkette und Rückgrat wurden zweifach sequenzdefinierte Makromoleküle erhalten. Diese wurden mittels Tandem Massenspektrometrie ausgelesen, wobei sich zeigte, dass es sich um interessante Verbindungen für die Datenspeicherung handelt, die durch die Erhöhung der frei wählbaren Einheiten pro Wiederholeinheit eine erhöhte Datenspeicherkapazität ermöglichen. In einem dritten Ansatz wurde die Passerini Reaktion mit der dazu orthogonalen TAD Diels-Alder Klick Reaktion in einem schutzgruppen-freien Ansatz kombiniert. Die wirksame und effiziente Kombination der beiden Reaktionen führte zu einem idealen iterativen Wachstum und erlaubte die schnelle Synthese von langen Sequenzen. Durch Übertragung des Ansatzes auf die Festphasensynthese konnte eine umfassende Vergleichsstudie von Festphasensynthese und der Synthese in Lösung durchgeführt werden, die die Vor- und Nachteile beider Strategien hervorhebt.

Die vorliegende Arbeit strebt danach, literaturbekannte Ansätze zur Sequenzdefinition, die auf der Passerini Reaktion basieren, in Vielseitigkeit und Anwendbarkeit der erhaltenen Makromoleküle zu übertreffen.

Table of Contents

Acknowledgements 5
Abstract I
Kurzzusammenfassung III
1 Introduction 1
2 Theoretical Background 3
  2.1 Sequence-definition in polymer chemistry 4
    2.1.1 Sequence-control versus sequence-definition and the goal of ultimate precision 4
    2.1.2 Inspired by Nature: synthetic sequence-defined biomacromolecules as prototypes for an emerging research field 6
    2.1.3 Synthesis of non-natural, sequence-defined macromolecules of uniform size 13
  2.2 Synthetic tools for achieving uniform macromolecules 39
    2.2.1 Multicomponent reactions 39
    2.2.2 An introduction to triazolinedione chemistry 53
3 Aims 59
4 Results and Discussion 61
  4.1 Synthesis of sequence-defined macromolecules using the monomer approach 61
    4.1.1 Synthesis of sequence-defined macrocycles and their use to evaluate the limits of ring-closing metathesis 63
    4.1.2 Dual sequence-definition by using the P-3CR 81
  4.2 Combining the P-3CR with Diels-Alder click chemistry for sequence-defined synthesis – a comparative study of solid and solution phase synthesis 101
5 Conclusion and Outlook 125
6 Experimental Section 127
  6.1 Materials 127
  6.2 Instrumentation 128

6.3 Experimental Procedures ... 131

6.3.1 Experimental procedures of Chapter 4.1.1 ... 131
6.3.2 Experimental procedures of Chapter 4.1.2 ... 225
6.3.3 Experimental Procedures Chapter 4.2 ... 325

7 Abbreviations ... 387
8 List of figures and schemes ... 391

8.1.1 Figures ... 391
8.1.2 Schemes ... 395
8.1.3 Tables ... 398
8.1.4 Figures and Tables of the experimental section ... 398

9 Appendix ... 403

9.1 Publications ... 403
9.2 Conference contributions ... 404

10 Bibliography ... 405

1 Introduction

Synthetic sequence-defined macromolecules play an emerging role in polymer chemistry, as they are a unique type of polymer. This field has been heavily inspired by nature's precision polymers, such as DNA, as these are synthetically unrivalled examples of sequence-definition.[1] In biopolymers, the perfectly defined primary structure is essential for the realisation of complex biochemical functions. In living organisms, highly complex processes like data storage in the genetic material[2-3] or enzymatic activity[4] are enabled by the defined arrangement of various monomer units in long sequences (*i.e.* the primary structure), which lead to secondary and higher ordered structures, highlighting the key to their functioning. The Watson-Crick base pairing leading to double helices[5] or the formation of precisely folded enzyme structures that allow substrate specific catalytic activity[4] are highly dependent on the sequence of the macromolecule. Ever since Staudinger understood that macromolecules are built from a series of covalently bound small repeating units[6] – the monomers – polymer chemists are striving for a similar control over a molecular structure as presented by Nature. A crucial feature of Nature's polymers is their uniformity, *i.e.* all polymer chains have the same length, mass (*i.e.* a molecular weight distribution of 1), and sequential arrangement of monomers, leading to defined three-dimensional structures. The first examples of a controlled chain growth of polymers were based on living/controlled polymerisations, such as cationic, [7] anionic,[8-9] and reversible deactivation radical polymerisations.[10-14] The development of these techniques allowed to control important parameters, such as molecular weight, the functionalities introduced, and the topology of the formed macromolecules. Although polymers with molecular weight distributions close to 1.0 were obtained using the above techniques, synthetic macromolecules of uniform size are still unreached and present a “holy grail” in polymer chemistry.[15] The field of sequence-defined polymerisations giving rise to sequence-defined structures of uniform size arose with Merrifield’s pioneering work on solid phase peptide synthesis in 1963.[16] He was later awarded the Nobel prize in 1984[17] and his concept was transferred to many other classes of polymers, such as peptoids,[18] glycopeptides,[19] or oligonucleotides[20]. Since then, many different natural and synthetic sequence-defined polymers have been targeted by researchers using various approaches including both, the solid[21-23] and liquid phase,[24-25] or on soluble supports.[26-27] The most popular liquid phase approaches include exponential iterative growth strategies,[25] bidirectional growth[24] or stepwise iterative procedures[27] and have allowed for varying the degree of control. Other more exotic approaches, such as single unit monomer insertions (SUMI)[28] based on radical reactions, or sequence-defined synthesis by using templates [29-30] molecular machine.[31-32] were described.

Up to date, only solution phase approaches bear the potential to allow an easy scale-up of the reactions in order to obtain sufficient quantities of material, which are crucial for some of the potential applications. For this reason, multicomponent reactions have been identified as a powerful tool for sequence-definition as they are highly efficient giving rise to high yields and as the inherent modular character of these reactions allow to easily introduce a variety of side chains into the polymer backbone.[27, 33-35] Several different growth modes have been investigated and on the one hand it was found that exponential- and bidirectional growth restrict the possible degree of control in the sequence order, while allowing for a fast build-up of long sequences. Stepwise iterative approaches, on the other hand, have shown to benefit from the highest possible degree of control, coming at the cost of a higher synthetic effort.[36]

Recently, the application of sequence-defined polymers as data storage devices has received a lot of attention, and the coding and decoding of information stored in synthetic molecules has become one of the hot topics in modern polymer chemistry.[37-41]

In this thesis, multicomponent reactions are used to further expand the toolbox available to polymer chemists for synthesising sequence-defined macromolecules. This is achieved by combining known multicomponent reactions with other versatile and efficient reactions, namely “Click reactions” and olefin metathesis. The herein developed approaches aim to develop more efficient synthetic procedures to achieve higher molecular weights, an increased degree of control compared to literature known approaches and novel, non-linear, architectures of sequence-defined macromolecules. Furthermore, the application of the macromolecules as data storage devices is also explored.

2 Theoretical Background

The current chapter serves as introductory chapter, covering the theoretical background of the main aspects of this thesis, which are concisely summarised. In the first part (Chapter 2.1), the origin and motivation behind the field of synthetic sequence-defined macromolecules is discussed, starting from the well-established synthesis of naturally occurring biopolymers, such as DNA or peptides. Subsequently, the state of the art in synthetic sequence-defined macromolecules is summarised by highlighting and discussing selected examples of current approaches towards sequence-definition as well as the achievements of leading working groups in this field. In the final section (Chapter 2.2) of this theoretical background chapter, the efficient and straightforward tools and techniques for achieving uniform and defined macromolecules, which are applied in this thesis, are presented. Thus, multicomponent reactions and their advantageous characteristics for defined synthesis are described. The Passerini three-component reaction (P-3CR) is introduced in detail, discussing the respective mechanism and applications in polymer chemistry. Finally, one example of highly efficient click chemistry, 1,2,4-triazoline-3,5-dione (TAD) chemistry, is presented, as it offers various desirable features for sequence-definition and was therefore combined with the well-established P-3CR within this thesis.

2.1 Sequence-definition in polymer chemistry

2.1.1 Sequence-control versus sequence-definition and the goal of ultimate precision

In a review published in 2013, sequence-controlled polymers were defined for the first time by Lutz, Ouchi, and Sawamoto.[39] They described sequence-controlled polymers as *"…macromolecules in which monomer units of different chemical nature are arranged in an ordered fashion"*. The definition shows that the term sequence-controlled can be considered as an umbrella term for any level of control within polymers, including not only perfectly defined macromolecules of uniform size, but also less defined polymers such as block- or even gradient copolymers. In order to distinguish between different levels of control, more strict definitions need to be made.[42-43] Sequence-controlled polymers can be further classified into disperse polymers and polymers of uniform size (see Figure 1).[42-43]

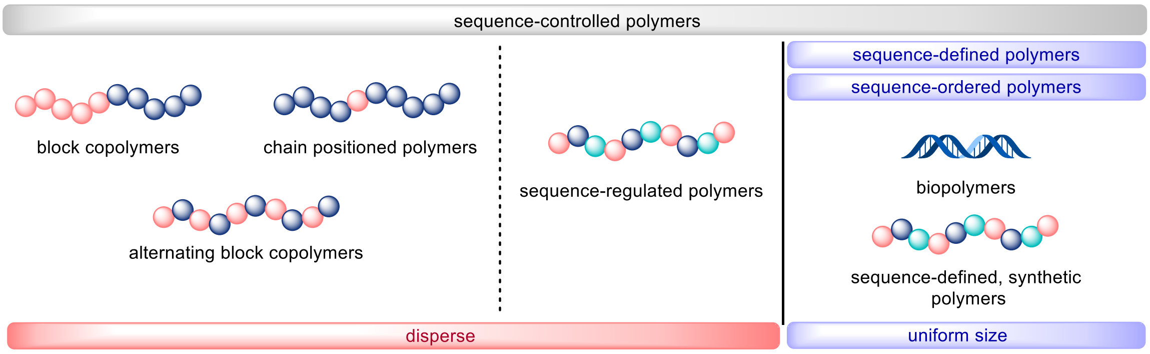
sequence-controlled polymers
sequence-defined polymers
sequence-ordered polymers
block copolymers
chain positioned polymers
sequence-regulated polymers
biopolymers
alternating block copolymers
sequence-defined, synthetic polymers
disperse
uniform size

Figure 1. Classification and definitions of polymers exhibiting different levels of control.

Sequence-controlled polymers include block copolymers, gradient copolymers, chain positioned polymers (in the ideal case, one different co-monomer unit in a homopolymer chain, but minimal variations typically exist due to the statistical nature of the applied synthesis techniques), but also sequence-regulated polymers that exhibit a higher degree of control albeit still being disperse.[44] The (molecular weight) dispersity is defined as shown in the formula below (with M_w being the weight average of the molar mass and M_n being the number average of the molar mass):[45]

$$Đ_M = M_w / M_n$$

In contrast to sequence-defined macromolecules which are strictly uniform in size and composition, sequence-controlled macromolecules with a dispersity close to 1.0 are not uniform in size albeit exhibiting a narrow size distribution. Furthermore, they feature minimal, but existing variation in the sequence order.[46] Sequence-defined polymers, on the other hand, include all kinds of macromolecules with a defined sequence of the monomer units as well as a defined chain length, thus being uniform in size.[42] They are sometimes also referred to as sequence-ordered polymers, since the nomenclature in the relatively young field of sequence-definition is not yet strictly defined.[47-48] According to the international union of pure and applied chemistry (IUPAC), such monodisperse sequence-defined macromolecules are called macromolecules of uniform size,[49] and are the focus of the present thesis. However, in the community, both words are still utilised interchangeably. Thus, the first part of this introductory theoretical background chapter highlights the most important examples of sequence-defined synthesis.

Before highlighting some examples of the state of the art within this field, the motivation and future targeted goals will be discussed. The field of sequence-definition is strongly inspired by nature, where highly defined macromolecules like DNA and certain proteins, *i.e.* enzymes, play important roles in living organisms. The sophisticated function of enzymes, for instance, which is strongly associated with the high definition of their primary structure (*i.e.* the sequence in which the constituent amino acids are linked to each other) – and as a consequence, their secondary and tertiary structure – has instigated the fascination behind sequence-defined synthesis. However, Nature's precision is unreached. By forming macromolecules with precise sequences of only four building blocks (*i.e.* nucleobases), the complex information, *i.e.* the building plan, needed to obtain a functioning organism is stored in highly defined macromolecules. Polypeptides, in addition, are able to catalyse complex biochemical reactions while offering high substrate specificity, thus catalysing only one single defined reaction.[4] Inspired by the precision and efficiency demonstrated by certain types of natural macromolecules, polymer chemists nowadays strive for greater control in synthetic polymers, albeit the control is often restricted to molecular weight or architecture. One century after Staudinger understood that polymers consist of monomer units that are covalently bound to each other to form a macromolecule, numerous achievements in polymer chemistry have been made.[6] An important step towards greater control in polymer synthesis was the development of living ionic polymerisations (living anionic polymerisation in particular)[8-10] and reversible-deactivation radical polymerisation (RDRP) techniques. The latter is especially advantageous because of its lower sensitivity to moisture and air, allowing for simpler reaction conditions. Such RDRP techniques include atom transfer radical polymerisation (ATRP), nitroxide-mediated radical polymerisation (NMP), and reversible addition-fragmentation chain transfer (RAFT) polymerisation enabled chemists to achieve control over the polymer molecular weight (distributions close to 1.0 can be achieved), architecture, and functionality.[10-14] However, the obtained products remain disperse. Meanwhile, several approaches towards sequence-defined macromolecules were developed, which will be introduced in the following section (see

Chapters 2.1.2 and 2.1.3). So far, the relatively young field of synthetic sequence-defined polymers is mostly driven by the development of novel and efficient approaches to synthesise such macromolecules, as well as the investigation of structure-property or structure-activity relationships, *i.e.* to understand how certain properties are affected by the structure. Sequence-definition in mainly achieved by side chain variation, but also a first example of introduction of sequence-definition by backbone variation has been reported. In the long term, properties that mimic the ones of the aforementioned biomacromolecules are envisioned, such as data storage capacity or enzyme-like catalytic activity. In that regard, attempts to use sequence-defined polymers for data storage have been developed demonstrating the challenges, but also showcasing the potential of synthetic polymers for specific applications in this field.

Nonetheless, the first examples of sequence-defined syntheses inspired by biomacromolecules were reported, setting the basis for the field as they allowed to develop key synthetic tools. In Chapter 2.1.2, the syntheses of three types of biomacromolecules, namely polypeptides, polypeptoids and oligonucleotides, will be discussed.

2.1.2 Inspired by Nature: synthetic sequence-defined biomacromolecules as prototypes for an emerging research field

The first approach towards sequence-defined synthesis was reported by Merrifield in 1963, who developed the solid phase peptide synthesis (SPPS),[16] for which he was later awarded with the Nobel prize.[17] The method allowed straightforward synthesis of oligopeptides and was later transferred to oligopeptoids[18] and oligonucleotides.[20] Furthermore, the procedure could be automated, allowing for fast synthesis of longer sequences in a straightforward fashion.[50] One of the main advantages of SPPS is the simple workup:[17] the products are separated by filtration. Furthermore, a large excess of reagents can be applied, facilitating quantitative conversions. The method also significantly reduces the loss of product or the formation of by-products.[17] The concept of SPPS benefits from an orthogonal protecting group strategy:[51] reactive functional groups need to be protected – the amine of the incoming amino acid is typically protected with a labile 9-fluorenyl methoxy carbonyl (Fmoc) group – the peptide synthesis follows an iterative coupling, washing, deprotecting, washing cycle. Thus, unwanted side reactions are avoided and only the desired coupling product is obtained. The commonly applied synthetic protocol follows a C→N strategy where the *C*-terminus of the first amino acid is reacted with the linker of the solid support. This synthesis procedure is depicted in Scheme 1. The first amino acid is coupled to the resin by a S_N2 reaction. Each coupling step is followed by a deprotection. The iterative cycle consists of a coupling and a deprotection step. The final peptide is obtained by cleavage from the solid support and by deprotection of the side groups and the *N*-terminus.[16]

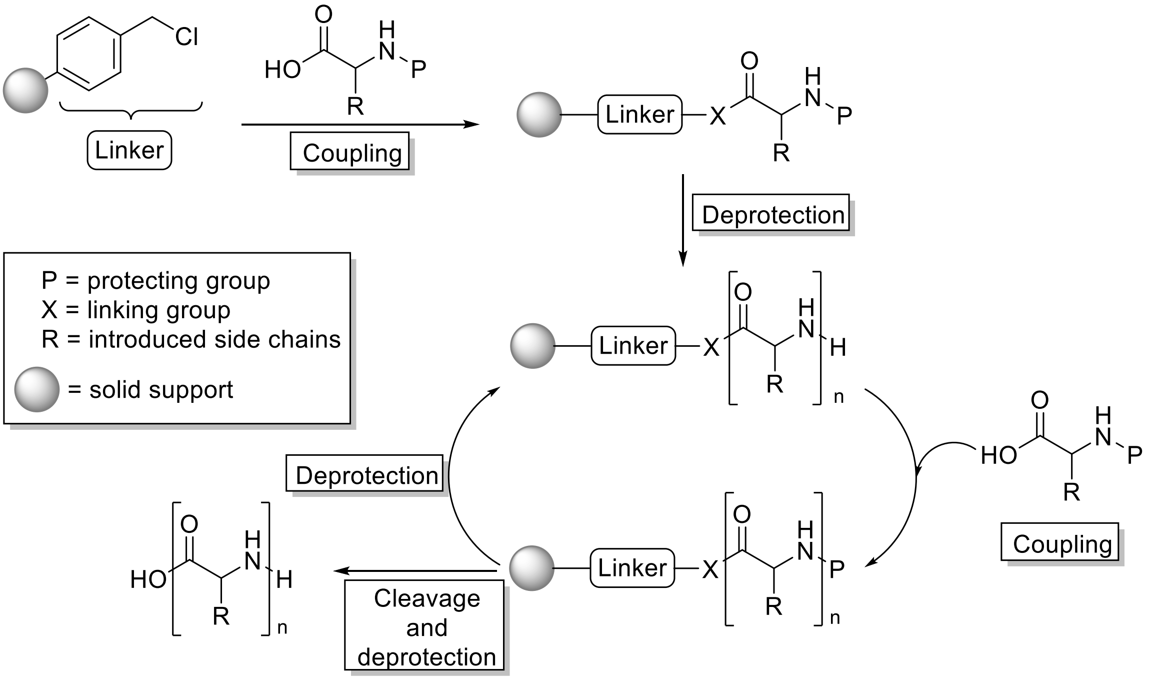
Linker
Coupling
Deprotection
P = protecting group
X = linking group
R = introduced side chains
= solid support
Cleavage and deprotection
Coupling
Deprotection

Scheme 1. Two-step iterative cycle of the SPPS, developed by Merrifield. [16, 51]

Highly crosslinked copolymers of styrene and 1,4-divinyl benzene or poly(acrylamide) are typically used as the solid support resin and are swollen in organic solvents in order to solvate the growing chain, thus making it accessible for the employed reagents (typical loadings of commercially available resin are between 0.2 – 1.0 mmol/g). Three examples of commonly used resin linkers are shown in Figure 2. The linker is usually attached to the resin by an ester or amide bond.[16]

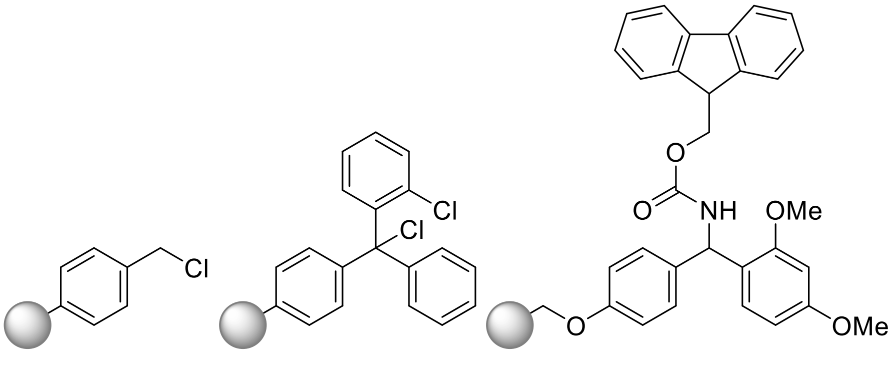

Figure 2. Three examples of commonly utilised resins used as solid support in SPPS. The chloromethyl resin, the 2-chlorotrityl chloride resin and the Rink amide resin are depicted.[52-54]

The SPPS cycle starts after the first amino acid has been attached to the linker which is in turn attached to the resin. In a first step, the temporary protection group on the *N*-terminus is cleaved.[16] Here, the base labile Fmoc protecting group is often used as temporary protecting group for the *N*-terminus.[51, 55] After deprotection the primary amine reacts with the activated acid group of the incoming *N*-terminus protected amino acid. The acid functionality needs to be activated in order to prevent an acid-base reaction between the acid and the amine and in order to allow the reaction to proceed under mild conditions.[17] By activating the carboxylic acid, an active ester is formed, accelerating the peptide bond formation by increasing the electrophilicity of the carboxy group. Furthermore, good leaving groups are introduced, further facilitating the reaction. The activation can be achieved by *N,N'*-dicyclohexylcarbodiimide (DCC) or phosphonium- or uronium-based coupling agents, such as benzotriazol-1-yl-oxytripyrrolidino phosphonium hexafluorophosphate (PyBOP) and 2-(1*H*-benzotriazol-1-yl)-1,1,3,3-tetramethyluronium hexafluorophosphate (HBTU).[56-60] After washing steps and filtration, chain extension can be performed by repeating the coupling-deprotection process. The desired oligopeptide is obtained upon cleavage from the solid phase. Because of the base-labile protecting group used on the *N*-terminus, the protecting groups used on the functional groups of the amino acids as well as the linker are commonly acid-labile, thereby ensuring orthogonality.[51] SPPS requires highly efficient reactions that achieve nearly quantitative conversions. Defective sequences, which can be caused by incomplete conversions as well as the formation of by-products, are difficult to separate after cleavage from the resin. Often, capping steps are required to quench the unreacted amino acids in order to prevent their reaction in later steps.[54]

Shortly after SPPS was first reported in 1965, Merrifield reported the automation of the process thus marking another breakthrough, not only in natural peptide synthesis,[50, 61] but, as the method was transferred to many other fields, also non-natural peptides,[62] glycopeptides,[19] oligonucleotides[20] or peptoids.[18]

In his first approach, Merrifield presented the synthesis of a tetramer,[16] but by careful optimisation longer sequences were also reported. For instance, Merrifield and colleagues synthesised bovine insulin, which is a sequence of 52 amino acids[63] and ribonuclease A, a sequence of 124 amino acids.[64] The invention of chemical ligation marks another milestone in the synthesis of enzymes.[65-66] Chemical ligation describes the covalent linkage of peptide fragments providing high yields and purities. By applying this concept, more than 300 biologically active proteins, that fold *in vitro*, were synthesised.[67] Thus, this method allows for the design of defined primary, secondary, and tertiary structures. By automation of the SPPS process and combination with chemical ligation concepts, the synthesis of HIV-1 protease (198 amino acids, *ca.* 22 kDa)[68] or even higher molecular weight peptides (e.g. an erythropoietin analogue containing 166 amino acids, *ca.* 55 kDa)[69] were realised, demonstrating that the SPPS method is an important tool for peptide synthesis and the synthesis of other uniform macromolecules, as the concept can be transferred to many other reactions.

Another class of biomacromolecules are the non-naturally occurring peptoids that, however, show biological activity. They are the *N*-substituted analogues of peptides, hence the side chain is not introduced at the C_{α}-position but bound to the nitrogen (compare Figure 3).[18]

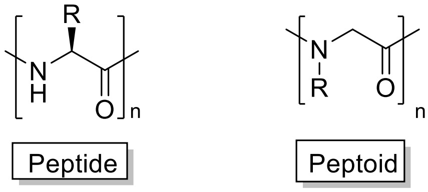

Figure 3. Comparison of the structure of naturally occurring peptides and non-natural peptoids.[18]

The different structure of peptoids leads to several interesting features of this class of macromolecules. In contrast to their *C*-substituted analogues, peptoids are not chiral, avoiding epimerisation issues during their synthesis.[70] Additionally, the formation of hydrogen bonds is prevented because of the *N*-substitution, resulting in conformationally unstable structures.[70] However, by introducing tailored side chains, secondary structures can be induced.[70-72] Such studies on initially conformationally unstable structures allow for detailed structure-property relationship investigations, which are interesting for the field of sequence-defined synthesis.[71-72] Peptoids exhibit better solubility in organic solvents compared to peptides due to their different backbone. Furthermore, they exhibit a higher proteolytic stability and are more resistant to enzymatic degradation.[70] Some peptoids show biological activity and, compared to peptides, are absorbed faster into cells. Such properties make them attractive candidates for medical and pharmacological applications where they are used as peptide mimics.[18]

Similar to peptides, peptoids can be synthesised on a solid support by coupling of mono-protected *N*-substituted glycine monomers.[18] However, due to the secondary amine of the peptoids, the coupling proceeds much slower, leading to the development of the so-called submonomer approach, which was first described by Zuckermann in 1992.[73] In this approach, the glycine repeating units are formed by the reaction of two so called submonomers, being an amine and a haloacetic acid. Advantageously, the reagents are commercially available and no backbone protecting groups are needed, thus making this process highly attractive.[73] The iterative cycle for the formation of a peptoid by SPPS is depicted in Scheme 2.[73] It starts with the reaction of a resin-bound secondary amine with a haloacetic acid upon activation with diisopropylcarbodiimide (DIC). This first acylation step is followed by a nucleophilic substitution, where the halide is replaced by an amine forming the first monomer unit. The subsequent acylation leads to a more reactive compound, compared to the corresponding secondary amine, thus significantly accelerating the reaction.[54]

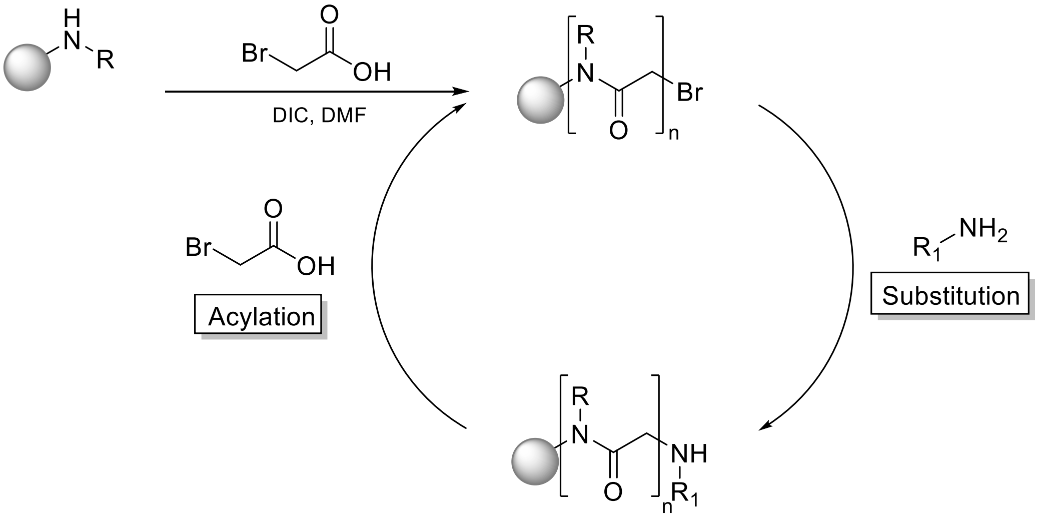

Scheme 2. Two-step iterative cycle for the preparation of peptoid using the submonomer approach which was reported by Zuckermann and co-workers in 1992.[73]

Alike the automated SPPS, the submonomer approach can be performed automatically on a peptide synthesiser.[54, 73] Polypeptoids containing up to 50 glycine units are routinely synthesised by automating the protocol.[74-76] This development facilitated investigations of the influence of the side chain on secondary structures.[71-72] By introduction of bulky α-chiral side chains, for instance by using (*S*)-*N*-(1-phenylethyl)glycine, the formation of α-helices is induced.[72, 77-79] Interestingly, analysis of the crystal structure of the helices provided new insight into the mechanism of helix formation. All amide bonds were found to be in *cis*-configuration while one turn in the helix was found to consist of three glycine repeating units.[80] Furthermore, introduction of more sterically-demanding side chains led to sharper peaks in the nuclear magnetic resonance (NMR) by reduction of the number of obtained conformational isomers.[81-83] Besides the formation of α-helices, β-sheet formation was also achieved. By mixing two oppositely charged 36-mers, self-assembly of the polypeptoids to two-dimensional nanosheets was achieved.[84] The well-investigated structure-property relationships of polypeptoids is particularly interesting for the further development of sequence-defined synthesis of various building blocks. Hence, the relatively well investigated structure property relationships of this interesting class of biomacromolecules represents an important example in sequence-defined synthesis.

Oligonucleotides represent the third class of sequence-defined biomacromolecules that will be briefly introduced within this chapter. The first report on oligonucleotide synthesis was published in 1965 by Letsinger and Mahadevan.[85] Nowadays, the synthesis is mainly conducted on solid support. The first report on automated DNA synthesis was published in 1985.[86-88] Thus, the synthesis of 98-mers and 120-mers was reported.[89-90] By the introduction of phosphoramidite chemistry, the protocol was significantly improved.[91] An example structure of a synthetic oligonucleotide is depicted in Figure 4.

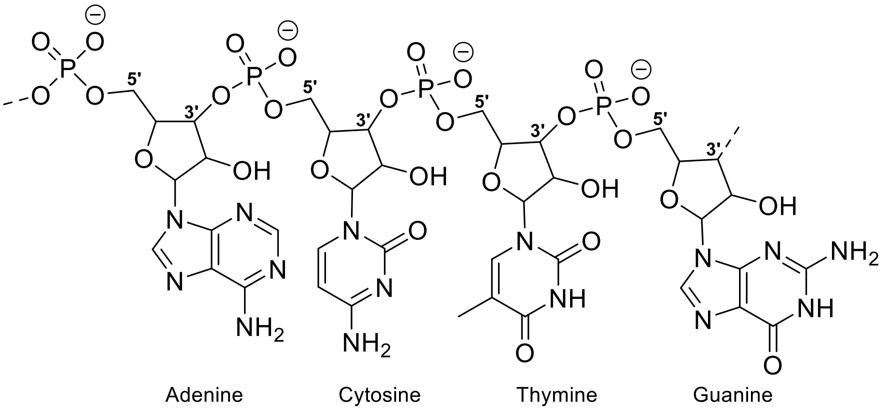

Figure 4. Structure of an oligonucleotide synthesised by applying the phosphoramidite approach. This example contains the four nucleobases: adenine, cytosine, thymine, and guanine.[92-93]

In synthetic chemistry, oligonucleotides are synthesised from the 3′ to the 5′ end in contrast to the natural synthetic process in biological systems. Similar to peptide synthesis, highly efficient and orthogonal protecting group strategies are required.[20] A resin-bound nucleoside is deprotected at its 5′ end.[93] The free hydroxy group is then reacted with a tetrazole-activated phosphoramidite, whereby a phosphite triester is obtained. The reagents are used in excess, similar to SPPS;[94] however, extensive capping steps are required since the coupling efficiency is low.[93] The capping step is followed by the oxidation of the phosphite triester to the more stable phosphotriester under mild reaction conditions using iodine and 2,6-lutidine as base.[95] Next, the iterative cycle consisting of deprotection, coupling, capping, and oxidation steps is repeated until the desired sequence is obtained.[93] Subsequently, the products are deprotected and cleaved from the resin. In the highly orthogonal protecting group strategy, different protecting groups are required for the exocyclic amine groups of the DNA bases,[93] the phosphite triester, and for cleaving the product from the solid support an additional linkage group is required (compare Figure 5). While thymine and uracil (one of the bases in ribonucleic acid) do not need protecting groups because they do not bear exocyclic amine groups, adenine, guanine, and cytosine require protecting, usually with base-labile benzoyl groups.[93] The 5′-hydroxy group is protected with an acid labile dimethoxytrityl group. The primary hydroxy group exhibits excellent regioselectivity and the cleavage is straightforward. In contrast to DNA, there is a 2′ hydroxy group present in ribonucleic acid (RNA). This group is commonly protected by a fluorine labile triisopropyl silyloxymethyl group (TOM group),[94] which allows RNA synthesis under conditions similar to those employed for DNA synthesis.[94, 96] The phosphotriester is protected *via* a base-labile cyanoethyl protecting group and a diisopropylamino group acts as leaving group during the coupling step.[20, 97-99]

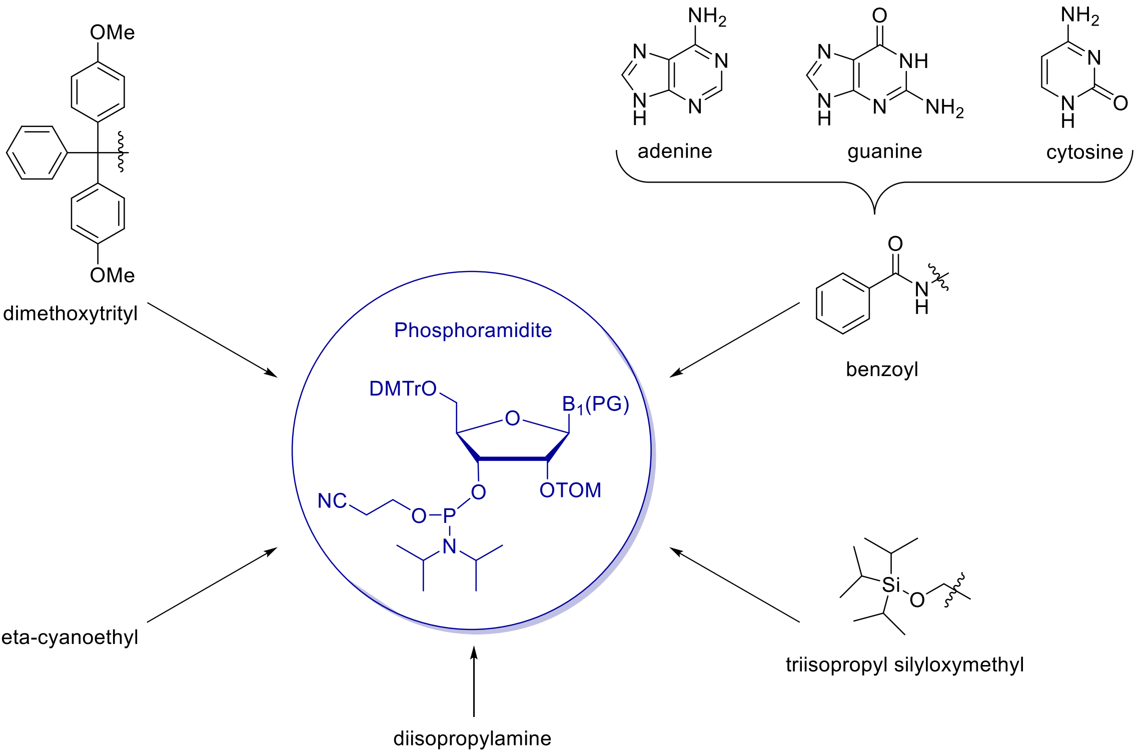
OMe
OMe
dimethoxytrityl
NH2
N
N
N
N
H
adenine
O
N
NH
N
N
NH2
H
guanine
NH2
N
N
O
H
cytosine
O
N
H
benzoyl
Phosphoramidite
DMTrO
O
B1(PG)
O
OTOM
NC
O
P
N
beta-cyanoethyl
Si
O
triisopropyl silyloxymethyl
diisopropylamine

Figure 5. Orthogonal protecting group strategy for the solid phase oligonucleotide synthesis commonly applied in the phosphoramidite approach.[93-94, 100]

It is noteworthy that, solely based on four building blocks (*i.e.* nucleobases) and the sequence in which these are linked, the genetic code is formed. This code dictates the functions responsible for life, e.g. protein synthesis, and represents a natural large capacity storage medium.[2-3] Its use as storage medium for digital data has also been reported.[37, 101-105] Conventional digital data storage is based on a binary code that allows the storage of one bit per repeat unit. DNA, on the other hand, owing to its four bases, offers a quaternary code, thus increasing the data storage capacity compared to conventional systems. In 2017, Ehrlich and Zielinski reported the use of DNA as a storage system: according to their calculations, $2.14 \cdot 10^6$ bytes can be encoded in oligonucleotides. They calculated an information density of 215 petabytes (10^{15}) per gram of DNA with 72,000 oligonucleotides (DP = 200) and were also able to read the stored information afterwards.[106]

In conclusion, many achievements towards synthetic biomacromolecules have been made, allowing to mimic nature and providing synthetic biomacromolecules for various different applications. Furthermore, some key synthesis tools can be transferred to non-natural macromolecules, thus paving the way for the synthesis of other classes of sequence-defined macromolecules.

2.1.3 Synthesis of non-natural, sequence-defined macromolecules of uniform size

In this section, different approaches towards sequence-defined non-natural macromolecules are presented. The chapter is divided in three sections based on the respective synthetic procedure: in the first section, syntheses on a solid support will be presented (see Chapter 2.1.3.1). The advantages and disadvantages of solid phase synthesis will be discussed in detail in this section followed by the synthetic approaches in solution (Chapter 2.1.3.2), highlighting the most important achievements in the synthesis of sequence-defined macromolecules in solution. Similarly to the previous sections, the respective advantages and disadvantages of solution phase approaches will be explained and discussed. In the third subsection of this chapter (Chapter 2.1.3.3), approaches that combine aspects of both previous methologies towards sequence-definition will be briefly introduced, including the synthesis on a soluble polymeric support, purification *via* fluorous solid phase extraction, and some more ‘exotic’ approaches such as the use of molecular machines or template-assisted approaches.

Parts of this chapter are based on the following review: Recent Progress in the Design of Monodisperse, Sequence-Defined Macromolecules, S. C. Solleder, R. V. Schneider, K. S. Wetzel, A. C. Boukis, M. A. R. Meier, *Macromol. Rapid Commun.* **2017**, *38*, 1600711.[36]

2.1.3.1 Solid supported synthesis

Perhaps the most widely applied synthetic approach to obtain sequence-defined macromolecules involves the use of solid supports, such as in the case of SPPS (described in more detail in Chapter 2.1.2). Solid phase approaches benefit from simple work-up procedures and the possibility to automate the synthesis, e.g. using commercial peptide synthesisers.[36] The products can be filtered off, while reagents that were used in excess or any formed smaller by-products can be washed away. However, in many reported syntheses, the products require purification once they are cleaved from the resin. This is because of incomplete reactions or side reactions, leading to inaccurate sequences. Capping steps can help to circumvent such errors, but 100% purity is hardly reached. Additionally, solid phase synthesis limits the applicability of the synthesised products because of the small scales of the reactions. On the other hand, the simple work-up saves time and labour, which makes solid phase approaches highly attractive as long sequences can be achieved within relatively short times. The most important advantage of solid-phase synthesis is the possibility to conduct the whole procedure automated on an adapted peptide synthesiser. Inspired by Zuckermann's submonomer approach[73] and by the SPPS developed by Merrifield,[16] several other approaches towards synthetic polymers were developed making benefit of solid supports.

The basic principle of peptide synthesis through the formation of amide bonds was implemented by Jiang and co-workers for the synthesis of uniform amide-bond-containing poly(ethylene glycol)s (PEGs) on a Rink amide solid support.[107] PEG containing amino acid building blocks were first synthesised in solution and subsequently applied in SPPA to obtain amide bond containing PEGs. A PEG 24-mer-amino acid was synthesised over 10 steps in an overall yield of 15%. However, yields for the coupled peptides obtained by SPPS were not reported. The synthesis of the PEG-amino acids was conducted on multigram scale and by coupling of the amino acids by SPPS molecular weights greater than 10,000 Da were reported. After cleavage from the solid support, high pressure liquid chromatography (HPLC) purification was required to obtain the products in high purity. Notably, not only high molecular weights were obtained, but also the final product was obtained in high purity. HPLC and matrix-assisted laser desorption ionization coupled to a time of flight detector (MALDI-ToF) analysis revealed high purity of the products.

Sleiman, Serpell, and colleagues reported the synthesis of sequence-defined macromolecules appended to DNA.[108] They used classic phosphoramidite chemistr,y[91] which was also applied in the synthesis of other DNA conjugates such as oligopyrenotide-,[109] oligonucleotide oligospermine-[110] and glycol-conjugates[111] appended to DNA. Using automated synthesis, oligonucleotides containing 19 nucleotides were prepared,[108] while small oligomers were then appended to the DNA strands. The conjugation was achieved by using the same automated phosphoramidite chemistry. The employed hydrophilic hexa(ethylene glycol) blocks and hydrophobic hexa(ethylene) blocks are commercially available as the corresponding dimethoxytrityl protected phosphoramidites. The hydrophobicity of the obtained oligomers was fine-tuned by variation of the number or sequence of the up to twelve attached blocks. Additionally, the self-assembly as well as the influence of the attached oligomers on the formation of higher order three-dimensional structures was studied.[112]

In another approach, the Sleiman group demonstrated the use of perfluorocarbon containing phosphoramidites for DNA strand synthesis, which was referred to as “DNA-teflon”.[113] Non-natural polymers were synthesised from two phosphoramidite building blocks bearing either hexa(ethylene glycol) or perfluorinated side chains. The two building blocks were coupled by automated phosphoramidite chemistry on a DNA synthesiser to form the desired copolymers. Electrospray ionisation mass spectrometry (ESI-MS) analysis confirmed the incorporation of up to ten units into a DNA 19-mer. The self-assembly of the "DNA-teflon" was investigated by dynamic light scattering (DLS) and atomic force microscopy, whereby spherical micelles with a perfluorocarbon core and DNA corona and narrow size distribution were observed.

An elegant approach was reported by Grate *et al.*, who exploited the nucleophilic substitution of cyanuric chlorides forming hexamers on a solid support.[21] For the oligomer synthesis, mono-substituted cyanuric chloride submonomers were first synthesised within one step in good yields and subsequently incorporated into the oligomer by reaction with a diamine between monomer additions (Scheme 3). Triazine-based sequence-defined oligomers with tailored side chains were formed without utilising any protecting groups, which was attributed to the decreasing reactivity of the cyanuric chloride chain-end with each reaction step. Sequence-defined hexamers were obtained in good overall yields of up to 75%. The products were characterised by various techniques, crucially showcasing their uniformity. The synthesis was conducted on a 50 mg scale, as typical for solid phase syntheses. Molecular dynamics simulations indicated that backbone interactions, such as hydrogen bonding or π-π-interactions, were present, which is especially interesting in terms of intermolecular self-assembly.

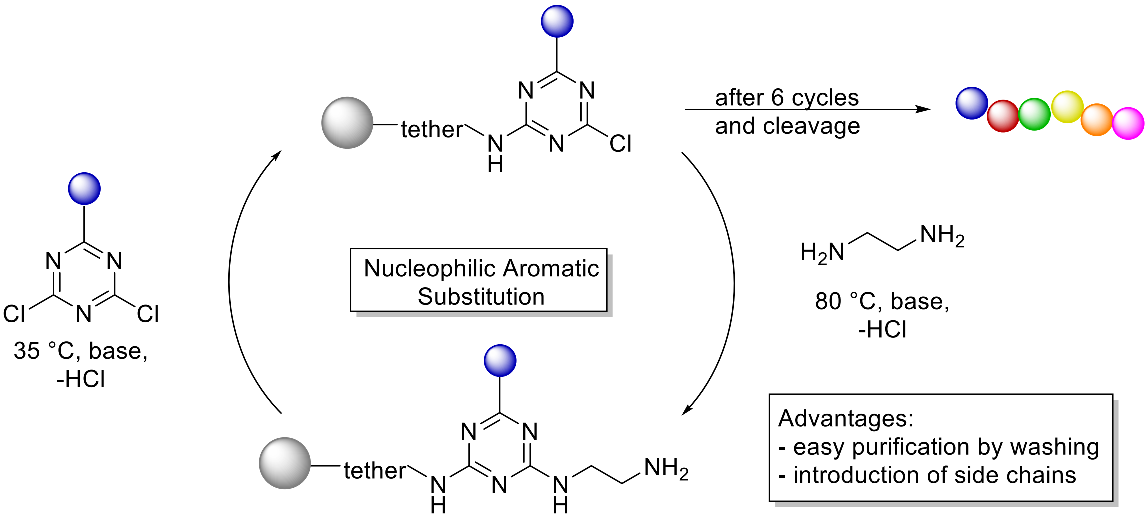

Scheme 3. Protecting group–free solid-phase synthesis exploiting the nucleophilic substitution of cyanuric chloride. With each reaction, the reactivity decreases, making elevated temperatures necessary and thereby avoiding protecting groups.[21]

Aiming at encoded macromolecular sequences for data storage, Lutz and co-workers have developed several systems that result in sequence-defined oligomers for such applications. In a first approach, the synthesis of phosphoramidite oligomers was conducted utilising a cross-linked polystyrene solid support, benefitting from the highly efficient and well established and optimised phosphoramidite coupling.[114] Non-natural phosphoramidite monomers were defined as 0, 1, and 1' in order to encode the oligomers. By performing the coupling reactions manually, sequence-defined oligomers with lengths between pentamers up to a 24-mer were achieved. The oligomers allowed for post-synthetic modification by copper-catalysed azide-alkyne cycloaddition (CuAAC) as terminal alkyne functions were incorporated. As a proof of principle, PEGylation of the polyphosphates was performed. The protocol was later extended by automating the coupling using a DNA synthesiser.[22] In the automated synthesis, two non-natural monomers were defined as 0 and 1 and the protocol of Beaucage and Caruthers was applied.[20, 91] Controlled pore glass was used as solid support and for the synthesis of long sequences, capping steps were inevitable. High coupling efficiencies were achieved within relatively short times of three to twelve hours depending on the length of the sequences (Figure 6).[22] It is noted that the approach required the synthesis of a primer sequence containing three thymine nucleotides that allowed the quantification of the formed oligomers by ultraviolet (UV) spectroscopy and facilitated characterisation by HPLC. Oligomers of different lengths with a degree of polymerisation (DP) of 16, 24, 56, and 104 were obtained. The read-out strategy of choice, which is of crucial importance for the success of the application of encoded oligomers in the field of data storage, included tandem-MS techniques,[115-116] NMR spectroscopy, or depolymerisation techniques.[117] The latter was later improved to further facilitate the read-out by carefully controlling the structure of the oligomers and introducing predetermined breaking points.[118] In another approach reported by Lutz, Charles, and co-workers, an orthogonal two-step iterative synthesis procedure on solid support was reported.[119] Phosphoramidite coupling was iterated with radical-radical couplings. Owing to the chemoselectivity of the two reactions, the procedure was conducted without the use of protecting groups. Two different building blocks were required to combine the reactions: a phosphoramidite monomer carrying an alkyl bromide and a hydroxyl-functionalised nitroxide. Five different phosphoramidite building blocks were synthesised two of which were used to encode the oligomers.

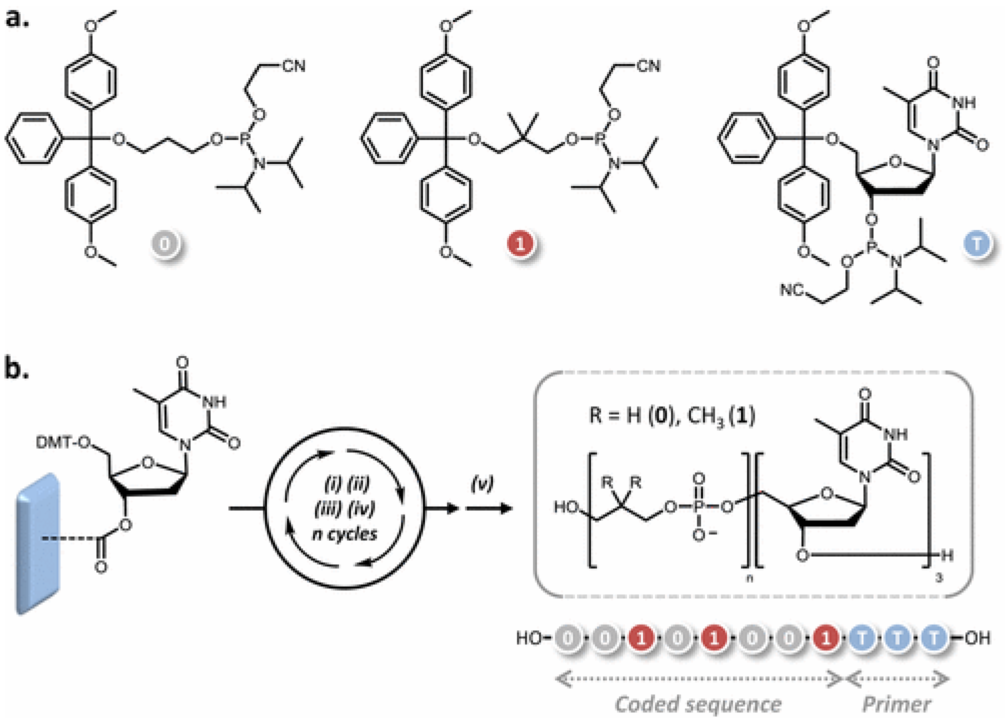

Figure 6. (a.) Phosphoramidite based monomers "0" and "1" to encode the macromolecules and the thymine containing nucleotide that formed the primer sequence facilitating the subsequent analysis. (b.) iterative approach on a solid support consisting of four steps: (i) Dimethoxy trityl (DMT) deprotection, (ii) coupling step, (iii) oxidation, (iv) capping. The final product is obtained by (v) cleavage from the solid support. Reprinted with permission from A. A. Ouahabi et al., ACS Macro Lett. ***2015****, 4, 1077-1080. Copyright © 2015 American Chemical Society.*[22]

In a first step, the phosphoramidite was immobilised on the solid support by reacting it with a hydroxy group. By an *in situ* oxidation, the phosphate was obtained. In the next step, the alkyl bromide was activated by using copper bromide, leading to the formation of a carbon-centred radical which was immediately trapped by the nitroxide. During the synthesis, labile alkoxyamide bonds were formed, which are easily cleaved, significantly facilitating the read-out by MS/MS since complex fragmentation patterns were thus avoided. Various oligomers with a DP up to 8 were obtained with this strategy. In another approach, which was also reported by Lutz and Charles *et al.*, the synthesis of encoded polyurethanes was described.[120] By applying an orthogonal iterative multistep growth strategy on solid phase, they realised the synthesis of polyurethanes with defined primary structures. A modified Wang resin was used and reacted with *N,N*-disuccinimidyl carbonate, yielding an unsymmetrically activated carbonate, which was subsequently converted in a chemoselective reaction with an amine to form the carbamate unit. Two different binary alphabets were defined and used to encode oligomers up to a length of 16 repeating units. The read-out was performed using tandem ESI mass spectrometry in negative mode.[121] In a later report, the oligo(urethanes) were used to evaluate their suitability as 2D molecular barcodes for labelling different commodity polymers,[122] and as *in vivo* recognition tags for implant identification.[123] The synthesis of oligo(alkoxyamine amide)s was demonstrated by the group of Lutz by using an orthogonal "AB+CD" strategy.[124] One of the monomers carried an amine and a nitroxide, the other was functionalised with an anhydride and an alkyl bromide. The orthogonal reactions resulted in a protecting group–free approach on solid support. Since the obtained products were thermally degradable due to their labile alkoxyamine bond, the fragmentation during thermal degradation could be easily analysed. As such, a large excess of (2,2,6,6-tetramethylpiperidin-1-yl)oxyl (TEMPO) was added as trapping agent, further facilitating the analysis of the fragments. The synthesis of pentamers and decamers was reported, albeit, owing to the bifunctional nature of the repeat units, the obtained products were only composed of 2.5 and five repeat units, thus are trimers and pentamers based on the numbering system used throughout this thesis. The fragmentation behaviour of the obtained products was studied in detail in positive and negative tandem ESI-MS mode.[115, 125] The group also investigated the specific optimisation of fragmentation patterns by introducing predetermined breaking points into the polymer that are cleaved during ESI-MS/MS analysis, thus avoiding complicated and unpredictable cleavages during the analysis.[126-127] Recently, the group of Lutz reported the preparation of thin films built from layers of digitally encoded polymers using a layer-by-layer strategy in order to increase the data storage capacity.[128] They encoded a sentence of 160 bytes and embedded the data into defined sequences of layers of nanofabricated multi-layered films. A library of 16 sequence-defined polyanions was generated by solid-phase phosphoramidite chemistry and used for deposition in a layer-by-layer manner with non-coded polycationic layers between the coded polyanion layers to form digitally encoded thin films. Each anion contained 10 bytes of information, resulting in the reported total of 160 bytes. To date, read-out and thus actual data storage of the layers has not been reported and thus the applicability of this approach remains inconclusive.

Du Prez and co-workers introduced thiolactone chemistry for the preparation of sequence-defined macromolecules. In their first approach, published in 2013, a two-step iterative cycle performed on a 2-chlorotrityl chloride resin was presented.[129] In the first step, the amine function of the resin was exploited to open a thiolactone ring by aminolysis, generating a thiol. The thiol was subsequently converted in a Thia-Michael addition with a thiolactone acrylamide. By using different primary amines in the aminolysis, different side chains were introduced. Due to the orthogonality of the two employed reactions, protecting groups were not required in this approach. A sequence-defined tetramer was obtained, but due to observed side reactions it was not possible to obtain sequences beyond the tetramer stage.

The approach was subsequently improved by using a thiolactone functionalised resin (see Scheme 4).[23] This was achieved by reacting the 2-chlorotrityl chloride resin with a hydroxyl thiolactone. The two-step iterative cycle was initiated with the selective ring-opening reaction of the immobilised thiolactone moiety using an amino alcohol. The generated thiol functionality was subsequently converted in a Thia-Michael addition using an acrylamide or an acrylate. Using this approach, various different side chains were introduced to the growing chain, whilst the approach greatly benefited from the high number of commercially available acrylamides and acrylates. Interestingly, this strategy also allowed for backbone definition by selecting different amino alcohols for the ring opening. The second step of the iterative cycle was the chain extension, which was achieved by reacting the hydroxy group with the isocyanato group of a previously synthesised thiolactone building block. By applying this improved approach, the DP of the oligomers was significantly improved and a set of different decamers was obtained. It is noteworthy that the robustness of the approach allowed its transfer to an adapted peptide synthesiser, thus performing the synthesis in an automated fashion. Therefore, the reaction conditions were carefully optimised by varying the stoichiometry, the solvent, and the reaction time in a comprehensive kinetic study, which was performed with the help of liquid chromatography-mass spectrometry (LC-MS). Using the automated process, another decamer was synthesised and compared to the manually obtained decamers. The reaction time was significantly reduced from five days to 33 hours by using the automated approach. However, minor impurities were observed in the analysis of the synthesiser derived decamers that were attributed to incomplete sequences by LC-MS analysis.

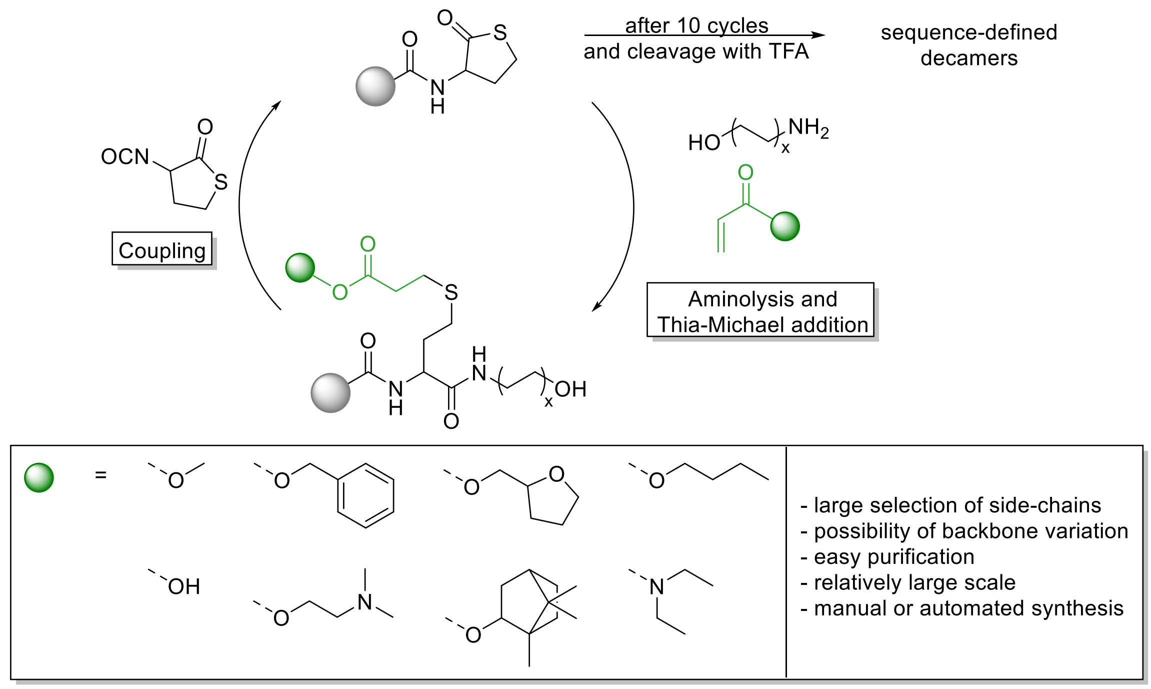
after 10 cycles
and cleavage with TFA
sequence-defined
decamers
Coupling
Aminolysis and
Thia-Michael addition
=
- large selection of side-chains
- possibility of backbone variation
- easy purification
- relatively large scale
- manual or automated synthesis

Scheme 4. Iterative two-step synthesis protocol for the formation of sequence-defined macromolecules based on thiolactone chemistry.[23]

In a solid-phase-based four-step protocol, consisting of aminolysis, a Thia-Michael addition, amidation, and a final coupling step, the synthesis of sequence-defined structures by thioacrylate chemistry was recently reported.[130] Various oligomers, up to the hexamer stage, carrying differently functionalised side chains were obtained by this strategy. The thiolactone-based approaches were also adapted for the conjugation of such oligomers to poly(ethylene glycol).[131-132]

In 2018, thiolactone based sequence-defined macromolecules were utilised in the field of data storage. This was demonstrated by the group of Du Prez who encoded a sentence as well as a 33 x 33 QR code into a set of oligomers. In order to achieve this, the encoding and read-out was automated with the help of a software. A Chemreader tool for reconstructing oligomer sequences based on tandem MS results as well as a Chemcoder for encoding data into oligomers was established. As depicted in Figure 7, the QR code represented a two-dimensional binary string which was translated into an oligomer sequence carrying different functionalities. In their work, they used the quick response (QR) code leading to the Wikipedia page of August Kekulé.

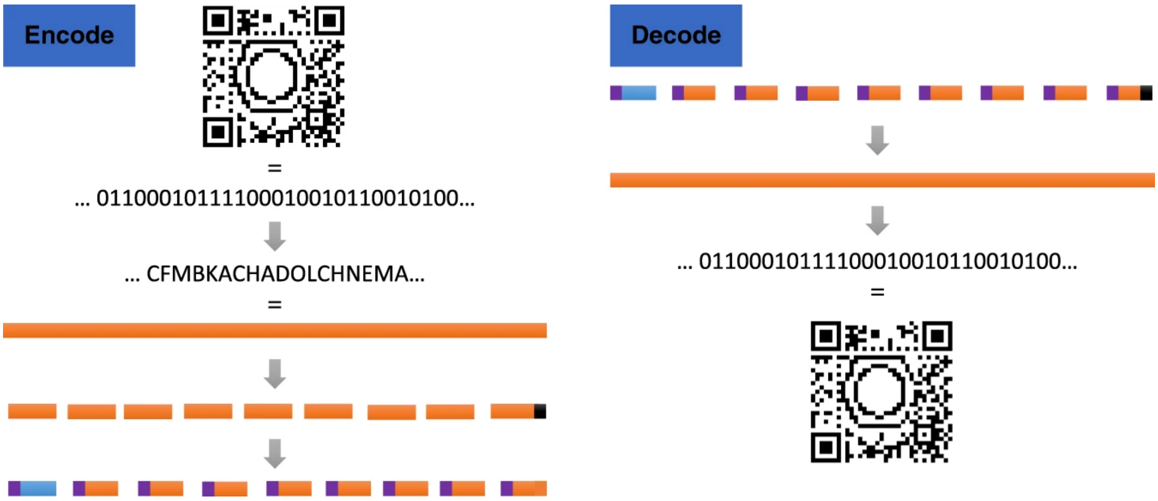

Figure 7. Illustration of the mechanism for encoding and decoding of a QR code works: the QR code as established by Du Prez and colleagues: the QR code was first translated into a bit string which was then transferred to a pentadecimal numerical system. The long sequence was divided into small fragments of defined sizes and marked with an index to reassign the order of the fragments later on. The index is marked in purple. Encoding was done automatically by a Chemcoder. The read-out was done by tandem MS and the results were automatically reconverted by the Chemreader resulting in the original QR code. The figure is reprinted from a publication of Martens et al., which is licensed under a Creative Commons Attribution licence.[40]

However, the required sequence was deemed too long to be efficiently synthesized. Thus, the sequence was cut into smaller fragments of a defined length, which were equipped with an index, enabling reassignment after the read-out. In total, 71 small oligomers with lengths up to hexamers were synthesised by the thiolactone strategy on a peptide synthesiser. Each oligomer represented a coded fragment, whereby the side chain functionality was introduced by using 15 different acrylate monomers. The read-out was performed by tandem MS analysis whilst the analysis of the obtained spectra was done automatically using the previously established Chemreader that enabled the identification of the most characteristic fragmentation patterns. Based on the index, which was assigned to the single oligomers by the Chemcoder, the oligomers were sorted in their original order, thus reconstructing the whole length of the original sequence. This sequence was in the end transferred to the QR code, leading to the website. The presented approach demonstrated the versatility and effectiveness of the thiolactone-based synthesis towards sequence-defined macromolecules. The easy functionalisation by the use of commercially available substrates and the possible transfer to automated processes render this approach attractive for further development in the field of sequence-defined polymers for data storage.

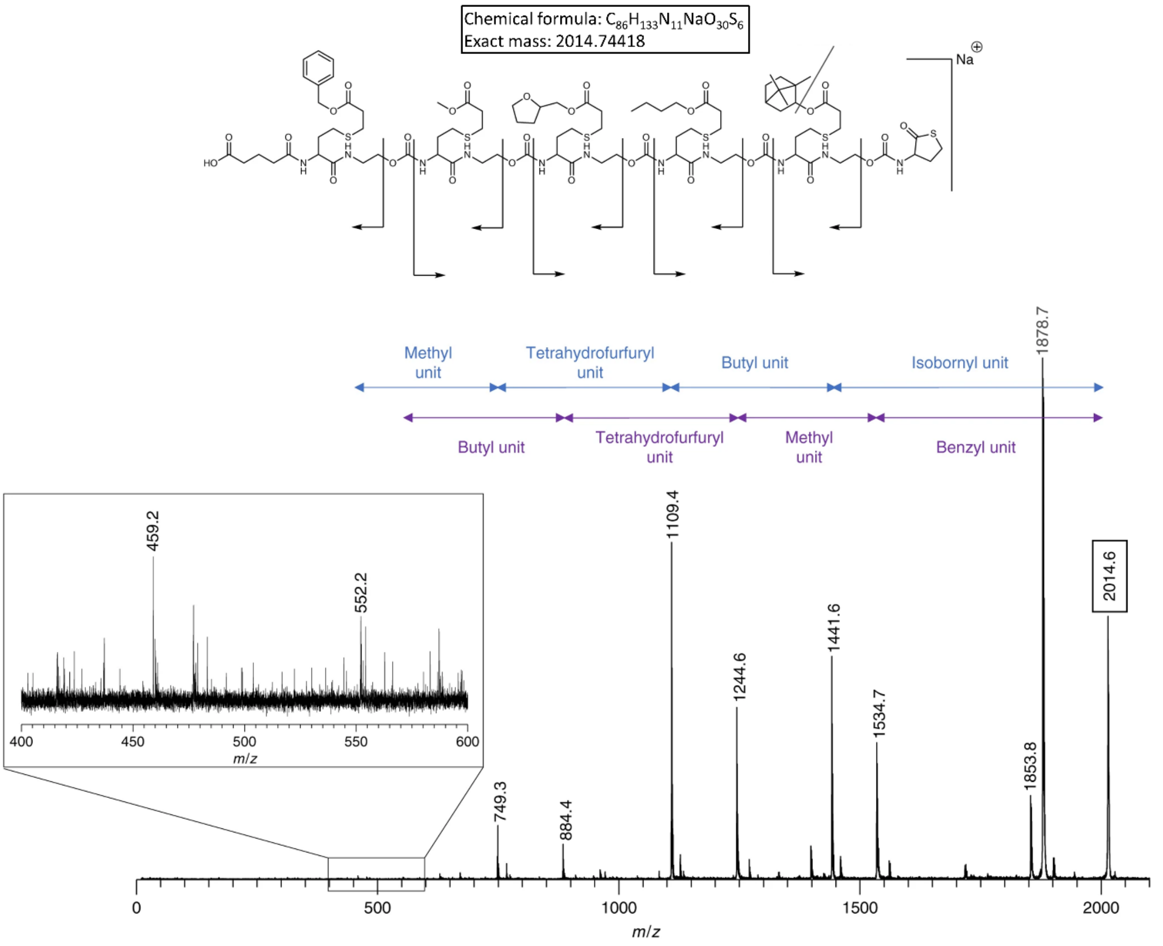

Figure 8. Read-out of the sequence of a pentamer using MALDI tandem MS/MS. Different characteristic fragmentation patterns were found (marked in blue and purple). The figure is reprinted from a publication of Martens et al., which is licensed under a Creative Commons Attribution licence.[40]

2.1.3.2 Solution-phase synthesis

Solution phase synthesis benefits from scalable reactions, facilitating subsequent analyses, compared to solid phase synthesis. Highly pure products can be obtained by employing efficient "click" chemistries, *i.e.* reactions that can provide quantitative yields, while reagents are used in stoichiometric ratios.[133] The latter is particularly important as, if reagents are used in excess, strenuous chromatographic procedures in order to purify the products are necessary. The purification can either be performed manually by column chromatography,[25, 27, 33-34, 134-135] or by automated chromatographic systems.[136-137] Generally, four different synthetic approaches towards sequence-defined macromolecules in solution can be considered: iterative exponential growth strategies (IEG), bidirectional growth strategies, single unit monomer insertions (SUMI), and stepwise iterative approaches. In the following section, all four approaches will be introduced and discussed, while selected representative examples of some of the leading working groups will be discussed.

In the IEG strategy, orthogonally protected monomers are separated into two parts, and subsequently, in each part, one protecting group is cleaved while the other remains protected. Then, the two parts (each deprotected on opposite sides) are reunited and reacted to form a dimer that is again separated into two parts and orthogonally deprotected. Using this approach, dimers can directly form tetramers that, once reacted, double in size to form the respective octamers, and so on. IEG benefits from the fast growth to large macromolecules. A drawback of this strategy is, however, that it is limited to repetitive or palindromic sequences. It is noted that in other synthetic fields, e.g. the field of conjugated, monodisperse macromolecules, this strategy is called divergent/convergent approach, describing exactly the same synthetic strategy. Within this theoretical background chapter, the focus will be on non-conjugated systems.[138]

The first report on IEG strategies was published as "molecular doubling" by Whiting and co-workers, in 1982.[139-140] They synthesised long aliphatic *n*-paraffin compounds of up to 400 carbon atoms in a purity of 92%. The group of Hawker later reported the synthesis of a uniform poly(ε-caprolactone) 64-mer in a purity of 96% in a good overall yield of 18% after 16 reaction steps. The strategy was later repeated to obtain a lactic acid-based 64-mer.[135, 141] In the second approach the overall yield dropped to 11%. However, it was reported that the oligomers were obtained in multigram scale and size exclusion chromatography (SEC) traces indicate excellent purity. Owing to the use of chiral substrates in the latter case, enantiomerically pure products were obtained. Poly(ethylene glycol)s (PEGs) have attracted considerable attention for their synthesis using IEG strategies.[142-144] Uniform PEGs are interesting candidates in drug delivery systems, since they are biocompatible and the well-defined structure affects the biological activity.[145] Furthermore, they are of especially high Interest as they serve as solid or soluble supports for the synthesis of other uniform, sequence-defined oligomers, thus significantly facilitating the purification and saving time and labour, while still maintaining the uniform character of the products. Johnson, Jamison, and Leibfarth demonstrated an interesting example of a semi-automated synthesis of oligo(ester)s.[146] This semi-automation allowed the automated separation of the reactants in two parts, orthogonal deprotection and subsequent CuAAC. The coupling products were purified by column chromatography before continuing with the next cycle. This semi-automated system was reported to be time-efficient as one iterative cycle required *ca.* one day and a monodisperse octamer was realised within three steps.

The group of Johnson introduced the IEG+ strategy that combines exponential growth with side chain control.[147] The reaction procedure is depicted in Scheme 5. It benefits from an enantiopure monomer that carries an epoxy group along with a TBDMS protected alkyne functionality. After the monomer was separated into two portions, the protecting group was removed on one portion of the monomers and the second portion was reacted with sodium azide to ring-open the epoxide. This resulted in an alcohol that was subsequently reacted with a functional bromine to introduce the desired side chain. The chain elongation was performed by CuAAC, while the introduction of different side chains was achieved by functionalisation of the generated secondary alcohol by ether- or esterifications. The advantages of this elegant strategy are its scalability, high yields, the possibility to introduce tailored side chains, and the stereocontrol, which is achieved by the use of a chiral monomer. After five reaction cycles, a sequence-defined 32-mer with a molecular weight over 6 kDa was obtained.

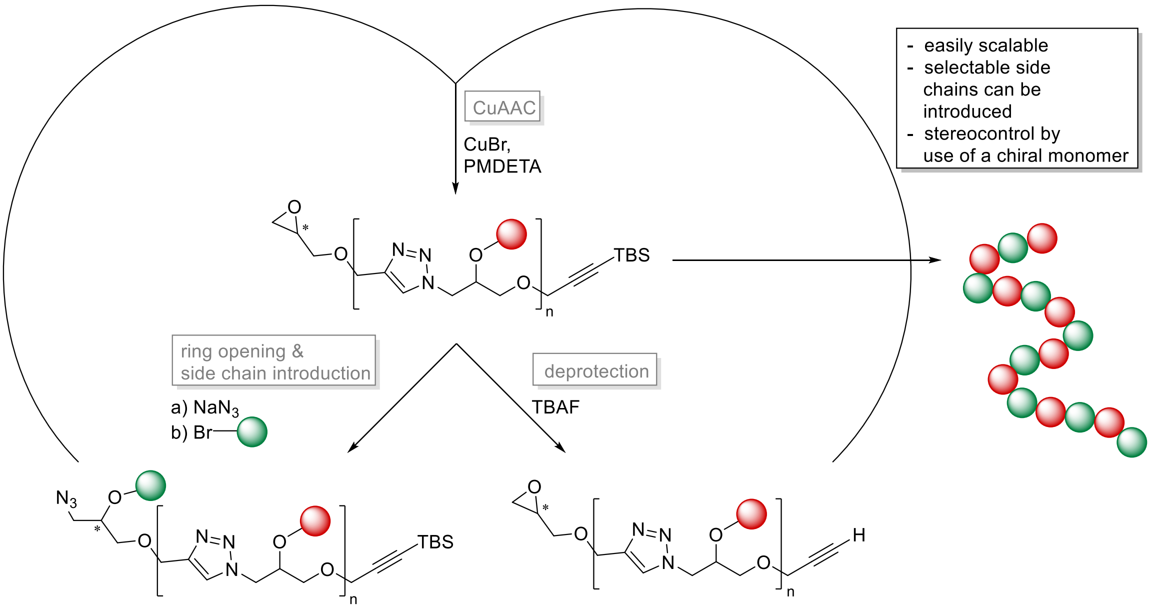

Scheme 5. In the approach from Johnson an enantiopure AB-monomer bearing an epoxy group and a TBDMS protected alkyne functionality is devided into two parts, one is deprotected, the other one is ring-opened, whereby a side chain can be introduced. Chain elongation is performed by recombining the two parts and repeating the iterative procedure until the desired product is obtained.[147]

In bidirectional growth strategies, a bifunctional core unit is used as the starting material. This allows the addition of two monomer units per iterative cycle and facilitates the synthesis of long sequences in fewer reaction steps compared to stepwise iterative approaches that start from a monofunctional stating material. By applying this strategy, symmetric products are obtained, which may be perceived as a restriction in terms of achievable control. Nonetheless, bidirectional growth is widely applied in monodisperse PEG synthesis, where the synthesis of dodecamers,[148] 29-mers,[149] and even 44-mers[150] have been reported. Jiang and co-workers reported a variation of the bidirectional growth approach towards uniform PEG:[151-152] they synthesised a macrocyclic monomer from commercially available tetra(ethylene glycol) with thionyl chloride and oxidised it to the corresponding sulfate. The macrocyclic monomer is ring-opened upon addition of two monomer units which, interestingly, avoids the use of protecting groups. A PEG 64-mer was achieved using this approach.

The group of Barner-Kowollik also applied the bidirectional growth strategy to prepare sequence-defined macromolecules by photochemical approaches. In 2015, they reported the synthesis of a sequence-defined symmetric decamer:[134] a bismaleimide served as core unit and was first reacted with the photoenol of a bifunctional monomer which also carried a sorbyl ester end group. The sorbyl ester end group was subsequently reacted *via* a Diels-Alder reaction with a second monomer. Besides the photochemically activated phenacylsulfide which reacted in the second step, the monomer also carried a furan-protected maleimide. This was removed *in vacuo* and the iterative cycle was repeated. By iterating the cycle five times, a sequence-defined decamer was obtained as shown by SEC and MALDI mass spectrometry. However, this approach did not allow for the introduction of different side chains to the growing oligomer. In a second approach, the same group demonstrated the introduction of different functionalities by synthesising a library of six different monomers carrying ester, alcohol, adamantly, and aromatic functionalities.[153] The AB-monomers were equipped with a furan-protected maleimide and an α-methyl benzaldehyde was photochemically activated to form a photoenol. The photoenol allowed for chain-elongation by Diels-Alder reaction. First, sequence-defined hexamers were synthesised that were subsequently reacted with monoprotected dimers to afford the symmetric decamers. The obtained products were carefully characterised by NMR, ultraviolet–visible (UV-Vis) spectroscopy, ESI-MS SEC, and MALDI-ToF-ToF-MS techniques.

In another approach recently published by the same working group, the bidirectional growth strategy was applied in a light-induced convergent approach using nitrile imine carboxylic acid ligation (NICAL) and Diels-Alder cycloaddition (see Scheme 6).[24] They synthesised two complementary monomer units. One monomer carried a visible light-responsive pyrene aryl tetrazole and a UV-responsive *o*-methylbenzaldehyde (*o*-MBA), while the other monomer was equipped with a fumarate and a carboxylic acid moiety. A bifunctional acid served as core unit. By iterating the two aforementioned reactions, symmetric sequence-defined oligomers, up to decamers, were obtained through a protecting group-free approach and characterised by SEC, ESI-MS, and NMR spectroscopy techniques. Interestingly, the two photosensitive groups of the first monomer allowed for chain extension by activation at distinct wavelengths.

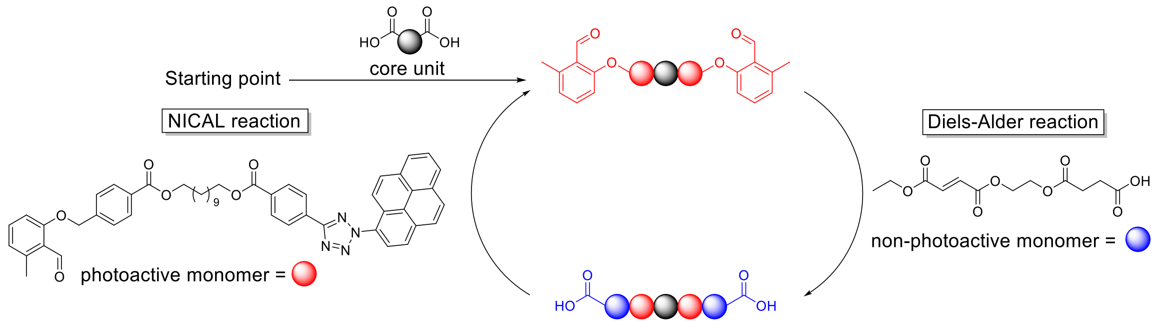
core unit
Starting point
NICAL reaction
Diels-Alder reaction
photoactive monomer =
non-photoactive monomer =
HO
OH
9

Scheme 6. Photochemical approach towards sequence-defined macromolecules using bidirectional growth strategies reported by Barner-Kowollik et al. The light-induced chain extension is achieved by switching between NICAL and Diels-Alder reactions while irradiating with distinct wavelengths.[24]

In a third approach, the photochemical approach of the Barner-Kowollik group was combined with a multicomponent reaction,[154] benefitting from the individual advantages of both chemistries. As such, *o*-MBA conjugation was combined with highly effective P-3CR reactions (see Scheme 7). Two linker molecules were designed: one bearing an *o*-MBA and a carboxylic acid group, and one carrying an isocyanide and a maleimide. The two linkers allowed to switch between the two chemistries. First, a set of different isocyanide-maleimide linkers were synthesised *via* P-3CRs and, by iterating the photoreaction and the P-3CR, sequence-defined macromolecules with a molecular weight of over 3,500 g/mol were obtained.

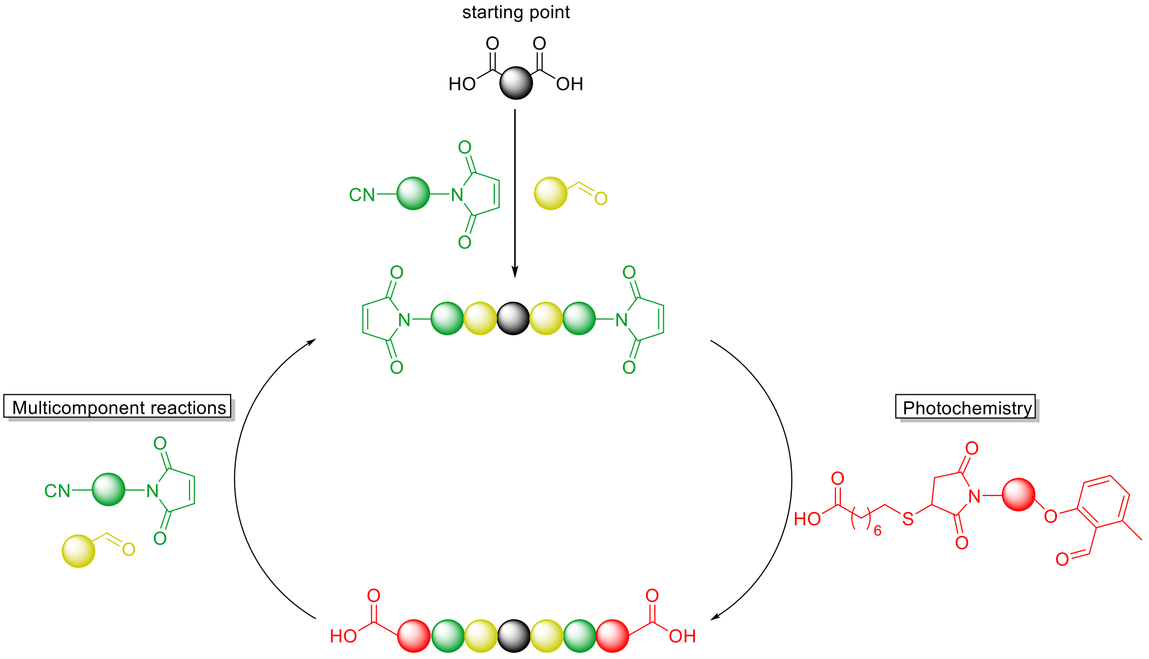
starting point
Multicomponent reactions
Photochemistry
CN
HO
OH
6
S

Scheme 7. Synthesis of sequence-defined oligomers by switching between photochemistry and multicomponent reactions. The combination of the two different methods was achieved by the design and synthesis of two AB-type linker molecules, that carried a reactive functional group for both of the reactions.[154]

Another interesting approach towards sequence-defined synthesis is the recently developed SUMI. The idea behind this approach is the drastic reduction of the reactivity of the growing chain in classical RDRP processes in order to allow only one monomer to be added. Alternatively, the monoaddition can be induced by adjusting the ratio of the reactants. In both cases, monoaddition was shown to be favoured over chain growth. In early reports, only a low DP was achieved using SUMI approaches. RAFT and atom transfer radical additions (ATRA) were investigated for SUMI approaches by different working groups but the yields were relatively low (usually below 30%, in some cases even below 1%) and the achieved DP was typically below 4.[155-159] Most approaches towards sequence-defined macromolecules use highly efficient “click” chemistries, leading to backbone structures other than common polymers, such as poly(acrylates). By using SUMI approaches, it is possible to synthesise defined structures while obtaining conventional polymer backbones. The group of Junkers recently conducted further investigations on SUMIs. In a first approach, they demonstrated the synthesis of two different tetramers exhibiting a defined sequence.[137] They were prepared by RAFT polymerisation using a commercially available chain transfer agent for the polymerisation of *n*-butyl acrylate. The reaction was quenched after ten minutes in order to only insert one monomer to the growing chain per chain growth step. Purification was achieved automatically by recycling SEC. The strategy was later extended for the formation of linear uniform 18- and 20-mer acrylates *via* RAFT polymerisation:[28] first, sequence-defined nonamers and decamers were prepared that were subsequently end-modified by aminolysis of the trithiocarbonate end group and subsequent oxidation to enable disulfide bridging, thus leading to the formation of the respective symmetric 18-mer and 20-mers with molecular weights of over 2,200 g/mol.

The same group also investigated SUMI approaches by using ATRP that also allowed the formation of acrylate-based backbones.[136] They used a common ATRP initiator that was employed together with copper(II)-bromide and tris[2-(dimethylamino)ethyl]amine. UV irradiation yielded the desired SUMI product as the main product on account of the reaction equilibrium being shifted towards the dormant species, thus switching off the light source stopped the polymerisation. The SUMI was observed by online Fourier-transform infrared spectroscopy (FT-IR) as the characteristic band of the vinyl bond of the acrylate was found to decrease in intensity, indicating the consumption of the monomer. A set of differently functionalised defined tetramers and pentamers was obtained. The group of Junkers demonstrated that SUMI approaches present a highly attractive tool for sequence-defined synthesis while — in contrast to iterative strategies — maintaining the backbone structure of classical polymers. Furthermore, it was shown that the approach exhibits tolerance towards different functional groups, while the reagents are commercially available.

Stepwise iterative approaches represent the last important solution-phase approach that is discussed within this thesis. Here, the oligomers are formed in a stepwise manner, whereby the monomers are attached one-by-one. Therefore, the preparation of high molecular weight oligomers requires more synthetic steps compared to bidirectional growth or IEG strategies. However, in terms of definition and sequence precision, they offer the most freedom as the side chains or backbone units can be varied in each iterative cycle and are not restricted to palindromic or symmetric sequences.[36]

Stepwise iterative approaches were applied for PEG synthesis as demonstrated by Livingston, Gaffney, and co-workers.[160-161] They synthesised PEGs from a three-arm star-shaped molecule using pre-synthesised protected octameric PEG building blocks and cleaved the arms after end-functionalisation to obtain the linear PEG. Using this approach, a 56-mer PEG was obtained in 14 steps with an overall yield of 20%. The trifunctional core functioned as protecting group and facilitated purification caused by an increased dissimilarity of the stars compared to the building blocks of lower molecular weight. The synthesis was performed on a multigram-scale, however, end-functionalisation and cleavage from the core was only performed in milligram-scale and reduced the overall yield to 13%. The purity of the obtained PEG was estimated by MALDI.

The group of Sawamoto reported an iterative approach taking advantage of radical intramolecular cyclisations.[162] They employed an initiator-monomer system, often referred to as inimer, which bears two cleavable bonds: an *N*-hydroxysuccinimidyl ester and an ortho-pyridyl disulfide. The ester was cleaved by reaction with primary amines and regenerated with acid halides in an esterification reaction, while the disulfide was cleaved in the presence of alkyl thiols and regenerated upon reaction with activated halides. When the ring system was opened, monoaddition of an acrylate was performed and the elongation was complete once the reversibly cleaved bonds are regenerated.

The use of multicomponent reactions in the synthesis of sequence-defined macromolecules was introduced by our group in 2014.[27] Multicomponent reactions (MCRs), like the Passerini three-component reaction (P-3CR) or the Ugi four-component reaction (U-4CR), which will be introduced in more detail in Chapter 2.2.1, are highly efficient tools for sequence-definition because of their modular character. The main advantages of such reactions are the one-pot procedure, the easy introduction of various side chains by selecting different components, the high yields, and the commercial availability of the reactants. These characteristics of MCRs make them an ideal tool in the synthesis of defined structures and there is a wealth of literature showcasing their potential in sequence-definition.[163]

In the first report, the P-3CR was combined with highly efficient thiol-ene reactions in an iterative approach.[27] The approach benefited from the orthogonality of the reactions, thus avoiding the use of protecting groups. As it only used commercially available reactants and in each iterative cycle one repeating unit was introduced, the P-3CR report can be compared with Zuckermann's submonomer approach for peptoid synthesis.[73] Stearic acid served as the starting unit, providing good solubility in organic solvents and subsequently reacted in a P-3CR with an isocyanide and 10-undecenal. The acid and the aldehyde component were used for chain elongation, while the isocyanide introduced the side chain. Furthermore, the aldehyde introduced a terminal double bond, which served as reactive site for the subsequent thiol-ene reaction. In that second reaction, 3-mercaptopropionic acid was used to introduce the acid functionality enabling the second P-3CR to proceed (Scheme 8). By varying the isocyanide in each iterative cycle, different functionalities were introduced. Using this approach, a sequence-defined tetramer carrying linear, branched, and cyclic aliphatic side chains was synthesised in seven steps in an overall yield of 26%. The synthesis was conducted in multigram scale. For purification, column chromatography was required after each P-3CR step. However, after the thiol-ene addition, only aqueous work-up was required to remove the excess of 3-mercaptopropionic acid. The same strategy was also transferred to a soluble PEG support, which was equipped with a carboxylic acid as starting point.[27] By performing the reaction on the support, the required time for purification was significantly shortened since column chromatography was avoided as the products were obtained by precipitation. A pentamer carrying five different side chains was obtained in an overall yield of 34%.

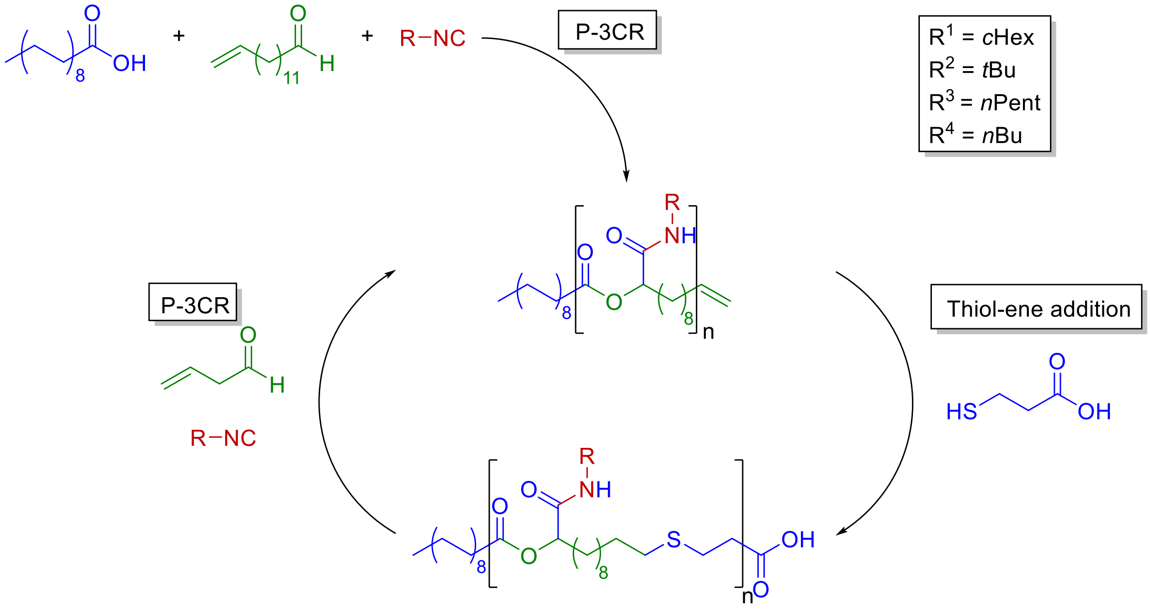

Scheme 8. Stepwise iterative approach using the P-3CR and subsequent thiol-ene addition.[27]

The MCR thiol-ene approach was also extended to the U-4CR, allowing for the introduction of two different side chains per repeat unit because of the additional fourth component.[33] Similarly to the P-3CR, the U-4CR is an IMCR, in which, additionally to the three components carboxylic acid, aldehyde, and isocyanide that react in the P-3CR, an amine is incorporated into the final product. The U-4CR will be discussed in more detail in Chapter 2.2.1.2. By iterating the U-4CR with the thiol-ene reaction, a sequence-defined tetramer was synthesised. In the first approach, the side chain was introduced by varying the amine component while *tert*-butyl isocyanide was used as fourth component. In a second approach, both components were varied at the same time, thus enabling dual side chain definition. The obtained pentamer was equipped with ten tailored side chains as two side chains per repeating unit were introduced. The final oligomer was obtained in nine steps in a moderate yield overall yield of 15%.

In another approach, the P-3CR thiol-ene approach was combined with thiolactone chemistry in a versatile convergent synthesis.[35] With this straightforward and scalable approach, it was possible to obtain high molecular weight oligomers of up to *ca.* 4600 g/mol bearing 15 individually selectable side chains in three coupling steps in multigram scale. Interestingly, multifunctional products were obtained bearing different functionalities, such as ester groups, furans, and aliphatic groups, which were introduced as side chains.

In order to further improve the overall yield, the strategy was modified (see Scheme 9): a tailored AB-monomer was employed in the P-3CR.[34] This monomer carried an isocyanide, which participated in the P-3CR, as well as a benzyl ester protected acid, which was released in the second step of the iterative cycle by hydrogenolysis. In contrast to the previous thiol-ene approach, the oligomer was grown through the acid and the isocyanide component, while the side chain was introduced by the aldehyde component. This was deemed beneficial since a larger variety of aldehydes is commercially available, compared to the previously used isocyanides. The approach is later referred to as monomer approach.

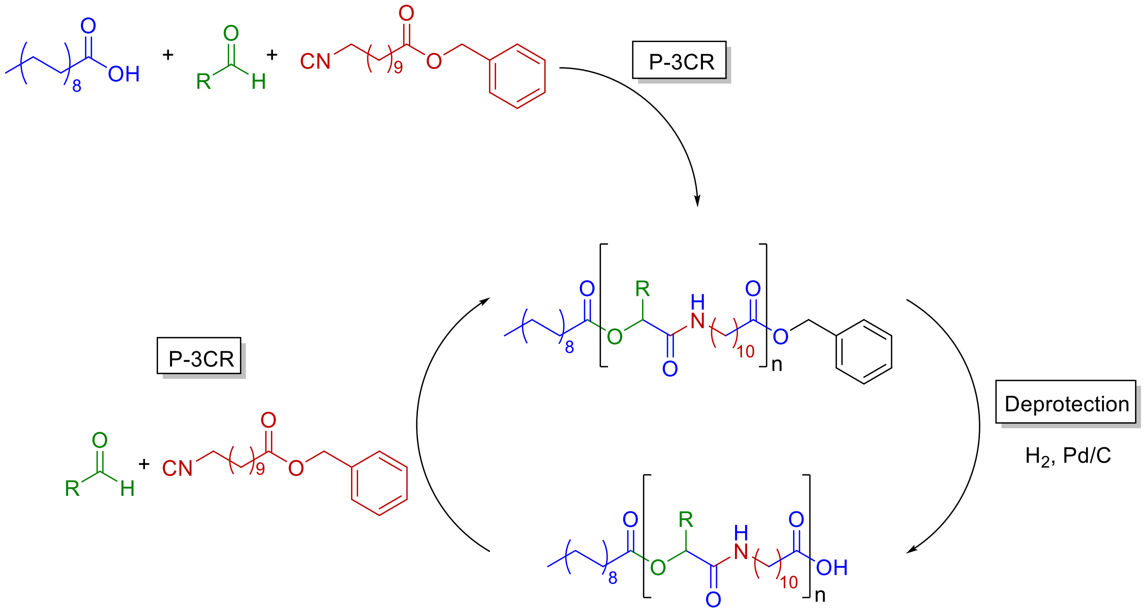

Scheme 9. AB-monomer approach using the P-3CR and a subsequent deprotection step in a two-step iterative cycle.[34]

Furthermore, the use of foul-smelling volatile isocyanides was avoided, making the approach more convenient. After the first P-3CR, column chromatography was required for purification. The subsequent deprotection step used palladium on activated charcoal as heterogeneous catalyst and the mixture was purged with hydrogen to yield the free acid. The catalyst was easily filtered off and, due to the quantitative reaction in this step, no further purification was required. Compared to the previous approach, the yields in the respective steps drastically increased, from 48%–94% to nearly quantitative yields. The increased yields facilitated to achieve higher molecular weights and longer sequences.

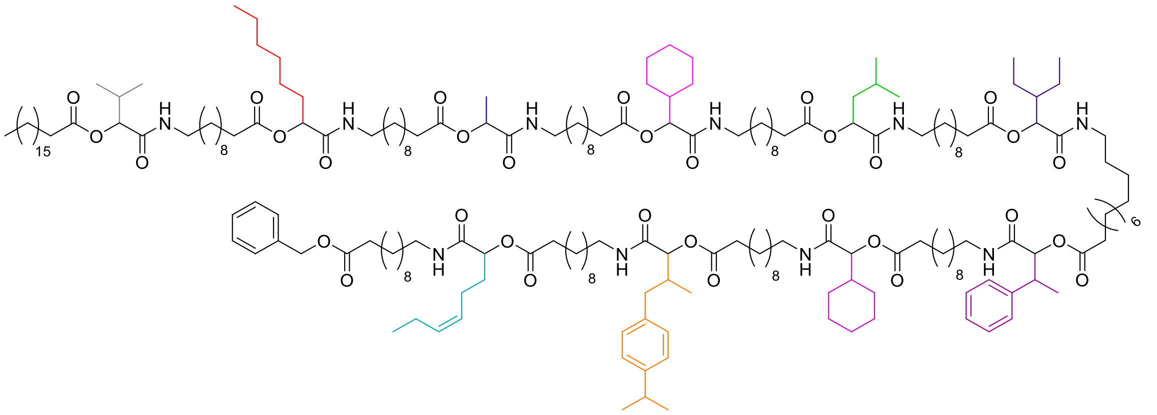

Figure 9. Structure of a sequence-defined decamer obtained by the monomer approach bearing ten different side chains.[34]

A sequence defined decamer carrying ten different side chains (Figure 9) was obtained within 19 steps in an overall yield of 44%. The synthesis was conducted in multigram scale thus yielding 2.4 g of the decamer. It is also noteworthy that the decamer was equipped with a terminal double bond, which was introduced as a side chain. The double bond allowed the coupling of two decamers by self-metathesis, thus doubling the molecular weight of the product. A symmetric sequence-defined 20-mer with a molecular weight of over 7000 g/mol was obtained in an overall yield of 21%. In terms of overall yield, scale and achievable DP, this strategy provided a substantial improvement compared to the MCR thiol-ene approach.[27, 33-34]

Meier and colleagues later introduced sequence-defined macromolecules obtained by MCRs to the field of data storage. In a first approach, small key molecules synthesised *via* the U-4CR were shown to be suitable candidates for advanced encryption in standard cryptography in combination with molecular steganography.[164-165] The required large structural variety was provided by utilizing a four-component reaction. By only considering commercially available starting compounds, an exemplary library of 130 components was established, leading to 500,000 key molecules if all possible permutations are taken into account. The synthesised key molecules were equipped with a perfluorinated side chain in order to facilitate extraction from various media. The molecular keys were hidden by adsorption onto paper, coffee, sugar or by dissolution in perfume or blood. After regeneration by extraction, the molecular keys were read out by ESI-MS/MS techniques, demonstrating the practicality of the presented approach. By recombining the by ESI-MS/MS obtained fragments, the structure of the initial molecule was reconstructed. The read-out was assisted by using assisted custom programmed read-out software. In order to unambiguously identify the molecule, the monoisotopic mass and three fragments were necessary. Further fragments were assigned and further confirmed the structure, however, they were not essential for successful read-out.

In another approach by our group, two MCRs, namely the Biginelli and the Passerini, were combined in a defined synthesis approach towards sequence-coded macromolecules for data storage.[38] Interestingly, by combining two MCRs, up to six different functional groups per repeating unit were introduced, resulting in high information density and an increase of data storage capacity. As such, up to 24 bits (=3 bytes) can be stored per repeating unit if a large library of 100 possible commercially available compounds is considered. The reaction scheme is shown in Scheme 10. First, a Biginelli acid was synthesised from ureido carboxylic acids with acetoacetate benzyl esters and an aldehyde. The acid was subsequently reacted with different aldehydes and diisocyanides in a P-3CR to yield a monomer with a benzyl ester-protected carboxylic acid and an isocyanide functionality which can be applied in the above discussed monomer approach. The monomer itself carried five selectable functionalities. The sixth functionality was added by the aldehyde component in the subsequent P-3CR of the iterative cycle. The iterative cycle, consisting of the P-3CR and the deprotection step, added one monomer after another while introducing an additional side chain. In the end, tetramers which encode 97 bits were obtained using this approach. The read-out was performed by tandem mass spectrometry: by identifying the characteristic fragmentation patterns, the structure of the macromolecule was reconstructed.

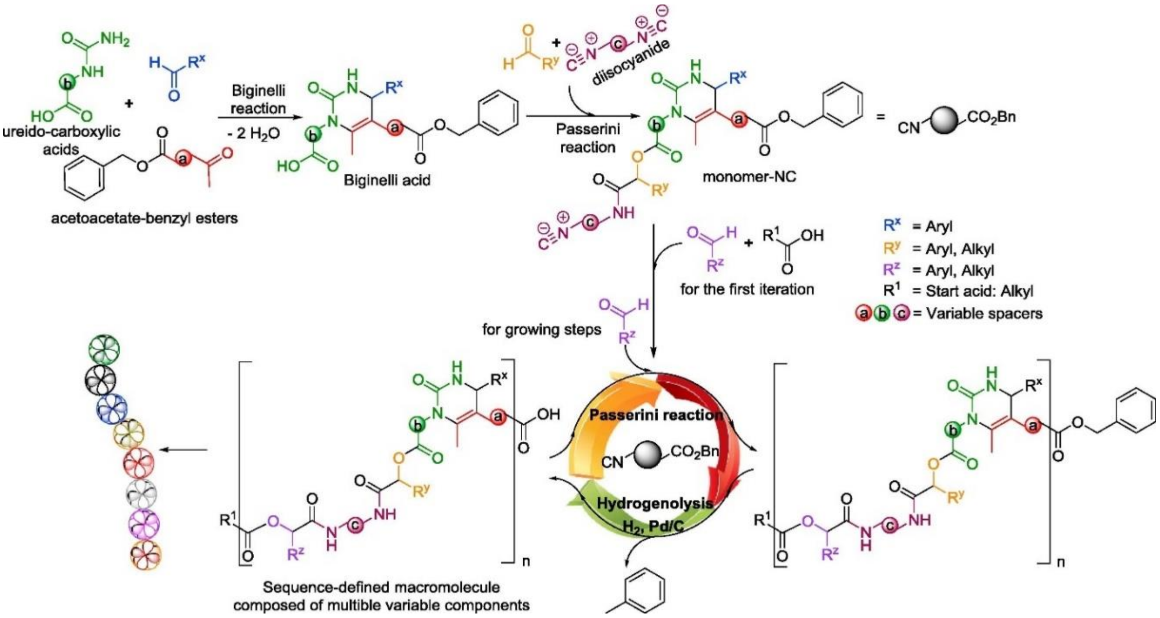
ureido-carboxylic acids
acetoacetate-benzyl esters
Biginelli reaction
- 2 H₂O
Biginelli acid
diisocyanide
Passerini reaction
monomer-NC
CN
CO₂Bn
for the first iteration
for growing steps
Rˣ = Aryl
Rʸ = Aryl, Alkyl
Rᶻ = Aryl, Alkyl
R¹ = Start acid: Alkyl
a b c = Variable spacers
Passerini reaction
Hydrogenolysis
H₂, Pd/C
Sequence-defined macromolecule composed of multible variable components
n

Scheme 10. Synthetic procedure for the synthesis of sequence-defined macromolecules as candidates for data storage materials offering a high data storage capacity owed to the combination of two powerful MCRs. Reprinted with permission from A. C. Boukis, M. A. Meier, Eur. Polym. J. 2018, 104, 32-38. Copyright © 2018 Elsevier.[38]

It has been shown that MCRs provide a powerful tool for introducing various functionalities independently to sequence-defined structures. The robustness and the simple synthesis procedures are important advantages of these reactions. Furthermore, due to their tolerance towards numerous functional groups, they allow combination of MCRs with different chemical approaches. Thus, the combined methodical advantages can be exploited in the synthesis of sequence-defined structures. The scalability allows for multigram synthesis and simple upscaling of the reaction, thus making the products interesting materials for various applications and paving the way for profound fundamental understanding by investigation of, for instance, structure- property or structure- activity relationships or by investigating the systematic formation of higher ordered structures.

2.1.3.3 Other synthetic approaches for the synthesis of sequence defined macromolecules

Besides the above discussed solid- and solution phase approaches towards sequence-defined macromolecules, several other approaches exist, which will be briefly introduced in this section. In sequence-defined syntheses, one of the most crucial steps is the purification, hence many investigations aim to optimise the purification steps. Two very interesting approaches are fluorous-supported approaches and the use of a soluble polymer support. Both approaches allow for homogeneous reaction conditions in solution, also implying solution phase characteristics like scalability, but in combination with a significantly simplified purification that makes such approaches very attractive. However, the cleavage from the soluble supports and subsequent separation of the product from the support can sometimes limit the scalability. The general concept of both approaches is illustrated in Figure 10.[36]

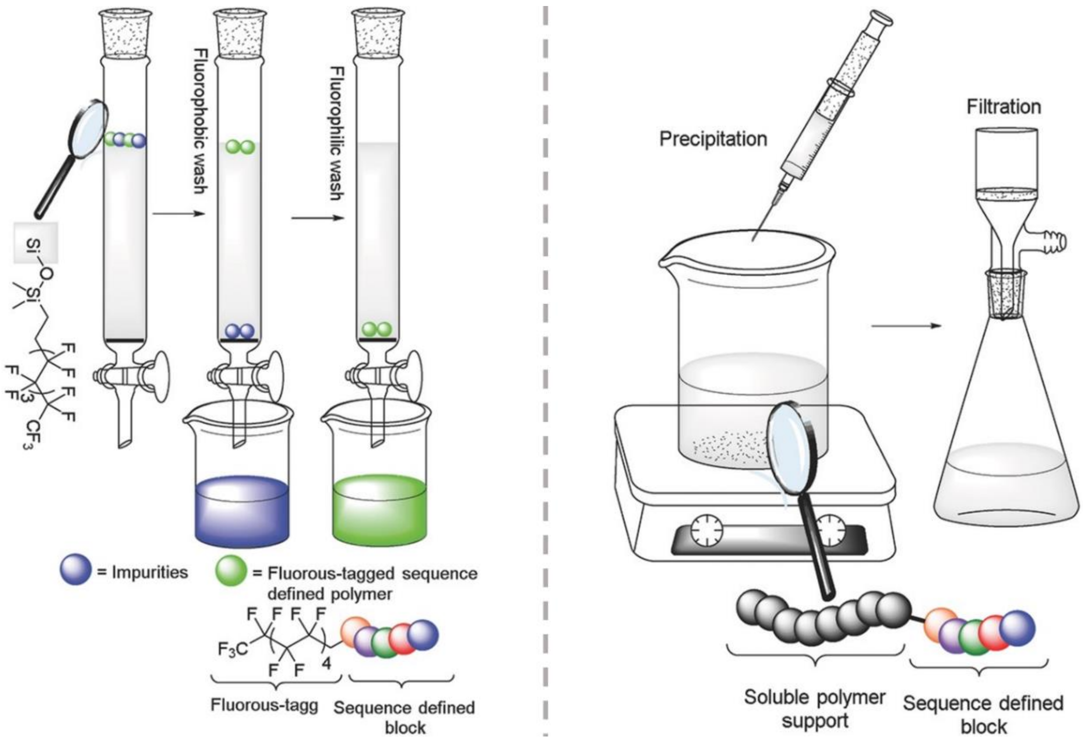
Fluorophobic wash
Fluorophilic wash
Si–O–Si
F F F F
F F
CF3
= Impurities
= Fluorous-tagged sequence defined polymer
F F F F
F3C
F F 4
Fluorous-tagg
Sequence defined block
Precipitation
Filtration
Soluble polymer support
Sequence defined block

Figure 10. Left: Fluorous solid phase extraction: the fluorous-tagged substrate is purified by using a column packed with silica gel equipped with perfluorinated alkyl chains. By using different solvents, the mixture is separated into a fluorophobic and a fluorophilic fraction. Right: the polymer is synthesised on a soluble polymer support in solution and can be purified by precipitation in another solvent, in which the impurities are soluble. Separation is achieved by simple filtration. Reprinted with permission from S. C. Solleder, et al., Macromol. Rapid Commun. ***2017****, 38, 1600711. Copyright © 2017 John Wiley and Sons.*[36]

Fluorous solid phase extraction (FSPE) can be performed as purification method:[166] The separation of fluorous-tagged molecules is based on fluorophilic and fluorophobic interactions. The principle is rather simple: a mixture of fluorine-containing compounds and non-fluorine containing compounds can be separated by using a commercially available fluorous stationary chromatographic phase. The mixture is loaded onto the fluorinated silica gel and first eluted with fluorophobic solvents, such as mixtures of methanol and water, acetonitrile and water, dimethyl formamide (DMF) and water, or pure dimethyl sulfoxide (DMSO). Fluorophobic solvents elute various organic compounds that do not contain fluorine. Afterwards, the column is flushed with fluorophilic solvents, yielding the product fraction containing a perfluorinated tag. Typical fluorophilic solvents are pure methanol, pure acetonitrile, or pure tetrahydrofuran (THF).[166] Several syntheses of sequence-defined macromolecules benefiting from FSPE have been reported, including the synthesis of uniform PEGs or macromolecules with defined side chains.[167-169]

The synthesis on soluble polymer supports is often referred to as polymer tethered synthesis.[170] The reactive site is immobilised on an anchor point of a soluble polymeric support. All chemical reactions are performed in solution, simplifying the scale-up and characterisation of intermediates. The formed products are obtained by precipitation in another solvent, in which the polymeric support is not soluble. However, cleavage from such supports can be critical, thus limiting the applicability of those approaches. Syntheses on soluble polymer supports have been reported by Meier, Lutz, and Badi among others.[1, 26-27, 124, 171-172]

Another approach towards defined structures is the template-mediated polymerisation. In the biosynthesis of DNA, the template-mediated synthesis plays an important role because the template strands recognise the complementary bases, thus bringing the building blocks into a defined order.[1] Most of the template-based approaches in synthetic polymer chemistry rely on DNA templates. Like in the natural process, the monomers are forced into a certain order, brought into near proximity by hybridisation and thus the synthesis of the targeted sequence is enabled.[173-175] The advantage of this approach is that the reactions proceed even at very low concentrations,[176-177] as by hybridisation, the reaction partners are brought into close proximity which induces locally a high concentration enabling the reaction to proceed. Coupling of oligonucleotides,[178] peptide nucleic acids[179] or reductive aminations between modified DNA oligomers[176] have been reported. Besides the DNA-templated polymerisation techniques, a few reports on non-DNA based templated polymerisations are available.[29, 180-182] Not all of the template-based approaches yield sequence-defined structures. Often, they only allow for sequence-regulated macromolecules.[182] The group of Sawamoto, for instance, reported on non-DNA based template approaches.[29-30, 181] Their approach, which is depicted in Scheme 11, provided access to sequence-regulated structures by radical polymerisation using a template initiator. The template initiator was equipped with two carbon-chlorine bonds in ortho position to each other, held in a rigid benzene framework. The haloether was used to generate and embed the template by cationic polymerisation as this allowed precise positioning of the monomers. The haloester was used for metal-assisted recognition of methacrylic acid (MAA), to form the complementary daughter polymer to the initial polymer by radical polymerisation. The building blocks are recognised by ionic recognition. Thus, the selective radical addition of MAA along an amine-functionalised or a crownether-functionalised template initiator is enabled.

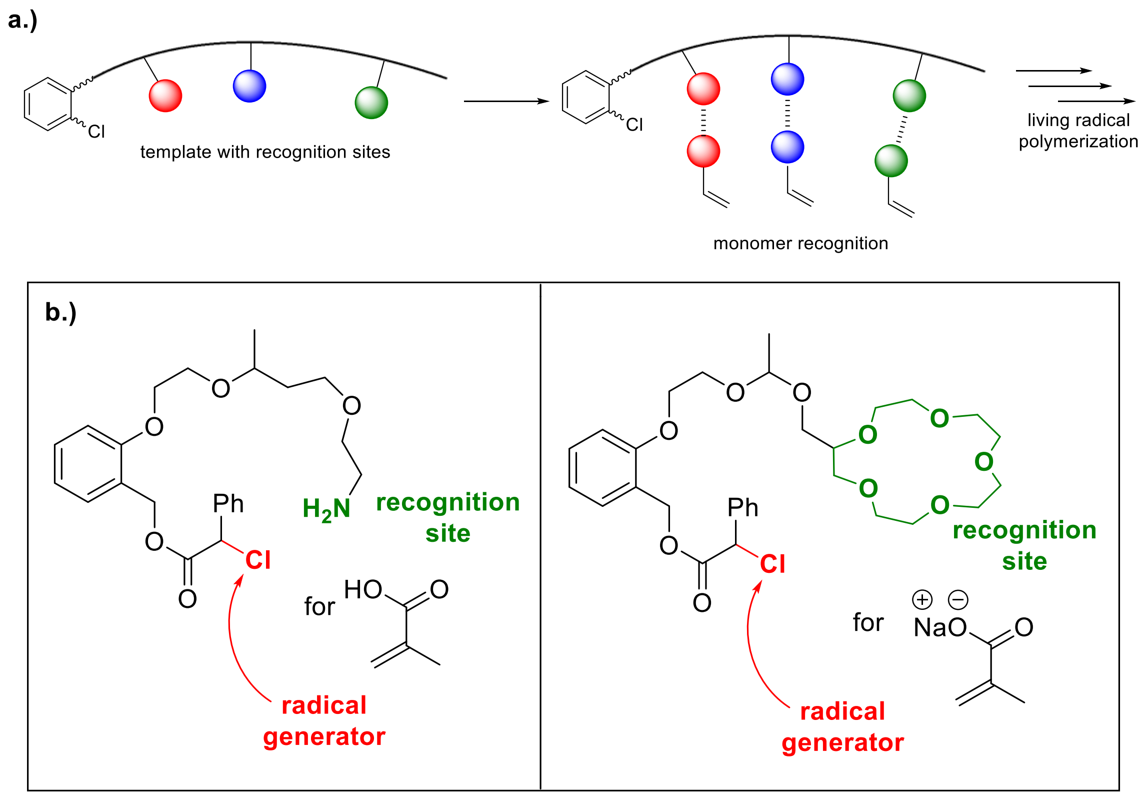
a.)
Cl
template with recognition sites
Cl
living radical
polymerization
monomer recognition
b.)
O
O
O
O
O
Ph
Cl
H2N
recognition
site
for
HO
O
radical
generator
O
O
O
O
O
Ph
Cl
O
O
O
O
O
recognition
site
for
⊕ ⊖
NaO
O
radical
generator

Scheme 11. (a) Template initiator which is used in the template-assisted living radical polymerisation process. (b) the selective radical addition of MMA monomers by the amine-functionalised and by a crown ether-functionalised template is depicted. The interaction with the template is based on ionic recognition.[181]

Undoubtedly, such approaches are very elegant; however, the disadvantage is that they are typically conducted in small scale of pmols to nmols[174, 181] and most of the efficient approaches are restricted to DNA-like structures. [177]

Another notable and elegant approach towards sequence-defined macromolecules is the use of molecular machines. Pioneering work in this field was done by Sauvage,[183] Stoddart,[184] and Feringa,[185] who were recently awarded with the Nobel Prize.[186] Molecular machines were later also used for the synthesis of defined macromolecules. Leigh and colleagues reported the synthesis of sequence-defined peptides by using a rotaxane-based molecular machine.[31-32] The desired amino acid sequence was synthesised and a macrocycle was designed. The macrocycle moved along the amino acid strand and recognised certain amino acids that were incorporated in a programmed order by successive native chemical ligation. Once the final amino acid is removed, the macrocycle is cleaved from the synthesised tetramer. The synthesis and composition of the molecular machine is illustrated in Scheme 12.

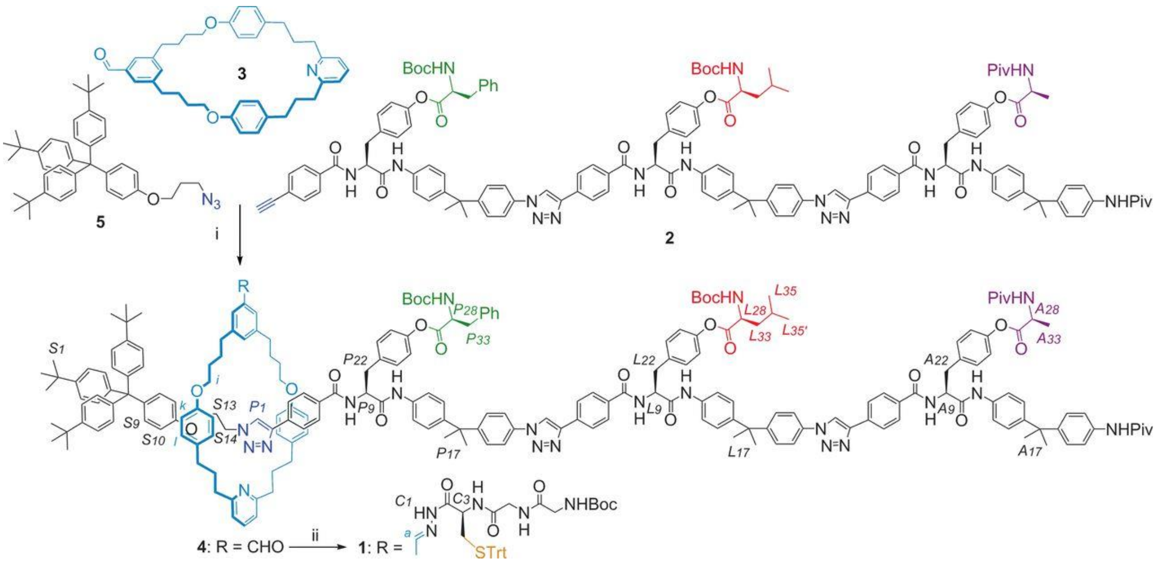

Scheme 12 The synthesis of a rotaxane-based molecular machine is depicted. It incorporates a strand with amino acid building blocks ***(2)****, and a macrocycle with one reactive site for attaching the reactive arm* ***(3)****. The terminal blocking group* ***(5)*** *prevents the threaded macrocycle from coming off the strand before all amino acids have been collected. Reprinted with permission from B. Lewandowski et al., Science 2013, 339, 189-193. Copyright © 2013 The American Association for the Advancement of Science.*[32]

Nonetheless, the pre-programmed amino acid strand represents a sequence-defined macromolecule itself and also needs to be synthesised in a stepwise manner. Furthermore, the approach can only be conducted in small scales and the overall yields are low.[32] The complexity of the synthesis, however, has not allowed the scaling up of the process and its consideration for further applications.

In conclusion, numerous and versatile approaches towards sequence-defined macromolecules have been developed by applying different methodologies. While solid phase-approaches benefit from a fast build-up of long sequences while being restricted to small scales, approaches in solution can be easily scaled up to multigram batches, however require strenuous chromatographic purification. All above discussed approaches have in common that highly efficient reactions are needed for achieving high conversions and yields to reach long sequences while avoiding defects and by-products. In the following section, different reactions that fulfil these requirements and thus are suitable for the synthesis of sequence-defined macromolecules will be presented.

2.2 Synthetic tools for achieving uniform macromolecules

Within this chapter, some efficient synthetic tools for achieving uniform and highly functional macromolecules are presented. The selection of the described approaches, tools, and chemistries is based on approaches used in this thesis. The general background, including the respective reaction mechanisms and potential application in related research areas, is discussed in detail. First, multicomponent reactions and in particular the herein used Passerini three-component reaction is described including a discussion on isocyanides and their reactivity (Chapter 2.2.1). Subsequently, a specific example of click chemistry and its advantageous characteristics are illustrated (Chapter 2.2.2).

2.2.1 Multicomponent reactions

Multicomponent reactions (MCRs) are efficient one-pot reactions, where three or more reactants are efficiently incorporated into one single product.[187] Most of the atoms of the starting components are incorporated into the final product, leading to the formation of complex structures.[188] MCRs provide some valuable characteristics, establishing them as “the logical choice” when it comes to sequence-definition.[189] The main advantages of MCRs include high atom efficiency, their convergent character, and the formation of many covalent bonds in a single reaction, forming complex structures without any intermediate stages that need to be purified.[188] Furthermore, according to the concept of an ideal synthesis, described by Wender *et al*., MCRs can be considered as “ideal reactions” because of the aforementioned high atom efficiency, the commercially available starting materials, the very simple reaction procedures, the high yields, as well as the (mostly) environmentally friendly reactants.[190] In the context of sequence-definition, the high yields and simple reaction procedures, which allow the formation of complex products in one step, should be considered as the main advantages of the reactions as they enable the synthesis of highly functionalised macromolecules and, by achieving high yields, the synthesis of long sequences is facilitated. Furthermore, as the products are formed in one step, MCRs are experimentally straightforward, avoiding time-consuming purification of intermediates. Due to the modular character of the reactions, they are very versatile and therefore commonly used in combinatorial chemistry: by varying the different components, large substance libraries can be synthesised and screened.[187]

In general, there are three main reaction types of MCRs, depending on their reaction mechanism, as depicted in Scheme 13.[187]

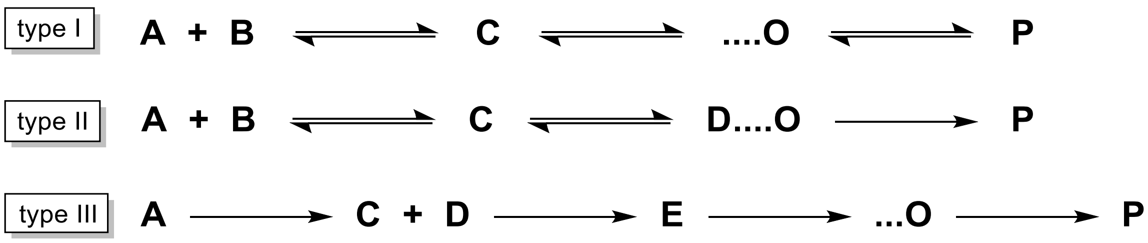

Scheme 13. MCRs are differentiated into three main types: In type I, all reactions are reversible, type II reactions have an irreversible last reaction step and in type III reactions, all reaction steps are irreversible,[187] *with* ***A, B****: starting material;* ***C, D, E, O****: intermediates and* ***P****: product.*

In type I reactions, all the reaction steps are reversible. Thus, type I reactions can result in low yields, depending on the equilibrium constants of the respective reaction steps. In type II reactions, the last irreversible step shifts the equilibrium towards the product side, which is advantageous in terms of yields. The ideal situation is provided by type III MCRS, which only consist of irreversible reaction steps. Such reactions are rarely found in synthetic chemistry, however, some biochemical reactions of the metabolism can be classified as this type of MCR. The transitions between the three types of MCRs are fluent and not every reaction can be strictly grouped into one of the categories.[187]

In the following section, the most important MCRs will be shortly introduced in chronological order before discussing isocyanide-based and especially the herein used Passerini reaction in more detail.

The first known multicomponent reaction was described by Strecker in 1850 (see Scheme 14a), which enables the straightforward synthesis of amino acids by a reaction of an aldehyde with hydrogen cyanide and ammonia. The formed α-aminonitrile is subsequently hydrolysed to yield the corresponding amino acid as a racemate.[191] To date, numerous asymmetric versions of the Strecker reaction, allowing the synthesis of enantiopure amino acids have been established.[192-193] Hantzsch developed a four-component reaction towards dihydropyridines in 1882 (see Scheme 14b).[194] The product is obtained by the reaction of two equivalents of β-ketoester, ammonia, and an aldehyde. The reaction is pharmaceutically applied in the synthesis of Nifedipin, which is a drug applied for treating angina and cardiovascular diseases.[187]

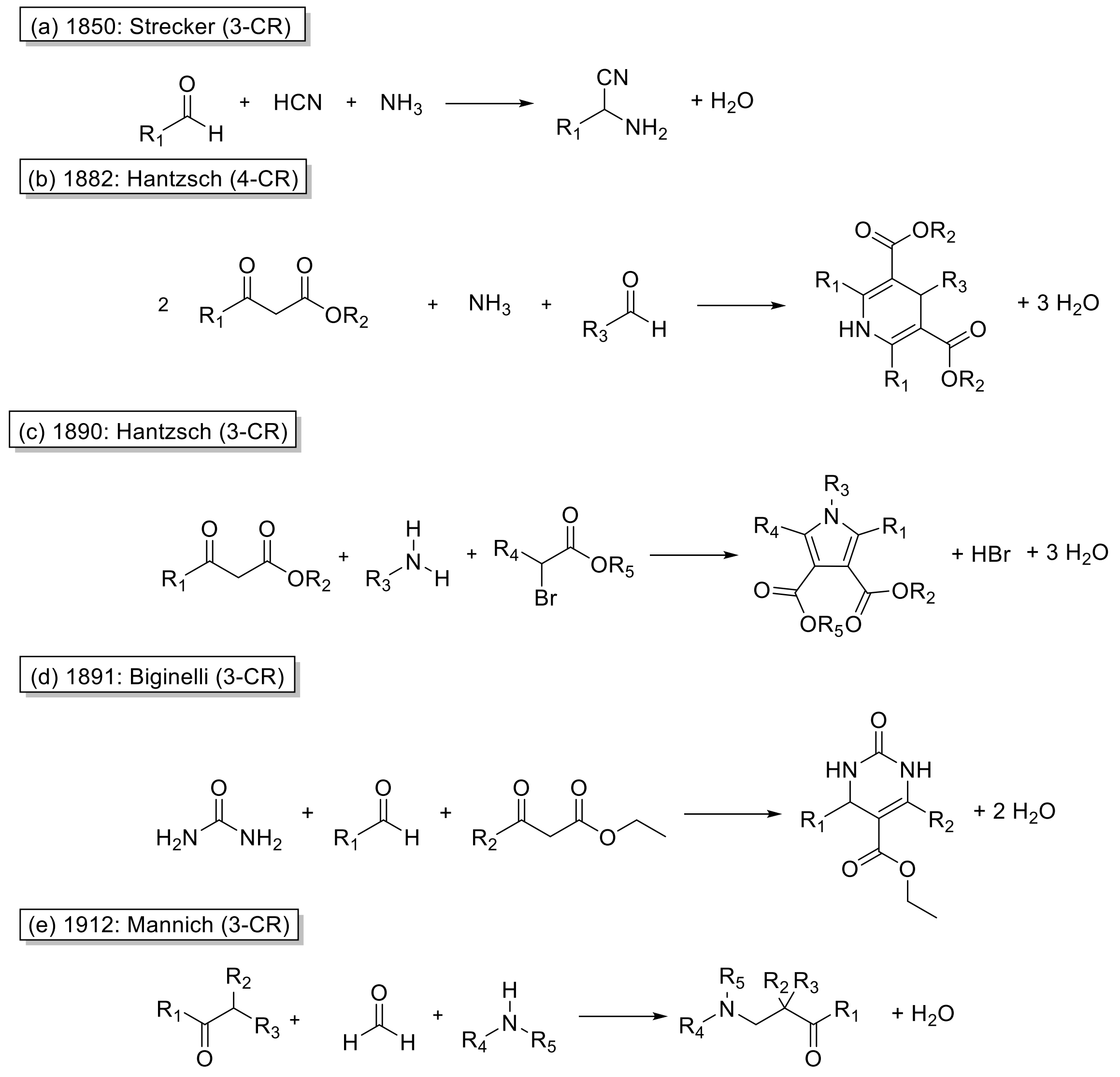
(a) 1850: Strecker (3-CR)
(b) 1882: Hantzsch (4-CR)
(c) 1890: Hantzsch (3-CR)
(d) 1891: Biginelli (3-CR)
(e) 1912: Mannich (3-CR)

Scheme 14. Examples of historically important MCRs in chronological order.[191, 194-197]

In 1890, another important three-component reaction was reported by Hantzsch: the Hantzsch pyrrole synthesis (see Scheme 14c).[195] In this reaction, α-haloketones are reacted with β-ketoesters and ammonia to form pyrroles[195] and the resulting products were found to be advantageous drugs, for instance, in malaria therapy.[198-199] The Biginelli three-component reaction was reported in 1891 (see Scheme 14d).[196] In this reaction, the aza-analogues of the Hantzsch dihydropyridines are formed by the reaction between an aldehyde, urea, and a β-ketoester. The products obtained in the Biginelli reaction are also pharmaceutically interesting, as they are, for example, used as antitumor agents and as calcium channel blockers.[200-201] The Mannich three-component reaction, which was reported in 1912, is another example of a historically important MCR. It involves the reaction of formaldehyde with amines and an oxo-component, which can be either an aldehyde or a ketone. After condensation of the formaldehyde with the amine to form the corresponding iminium ion, the iminium ion is attacked by the oxo-component and a β-aminocarbonyl is formed.[197] The Mannich reaction is widely applied in alkaloid synthesis.[202]

There are two other important subclasses of MCRs, namely metal-catalysed MCRs[203-206] and isocyanide-based MCRs (IMCRs). Since the latter is a highly valuable tool for introducing various functionalities into sequence-defined macromolecules, the following section focusses on this subclass by first introducing isocyanides and their outstanding reactivity and subsequently presenting two IMCRs: the Ugi four-component reaction (U-4CR) and the Passerini three-component reaction (P-3CR).

2.2.1.1 Isocyanides – a functionality with remarkable reactivity

The remarkable reactivity of isocyanides is a consequence of the reactivity of the formally divalent carbon atom.[187] This isocyanide reactivity is only comparable to that of carbenes and carbon monoxide. Their reactivity can be explained by the two resonance structures, depicted in Figure 11. One of the mesomeric resonance structures features a divalent carbon atom (Figure 11, left), similar to that found in carbenes, for instance. The second one, being a zwitterionic structure (Figure 11, right), leads to their ability to undergo α-additions, meaning that isocyanides react as nucleophiles, whereby the carbon is transformed into an electrophile, allowing a nucleophilic attack, the so called α-addition, at the same position. Isocyanides exhibit α-acidity, which is further increased if electron withdrawing groups (EWGs) are introduced in the α-position.[187] Furthermore, by introducing EWGs, the zwitterionic character is increased, further facilitating the formation of radicals.[187]

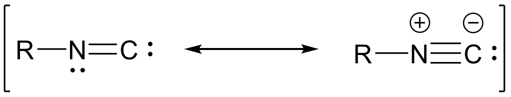

Figure 11. The mesomeric resonance structures of isocyanides include a zwitterionic configuration as well as a carbene like structure.

Chatani *et al.* reported that isocyanides are able to undergo [4+1] cycloadditions with α,β-unsaturated carbonyls[207] and are used in the synthesis of heterocycles like imidazoles, pyrroles, and oxazoles,[208-210] as well as of steroids.[211] Upon initiation with Brønstedt and Lewis acids, isocyanides are easily polymerisable. Polymerisation can also be achieved by decomposition of metal-isocyanide complexes.[212-213]

Volatile isocyanides of low molecular weight exhibit a strong and unpleasant odour, which decreases with increasing molecular weight.[187, 214] They hydrolyse in acidic media but are stable in under basic conditions.

Isocyanides are also found in nature, where terrestrial isocyanides can be distinguished from marine isocyanides. Terrestrial isocyanides are derived from amino acids, whereas marine ones are terpene-based.[215-216] Many naturally occurring isocyanides have been isolated and are interesting due to their antibiotic or fungicidal behaviour.[216] The first isolation of a naturally occurring isocyanide was reported in 1950 by Rothe, who extracted the antibiotic isocyanide metabolite Xanthocillin from Penicillium notatum Westling - a terrestrial isocyanide built from tyrosine units.[217] An example of a typical marine diterpenoid isocyanide (Kalihinene) is depicted in Figure 12, together with the aforementioned terrestrial Xanthocillin, which interestingly exhibits antibiotic properties.[218]

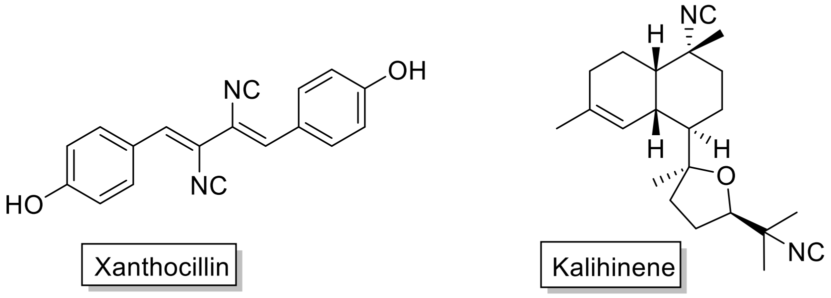

Xanthocillin

Kalihinene

Figure 12. Examples of two naturally occurring isocyanides.[217-218]

To date, several synthetic routes towards isocyanides are described. In 1859, Lieke accidentally synthesised an isocyanide for the first time.[214] He reacted allyl iodide with silver cyanide and obtained allyl isocyanide instead of allyl cyanide, which is what he intended to synthesise.[214] Only several years later, in 1868, Gaultier proved that the isocyanide was synthesised instead, by hydrolysing the product to the corresponding formamide.[219] In case the nitrile had been prepared, the corresponding carboxylic acid would have been formed.[219] Hofmann reported another route towards isocyanides in 1867 by reacting primary amines with chloroform in the presence of potassium hydroxide.[220]

Nearly 100 years later, a novel route to synthesise isocyanides was reported by Ugi.[221] He dehydrated *N*-formamides by using phosgene in the presence of bases. Ever since, this synthesis strategy is the method of choice for isocyanide synthesis and significantly contributed to the development in the field of IMCRs. Although phosgene is highly toxic, it is still utilised as dehydration agent in industrial processes on account of its low price. However, in lab scale, it has been replaced by other less toxic dehydration agents, such as triphosgene, diphosgene, or phosphoryl trichloride.[222-224] Since Dömling *et al.* discovered the value of the Leuckart-Wallach reaction as tool for the synthesis of *N*-formamides, the number of synthetically accessible isocyanides has drastically increased.[225] Recently, they also reported a procedure using triphosgene as *in situ* dehydration agent in order to avoid the unpleasant smell of the isocyanides and proved the compatibility with IMCRs by applying it to several IMCRs.[226] The discussed approaches towards isocyanides are shown in Scheme 15.

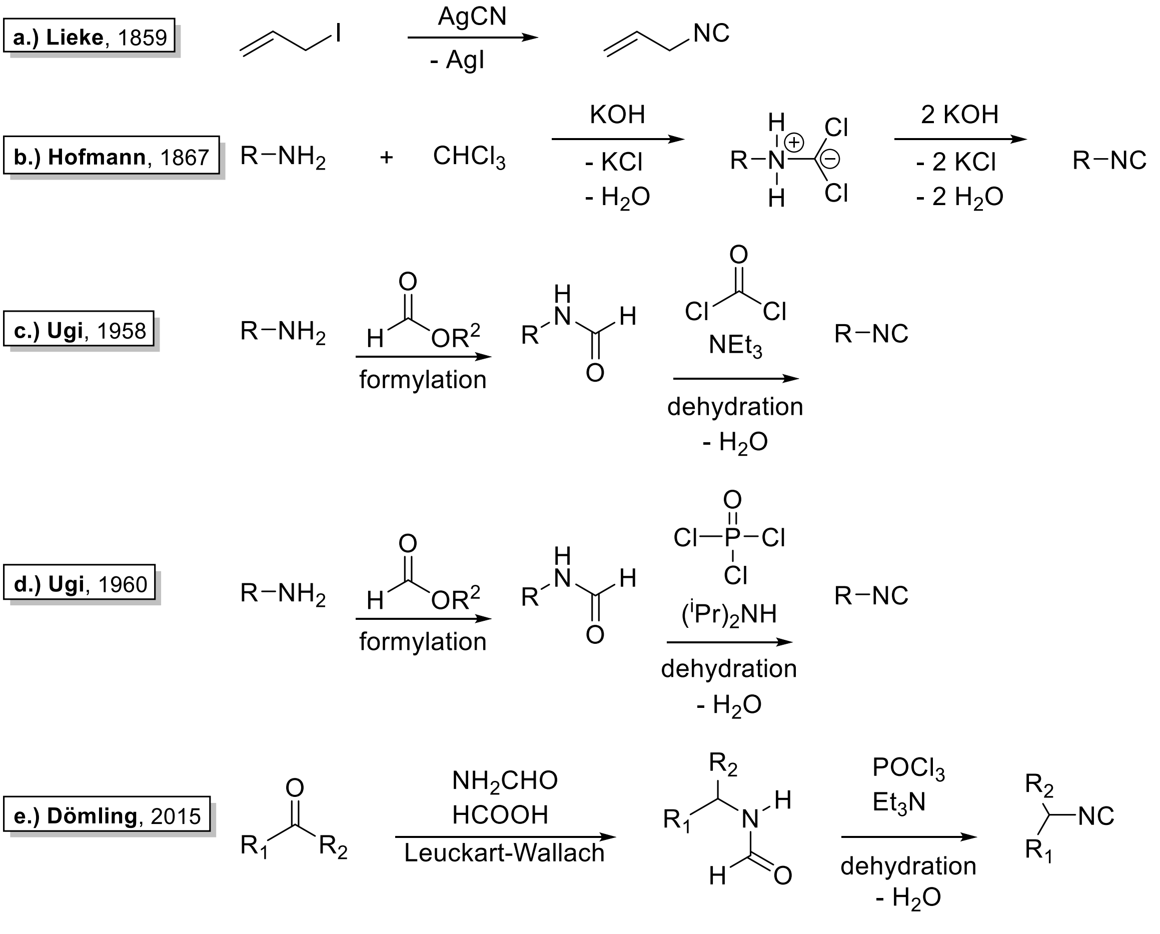
a.) Lieke, 1859
AgCN
- AgI
NC
b.) Hofmann, 1867
R−NH2
CHCl3
KOH
- KCl
- H2O
2 KOH
- 2 KCl
- 2 H2O
R−NC
c.) Ugi, 1958
formylation
NEt3
dehydration
- H2O
d.) Ugi, 1960
(iPr)2NH
e.) Dömling, 2015
NH2CHO
HCOOH
Leuckart-Wallach
POCl3
Et3N

Scheme 15. Different routed towards isocyanides in chronological order.[214, 220-221, 225]

Many important achievements towards the efficient synthesis of isocyanides have been made, which allow the formation of various different isocyanide compounds in good yields while being easy to handle reaction procedures. Nowadays, in synthetic laboratories, the procedure reported by Ugi is the method of choice. In the following part, the useful reactivity of isocyanides in isocyanide-based MCRs and polymer chemistry will be showcased.

2.2.1.2 Isocyanide-based multicomponent reactions

There are two important IMCRs which will be introduced here: The Passerini three-component reaction and the Ugi four-component reaction. Both reactions are depicted in Scheme 16. The P-3CR was reported in 1921 and is the first described IMCR.[227] As illustrated below, a carboxylic acid, an aldehyde, and an isocyanide are reacted to form one single product without any side products by incorporating every atom of the starting materials. In the U-4CR, an amine is added as fourth component forming α-acylaminoamides.[228-229] Thus, in the U-4CR, a fourth functionality can be introduced to the product within one reaction step, allowing the formation of complex and highly functionalised products. The U-4CR was discovered in 1959 by Ivar Ugi. [228-229]

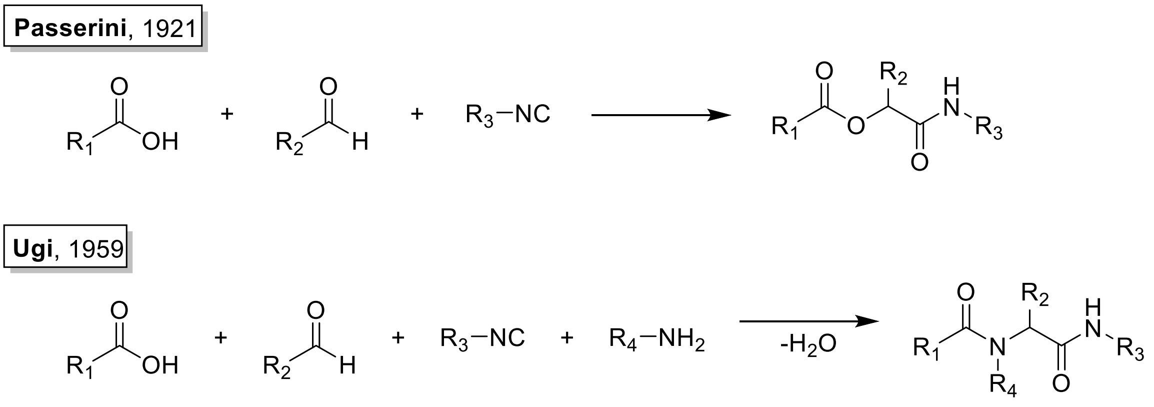

Scheme 16. Reaction equations of the two important IMCRs: The P-3CR and the U-4CR.[227-229]

Before discussing the P-3CR in more detail in Chapter 2.2.1.3, which is used within this thesis, the U-4CR will be briefly introduced. The reaction will be explained with the aid of its mechanism (see Scheme 17), which differs from that of the P-3CR (compare Scheme 18). The reaction starts with the formation of the imine by the reaction of the aldehyde and the amine. Interestingly, it was found that the preformation of the imine can have advantageous effects on the obtained yield.[187] Subsequently, the imine is activated by protonation by the carboxylic acid. In the next step, the α-addition of the isocyanide takes place. The nucleophilic attack results in a nitrilium species[230] which is converted into an imidate through nucleophilic attack at the same position by the deprotonated carboxylic acid. The product is formed after a final rearrangement, the so-called Mumm rearrangement, which was first reported in 1910. Due to the last irreversible step, the U-4CR can be classified as type II MCR (see Scheme 13).[187] In contrast to the P-3CR, U-4CR reactions are performed in protic solvents, such as methanol, as they proceed more efficiently under such conditions.[187] The U-4CR plays an important role in combinatorial chemistry as well as in synthetic and pharmaceutical chemistry as highly functionalised products are obtained in straightforward one-pot procedures.[231]

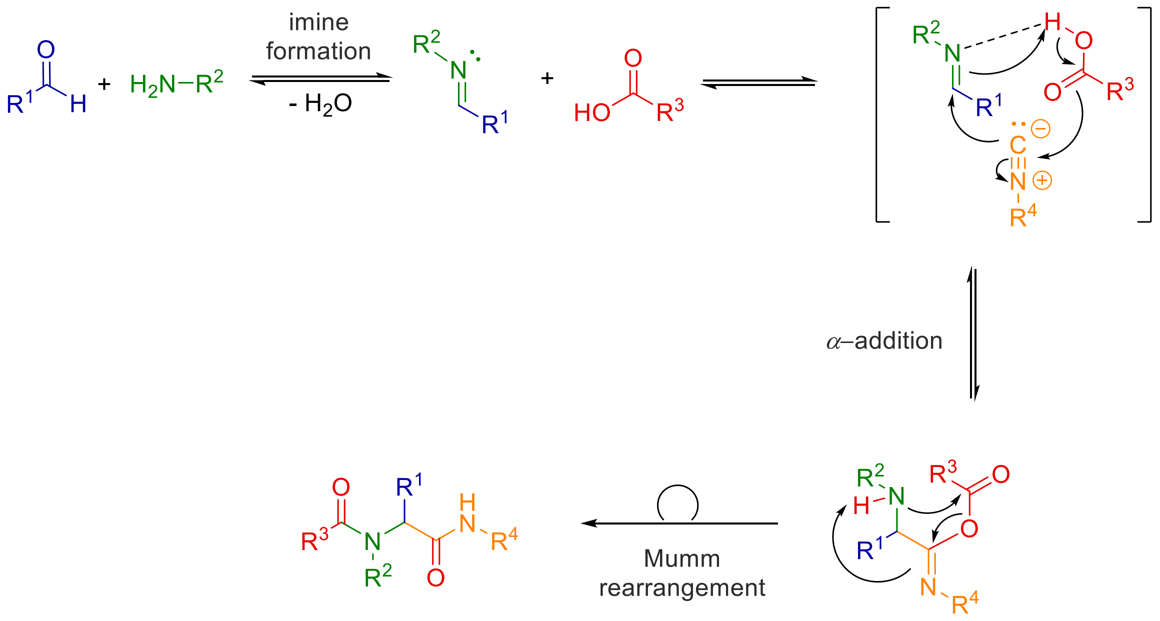

Scheme 17. Commonly accepted mechanism of the U-4CR, first introduced by Ivar Ugi in 1961. First, the imine is formed, which is then activated by protonation. The isocyanide is introduced via α-addition and the α-acylaminoamide product is formed upon Mumm rearrangement.[187, 228-229]

The efficient and straightforward U-4CR offers a powerful platform for a magnitude of different applications in combinatorial-, organic-, and polymer chemistry. In Chapter2.1.3.2, its importance in various sequence-defined syntheses has already been shown.

2.2.1.3 The Passerini three-component reaction

As mentioned above, the Passerini three-component reaction was first reported in 1921 by the Italian chemist Mario Passerini and is the first known IMCR.[227] The P-3CR is a one-pot reaction that benefits from simple reaction conditions as it is conducted at room temperature in aprotic solvents, such as dichloromethane (DCM). The three components are used in high concentrations to achieve high yields.[187] The reaction has been known for nearly 100 years, but its mechanism remains topic of current research as it has not been fully understood yet. The first mechanism was proposed by Passerini himself and it is still widely accepted.[227] It starts with the activation of the aldehyde by formation of hydrogen bonds with the carboxylic acid. Subsequently, the isocyanide undergoes α-addition thereby forming a cyclic transition state. A proton is transferred from the carboxylic acid to the aldehyde and the product is formed *via* a final rearrangement. The described mechanism is shown in Scheme 18. Several kinetic investigations on the P-3CR performed by Ugi[232] and Baker[233] support the suggested mechanism. Like the U-4CR, the P-3CR can be classified as a type II MCR because of the irreversible last step.[187]

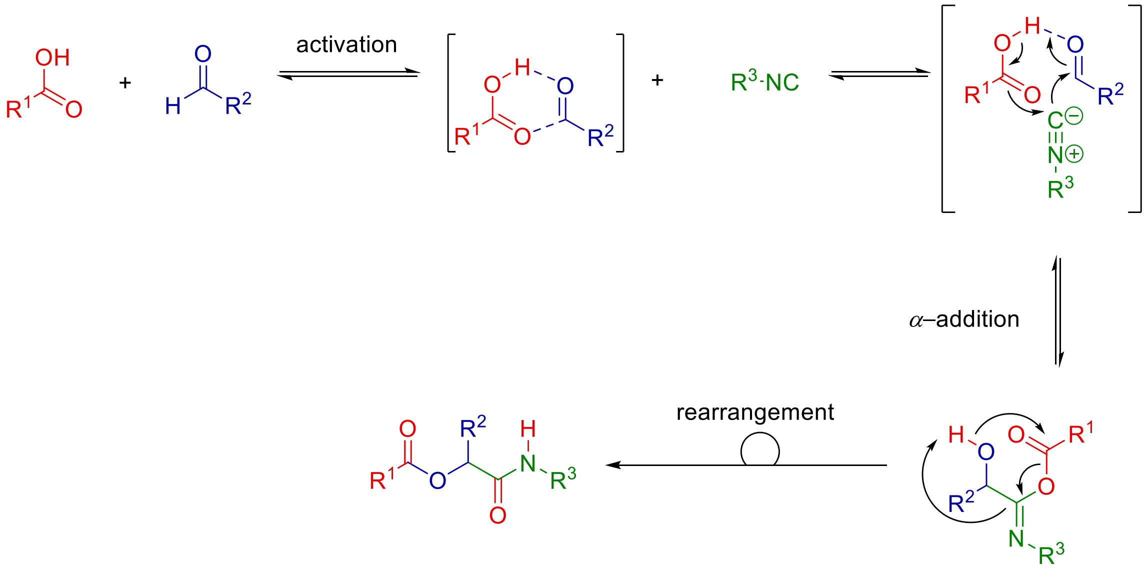

Scheme 18. Proposed mechanism of the P-3CR which was later supported by kinetic investigations by Ugi and Baker.[227, 232-233] *It starts with activation of the aldehyde by hydrogen bonds, which allows for subsequent α-addition to form a cyclic transition state. The product is formed via final rearrangement.*

As already discussed, there is still uncertainty about the actual mechanism of the P-3CR. In another proposed mechanism reported by Eholzer in 1965, the isocyanide is first protonated by the carboxylic acid, an assumption based on the fact that the P-3CR proceeds faster in the presence of mineral acids as catalysts.[234] These findings are in agreement with a publication reporting accelerated P-3CRs in water.[235] However, they are at odds with the observation that P-3CRs are accelerated in non-polar, protic solvents, as reported by Ugi.[236] Based on calculations in the gas phase, another mechanism was postulated in 2011 involving a fourth component (see Scheme 19).[237] The mechanism involves two carboxylic acids; however, the second acid component acts like a catalyst and the reaction could be described as an organo-catalysed three-component reaction rather than a four-component reaction. According to this mechanism, the activation step and the α-addition proceed as shown in the previously discussed mechanism (compare Scheme 18). However, the rearrangement involves a second carboxylic acid, because the calculated energy of the transition state is significantly lower if a second acid molecule is involved and the product is thus formed *via* a cyclic transition state. The postulated mechanism was later supported by density functional theory (DFT) calculations.[238]

Although the mechanism of the P-3CR is not yet fully understood, the reaction is widely applied in preparative chemistry. Due to the modular character of MCRs, the achievable structural diversity in one single step is incomparably wide in scope, making these reactions an attractive tool for many different applications. Since pharmaceutically active compounds are easily accessible by P-

3CR, it is also applied in medical chemistry, as well as in combinatorial chemistry, where large substance libraries are synthesised.[188, 239]

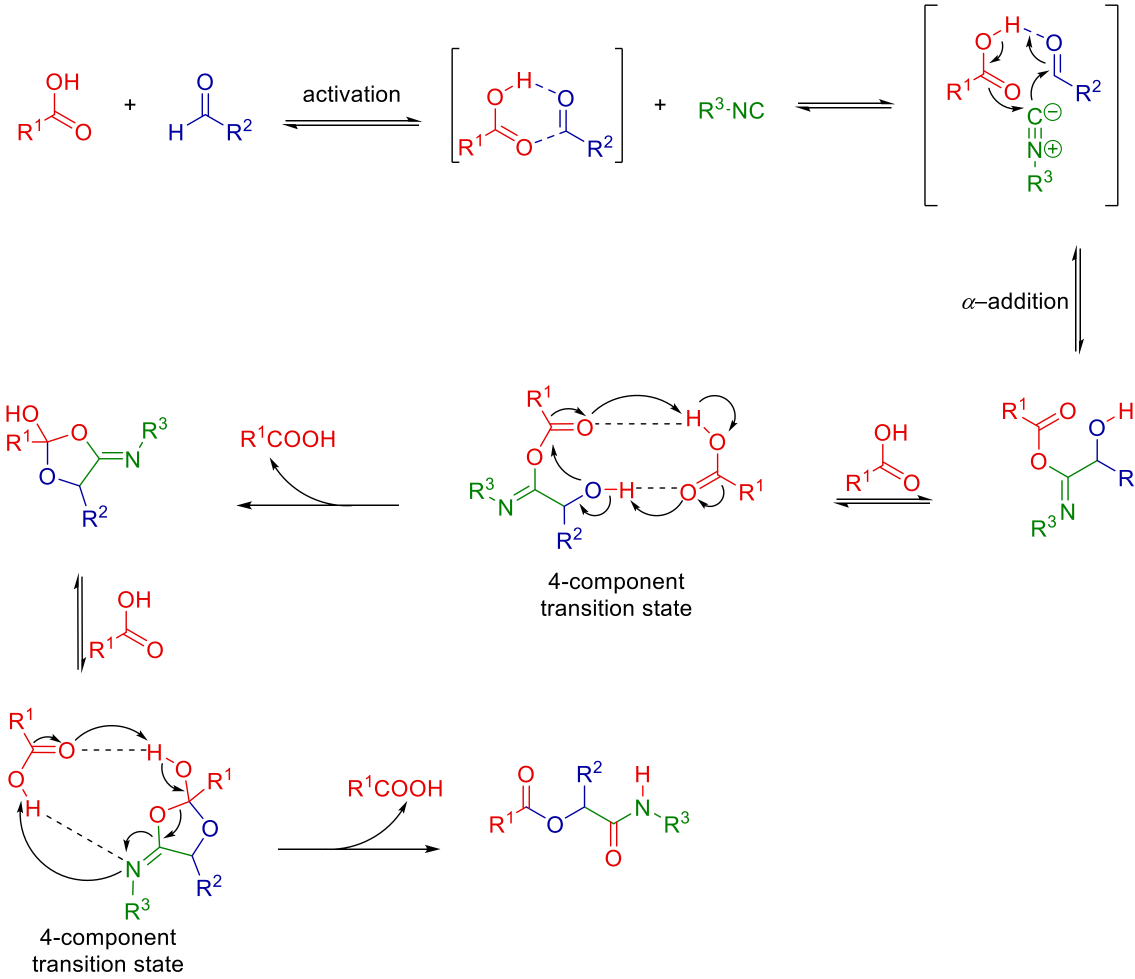

Scheme 19. Proposed mechanism of the P-3CR by Maeda et al. involving two carboxylic acids. The mechanism was developed based on quantum mechanical calculations in the gas phase.[237] DFT calculations supported the postulated mechanism later.[238]

Many different variations of the classic P-3CR have been reported. They include substitutions of the mentioned components by other functional groups: the carboxylic acid, for example, was replaced by alcohols which was achieved at elevated temperatures using Lewis acids as catalysts, thus α-alkoxy amide derivatives were formed.[240-242] Such Lewis acids are indium (III)- or bismuth (III) triflate and aluminium (III) chloride. Furthermore, 2-nitrophenols were applied without any catalyst to yield the corresponding *o*-arylative Passerini product.[243] In this case, another rearrangement step takes place: the so-called Smiles rearrangement. By basic treatment of the amide moiety, a second Smiles rearrangement can be induced and 1,4-benzoxazinones were obtained.[244] The acid component could also be replaced by water resulting in the formation of α-hydroxy amides.[245] The reaction with water as acid component can be catalysed by adding small amounts of boronic acids.[246] Another interesting P-3CR variation benefited from alcohols, that were used as surrogates for aldehydes and were oxidised *in situ*. This is especially interesting with regard to the commercial availability of aldehydes and their poor stability, as they tend to autooxidise. The first example of *in situ* oxidation of alcohols with subsequent P-3CR was reported by Zhu and colleagues.[247] They used 2-iodoxybenzoic acid (IBX) as oxidising agent and performed the reaction in THF reaching high yields of up to 93%. Different variants of the P-3CR replacing one of the components are depicted in Scheme 20. In another example, the carboxylic acid was replaced by hydrazoic acid, providing a straightforward access to tetrazole derivatives.[232] The hydrazoic acid was later replaced by trimethylsilyl azide, offering a less explosive and less toxic alternative.[248] Enantioselective variants of the P-3CR are reported as well.[249] Enantioselectivity can either be achieved with the help of asymmetric catalysts[250] or by utilising chiral components. There are variants demonstrating the use of chiral carboxylic acids, aldehydes as well as isocyanides, offering manifold pathways towards stereoselectivity.[251-253]

Besides the replacement of the carboxylic acid, there are also variants of the P-3CR replacing the aldehyde. This can be achieved using ketenes and acyl isocyanates, for example, leading to α,γ-diketo-carboxamides and *N*,*N*-diacyloxamides, respectively.[254-255] The third component, the isocyanide is crucial for the reaction and there are not many variations reported. The only possibility is the use of convertible isocyanides, meaning that another (sometimes protected) reactive groups is incorporated in the isocyanide component, which allows for post-modification of the Passerini scaffold.[256-260]

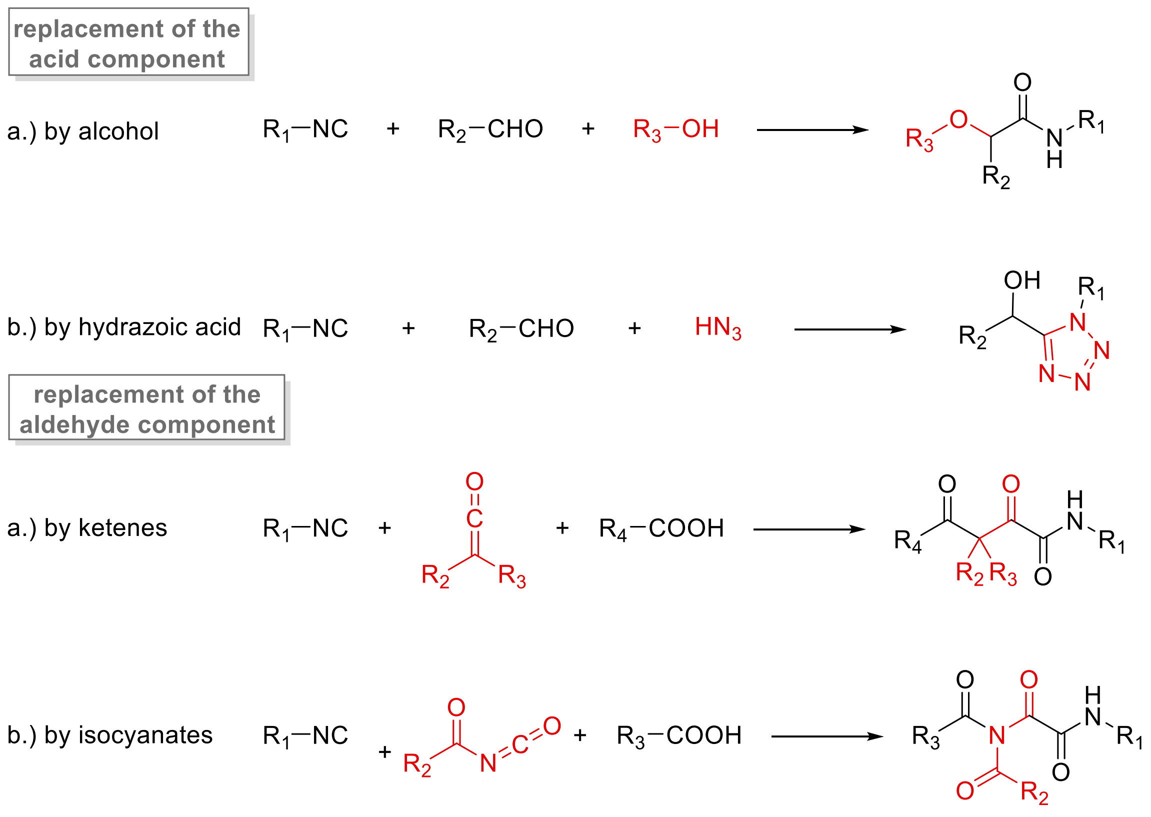
replacement of the acid component
a.) by alcohol
b.) by hydrazoic acid
replacement of the aldehyde component
a.) by ketenes
b.) by isocyanates

Scheme 20. Different variants of the P-3CR, replacing the acid or the aldehyde component by other functional groups which demonstrates the versatility of the reaction.

The synthesis of cyclic compounds using the P-3CR has also been reported, further substantiating the versatility of this reaction. Ring-closing is achieved by reacting hetero-bifunctional components with the third component. The first example of such two-component three-centre reactions was reported in 1923, only shortly after the reaction was first reported.[261] Passerini reported the cyclization of 2-acetylbenzoic acid with various isocyanides, yielding differently functionalised small cycles. A similar reaction was reported by Li *et al*. who replaced the ketone by a more reactive aldehyde.[262] The method allows the synthesis of lactones in different sizes by regulating the size of the spacer between acid and oxo component.

2.2.1.4 The use of the P-3CR and other MCRs in polymer chemistry

For a long time, the use of multicomponent reactions in general and the P-3CR in particular was limited to the fields of synthetic organic chemistry, combinatorial chemistry, and pharmaceutical/medicinal chemistry. However, the attractive characteristics of these reactions led to a growing interest in the field of polymer chemistry. Besides the aforementioned features of MCRs, namely being highly atom efficient, easy to perform one-pot procedures, readily available starting materials, and chemical diversity, the P-3CR is also highly efficient without side reactions, thus making it attractive in polymer syntheses.

In general, there are three different ways how organic reactions can be transferred to the field of polymers. First, the reaction itself can be used to synthesise polymers. This can either be achieved by synthesising monomers bearing polymerisable end groups, which are subsequently used in a polymerisation reaction, or by using the reaction itself for the polymerisation process. The latter is achieved by using bifunctional monomers in the MCR. However, organic reactions can also be used for post-polymerisation modifications on pre-formed polymers. For this purpose, functional polymers with one or more reactive sites that are suitable to be converted in an MCRs need to be present.[263-265]In the following section, different approaches towards polymer chemistry applying the P-3CR and other MCRs will be presented.

The first report on monomer synthesis *via* P-3CR was published in 2010.[266] The group of Gianneschi and Yang used convertible isocyanides in the MCR which allowed the synthesis of α-hydroxy carboxylic acid monomers upon cleavage. The monomers were incorporated into poly(α-hydroxy carboxylic acid)-copolymers. Our group reported the synthesis of monomers bearing terminal double bonds which were suitable for acyclic diene metathesis polymerisation (ADMET). The monomers were not only formed *via* P-3CR,[267] but also *via* U-4CR.[268] Depending on the applied MCR, the polymers were obtained as polyesters with amide side chains or polyamides with amide side chains, respectively. Similarly, asymmetric α,ω-dienes have been formed by the P-3CR and excellent head-to-tail selectivity was reported.[269-270] Furthermore, acrylate and acrylamide monomers have been synthesised and applied in free radical polymerisations offering access to polymers with interesting material properties.[271-272] By careful selection of the components in the MCR, the glass transition temperature (T_g) and the thermoresponsive behaviour, such as the upper critical solution temperature, were fine-tuned. Similarly, the U-4CR was also applied for monomer synthesis. There are also examples reported using the Biginelli and the Hantzsch reaction.[273-274]

The P-3CR can also be conducted as polymerisation method. This was achieved for the P-3CR[267] as well as for the U-4CR.[275] By utilising bifunctional molecules as monomers, polyaddition can be induced, leading to the formation of polymers. The P-3CR polymerisation was first reported in 2011.[267] Dicarboxylic acids and bifunctional aldehydes were polymerised with different monofunctional isocyanides, allowing for functionalisation of the polymer. Using this combination of starting materials, poly(esters) with amide side chains are obtained,[267] whereas poly(ester-amides) were obtained when dicarboxylic acids, bifunctional isocyanides and monofunctional aldehydes are used.[44] The third possible combination of the components uses dialdehydes and diisocyanides combined with monofunctional acids yielding poly(amides) with ester side chains.[276] The three different possible combinations of the components are depicted in Scheme 21. Another elegant polymerisation technique is the P-3CR polymerisation using a bifunctional AB-monomer. This was achieved by polymerising a monomer bearing both a carboxylic acid and an aldehyde moiety with different isocyanides.[277] The approach allows for investigation of the influence of the introduced side chains. Furthermore, sequential introduction of different side chains by P-3CR polymerisation was reported. This was achieved by Li and co-workers, who synthesised sequence-defined macromonomers which were subsequently polymerised in a P-3CR polymerisation.[278] Apart from linear polymeric structures, the synthesis of star-shaped block copolymers with adjustable block length and selectable side chains was reported.[279]

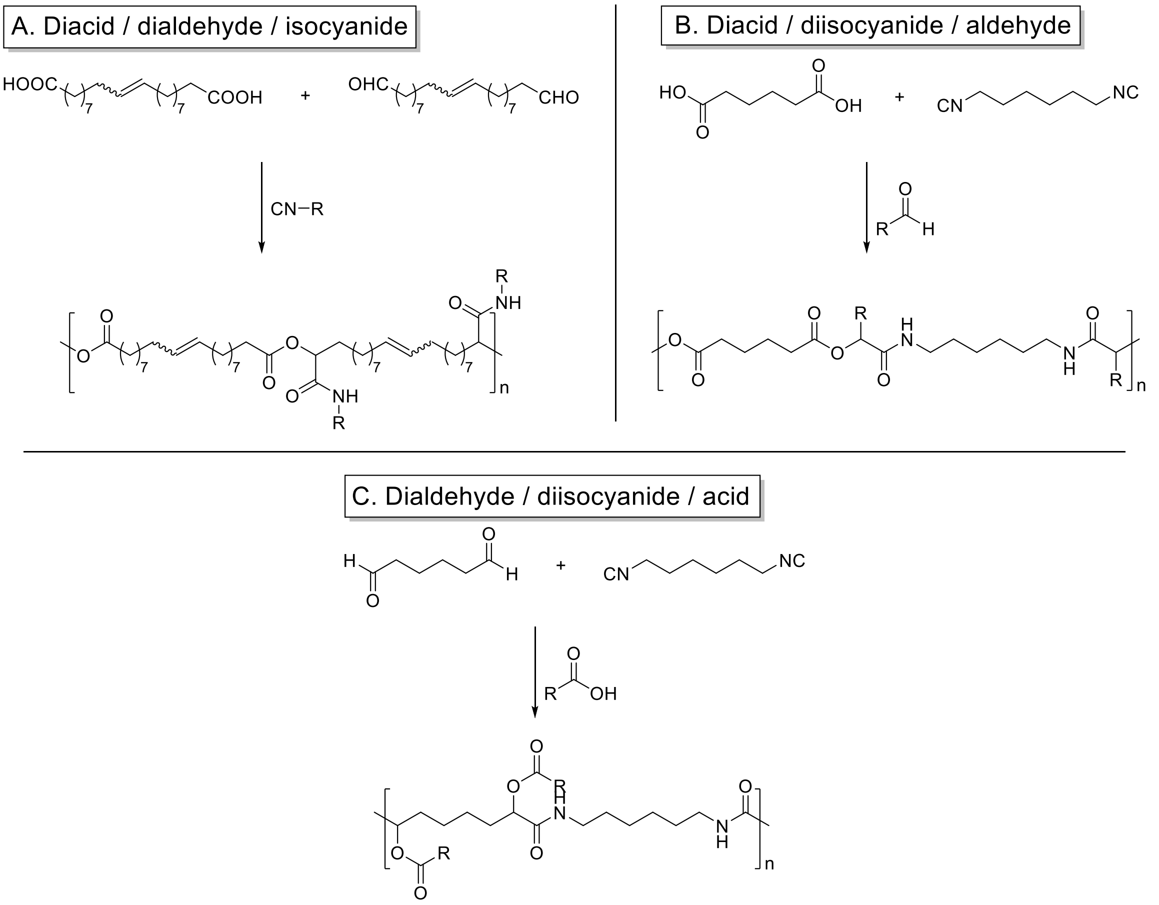
A. Diacid / dialdehyde / isocyanide
B. Diacid / diisocyanide / aldehyde
C. Dialdehyde / diisocyanide / acid
HOOC
COOH
OHC
CHO
7
CN–R
HO
OH
CN
NC
R
H
O
NH
n
H
N
OH

Scheme 21. Three different ways of P-3CR polymerisation, using different combinations of bifunctional components leading to different polymeric scaffolds.

In 2016, our group reported a polymerisation technique using the Biginelli reaction. Diacetoacetates, dialdehydes, and urea, all of which can be obtained from renewable resources, were reacted in a Biginelli-type step-growth reaction and high molecular weight polymers with high T_g and thermal stability were achieved.[280]

In conclusion, the versatility, robustness, and the simple synthesis procedures make the P-3CR an attractive tool for sequence-defined synthesis. The reaction allows for high, nearly quantitative yields, which is crucial if long sequences are targeted. Furthermore, no side products are formed, leading to easy purification procedures, where only the excess of the components needs to be separated from the growing oligomers. Finally, the modular character of multicomponent reactions in general allows introducing of various different functionalities by utilizing commercially available reagents, thus leading to sequence-definition. The importance of the P-3CR in the field of sequence-definition has already been showcased in Chapters 2.1.3.1 and 2.1.3.2.

2.2.2 An introduction to triazolinedione chemistry

As already discussed above, the P-3CR, as multicomponent reactions in general, is a very effective tool in sequence-defined synthesis. In one of the approaches developed within this thesis (see Chapter 4.2), the P-3CR is combined with the ultrafast and efficient 1,2,4-triazoline-3,5-dione (TAD) chemistry, which can be considered as click reaction. Therefore, in this chapter, the chemistry of triazolinediones will be introduced by showing different synthesis procedures of TAD, explaining the extraordinary reactivity of TAD, and finally giving some application examples.

The term "click" chemistry was coined by Sharpless in 2001.[133] The main advantages of click chemistry include the wide range of substrates, high yields, fast reactions, inoffensive by-products, and easy purifications, all of which are valuable characteristics for macromolecular sequence-definition.[281] TAD is one notable example in the field of click chemistry.[282] Apart from the aforementioned characteristics, the fact that it provides a visual feedback due to the vivid red colour of the TAD molecule[282-283] makes it an ideal reaction partner when striving for sequence-definition. In the pioneering work of Thiele and Stange from 1894, TAD was reported for the first time.[284] They reported a route towards the dihydro derivative of TAD, the 1,2,4-triazolidine-3,5-dione, or the so-called urazole. However, at the time, oxidation or reduction reactions were often applied to clarify the structure and prove the success of the synthesis protocol. Thus, the last step of the urazole synthesis was an oxidation, yielding a vividly red-coloured solution, which can be explained by the formation of TAD (see Scheme 22).[284-286]

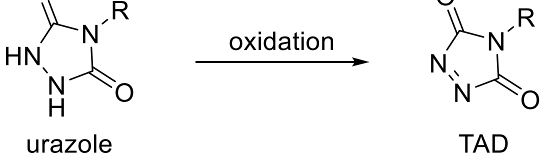

Scheme 22. Oxidation of the urazole precursor leads to the corresponding TAD compound.

Due to the extraordinarily high reactivity of TAD molecules, which caused stability issues and the problematic isolation of the pure compound, they were rarely used or even synthesised for a long time.[287-288] To date, the exclusively followed synthesis route towards TAD entails the oxidation of their bench-stable urazole precursors. Nowadays, TAD compounds are well-known for their instantaneous reaction with cyclopentadiene.[288] Even at very low temperatures of -78 °C, the reaction proceeds within seconds. Therefore, they are considered as the most reactive dienophiles and enophiles, while still bench-stable.[289] The extreme reactivity of TAD is attributed to the locked *cis*-azo configuration (see Scheme 23).[288, 290] If the reactivity is compared to other azodicarbonyl dienophiles, it is found that the *cis*-configuration drastically accelerates the reaction when the dienophiles are reacted with cyclopentadiene in a Diels-Alder reaction.[291]

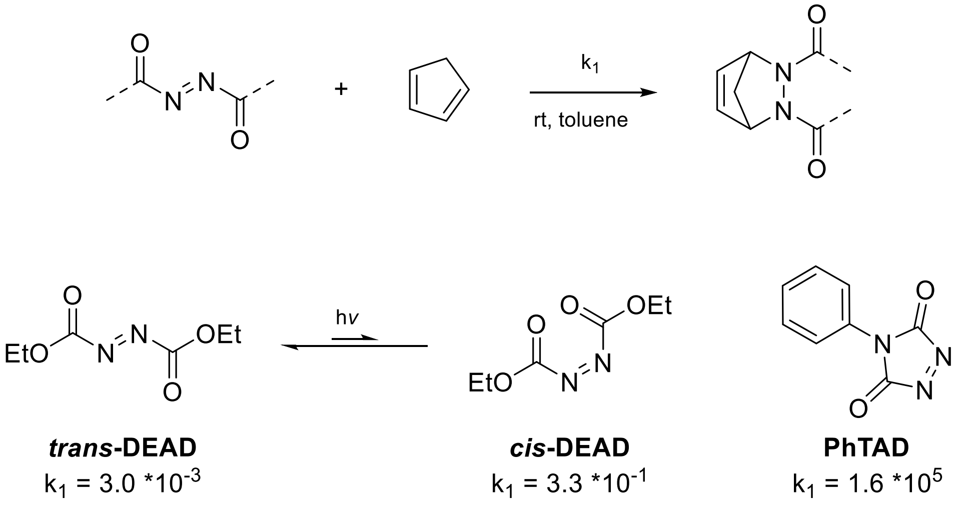

Scheme 23. The different rate coefficients (L mol^{-1} s^{-1}) in the Diels-Alder reaction with cyclopentadiene at room temperature in toluene. Three different aza-dienophiles are compared, namely cis- and trans-DEAD and phenyl TAD.[291]

As depicted in Scheme 22, TAD compounds are obtained upon oxidation of their urazole precursors. The first report on the synthesis of such a precursor was published by Thiele and describes the reaction of a mixture of biurea and aniline hydrochloride.[284] The reaction was heated to 200 °C and besides the considerable amount of a diphenylurea side product, the substrate scope was very limited because of the harsh reaction conditions. Zinner and Deucker reported another synthesis procedure towards urazoles applying significantly milder reaction conditions in 1961.[292] They reported the cyclisation of 4-substituted 1-(ethoxycabonyl)semicarbazides, also referred to as semicarbazides, which in turn were obtained from isocyanates and ethylcarbazate. In this reaction, high yields were obtained under much milder conditions. The two routes towards urazole are depicted in Scheme 24.

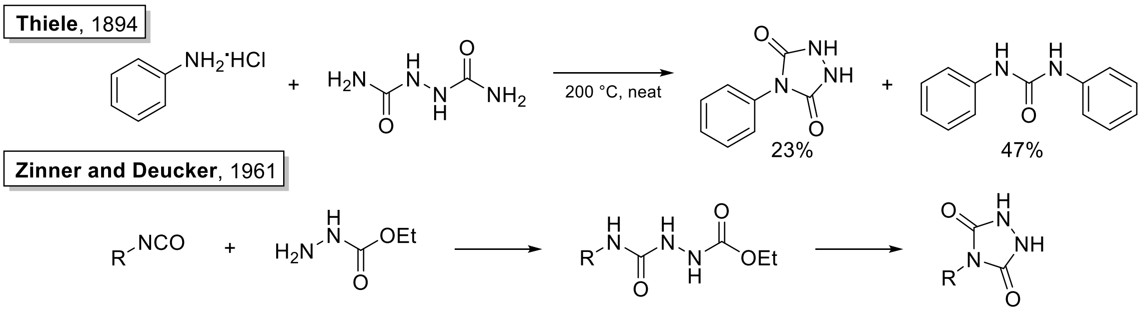

Scheme 24. Two synthetic routes towards the urozole precursor. Thiele developed the first urazole synthesis by reacting biurea with aniline hydrochloride. The more efficient and modern pathway was later reported by Zinner and Deucker.[284, 292]

However, the synthesis procedure did not gain much attention until Cookson used it and performed a final oxidation step, reporting the first efficient isolation of phenyl-TAD.[293] Nowadays, the whole reaction sequence, including the final oxidation, is commonly referred to as Cookson method[294] with phenyl-TAD being the so-called Cookson's reagent.[295-296] However, the substrate scope was still limited due to the limited commercial availability of isocyanates. Along with continuous improvements in isocyanate synthesis, several novel routes were developed. One method describes the conversion of carboxylic acids into acyl azides,[297] which underwent a Curtius rearrangement to yield isocyanates.[298-300] Another route towards isocyanates is the reaction of amines with phosgene.[301-302] Nowadays, isocyanate-free and more environmentally friendly methods are also reported.[294, 303-304] In order to further broaden the substrate scope, post modification reactions are applied and thus functional groups that would interfere with the urazole synthesis can be introduced.[283, 305-306]

The subsequent oxidation towards the final TAD compounds represents the bottleneck in TAD synthesis due to several reasons.[282] First, the chemoselectivity of the oxidant is important in order to avoid the formation of additional unwanted TAD compounds or other by-products as the isolation of TAD can often be protracted. Another problem is the high reactivity of the formed TAD. Therefore, *in situ* generation of TAD is often preferred, thus it is crucial that both the oxidant and its corresponding reduced form do not react with TAD. One important oxidation procedure in TAD synthesis (see Scheme 25) is concentrated nitric acid.[284, 307] However, aqueous work-up procedures are often necessary to remove by-products, which is problematic due to limited stability of TAD towards hydrolysis.

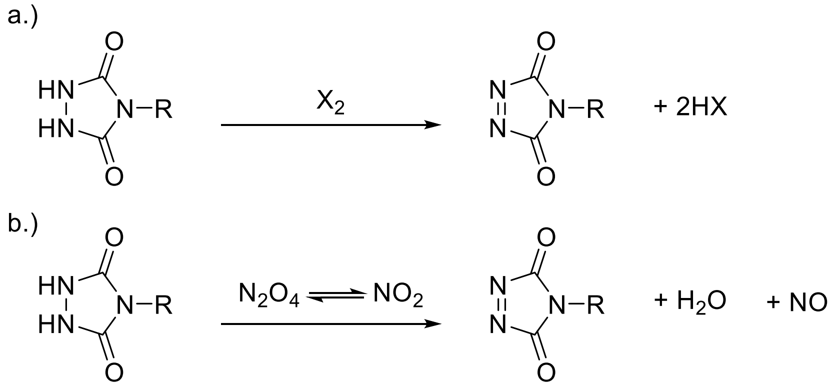

Scheme 25. The oxidation of urazole to the corresponding TAD compound can either be achieved by halogens or by dinitrogen tetroxide.

Another procedure, which is depicted in Scheme 25, uses gaseous dinitrogen tetroxide (N_2O_4)[308] which is in equilibrium with nitrogen dioxide[309] and provides much milder oxidation conditions while avoiding acids. The procedure was developed by Stickler and Pirkle and yields TAD in quantitative yields without any by-products or leaving any traces of other reagents.[308] The reaction is typically performed in polar solvents with a desiccant in order to trap the formed water during the reaction. The main disadvantages of this strategy are the high toxicity of the gas as well as its high cost and the fact that the quality of the gas is often not reliable. Novel approaches therefore focus on *in situ* generation of neat N_2O_4[310] or on heterogeneous catalysis where N_2O_4 is either adsorbed or complexed on a solid support.[311-314] Besides the nitrogen-based oxidation reagents, halogens and their derivatives are suitable oxidation agents. The oxidation of urazole towards TAD using elemental chlorine[306] or bromine[289] has been reported, but also derivatives that *in situ* form halogens have been used. *Tert*-butyl hypochlorite in dry acetone,[288] *N*-bromosuccinimide (NBS),[315-316] the tetrameric complex of 1,4-diazabicyclo[2.2.2]octane with bromine (DABCO-Br)[314, 317-318] and trichloroisocyanuric acid (TCICA)[319] have been used, for example (Figure 13).

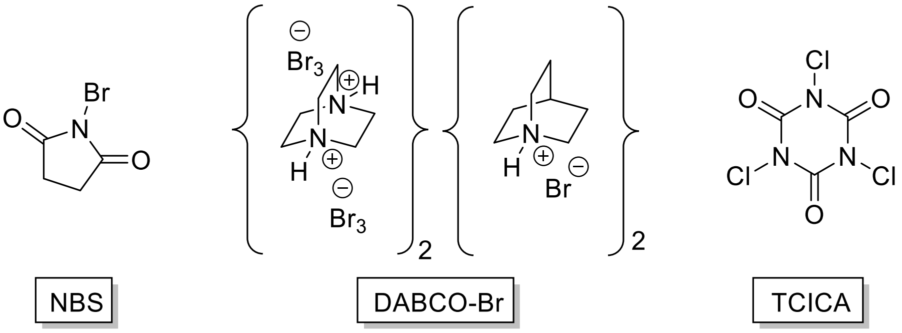

Figure 13. Some commonly applied oxidation reagents that are used for the oxidation of urazole to form TAD: NBS: N-bromosuccinimide; DABCO-Br: tetrameric 1,4-diazabicyclo[2.2.2]octane-bromine; TClCA: trichloroisocyanuric acid.

TAD compounds are considered to be the structural analogue of maleimides, which are more widely known and well established in synthetic chemistry.[320-321] In TAD compounds, the C=C double bond is replaced by a N=N double bond, leading to a up to six magnitudes higher reactivity in Diels-Alder reactions with cyclopentadiene compared to the corresponding maleimides.[291, 321] They show a high reactivity not only in Diels-Alder reactions,[290] but also in Alder-Ene reactions,[322] [2+2] cycloadditions,[323] and electrophilic aromatic substitutions. The four typical thermal reactions of TAD are shown in Scheme 26.

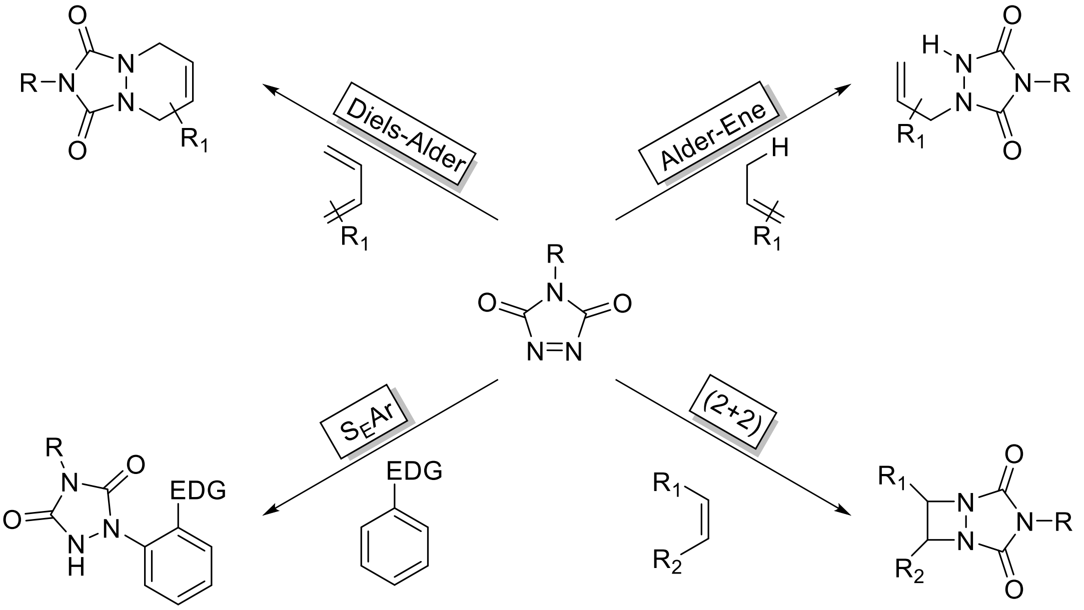

Scheme 26. The four general thermal TAD-based reactions: Diels-Alder reaction, Alder-Ene reaction, [2+2] cycloaddition and electrophilic aromatic substitution (S_EAr).

The Diels-Alder reaction is one of the most efficient and most adopted C-C bond-forming reactions and is extremely tolerant towards a variety of functional groups.[288, 324] This makes the reaction a very attractive tool in sequence-defined synthesis and was therefore the reaction of choice within this work (see Chapter 4.2). In combination with TAD, which acts as a reactive dienophile,[325] it was used as a powerful tool for quantitative chain elongation in the herein presented synthesis protocol. One notable example, shown in Scheme 27, demonstrates the speed of this click reaction even at ambient temperature: when TAD reacts with styrene, a 2:1 Diels-Alder adduct is formed quantitatively, even though the reagents are used in equimolar ratios.[290]

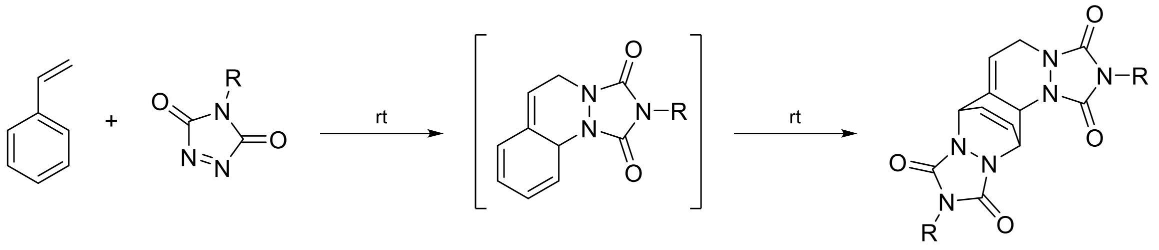

Scheme 27. The equimolar Diels-Alder reaction of styrene and TAD demonstrates the extraordinary reactivity of TAD as it yields a 1:2 adduct via a reactive intermediate.

Because of the two strong chromophores, *i.e.* the azo and the carbonyl group, which not only are in close proximity but also connected by conjugation,[326] TAD not only reacts in the already discussed thermal reactions, but also offers an extraordinary photochemical reactivity.[327] The two excitations are accomplished by UV- or visible light and can be assigned to the π → π* and the n → π* transition,[326] the latter being responsible for the typical red-purple colour of TAD compounds. In contrast to the thermal reactions of TAD, the photochemical ones are less explored.[328] In general, there are reports on four different types of photochemical TAD reactions: photolysis,[329] photo polymerisation,[330] α-photoaddition to (thio)ethers,[330] and light-induced [4+2] cycloaddition reactions.[328, 331-333] Due to its exceptional reactivity and click behaviour,[133, 334] TAD is widely applied in polymer synthesis.[283] It is used as polydiene modifier as well as a crosslinker.[283] Reports are available on irreversible and reversible TAD-based polymer (bio)conjugation reactions[335-336] while it has also been applied in the synthesis of healable or recyclable materials.[283]

The high reactivity of TAD and the potential to obtain quantitative yields within short reaction times in combination with the wide substrate scope make it an interesting substrate for sequence-defined macromolecular synthesis. Its reactivity is orthogonal to that of the P-3CR, showcasing another important advantage for its use in combination with IMCR reactions, as it can be applied in protecting group free approaches. As discussed in Section 2.1, the efficiency of a reaction is one of the most important criteria for the successful synthesis of long sequences. Hence, TAD click chemistry is an ideal reaction to be introduced to sequence-defined synthesis as it reacts selectively with non-activated electron rich olefin substrates, which does not interfere with the herein used P-3CR.

3 Aims

In this thesis, novel strategies towards defined macromolecules exhibiting various structures and architectures were investigated by using the Passerini three-component reaction (P-3CR). The P-3CR is a well-established and powerful tool in the field of sequence-defined polymer synthesis, as it provides the possibility to tailor the polymer side chains in a high-yielding, up-scalable one-pot procedure. It will be shown that, in combination with other reactions, such as 1,2,4-triazoline-3,5-dione (TAD) Diels-Alder click reactions or ring-closing metathesis, the versatility of literature-known approaches can be exceeded. Despite the above-mentioned advantages, current methodologies introduce the sequence *via* the side chain only, lack the facile synthesis of large macromolecules (>5 kDa), and often require deprotection steps. Herein, three novel approaches are described addressing these issues. The first two are based on precisely designed AB-type monomers, bearing an isocyanide and a benzyl ester protected acid. From these sequence-defined macromolecules were obtained by using the isocyanide moiety in a P-3CR, while the subsequent deprotection of the benzyl ester released the free acid enabling an iterative reaction cycle. The third approach combines two orthogonal chemistries of TAD and the P-3CR reaction to synthesise sequence-defined polymers both in solution and the solid phase.

The first approach applies a bidirectional growth strategy to AB-type monomers. Starting from bifunctional carboxylic acids, defined side chains were introduced through the aldehyde component and long sequences were reached in fewer reaction steps compared to published procedures that use stepwise iterative procedures, as the oligomer was grown bidirectionally. By applying this two-step iterative cycle, linear, symmetric precursors of different lengths as well as side groups were synthesised and were end-functionalised with double bonds. This enabled a subsequent ring-closing metathesis (RCM) of these precursors, leading to large sequence-defined macrocycles containing more than 150 ring atoms. Importantly, structure-activity relationship investigations for these RCM reactions were possible through the use of sequence-defined precursors, and clear trends were observed with respect to ring-size and the type of side group, highlighting the limits of RCM. These trends could only be established thanks to the uniform nature of the precursors, and the formed macrocycles are the first examples of sequence-defined oligomers with a non-linear architecture.

In the second approach, dual sequence-defined oligomers were targeted in order to further increase the structural versatility achievable *via* P-3CR reactions for sequence-defined polymers. First, a library of nine different AB-monomers, with different backbone moieties, was investigated in terms of their suitability for the synthesis of sequence-defined structures. That way, the introduction of sequences into the oligomer, which is normally achieved using side-chain variation, was possible using the backbone. In a second step, a twofold variation of the monomer structure was performed, leading to monomers which differ in both the backbone and the sidechain, which allowed to synthesise dual sequence-defined oligomers. Importantly, both the monomer side chain and backbone could be varied independently of one another. The obtained uniform macromolecules are interesting for data storage applications, as a significant increase in the number of permutations is possible compared to previous systems. Sequential read-out by tandem mass spectrometry revealed typical fragmentation patterns, highlighting the capability and suitability of such dual sequence-defined macromolecules to increase the data storage capacity of synthetic macromolecules.

Finally, a novel approach towards large sequence-defined macromolecules was developed by combining efficient and fast TAD Diels-Alder click reactions with the P-3CR. The two orthogonal reactions allowed a protecting group free synthesis of sequences of up to 18 repeat units with a molecular weight of over 11 kDa. Furthermore, a comprehensive comparison of this solution-based approach with the analogous solid phase reactions provided new insights into such stepwise iterative methodologies.

Overall, this thesis expands the versatility of P-3CR reactions for precisely-defined macromolecules and simultaneously highlights the power of this reaction platform in the field of sequence-definition.

4 Results and Discussion

4.1 Synthesis of sequence-defined macromolecules using the monomer approach

In this Chapter, the synthesis of sequence-defined macromolecules of different architecture and different degree of definition is discussed by applying the same synthesis strategy. The utilized approach is making benefit from specifically designed AB-type monomers, bearing an isocyanide functionality as well as a benzyl ester protected carboxylic acid. The isocyanide is reactive in the P-3CR which is a well-established reaction in the field of sequence-definition[34-35, 337] and meanwhile the “logical choice” to synthesise highly defined structures in high purity, yield and scale in solution. After the first P-3CR, the benzyl ester moiety can be cleaved by hydrogenolysis, releasing the free acid, which can undergo a second P-3CR. By repeating this two-step iterative cycle several times, sequence-defined structures of uniform size can be obtained.

The approach is applied for the synthesis of symmetric linear oligomers, which served as precursors for the template free synthesis of ultralarge macrocycles, which were formed by RCM. Moreover, dual sequence-control was achieved with this approach by also altering the backbones of the AB-monomers. This led to a significantly enhanced degree of definition per repeat unit.

4.1.1 Synthesis of sequence-defined macrocycles and their use to evaluate the limits of ring-closing metathesis

Parts of this chapter and the associated parts in the experimental section were published before: Monodisperse, sequence-defined macromolecules as tool to evaluate the limits of ring-closing metathesis, Katharina S. Wetzel and Michael A. R. Meier, Polym. Chem., **2019**, *10*, 2716-2722.[338] Parts of this project have been started during the Master's thesis of Katharina Wetzel.[339] The project was later continued during the PhD thesis. Footnotes in the experimental section mark the respective molecules that have been synthesised during the Master's thesis and provide detailed differentiation between Master's and PhD thesis.

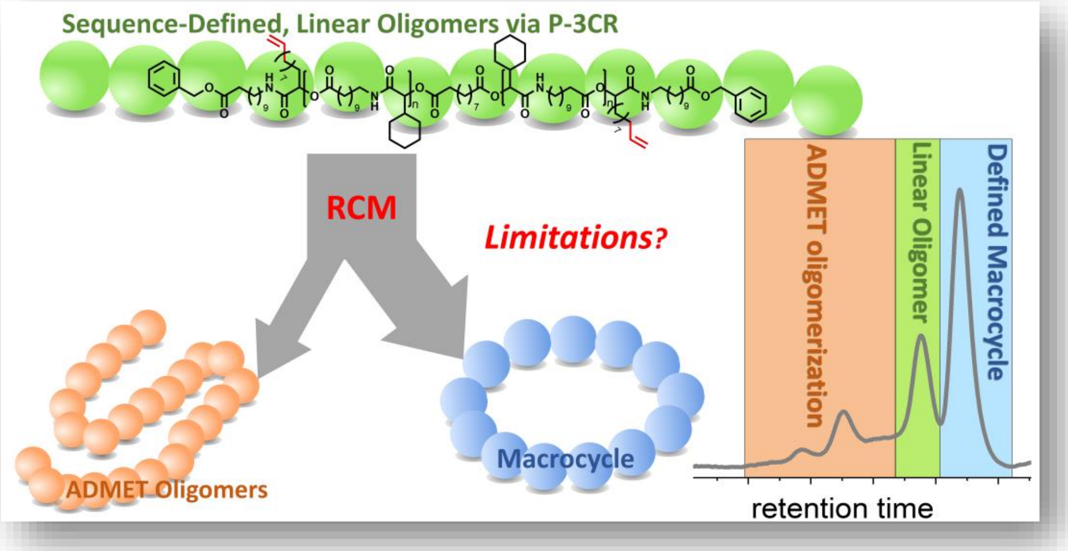

Abstract:

Sequence-defined macromolecules of uniform size unlock the door to many new applications in polymer chemistry, such as structure/property or structure/activity relationship investigations, which cannot be conducted accurately, if the investigated macromolecules exhibit dispersity. Within this chapter, a first example of the efficient and template-free synthesis of sequence-defined, uniform cyclic oligomers that are significantly larger than conventional large macrocycles (here >150 backbone atoms) is discussed. Linear uniform precursors were synthesised using the monomer approach and subsequently utilised to evaluate the limits of RCM, manifesting clear trends depending on the ring size and introduced side chains. Furthermore, the synthesis of the macrocycles described in this chapter are the first example of a sequence-defined synthesis of a polymer architecture other than linear macromolecules.

Within this chapter, an efficient and fast template-free approach towards large sequence-defined macrocycles of up to 152 ring atoms, bearing flexible backbones and tailored side chains is described. First, some other approaches towards large macrocycles will be discussed as this has not been done in the introductory chapter (Chapter 2). Furthermore, olefin metathesis in general and especially ring-closing metathesis which was applied in this project, will be briefly introduced before the results will be presented.

In the last years, more and more investigations on polymeric architectures were conducted, which lead to a growing understanding on how the molecular architecture fundamentally affects the material properties.[340] Those investigations included various different architectures, such as linear polymers, polymer brushes, star polymers, ladder polymers, dendrimers, hyperbranched polymers and polymer networks. Since the end groups of linear, non-cyclic polymers have a significant influence on the materials properties, their end group-free analogous macrocyclic oligomers have gained growing interest.[341-342] In general, two main methods for synthesising macrocyclic polymers are available: as ring-expansion polymerisations[151, 343-344] and end-to-end cyclisation of linear precursors. The latter can be further divided into unimolecular reactions of α,ω-heterofunctional polymers[345-347] and bimolecular reactions of α,α'-homodifunctional polymers.[348-350] However, the obtained macrocycles are either uniform in size but relatively small (3-13 bonds along the backbone)[340] or disperse in size.[342] Within this project, RCM was performed for the cyclisation of large cycles. In organic chemistry, however, RCM is mostly applied for the preparation of smaller rings with up to seven ring atoms.[351] But also, the synthesis of larger rings containing eight to eleven ring atoms was reported. Such rings are referred to as medium sized rings in literature.[352-353] The so-called large macrocycles typically consist of twelve to fifteen ring atoms,[352-353] but there are also reports on even larger cycles. Besides, also more complex polycyclic systems were obtained.[354] The advantage of RCM is that versatile structures can be obtained by cyclisation of previously synthesised linear precursors which can be obtained by many different approaches.[352-353, 355] The only requirement is the final functionalisation with terminal double bonds. The yields in RCM vary from very low to nearly quantitative and are highly dependent on the substrates.[352-353, 355] Several examples on macrocyclic biomacromolecules were reported. The synthesis of cyclic peptides or DNA is well known and established.[356-359] Cyclic peptides usually consist of four to six amino acids thus forming smaller rings,[360] while impressive examples of ultra large DNA cycles were reported.[361] It is important to mention that such cycles are formed by using rigid precursors exhibiting an appropriate geometry, leading to preorganisation and thus facilitating the cyclisation reaction. Such preorganisation can be achieved by different concepts such as ligands, hydrogen bonds, or rigid architectures and is thus a powerful tool, which is widely applied to achieve efficient macrocyclisation.[362] On the other hand, macrocycles with a molecular weight in the range of polymers (for example cyclic polythiolactones with a molecular weight of up to 13 kDa)[363] are obtained by cyclisation of polymeric precursors which in turn were obtained by controlled radical polymerisation (*i.e.* ATRP polystyrene oligomers with a relatively low polydispersity index (PDI) < 1.2).[364] Macrocycles that are both, large and uniform in size, were developed in the field of catenanes.[365-366] Here, the use of a metal ion template, which preorganised the linear precursors by ligand coordination was inevitable.[367-371] However, one very interesting exception was reported by Alabi and colleagues. They impressively demonstrated the synthesis of defined macrocycles consisting of up to 56 ring atoms by applying an iterative approach.[372] The synthesis of oligo(thioetheramide) macrocycles *via* a one-pot acid-catalysed cascade reaction was reported. The linear oligomers synthesised on a liquid fluorous support, allowing the fast monomer addition in solution and facilitating the purification procedure.

Within this project, RCM is used for the final cyclisation reaction. Olefin metathesis is one of the most powerful tools for the formation of C-C double bonds in organic chemistry.[373] The reaction scheme is depicted below in Scheme 28.

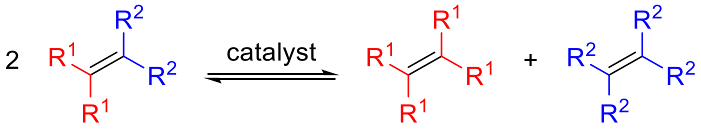

Scheme 28. General reaction scheme of olefin metathesis.[374]

In 2005, Chauvin, Grubbs and Schrock were awarded with the Nobel Prize in chemistry for the proposal of the correct reaction mechanism (Chauvin) and for the development of new efficient catalysts.[375-377] The word metathesis is derived from the two Greek words *meta* and *tithemi*, which mean change and place.[378] This also describes the reaction in a chemical sense since the alkylidene groups between two double bonds are exchanged in an olefin metathesis reaction. During the reaction, the carbon-carbon double bonds are rearranged by using a metal carbene complex as catalyst. It was discovered accidentally in 1964 by two industrial chemists at Philips Petroleum, who performed studies on Ziegler polymerisations.[378] After several proposals on the mechanism which were refuted, the correct mechanism was proposed by Yves Chauvin in 1971.[379-380] It undergoes several metallocyclobutane and carbene complexes and is depicted in Scheme 29.

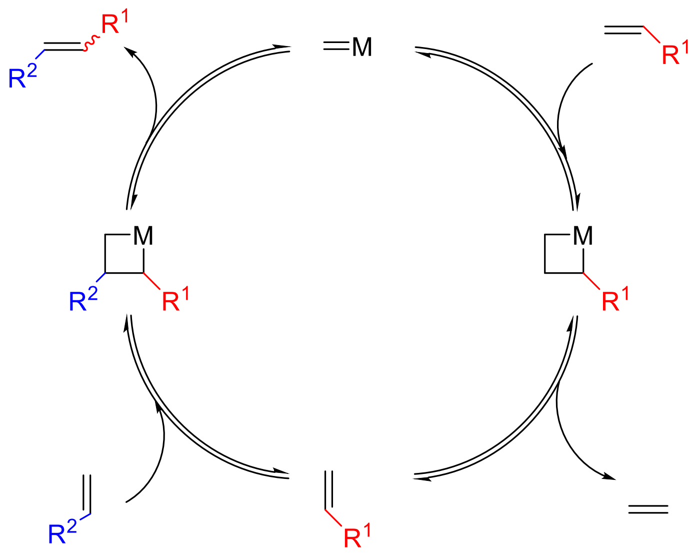

Scheme 29. Reaction mechanism of olefin metathesis, which was proposed by Yves Chauvin.[379]

There are three different main types of olefin metathesis, which can further be divided in subtypes (see Scheme 30).[381] The first type (Type A) is ring-opening metathesis (ROM) and ring-opening metathesis polymerisation (ROMP). The driving force in this type of reaction is the release of ring strain of a cyclic olefin. Together with a non-cyclic diene, ROM takes place, whereas ROMP takes place, if only cyclic olefins are reacted. The reversal of ROM is the RCM (type B). Since it is an equilibrium reaction, RCM and ROM are competing. The formation of the desired product can be forced by adjusting the reaction conditions: in RCM reactions with terminal double bonds, ethylene is released, thus by removing the ethylene from the reaction mixture, the equilibrium can be shifted. In RCM reactions, again, two subtypes are described which occur depending on the concentration in which the reaction is conducted. In high concentration, the acyclic diene metathesis (ADMET) is favoured forming polymers, whereas in low concentrations rings are formed *via* RCM. The ADMET and RCM reaction are competing reactions. Thus, the reaction conditions need to be carefully adjusted and optimised in order to supress the unwanted side reaction. However, in case of RCM, it is very challenging to completely avoid the ADMET side reaction. The third type of metathesis reaction (type C) is the reaction of acyclic olefins. In case of identical olefins, it is referred to as self-metathesis, whereas it is called cross-metathesis when two different olefins undergo the reaction. In general, it is advantageous for all the reaction types when the metathesis between olefins with terminal double bonds is performed because in this case, ethylene is released during the reaction as volatile side product, enabling to shift the equilibrium towards the products side, thus increasing the conversion and yield.

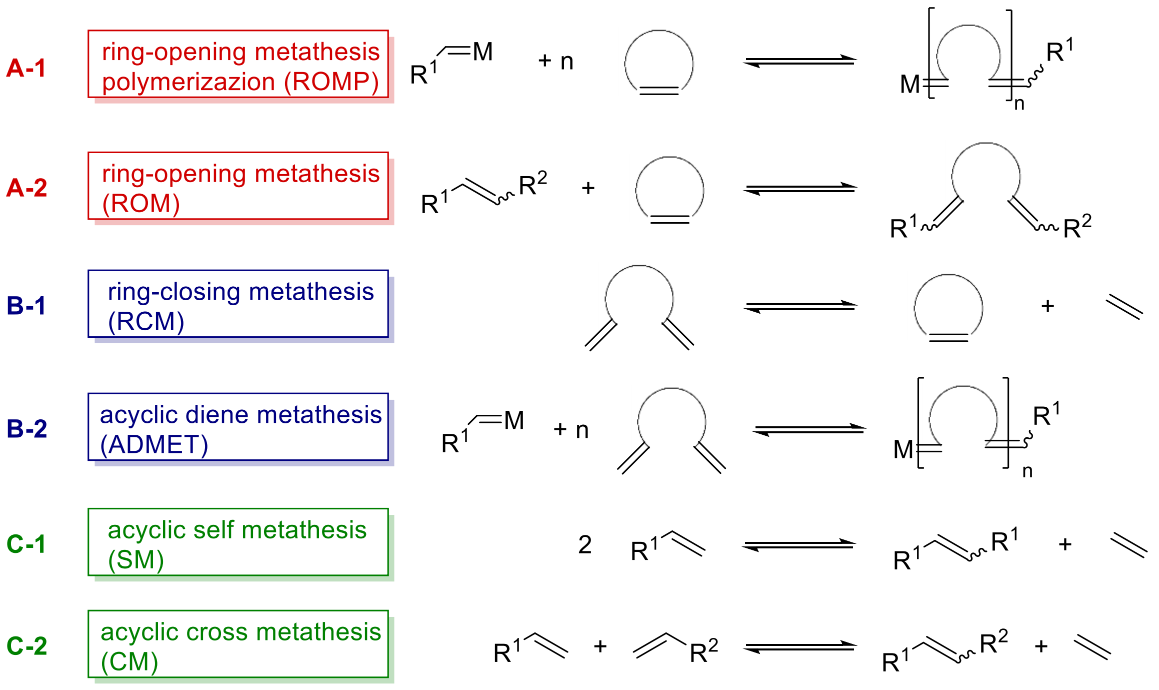
A-1
ring-opening metathesis polymerizazion (ROMP)
R1 =M
+ n
M
n
R1
A-2
ring-opening metathesis (ROM)
R1 R2
+
R1
R2
B-1
ring-closing metathesis (RCM)
+
B-2
acyclic diene metathesis (ADMET)
R1 =M
+ n
M
n
R1
C-1
acyclic self metathesis (SM)
2
R1
R1 R1
+
C-2
acyclic cross metathesis (CM)
R1
+
R2
R1 R2
+

Scheme 30. The three different types of olefin metathesis: Ring-opening metathesis (type A), ring-closing metathesis (type B) and self- or cross-metathesis (type C)[381]

For the wide applicability of the metathesis reaction, the design of efficient and stable catalysts was the most crucial and innovative improvement.[382-386] Various different molybdenum-alkylidene complexes were introduced as new catalysts by Schrock.[384-386] They have proven to be highly efficient catalysts and even suitable to catalyse sterically hindered substrates. The reactive site of such catalysts is the Schrock carbene that is stabilised *via* different ligands depending on the catalyst.

Grubbs, on the other hand, demonstrated the power of ruthenium-based catalysts compared to other transition metals. The main advantage is their tolerance against moisture and air.[373] The Grubbs 1st generation catalyst was commercialised in 1995 already.[382] Later on, also other derivatives of this ruthenium-based catalyst were commercialised. Some of the commercially available catalysts are depicted in Figure 14.

Even with the more stable Grubbs catalysts, degassing of the reaction mixture is still beneficial. Olefin metathesis reactions are mostly conducted in DCM or toluene. However, the reaction can also be performed in many other solvents like acetone, chlorinated benzenes, diethyl ether, ethyl acetate, methanol or THF. The ideal catalyst loading highly depends on the substrates. Typically, 0.1 to 5 mol% of catalyst are applied but also catalyst loadings of up to 60% are reported. The reaction temperature ranges between 25 and 50 °C.[387]

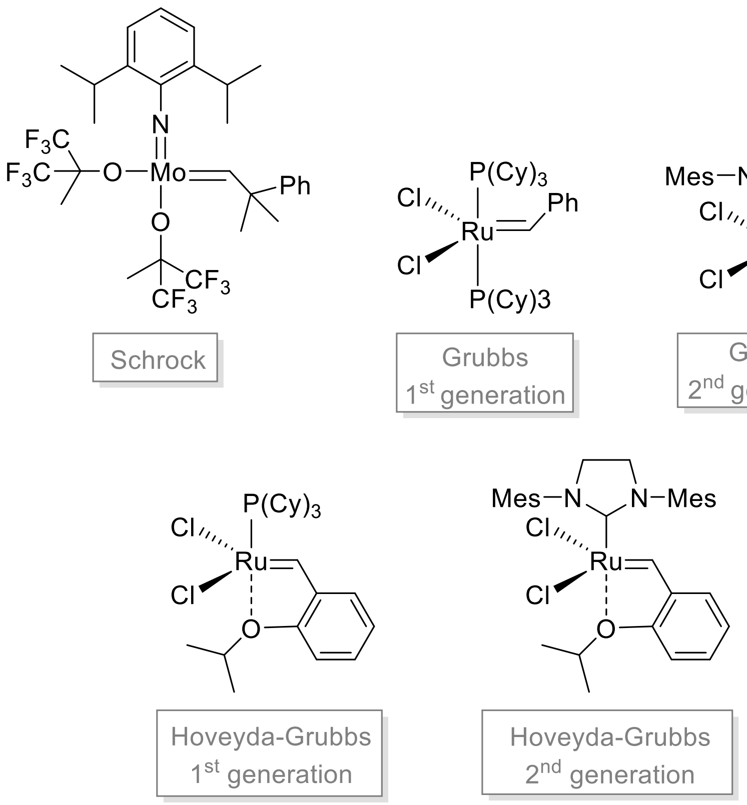

Figure 14. Selection of the most important commercially available catalysts for olefin metathesis.

To form the uniform macrocycles within this project, linear and symmetric oligomers bearing tailored side chains were first synthesised as precursors *via* the adapted monomer approach.[34] The oligomers were formed in a two-step iterative cycle consisting of the P-3CR and a subsequent deprotection step (see Scheme 32). Apart from the AB-monomer (**M1**), which bears an isocyanide and a benzyl ester protected acid, and which is thus synthesised in three steps from the corresponding amino acid[34] (see experimental section for details, Chapter 6.3.1), all used substances are commercially available.

The isocyanide monomer **M1** was synthesised according to a previously reported procedure from 11-aminoundecanoic acid **1a**. The synthesis is illustrated in Scheme 31. In a first step, the benzyl ester ammonium salt **2a** was formed by reacting the amino acid **1a** with benzyl alcohol **3** in the presence of thionyl chloride **4**. Subsequently, the *N*-formylation was performed using trimethyl orthoformate **5** as formylation agent. The last dehydration step with phosphoryl trichloride **6** and an amine base **7** yields the isocyanide monomer **M1**. During the synthesis, the monomer was analysed by proton and carbon NMR, by mass spectrometry and by infrared (IR) spectroscopy. Interestingly, the isocyanide group gives a very characteristic bond in the IR at around 2145 cm^{-1}, thus providing a very easy proof of the successful isocyanide formation. The ammonium salt **2a** was obtained in a yield of 95%, the crude *N*-formamide **8a** was obtained in quantitative yield and the final monomer **M1** needed to be purified by column chromatography leading to a yield of 67%. Thus, the product was obtained in an overall yield of 64%. The synthesis was performed on a 15-gramm scale.

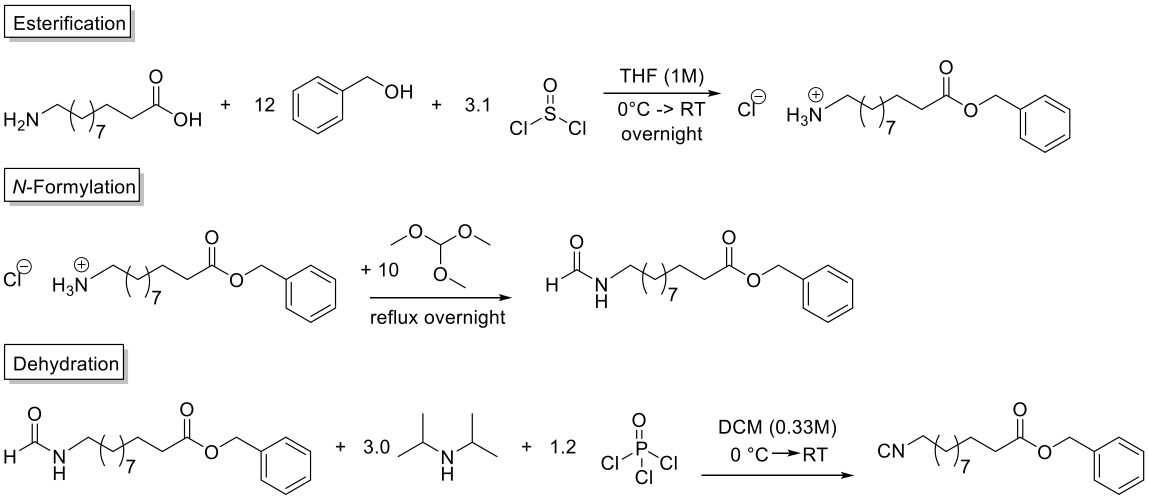

*Scheme 31. Three-step synthesis of the AB-monomer **M1** bearing an isocyanide and a benzyl ester protected acid.*

As discussed in Chapter 2.1.3.2 and in the introduction to this Chapter, it was previously shown, that this strategy allows the synthesis of highly functionalised oligomers of high purity on a multigram scale.[34] Therefore, it was decided not to vary the side chains within one macromolecule anymore, but to synthesise various macromolecules of different sizes carrying different side chains. Here, a bifunctional carboxylic acid as starting material (see Scheme 32, *i.e.* bidirectional growth, compare Chapter 2.1.3.2) reduced the overall reaction time. As such, linear oligomers of different lengths (**LO**$_{2,4,6,8,10}$, see Scheme 32) carrying three different side chains (namely ethyl, cyclohexyl or isopropyl, see Scheme 32) were synthesised.

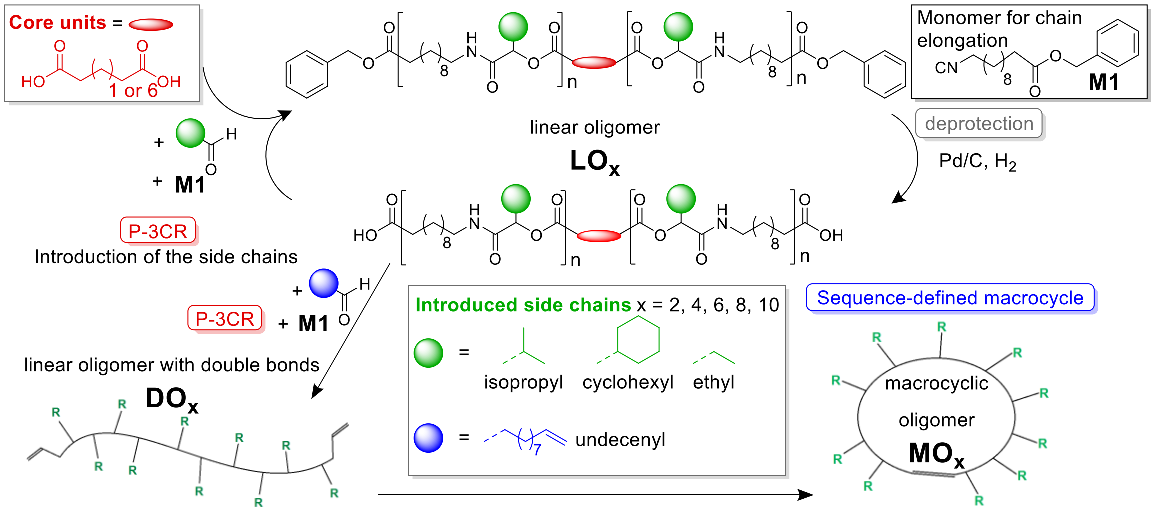
Core units =
HO
OH
1 or 6
+ M1
P-3CR
Introduction of the side chains
linear oligomer
LO$_x$
Monomer for chain elongation
CN
8
M1
deprotection
Pd/C, H$_2$
HO
OH
n
+ M1
P-3CR
linear oligomer with double bonds
DO$_x$
Introduced side chains x = 2, 4, 6, 8, 10
isopropyl
cyclohexyl
ethyl
undecenyl
Sequence-defined macrocycle
macrocyclic oligomer
MO$_x$
R

Scheme 32. General reaction scheme for the synthesis of sequence-defined linear precursors, which served as starting material for the synthesis of uniform macrocycles. The linear oligomers are formed in a two-step iterative cycle consisting of the P-3CR and a deprotection step. Cyclisation is performed via RCM after introduction of two terminal olefin functionalities.

Initially, glutaric acid **9** was used as starting material, but in the first P-3CR the yield was relatively low (69-86%, depending on the side chain). Therefore, glutaric acid **9** was later replaced by the longer sebacic acid **10** leading to significantly increased yields of 97-99%. Four different oligomers were synthesised: two with glutaric acid **9** as starting material and ethyl or cyclohexyl side chains and two with sebacic acid **10** as core unit carrying cyclohexyl or isopropyl side chains. The P-3CRs were conducted in DCM at a concentration of 0.5 M at room temperature. Monomer **M1** and the aldehyde components (propanal **11a**, cyclohexanal **11b**, or isobutyraldehyde **11c**) were added in a small excess of 1.5 eq. relative to the acid groups, thus, 3.0 eq. of these components were added relative to the diacid (**9** or **10**). After a reaction time of 24 hours, the crude products were purified by column chromatography to obtain the pure dimers **LO**$_2$ in nearly quantitative yields (*i.e.* 100% by NMR spectroscopy, 98-99% purity by SEC, see Figure 16).

The oligomer synthesis was performed in gram scale (*i.e.* product **LO**$_8$ was obtained with a yield of 2.5 g). The products were characterised after each reaction step by proton and carbon NMR spectroscopy, IR spectroscopy, mass spectrometry and SEC to verify the structure of the obtained products as well as their dispersity (compare Figure 15 and Figure 16 and see experimental section Chapter 6.3.1 for the respective set of analytical data of all the obtained products). In the second reaction of the iterative cycle, the benzyl ester protecting groups were removed by hydrogenolysis in a quantitative manner. Upon complete deprotection, a second P-3CR can be performed on account of the newly formed dicarboxylic acid. By applying this iterative strategy, symmetric oligomers of a length of up to ten units were synthesised. In the third P-3CR, the reaction time was extended to 48 hours to ensure full conversion, while for the deprotection step, the concentration was decreased with increasing length of the oligomers to address the increased viscosity and ensure full conversion (see experimental section for details, Chapter 6.3.1).

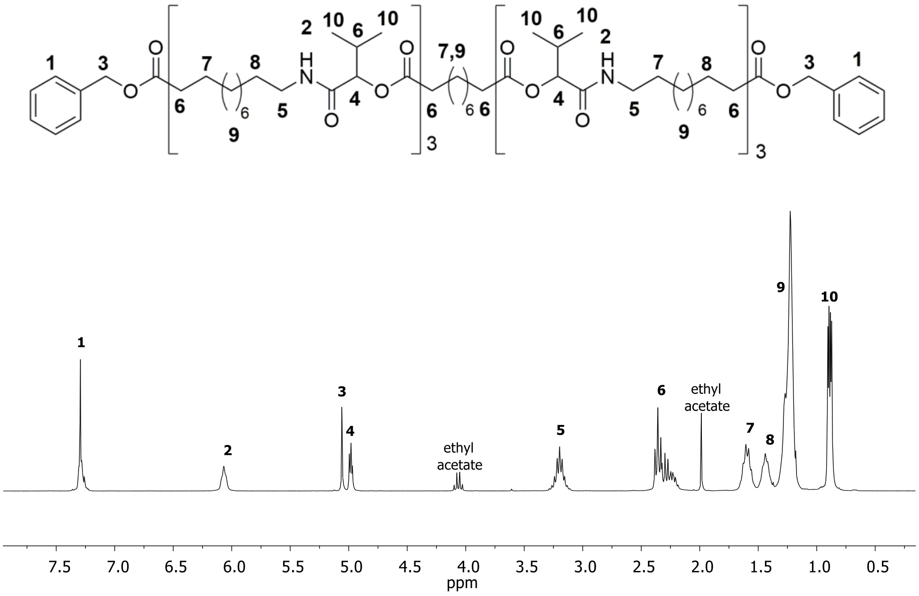

Figure 15. Example of a fully assinged NMR spectrum of a symmetric hexamer carrying isopropyl side chains.

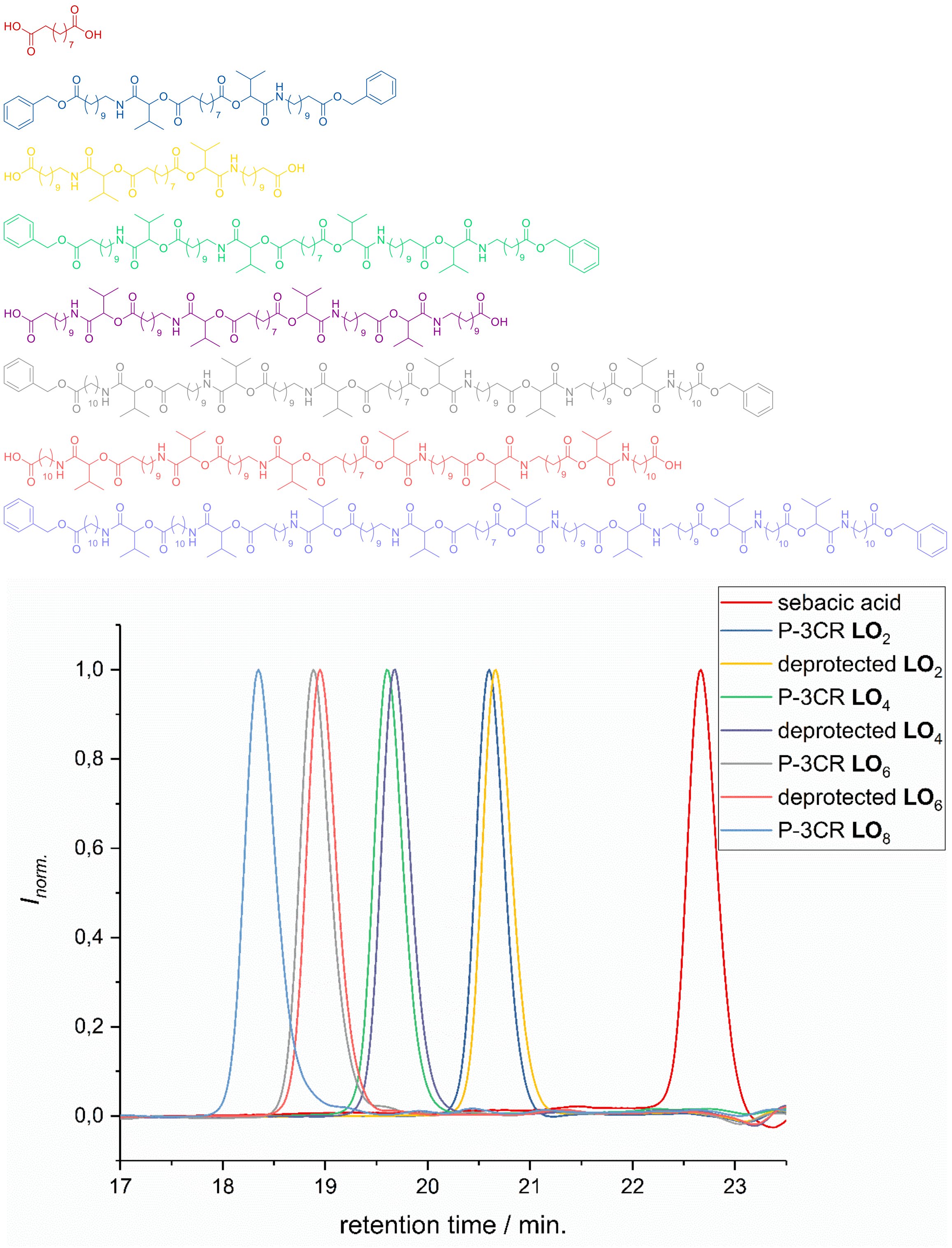

*Figure 16. Structures and the results of the SEC analysis of the linear protected and deprotected oligomers (**LO**$_{2, 4, 6, 8}$) carrying isopropyl side chains. The structures and respective SEC traces are assigned by the same colour code. The SEC traces clearly verify the uniform size distribution of the obtained products.*[*]

---

[*] SEC measurements were performed on system A. See SI for detailed device information.

Having the linear oligomers (**LO**$_x$) in hands, the next step was to functionalise these oligomers with terminal double bond on both ends in order to obtain the final double bond functionalised linear oligomers (**DO**$_x$). This was achieved by separating small amounts (300-900 mg) of the deprotected oligomers (**LO**$_x$) at different stages of the synthesis from the product and reacting them in one last P-3CR with 10-undecenal **11d**, in order to introduce two terminal double bonds to the final linear oligomer (**DO**$_x$). The introduction of the double bonds always marked the final reaction before macrocyclisation for the respective oligomer **DO**$_x$. The remaining **LO**$_x$ was used to continue the synthesis towards higher molecular weight oligomers, with the introduction of the double bonds taking place at a later stage. Thus, symmetric uniform dimers, tetramers, hexamers, octamers, and decamers, containing tailored side chains as well as terminal double bonds (**DO**$_x$) were obtained. The different **DO**$_x$ were carefully characterised by all the different characterisation methods. As an example, the SEC analysis of the end-functionalised final linear precursors (**DO**$_{2,4,6,8}$) carrying cyclohexyl side chains, is shown in Figure 17. As can be seen in the SEC traces, the samples contain minor impurities. However, since the percentage of the impurities is in all cases below 3%, the precursors were converted without further purification.

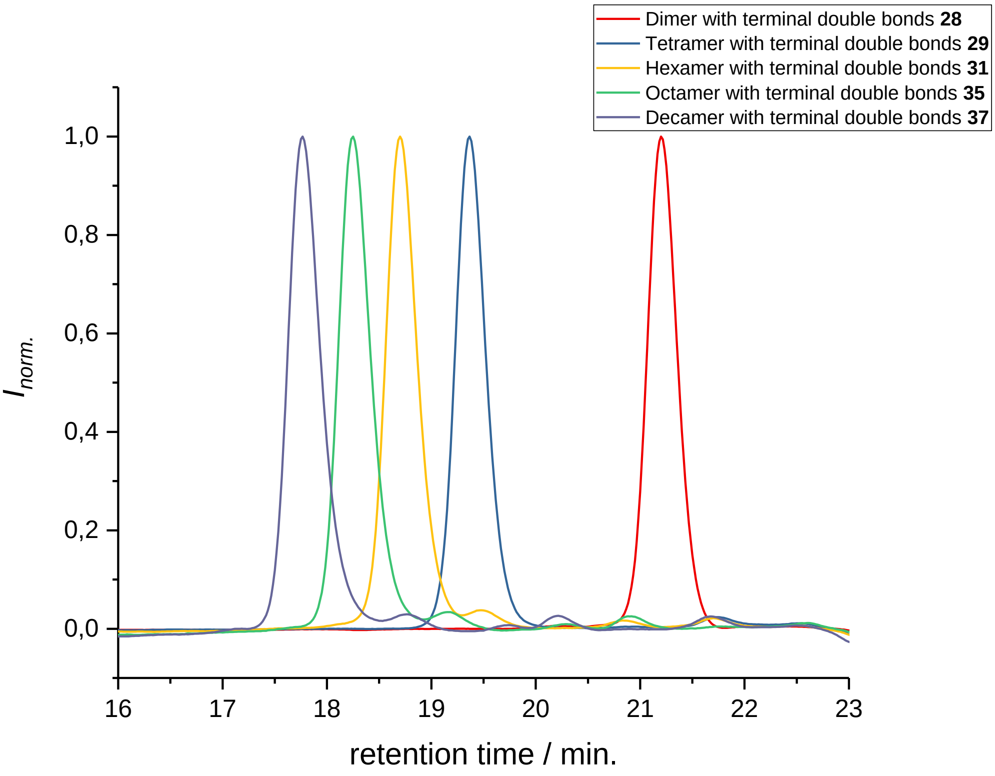

*Figure 17. SEC characterisation of the final linear precursors **DO**$_{2,4,6,8}$ carrying cyclohexyl side chains. All the oligomers are end-functionalised with terminal double bonds, allowing for subsequent macrocyclisation.*[*]

---

[*] SEC measurements were performed on system A. See SI for detailed device information.

In the following table, the results of the stepwise synthesis of a symmetric, sequence-defined decamer with cyclohexyl side chains are summarised as an example. The final product is the end-functionalised precursor with terminal double bonds, that can be used for the macrocyclisation reaction in the subsequent RCM reaction.

Table 1. summary of the results of each reaction step during the synthesis of a linear precursor bearing terminal double bonds which is functionalised with cyclohexyl side chains.

Reaction	Product	Formula	Yield [%]	m/z calc.	m/z found
1st P-3CR	dimer (**LO**$_2$)	$[C_{62}H_{97}N_2O_{10}]^+$	97[a]	1029.7138	1029.7137
1st deprotection	deprotected dimer (**LO**$_2$)	$[C_{48}H_{84}N_2O_{10}Na]^+$	quant.[b]	871.6018	871.6019
2nd P-3CR	tetramer (**LO**$_4$)	$[C_{100}H_{162}N_4O_{16}Na]^+$	91[a]	1698.1878	1698.1914
2nd deprotection	deprotected tetramer (**LO**$_4$)	$[C_{86}H_{150}N_4O_{16}Na]^+$	98[b]	1518.0939	1518.0933
3rd P-3CR	hexamer (**LO**$_6$)	$[C_{138}H_{228}N_6O_{22}Na]^+$	97[a]	2344.6799	2344.6778
3rd deprotection	deprotected hexamer (**LO**$_6$)	$[C_{124}H_{216}N_6O_{22}Na]^+$	94[b]	2164.5860	2164.5895
4th P-3CR	octamer (**LO**$_8$)	$[C_{176}H_{294}N_8O_{28}Na]^+$	99[a]	2991.1720	2991.1691
4th deprotection	deprotected octamer (**LO**$_8$)	$[C_{162}H_{282}N_8O_{28}Na]^+$	78[b]	2811.0781	2811.0787
5th P-3CR	decamer (**DO**$_{10}$)	$[C_{222}H_{376}N_{10}O_{34}Na_2]^{2+}$	99[a]	1886.3893	1886.4028

[a] *after column chromatography,* [b] *after filtration*

The introduced terminal double bonds were exploited for the formation of sequence-defined macrocycles (**MO**$_x$) *via* RCM (see Scheme 32). Grubbs 1st generation catalyst **12** was chosen, since it catalyses the RCM reaction, while minimising the ring-opening polymerisation of the formed cycles.[388-389] Furthermore, it does not show olefin isomerisation side reactions, which are very pronounced for the 2nd generation catalyst and can only be suppressed to some extent (and would thus lead to dispersity in our system).[390-391] Initially, the RCM reaction of a **DO**$_8$ carrying cyclohexyl side chains was investigated, the crude product (**MO**$_8$) was analysed by size exclusion chromatography coupled to electrospray ionisation mass spectrometry (SEC-ESI-MS) and a relatively low conversion towards the macrocycle of around 32% was determined. The reaction was thus optimised by adding the same amount (10 mol%) of catalyst four times during the reaction, thus increasing the total amount of catalyst to 40 mol%. This catalyst concentration is relatively high, if compared with typical catalyst concentrations of 1-5 mol% for the synthesis of smaller cycles; however, if larger or highly functionalised molecules were cyclised, also higher catalyst concentrations of up to 60 mol% are reported.[352] After this optimisation, all RCM reactions were performed under identical conditions in order to evaluate the influence of the side chains or the oligomer length on the conversion towards the macrocycle. The reactions were carried out in high dilution (*ca.* 5×10^{-4} mol/L in chloroform) in order to prevent ADMET, using Grubbs 1st generation catalyst **12**, which was added in four aliquots in the course of the reaction (4×10 mol%). The desired macrocycles were obtained after five hours at 45 °C. Remarkably, the reactivity of the catalyst is sufficient to achieve high conversion even at such low concentrations.[352]

The ^{1}H NMR spectra of **MO$_4$**, carrying isopropyl side chains, as well as its precursor, **DO$_4$**, are exemplarily depicted in Figure 18. In spectrum **A**, showing **DO$_4$** before the cyclisation reaction, the two characteristic signals of the terminal double bonds are clearly visible, which disappear completely in spectrum **B** of **MO$_4$** after cyclisation while a new peak for the internal double bond protons arises, indicating full conversion towards the desired product.

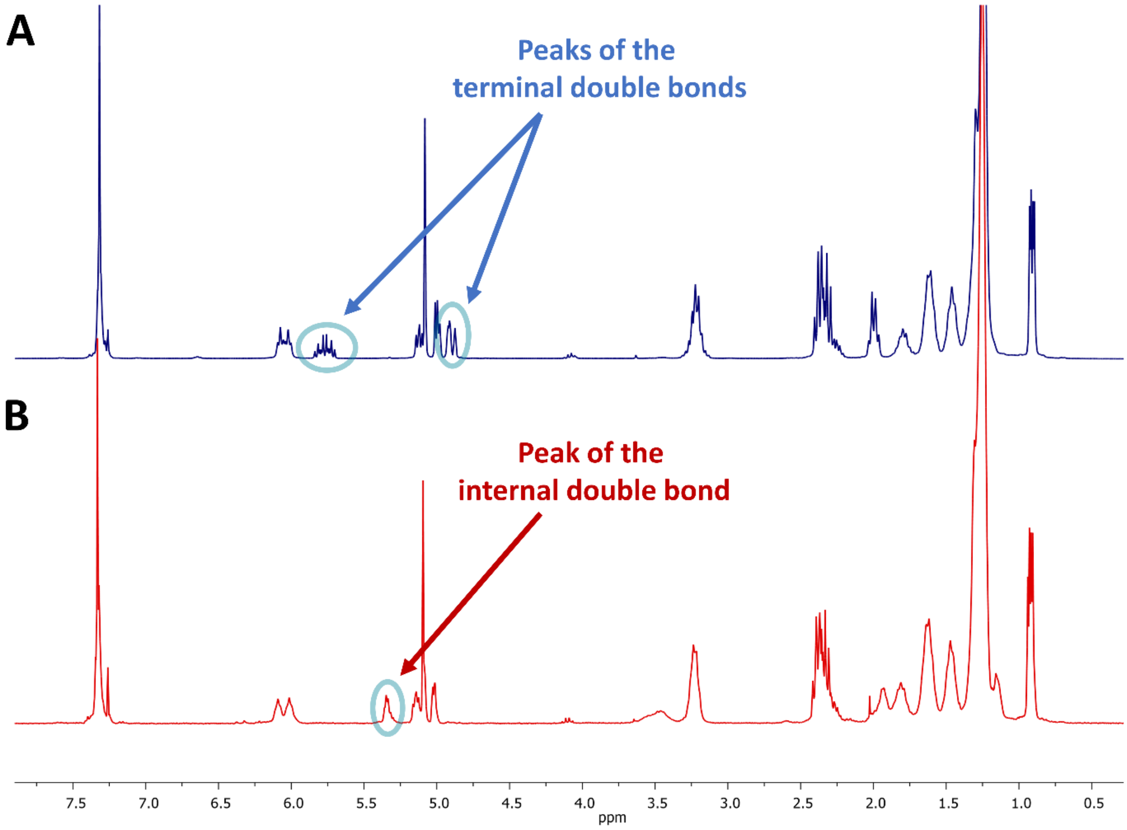

*Figure 18. ^{1}H NMR comparison of a **LO$_4$** (**A**) and a **MO$_4$** (**B**) carrying isopropyl side chains. In the first ^{1}H NMR spectrum, the signals of the terminal double bonds are clearly observed, whereas in the spectrum on the bottom, these signals disappear completely and the signal of the newly formed internal double bond appears, indicating full conversion towards **MO$_4$**.*

SEC analysis, on the other hand, revealed that the conversion of $\mathbf{LO_4}$ towards $\mathbf{MO_4}$ was only 91%. Besides the product, traces of ADMET side product are present as well as unreacted $\mathbf{LO_4}$, which remained in the crude product. The comparison of the NMR and SEC results thus clearly demonstrated the importance of SEC characterisation for macromolecules exhibiting uniform size distribution, because only the latter provides sufficient resolution to prove the absence of tiny amounts of impurities, which is essential and can otherwise not be provided by any other characterisation technique. During RCM, the terminal double bond is formed in *cis* and *trans*-configuration, but the ratio between the two isomers cannot be determined by SEC, which shows the limits of the technique. However, SEC allows for precise analysis of the uniformity in size.
By analysing the crude products by SEC-ESI-MS, the different peaks in the SEC chromatogram could be assigned with the help of the mass spectrum. An example of such an analysis is shown in Figure 19 for a crude macrocyclic octamer with cyclohexyl side chains ($\mathbf{MO_8}$).

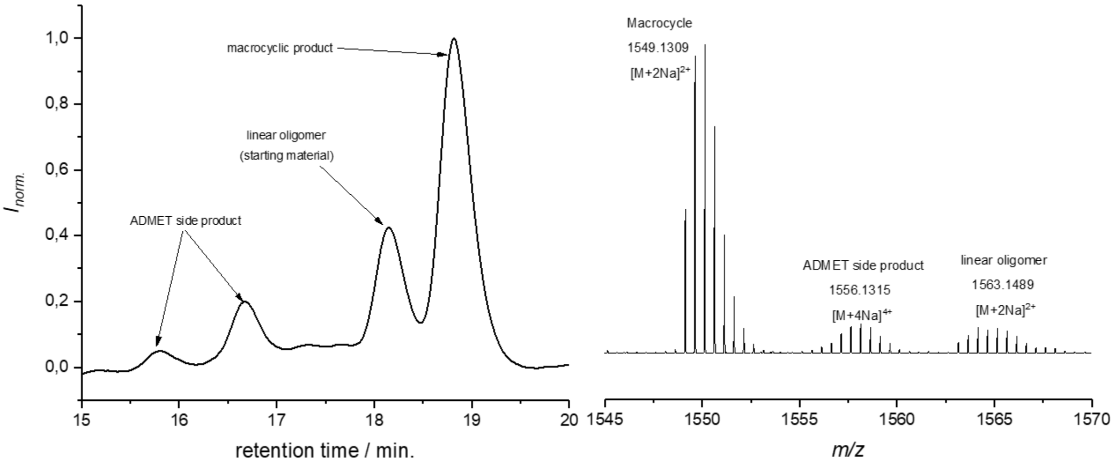

Figure 19. SEC-ESI-MS analysis of a crude macrocyclic octamer $\mathbf{MO_8}$ *with cyclohexyl side chains. Left: SEC trace with assignment of the respective peaks. The peaks could be assigned with the help of the mass spectrum, which is shown on the right.*

The crude macrocyclic products $\mathbf{MO_X}$ were thus characterised and compared by SEC-ESI-MS analysis. Surprisingly, the side chains did not influence the conversion significantly. The length of the oligomers, on the other hand, resulted in a considerable difference in conversion as observed by SEC (see Figure 20, left): for the dimer ($\mathbf{DO_2}$), nearly quantitative conversion towards the desired macrocycle ($\mathbf{MO_2}$) was obtained, whereas lower conversions were observed when longer oligomers underwent the RCM reaction. For the decamer ($\mathbf{MO_{10}}$), 51% conversion towards the macrocycle was achieved, which is the lowest conversion compared to the smaller macrocycles ($\mathbf{MO}_{2,\ 4,\ 6,\ 8}$). Furthermore, ADMET oligomerisation could be fully prevented in case of ($\mathbf{DO_2}$), whereas significant amounts of the ADMET side product were obtained in the RCM reaction of ($\mathbf{DO_{10}}$) (*ca.* 17%, according to SEC analysis).

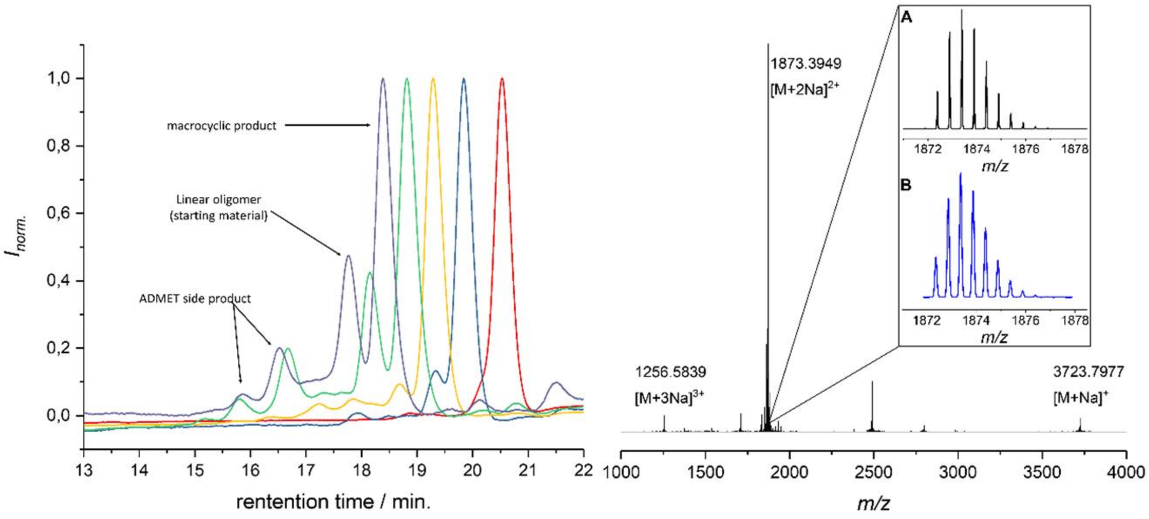

*Figure 20. Left: SEC analysis results of the crude macrocyclic products with cyclohexyl side chains and sebacic acid **10** as core unit, revealing the influence of the size of the oligomer on the conversion towards the macrocycle. For the decamer **MO**$_{10}$, a detailed description of the obtained products is depicted exemplary. The different species were identified by SEC-ESI-MS analysis. Right: SEC-ESI-MS analysis of the macrocyclic decamer **MO**$_{10}$ bearing cyclohexyl side chains. The single, double and triple charged sodium cations are clearly observed. The expanded region (panel A) shows the apparent isotopic pattern (black) which was found to be in good agreement with the calculated one (blue, panel B), obtained by the program mMass.*

Isolation of the macrocyclic product (from the linear oligomer and the ADMET side product) by column chromatography was not successful due to the similar polarity of the compounds. Purification by preparative SEC was also considered; however, the resolution was low compared to that of the oligomer-specific SEC columns used for characterisation. Nonetheless, characterisation of the crude macrocyclic products by SEC-ESI-MS analysis was found adequate to determine the ratio between linear starting material (**DO**$_{x}$), macrocyclic product (**MO**$_{x}$), and ADMET side product, but also to support the successful formation of the desired sequence-defined macrocycles arising from the advantageous combination of the ESI-MS and the SEC data. For the decamer **MO**$_{10}$, for example, three peaks were observed, the one at a retention time of 14.36 minutes belonging to the ADMET side product and the one at 15.33 minutes belonging to **DO**$_{10}$. The ESI-MS spectrum of the product fraction at 15.86 minutes showed a single isotopic distribution with a maximum at 1873.3949 m/z, which corresponds to the Na^{2+} adduct of the cyclised MO$_{10}$ ($[C_{220}H_{372}O_{34}N_{10}Na_2]^{2+}$, see Figure 20, right) It is noteworthy that large macrocycles, composed of up to 152 ring backbone atoms, were obtained (see Figure 21, left). In Figure 21 (right), the RCM towards two **MO**$_{8}$ with different side chains are compared exemplarily regarding conversion towards the desired macrocycle and the ADMET side product, revealing low dependence on the side-chains. Furthermore, Figure 21 (left) reveals that the conversion towards the macrocycle is relatively independent from the applied side-groups for different ring-sizes. On the other hand, the conversion strongly depends on the size of the macrocycle.

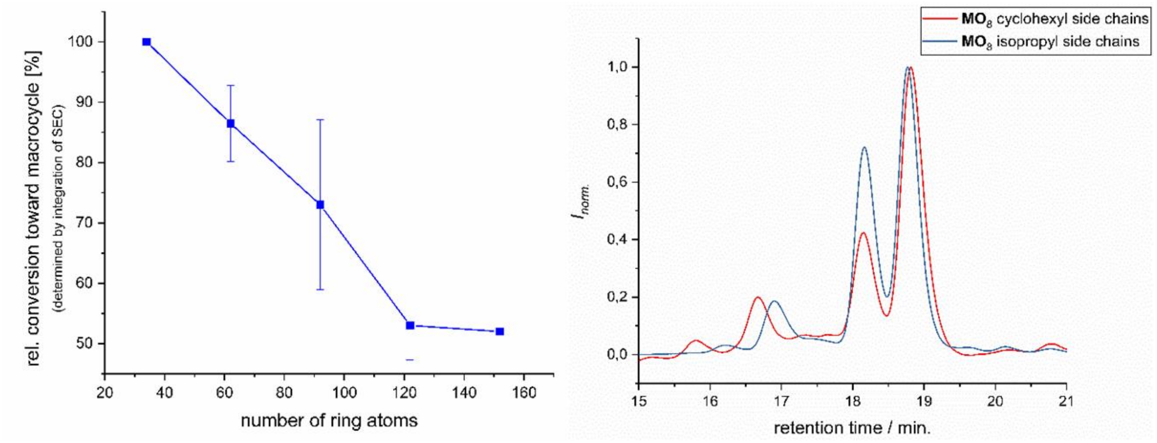

Figure 21. Left: Dependence of the oligomer size on the conversion towards the desired macrocycle. The mean values and standard deviation of the conversions for **MO$_{2,4,6,8,10}$** *are displayed; the line is only drawn to guide the eye.* **MO$_2$** *and* **MO$_{10}$** *do not have a standard deviation since they were not synthesised with different side chains. Right: Comparison of the conversion towards the macrocycles* **MO$_8$** *carrying different side chains, namely cyclohexyl and isopropyl by SEC analysis. The conversion is 57 and 49% for* **MO$_8$** *carrying cyclohexyl and isopropyl side chains, respectively.** *The peaks were identified by SEC-ESI-MS to be* **MO$_8$**, **LO$_8$**, *and the two ADMET side products (***LO$_8$***)$_2$ and (***MO$_8$***)$_3$, from higher to lower retention time.*

Interestingly, such conclusions could not be drawn if disperse oligomers were studied for their cyclisation tendency,[41] as (i) resolution in SEC would certainly be too poor to allow for a proper integration (compare Figure 20, left and Figure 21, right) and (ii) molecular weight dispersity would introduce a significant error in the abscissa of Figure 21, left. Considering, for example, a typical dispersity of controlled radical polymerisation of Đ ~ 1.2, a mass of 3724 *m/z* with 152 ring atoms (**MO**$_{10}$) would translate to a dispersity in ring size of 35 ring atoms.

Even in a system devoted to high resolution oligomer analysis, as applied here, peaks would overlap and integration would be infeasible if a disperse system was utilised. This can be seen very clearly in Figure 22, where the SEC curve of a crude macrocyclic octamer is compared to three different narrow PMMA standards with very low dispersity as they are commonly used for SEC calibration. In the crude macrocyclic octamer, four different species are detectable, which can be identified by SEC-ESI-MS measurements to be the macrocycle **MO$_8$**, the linear precursor oligomer **LO$_8$**, and two ADMET by-products (**LO$_8$**)$_2$ and (**LO$_8$**)$_3$ (from higher to lower retention time). Since these peaks are well separated, integration is possible. If such studies were performed with disperse precursors (see PMMA standards below for relatively narrowly dispersed model compounds), the obtained mixture of products, starting material and by-products were not separately detectable in SEC.

---

* SEC measurements were performed on system A. See SI for detailed device information.

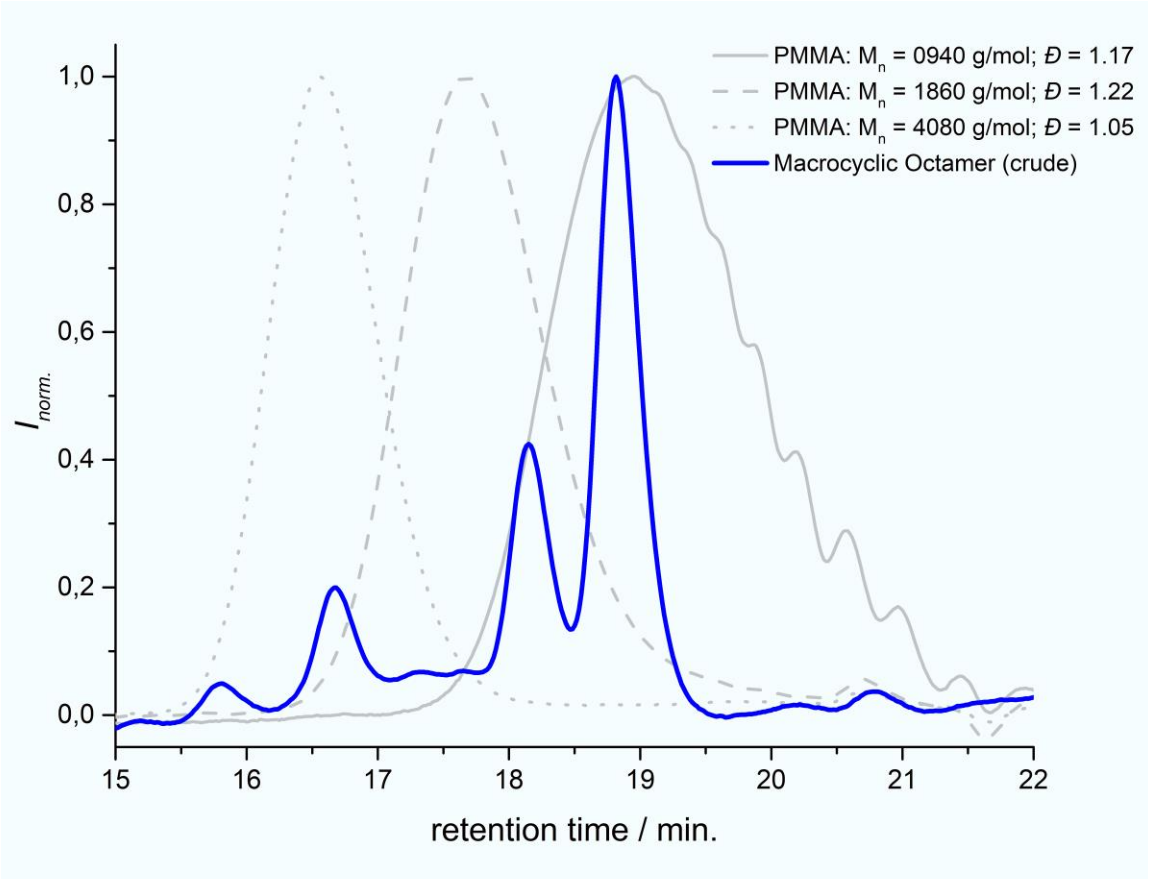

Figure 22. SEC comparison of a crude macrocyclic octamer with three different narrow PMMA standards, that are commonly used for SEC calibration. In the crude product, four different species are detectable, which can be identified by SEC-ESI-MS analysis.[*]

Macromolecules of uniform size, on the other hand, allow for easy analysis by integration of the SEC traces if oligomer-specific columns with sufficient resolution are utilised (compare Figure 22). In summary, it was demonstrated that the applied approach is suitable for the template-free synthesis of sequence-defined large macrocycles. This is furthermore the first example of sequence-defined macromolecules that are employed for the synthesis of another polymer architecture than linear macromolecules. The synthetic procedure allowed the introduction of different tailored side chains as well as long aliphatic backbones to the macrocyclic backbone. During RCM, clear trends were observed, offering the possibility to identify the limits of RCM regarding conversion as well as to determine clear structure-activity relationships, here the dependence of RCM on the length of the linear oligomer and on the side chains. Indeed, the side chains did not influence the conversion significantly, whereas the length of the oligomer greatly influenced the reaction yield. Interestingly, RCM in a powerful tool for macrocycle synthesis, even in very low concentrations and if very large cyclic compounds with more than 150 ring atoms are targeted. This study serves as a model and example of application possibilities of sequence-defined macromolecules of uniform size to determine quantitative structure property/activity relationships, which cannot be analysed accurately if disperse systems are utilised.

---

[*] SEC measurements were performed on system A. See SI for detailed device information.

4.1.2 Dual sequence-definition by using the P-3CR

The ESI-MS/MS experiments of this project were performed in cooperation with Maximiliane Frölich. The synthetic and characterisation part of the sequence-defined oligomers was solely performed by Katharina Wetzel, whereas the ESI-MS/MS readout was performed by Maximiliane Frölich. Some of the monomers were synthesised by Vertiefer-students under lab supervision of Katharina Wetzel. Footnotes in the experimental part mark the respective molecules that have been synthesised by the students and provide detailed differentiation.

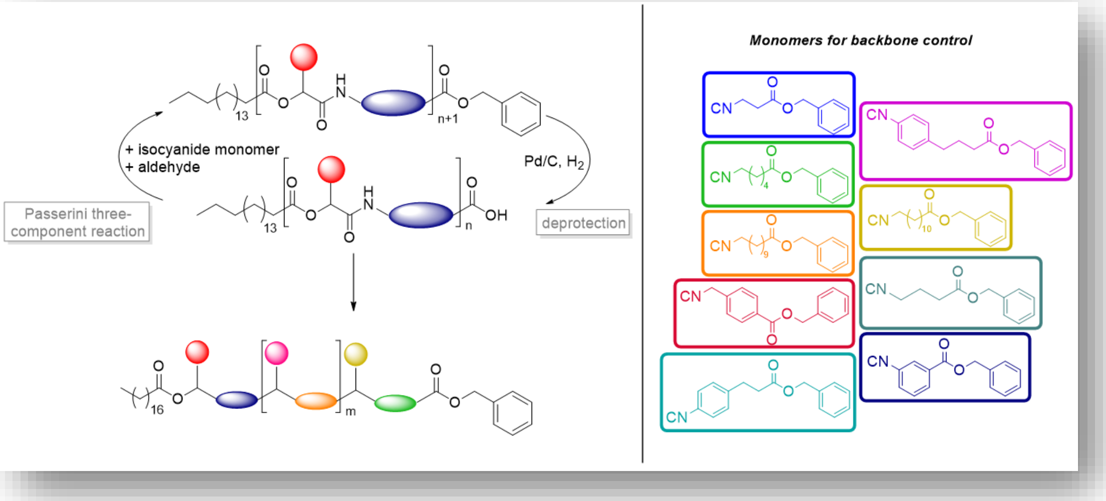
+ isocyanide monomer
+ aldehyde
Passerini three-component reaction
Pd/C, H₂
deprotection
Monomers for backbone control

Abstract:

An approach towards dual sequence-defined linear macromolecules by using the P-3CR is presented within this chapter. By using a specifically designed AB-type monomer, it was already demonstrated by our group, that large macromolecules carrying many different side groups at predefined positions can be synthesised in large scale and excellent purity.[34] *Within this project, an even higher degree of definition was achieved by not only defining the side chain, but also the backbone moiety in each repeating unit. Dual sequence-definition was thus achieved by varying the aldehyde component and the AB-monomer at the same time in each P-3CR. In order to do so, nine different monomers were synthesised from the corresponding amino acid. Applying them in a two-step iterative cycle led to uniform high molecular weight oligomers, which were utilized for the first tandem ESI-MS fragmentation investigations, showing the expected fragmentation pattern.*[392] *Thus, these macromolecules are suitable for applications in data storage systems, drastically increasing number of permutations, and thus the data storage capacity compared to previous systems developed by our group.*[393-394]

Within this chapter, the synthesis of dual sequence-defined macromolecules is described. The previously developed monomer approach was adapted and the aldehyde component as well as the AB-monomer were varied in each iterative cycle instead of only varying the aldehyde component. Thus, dual sequence-definition was achieved. By variation of the aldehyde in each P-3CR, different side chains were introduced, as demonstrated before.[34] If additionally to the aldehyde, the AB-monomer is varied, dual sequence-definition is achieved. The generally applied two step iterative cycle consisted, similarly to the previously described approach (compare Chapter 4.1.1), of the P-3CR and a subsequent deprotection step, as can be seen in Scheme 33. Starting from stearic acid **13**, linear macromolecules exhibiting different degrees of control were synthesised by defining either the backbone or both, the backbone and the side chain.

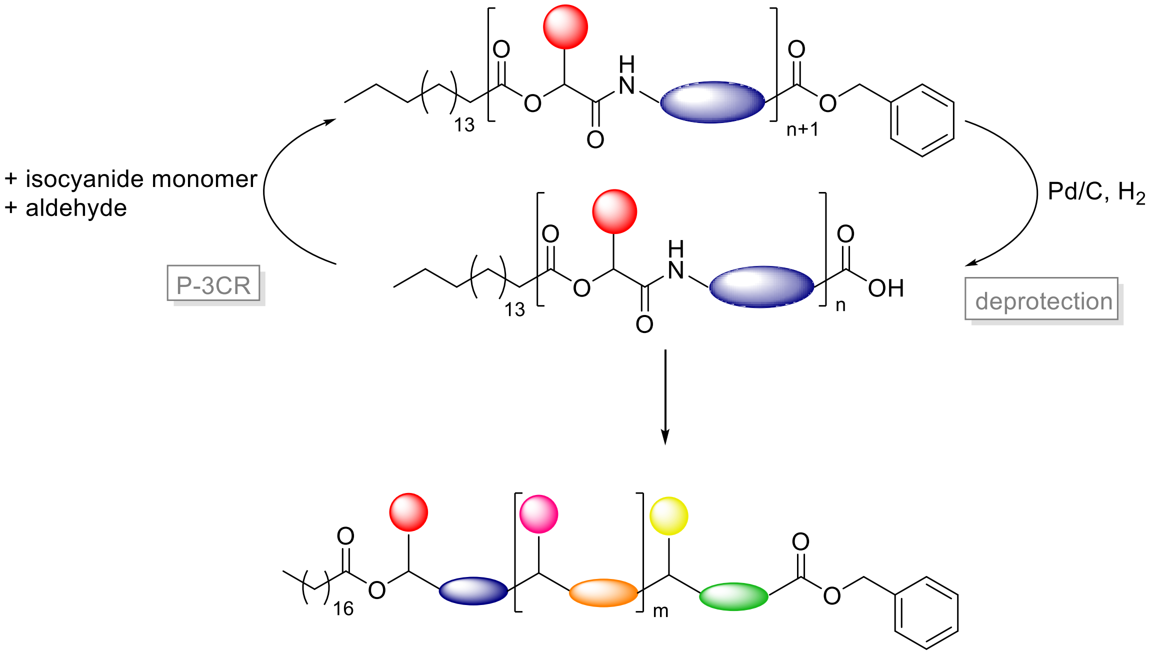

Scheme 33. Two-step iterative reaction cycle for the synthesis of dual-sequence-defined macromolecules, which allows to control the backbone as well as the side chain at the same time.

Commercially available aldehydes were thus utilised to achieve side chain control. A library of eleven different aldehydes was established as potential components for introducing the side chains, amongst them aldehydes bearing cyclic, branched and linear aliphatic groups of different lengths, as well as an aromatic compound. The library of potential aldehyde components is depicted in Figure 23 (right hand side). To furthermore achieve backbone control, a set of different AB-type monomers (see Figure 23, left hand side) needed to be synthesised in three to four reaction steps from the corresponding amino acids. The synthesis protocol was adapted from the protocol of monomer **M1**, which can be transferred to various different amino acids (see Chapter 6.3.2.1 for experimental details).

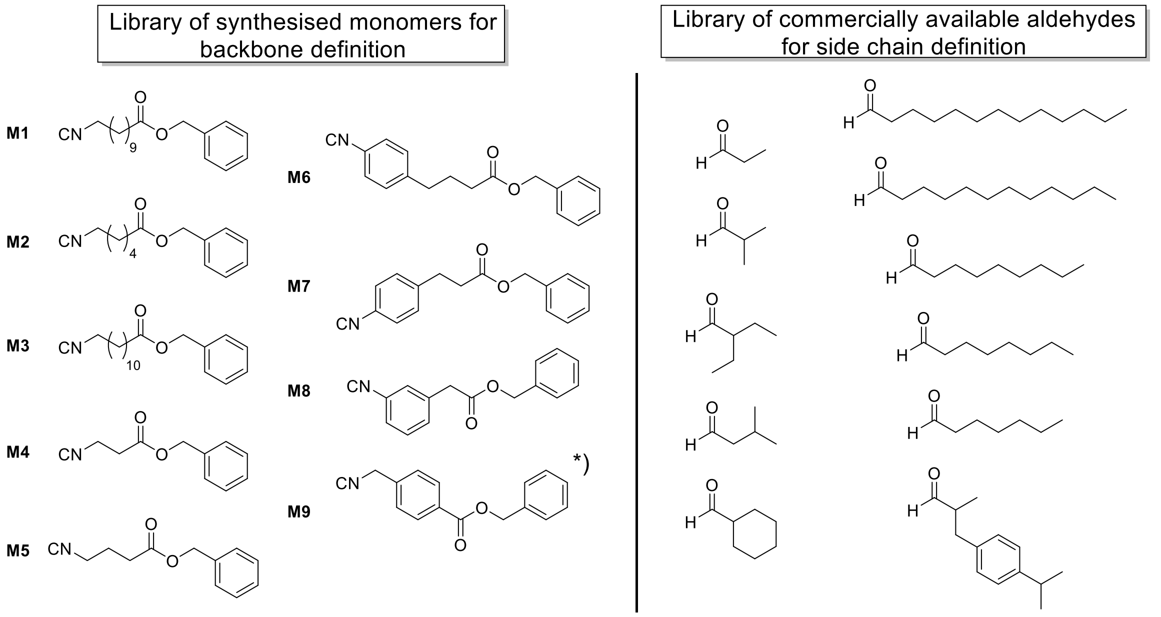
Library of synthesised monomers for backbone definition
Library of commercially available aldehydes for side chain definition
M1
M2
M3
M4
M5
M6
M7
M8
M9
*)

*Figure 23. Left: library of the AB-type monomers **M1** – **M9** that were synthesised from the corresponding amino acid in three steps; (*) in case of **M9**, the synthesis is performed via a four-step procedure. By variation of the monomers, different backbone moieties can be introduced to the macromolecules. Right: library of commercially available aldehydes applied to introduce different side chains to the oligomers.*

Applying this three-step synthesis protocol, seven new monomers (**M2** – **M8**) were successfully synthesised. Starting from the amino acids (amino acids **1b-h**, see experimental section Chapter 6.3.2.1), an esterification was performed as a first step. Therefore, the amino acid was suspended in THF and a large excess of benzyl alcohol **3** was added. The subsequent addition of thionyl chloride **4** was performed dropwise at 0 °C. While stirring the reaction mixture over night at room temperature, it turned into a clear solution, indicating product formation. The product (benzyl esters **2b-h**) was precipitated by pouring the reaction mixture into cold diethyl ether and storing it in the freezer. After filtration and washing with small amounts of cold diethyl ether, the product was obtained. In the first step, usually high yields above 80% up to 99% were achieved. However, for one of the monomers (**M8**) bearing a small aromatic backbone with the two different functional groups attached to the aromatic ring in meta position, a significantly reduced yield of 56% was obtained in the first step. This might be caused by steric hindrance.

The next synthesis step for monomers **M1** – **M8** was the *N*-formylation yielding the *N*-formamide compound (**8a-h**) was achieved by dissolving the ammonium salt (compounds **2a-i**) in trimethyl orthoformate **5** and heating it under reflux overnight. After evaporation of the solvent, the crude product was obtained, which was used without further purification in the next reaction step in case of the synthesis of monomers **M1**, **M3**, **M5**, **M7** and **M8**. However, for the monomers, **M2**,

M4 and **M6**, column chromatography was required after this step. The last synthetic step was the formation of the isocyanide, which was achieved by dehydration of the formamide group by using phosphoryl trichloride **6** and diisopropylamine **7**. The whole reaction scheme for the three-step synthesis of monomers **M1** – **M8** is depicted exemplarily for monomer **M2** in Scheme 34.

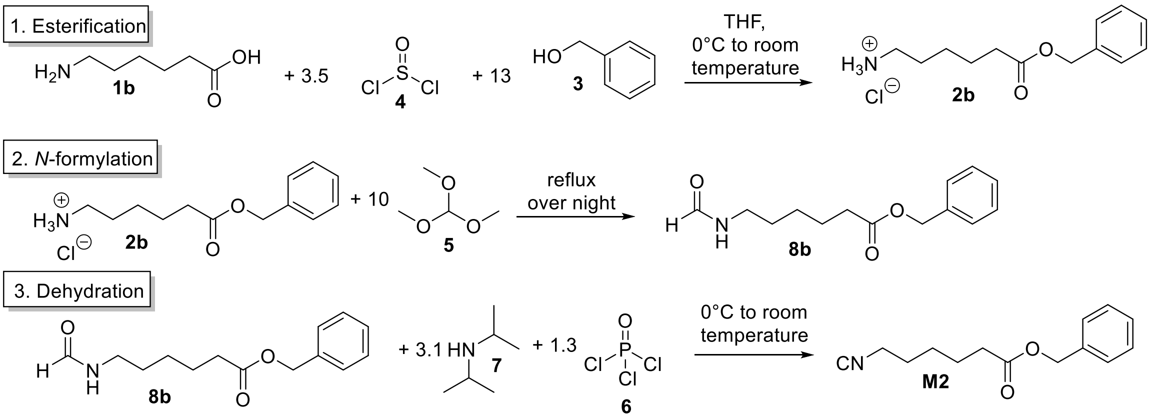

*Scheme 34. Three-step synthesis procedure for the synthesis of monomer **M2** consisting of the esterification, the N-formylation and a final dehydration step. The synthesis procedure was applied in the synthesis of monomers **M1** – **M8**.*

All the different monomers **M1**-**M8** were thoroughly characterised by proton and carbon NMR, mass spectrometry and IR spectroscopy in order to verify their structure. Before they were used in the oligomer synthesis, they were also analysed by SEC, which is equipped with columns specifically designed for measuring oligomers. In Figure 24, the NMRs of each of the reaction steps towards monomer **M2** is depicted exemplarily. In the spectrum of the first reaction step (blue trace), signals 1 and 2 indicate the successful formation of the benzyl ester **2b**, while the other signals represent the CH_2 groups of the backbone. The successful *N*-formylation towards compound **8b** is unambiguously visible in the green spectrum. Two new signals arise as a result of the *N*-formamide group: signal 1 was assigned to the proton at the carbonyl, and signal 3 was assigned to the proton at the nitrogen. Interestingly, signal 1 is split into two signals. A singlet and a doublet are visible at around 8.00 ppm (signal 1). This is caused by the partial double bond character of the *N*-formamide. The two signals represent the *cis*- and the *trans*-isomers. In the spectrum of the final product **M2** (red trace), the signals at *ca.* 8 ppm disappear again, while the isocyanide is formed. Signal 3 is shifted to the low field if compared to the blue spectrum, indicating the successful formation of the isocyanide. The measured mass is in good agreement with the calculated value (compare Table 2) the IR shows a characteristic band of the isocyanide at 2146.5 cm^{-1}. Thus, IR spectroscopy provides the final proof of the successful isocyanide formation.

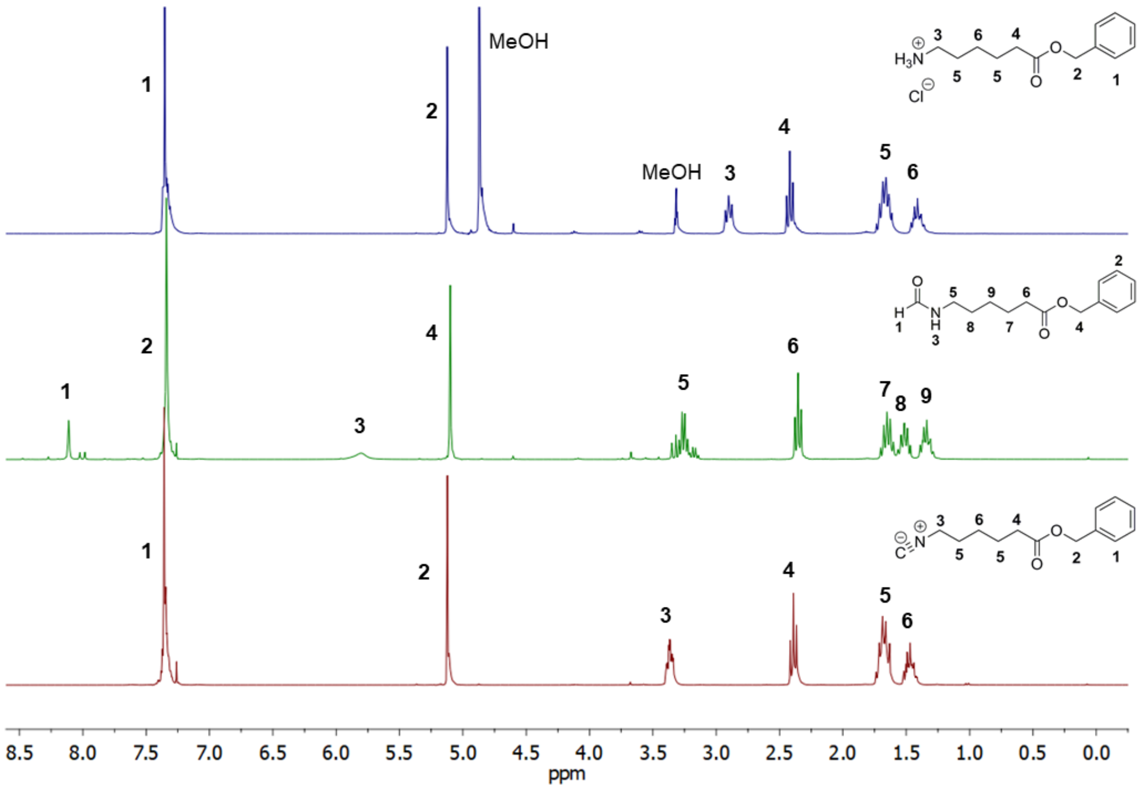

Figure 24. Example of the evolution in the proton NMR spectrum during the monomer synthesis. The three spectra show the intermediates ***2b*** *and* ***8b*** *(blue: esterification; green: N-formylation) and the final product* ***M2*** *(red: dehydration).*

If the acid functionality is directly connected to an aromatic ring, like it is the case with 4-(aminomethyl)benzoic acid **1i**, it was found that it is not reactive in the esterification reaction with benzyl alcohol **3**. In order to circumvent the low reactivity that led to very low yields, a fourth reaction step was introduced (see Scheme 35 and refer to Chapter 6.3.2.1 for detailed information). In a first step, the esterification was performed, using methanol as solvent instead of THF and benzyl alcohol **3**. Thus, the methyl ester **14** was obtained. After the *N*-formylation step towards the N-formamide **15**, the new reaction step, being a transesterification with benzyl alcohol **3**, was inserted to yield again the benzyl ester *N*-formamide **16**. The transesterification was performed using 20 mol% 1,8-Diazabicyclo[5.4.0]undec-7-en (DBU) **17** as a catalyst at 150 °C for five hours, while methanol was released and distilled off. The crude intermediate was purified by column chromatography before the dehydration was performed as the last step.

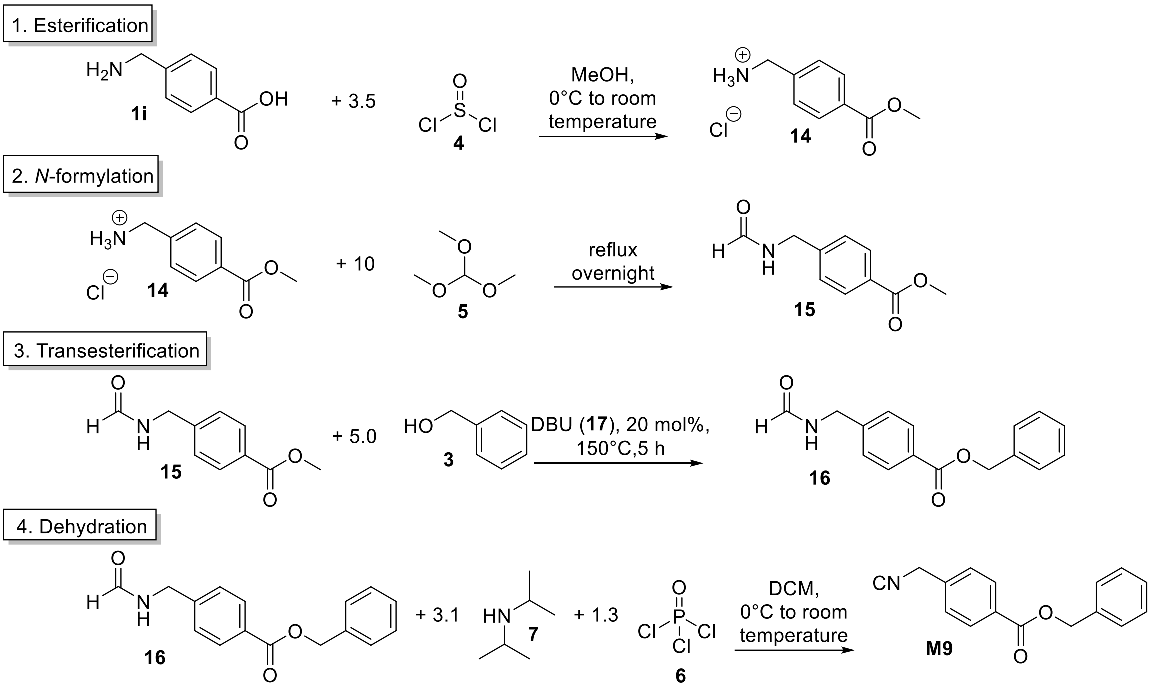
1. Esterification
1i
+ 3.5
4
MeOH,
0°C to room
temperature
14
2. N-formylation
14
+ 10
5
reflux
overnight
15
3. Transesterification
15
+ 5.0
3
DBU (17), 20 mol%,
150°C,5 h
16
4. Dehydration
16
+ 3.1
7
+ 1.3
6
DCM,
0°C to room
temperature
M9

*Scheme 35. Four-step synthesis procedure for the synthesis of monomer **M9**, including the esterification with methanol to form the methyl ester and a transesterification as an additional third step.*

The NMRs of the intermediates and the final product **M9** is shown in Figure 25. In the spectrum of the first esterification step (read trace), the methyl ester **14** gives a characteristic signal at around 3.8 ppm. In the next step, the *N*-formamide peak of substance **15** arises (signal 1, green trace). In the third transesterification step, signals 3 and 4 prove the successful insertion of the benzyl group (turquoise trace, substance **16**) and in the final product **M9** (purple trace), the formamide signal disappears, while signal 4 is significantly shifted to the low field, indication the formation of the isocyanide. Again, the characteristic isocyanide peak is visible in the IR spectrum at 2149.4 cm^{-1}, proving the success of the last step.

The results of the synthesis of the nine different monomers with all their intermediates are summarised in Table 2. It is noteworthy that moderate to high overall yields were achieved for all the different monomers. The monomer syntheses were performed in multigram scale of up to 15 grams.

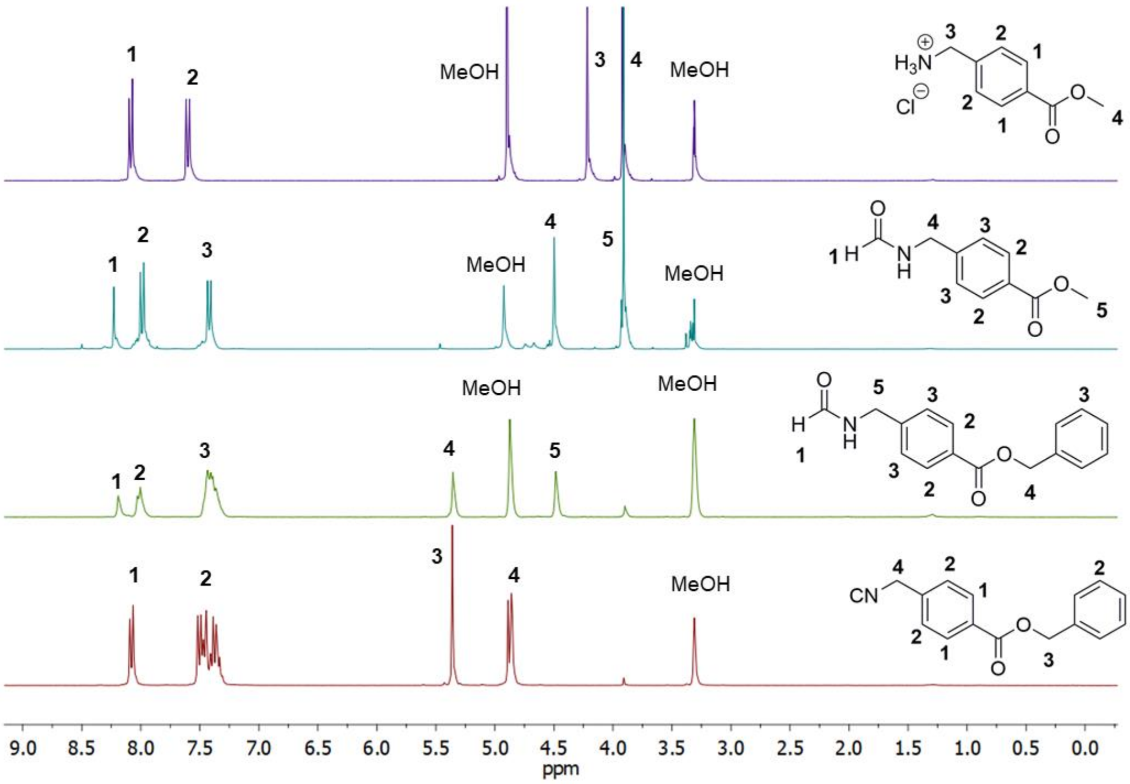

*Figure 25. Example of the evolution in the NMR spectra during the monomer synthesis. The spectra of the three intermediates (purple: methyl ester, turquoise: N-formamide, green: benzyl ester) as well as of the final product **M9** (red) are depicted.*

Having the monomers **M1** – **M9** in hands, the reactivity of some of the monomers was investigated in a P-3CR with a subsequent deprotection in order to ensure their potential usefulness in the oligomer synthesis. The monomers **M3**, **M5**, **M6**, **M7** and **M9** were used to evaluate the reactivity in the two reaction. It was found that all of them were reactive in both of the reactions (*i.e.* deprotection and P-3CR, see Chapter 6.3.2.1 for detailed experimental procedures). Thus, such test reactions were not performed for the other monomers and they were directly used for the oligomer synthesis.

*Table 2. Summary of the results of the monomer syntheses of monomers **M1** – **M9** with all their intermediates.*

Monomer	Reaction step	Yield [%]	m/z $_{\text{calc.}}$	m/z $_{\text{found}}$
Monomer 1	Esterification	95[a]	292.2271	292.2271
	N-formylation	quant.[b]	320.2220	320.2222
	Dehydration	67[c]	302.2115	302.2113
Overall yield		64		
Monomer 2	Esterification	96[a]	222.1489	222.1489

	N-formylation	73[c]	250.1438	250.1437
	Dehydration	74[c]	232.1332	232.1331
Overall yield		52		
Monomer 3	Esterification	75[a]	306.2443	306.2431
	N-formylation	quant.[b]	334.2382	334.2384
	Dehydration	32[c]	316.2271	316.2272
Overall yield		24		
Monomer 4	Esterification	81[a]	180.1103	180.1104
	N-formylation	52[c]	208.0968	208.0967
	Dehydration	74[c]	188.0712	188.078710
Overall yield		31		
Monomer 5	Esterification	89[a]	194.1181	194.1181
	N-formylation	91[b]	221.1052	221.1050
	Dehydration	69[c]	204.1025	204.1024
Overall yield		56		
Monomer 6	Esterification	78[a]	270.2135	270.2137
	N-formylation	72[c]	298.1443	298.1439
	Dehydration	68[c]	280.1338	280.1336
Overall yield		38		
Monomer 7	Esterification	93[a]	256.1338	256.1337
	N-formylation	99[b]	284.1287	284.1288
	Dehydration	55[c]	266.1181	266.1182
Overall yield		51		
Monomer 8	Esterification	56[a]	242.1181	242.1181
	N-formylation	quant.[b]	270.1130	270.1132
	Dehydration	39[c]	252.1025	252.1024
		22		
Monomer 9	Esterification	88[a]	166.0863	166.0863
	N-formylation	93[b]	193.0733	193.0736
	Transesterification	44[c]	270.1130	270.1132
	Dehydration	76[c]	252.1025	252.1026
Overall yield		27		

[a] after purification by washing, [b] crude, [c] after purification by column chromatography.

Since it has been demonstrated before that long sequences with or without side chain variation can be achieved in high overall yields and scale by applying the monomer approach,[34] the next step was to investigate, if the backbone can be varied by utilising the previously synthesised monomers in the same approach.

Thus, an oligomer was synthesised by varying the monomer in each reaction cycle (see Chapter 6.3.2.2.1 for detailed experimental procedures). The aldehyde component, on the other hand, was not varied. Isobutyraldehyde **11c** was used as aldehyde component for the whole synthesis, thus isopropyl side chains were introduced. The reaction conditions were adapted from previous protocols, utilising the P-3CR with subsequent deprotection.[34, 338-339] Stearic acid **13** was used as starting moiety and the reaction was performed in DCM. The aldehyde and monomer components were used in small excess relative to the carboxylic acid. The reaction was stirred at room temperature for 24 hours and the product **18** was obtained after purification by column chromatography. The product **18** was obtained in excellent yield (98%) and purity which was confirmed by proton and carbon NMR, mass spectrometry, IR spectroscopy and by SEC chromatography. The second deprotection step was performed in ethyl acetate using palladium on activated charcoal **19** as heterogeneous catalyst. The mixture was purged with hydrogen by using several balloons. Full conversion was ensured by TLC and SEC analysis, which showed a shift towards higher retention times, thus lower molecular weight. Furthermore, the cleavage of the benzyl ester was observed by NMR, were the signals of the benzyl group at around 7.5 ppm (aromatic protons) and 5.2 ppm (CH_2-group) disappeared. The product **20** was obtained by filtering off the catalyst and evaporating the solvent. After each reaction step, a full characterisation was performed using NMR, SEC, mass spectrometry and IR spectroscopy. By iteration of the reaction cycle, defined sequences were obtained. Starting with monomer **M1**, the monomers were inserted in the following order: **M2**, **M9**, **M4**, **M5**, **M7**, and **M3** to afford a backbone-defined heptamer **21**. From the fifth deprotection on, the solvent was changed from ethyl acetate to THF, due to solubility issues. The deprotected acid of the growing oligomers was barely soluble in ethyl acetate, thus hindering the successful deprotection, as the reaction mixture became more and more viscous or in some cases solid. Therefore, purging the reaction with hydrogen balloons was at some point not possible anymore and the solvent needed to be changed. As both the starting material and the deprotected product were soluble in THF also at higher molecular weight of the oligomers, THF proved to be a suitable solvent for the reaction. In Figure 26, the growing oligomers are depicted after each P-3CR (top) and the respective SEC trace is shown in the chromatogram below, clearly proving the high purity of the obtained oligomers. In the last P-3CR, minor impurities of *ca.* 4% were visible in the SEC trace.

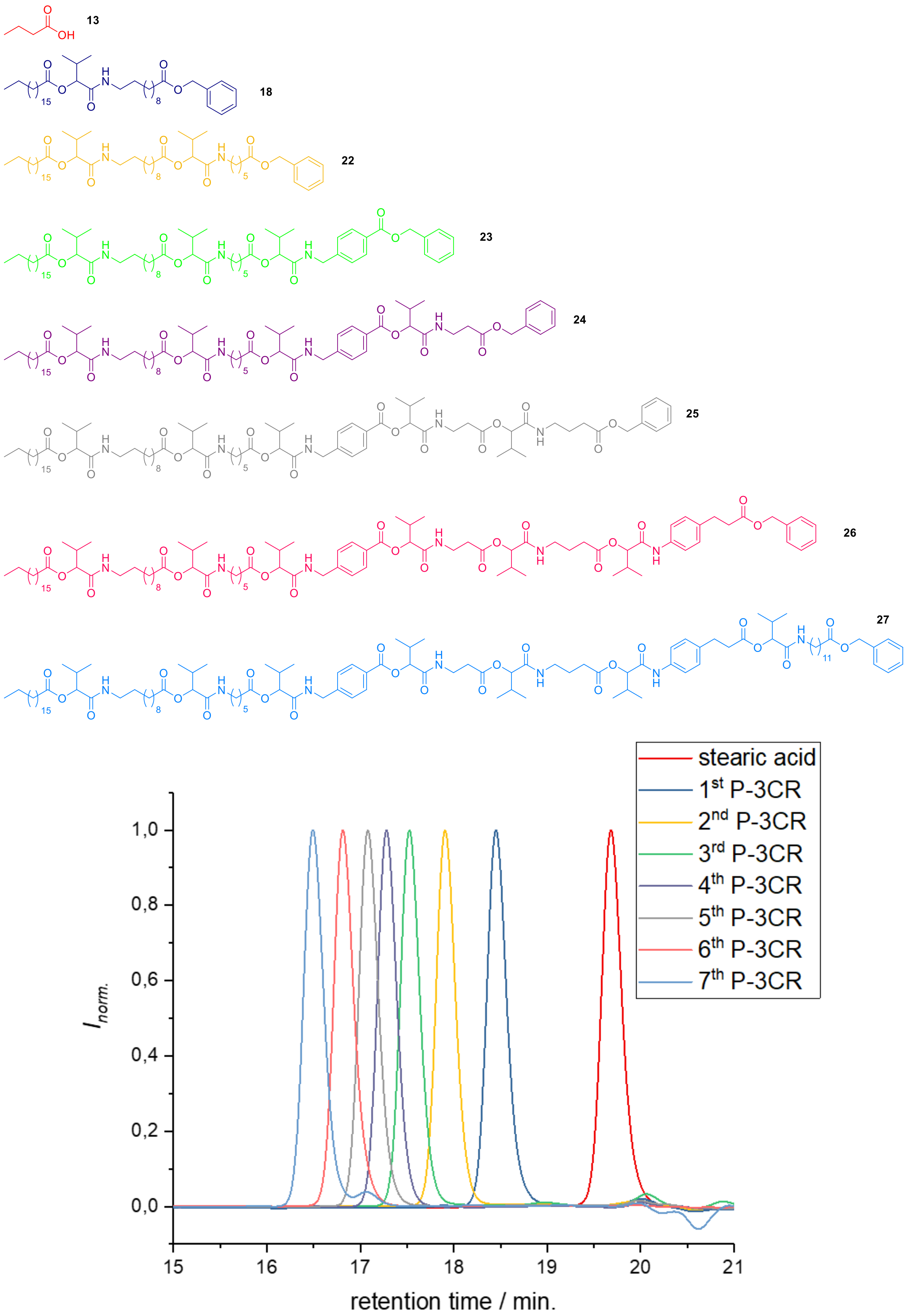

Figure 26. Top: the molecule structure of the growing oligomers after each P-3CR up to the heptamer stage, where the monomers were inserted step by step in the following order: ***M1****,* ***M2****,* ***M9****,* ***M4****,* ***M5****,* ***M7****, and* ***M3****. Bottom: the SEC results after each P-3CR are verifying the purity of the products. For the assignment of the oligomers, refer to the colour code.*

Besides the characterisation by SEC, the oligomers were also analysed by proton and carbon NMR spectroscopy and mass spectrometry. In the proton NMR spectrum, all peaks were assigned with the help of two-dimensional NMR techniques (COSY, HMBC, HSQC). The ESI mass spectrum of the pure hexamer **26** is depicted in Figure 27 as an example. In the mass spectrum, the sodium ion is observed as the main peak, further proving the purity of the molecule. By zooming in, the measured isotopic pattern (black) can be compared with the calculated one (blue), which was obtained by the program mMass. As can be seen below, the isotopic patterns are in good agreement with each other, clearly confirming the structure of the sequence-defined macromolecule **26**.

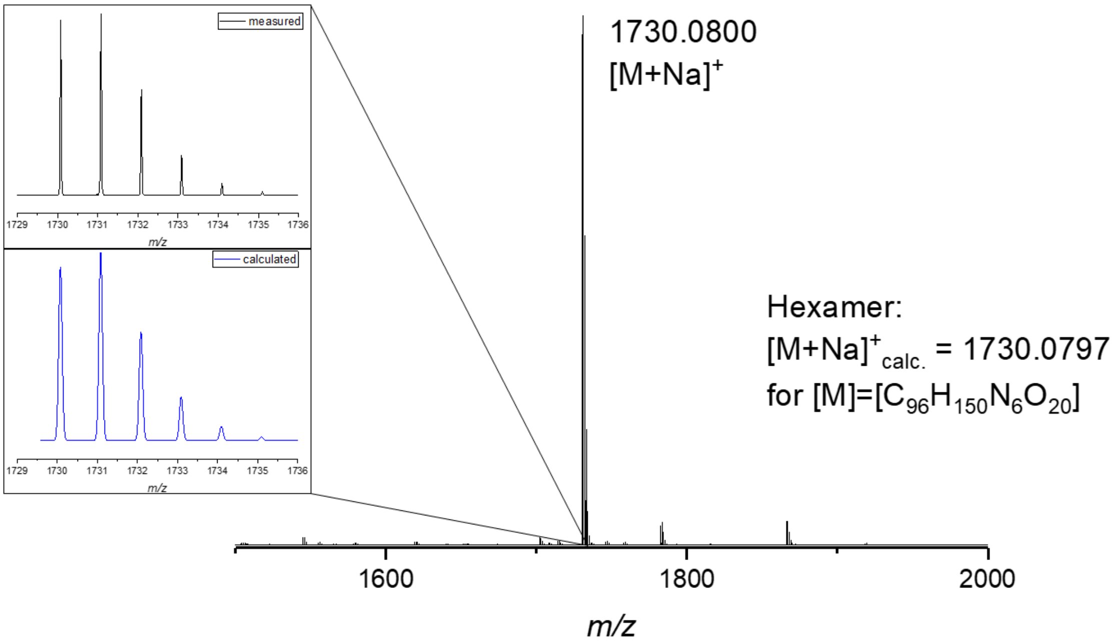

Figure 27. Mass spectrum of the backbone-defined hexamer ***26****: the singly charged sodium ion was found to be the main peak, indicating high purity of the product. The measured isotopic pattern (black) can be compared with the calculated one obtained by mMass (blue), revealing that they are in good agreement.*

In the following Table 3, the results of the backbone-defined oligomer synthesis are summarised. The table indicates the monomers that were utilised in the respective reaction steps, gives the yield of each step, and compares the calculated mass with the one that was found. The overall yield of this backbone defined heptamer **21** was 31% over 14 reaction steps and is slightly lower if compared to the previous monomer approach, where the side chain was varied. This might result from the aromatic scaffolds of the monomers, which make the reactive site more difficult to access during the reaction. Furthermore, the oligomer became more and more polar with growing length, which made the purification by column chromatography increasingly difficult.

Table 3. Summary of the backbone-defined oligomer synthesis.

Product	Applied monomer	Yield [%]	m/z $_{\text{calc.}}$	m/z $_{\text{found}}$
1st P-3CR **18**	**M1**	98[a]	658.5405	658.5404
1st deprotection **20**		87[b]	568.4936	568.4935
2nd P-3CR **22**	**M2**	98[a]	871.6770	871.6764
2nd deprotection **27**		93[b]	781.6300	781.6297
3rd P-3CR **23**	**M9**	99[a]	1104.7822	1104.7826
3rd deprotection **28**		81[b]	1014.7352	1014.7343
4th P-3CR **24**	**M4**	92[a]	1275.8717	1275.8743
4th deprotection **29**		99[b]	1185.8248	1185.8254
5th P-3CR **25**	**M5**	82[a]	1460.9769	1460.9792
5th deprotection **30**		97[b]	1370.9300	1370.9318
6th P-3CR **26**	**M7**	85[a]	1708.0978	1708.0978
6th deprotection **31**		99[b]	1618.0508	1618.0494
7th P-3CR **32**	**M3**	92[a]	2005.3282	2005.3289
7th deprotection **21**		81[b]	1915.2812	1915.2852
Overall yield	31% over 14 reaction steps			

[a] *after column chromatography,* [b] *after filtration.*

The backbone-defined heptamer **21** clearly demonstrated the suitability of the different monomers for achieving backbone definition, thus increasing the degree of structural variability as well as the general versatility of the P-3CR monomer approach.

As a next step, the two types of control achieved by this approach, e.g. side chain and backbone control, should be combined in order to introduce defined side chains as well as backbone moieties into each repeating unit. Therefore, a new oligomer was synthesised while varying both the AB-monomer and the aldehyde component independently in each step (see Chapter 6.3.2.2.2 for detailed experimental procedures). Again, stearic acid **13** was used as starting point and monomer **M1** and isobutyraldehyde **11c** were used in the first P-3CR. The reaction conditions in both of the reactions remained unchanged. Only in the deprotection step, THF was used from the beginning of the oligomer synthesis.

In Figure 28, the structures of the obtained oligomers up to the pentamer stage and the corresponding SEC results of all reaction steps are shown. For the synthesis, the monomers **M1**, **M7**, **M5**, **M8** and **M3** were used. Isobutyraldehyde **11c**, isovaleraldehyde **11e**, octanal **11f**, dodecanal **11g** and 2-phenylpropanal **11h** served as aldehyde components.

The SEC traces clearly prove the purity of the oligomers. From the deprotected tetramer stage on, a small shoulder towards higher retention time was observed, which could not be separated. The shoulder became even more prominent in the next Passerini step. It is noteworthy that also in the backbone-defined oligomer, the shoulder arose when the long aliphatic **M3** monomer was utilised. Probably, the problems are caused by minor undetectable impurities in the monomer compound and could be avoided by using other monomers.

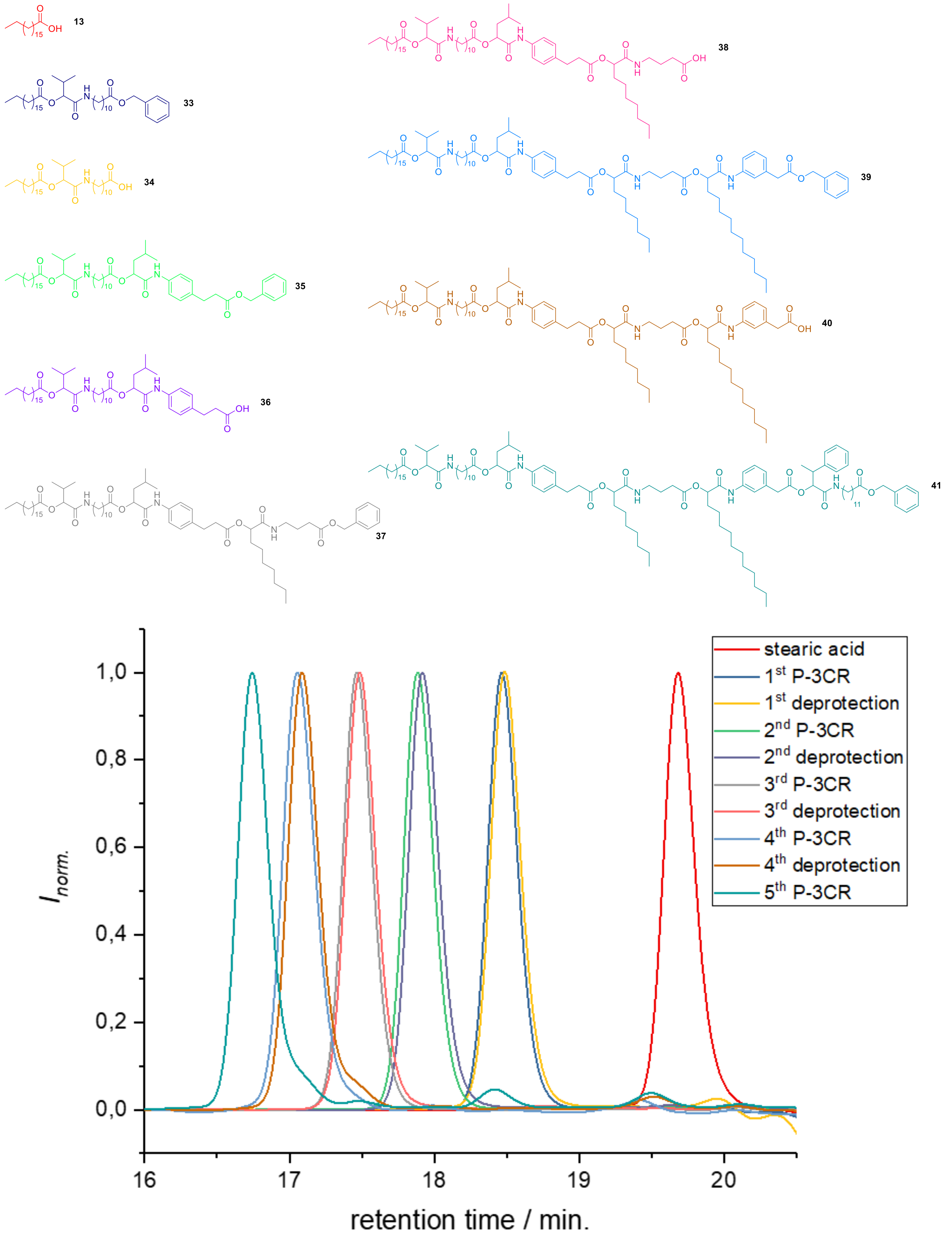

*Figure 28. Top: the molecule structure of stearic acid **13** and the growing oligomers **33** - **41** after each P-3CR and deprotection up to the pentamer stage, where the monomers were inserted step by step in the following order: **M1**, **M7**, **M4**, **M8**, and **M3**. Isobutyraldehyde **11c**, isovaleraldehyde, octanal, dodecanal and 2-phenylpropanal **11h** were used to introduce different side chains. Bottom: the SEC results after each P-3CR and deprotection step are verifying the purity of the products. For the assignment of the oligomers, refer to the colour code.*[*]

---

[*] SEC measurements of Chapter 4.1.2 were performed on system B. See SI for detailed device information.

Besides the characterisation by SEC, the oligomers were also analysed by proton and carbon NMR spectroscopy, and mass spectrometry after each step. In Figure 29, the mass spectrum of the pure deprotected tetramer **40** is depicted. Both, the protonated ion and the sodium ion, are visible in this case, while the protonated ion represents the main peak. If the measured isotopic pattern (black) is compared with the calculated one obtained by mMass, an excellent agreement can be observed, further proving the structure of the obtained product.

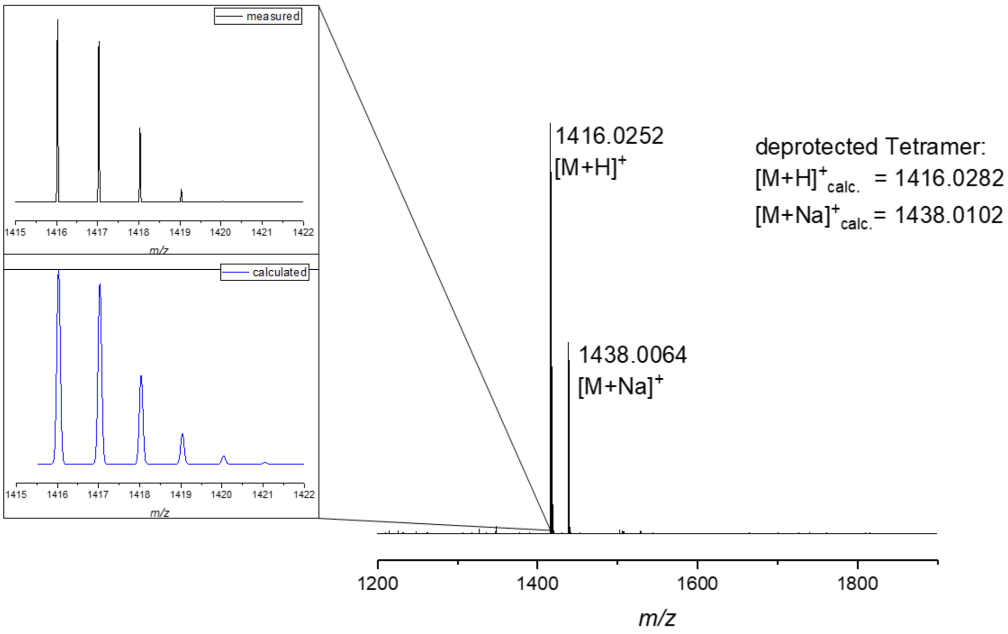

Figure 29. Mass spectrum of the backbone-defined deprotected tetramer: the protonated ion and the singly charged sodium ion was found in the spectrum, indicating the high purity of the product. The measured isotopic pattern (black) can be compared with the calculated one obtained by mMass (blue), revealing that they are in very good agreement.

Table 4 briefly summarises the results during the dual sequence-defined synthesis of macromolecule **41**. The applied monomer compound as well as the aldehyde component that is used in each P-3CR is given. The calculated and the found masses are compared and the yield of each synthesis step is given. With 23%, the overall yield of the dual sequence-defined oligomer was a bit lower compared to the backbone defined macromolecule. This might be due to the more difficult separation of the compounds that were used in excess from the oligomer if compared to the side chain variation, where purification became easier with increasing oligomer length.[34]

Table 4. Summary of the results obtained in the synthesis of dual sequence-defined macromolecules. The applied monomer and aldehyde component, as well as the yields, applied purification strategy and the calculated and found masses are given.

Product	Applied monomer	Applied aldehyde	Yield [%]	m/z $_{\text{calc.}}$	m/z $_{\text{found}}$
1st P-3CR **33**	**M1**	Isobutyraldehyde**11c**	98[a]	658.5405	658.5391
1st deprotection **34**			99[b]	568.4936	568.4922
2nd P-3CR **35**	**M7**	Isovaleraldehyde	65[a]	919.6770	919.6747
2nd deprotection **36**			99[b]	829.6300	829.6279
3rd P-3CR **37**	**M4**	Octanal	47[a]	1160.8448	1160.8435
3rd deprotection **38**			99[b]	1070.7978	1070.7958
4th P-3CR **39**	**M8**	Dodecanal	quant[a]	1506.0752	1506.0745
4th deprotection **40**			99[b]	1416.0282	1416.0226
5th P-3CR **41**	**M3**	2-phenyl-propanal	81[a]	1865.3212	1865.3248
Overall yield	23% over nine reaction steps				

[a] after purification by column chromatography, [b] after filtration.

As already mentioned in the introduction, the dual sequence-defined macromolecules were exploited for sequential read-out by tandem ESI-MS/MS. Nowadays, information technology is based on the binary code of “0” and “1”, which originates from switches and triggers “off” and “on”. For encoding information into such a system, very long sequences are required. However, if instead of a binary system, a quaternary system, like the four DNA bases, is used, shorter sequences are required for encoding the same amount of information into the strand.[395] If the different data storage systems are compared, an important benchmark is the number of permutations. In a binary system for example, a sequence of eight binary digits is 1 byte, which is 8 bit or 2^8, thus 256 permutations. In a quaternary system, on the other hand, shorter sequences are required to achieve the same number of permutations: 4^4 =256, thus only tetramers would be required to achieve the same storage capacity. The increase of data storage capacity, or the achievable number of permutations, is therefore an important topic in current research. As reported before by our group, molecules obtained by MCRs can used for data storage.[38, 164-165, 392] In a previous work, it was demonstrated that the well-established monomer approach is suitable for applications in data storage if different side groups are defined as an alphabet, where information can be encoded and successfully be read-out afterwards.[392] The read-out was later computer assisted, which facilitated the process drastically. Another advantage, of that approach was the robust, straightforward and fast synthesis procedure. However, this approach only allowed to vary one side group per repeating unit, with led to a limited number of permutations. If the library of eleven commercially available aldehyde components, which was utilised in this work, was applied as an alphabet, and a sequence of four repeating units was established, this would correspond to 11^4 = 14.641 permutations.

By applying the dual sequence-defined macromolecules for data storage, this number can be significantly extended, since now the backbone and the side chains can be varied independently at the same time. Eleven possible side chains plus nine possible backbone moieties lead to $(11{\cdot}9)^4$ = 96.059.601 permutations, which is a notable increase compared to the previous system. The permutations can be translated into bit and byte terminology by the following equations:

$$bit = \frac{\log\left(n_{permutations}\right)}{\log\,(2)}$$

And

$$8\ bits = 1\ byte$$

Thus, the permutations translate to 26,5 bits, which in turn translates to 3.31 bytes storage capacity of a tetramer. Having the dual sequence-defined tetramers **39** in hand, they were used for tandem mass spectrometry to identify the predominant fragmentation patterns. Interestingly, it was found that the fragmentation pattern does not differ significantly from the oligomers, where only the side chain is varied. In Figure 30, the α-fragmentation from both ends of the tetramer is depicted. By recombination of the fragments, the initial structure can be retraced, enabling the successful read-out of the sequence. Besides the α-fragmentation, also McLafferty rearrangement was observed as expected.

This was an important result of the first fragmentation investigations, as it potentially allows the transfer to the already established automated read-out process, that benefits from a software which was specifically designed for the read out of those molecules.

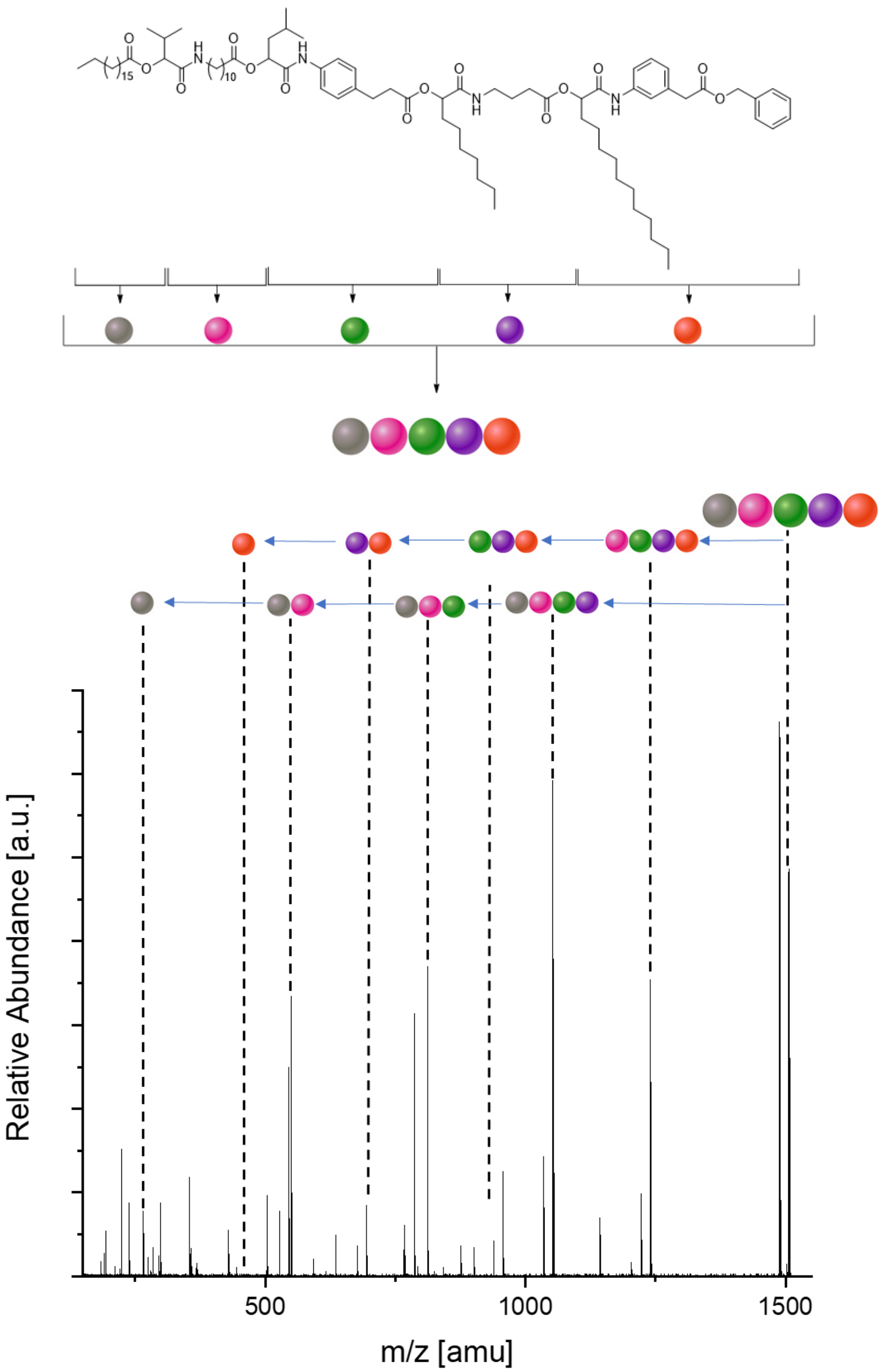

*Figure 30. Fragmentation of the dual sequence-defined tetramer **39** by tandem mass spectrometry revealing the expected fragmentation pattern. In the spectrum, the α-fragmentation from both ends of the oligomer is depicted. By recombining the fragments, the initial structure of the tetramer can be retraced. A detailed list of all fragments is depicted in the experimental section (Chapter 6.3.2.2.3, Table S 2)*

In summary, it was demonstrated that a large library of different monomers was successfully established and applied in the synthesis of sequence-defined macromolecules. The well-established monomer approach was adapted and enhanced to first synthesise a backbone defined macromolecule and proof the suitability of the different monomers for this approach. Furthermore, dual sequence-defined macromolecules, having independently selectable side chains and backbone moieties, were synthesised. The dual sequence-defined oligomers were successfully applied for sequential read out *via* tandem mass spectrometry, significantly increasing the data storage capacity compared to the previously established system.

4.2 Combining the P-3CR with Diels-Alder click chemistry for sequence-defined synthesis – a comparative study of solid and solution phase synthesis

Parts of this chapter and the associated parts in the experimental section were published before: Direct Comparison of Solution and Solid Phase Synthesis of Sequence-Defined Macromolecules, Joshua O. Holloway, Katharina S. Wetzel, Steven Martens, Filip E. Du Prez, Michael A. R. Meier, *Polym. Chem.*, **2019**, *10*, 3859-3867.[163] (The first two authors contributed equally to this work)

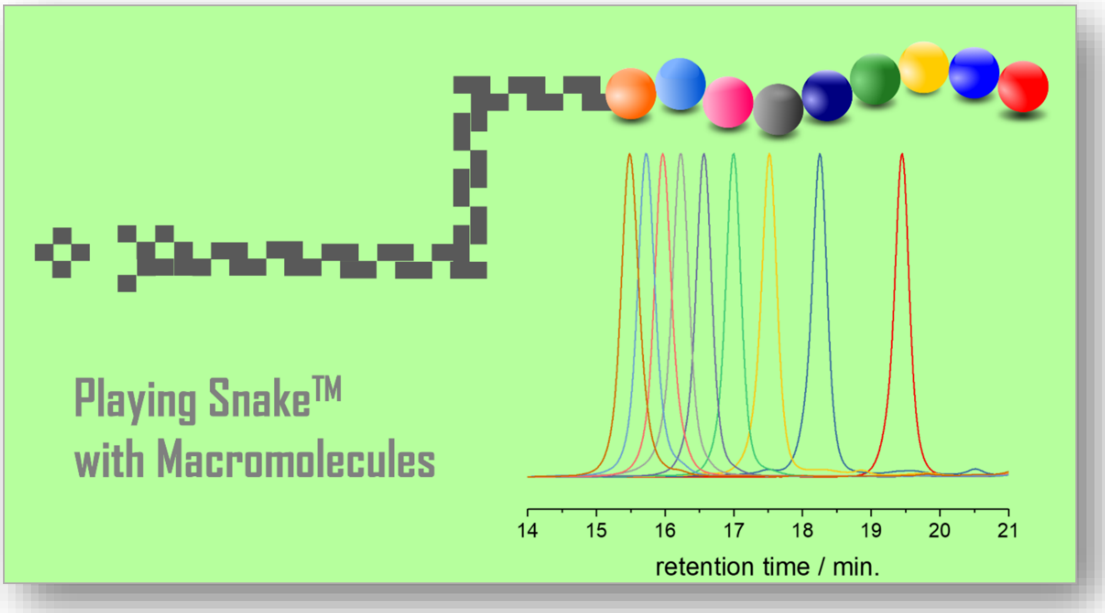

Abstract:

The synthesis of perfectly defined macromolecules of uniform size is one of the challenges faced by polymer chemists today. Such precision synthesis requires a fundamentally different approach to conventional polymer synthesis, but in turn can unlock the door to many new applications. Within this chapter, the combination of ultra-fast "click" reactions using TAD with the highly efficient and versatile Passerini three-component reaction is discussed. This new approach not only resulted in the synthesis of monodisperse, sequence-defined macromolecules of high purity and molecular weight (> 7,000 Da), but also offered new insights into the iterative synthesis of sequence-defined macromolecules in general, as a detailed comparative study of the same chemistry protocols carried out on solid phase as well as in solution is presented.

The combination approach was performed as a collaboration project with the working group of Prof. Filip Du Prez, whereas the synthetic part was carried out at Ghent University (Belgium) Solution phase synthesis and the synthesis of linker molecule **L1** was performed by Katharina S. Wetzel, whereas solid phase synthesis and the synthesis of linker molecule **L2** was performed by Joshua O. Holloway. Both approaches served as the basis for the comparative study and are crucial for the conclusions that were drawn. Thus, both approaches will be discussed within this chapter with a detailed focus on the solution phase synthesis as it was carried out by the author. Footnotes in the experimental part mark the respective molecules that have been synthesised by the cooperation partner and provide detailed differentiation.

A new strategy combining the – in this field well-established – P-3CR with the fast and efficient TAD-based Diels-Alder chemistry to obtain sequence-defined structures of high molecular weight and excellent purity is investigated. Since only a few examples exist to date, the use of Diels-Alder reactions for sequence-defined synthesis remains very limited, as only a few examples exist to date.[134, 153, 396-397] Compared to previously reported approaches, the combination approach presented in this chapter was proven to be a powerful tool for targeting sequence-definition, significantly improving the efficiency and speed of the synthesis by combining these two versatile and efficient orthogonal reactions. Additionally, the combination approach allowed the same synthesis protocol to be carried out on solid phase as well as in solution. Hence, a comprehensive study of the two approaches, discussing the advantages and disadvantages of both strategies, is presented in the current section.

In order to combine the two chemistries, namely P-3CR and TAD Diels-Alder cycloaddition, two AB-type linker molecules (**L1** and **L2**) were designed and synthesised in four reaction steps (see experimental section, Chapter 6.3.3.1, for further details). Subsequently, the linker molecules were employed in a two-step iterative cycle consisting of the two orthogonal reactions, resulting in sequence-defined macromolecules. **L1**, equipped with an isocyanide and a conjugated diene, was synthesised *via* a four-step protocol starting from 11-amino undecanoic acid **1a**, as illustrated in Scheme 36. An esterification with methanol was carried out in the first step to form **42**, followed by an *N*-formylation using trimethyl orthoformate **5**, yielding **43**. In the next step, the isocyanide **44** was formed *via* dehydration using phosphoryl trichloride **6** and the targeted compound was obtained by a transesterification with sorbic alcohol **45** forming the product **L1**. The synthesis was carried out on a 15-gram scale with an overall yield of 65%. Isolated yields and the measured exact mass after each reaction step of the synthesis of linker molecule **L1** are summarised in Table 5.

*Table 5. Overview of the isolated yields and the exact masses obtained after each synthetic step in the synthesis of linker molecule **L1**.*

Reaction/ product	isolated yield	$m/z_{\text{calc.}}$	m/z_{found}
Esterification/ **42**	quantitative[a]	215.1885	215.1885
N-Formylation/ **43**	98%[b]	243.1834	243.1835
Dehydration/ **44**	70%[c]	225.1729	225.1729
Transesterification/ **L1**	95%[c]	292.2198	292.2198
Overall yield	65%		

[a] after precipitation and washing, [b] crude, [c] after column chromatography

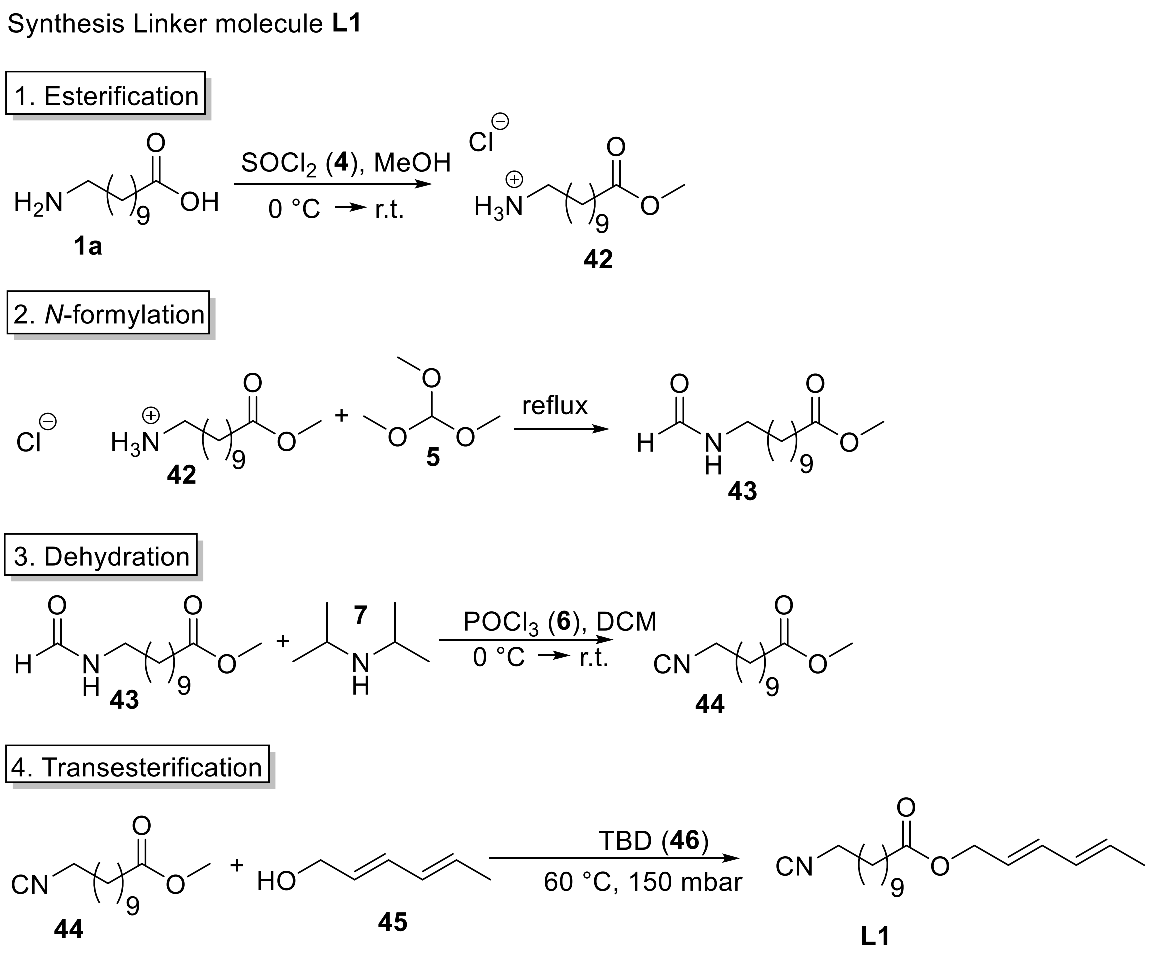
Synthesis Linker molecule L1
1. Esterification
1a
SOCl2 (4), MeOH
0 °C → r.t.
42
2. N-formylation
42
5
reflux
43
3. Dehydration
43
7
POCl3 (6), DCM
0 °C → r.t.
44
4. Transesterification
44
45
TBD (46)
60 °C, 150 mbar
L1

*Scheme 36. Synthesis of linker molecule **L1** containing an isocyanide and a diene moiety. In a first step, an esterification with methanol is carried out, followed by an N-formylation and the dehydration to form the isocyanide. The targeted compound **L1** is obtained via transesterification using sorbic alcohol.*

Each intermediate (compounds **42** – **44**) and the final product **L_1** was characterised by proton and carbon NMR techniques, mass spectrometry, and IR spectroscopy. It is noteworthy that isocyanides cause a very characteristic IR band visible at 2145 cm^{-1} as illustrated in Figure 31. The band in the IR spectrum resulting from the isocyanide group enabled kinetic studies of the P-3CR *via* online IR spectroscopy giving new insights into the reaction. As a result, the kinetic studies allowed for further optimisation of the reaction times, thus significantly reducing the reaction time in the solution phase synthesis.

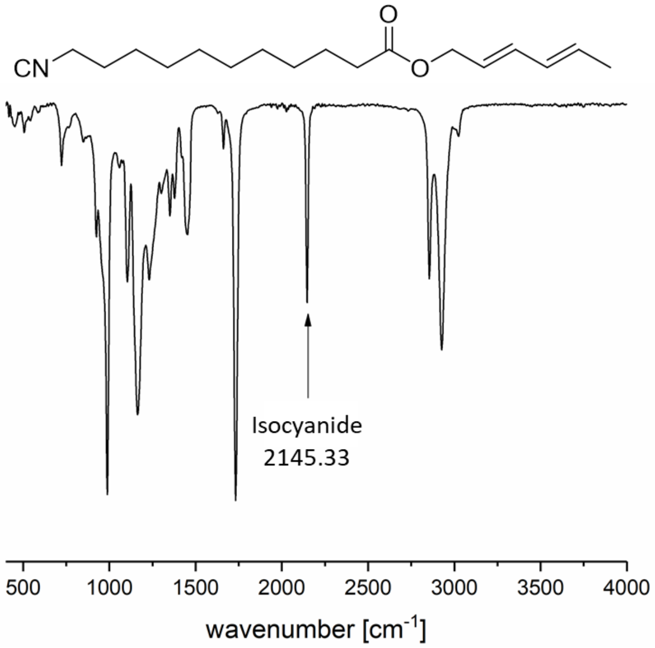

*Figure 31. IR spectrum of the final linker molecule **L1** showing a characteristic isocyanide band at 2145 cm^{-1}.*

L2, containing both, *i.e.* the TAD and the carboxylic acid moieties, was synthesised on 2-gram scale *via* a four-step synthesis with an overall yield of 27% referring to the corresponding urazole compound **47** (the precursor of TAD). The TAD moiety is obtained by oxidation of its respective bench-stable urazole **47** compound in a subsequent reaction step. Therefore, **L2** was obtained by oxidising the urazole **47** in small batches on demand to avoid any undesired degradation, as the stability of the TAD-functionality can vary from hours to months depending on its substituents and purity.[282] The synthesis procedure of **L2** is depicted in Scheme 37 and the overview of isolated yields as well as the exact masses of each synthesis step are summarised in Table 6.

*Table 6. Summary of the results obtained after each synthetic step in the synthesis of the linker molecule **L2**.*

reaction	isolated yield	m/z $_{\text{calc.}}$	m/z $_{\text{found}}$
ethyl phenyl hydrazine-1,2-dicarboxylate **48**	64%[a]	225.0870	225.0872
hexanoic acid semicarbazide **49**	64%[a]	262.1403	262.1396
Urazole **47**	67%[b]	216.0984	216.0981
TAD **L2**	quant. conversion[b]	214.0822	214.1879
Overall yield	27%		

[a] *precipitation,* [b] *crude*

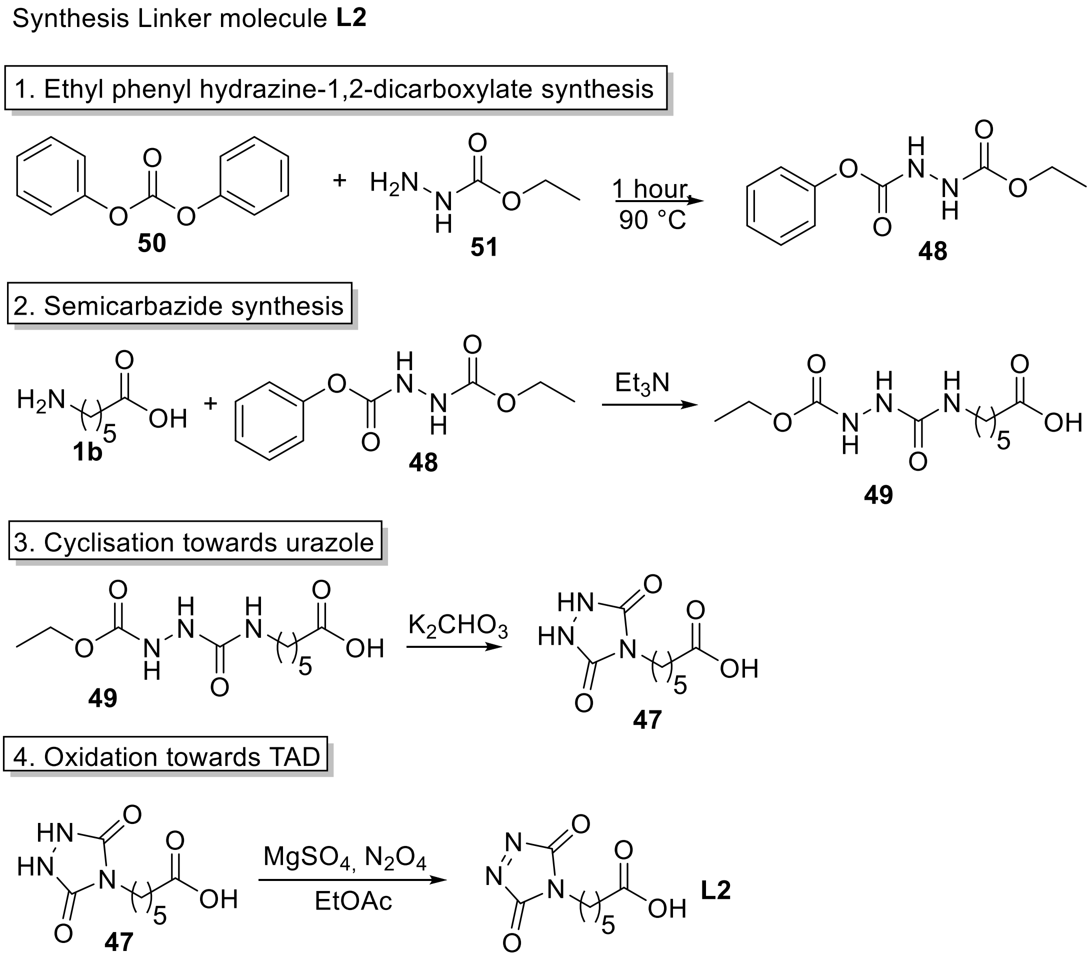
Synthesis Linker molecule L2
1. Ethyl phenyl hydrazine-1,2-dicarboxylate synthesis
50
51
1 hour, 90 °C
48
2. Semicarbazide synthesis
1b
48
Et3N
49
3. Cyclisation towards urazole
49
K2CHO3
47
4. Oxidation towards TAD
47
MgSO4, N2O4
EtOAc
L2

*Scheme 37. Synthesis of the linker molecule **L2** containing a TAD moiety as well as a carboxylic acid.*

The linker molecules **L1** and **L2** contained one moiety that reacts in a Diels-Alder reaction (TAD and a diene) and a second group that is active in the P-3CR (carboxylic acid and isocyanide), respectively, allowing a protecting group-free, iterative approach benefiting from the two orthogonal reactions. The conjugated diene structure in **L1** is a suitable reaction partner for the irreversible TAD Diels-Alder cycloaddition and it is known to be extremely fast and efficient.[282-283] As the third component for the P-3CR, three aldehydes were used from commercially available sources to provide different functionalities. It was already demonstrated previously by our group that a large variety of side chains can be introduced to the oligomeric backbone by varying the aldehyde component in the P-3CR. In the current study, a limited number of three different aldehydes was employed to generate "[ABC]x"-sequences and thus achieve the desired sequence-definition.

Using **L1** and **L2**, a two-step, iterative cycle was developed, consisting of a TAD Diels-Alder reaction, followed by a P-3CR (Scheme 38). Both reactions reached quantitative conversions as well as high yields and were carried out both on the solid phase and in solution. As a result, a sequence-defined dodecamer **52** was obtained on solid phase, while a sequence-defined nonamer **53** was obtained in solution. Apart from the starting block, almost identical sequences were synthesised in both cases. Stearic acid **13** was used as the starting molecule for the solution phase synthesis to facilitate subsequent purifications, as it reduced the polarity of the oligomers. The obtained products were carefully compared with those obtained on solid support regarding yield, purity, reaction time, degree of polymerisation, purification method and scale. An overview of the synthesis strategy is provided in Scheme 38.

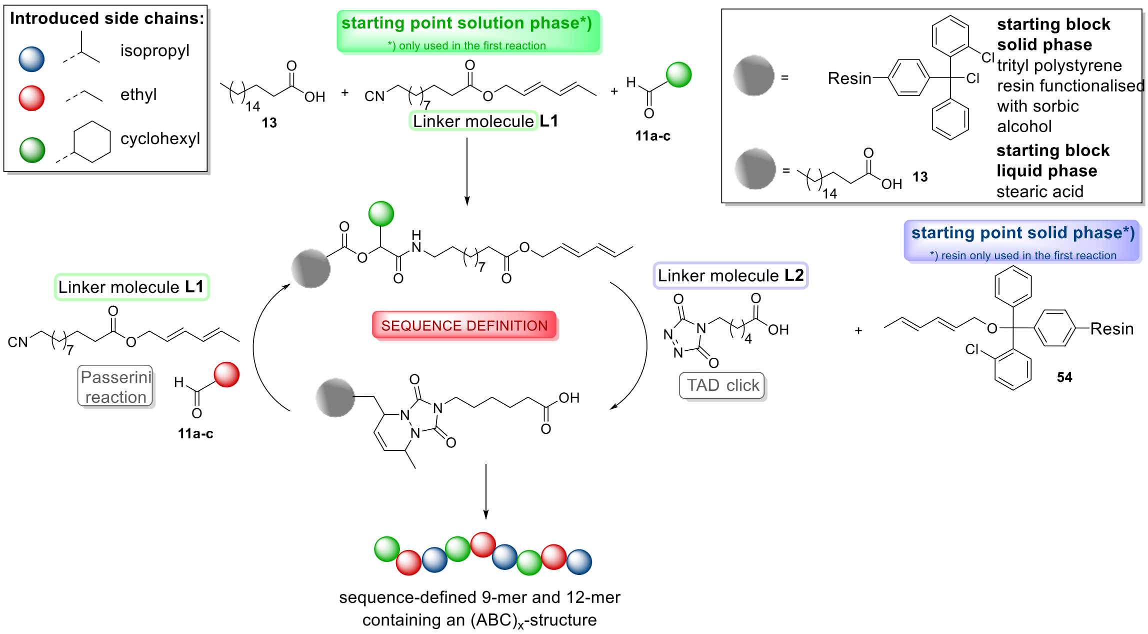
Introduced side chains:
isopropyl
ethyl
cyclohexyl
starting point solution phase*)
*) only used in the first reaction
13
Linker molecule L1
11a-c
Resin
starting block solid phase
trityl polystyrene resin functionalised with sorbic alcohol
starting block liquid phase
stearic acid
13
starting point solid phase*)
*) resin only used in the first reaction
Linker molecule L1
Passerini reaction
11a-c
SEQUENCE DEFINITION
Linker molecule L2
TAD click
54
sequence-defined 9-mer and 12-mer containing an (ABC)x-structure

*Scheme 38. Two-step iterative reaction cycle consisting of the P-3CR and the TAD Diels-Alder reaction, which was employed to synthesise sequence-defined macromolecules on solid phase and in solution. Box top left: different side chains that were introduced to achieve sequence-definition, box top right: two different starting points for solid (resin) and solution phase (stearic acid **13**), respectively.*

For the solution phase synthesis, stearic acid **13** was used as starting substrate, which was first reacted with an aldehyde moiety and the isocyanide group of linker molecule **L1** in a P-3CR. The side chains were introduced by varying the aldehyde component in each P-3CR. Therefore, the commercially available aldehydes propanal **11a**, isobutyraldehyde **11c**, and cyclohexane carboxaldehyde **11b** were used alternatively for the sequence variation to build uniform [ABC]x sequenced macromolecules.

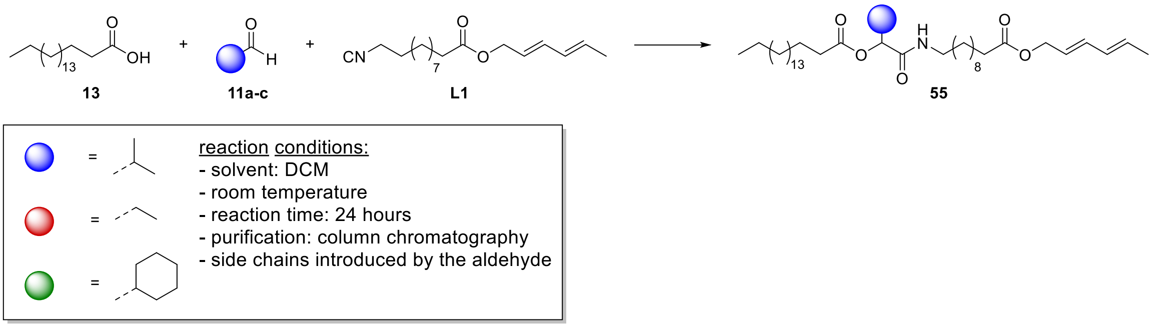

reaction conditions:
- solvent: DCM
- room temperature
- reaction time: 24 hours
- purification: column chromatography
- side chains introduced by the aldehyde

Scheme 39. The P-3CRs that were performed, employing the three aldehydes propanal ***11a****, isobutyraldehyde* ***11c****, and cyclohexane carboxaldehyde* ***11b****, and screened by online IR in order to optimise the reaction conditions for further reactions.*

First, the kinetics of the P-3CR were investigated. Earlier works on the P-3CR never investigated reaction times and typically reported reaction conduction for 24 hours to ensure full conversion.[34-35, 337] To study this, the three different aldehyde compounds **11a-c** were reacted with stearic acid **13** and linker molecule **L1** and the reactions were screened by online IR (see Scheme 39, Figure 32 and experimental section Chapter 6.3.3 for more details). The IR band of the isocyanide at 2145 cm^{-1} was the most characteristic one in the spectrum and thus used for monitoring. Since the isocyanide was used in excess, full conversion was indicated when the intensity of the isocyanide band reached a plateau as shown in Figure 32 and Figure 33. The decrease of the intensity of the isocyanide band was plotted separately for each of the three Passerini reactions in order to compare the results. In Figure 33, the evolution of the intensity obtained by the P-3CR with propanal **11a** as aldehyde component is shown exemplarily. In this case, the plateau was reached after five hours. Overall, a plateau limit was determined for all aldehydes after a reaction time of four to six hours. The Passerini products were purified by column chromatography achieving yields of 96 - 98%. Nevertheless, further P-3CRs were typically stirred for eight to ten hours to ensure full conversion, and thus offering a significant time advantage over previous approaches.

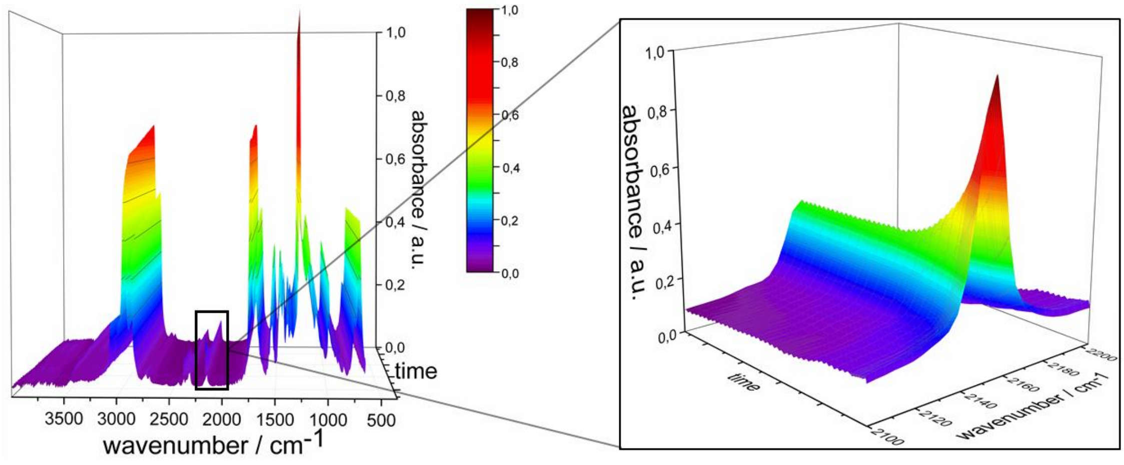

Figure 32. Left: Example of an online IR measurement during a P-3CR highlighting the isocyanide absorption band at 2145 cm^{-1}. Right: By zooming in, the decrease of the absorbance of the isocyanide peak is clearly observed.

In the next step, the first TAD Diels-Alder reaction was performed (see Scheme 40). Since TAD compounds have an intense pink/red colour, which disappears as they are consumed, a visual feedback was observed during the reaction. Hence, the linker molecule **L2** was added in small stoichiometric excess to the reaction mixture and the reaction was conducted as a titration. As soon as the colour slightly remained, the consumption was considered to be complete and the crude product was directly used for the subsequent P-3CR. The straightforward reaction protocol also resulted in a significant advance in time and ease of the procedure. Most importantly, a purification step is circumvented by the combination of TAD with P-3CR. By iterating the two-step cycle several times, sequence-defined oligomers were synthesised.

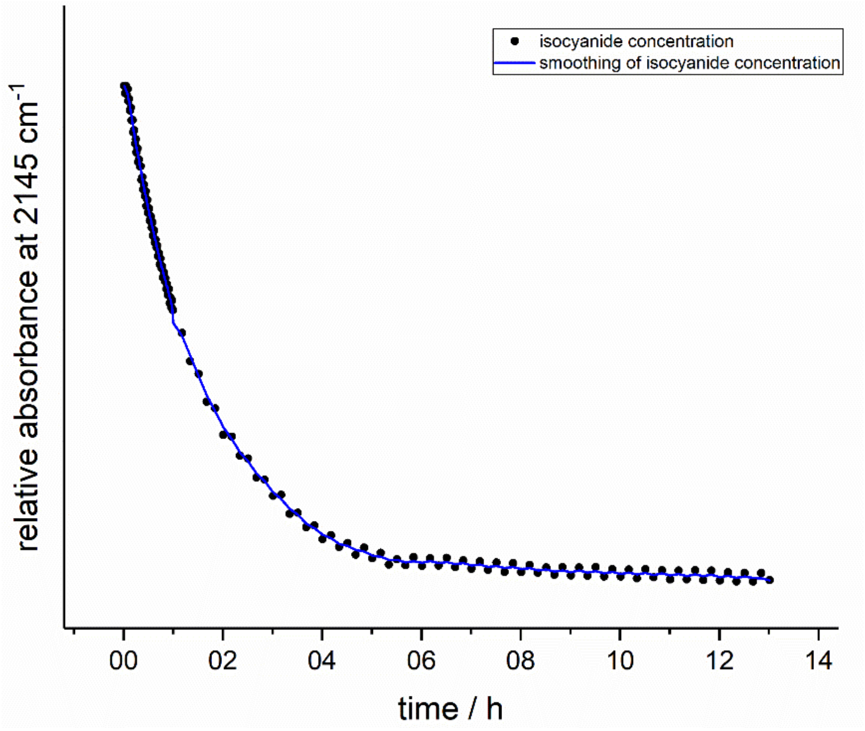

*Figure 33. Online IR analysis of the P-3CR with stearic acid **13**, linker molecule **L1** and propanal **11a** depicting the absorbance decrease of the isocyanide band at 2145.33 cm^{-1} with time. Reaching the plateau indicates full conversion, since **L1** was used in excess. The reaction is complete after 5h20min.*

During the fifth reaction cycle, the online IR measurement was repeated (see experimental section Chapter 6.3.3), confirming an expected slowing-down of the reaction because of possible increasing chain entanglement, thus leading to less accessible end groups. The reaction was observed to be complete after 16 hours. As a consequence, the reaction time was extended to 24 and eventually to 48 hours in further P-3CRs, for making higher molecular weight oligomers accessible. By applying these reaction conditions, a sequence-defined nonamer **53** was obtained.

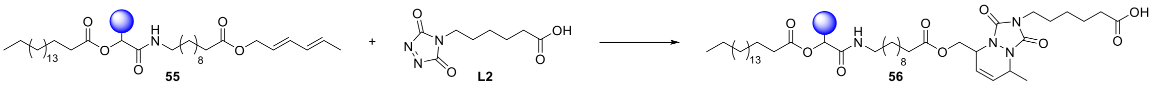

*Scheme 40. TAD Diels- Alder reaction using the linker molecule **L2**. In the first reaction cycle, ethyl side chains were introduced to the molecule via a P-3CR.*

After each P-3CR step, the obtained product was carefully characterised by proton and carbon NMR spectroscopy, IR spectroscopy, mass spectrometry, SEC, SEC-MS and LC-MS analysis. SEC was the most crucial technique to confirm the (mono)dispersity and thus purity of the products. However, SEC analysis (see Scheme 41) revealed that a side reaction had occurred. The SEC measurements were performed using refractive index detectors and the columns used were specifically designed for low molecular weight molecules (100-60,000 Da). The side reaction was not detectable by NMR spectroscopy nor LC-MS analysis. In contrast, even traces of impurities were clearly visible in the SEC chromatogram.

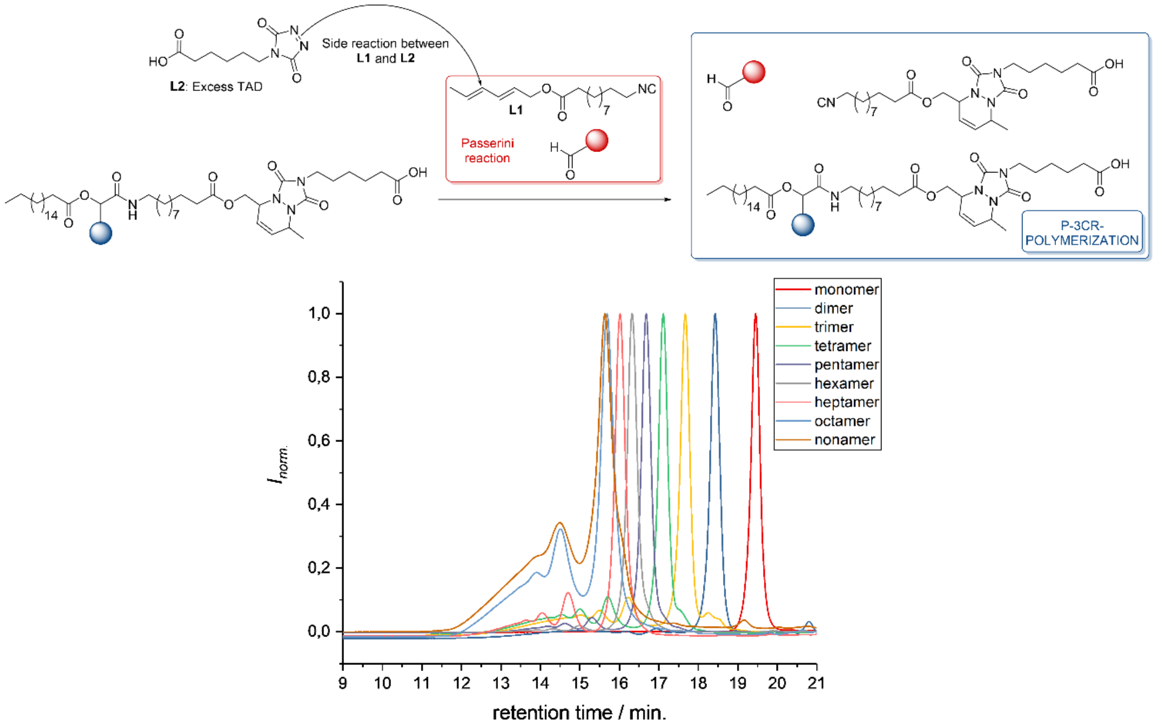

*Scheme 41. Side reaction that occurred between the excess of TAD-COOH molecule **L2,** and the diene isocyanide linker molecule **L1,** leading to an undesired Passerini polymerisation with present aldehydes. SEC traces of the obtained P-3CR polymerisation products. The solution phase synthesis enabled successful identification of the side reaction allowing for further optimisation.**

Starting from the trimer stage, side products of lower retention time, thus higher molecular weight, were obtained, which could not be separated from the product. Over the course of the subsequent reactions, the amount of polymeric side product increased drastically. The reaction mixture of the targeted compound consisted of 46% side product and only 54% sequence-defined nonamer **53**. Furthermore, the side reaction was also observed on the solid phase, albeit to a much lesser extent (see below). Therefore, initial focus was set on optimising the reaction conditions for the solution phase reactions, as the impurity was much more pronounced there. Later, the optimised reaction conditions were applied to the solid-phase approach in order to avoid the undesired side reaction. It is noteworthy that only the solution phase approach enabled a large-scale synthesis of the sequence-defined oligomers, thus allowing for full characterisation after each reaction step. As a consequence, the recurring side reactions could be identified and the reaction progress was understood. The reaction mixture containing both, the side product and the sequence-defined oligomers, was analysed by SEC-ESI-MS and the side product was identified to be the product of a P-3CR polymerisation, occurring because of the small excess of TAD compound remaining after each reaction cycle (Scheme 41). Despite the absence of the pink colour, a trace of TAD-COOH **L2** was still present after evaporation of the solvent from the reaction mixture. The two linker molecules **L1** and **L2** underwent a Diels-Alder click reaction with each other, forming a new AB-type linker molecule carrying a carboxylic acid and isocyanide moiety, which reacted in a P-3CR polymerisation, together with the aldehyde compounds and the sequence-defined oligomer.

---

* SEC measurement was performed at Ghent University (System C). See SI for detailed device information.

To prevent the undesired polymerisation, the reaction conditions were adjusted by adding a non-functional alkene (20 µL of dimethylbut-2-ene **57**) after the TAD addition reaction to quench the excess of linker **L2** *via* an Alder-Ene type reaction.[282-283] The addition of the non-functional alkene **57** resulted in an immediate disappearance of the remaining pink colour and the reaction was then continued with the subsequent P-3CR. Because of the better scalability of the reactions in solution, the optimisation was first performed for the solution phase approach, as it offered the straightforward possibility to investigate the dispersity after every iterative cycle. Afterwards, the optimised conditions were transferred to the solid phase approach. The scalability turned out to be one of the main advantages of the solution phase approach as it contributed to a better understanding of the P-3CR and the polymerisation side reaction. Without identifying the occurring side reaction in solution, it would have been impossible to successfully optimise the reaction conditions. By applying the optimised reaction conditions, the side reaction was prevented and a sequence-defined nonamer **53** of very high purity (>> 99%) was successfully synthesised in solution. The nonamer **53**, with a molecular weight of 5340.02 g·mol^{-1}, was synthesised in 17 reaction steps with an overall yield of 18% (180 mg). SEC analysis verified the high purity of the final product (Figure 5). In SEC-ESI-MS analysis, the mass of the doubly (m/z 2670.97), triply (m/z 1780.99) and quadruply (m/z 1335.86) protonated ions as well as the respective sodium ions were detected and the isotopic pattern was compared with the calculated one, confirming the structure of the product. The nonamer was further analysed by NMR- and IR spectroscopy, as well as by high resolution mass spectrometry, all confirming the high purity of the macromolecule.

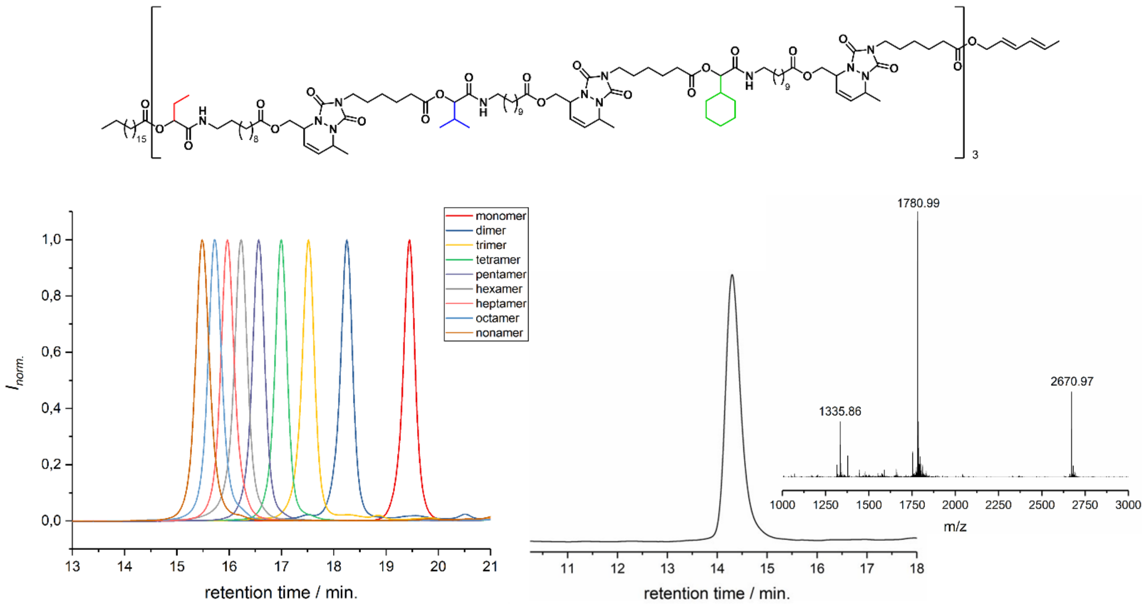

Figure 34. Top: structure of the [ABC]$_3$ sequence-defined nonamer ***53*** *with three different side chains. Bottom left: SEC analysis of the obtained products from the optimised iterative synthesis cycle. The SEC results show the successful prevention of the side reaction and verify the high purity of the products. Bottom right: SEC-ESI-MS analysis of the nonamer showing the chromatogram and the corresponding mass spectrum at a retention time of 14 min 30 s. The assigned mass peaks correspond to the nonamer mass plus two, three and four protons.*[*]

Two-dimensional NMR techniques enabled the assignment of all peaks in the proton NMR. The spectrum is depicted in Figure 35. The most characteristic signals are the ones resulting from the double bonds and the ones of the amide bond at around 5.8 ppm (signal 1). Furthermore, there are two characteristic backbone signals at 5.0 ppm (signal 2 and 3), which were assigned to the branching point towards the side chains. Thus, the successful introduction of additional side chains could easily be verified by integration of this peak. Signals 8 and 9 were assigned to the CH$_2$ groups next to the nitrogen and proton signal 16 was assigned to the terminal CH$_3$ groups.

---

[*] SEC measurement was performed at Ghent University (System C). See SI for detailed device information.

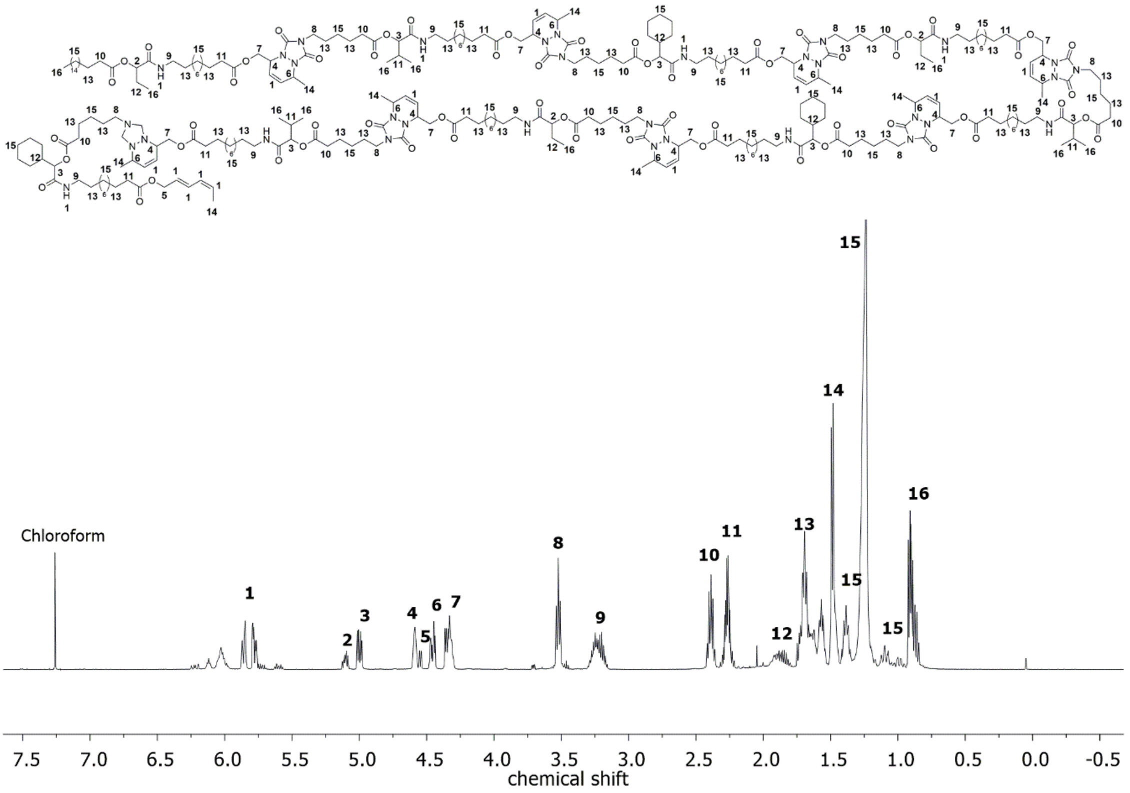

*Figure 35. Proton NMR spectrum of the sequence-defined nonamer **53** synthesised in solution exhibiting an [ABC]$_3$ structure recorded in CDCl$_3$ at 500 MHz.*

The large scale of the solution phase approach allowed for further increasing the molecular weight by coupling two nonamers together using a bis-TAD core molecule **58**, as depicted in Scheme 42. First, the reaction conditions were carefully optimised by coupling two monomers **55** in order not to waste too much of the nonamer **53** for the investigation of the best reaction conditions.

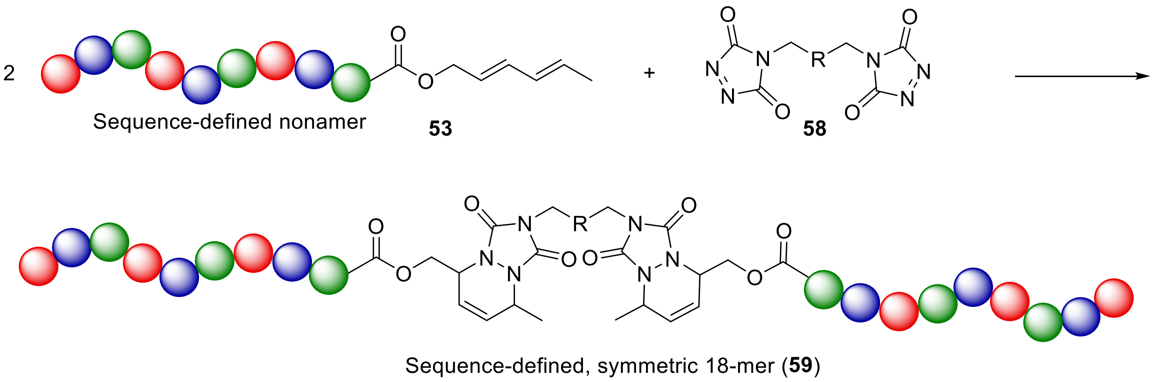

*Scheme 42. Coupling of two sequence-defined nonamers **53** using bis-TAD **58** as a method for increasing the molecular weight of sequence-defined macromolecules.*

Two different solvents, the monomer- (**55**) and the bis-TAD (**58**) concentration, as well as different reaction times were screened (see Table 7).

Table 7. Condition screening for the coupling reaction of two monomers using bis-TAD.

solvent	c (monomer) [mol/L]	c (bis-TAD) [mol/L]	reaction time	conversion
acetone	0.0005	0.036	TAD addition at once, 15 minutes	84%
acetone	0.00025	0.036	TAD addition at once, 15 minutes	84%
acetone	0.000125	0.00036	TAD addition at once, 15 minutes	94% , 17% dead chains
acetone	0.001	0.0045	0.4 eq. added, stirred for 3 h, 0.1 eq. added	90%
dry EtOAc	0.002	0.0072	0.45 eq. added, stirred for 2.5h, 0.1 eq. added	99%

The reactions were performed on a 50 mg scale and the crude products were analysed by SEC without quantifying the yield. The conversion given in Table 7 was determined by integration of the SEC trace. It was found that nearly quantitative conversion towards the symmetric dimer **60** was obtained if the monomer **55** was first dissolved in dry ethyl acetate in a concentration of 0.002 mol/L. Subsequently, 0.45 eq. of the bis-TAD compound **58**, dissolved in dry ethyl acetate were added dropwise to the solution and stirred for three hours at room temperature. Another 0.1 eq. of bis--TAD **58** dissolved in dry ethyl acetate were added and the reaction was stirred for another 30 minutes at room temperature. In the SEC, negligible impurities were observed after the reaction as illustrated in Figure 36. However, the purity is still very high (around 96% according to SEC).

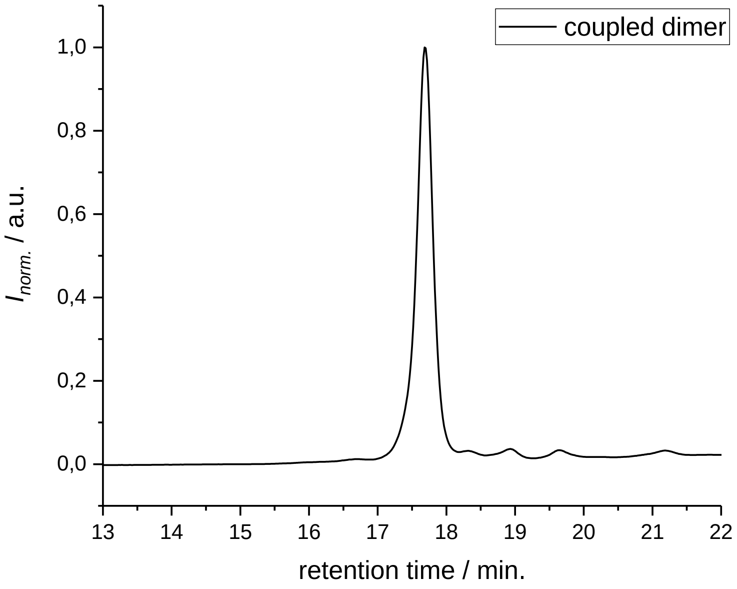

*Figure 36. SEC analysis of the symmetric coupled dimer **60**. The SEC trace is clearly visualising that the product was obtained in high purity.*[*]

After optimisation of the reaction conditions, which allowed for obtaining high conversion towards the coupled dimer **60**, the reaction conditions were applied for the coupling of two nonamers **53**. The reaction was performed on a 50 mg scale and the crude 18-mer **59** was analysed by SEC and SEC-ESI-MS to verify the structure of the obtained product as depicted in Figure 37. The spectra obtained for the nonamer coupling indicate that the conversion was significantly lower compared to the monomer coupling. Besides the main peak at a retention time of 13.4 min, which corresponds to the product as confirmed by mass spectrometry analysis and the obtained isotopic pattern (see Figure 37), there is also a smaller peak towards higher retention time, thus lower molecular weight. According to SEC-ESI-MS, the peak at higher retention time corresponds to a single nonamer coupled to a bis-TAD core unit. Because of the slower coupling reaction, compared to the monomer coupling, and the low stability of the bis-TAD compound, the second unreacted TAD moiety degraded, leading to a considerable amount of dead-chains in the crude product. Purification of the 18-mer **59** by column chromatography was not possible as the difference in polarity was too low, preventing a successful separation.

---

[*] SEC measurement was performed at Ghent University (system C). See SI for detailed device information.

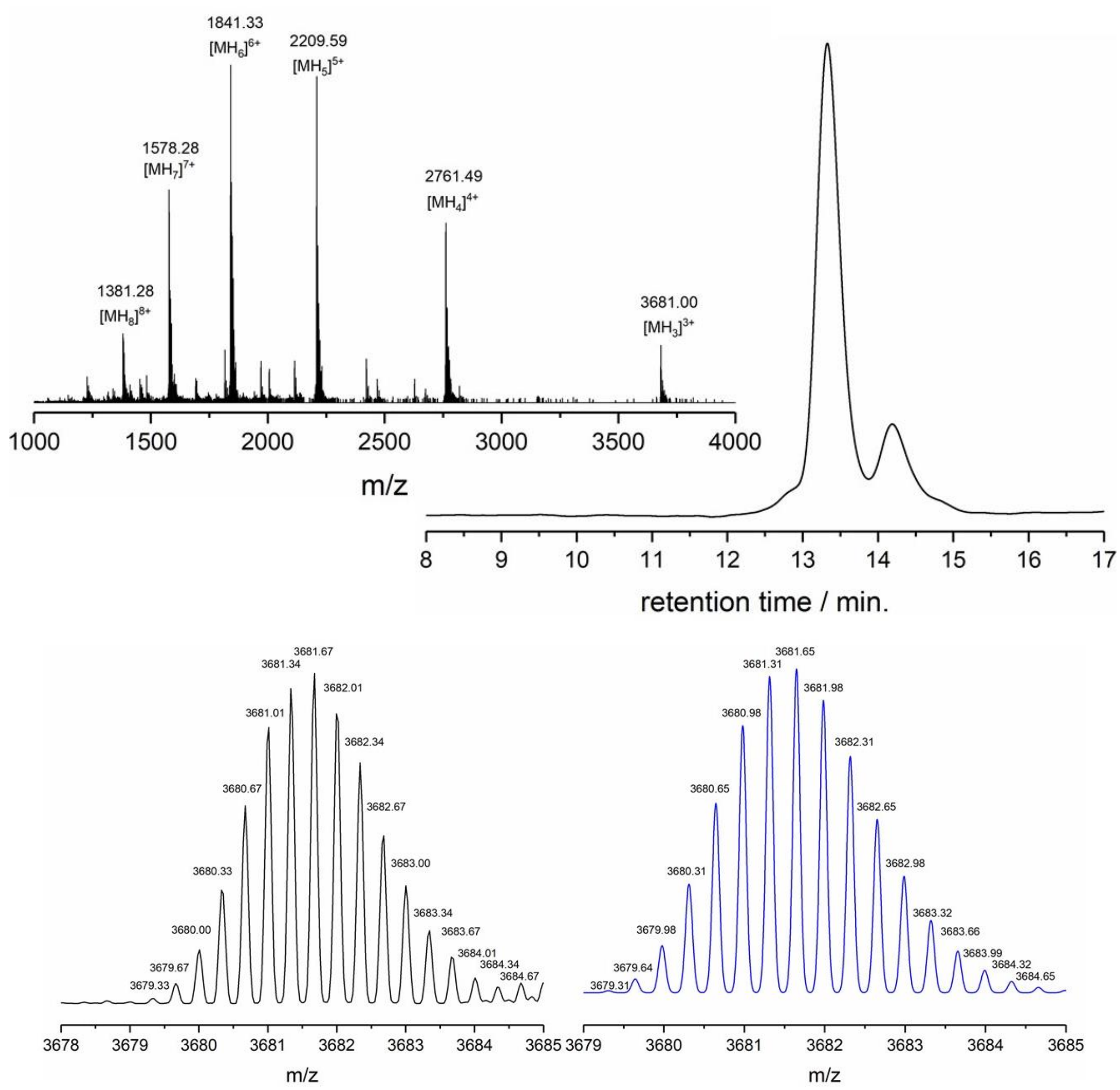

*Figure 37. Top: SEC-ESI-MS analysis of the bis-TAD coupled 18mer **59**. The mass spectrum corresponds to the retention time of the main peak at a retention time of 13.4 min. The three to eight-fold charged protonated 18-mer ions are clearly observed. Bottom: Comparison of the measured (black) with the calculated isotopic pattern (blue), which are in very good agreement clearly proving the structure of the 18-mer.*

It is important to note that the symmetric 18-mer **59** was obtained as the main product and it is noteworthy that by coupling of two nonamers **53** a sequence-defined macromolecule with a molecular weight of 11 042 g/mol is obtained, which is significantly higher compared to previous approaches obtained by the P-3CR.

As mentioned before, the developed synthesis protocol was transferred to the solid phase after optimisation of the reaction conditions. The solid phase synthesis was performed on a 2-chlorotrityl chloride functionalised resin **54** as starting point. An important advantage of this kind of resin are the very mild cleavage conditions (1% trifluoroacetic acid **61** (TFA) in DCM), that prevent unwanted side reactions such as degradation of ester bonds formed by the P-3CR. For the solid phase, the resin was first loaded with sorbic alcohol **45** to provide a suitable reaction site for the first irreversible Diels-Alder reaction. The functionalisation of the resin with sorbic alcohol **45** was adapted from an earlier reported method.[23] For subsequent cycles, the dienophile reactive site is provided by the diene-isocyanide linker molecule **L1**. Starting from the functionalised resin **54** and a monomer **62**, a sequence-defined dimer **63** and trimer **64** were first synthesised separately to confirm the success of the protocol outlined in Scheme 38. The investigation was done by analysing the conversion and the purity of the obtained products *via* LC-MS analysis (Figure 38a). Furthermore, the synthesis of the monomer **62**, dimer **63**, and trimer **64** enabled the complete characterisation of the whole ABC-type sequence by NMR spectroscopy and high-resolution mass spectrometry (HRMS) (see experimental section, Chapter 6.3.3). The three structures were fully resolved by ^{1}H and ^{13}C NMR spectroscopy techniques with the aid of 2D NMR analysis. NMR spectroscopy along with SEC and LC-MS techniques proved the structure of the sequence-defined oligomers and later aided the final analysis of the dodecamer by NMR spectroscopy. After having characterised the first part of the sequence and thus having proven the successful transfer to the solid phase, the protocol was repeated in order to synthesise longer sequences, resulting in an $[ABC]_3$-nonamer and an $[ABC]_4$-dodecamer. To obtain comparable results for the comparative study, the same three aldehydes **11a-c** as in the solution phase approach were used alternatingly in the solid phase approach to introduce the identical side groups.

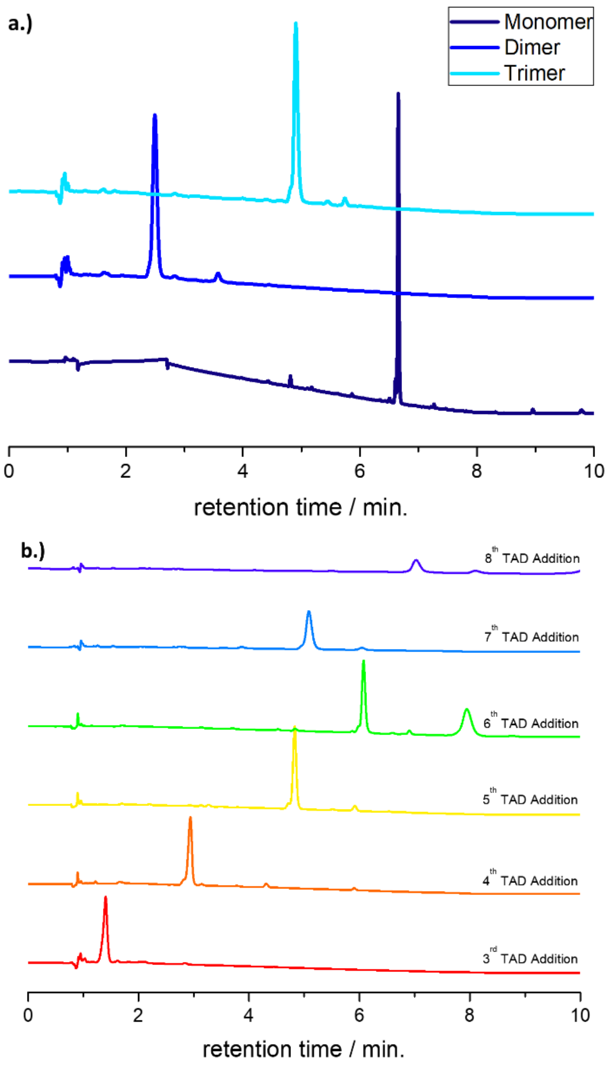

*Figure 38. a) LC-MS chromatograms at λ=214 nm of phenyl-TAD capped monomer **62**, dimer **63** and trimer **64**, demonstrating excellent conversion and purity. The monomer was processed at a solvent gradient of 0 → 100% acetonitrile → water, the dimer **63** and trimer **64** were processed at a 75 → 100% gradient on account of their decreased polarity. The reduced gradient results in a lower retention time for the molecule. b) LC-MS chromatograms at λ=214 nm of the TAD molecule (**L2**) addition step. The increased polarity resulting from the carboxylic acid end-group made the TAD addition step much easier to analyse by LC-MS than the P-3CR step. By following the same step in the cycle, one can see a shift in retention time as the molecular weight increases. It should be noted that the shift in retention time does not continue in a liner fashion because the solvent gradient was changed from 75-100% to 90-100% after the 6th cycle. (See Figure S3 for LC-MS chromatograms of each step in the cycle).*

One of the most important advantages of solid phase chemistry is the possibility to work with large excesses of reagents to ensure 100% conversion, since purification is simplified massively by just washing unwanted starting material away. Particularly for sequence-defined synthesis, simple purification is highly advantageous, as long sequences require a high number of iterative synthesis steps. The simple workup of the products results in a time and labour-saving approach compared to purification *via* column chromatography. Furthermore, the synthesis can, in principle, be automated, further accelerating the process.[23, 398] The high reactivity of TAD molecules required only two equivalents of **L2** for the TAD addition step, which is notably low for solid phase synthesis, compared to other reported procedures [23, 130, 399] with shaking for only 5 minutes at room temperature to ensure 100% conversion. The conversion was quantified by LC-MS (see experimental section chapter 6.3.3).

In the first P-3CR on solid phase, the reaction time was optimised by following the reaction progress *via* LC-MS. Interestingly, the reaction was much faster than anticipated as it was complete within 30 minutes reaching up to twelve times faster than in solution. The equivalents of reagents were increased 10-fold with respect to the solution phase reaction conditions which is in line with previous solid phase reactions of the Du Prez working group.[23, 130, 399] The fast conversion of the reactants on solid phase is a direct result of the high excess of reagents. Since LC-MS analysis after each cycle showed a slowing down of the reaction as the oligomer grew larger, the reaction time was increased every 3-4 cycles by 30 minutes. The kinetic behaviour was expected as it is known from the solution phase kinetics (see above) that the reaction slows down with increasing oligomer length.

The main disadvantage of solid phase chemistry is its limited scale. In the current approach, reactions were carried out on 50 mg of resin **54**, yielding 14.4 mg of the dodecamer **52**, once cleaved from the resin. The small scale resulted in a limited range of characterisation techniques available to use, which made optimisation on solid phase too difficult. The reactions were followed by LC-MS as this technique only requires very small amounts of the sample. Nonetheless, because of the high molecular weight oligomers achieved here (7200 Da), compared to our previous reported works (*ca.* 4000 Da),[23, 35, 130, 399] the limitations of the used LC-MS equipment became clear, as displayed in Figure 38b, by the 7th TAD addition step (*ca.* 3800 Da). In general, LC-MS was much more useful after the TAD-COOH addition reaction in the iterative cycle, as the more polar end-group resulted in a lower retention time in the LC. After the P-3CR step of the 4th cycle, LC-MS analysis became unsuitable as the long, non-polar carbon chain from the linker molecule **L1** resulted in a too high retention time for accurate and quantitative analysis. Even with a reduced solvent gradient from acetonitrile to water of 75-100% and eventually 90-100% instead of the usual 0-100% did not significantly decrease the retention time. Therefore, the sequence was eventually continued without intermediate analysis and the final dodecamer **52** was analysed by IR, NMR spectroscopy and SEC once cleaved from the resin. Half of the reaction sample at the nonamer **65** stage was taken for intermediate analysis and the reaction was continued to the dodecamer **52** with the remaining 25 mg of resin.

In order to compare the solid phase results with the solution phase approach, analysis of the solid phase synthesised trimer **64**, nonamer **65** and dodecamer **52** was also conducted by SEC (see Figure 39, left). SEC was the preferred method of analysis for the oligomers synthesised in solution, as this approach allows for a bigger reaction scale enabling sampling after each cycle and the above-mentioned problems of the LC-MS analysis could be overcome. Thus, one could easily compare both the purity and (mono)dispersity of the obtained oligomers. In order not to lose material during the synthesis of the dodecamer **52**, a separate trimer **64** was synthesised for SEC analysis, as this could be quickly done within just three hours *via* the solid phase approach. For each of the oligomers, the conjugated diene chain end was "end-capped" with phenyl-TAD **66** before SEC analysis, to prevent any further side reaction or cleavage of the ester bond induced by acid hydrolysis during cleavage from the solid phase resin. SEC analysis revealed a small amount of impurity of the nonamer **65** and dodecamer **52** being dead chains (14%) and the polymerisation side-product (12%), that was previously also observed in solution. Thus, the final product **52** was obtained in a purity of 74%, applying the initial reaction conditions.

In case of the solid phase approach, the same Passerini polymerisation side reaction as in solution was observed, but to a significantly smaller extend. However, solid phase synthesis did not allow for identification or optimisation of the reaction. Hence, performing the reactions in solution was crucial to further understand the observed side-reactions (see above) and to optimise the procedure. After having applied the initial reaction conditions (no quenching of unreacted TAD **L2**) on the solid phase approach, the optimised conditions (quenching any excess of unreacted TAD **L2** with 2,3-dimethylbutene **57**) were also transferred to the solid phase approach. A new nonamer **65** was synthesised to verify that the optimisation worked for both approaches. A significant increase in the purity was confirmed by SEC (see Figure 39). The product was also analysed by SEC-ESI-MS to further confirm the structure. The purity of the sequence-defined nonamer **65** increased from 74% to 84% as a result of the optimised conditions. The previously observed polymerisation side reaction was successfully suppressed to a minimum. However, minor impurities were still observed and could be attributed to the fact that whilst theoretically solid-phase synthesis facilitates 100% conversion, in practice it is often slightly lower, depending on the handling of the resin. That, combined with the multi-step, iterative nature of this protocol, results in a small amount of lower molecular weight products (dead chains) still present in the LC-MS chromatogram of the oligomers, as can be seen in Figure 39 (right). One could potentially attribute the lower molecular weight impurities to human error, as it has been reported that automation introduces more consistency into iterative approaches, thus improving purity and reproducibility.[398]

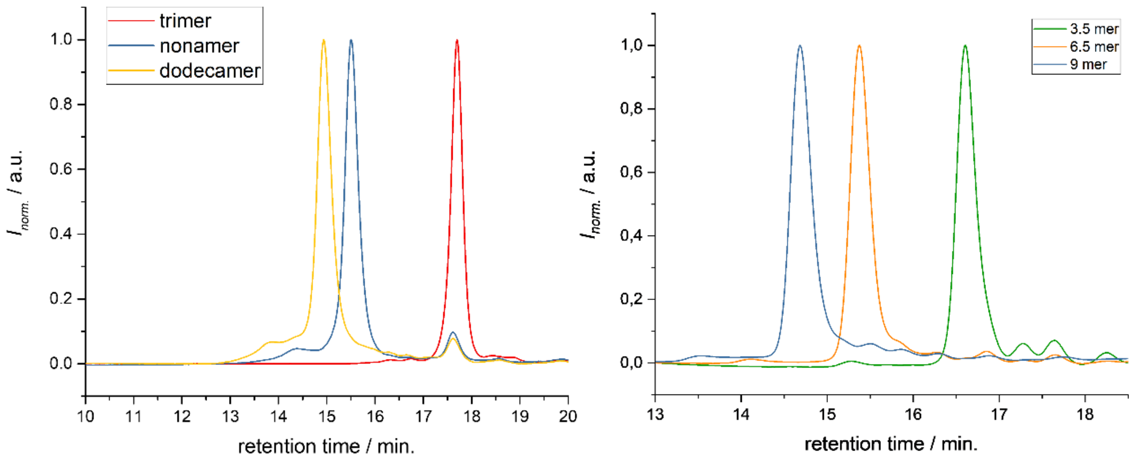

*Figure 39. Left: Evolution of the solid phase synthesised oligomer from trimer **64** through to nonamer **65** and dodecamer **52** before optimisation. In the chromatogram of the nonamer **65**, and even more in the one of the dodecamer **52**, a minor high molecular weight side-product is observed (left of the main peak), while a dead chain from the trimer level of the synthesis (right of the main peak) is also present.** *Right: SEC analysis of the solid phase synthesised oligomers after optimisation, depicting the 3.5 mer **67**, 6.5 mer **68** and nonamer **65**. The P-3CR polymerisation side product was significantly reduced following the successful application of the optimisation conditions.*†

In summary, a new approach towards sequence-defined macromolecules was developed, combining the advantages of the P-3CR with the very efficient and ultra-fast TAD chemistry. A careful comparison of this approach carried out in solution as well as on solid phase is given in Table 8. In solution, following the successful application of the optimisation conditions, 180 mg of a uniform nonamer **53** with a purity of >99% was obtained in 17 reaction steps, with an overall yield of 18%. P-3CRs were carried out over a reaction time of 8 to 48 hours, while TAD Diels-Alder reactions were complete in less than 5 minutes. The products were purified by column chromatography, which is effective, but time consuming. Here, the reactions were typically carried out on a 200 mg scale but, theoretically, the synthesis could easily be scaled up to multigram scale, which is a main advantage of solution phase, as optimisation or applications are only feasible if enough material is obtained.

---

* SEC measurement was performed at Ghent University (system C). See SI for detailed device information.

† SEC measurement was performed at KIT in Karlsruhe (system B). See SI for detailed device information.

Table 8. Direct comparison of the two synthesis techniques (i.e. solid phase and solution phase chemistries).

	Solid phase	Solution phase
yield [%]	5	18
purity [%]	84	>99
scale	50 mg	200 mg
degree of polymerisation	9*	9
purification method	washing	column chromatography
reaction time	<5 min.,$^{a)}$ 30-120 min.$^{b)}$	5 min.,$^{a)}$ 8-48 h$^{b)}$
overall required time	2 days	3 weeks

** Prior to optimisation, a degree of polymerisation of 12 was achieved. Reaction time for $^{a)}$ TAD Diels-Alder reaction and $^{b)}$ P-3CR.*

On solid phase, on the other hand, a dodecamer **52**, was synthesised in 25 steps with an overall yield of 5% (14.4 mg). The synthesis was performed using 50 mg of loaded resin and the final product was first obtained with a purity of 74%, because of a P-3CR polymerisation as a side reaction. This side reaction was originally observed to a much greater extent with the solution phase approach. However, simple reaction optimisation in solution showed how the side reaction could be successfully prevented, leading to a very practical and quick build-up of oligomers. Accordingly, the optimisation was later successfully transferred to the solid phase approach to synthesise a sequence-defined nonamer **65**, where the purity was significantly increased to 84%. The most important advantage of the solid phase approach is the required time, not only for the reactions themselves, but also for the purification. P-3CRs were performed within 30 to 120 minutes, while TAD Diels-Alder reactions reached full conversions in less than five minutes. The products were purified by simple washing procedures. Thus, working on a solid support simplifies and accelerates the synthesis and workup procedure significantly. The synthesis of a nonamer in solution requires approximately three weeks, whereas the same molecule synthesised on a solid support can be obtained within two days. The purity of the oligomers obtained on solid phase was, however, slightly lower compared to the oligomers obtained in solution.

The comprehensive study presented here, clearly demonstrates the power of combining click chemistry with multicomponent reactions. This combination leads to an ideal situation for iterative growth and multifunctionalisation of macromolecules, significantly improving already reported procedures in terms of purity, time and transferability between approaches for scalability. The current comparative study, also demonstrates very nicely that many different and versatile chemistries can be carried out on both the solid phase and in solution. The user choice for the appropriate procedure should be guided by decisions of synthesis speed, potential for library synthesis, required purity and necessary scale.

5 Conclusion and Outlook

Multi-component reactions (MCRs), and the Passerini three-component reaction (P-3CR) in particular, are valuable tools for the synthesis of sequence-defined macromolecules of different architecture and structure. The straightforward and sequential built-up of defined sequences on a large scale, with high yields and purity is possible using these platforms. Moreover, the modular character of the P-3CR allows for a high structure versatility with respect to the side chains and backbone of the oligomers, making it the method-of-choice for the synthesis of sequence-defined macromolecules. Nonetheless, the use of such polymers for applications such as data storage is still hampered by the laborious purification procedures and the limited scalability of these approaches.

This thesis highlights that the P-3CR allows for the sequence-defined synthesis of high molecular weight oligomers in high purity and yield *via* different strategies, especially in combination with other reactions. In chapter 4.1.1 of this thesis, sequence-defined polymers bearing terminal double bonds were synthesised using P-3CRs and were subsequently ring-closed into unprecedented macrocyclic structures. Furthermore, the uniform linear precursors were used for structure-activity relationship investigations during RCM reactions, which allowed to uncover clear trends regarding the limits of such RCMs, inaccessible with analogous disperse precursors, thus demonstrating a possible application of sequence-defined materials.

The ability of increasing the degree of definition for P-3CR reactions was then demonstrated by varying both the side chain and the backbone of the oligomers (Chapter 4.1.2). In each iterative cycle, the aldehyde component and as well as the isocyanide monomer were varied in order to achieve dual sequence-definition of the side chain and the backbone. This approach allowed to increase the degree of definition significantly and holds the promise of multiplying the data storage capacity of such macromolecules.

In the last part of this thesis (Chapter 4.2), a new strategy towards sequence-defined macromolecules was developed by introducing TAD Diels-Alder click chemistry to the P-3CR. This powerful combination of two orthogonal reactions leads to an ideal situation for iterative growth and multifunctionalisation of macromolecules, significantly improving already reported procedures in terms of purity and time. Furthermore, the same chemistry was conducted on solid phase and in solution, and a detailed comparison for these two important and frequently used synthetic strategies in the field of sequence-defined macromolecules, and in polymer chemistry in general, was established. Importantly, oligomers of very high molecular weight were obtained *via* both approaches, and a sequence-defined 18-mer with a molecular weight of over 11 kDa could be obtained using the solution-based approach.

Overall, these synthetic pathways open up new routes to sequence-defined polymers *via* the P-3CR. Further investigations are necessary to reach even higher degrees of control as well as higher densities of functional groups per repeating unit, enhancing the potential of sequence-defined macromolecules for data storage applications. Improvements are also necessary for the read-out strategy of such code-containing macromolecules, as the currently used tandem mass spectrometry destroys the sample, and non-destructive alternatives, such as novel NMR spectroscopy analysis methods, would allow for the re-use of the polymer. Besides the full control over the side chains and the backbone, the introduction of chiral centres into the sequence would allow to investigate the influence of chirality on material properties. This would establish a new dimension in the field of sequence-defined macromolecules and lead to new synthetic challenges , such as chirality control during the synthesis Ultimately, this could lead to artificial secondary structures of sequence-defined polymers which, in combination with the introduction of catalytically active sites into such macromolecules, would allow for the synthesis of artificial enzymes and pave the way towards promising applications in biology and medicine.

6 Experimental Section

6.1 Materials

The following chemicals were used as received from the following suppliers unless otherwise noted: 11-aminoundecanoic acid **1a** (97%, Sigma-Aldrich), 6-aminohexanoic acid **1b** (≥ 99%, VWR), 12-aminododecanoic acid **1c** (98%, ChemPur), β-alanine **1d** (99%, Sigma-Aldrich), 4-aminobutyric acid **1e** (≥ 99%, Sigma-Aldrich), 4-(4-aminophenyl)butanoic acid **1f** (≥ 95%, ChemPur), 3-(4-aminophenyl)propanoic acid **1g** (97%, ChemPur), 3-aminophenyl acetic acid **1h** (97%, Sigma-Aldrich), 4-(aminomethyl)benzoic acid **1i** (97%, Sigma-Aldrich), benzyl alcohol **3** (99%, Sigma-Aldrich), thionyl chloride **4** (99%, Sigma-Aldrich), trimethyl orthoformate **5** (99%, Sigma-Aldrich), phosphoryl trichloride **6** (99%, Sigma-Aldrich), diisopropylamine **7** (DIPEA) (> 99.5%, Sigma-Aldrich), glutaric acid **9** (99%, Sigma-Aldrich), sebacic acid **10** (99%, Sigma-Aldrich), hydrochloric acid in 1,4-dioxane (*ca.* 4 mol/L, Tokyo Chemical Industry), hydrochloric acid (36 wt%, Chem Lab NV), propanal **11a** (> 98%, Tokyo Chemical Industry and 97%, Sigma-Aldrich), cyclohexanal **11b** (97%, Alfa Aesar and > 98%, Tokyo Chemical Industry), isobutyraldehyde **11c** (98%, Sigma-Aldrich and >98%, Tokyo Chemical Industry), 10-undecenal **11d** (90%, SAFC and 90% Sigma-Aldrich), isovaleraldehyde **11e** (≥ 98%VWR), octanal **11f** (99%, Sigma-Aldrich), dodecanal **11g** (≥ 95%, VWR), 2-phenylpropanal **11h** (98%, Fisher Scientific), Grubbs 1st generation catalyst **12** (97%, Sigma-Aldrich), stearic acid **13** (98%, Tokyo Chemical Industry), palladium on activated charcoal

19 (10% palladium basis, Sigma-Aldrich), *trans*,*trans*-2,4-hexadien-1-ol (sorbic alcohol) **45** (97%, Sigma-Aldrich and 98%, Alfa Aesar), 1,5,7-triazabicyclo[4.4.0]dec-5-ene (TBD) **46** (98%, Sigma-Aldrich), diphenyl carbonate **50** (99%, Acros Organics), Ethyl carbazate **51** (97%, Tokyo Chemical Industry), 2-chlorotrityl chloride resin **54** (100-200 mesh, 1% DVB, 1.6 mmol/g, Iris Biotech GmbH), 2,3-dimethylbut-2-ene **57** (≥ 99.9%, Sigma-Aldrich), trifluoroacetic acid **61** (TFA, peptide grade, Iris Biotech GmbH), *p*-benzoquinone **69** (> 98%, Sigma-Aldrich), ethyl vinyl ether **70** (99%, Sigma Aldrich), triethylamine **81** (99%, anhydrous, Acros Organics), pyridine **82** (99.5%, anhydrous, Acros Organics), dinitrogen tetroxide (Gerling Holz & Co, Germany), hydrogen (99,999%, Air Liquide), TLC silica gel F_{254} (Sigma-Aldrich), Silica gel 60 (0.040 - 0.063, Sigma-Aldrich and Rocc), cerium(IV)-sulfate (99%, Sigma-Aldrich), phosphomolybdic acid hydrate (99%, Sigma-Aldrich), sodium carbonate (98%, Sigma-Aldrich), sodium hydrogen carbonate (> 95%, Sigma-Aldrich), sodium sulfate (> 99%, anhydrous, Sigma-Aldrich),. potassium carbonate (≥ 99%, Carl Roth), magnesium sulfate (≥ 99%, Carl Roth), MeCN-d3 (≥ 99.8%, Euriso-top), DMSO-d6 (≥ 99.8%, Euriso-top), MeOH-d4 (≥ 99.8%, Euriso-top), CDCl3 (≥ 99.8%, Euriso-top), anhydrous ethyl acetate (99.8%, Sigma-Aldrich), acetonitrile (HPLC grade ≥ 99.9%, Sigma-Aldrich), chloroform (HPLC grade ≥ 99.9%, Sigma-Aldrich), dichloromethane (DCM, HPLC grade ≥ 99.9%, Sigma-Aldrich), methanol (HPLC grade 99.8%, Acros Organics), dimethylformamide (DMF, 99.8%, anhydrous, Acros Organics), tetrahydrofuran (THF, 99.5%, extra dry over molecular sieves, Acros Organics), ethanol (analytical reagent grade, Fisher Scientific), diethyl ether (analytical reagent grade, Fisher Scientific), hexane (technical grade, Univar), ethyl acetate (technical grade, Univar). All solvents were used without further purification, unless otherwise noted. Water, when used in the synthesis, was de-ionised.

6.2 Instrumentation

NMR ^{1}H spectra were recorded at the Karlsruhe Institute of Technology (KIT, Germany) on a Bruker AVANCE DRX at 500 MHz and ^{13}C-NMR Attached Proton Test (APT) spectra were recorded at 125 MHz. $CDCl_3$ or CD_3OD were used as solvents. Chemical shifts are presented in parts per million (δ) relative to the resonance signal at 7.26 ppm (^{1}H, $CDCl_3$) and 77.16 ppm (^{13}C, $CDCl_3$) or 3.31 ppm (^{1}H, CD_3OD) and 49.00 ppm (^{13}C, CD_3OD), respectively.

NMR ^{1}H spectra were recorded at Ghent University (UGent, Belgium) on a Bruker Avance 300, a Bruker Avance 400, Bruker Avance 500 or a Bruker Avance II 700 and ^{13}C-NMR Attached Proton Test (APT) spectra were recorded at 100 MHz on a Bruker Avance 400. DMSO-d_6, CD_3OD, $CDCl_3$ or CD_3CN were used as solvents. Chemical shifts are presented in parts per million (δ) relative to the resonance signal at 2.50 ppm (^{1}H, DMSO-d_6) and 39.51 ppm (^{13}C, DMSO-d_6), 3.31 ppm (^{1}H, CD_3OD)

and 49.00 ppm (^{13}C, CD_3OD), 7.26 ppm (^{1}H, $CDCl_3$) and 77.16 ppm (^{13}C, $CDCl_3$) or 1.94 ppm (^{1}H, CD_3CN) and 118.26 ppm (^{13}C, CD_3CN), respectively.

Coupling constants (*J*) are reported in Hertz (Hz). All measurements were recorded in a standard fashion at 25 °C unless otherwise stated. Full assignment of structures was aided by 2D NMR analysis (COSY, HSQC and HMBC).

Oligomers were characterized on a Varian 390-LC **gel permeation chromatography (GPC)** system (**System A**) equipped with a LC-290 pump (Varian), refractive index detector (24 ° C), PL AS RT GPC-autosampler (Polymer laboratories) and a Varian Pro Star column oven Model 510, operating at 40 ° C. For separation, two SDV 5 µm linear S columns (8 × 300 mm) and a guard column (8 × 50 mm) supplied by PSS, Germany, were used. Tetrahydrofuran (THF) stabilized with butylated hydroxytoluene (BHT, HPLC-SEC grade) supplied by Sigma Aldrich was used at a flow rate 1.0 mL min-1. Calibration was carried out with linear poly(methyl methacrylate) standards (Agilent) ranging from 875 to 1 677 000 Da. Detection was done by a refractive index detector operating in THF (flow rate 1.0 mL min^{-1}).

Size Exclusion Chromatography (SEC) measurements were performed on a SHIMADZU Size Exclusion Chromatography (SEC) system (**System B**) equipped with a SHIMADZU isocratic pump (LC-20AD), a SHIMADZU refractive index detector (24°C) (RID-20A), a SHIMADZU autosampler (SIL-20A) and a VARIAN column oven (510, 50°C). For separation, a three-column setup was used with one SDV 3 µm, 8×50 mm precolumn and two SDV 3 µm, 1000 Å, 3×300 mm columns supplied by PSS, Germany. Tetrahydrofuran (THF) stabilized with 250 ppm butylated hydroxytoluene (BHT, ≥99.9%) supplied by SIGMA-ALDRICH was used at a flow rate of 1.0 mL min^{-1}. Calibration was carried out by injection of eight narrow polymethylmethacrylate standards ranging from 102 to 58300 kDa.

Oligomers were characterised at Ghent University (UGent, Belgium, **System C**) on a Waters **Size Exclusion Chromatography (SEC)** system equipped with a Waters 1515 isocratic pump, Waters 2410 refractive index detector (24 °C), Waters 717plus autosampler and a Waters 2487 dual λ absorbance UV detector and column oven. For separation, a three-column setup was used with one SDV 3 µm, 8×50 mm precolumn and two SDV 3 µm, 1000 Å, 8×300 mm columns supplied by PSS, Germany. Tetrahydrofuran (THF) stabilized with butylated hydroxytoluene (BHT, HPLC-SEC grade) supplied by Biosolve was used at a flow rate 1.0 mL min^{-1}. Calibration was carried out by three injections of a mixture of narrow polystyrene standards ranging from 162 to 38640 kDa.

SEC-ESI-MS spectra were recorded on a Q Exactive (Orbitrap) mass spectrometer (Thermo Fisher Scientific, San Jose, CA, USA) equipped with a HESI II probe. The instrument was calibrated in the *m/z* range 74–1822 using premixed calibration solutions (Thermo Scientific). A constant spray voltage of 4.6 kV, a dimensionless sheath gas of 8, and a dimensionless auxiliary gas flow rate of 2 were applied. The capillary temperature and the S-lens RF level were set to 320 °C and 62.0, respectively. The Q Exactive was coupled to an UltiMate 3000 UHPLC System (Dionex, Sunnyvale, CA, USA) consisting of a pump (LPG 3400SD), autosampler (WPS 3000TSL), and a thermostated column department (TCC 3000SD). Separation was performed on two mixed bed size exclusion chromatography columns (Polymer Laboratories, Mesopore 250 × 4.6 mm, particle diameter 3 µm) with precolumn (Mesopore 50 × 4.6 mm) operating at 30 °C. THF at a flow rate of 0.30 $\mathrm{mL \cdot min^{-1}}$ was used as eluent. The mass spectrometer was coupled to the column in parallel to a RI-detector (RefractoMax520, ERC, Japan). 0.27 $\mathrm{mL \cdot min^{-1}}$ of the eluent were directed through the RI-detector and 30 $\mathrm{\mu L \cdot min^{-1}}$ infused into the electrospray source after post-column addition of a 100 µM solution of sodium iodide in methanol at 20 $\mathrm{\mu L \cdot min^{-1}}$ by a micro-flow HPLC syringe pump (Teledyne ISCO, Model 100DM). A 20 µL aliquot of a polymer solution with a concentration of 2 $\mathrm{mg \cdot mL^{-1}}$ was injected onto the HPLC system.

Orbitrap Electrospray-Ionisation Mass Spectrometry (ESI-MS) mass spectra were recorded on a Q Excative (Orbitrap) mass spectrometer (Thermo Fisher Scientific, San Jose, CA, USA) equipped with an atmospheric pressure ionisation source operating in the nebuliser assisted electrospray mode. The instrument was calibrated in the m/z-range 150-2000 using a standard containing caffeine, Met-Arg-Phe-Ala acetate (MRFA) and a mixture of fluorinated phosphazenes (Ultramark 1621, all from Sigma Aldrich). A constant spray voltage of 3.5 kV, a dimensionless sheath gas of 6, and a sweep gas flow rate of 2 were applied. The capillary voltage and the S-lens RF level were set to 68.0 V and 320°C, respectively.

Electron ionisation (EI) For the measurements that were performed with the electron ionisation (EI) method, an instrument by Finnigan, model MAT 90 (70 eV), was used with 3-nitrobenzyl alcohol (3-NBA) as matrix. For the interpretation of the spectra, molecular peaks $[M]^+$, peaks of pseudo molecules $[M+H]^+$ and characteristic fragment peaks are indicated with their mass to charge ratio (*m/z*) and their intensity in percent, relative to the most intense peak (100%).

Fast atom bombardment (FAB) mass spectra were recorded on a *Finnigan* MAT 95 instrument. The protonated molecule ion is expressed by the term: $[(M+H)]^+$.

High Resolution Mass Spectroscopy (HRMS) spectra were collected at UGent using an Agilent 6220 Accurate-Mass time-of-flight (TOF) equipped with a multimode ionisation (MMI) source.

Liquid Chromatography-Mass Spectrometry (LC-MS) spectra were recorded on an Agilent technologies 1100 series LC/MSD system equipped with a diode array detector and single quad MS detector (VL) with an electrospray source (ESI-MS) for classic reversed phase LC-MS and MS analysis. Analytic reversed phase HPLC (high-performance liquid chromatography) was performed with a Phenomenex Kmetex C18 (2) column with a solid core at 35 °C and a flow rate of 1.5 mL/min

(5 µ, 150 x 4.6 mm) using a solvent gradient (0 → 100% acetonitrile in H_2O in 6 min) and the eluting compounds were detected *via* UV-detection (λ = 214 nm).

Infrared spectra (IR) were recorded at the KIT on a Bruker Alpha-p instrument in a frequency range from 3998 to 374 cm^{-1} applying KBr and Attenuated Total Reflection (ATR) technology or at UGent on a Perkin Elmer FTIR SPECTRUM 1000 spectrometer with ATR with a PIKE Miracle ATR unit.

All **thin layer chromatography** experiments were performed on silica gel coated aluminium foil (silica gel 60 F_{254}, Sigma-Aldrich). Compounds were visualized by staining with Seebach-solution (mixture of phosphomolybdic acid hydrate, cerium(IV)-sulfate, sulfuric acid and water).

6.3 Experimental Procedures

6.3.1 Experimental procedures of Chapter 4.1.1

6.3.1.1 Monomer synthesis of monomer 1

Synthesised according to previously reported procedure[34]

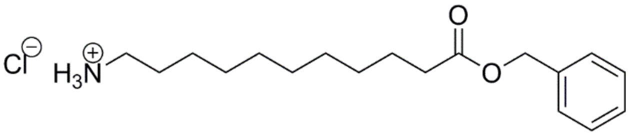

11-aminoundecanoic acid **1a** (15.0 g, 74.8 mmol, 1.0 eq.) was suspended in 75 mL THF. Subsequently, benzyl alcohol **3** (96.7 g, 0.89 mol, 12 eq.) was added and the suspension was cooled to 0 °C. Thionyl chloride **4** (16.6 mL, 27.4 g, 0.23 mol, 3.1 eq.) was added dropwise. After addition of the thionyl chloride **4**, the solution was warmed to room temperature and stirred overnight. The yellow solution was then poured into 500 mL diethyl ether and stored in the freezer for one hour. The product was filtered off and another 500 mL diethyl ether were added and the suspension was stored in the freezer for another hour. The product was filtered off and dried under high vacuum. 11-(Benzyloxy)-11-oxoundecan-1-aminium chloride **2a** was obtained in a yield of 95% (20.7 g, 71.1 mmol) as a white solid.

^{1}H-NMR: (300 MHz, CD_3OD) δ /ppm: 7,33 (s, 5H, 5 CH aromatic, ^{1}); 5,09 (s, 2H, CH_2, ^{2}); 2,90 (t, J = 7.5 Hz, 2H, CH_2, ^{3}); 2,34 (t, J = 7,3 Hz, 2H, CH_2, ^{4}); 1,61 (s, 4H, 2 CH_2, ^{5}); 1,31 (m, 12H, 6 CH_2, ^{6}).

^{13}C NMR (75 MHz, CD_3OD) δ /ppm: 175.2, 137.7, 129.5, 129.5, 129.2, 129.2, 67.1, 40.8, 35.0, 30.4, 30.3, 30.2, 30.1, 28.5, 27.4, 26.0.

HRMS-FAB-MS of $[C_{18}H_{30}NO_2]^+$: calculated: 292.2271, found: 292.2271.

IR (ATR platinum diamond): ν /cm^{-1} = 2916.5, 2847.7, 1737.2, 1601.6, 1527.7, 1495.8, 1462.9, 1385.9, 1359.8, 1332.2, 1307.4, 1278.9, 1246.1, 1208.4, 1152.0, 1043.3, 992.7, 959.9, 810.1, 742.7, 722.1, 695.3, 580.3, 509.3, 416.3.

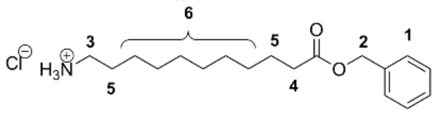
$Cl^{\ominus}$
$H_3\overset{\oplus}{N}$
3
6
5
O
2
1
5
4
O

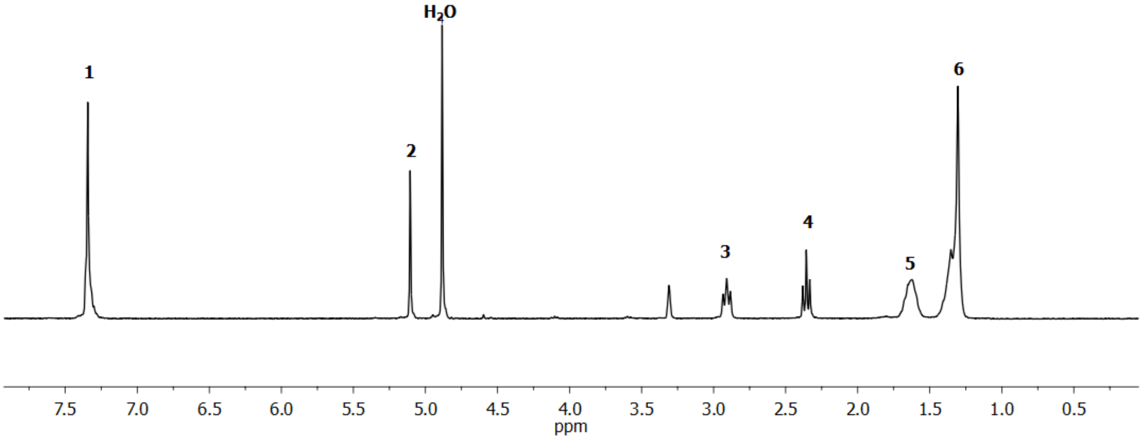

Synthesised according to previously reported procedure.[34]

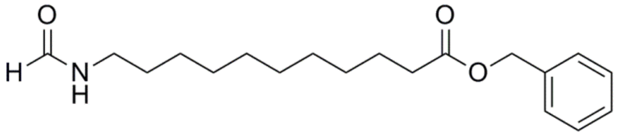

11-(Benzyloxy)-11-oxoundecan-1-aminium chloride **2a** (21.3 g, 64.7 mmol, 1.0 eq.) was dissolved in trimethyl orthoformate **5** (71 mL, 68.9 g, 0.65 mol, 10 eq.) and heated to 100 °C. The reaction mixture was refluxed overnight at 100 °C. Trimethyl orthoformate **5** was then removed under reduced pressure and the crude product **8a** (21.9 g) was used without further purification.

^{1}H NMR (300 MHz, $CDCl_3$) δ /ppm: 8.22 – 7.97 (m, 1H, CH, ^{1}), 7.37 (m, 5H aromatic, ^{2}), 5.61 (s, 1H, NH, ^{3}), 5.10 (s, 2H, CH_2, ^{4}), 3.42 – 3.11 (m, 2H, CH_2, ^{5}), 2.41 – 2.28 (t, J = 7.5 Hz, 2H, CH_2, ^{6}), 1.91 – 1.41 (m, 4H, $2CH_2$, ^{7}), 1.26 (s, 12H, 6 CH_2, ^{8}).

^{13}C NMR (75 MHz, $CDCl_3$) δ /ppm: 173.8, 164.7, 161.3, 136.2, 128.6, 128.2, 66.1, 41.8, 38.2, 34.4, 31.3, 29.5, 29.4, 29.3, 29.2, 29.1, 26.9, 26.4, 25.0.

HRMS-FAB-MS of $[C_{19}H_{30}NO_3]^+$: calculated: 320.2220, found: 320.2222.

IR (ATR platinum diamond): ν / cm^{-1} = 3264.9, 3068.1, 2913.6, 2848.1, 1732.5, 1651.1, 1555.4, 1470.5, 1449.3, 1417.1, 1379.2, 1329.5, 1299.2, 1267.1, 1233.0, 1199.5, 1159.1, 1054.8, 996.7, 938.2, 866.1, 825.1, 806.2, 752.8, 718.3, 695.3, 608.9, 519.5, 487.1, 451.5.

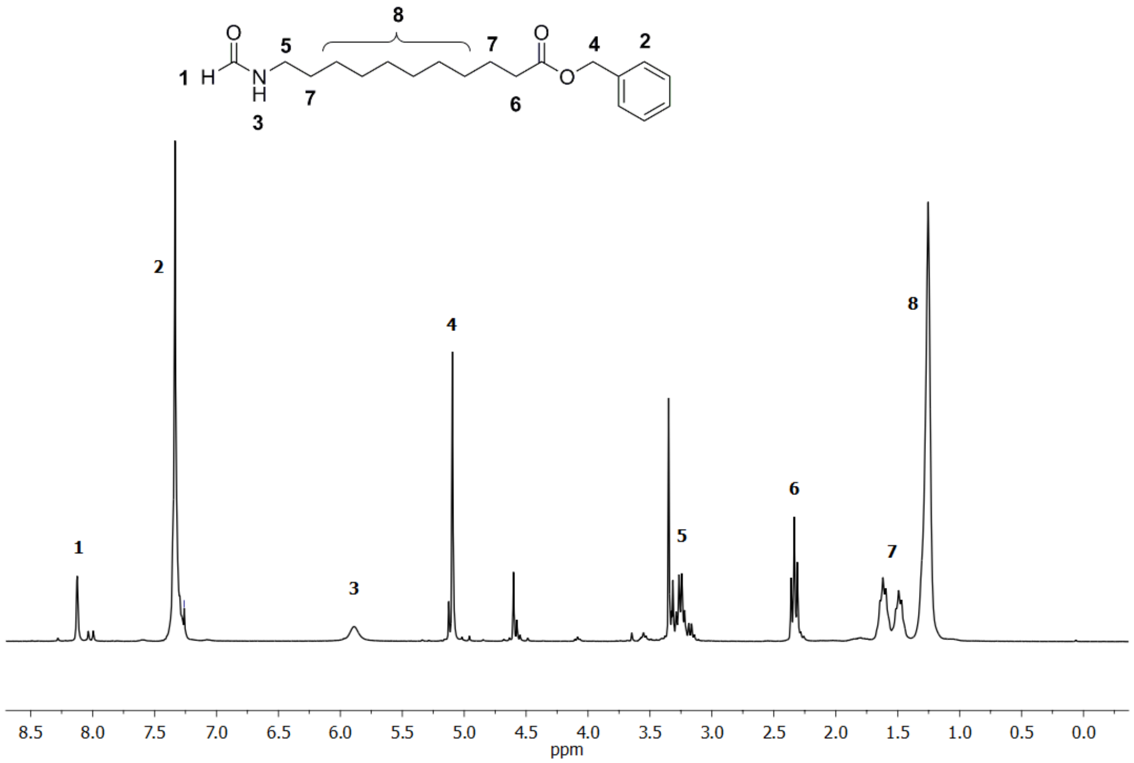

Synthesised according to previously reported procedure.[34]

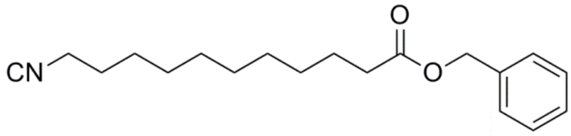

Benzyl-11-formamidoundecanoate **8a** (19.6 g, 61.2 mmol, 1.0 eq.) was dissolved in 185 mL DCM (0.33 M). Diisopropylamine **7** (26.7 mL, 19.2 g, 0.190 mol, 3 eq.) was added and the reaction mixture was cooled to 0 °C in an ice bath. Subsequently, phosphoryl trichloride **6** (6.7 mL, 11.3 g, 73.5 mmol, 1.2 eq.) was added dropwise and the reaction mixture was then stirred at room temperature for two hours. Subsequently, the mixture was cooled in an ice bath and the reaction was quenched by addition of sodium carbonate solution (20%, 75 mL) at 0 °C. After stirring for 30 minutes at room temperature, 50 mL DCM and 50 mL water were added. After separation of the aqueous phase, the organic layer was washed with water (3 × 80 mL) and brine (80 mL). The organic layer was dried over sodium sulfate and the solvent was removed under reduced pressure. The crude product was purified by column chromatography (hexane / ethyl acetate 19:1 → 8:1). The product **M1** was obtained as slightly yellow oil in a yield of 67% (12.3 g, 41.0 mmol).

^{1}H NMR (300 MHz, $CDCl_3$) δ /ppm: 7.40 – 7.28 (m, 5CH aromatic, ^{1}), 5.11 (s, 2H, CH_2, ^{2}), 3.47 – 3.25 (m, 2H, CH_2, ^{3}), 2.35 (t, *J* = 7.5 Hz, 2H, CH_2, ^{4}), 1.65 (m, 4H, 2 CH_2, ^{5}), 1.51 – 0.99 (m, 12H, 6 CH_2, ^{6}).

^{13}C NMR (75 MHz, $CDCl_3$) δ /ppm: 173.8, 155.8, 155.7, 155.6, 136.2, 128.6, 128.3, 66.2, 41.7, 41.6, 41.6, 34.4, 29.4, 29.3, 29.2, 29.2, 28.8, 26.4, 25.0.

HRMS-FAB-MS of $[C_{19}H_{28}NO_2]^+$: calculated: 302.2115, found: 302.2113.

IR (ATR platinum diamond): ν / cm^{-1} = 3032.1, 2924.6, 2853.5, 2145.5 (isocyanide), 1732.4, 1496.9, 1454.3, 1380.2, 1350.0, 1211.7, 1160.2, 1100.4, 1001.0, 735.3, 696.7, 578.4, 494.9.

***R*$_f$**: (hexane / ethyl acetate 5:1) = 0.55.

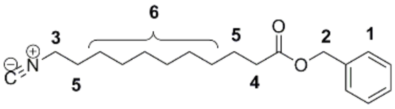
6
3
5
O
2
1
C
N
5
4

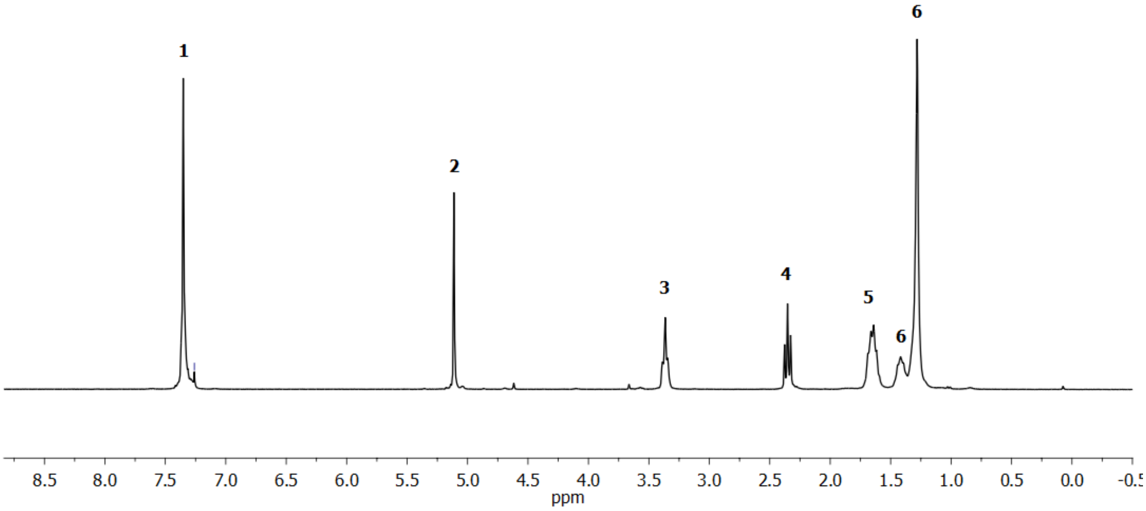
1
2
3
4
5
6
6
8.5
8.0
7.5
7.0
6.5
6.0
5.5
5.0
4.5
4.0
3.5
3.0
2.5
2.0
1.5
1.0
0.5
0.0
-0.
ppm

6.3.1.2 Oligomer synthesis

Oligomer synthesis with propanal as side chain[*]

1st Passerini reaction: Synthesis of Dimer $\mathbf{LO_{2a}}$

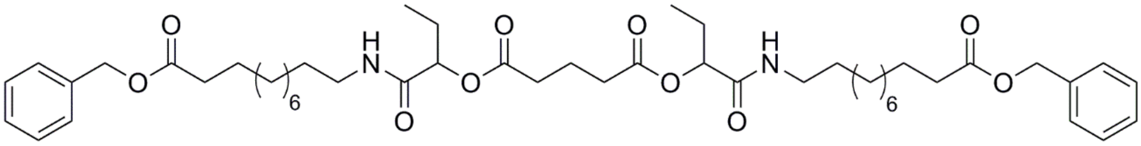

Glutaric acid **9** (300 mg, 2.27 mmol, 1.0 eq.) was suspended in DCM (4.6 mL, 0.5 M). Subsequently, propanal **11a** (0.59 mL, 0.47 g, 8.18 mmol, 3.6 eq.) and monomer **M1** (2.05 g, 6.80 mmol, 3.0 eq.) were added and the reaction mixture was stirred at room temperature for 48 h. The solvent was removed under reduced pressure and the crude product was purified by column chromatography (hexane / ethyl acetate 9:1 → 1:1) to obtain the desired product $\mathbf{LO_{2a}}$ in a yield of 69% (1.33 g, 1.57 mmol) as a yellowish oil.

^{1}H NMR (300 MHz, $CDCl_3$) δ / ppm: 7.43 – 7.28 (m, 10CH aromatic, ^{1}), 6.28 – 6.01 (m, 2H, NH, ^{2}), 5.11 (s, 6H, 2 CH_2, 2 CH, ^{3}), 3.37 – 3.09 (m, 4H, 2 CH_2, ^{4}), 2.50 (t, J = 7.0 Hz, 4H, 2 CH_2, ^{5}), 2.34 (t, J = 7.5 Hz, 4H, 2 CH_2, ^{6}), 2.03 (m, 2H, CH_2, ^{7}), 1.88 (m, 4H, 2 CH_2, ^{8}), 1.68 – 1.56 (m, 4H, 2 CH_2, ^{9}), 1.48 (m, 4H, 2 CH_2, ^{10}), 1.26 (s, 24H, 12 CH_2, ^{11}), 0.92 (t, J = 7.4 Hz, 6H, 2 CH_3, ^{12}).

^{13}C NMR (75 MHz, $CDCl_3$) δ / ppm: 173.8, 172.0, 171.8, 169.5, 136.3, 128.7, 128.3, 75.3, 66.2, 39.4, 34.4, 33.1, 33.0, 29.7, 29.6, 29.5, 29.3, 29.2, 27.0, 25.2, 25.1, 20.2, 20.2, 9.2, 9.2.

HRMS-FAB-MS of $[C_{49}H_{75}N_2O_{10}]^+$: calculated: 851.5416 found: 851.5417.

IR (ATR platinum diamond): ν / cm^{-1} = 3303.7, 2924.4, 2852.5, 1733.9, 1654.6, 1533.9, 1454.6, 1379.5, 1229.1, 1148.7, 1100.4, 967.7, 734.7, 696.6.

***R*f** : (hexane / ethyl acetate 2:3) = 0.79.

---

[*] This oligomer was synthesised by Katharina Wetzel during the Master thesis [339]

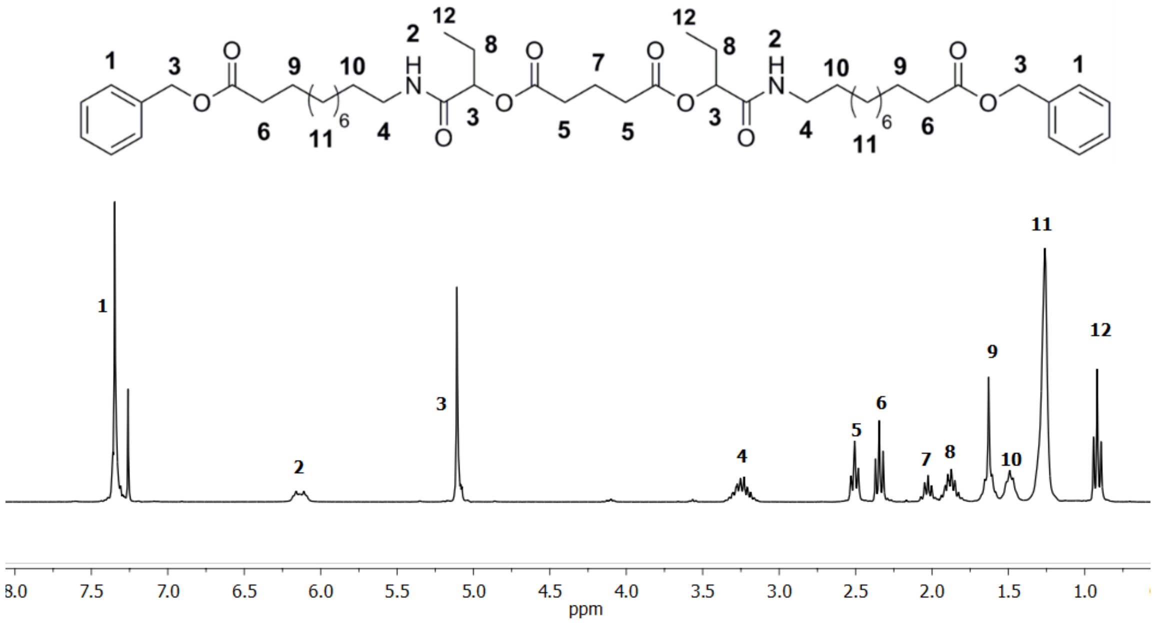
1
2
3
4
5
6
7
8
9
10
11
12
8.0
7.5
7.0
6.5
6.0
5.5
5.0
4.5
4.0
3.5
3.0
2.5
2.0
1.5
1.0
ppm

1st deprotection: Synthesis of Dimer LO_{2b}

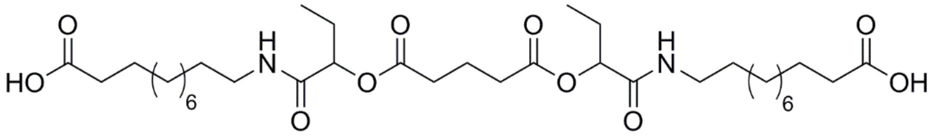

Substance **LO_{2a}** (1.09 g, 1.28 mmol, 1.0 eq) was dissolved in 2.2 mL ethyl acetate (0.5 M) and palladium on activated charcoal **19** (0.11 g, 10 wt%) was added. The reaction mixture was purged with hydrogen (balloon) and then stirred overnight under hydrogen atmosphere. The heterogeneous catalyst was removed by filtration and the solvent was evaporated under reduced pressure to afford the product **LO_{2b}** without further purification in a yield of 96% (0.82 g, 1.22 mmol) as a highly viscous, colourless oil.

^{1}H NMR (300 MHz, $CDCl_3$) δ / ppm: 6.30 (m, 2H, NH, ^{1}), 5.09 (t, J = 5.7 Hz, 2H, 2 CH, ^{2}), 3.35 – 3.11 (m, 4H, 2 CH_2, ^{3}), 2.50 (t, J = 7.0 Hz, 4H, 2 CH_2, ^{4}), 2.32 (t, J = 7.4 Hz, 4H, 2 CH_2, ^{5}), 2.07 – 1.94 (m, 2H, CH_2, ^{6}), 1.93 – 1.77 (m, 4H, 2 CH_2, ^{7}), 1.60 (m, 4H, 2 CH_2, ^{8}), 1.46 (m, 4H, 2 CH_2, ^{9}), 1.26 (s, 24H, 12 CH_2, ^{10}), 0.91 (t, J = 7.4 Hz, 6H, 2 CH_3, ^{11}).

^{13}C NMR (75 MHz, $CDCl_3$) δ / ppm: 179.2, 172.1, 171.9, 169.8, 75.3, 39.5, 34.2, 33.1, 32.9, 29.6, 29.4, 29.3, 29.2, 29.2, 29.1, 26.9, 25.2, 24.9, 20.2, 9.21, 9.2.

HRMS-FAB-MS of $[C_{35}H_{63}N_2O_{10}]^+$: calculated: 671.4477 found: 671.4479.

IR (ATR platinum diamond): ν /cm^{-1} = 3291.4, 2921.3, 2850.7, 1734.8, 1698.0, 1653.6, 1544.4, 1435.7, 1376.5, 1234.7, 1145.4, 1104.3, 1047.3, 963.6, 909.1, 722.4, 679.6.

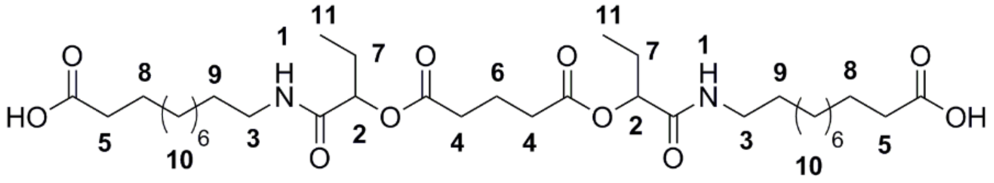
HO
O
5
8
10
6
9
3
1
H
N
O
11
7
2
O
O
4
6
4
O
O
11
7
2
O
1
H
N
3
9
10
6
8
5
O
OH

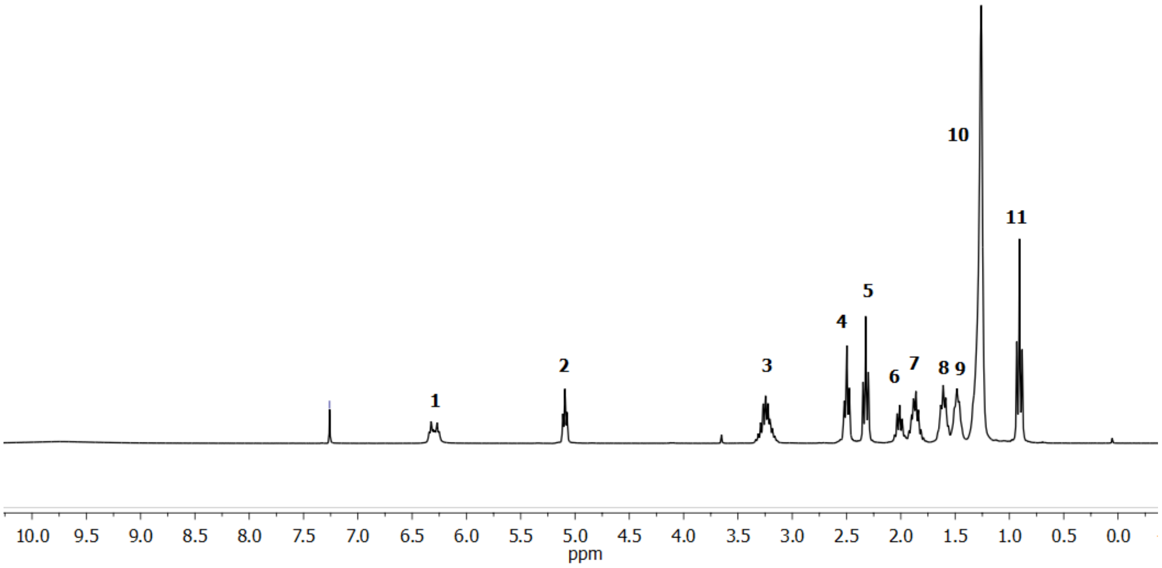
1
2
3
4
5
6
7
8
9
10
11
10.0
9.5
9.0
8.5
8.0
7.5
7.0
6.5
6.0
5.5
5.0
4.5
4.0
3.5
3.0
2.5
2.0
1.5
1.0
0.5
0.0
ppm

2nd Passerini reaction: Synthesis of tetramer **LO$_{4a}$**

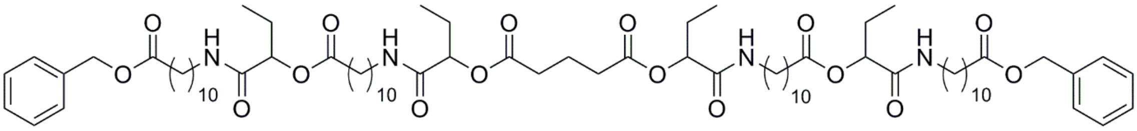

Substance **LO$_{2b}$** (0.78 g, 1.17 mmol, 1.0 eq.) was dissolved in DCM (3.5 mL, 0.33 M). Subsequently, propanal **11a** (0.25 mL, 0.20 g, 3.51 mmol, 3.0 eq.) and monomer **M1** (1.07 g, 3.51 mmol, 3.0 eq.) were added. The reaction mixture was stirred at room temperature for 48 h. The solvent was evaporated under reduced pressure and the crude product was purified by column chromatography (hexane / ethyl acetate 4:1 → 1:6). The desired product **LO$_{4a}$** was obtained in a yield of 89% (1.45 g, 1.04 mmol) as a yellowish, viscous oil.

^{1}H NMR (400 MHz, CDCl$_3$) δ / ppm: 7.38 – 7.27 (m,10H, CH, aromatic,^{1}), 6.24 (t, J = 5.7 Hz, 1H, NH, ^{2}), 6.18 (t, J = 5.7 Hz, 1H, NH, ^{2}), 6.06 (t, J = 5.3 Hz, 2H, 2 NH, ^{2}), 5.16 – 5.02 (m, 8H, 4 CH, 2 CH$_2$, ^{3}), 3.32 – 3.15 (m, 8H, 4 CH$_2$, ^{4}), 2.54 – 2.44 (m, 4H, 2 CH$_2$, ^{5}), 2.41 – 2.29 (m, 8H, 4 CH$_2$, ^{6}), 2.01 (m, 2H, CH$_2$, ^{7}), 1.95 – 1.77 (m, 8H, 4 CH$_2$, ^{8}), 1.68 – 1.56 (m, 8H, 4 CH$_2$, ^{9}), 1.53 – 1.43 (m, 8H, 2 CH$_2$, ^{10}), 1.26 (s, 48H, 24 CH$_2$, ^{11}), 0.90 (m, 12H, 4 CH$_3$, ^{12}).

^{13}C NMR (101 MHz, CDCl$_3$) δ / ppm: 173.8, 172.5, 172.0, 171.8, 169.7, 169.5, 136.2, 128.6, 128.3, 128.2, 75.2, 74.9, 66.2, 39.4, 39.3, 34.4, 34.4, 33.0, 32.9, 29.7, 29.5, 29.4, 29.3, 29.2, 29.2, 26.9, 25.2, 25.2, 25.0, 20.2, 20.2, 9.2, 9.2, 9.1.

HRMS-FAB-MS of [$C_{79}H_{129}N_4O_{16}$]$^+$: calculated: 1389.9 found: 1388.9.

IR (ATR platinum diamond): ν /cm^{-1} = 3305.3, 2923.8, 2852.3, 1735.6, 1653.9, 1533.6, 1455.2, 1377.5, 1230.1, 1150.3, 1100.3, 1047.9, 971.1, 732.0, 696.8.

***R*$_f$** (hexane / ethyl acetate 1:2) = 0.73.

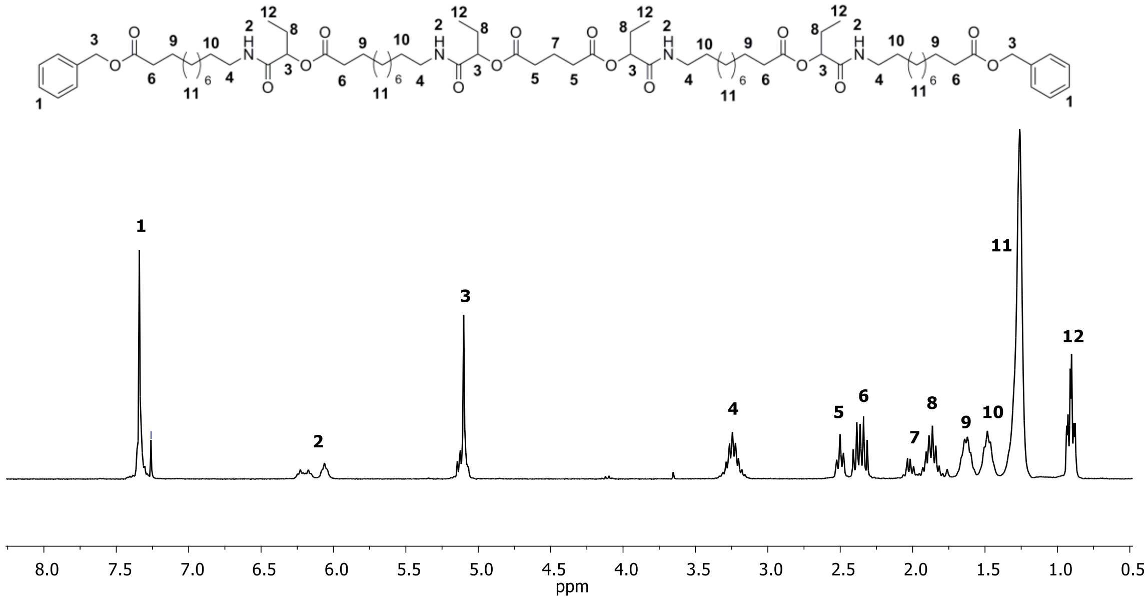
1
2
3
4
5
6
7
8
9
10
11
12
8.0
7.5
7.0
6.5
6.0
5.5
5.0
4.5
4.0
3.5
3.0
2.5
2.0
1.5
1.0
0.5
ppm

2nd deprotection: Synthesis of Tetramer LO$_{4b}$

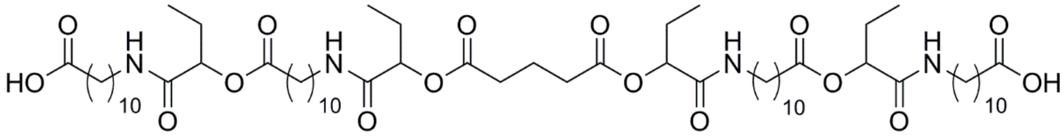

Substance **LO$_{4a}$** (1.35 g, 0.97 mmol, 1.0 eq.) was dissolved in ethyl acetate (2 mL, 0.5 M) and palladium on activated charcoal **19** (0.14 g, 10 wt%) was added. The reaction mixture was purged with hydrogen (balloon) and stirred overnight under hydrogen atmosphere. The heterogeneous catalyst was removed by filtration and the solvent was evaporated under reduced pressure to afford the product **LO$_{4b}$** without further purification in a yield of 99% (1.16 g, 0.96 mmol) as highly viscous colourless oil.

^{1}H NMR (400 MHz, $CDCl_3$) δ / ppm: 6.33 (m, 2H, 2 NH, ^{1}), 6.13 (t, J = 5.4 Hz, 2H, 2 NH, ^{1}), 5.18 – 5.04 (m, 4H, CH, ^{2}), 3.33 – 3.15 (m, 8H, 4 CH_2, ^{3}), 2.54 – 2.46 (m, 4H, 2 CH_2, ^{4}), 2.42 – 2.27 (m, 8H, 4 CH_2, ^{5}), 2.06 – 1.95 (m, 2H, CH_2, ^{6}), 1.93 – 1.76 (m, 8H, 4 CH_2, ^{7}), 1.69 – 1.55 (m, 8H, 4 CH_2, ^{8}), 1.54 – 1.40 (m, 8H, 4 CH_2, ^{9}), 1.26 (s, 48H, 24 CH_2, ^{10}), 0.96 – 0.84 (m, 12H, 4 CH_3, ^{11}).

^{13}C NMR (101 MHz, $CDCl_3$) δ / ppm: 178.2, 172.6, 172.1, 172.0, 169.9, 169.9, 75.3, 74.9, 39.5, 39.3, 34.4, 34.1, 33.1, 32.9, 29.8, 29.6, 29.6, 29.5, 29.4, 29.3, 29.2, 29.2, 29.1, 26.9, 26.8, 25.2, 25.2, 25.1, 24.7, 20.2, 20.2, 9.22, 9.2, 9.2.

FAB-MS of $[C_{65}H_{117}N_4O_{16}]^+$: calculated: 1209.8 found: 1209.1.

IR (ATR platinum diamond): ν /cm^{-1} = 3303.8, 2923.8, 2852.8, 1737.9, 1650.3, 1540.3, 1458.9, 1376.9, 1231.7, 1151.8, 1101.2, 1048.7, 970.9, 721.9.

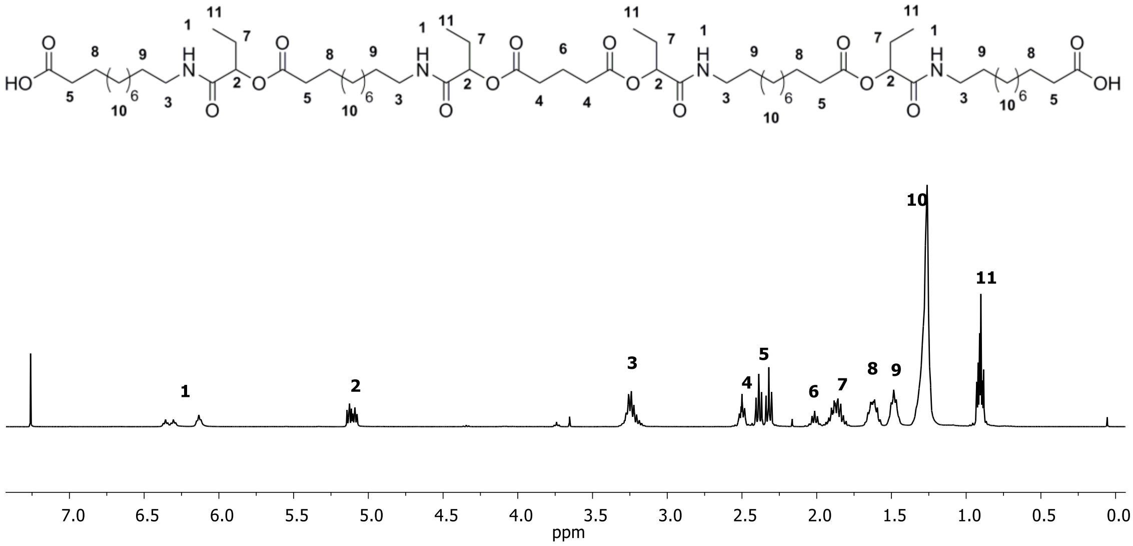
HO
OH
H
N
O
1
2
3
4
5
6
7
8
9
10
11
7.0
6.5
6.0
5.5
5.0
4.5
4.0
3.5
3.0
2.5
2.0
1.5
1.0
0.5
0.0
ppm

3rd Passerini reaction: Synthesis of Hexamer **LO_{6a}**

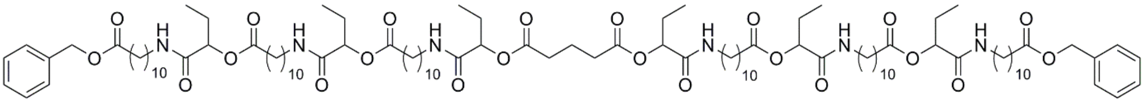

Substance **LO_{4b}** (1.04 g, 0.86 mmol, 1.0 eq.) was dissolved in DCM (1.8 mL, 0.43 M) and propanal **11a** (0.19 mL, 0.15 g, 2.57 mmol, 3.0 eq.) and monomer **M1** (1.07 g, 3.51 mmol, 3.0 eq.) were added. The reaction mixture was stirred at room temperature for 24 h. Again, propanal **11a** (0.05 mL, 40 mg, 0.69 mmol, 0.80 eq.) was added and the reaction mixture was stirred at room temperature for another 24 h. The solvent was evaporated under reduced pressure and the crude product was purified by column chromatography (hexane / ethyl acetate 5:1 → 1:8). The desired product **LO_{6a}** was obtained in a yield of 75% (1.23 g, 0.64 mmol) as yellowish, highly viscous oil.

^{1}H NMR (600 MHz, $CDCl_3$) δ / ppm: 7.39 – 7.27 (m, 10H, CH, aromatic, ^{1}), 6.28 – 6.00 (m, 6H, 6 NH, ^{2}), 5.19 – 5.04 (m, 10H, 2 CH_2, 6 CH, ^{3}), 3.32 – 3.13 (m, 12H, 6 CH_2, ^{4}), 2.54 – 2.46 (m, 4H, 2 CH_2, ^{5}), 2.42 – 2.27 (m, 12H, 6 CH_2, ^{6}), 2.05 – 1.97 (m, 2H, CH_2, ^{7}), 1.94 – 1.78 (m, 12H, 6 CH_2, ^{8}), 1.63 (m, 12H, 6 CH_2, ^{9}), 1.52 – 1.43 (m, 12H, 6 CH_2, ^{10}), 1.27 (s, 72H, 36 CH_2, ^{11}), 0.91 (m, 18H, 6 CH_3, ^{12}).

^{13}C NMR (151 MHz, $CDCl_3$) δ / ppm: 173.8, 172.6, 172.6, 172.0, 171.9, 169.8, 169.7, 169.6, 136.2, 128.7, 128.3, 128.3, 75.3, 74.9, 66.2, 39.4, 39.4, 39.3, 39.3, 34.4, 34.4, 33.1, 33.0, 29.7, 29.6, 29.5, 29.3, 29.3, 29.2, 27.0, 25.3, 25.2, 25.1, 25.1, 20.2, 20.2, 9.2, 9.2, 9.2, 9.2.

HRMS-FAB-MS of $[C_{109}H_{183}N_6O_{22}]^+$: calculated: 1928.3380 found: 1928.33352.

IR (ATR platinum diamond): ν /cm^{-1} = 3294.3, 2922.7, 2851.2, 1735.6, 1655.4, 1536.3, 1455.1, 1164.8, 696.8.

R_f (hexane / ethyl acetate 1:2) = 0.56.

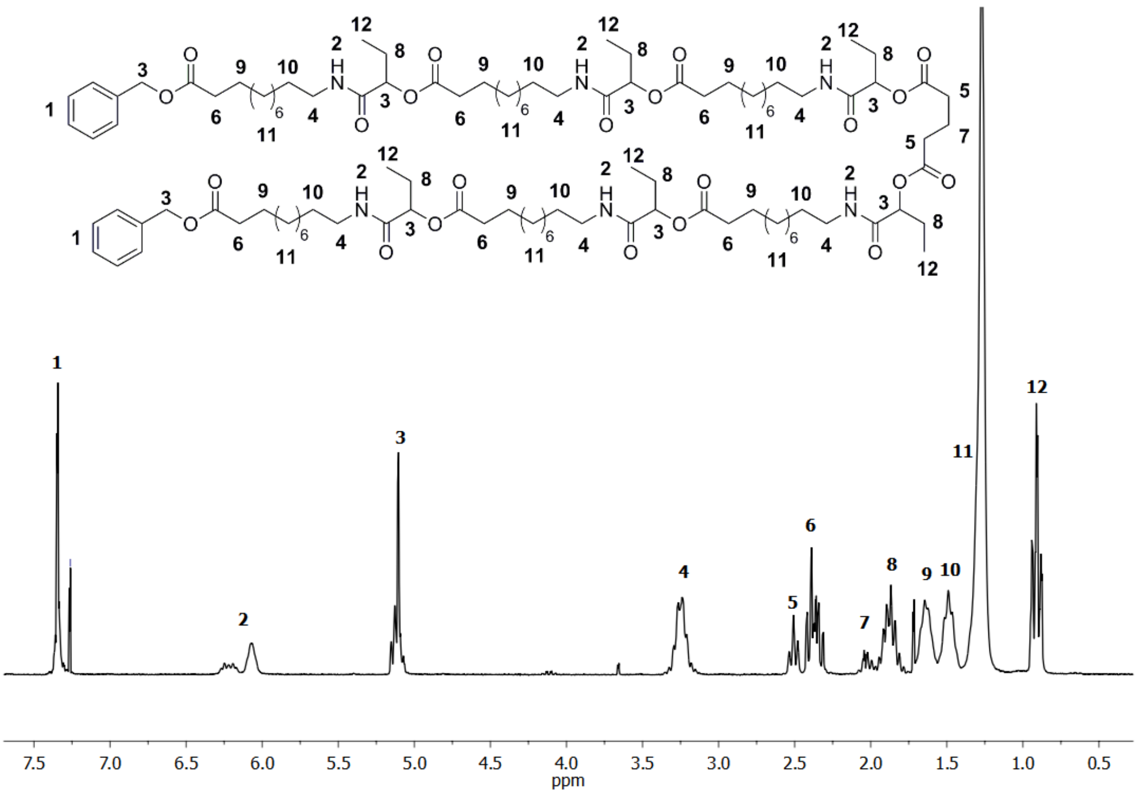
1
2
3
4
5
6
7
8
9
10
11
12
7.5
7.0
6.5
6.0
5.5
5.0
4.5
4.0
3.5
3.0
2.5
2.0
1.5
1.0
0.5
ppm

3rd deprotection: Synthesis of Hexamer LO$_{6b}$

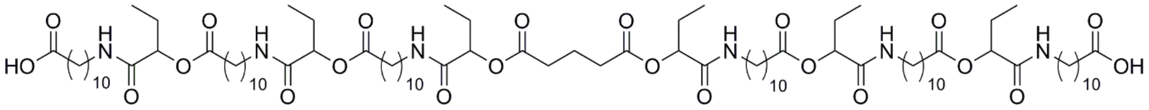

Substance **LO$_{6a}$** (1.12 g, 0.58 mmol, 1.0 eq.) was dissolved in ethyl acetate (5 mL, 0.22 M) and palladium on activated charcoal **19** (0.11 g, 10 wt%) was added. The reaction mixture was purged with hydrogen (balloon) and stirred overnight under hydrogen atmosphere. The heterogeneous catalyst was removed by filtration and the solvent was evaporated under reduced pressure to afford the product **LO$_{6b}$** without further purification in quantitative yield (1.02 g, 0.58 mmol) as highly viscous, lightly yellowish oil.

^{1}H NMR (600 MHz, CDCl$_3$) δ / ppm: 6.44 – 6.08 (m, 6H, 6 NH, ^{1}), 5.14 – 5.01 (m, 6H, 6 CH, ^{2}), 3.29 – 3.16 (m, 12H, 6 CH$_2$, ^{3}), 2.50 – 2.43 (m, 4H, 2 CH$_2$, ^{4}), 2.37 (t, J = 7.5 Hz, 8H, 4 CH$_2$, ^{5}), 2.30 (t, J = 7.5 Hz, 4H, 2 CH$_2$, ^{5}), 2.04 – 1.95 (m, 2H, CH$_2$, ^{6}), 1.92 – 1.78 (m, 12H, 6 CH$_2$, ^{7}), 1.66 – 1.55 (m, 12H, 6 CH$_2$, ^{8}), 1.50 – 1.44 (m, 12H, 6 CH$_2$, ^{9}), 1.25 (m, 72H, 36 CH$_2$, ^{10}), 0.93 – 0.84 (m, 18H, 6 CH$_3$, ^{11}).

^{13}C NMR (151 MHz, CDCl$_3$) δ / ppm: 177.8, 172.6, 172.6, 172.0, 171.9, 167.0, 169.9, 169.8, 169.8, 75.2, 74.9, 39.4, 39.4, 39.3, 39.3, 34.4, 34.3, 34.1, 33.0, 32.9, 29.8, 29.6, 29.5, 29.5, 29.4, 29.4, 29.3, 29.3, 29.3, 29.2, 29.2, 29.1, 29.1, 26.9, 26.9, 26.9, 25.2, 25.2, 25.0, 25.0, 24.9, 20.2, 20.1, 9.2, 9.2, 9.1.

HRMS-FAB-MS of [$C_{95}H_{171}N_6O_{22}$]$^+$: calculated: 1748.2441 found: 1748.2413.

IR (ATR platinum diamond): ν /cm^{-1} = 3304.9, 2923.3, 2852.5, 1737.7, 1650.5, 1537.1, 1460.0, 1375.0, 1160.3, 1100.5, 973.1, 721.0.

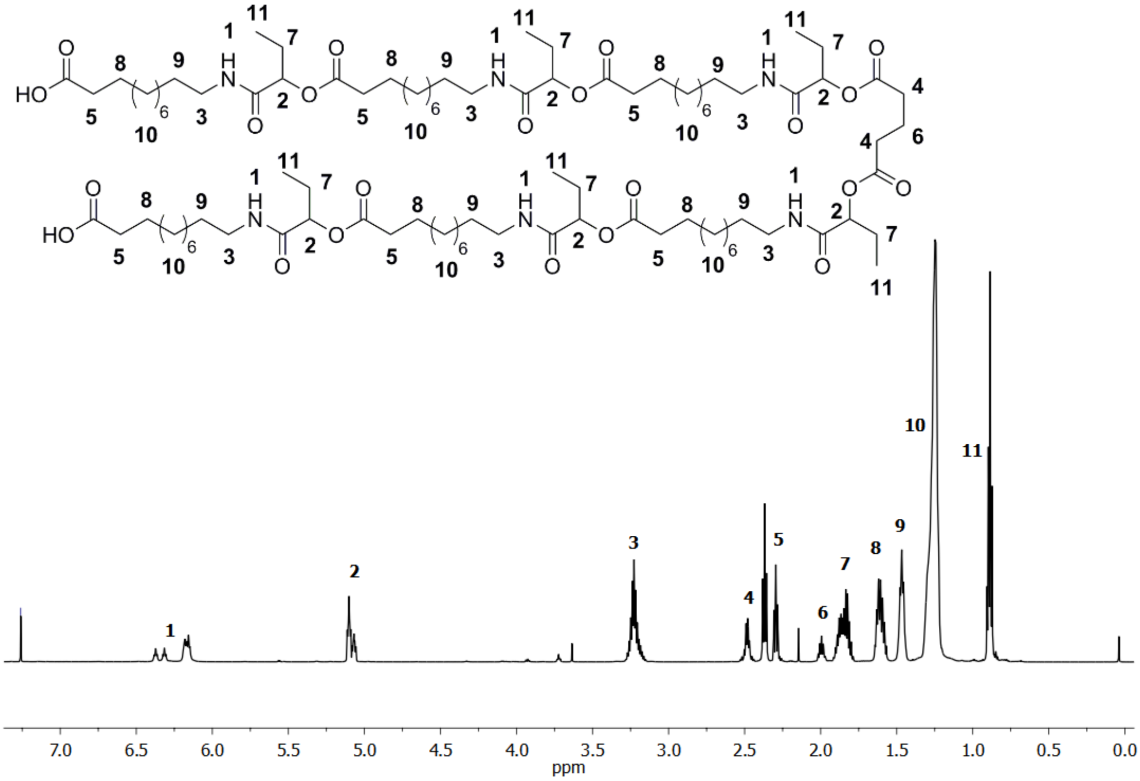
HO
O
HN
OH
1
2
3
4
5
6
7
8
9
10
11
7.0
6.5
6.0
5.5
5.0
4.5
4.0
3.5
3.0
2.5
2.0
1.5
1.0
0.5
0.0
ppm

4th Passerini reaction: Synthesis of Octamer **LO_{8a}**

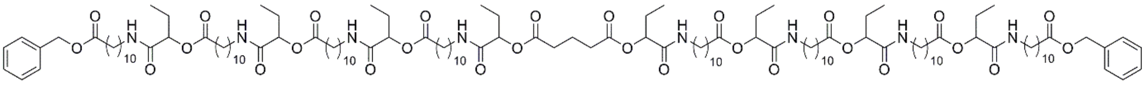

Substance **LO_{6b}** (0.49 g, 0.28 mmol, 1.0 eq.) was dissolved in DCM (1 mL, 0.27 M) and propanal **11a** (84 µL, 68 mg, 1.17 mmol, 4.2 eq.) and monomer **M1** (0.27 g, 0.90 mmol, 3.2 eq.) were added. The reaction mixture was stirred at room temperature for 48 hours. The solvent was evaporated under reduced pressure and the crude product was purified by column chromatography (hexane / ethyl acetate 1:1 → 1:9). The desired product **LO_{8a}** was obtained in a yield of 85% (0.58 g, 0.24 mmol) as turbid, highly viscous oil.

^{1}H NMR (400 MHz, $CDCl_3$) δ / ppm: 7.37 – 7.27 (m, 10H, CH, aromatic, ^{1}), 6.38 – 6.06 (m, 8H, 8 NH, ^{2}), 5.13 – 5.03 (m, 12H, 2 CH_2, 8 CH, ^{3}), 3.30 – 3.13 (m, 16H, 8 CH_2, ^{4}), 2.53 – 2.45 (m, 4H, 2 CH_2, ^{5}), 2.34 (m, 16H, 8 CH_2, ^{6}), 2.04 – 1.95 (m, 2H, CH_2, ^{7}), 1.93 – 1.75 (m, 16H, 8 CH_2, ^{8}), 1.68 – 1.55 (m, 16H, 8 CH_2, ^{9}), 1.45 (m, 16H, 8 CH_2, ^{10}), 1.23 (m, 96H, 48 CH_2, ^{11}), 0.93 – 0.81 (m, 24H, 8 CH_3, ^{12}).

^{13}C NMR (101 MHz, $CDCl_3$) δ / ppm: 173.7, 172.5, 172.5, 172.0, 171.8, 169.7, 169.7, 169.6, 169.6, 136.2, 128.6, 128.2, 128.2, 75.2, 74.8, 66.1, 39.3, 39.2, 34.4, 34.3, 33.0, 32.9, 29.7, 29.6, 29.5, 29.4, 29.3, 29.1, 26.9, 25.2, 25.2, 25.0, 20.2, 20.1, 9.2, 9.2, 9.1.

FAB-MS of $[C_{139}H_{237}N_8O_{28}]^+$: calculated: 2466.7 found: 2466.4.

IR (ATR platinum diamond): ν /cm^{-1} = 3294.3, 2923.6, 2852.3, 1737.2, 1654.3, 1535.2, 1455.9, 1375.3, 1231.4, 1161.9, 1101.0, 1048.4, 973.2, 721.9, 696.9, 412.8.

R_f (hexane / ethyl acetate 1:4) = 0.70.

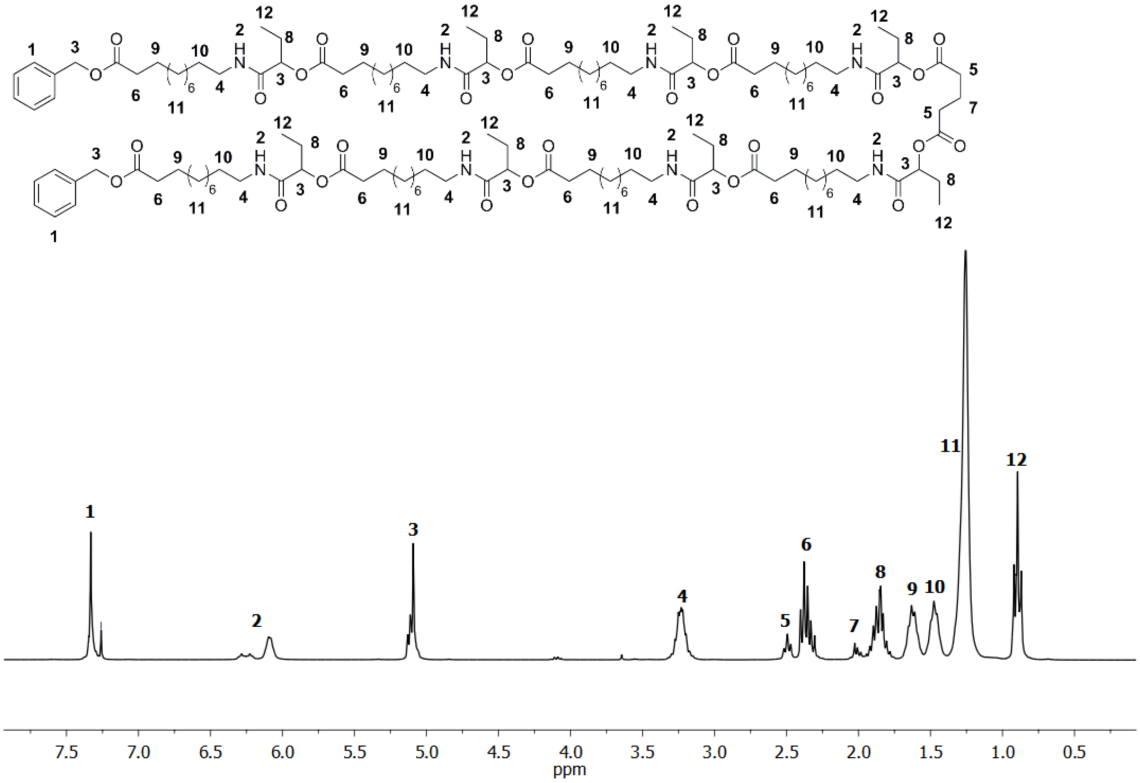
1
2
3
4
5
6
7
8
9
10
11
12
7.5
7.0
6.5
6.0
5.5
5.0
4.5
4.0
3.5
3.0
2.5
2.0
1.5
1.0
0.5
ppm

Oligomer synthesis with cyclohexane carboxaldehyde side chains*

1st Passerini reaction: Synthesis of Dimer LO$_{2c}$

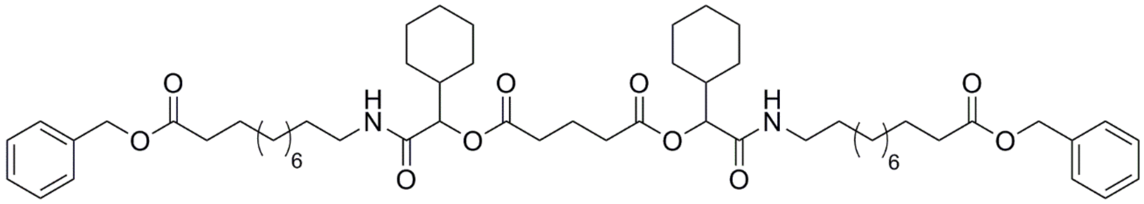

Glutaric acid **9** (400 mg, 3.03 mmol, 1.0 eq.) was suspended in DCM (6 mL, 0.5 M). Subsequently, cyclohexane carboxaldehyde **11b** (1.1 mL, 1.02 g, 9.08 mmol, 3.0 eq.) and monomer **M1** (2.75 g, 9.12 mmol, 3.0 eq.) were added and the reaction mixture was stirred at room temperature for 24 hours. The solvent was removed under reduced pressure and the crude product was purified by column chromatography (hexane / ethyl acetate 8:1 → 1:3) to obtain the desired product **LO$_{2c}$** in a yield of 86% (2.48 g, 2.59 mmol) as a brown-orange oil.

^{1}H NMR (400 MHz, CDCl$_3$) δ / ppm: 7.42 – 7.29 (m, 10H, CH aromatic, ^{1}), 6.12 (m, 2H, 2 NH, ^{2}), 5.10 (s, 4H, 2CH$_2$, ^{3}), 4.98 (t, J = 4.7 Hz, 2H, 2 CH, ^{4}), 3.38 – 3.11 (m, 4H, 2 CH$_2$, ^{5}), 2.58 – 2.43 (m, 4H, 2 CH$_2$, ^{6}), 2.34 (t, J = 7.5 Hz, 4H, 2 CH$_2$, ^{7}), 2.09 – 1.99 (m, 2H, CH$_2$, ^{8}), 1.99 – 1.87 (m, 2H, 2 CH, ^{8}), 1.81 – 1.55 (m, 16H, 8CH$_2$, ^{9}), 1.54 – 1.39 (m, 4H, 2CH$_2$, ^{10}), 1.34 – 0.91 (m, 32H, 16 CH$_2$, ^{11}).

^{13}C NMR (101 MHz, CDCl$_3$) δ / ppm: 173.8, 172.1, 172.0, 169.1, 136.2, 128.7, 128.3, 78.2, 66.2, 40.1, 40.1, 39.4, 39.4, 34.4, 33.1, 31.0, 29.7, 29.6, 29.5, 29.3, 29.2, 27.5, 27.0, 26.2, 26.1, 26.0, 25.1.

HRMS-FAB-MS of [C$_{57}$H$_{87}$N$_2$O$_{10}$]$^+$: calculated: 959.6355, found: 959.6354.

IR (ATR platinum diamond): ν/cm^{-1} = 2925.1, 2852.9, 1735.3, 1435.0, 1357.3, 1165.2, 697.7.

***R*$_f$** (hexane / ethyl acetate 1:1) = 0.73.

---

[*] This oligomer was synthesised by Katharina Wetzel during the Master thesis [339]

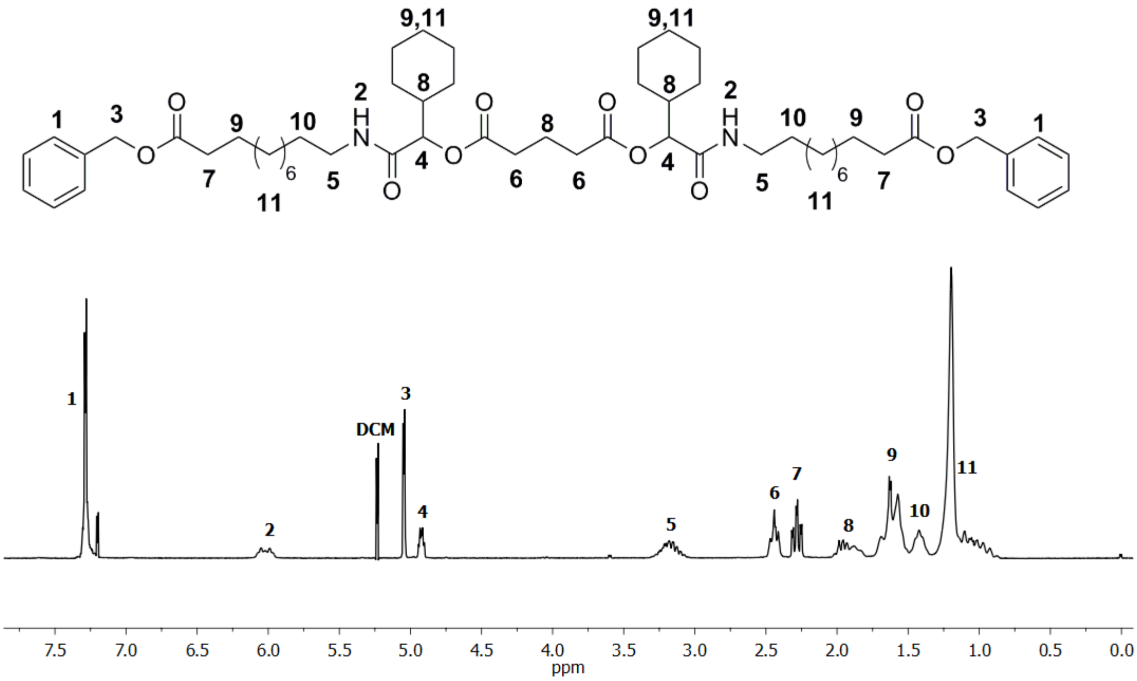
9,11
8
1
3
9
10
2
7
11
5
4
6
DCM
ppm
7.5
7.0
6.5
6.0
5.5
5.0
4.5
4.0
3.5
3.0
2.5
2.0
1.5
1.0
0.5
0.0

1st deprotection: Synthesis of Dimer $\mathbf{LO_{2d}}$

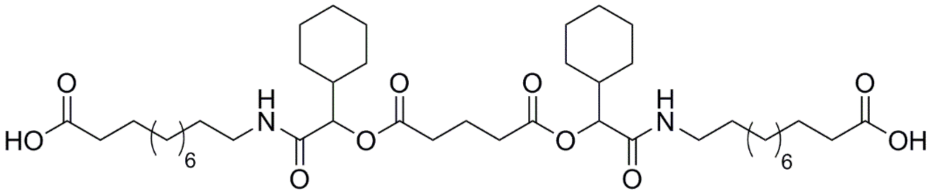

Substance $\mathbf{LO_{2c}}$ (2.31 g, 2.41 mmol, 1.0 eq.) was dissolved in ethyl acetate (4.9 mL, 0.5 M) and palladium on activated charcoal **19** (0.24 g, 10 wt%) was added. The reaction mixture was purged with hydrogen (balloon) and then stirred overnight under hydrogen atmosphere. The reaction mixture became solid over night and was dissolved in THF. The heterogeneous catalyst was removed by filtration and the solvent was evaporated under reduced pressure to afford the product $\mathbf{LO_{2d}}$ without further purification in a yield of 94% (1.76 g, 2.26 mmol) as highly viscous, yellowish oil.

^{1}H NMR (400 MHz, $CDCl_3$) δ / ppm: 6.33 – 6.15 (m, 2H, 2 NH, ^{1}), 4.96 (m, 2H, 2 CH, ^{2}), 3.35 – 3.09 (m, 4H, 2 CH_2, ^{3}), 2.57 – 2.40 (m, 4H, 2 CH_2, ^{4}), 2.35 – 2.25 (m, 4H, 2 CH_2, ^{5}), 2.04 – 1.82 (m, 4H, 2 CH, CH_2, ^{6}), 1.76 – 1.54 (m, 16H, 8 CH_2, ^{7}), 1.45 (m, 4H, 2 CH_2, ^{8}), 1.37 – 0.89 (m, 34H, 17 CH_2, ^{9}).

^{13}C NMR (101 MHz, $CDCl_3$) δ / ppm: 179.1, 172.2, 172.1, 169.4, 78.1, 40.0, 40.0, 39.4, 39.4, 34.2, 33.1, 32.9, 29.8, 29.5, 29.4, 29.3, 29.2, 29.21, 29.1, 27.5, 26.9, 26.1, 26.1, 25.9, 24.8, 20.3, 20.2.

HRMS-FAB-MS of $[C_{43}H_{75}N_2O_{10}]^+$: calculated: 779.5416, found: 779.5417.

IR (ATR platinum diamond): ν /cm^{-1} = 2922.9, 2851.6, 1735.9, 1644.5, 1540.6, 1448.9, 1373.8, 1142.1, 1100.5, 983.9, 721.6, 430.1.

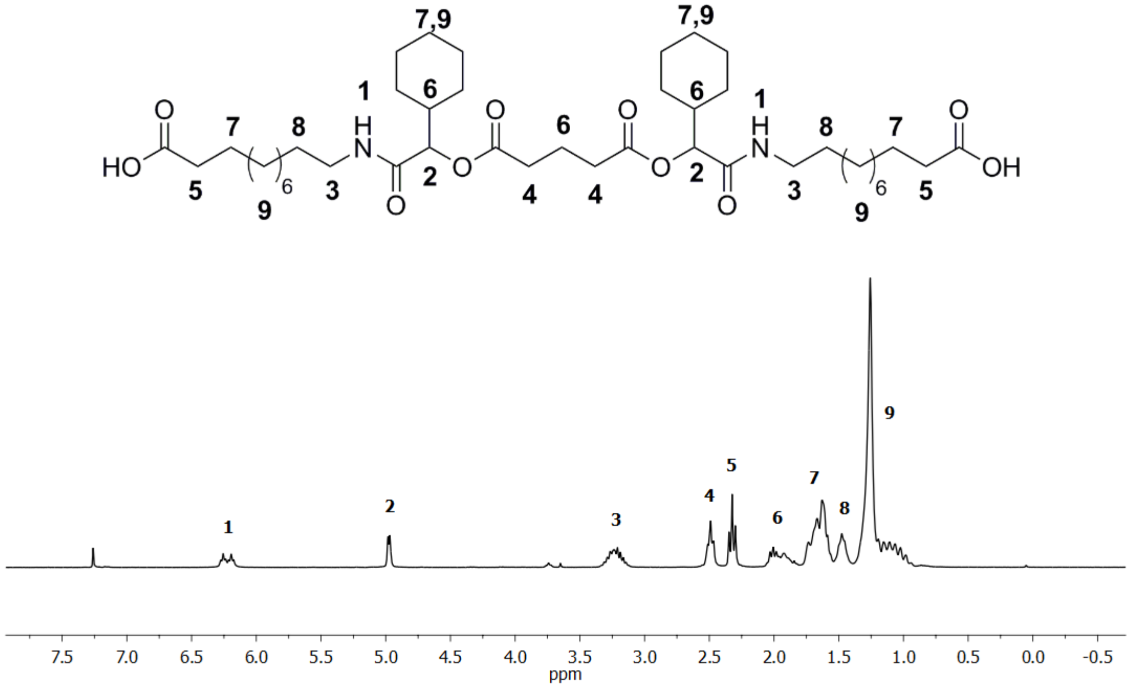
7,9
6
1
HO
O
5
7
6
9
8
3
H
N
O
2
O
O
4
6
4
O
O
2
O
H
N
1
3
8
6
9
7
5
O
OH
1
2
3
4
5
6
7
8
9
7.5
7.0
6.5
6.0
5.5
5.0
4.5
4.0
3.5
3.0
2.5
2.0
1.5
1.0
0.5
0.0
-0.5
ppm

2nd Passerini reaction: Synthesis of Tetramer **LO$_{4c}$**

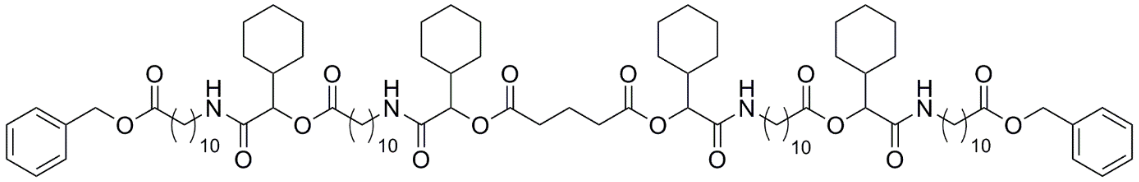

Substance **LO$_{2d}$** (1.57 g, 2.02 mmol, 1.0 eq.) was dissolved in DCM (4.0 mL, 0.5 M). Subsequently, monomer **M1** (1.83 g, 6.09 mmol, 3.0 eq.) and cyclohexane carboxaldehyde **11b** (0.75 g, 6.69 mmol, 3.3 eq.) were added and the reaction mixture was stirred at room temperature for 24 hours. The solvent was removed under reduced pressure and the crude product was purified by column chromatography (hexane / ethyl acetate 2:1 → 1:3) to obtain the desired product **LO$_{4c}$** in a yield of 91% (2.96 g, 1.84 mmol) as an orange, highly viscous oil.

^{1}H NMR (600 MHz, CDCl$_3$) δ / ppm: 7.38 – 7.26 (m, 10H, CH, aromatic, ^{1}), 6.26 – 5.95 (m, 4H, 4 NH, ^{2}), 5.08 (s, 4H, 2 CH$_2$, ^{3}), 5.02 – 4.92 (m, 4H, 4 CH, ^{4}), 3.31 – 3.12 (m, 8H, 4 CH$_2$, ^{5}), 2.53 – 2.44 (m, 4H, 2 CH$_2$, ^{6}), 2.42 – 2.29 (m, 8H, 4 CH$_2$, ^{7}), 2.05 – 1.87 (m, 6H, 4 CH, CH$_2$, ^{8}), 1.77 – 1.54 (m, 24H, 12 CH$_2$, ^{9}), 1.46 (m, 8H, 4 CH$_2$, ^{10}), 1.38 – 0.89 (m, 72H, 36 CH$_2$, ^{11}).

^{13}C NMR (151 MHz, CDCl$_3$) δ / ppm: 173.7, 172.6, 172.1, 171.9, 169.3, 169.1, 136.2, 128.6, 128.2, 128.2, 78.1, 78.1, 66.1, 40.0, 40.0, 39.3, 39.3, 39.2, 34.4, 34.3, 33.0, 32.9, 29.6, 29.5, 29.5, 29.5, 29.4, 29.4, 29.3, 29.2, 29.2, 29.1, 27.4, 27.4, 26.9, 26.9, 26.1, 26.1, 26.0, 25.9, 25.0, 25.0, 20.3, 20.2.

FAB-MS of [$C_{95}H_{153}N_4O_{16}$]$^+$: calculated: 1606.1 found: 1606.1.

IR (ATR platinum diamond): ν /cm^{-1} = 3304.9, 2922.7, 2851.2, 1735.8, 1651.2, 1532.9, 1449.3, 1373.9, 1231.0, 1148.6, 1100.8, 984.3, 733.6, 696.4, 577.8, 453.9, 429.6.

***R*$_f$** (hexane / ethyl acetate (2:3)) = 0.68.

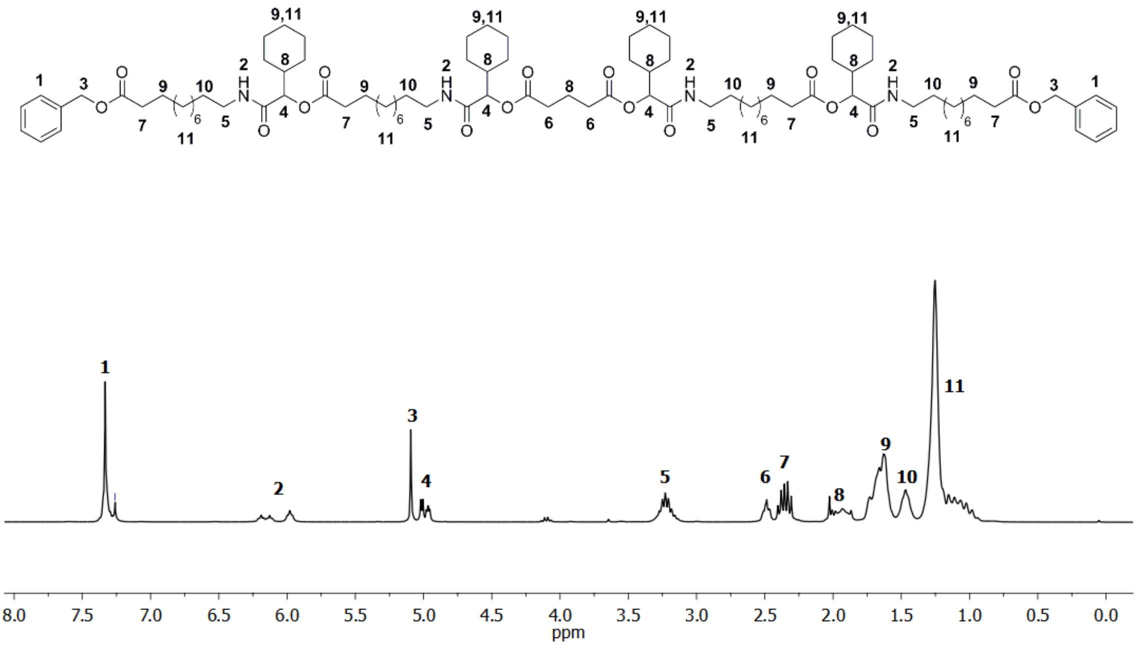
9,11
8
1
2
3
4
5
6
7
10
11
H
N
O
1
2
3
4
5
6
7
8
9
10
11
8.0
7.5
7.0
6.5
6.0
5.5
5.0
4.5
4.0
3.5
3.0
2.5
2.0
1.5
1.0
0.5
0.0
ppm

2nd deprotection: Synthesis of Tetramer $\mathbf{LO_{4d}}$

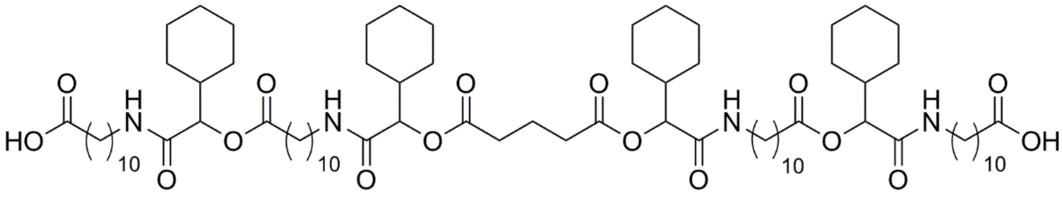

Substance $\mathbf{LO_{4c}}$ (2.73 g, 1.70 mmol, 1.0 eq.) was dissolved in ethyl acetate (5.5 mL, 0.3 M) and palladium on activated charcoal **19** (0.27 g, 10 wt%) was added. The reaction mixture was purged with hydrogen (balloon) and then stirred overnight under hydrogen atmosphere. The heterogeneous catalyst was removed by filtration and the solvent was evaporated under reduced pressure to afford the desired product $\mathbf{LO_{4d}}$ without further purification in a yield of 94% (2.28 g, 1.60 mmol) as highly viscous, orange oil.

^{1}H NMR (600 MHz, $CDCl_3$) δ / ppm: 6.36 – 6.00 (m, 4H, 4 NH, ^{1}), 5.06 – 4.89 (m, 4H, 4 CH, ^{2}), 3.30 – 3.09 (m, 8H, 4 CH_2, ^{3}), 2.53 – 2.42 (m, 4H, 2 CH_2, ^{4}), 2.40 – 2.24 (m, 8H, 4 CH_2, ^{5}), 2.03 – 1.76 (m, 6H, 4 CH, CH_2, ^{6}), 1.73 – 1.50 (m, 24H, 12 CH_2, ^{7}), 1.46 (s, 8H, 4 CH_2, ^{8}), 1.35 – 0.91 (m, 72H, 36 CH_2, ^{9}).

^{13}C NMR (151 MHz, $CDCl_3$) δ / ppm: 178.2, 172.7, 172.2, 172.1, 169.5, 169.4, 78.1, 68.0, 40.0, 39.4, 39.2, 34.3, 34.1, 33.1, 32.9, 29.6, 29.5, 29.4, 29.3, 29.2, 29.1, 27.5, 27.5, 27.4, 27.0, 26.9, 26.1, 26.0, 25.7, 25.1, 24.9, 20.3, 20.2.

HRMS-FAB-MS of $[C_{81}H_{141}N_4O_{16}]^+$: calculated: 1426.0337, found:1426.0304.

IR (ATR platinum diamond): ν /cm^{-1} = 3305.2, 2922.5, 2851.4, 1737.0, 1649.3, 1537.0, 1449.0, 1372.1, 1146.4, 1100.8, 984.7, 893.0, 720.7, 430.4.

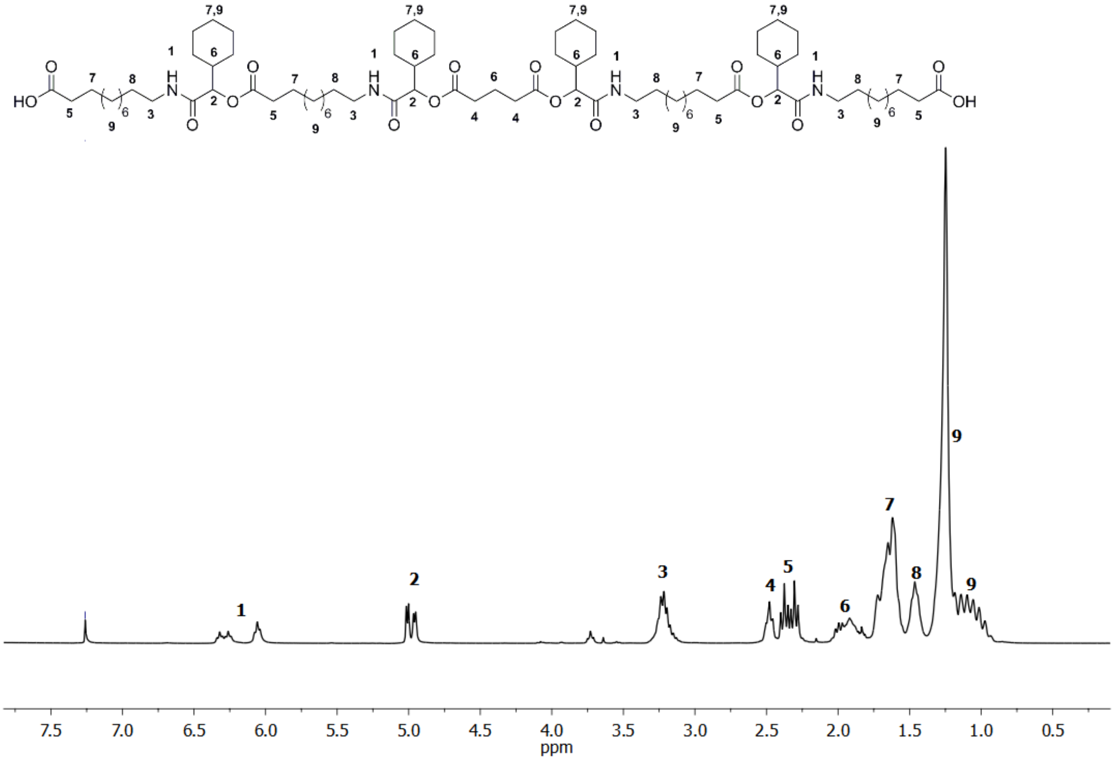
HO
OH
1
2
3
4
5
6
7
8
9
7,9
ppm
7.5
7.0
6.5
6.0
5.5
5.0
4.5
4.0
3.5
3.0
2.5
2.0
1.5
1.0
0.5

3rd Passerini reaction: Synthesis of Hexamer LO$_{6c}$

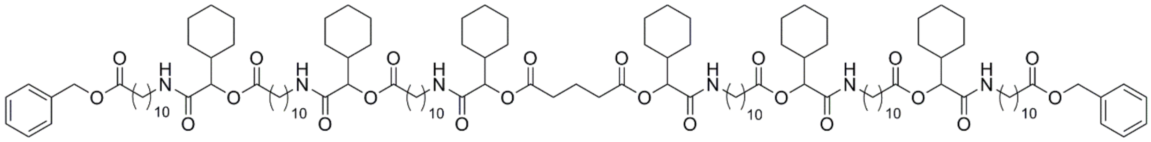

Substance **LO$_{4d}$** (2.09 g, 1.47 mmol, 1.0 eq.) was dissolved in DCM (3.0 mL, 0.5 M). Subsequently, monomer **M1** (1.35 g 4.40 mmol, 3.0 eq.) and cyclohexane carboxaldehyde **11b** (0.50 g 4.40 mmol, 3.0 eq.) were added and the reaction mixture was stirred at room temperature for 24 hours. The solvent was removed under reduced pressure and the crude product was purified by column chromatography (cyclohexane / ethyl acetate 2:1 → 1:2) to obtain the desired product **LO$_{6c}$** in a yield of 91% (3.00 g, 1.33 mmol) as an orange, highly viscous oil.

^{1}H NMR (400 MHz, $CDCl_3$) δ / ppm: 7.37 – 7.26 (m, 10H, CH, aromatic, ^{1}), 6.30 – 5.97 (m, 6H, 6 NH, ^{2}), 5.08 (s, 4H, 2 CH_2, ^{3}), 5.03 – 4.91 (m, 6H, 6 CH, ^{4}), 3.30 – 3.06 (m, 12H, 6 CH_2, ^{5}), 2.50 – 2.42 (m, 4H, 2 CH_2, ^{6}), 2.39 – 2.27 (m, 12H, 6 CH_2, ^{7}), 2.04 – 1.85 (m, 8H, 6 CH, CH_2, ^{8}), 1.79 – 1.52 (m, 36H, 18 CH_2, ^{9}), 1.44 (m, 12H, 6 CH_2, ^{10}), 1.33 – 0.89 (m, 108H, 54 CH_2, ^{11}).

^{13}C NMR (101 MHz, $CDCl_3$) δ / ppm: 173.7, 172.6, 172.1, 171.9, 169.3, 169.3, 169.1, 136.2, 128.6, 128.2, 128.2, 78.1, 78.0, 66.1, 40.0, 39.9, 39.3,39.2, 34.6, 34.3, 33.0, 32.9, 29.6, 29.5, 29.4, 29.3, 29.2, 29.1, 27.4, 26.9, 26.1, 26.1, 26.0, 25.9, 25.0.

FAB-MS of $[C_{133}H_{219}N_6O_{22}]^+$: calculated: 2252.6, found: 2252.9.

IR (ATR platinum diamond): ν /cm^{-1} = 3304.9, 2922.4, 2851.1, 1736.6, 1650.8, 1533.0, 1449.3, 1373.6, 1230.5, 1150.6, 1100.9, 985.1, 844.4, 731.1, 696.4, 577.3, 428.7.

***R*$_{f}$** (cyclohexane / ethyl acetate 2:3) = 0.68.

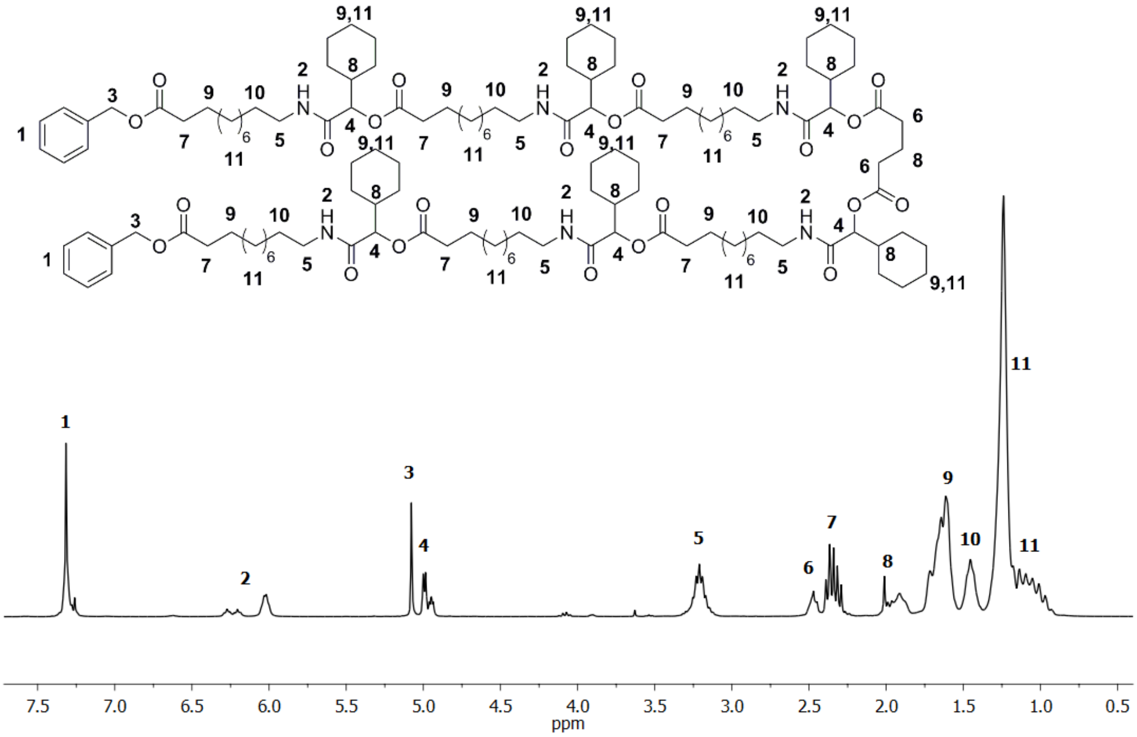
1
2
3
4
5
6
7
8
9
10
11
7.5
7.0
6.5
6.0
5.5
5.0
4.5
4.0
3.5
3.0
2.5
2.0
1.5
1.0
0.5
ppm

3rd deprotection: Synthesis of Hexamer $\mathbf{LO_{6d}}$

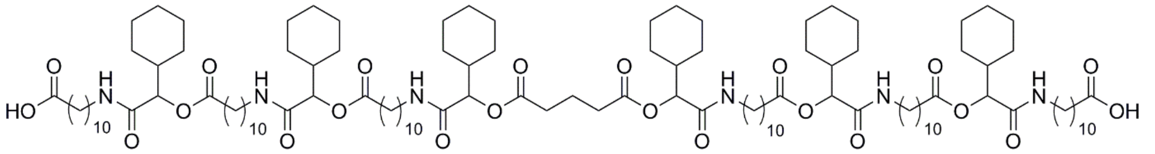

Substance $\mathbf{LO_{6c}}$ (2.83 g, 1.25 mmol, 1.0 eq.) was dissolved in ethyl acetate (4.2 mL, 0.15 M) and palladium on activated charcoal **19** (0.22 g, 8 wt%) was added. The reaction mixture was purged with hydrogen (balloon) and then stirred overnight under hydrogen atmosphere. The heterogeneous catalyst was filtered off and the solvent was evaporated under reduced pressure to obtain the product $\mathbf{LO_{6d}}$ without further purification in a yield of 82% (2.12 g, 1.02 mmol) as highly viscous, yellowish oil.

^{1}H NMR (400 MHz, $CDCl_3$) δ / ppm: 6.34 – 5.97 (m, 6H, 6 NH, ^{1}), 5.05 – 4.89 (m, 6H, 6 CH, ^{2}), 3.36 – 3.10 (m, 12H, 6 CH_2, ^{3}), 2.52 – 2.44 (m, 4H, 2 CH_2, ^{4}), 2.41 – 2.21 (m, 12H, 6 CH_2, ^{5}), 2.05 – 1.84 (m, 8H, 6 CH, CH_2, ^{6}), 1.78 – 1.54 (m, 36H, 21 CH_2, ^{7}), 1.53 – 1.38 (m, 12H, 6 CH_2, ^{8}), 1.37 – 0.89 (m, 108H, 53 CH_2, ^{9}).

^{13}C NMR (101 MHz, $CDCl_3$) δ / ppm: 177.9, 172.8, 172.7, 172.2, 172.1, 169.5, 169.3, 78.1, 40.1, 40.0, 39.4, 39.3, 34.4, 34.1, 33.1, 32.9, 29.6, 29.5, 29.4, 29.3, 29.2, 29.1, 27.5, 27.4, 27.0, 26.9, 26.2, 26.1, 26.0, 25.1, 24.9, 20.3, 20.2.

FAB-MS of $[C_{119}H_{206}N_6O_{22}]^+$: calculated: 2072.5, found:2072.8.

IR (ATR platinum diamond): ν /cm^{-1} = 3293.2, 2922.4, 2851.2, 1737.7, 1650.2, 1536.9, 1449.0, 1371.4, 1149.1, 1100.7, 985.4, 892.9, 720.8, 428.5.

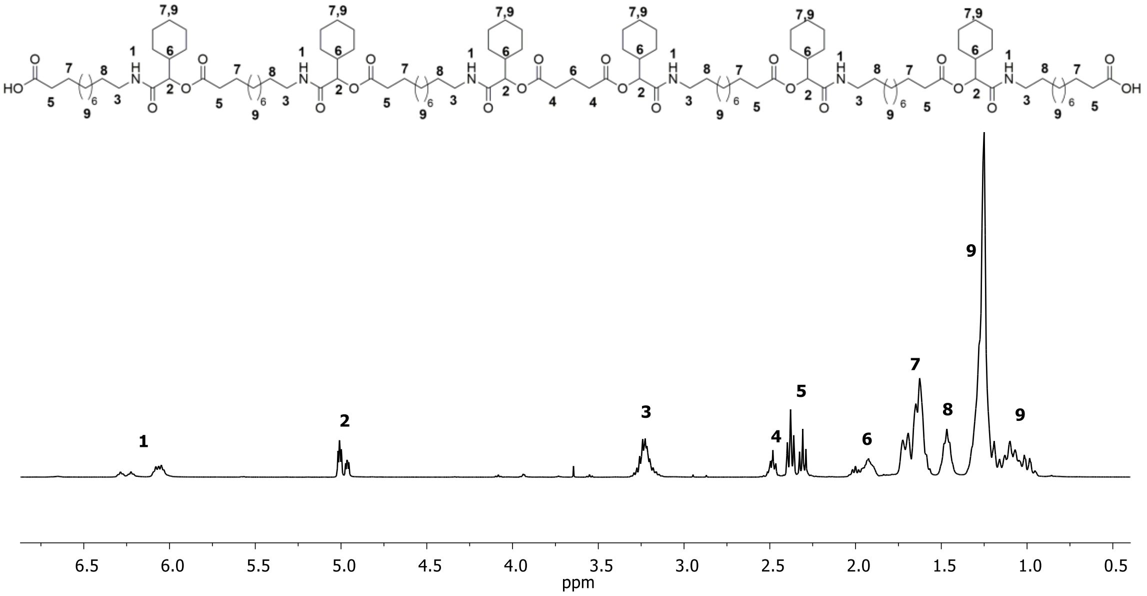
7,9
6
1
2
3
4
5
7
8
9
HO
OH
O
N
H
1
2
3
4
5
6
7
8
9
6.5
6.0
5.5
5.0
4.5
4.0
3.5
3.0
2.5
2.0
1.5
1.0
0.5
ppm

Synthesis of oligomers with sebacic acid 10 as core unit

1st Passerini reaction: Synthesis of Dimer LO_{2e}

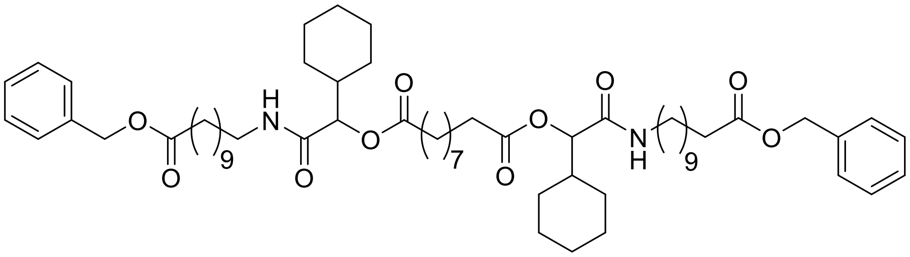

Sebacic acid **10** (776 mg, 3.85 mmol, 1.0 eq.) was suspended in DCM (7.6 mL, 0.5 M). Subsequently, cyclohexane carboxaldehyde **11b** (1.4 mL, 1.29 g, 11.5 mmol, 3.0 eq.) and monomer **M1** (3.48 g, 11.5 mmol, 3.0 eq.) were added and the reaction mixture was stirred at room temperature for 24 hours. The solvent was removed under reduced pressure and the crude product was purified by column chromatography (cyclohexane / ethyl acetate 5:1 → 1:1) to obtain the desired product **LO_{2e}** in a yield of 97% (3.84 g, 3.73 mmol) as a yellowish oil.

^{1}H NMR (300 MHz, $CDCl_3$) δ / ppm: 7.49 – 7.27 (m, 10H, CH, aromatic, ^{1}), 5.96 (t, J = 5.7 Hz, 2H, ^{2}), 5.10 (s, 4H, ^{3}), 5.01 (d, J = 4.7 Hz, 2H, ^{4}), 3.40 – 3.11 (m, 4H, ^{5}), 2.48 – 2.23 (m, 8H, ^{6}), 2.00 – 1.85 (m, 2H, ^{7}), 1.79 – 1.56 (m, 16H, ^{8}), 1.53 – 1.41 (m, 4H, ^{9}), 1.39 – 0.88 (m, 44H, ^{10}).

^{13}C NMR (75 MHz, $CDCl_3$) δ / ppm: 173.76, 172.58, 169.26, 136.21, 128.62, 128.24, 77.73, 66.15, 40.06, 39.24, 34.40, 34.33, 29.66, 29.53, 29.42, 29.29, 29.18, 29.14, 27.40, 26.93, 26.16, 26.08, 25.96, 25.02.

HRMS-FAB-MS of $[C_{62}H_{97}N_2O_{10}]^+$: calculated: 1029.7138, found: 1029.7136.

IR (ATR platinum diamond): ν/cm^{-1} = 2925.1, 2852.9, 1735.3, 1435.0, 1357.3, 1165.2, 697.7.

R

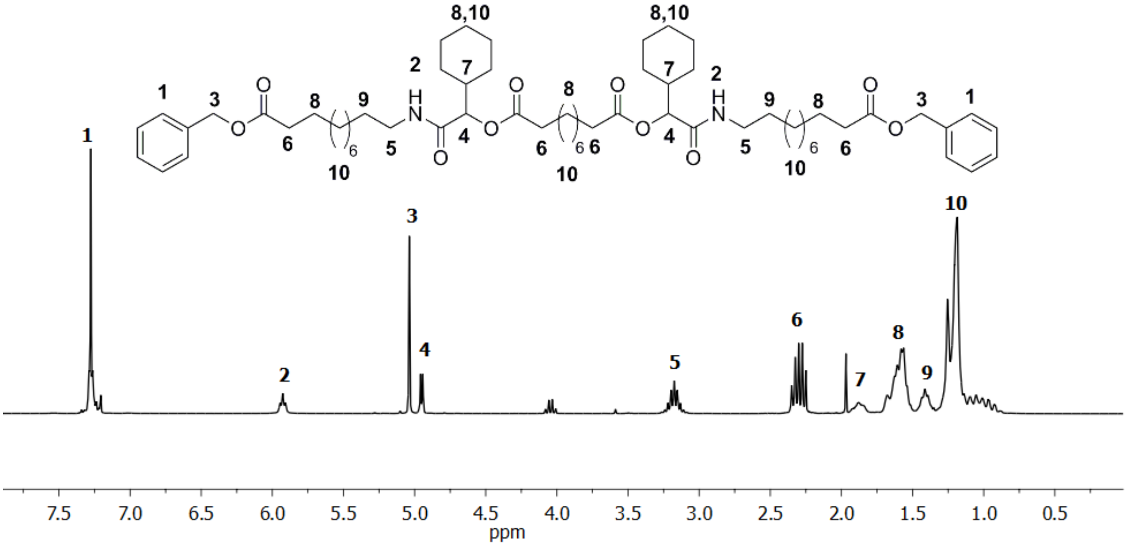

1st deprotection: Synthesis of Dimer LO$_{2f}$

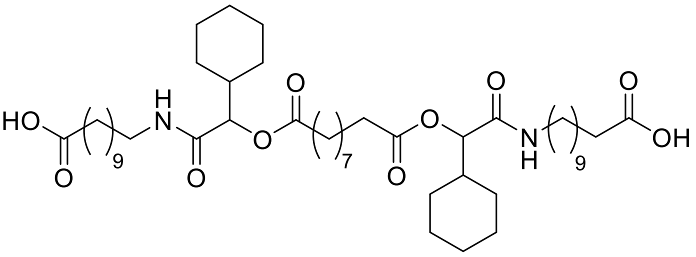

Substance **LO$_{2e}$** (3.61 g, 3.51 mmol, 1.0 eq.) was dissolved in ethyl acetate (7.0 mL, 0.5 M) and palladium on activated charcoal **19** (0.36 g, 10 wt%) was added. The reaction mixture was purged with hydrogen (balloon) and then stirred overnight under hydrogen atmosphere. The reaction mixture became solid over night and was dissolved in THF. The heterogeneous catalyst was filtered off and the solvent was evaporated under reduced pressure to afford the product **LO$_{2f}$** without further purification in a quant. yield (2.98 g, 3.51 mmol) as highly viscous, yellowish oil.

^{1}H NMR (300 MHz, CDCl$_3$) δ / ppm: 6.03 (t, *J* = 5.4 Hz, 2H, ^{1}), 5.01 (d, *J* = 4.7 Hz, 2H, ^{2}), 3.36 – 3.09 (m, 4H, ^{3}), 2.52 – 2.18 (m, 8H, ^{4}), 2.03 – 1.84 (m, 2H, ^{5}), 1.78 – 1.53 (m, 16H, ^{6}), 1.43 (dd, *J* = 20.1, 6.3 Hz, 4H, ^{7}), 1.38 – 0.88 (m, 44H, ^{8}).

^{13}C NMR (75 MHz, CDCl$_3$) δ / ppm: 179.28, 172.69, 169.51, 157.13, 132.52, 101.48, 77.75, 40.02, 39.29, 34.33, 34.14, 29.57, 29.45, 29.33, 29.29, 29.22, 29.15, 29.07, 27.42, 27.21, 27.01, 26.88, 26.16, 26.07, 25.95, 25.00, 24.79.

HRMS-ESI-MS of [$C_{48}H_{84}N_2O_{10}Na$]$^+$: calculated: 871.6018, found: 871.6019.

IR (ATR platinum diamond): ν /cm^{-1} = 2922.9, 2851.6, 1735.9, 1644.5, 1540.6, 1448.9, 1373.8, 1142.1, 1100.5, 983.9, 721.6, 430.1.

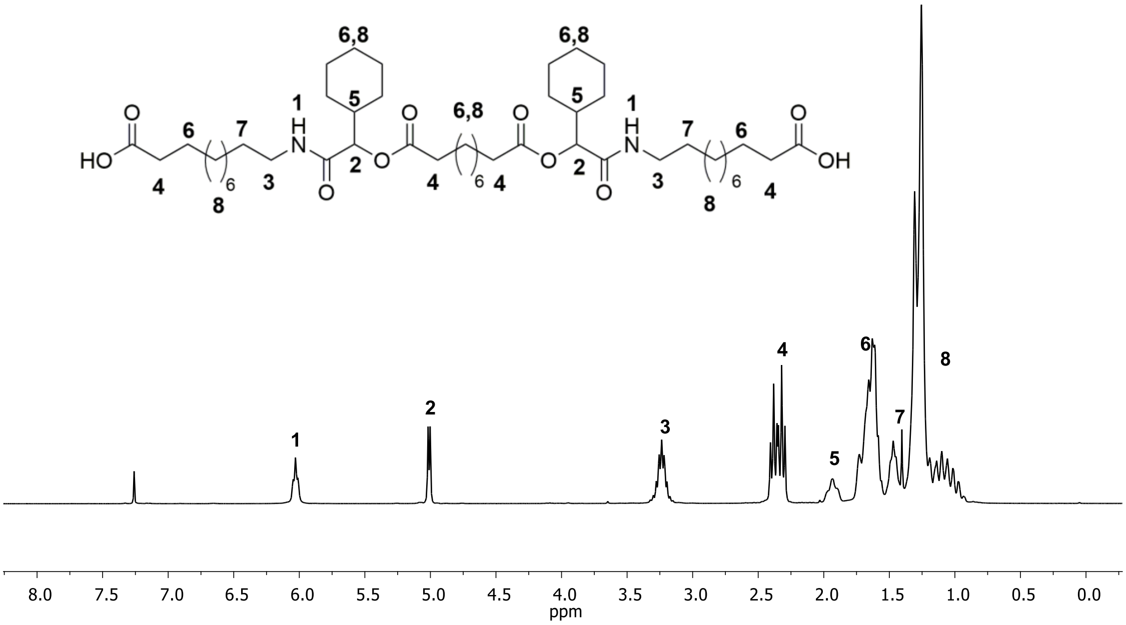

2nd Passerini reaction: Synthesis of Tetramer $\mathbf{LO_{4e}}$

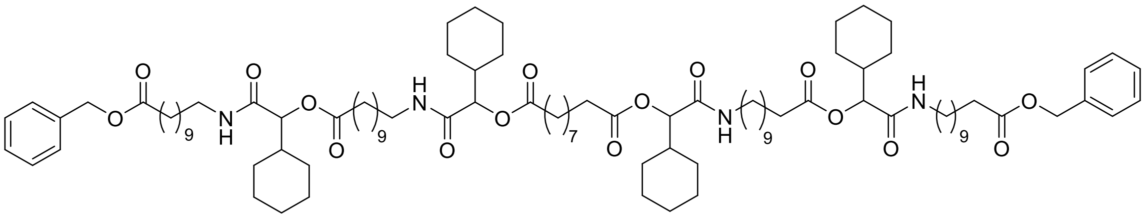

Substance $\mathbf{LO_{2f}}$ (2.41 g 2.83 mmol, 1.0 eq.) was dissolved in DCM (5.6 mL, 0.5 M). Subsequently, monomer **M1** (2.56 g, 8.49 mmol, 3.0 eq.) and cyclohexane carboxaldehyde **11b** (0.95 g 8.49 mmol, 3.0 eq.) were added and the reaction mixture was stirred at room temperature for 24 hours. The solvent was removed under reduced pressure and the crude product was purified by column chromatography (cyclohexane / ethyl acetate 3:1 → 1:2) to obtain the desired product $\mathbf{LO_{4e}}$ in a yield of 91% (4.29 g, 2.55 mmol) as a yellowish, highly viscous oil.

^{1}H NMR (300 MHz, $CDCl_3$) δ / ppm: 7.43 – 7.27 (m, 10H, ^{1}), 6.01 (t, J = 5.5 Hz, 4H, ^{2}), 5.08 (s, 4H, ^{3}), 4.99 (t, J = 4.3 Hz, 4H, ^{4}), 3.36 – 3.08 (m, 8H, ^{5}), 2.49 – 2.18 (m, 12H, ^{6}), 1.93 (m, 4H, ^{7}), 1.78 – 1.54 (m, 28H, ^{8}), 1.44 (m, 8H, ^{9}), 1.36 – 0.80 (m, 80H, ^{10}).

^{13}C NMR (75 MHz, $CDCl_3$) δ / ppm: 173.70, 172.59, 172.56, 171.17, 169.25, 136.16, 128.57, 128.18, 77.69, 77.65, 66.09, 60.42, 40.02, 39.18, 34.35, 34.31, 34.27, 29.61, 29.49, 29.38, 29.25, 29.14, 29.11, 27.38, 27.35, 26.89, 26.12, 26.04, 25.92, 25.02, 24.98, 21.08, 14.24.

HRMS-ESI-MS of $[C_{100}H_{162}N_4O_{16}Na]^+$: calculated: 1698.1878 found: 1698.1914.
$[C_{100}H_{162}N_4O_{16}Na_2]^{2+}$: calculated: 860.5885 found: 860.5882.

IR (ATR platinum diamond): ν /cm^{-1} = 3304.9, 2922.7, 2851.2, 1735.8, 1651.2, 1532.9, 1449.3, 1373.9, 1231.0, 1148.6, 1100.8, 984.3, 733.6, 696.4, 577.8, 453.9, 429.6.

***R*$_f$** (cyclohexane / ethyl acetate 3:2) = 0.50.

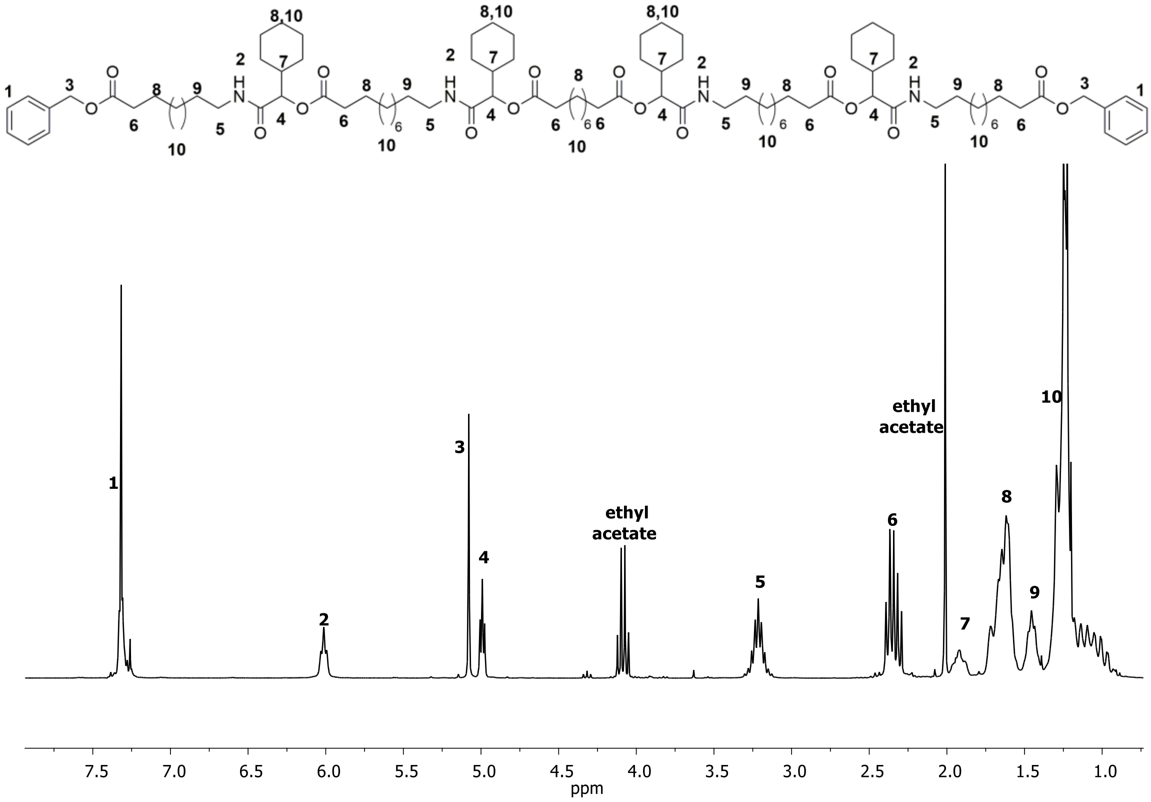
8,10
7
2
1
3
6
8
9
10
5
4
6
ethyl acetate
1
2
3
4
5
6
7
8
9
10
7.5
7.0
6.5
6.0
5.5
5.0
4.5
4.0
3.5
3.0
2.5
2.0
1.5
1.0
ppm

2nd deprotection: Synthesis of Tetramer **LO$_{4f}$**

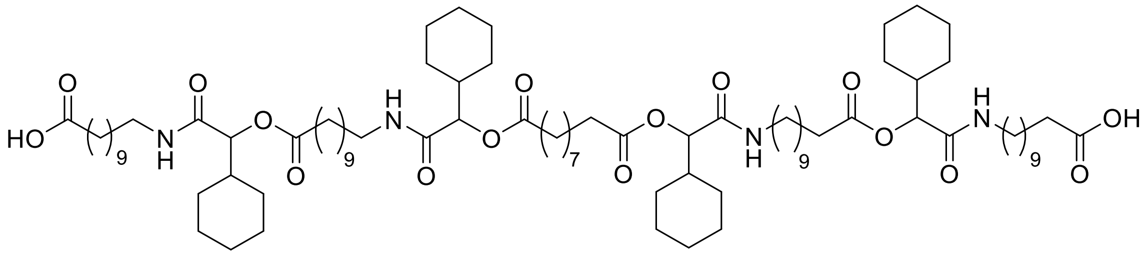

Substance **LO$_{4e}$** (3.89 g, 2.32 mmol, 1.0 eq.) was dissolved in ethyl acetate (5.0 mL, 0.5 M) and palladium on activated charcoal **19** (0.39 g, 10 wt%) was added. The reaction mixture was purged with hydrogen (balloon) and then stirred overnight under hydrogen atmosphere. The heterogeneous catalyst was removed by filtration and the solvent was evaporated under reduced pressure to afford the desired product **LO$_{4f}$** without further purification in a yield of 98% (3.39 g, 2.26 mmol) as highly viscous, orange oil.

^{1}H NMR (300 MHz, CDCl$_3$) δ / ppm: 6.05 (d, J = 5.7 Hz, 4H, ^{1}), 5.11 – 4.89 (m, 4H, ^{2}), 3.35 – 3.08 (m, 8H, ^{3}), 2.56 – 2.15 (m, 12H, ^{4}), 1.97 (m, 4H, ^{5}), 1.81 – 1.52 (m, 28H, ^{6}), 1.43 (m, 8H, ^{7}), 1.37 – 0.79 (m, 80H, ^{8}).

^{13}C NMR (75 MHz, CDCl$_3$) δ / ppm: 178.35, 172.68, 169.46, 157.05, 133.81, 126.28, 113.98, 101.39, 77.76, 77.71, 40.03, 39.84, 39.30, 39.25, 34.36, 34.31, 34.10, 29.62, 29.54, 29.45, 29.34, 29.26, 29.22, 29.13, 29.10, 27.82, 27.45, 27.40, 26.92, 26.89, 26.16, 26.07, 25.96, 25.08, 24.99, 24.84.

HRMS-ESI-MS of $[C_{86}H_{150}N_4O_{16}Na]^+$: calculated: 1518.0939, found: 1518.0933.
$[C_{86}H_{150}N_4O_{16}Na_2]^{2+}$: calculated: 770.5416, found: 770.5398.

IR (ATR platinum diamond): ν /cm^{-1} = 3305.2, 2922.5, 2851.4, 1737.0, 1649.3, 1537.0, 1449.0, 1372.1, 1146.4, 1100.8, 984.7, 893.0, 720.7, 430.4.

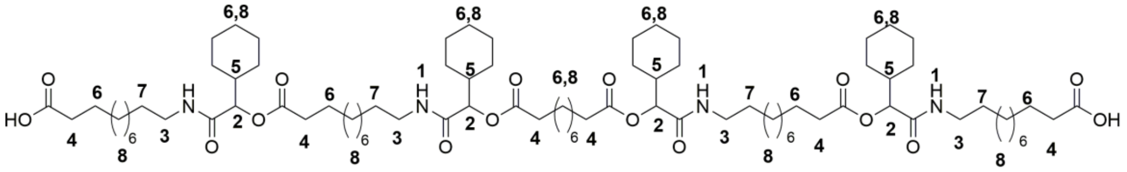
6,8
5
1
2
3
4
6
7
8
HO
OH
N
H
O

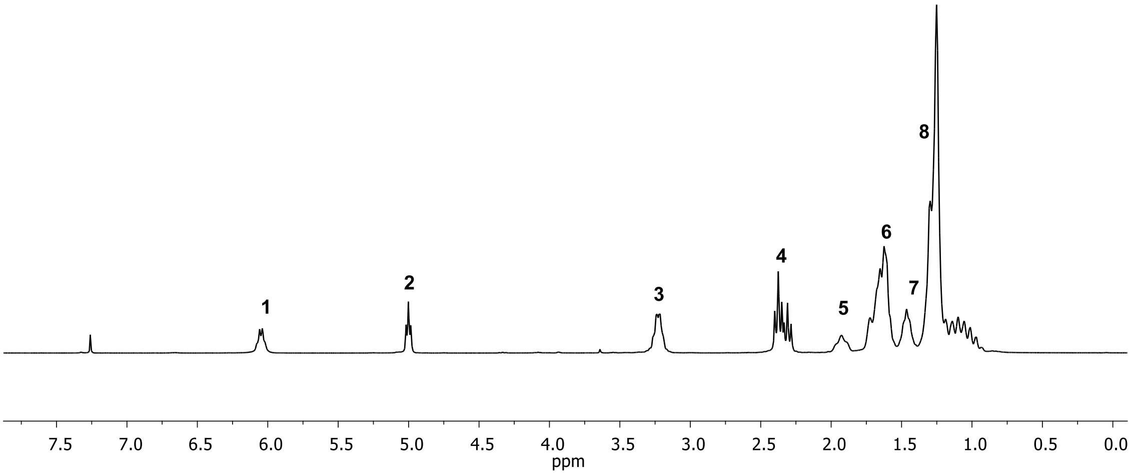
1
2
3
4
5
6
7
8
7.5
7.0
6.5
6.0
5.5
5.0
4.5
4.0
3.5
3.0
2.5
2.0
1.5
1.0
0.5
0.0
ppm

3rd Passerini reaction: Synthesis of Hexamer LO_{6e}

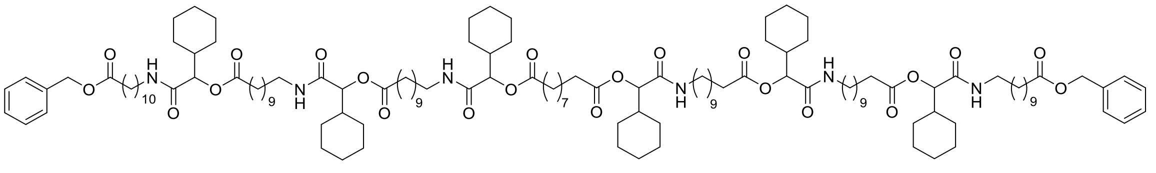

Substance $\mathbf{LO_{4f}}$ (2.38 g, 1.58 mmol, 1.0 eq.) was dissolved in DCM (4.8 mL, 0.33 M). Subsequently, monomer **M1** (1.44 g 4.77 mmol, 3.0 eq.) and cyclohexane carboxaldehyde **11b** (0.53 g, 4.77 mmol, 3.0 eq.) were added and the reaction mixture was stirred at room temperature for 48 hours. The solvent was removed under reduced pressure and the crude product was purified by column chromatography (cyclohexane / ethyl acetate 7:1 → 1:3) to obtain the desired product $\mathbf{LO_{6e}}$ in a yield of 97% (3.58 g, 1.54 mmol) as a yellowish, highly viscous oil.

^{1}H NMR (300 MHz, $CDCl_3$) δ / ppm: 7.39 – 7.21 (m, 10H, ^{1}), 6.05 (s, 6H, ^{2}), 5.06 (s, 4H, ^{3}), 4.97 (t, J = 4.2 Hz, 6H, ^{4}), 3.32 – 3.04 (m, 12H, ^{5}), 2.44 – 2.24 (m, 16H, ^{6}), 1.88 (m, 6H, ^{7}), 1.65 (m, 40H, ^{8}), 1.51 – 1.36 (m, 12H, ^{9}), 1.35 – 0.83 (m, 116H, ^{10}).

^{13}C NMR (75 MHz, $CDCl_3$) δ / ppm: 173.65, 172.57, 171.12, 169.22, 136.14, 128.54, 128.14, 77.65, 77.59, 66.05, 60.38, 39.99, 39.15, 34.31, 34.27, 34.23, 29.58, 29.46, 29.36, 29.23, 29.13, 29.10, 27.33, 27.15, 26.86, 26.09, 26.01, 25.90, 24.99, 24.94, 21.04, 14.21.

HRMS-ESI-MS of $[C_{138}H_{228}N_6O_{22}Na]^+$: calculated: 2344.6799, found: 2344.6778.
$[C_{138}H_{228}N_6O_{22}Na_2]^{2+}$: calculated: 1183.8346, found: 1183.8368.

IR (ATR platinum diamond): ν /cm^{-1} = 3304.9, 2922.4, 2851.1, 1736.6, 1650.8, 1533.0, 1449.3, 1373.6, 1230.5, 1150.6, 1100.9, 985.1, 844.4, 731.1, 696.4, 577.3, 428.7.

***R*$_f$** (cyclohexane / ethyl acetate 2:1) = 0.51.

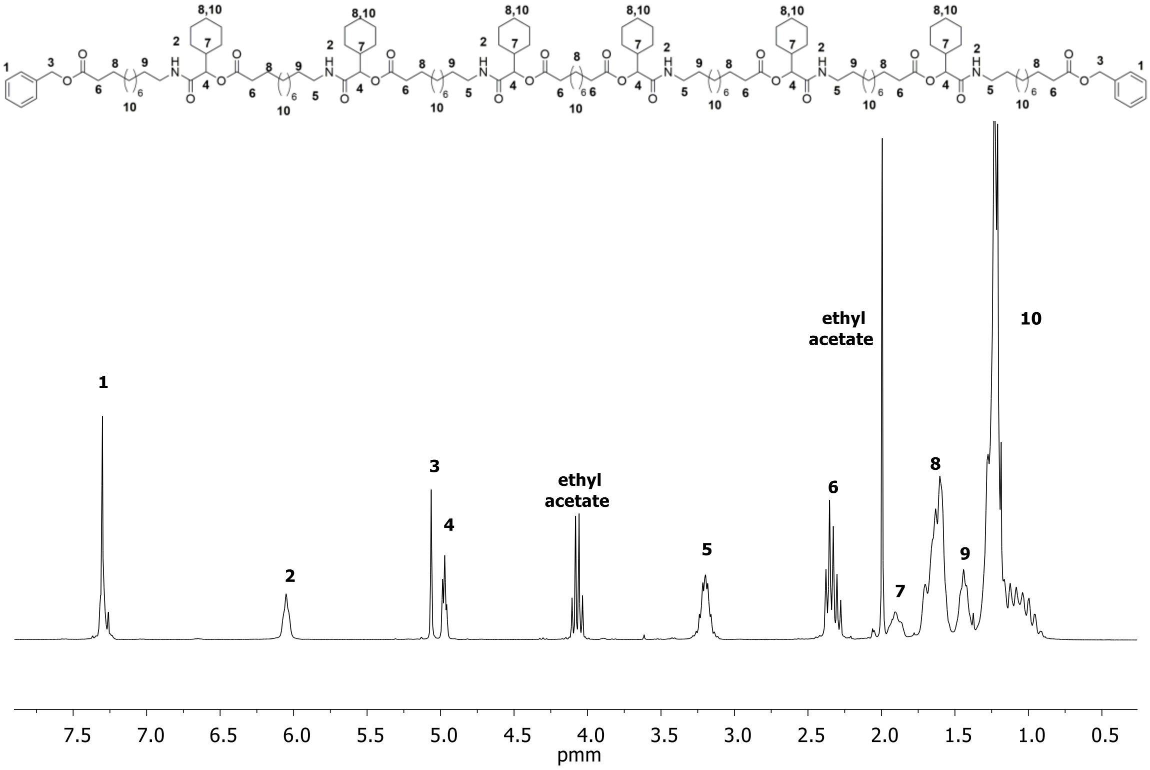
1
2
3
4
ethyl
acetate
5
6
ethyl
acetate
7
8
9
10
8,10
7.5
7.0
6.5
6.0
5.5
5.0
4.5
4.0
3.5
3.0
2.5
2.0
1.5
1.0
0.5
pmm

3rd deprotection: Synthesis of Hexamer $\mathbf{LO_{6f}}$

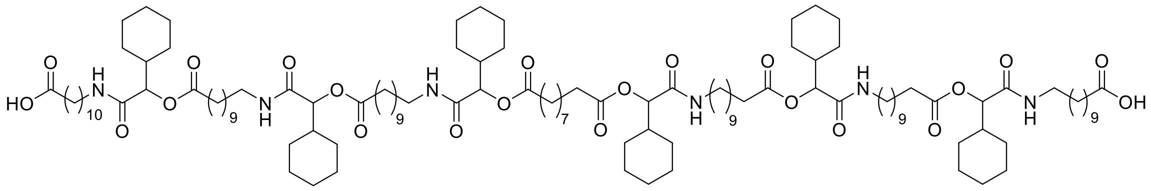

Substance $\mathbf{LO_{6e}}$ (3.24 g, 1.39 mmol, 1.0 eq.) was dissolved in ethyl acetate (4.5 mL, 0.3 M) and palladium on activated charcoal **19** (0.32 g, 10 wt%) was added. The reaction mixture was purged with hydrogen (balloon) and then stirred overnight under hydrogen atmosphere. The heterogeneous catalyst was filtered off and the solvent was evaporated under reduced pressure to obtain the product $\mathbf{LO_{6f}}$ without further purification in a yield of 94% (2.80 g, 1.31 mmol) as highly viscous, yellowish oil.

^{1}H NMR (300 MHz, $CDCl_3$) δ / ppm: 6.08 (m, 6H, ^{1}), 4.98 (m, 6H, ^{2}), 3.20 (m, 12H, ^{3}), 2.32 (m, 16H, ^{4}), 1.84 (m, 6H, ^{5}), 1.60 (m, 40H, ^{6}), 1.45 (m, 12H, ^{7}), 1.34 – 0.78 (m, 116H, ^{8}).

^{13}C NMR (75 MHz, $CDCl_3$) δ / ppm: 177.76, 172.64, 169.41, 156.85, 134.14, 133.85, 126.08, 113.51, 101.20, 77.67, 40.00, 39.65, 39.24, 34.30, 34.06, 29.57, 29.49, 29.39, 29.22, 29.09, 27.39, 26.88, 26.11, 26.03, 25.92, 25.02, 24.95, 24.84.

HRMS-ESI-MS of $[C_{124}H_{216}N_6O_{22}Na]^+$: calculated: 2164.5860, found: 2164.5895.
$[C_{124}H_{216}N_6O_{22}Na_2]^{2+}$: calculated: 1093.7876, found: 1093.7906.

IR (ATR platinum diamond): ν /cm^{-1} = 3293.2, 2922.4, 2851.2, 1737.7, 1650.2, 1536.9, 1449.0, 1371.4, 1149.1, 1100.7, 985.4, 892.9, 720.8, 428.5.

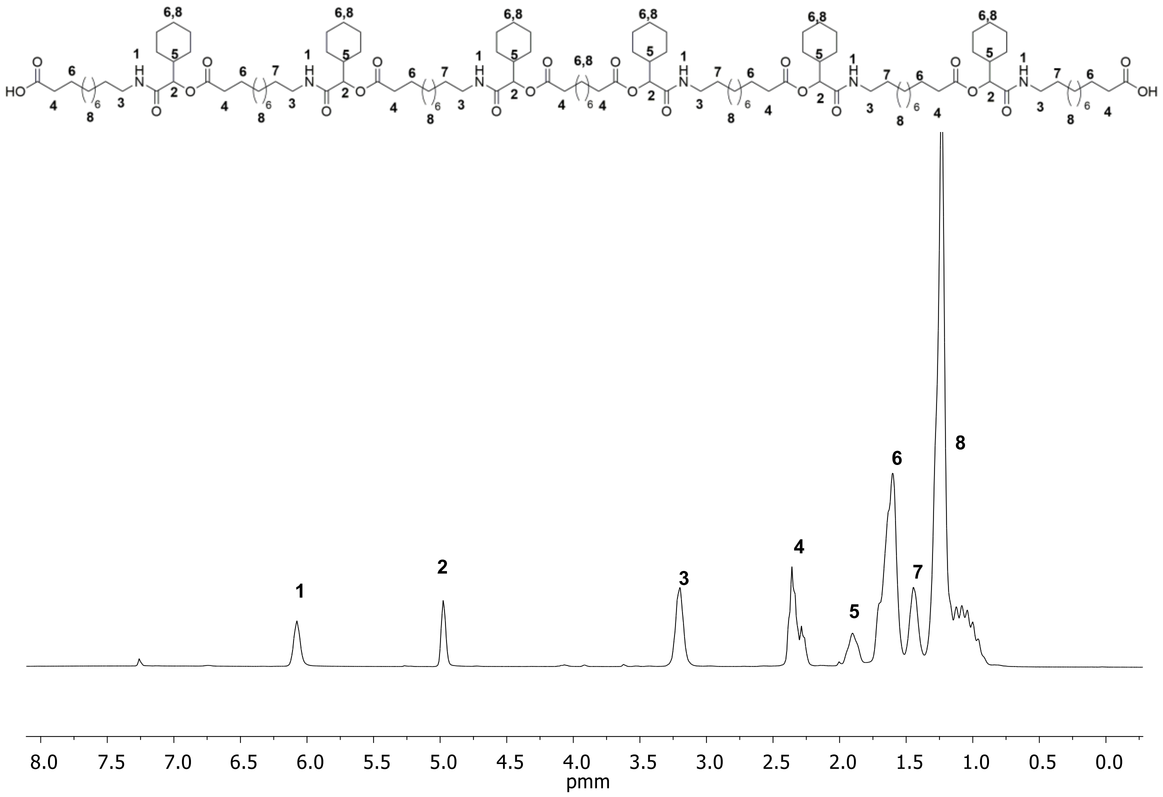
HO
OH
1
2
3
4
5
6
7
8
6,8
1
2
3
4
5
6
7
8
8.0
7.5
7.0
6.5
6.0
5.5
5.0
4.5
4.0
3.5
3.0
2.5
2.0
1.5
1.0
0.5
0.0
pmm

4th Passerini reaction: Synthesis of Octamer $\mathbf{LO_{8e}}$

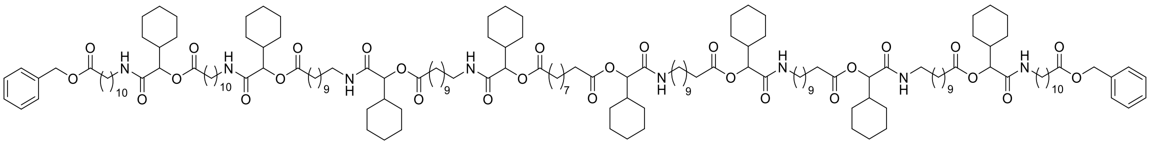

Substance $\mathbf{LO_{6f}}$ (1.94 g, 0.90 mmol, 1.0 eq.) was dissolved in DCM (2.0 mL, 0.5 M). Subsequently, monomer **M1** (0.82 g, 2.71 mmol, 3.0 eq.) and cyclohexane carboxaldehyde **11b** (0.33 g, 2.71 mmol, 3.0 eq.) were added and the reaction mixture was stirred at room temperature for 48 hours. The solvent was removed under reduced pressure and the crude product was purified by column chromatography (cyclohexane / ethyl acetate 5:1 → 0:1) to obtain the desired product $\mathbf{LO_{8e}}$ in a yield of 99% (2.70 g, 0.90 mmol) as an orange, highly viscous oil.

^{1}H NMR (300 MHz, $CDCl_3$) δ / ppm: 7.30 (s, 10H, ^{1}), 6.09 (m, 8H, ^{2}), 5.03 (s 4H, ^{3}), 4.98 (m, 8H, ^{4}), 3.19 (m, 16H, ^{5}), 2.47 – 2.21 (m, 20H, ^{6}), 1.90 (m, 8H, ^{7}), 1.75 – 1.52 (m, 52H, ^{8}), 1.40 (m, 16H, ^{9}), 1.34 – 0.68 (m, 152H, ^{10}).

^{13}C NMR (75 MHz, $CDCl_3$) δ / ppm: 173.65, 172.57, 169.23, 163.04, 156.88, 136.14, 128.53, 128.15, 128.13, 77.62, 66.05, 60.38, 39.99, 39.15, 34.32, 34.27, 34.23, 29.58, 29.46, 29.36, 29.22, 29.12, 29.10, 29.07, 27.34, 26.85, 26.09, 26.01, 25.90, 24.99, 24.94, 21.04, 14.21.

HRMS-ESI-MS of $[C_{176}H_{294}N_8O_{28}Na]^+$: calculated: 2991.1720, found:2991.1691.
$[C_{176}H_{294}N_8O_{28}Na_2]^{2+}$: calculated: 1507.0806, found: 1507.0835.
$[C_{176}H_{294}N_8O_{28}Na_3]^{3+}$: calculated: 1012.3835, found: 1012.3814.

IR (ATR platinum diamond): ν /cm^{-1} = 3295.1, 2923.1, 2851.9, 1737.7, 1651.1, 1534.4, 1449.8, 1372.8, 1158.9, 1101.2, 986.3, 723.0, 697.0, 578.2, 430.6.

R_f (cyclohexane / ethyl acetate 1:1) = 0.57.

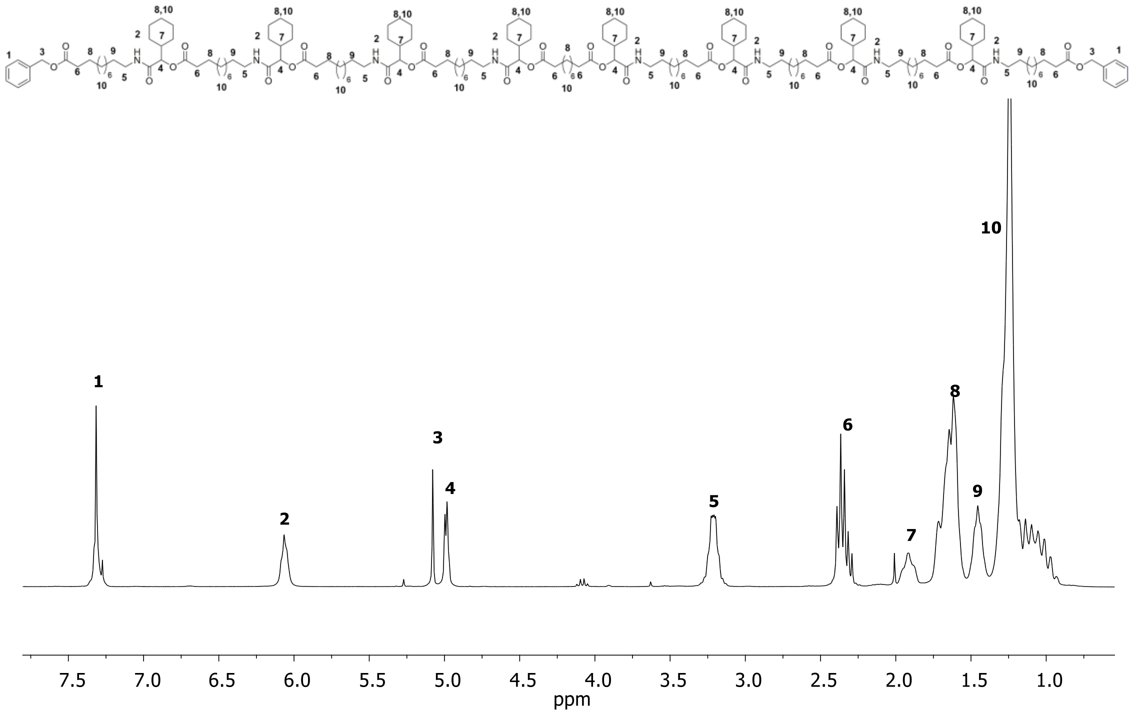
1
2
3
4
5
6
7
8
9
10
7.5
7.0
6.5
6.0
5.5
5.0
4.5
4.0
3.5
3.0
2.5
2.0
1.5
1.0
ppm

4th deprotection: Synthesis of Octamer **LO$_{8f}$**

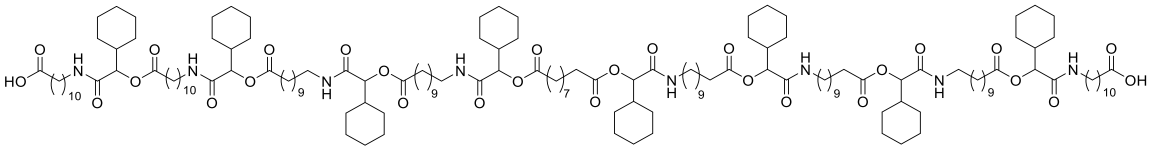

Substance **LO$_{8e}$** (2.51 g 0.85 mmol, 1.0 eq.) was dissolved in a mixture of 5.0 mL ethyl acetate and 0.5 mL methanol and palladium on activated charcoal **19** (0.25 g, 10 wt%) was added. The reaction mixture was purged with hydrogen (balloon) and then stirred overnight under hydrogen atmosphere. The heterogeneous catalyst was filtered off and the solvent was evaporated under reduced pressure to obtain the product **LO$_{8f}$** without further purification in a yield of 78% (1.82 g, 0.65 mmol) as highly viscous, yellowish oil.

^{1}H NMR (300 MHz, CDCl$_3$) *δ* / ppm: 6.10 (s, 8H, ^{1}), 4.96 (s, 8H, ^{2}), 3.19 (m, 16H, ^{3}), 2.31 (m, 20H, ^{4}), 1.83 (m, 8H, ^{5}), 1.75 – 1.52 (m, 52H, ^{6}), 1.39 (m, 16H, ^{7}), 1.32 – 0.81 (m, 152H, ^{8}).

^{13}C NMR (75 MHz, CDCl$_3$) *δ* / ppm: 185.58, 182.89, 180.29, 177.43, 172.64, 169.39, 162.97, 156.81, 134.14, 133.28, 117.84, 78.21, 77.51, 77.03, 45.76, 39.96, 39.62, 39.20, 34.27, 34.05, 29.47, 29.37, 29.19, 27.39, 26.84, 26.06, 24.98, 15.00.

HRMS-ESI-MS of $[C_{162}H_{282}N_8O_{28}Na]^+$: calculated: 2811.0781, found: 2811.0787.
$[C_{162}H_{282}N_8O_{28}Na_2]^{2+}$: calculated: 1417.0337, found: 1417.0364.
$[C_{162}H_{282}N_8O_{28}Na_3]^{3+}$: calculated: 952.3522, found: 952.3505.

IR (ATR platinum diamond): ν /cm^{-1} = 3292.9, 2922.5, 2851.7, 1738.4, 1649.2, 1535.2, 1449.4, 1371.8, 1159.6, 1100.9, 986.3, 722.1, 430.8.

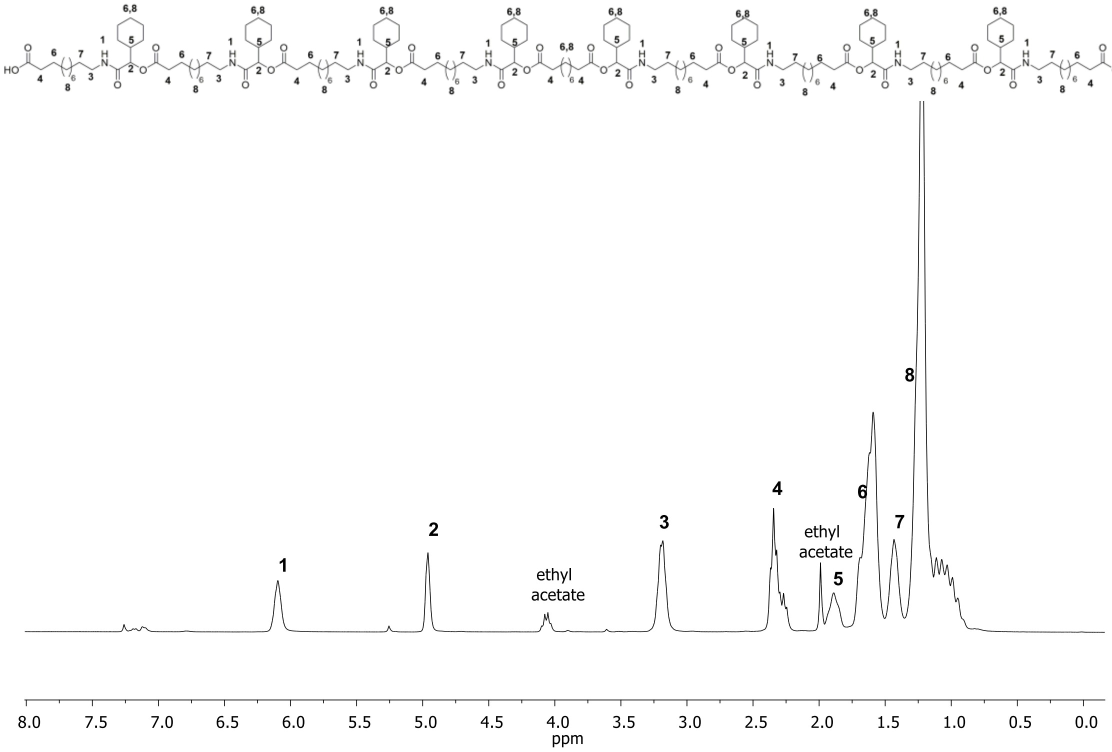

Oligomer with isopropyl side chains and sebacic acid 10 as core unit

1st Passerini reaction: Synthesis of Dimer LO$_{2g}$

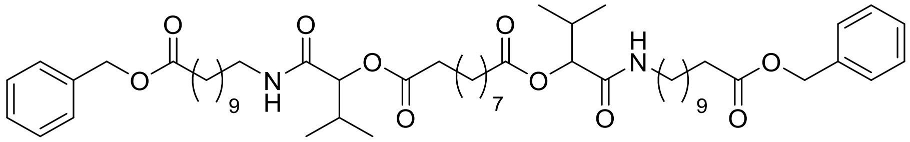

Sebacic acid **10** (700 mg, 3.46 mmol, 1.0 eq.) was dissolved in DCM (7.0 mL, 0.5 M). Subsequently, monomer **M1** (3.13 g, 10.4 mmol, 3.0 eq.) and isobutyraldehyde **11c** (0.95 mL, 75.0 mg, 10.4 mmol, 3.0 eq.) were added and the reaction mixture was stirred at room temperature for 24 hours. The solvent was removed under reduced pressure and the crude product was purified by column chromatography (cyclohexane / ethyl acetate 5:1 → 1:1) to obtain the desired product **LO$_{2g}$** in a yield of 99% (3.27 g, 3.45 mmol) as a yellowish, highly viscous oil.

^{1}H NMR (300 MHz, CDCl$_3$) δ / ppm: 7.42 – 7.27 (m, 10H, ^{1}), 5.98 (t, *J* = 5.6 Hz, 2H, ^{2}), 5.10 (s, 4H, ^{3}), 5.03 (d, *J* = 4.5 Hz, 2H, ^{4}), 3.36 – 3.12 (m, 4H, ^{5}), 2.46 – 2.19 (m, 10H, ^{6}), 1.62 (m, 8H, ^{7}), 1.54 – 1.40 (m, 4H, ^{8}), 1.26 (m, 32H, ^{9}), 0.92 (dd, *J* = 6.9, 3.1 Hz, 12H, ^{10}).

^{13}C NMR (75 MHz, CDCl$_3$) δ / ppm: 173.75, 172.59, 169.33, 136.20, 128.61, 128.23, 78.04, 66.13, 39.24, 34.39, 34.31, 30.59, 29.65, 29.50, 29.40, 29.27, 29.17, 29.12, 26.91, 25.01, 18.86, 17.07.

HRMS-FAB-MS of [$C_{56}H_{89}O_{10}N_2$]$^+$: calculated: 949.6512, found: 949.6510.

IR (ATR platinum diamond): ν /cm^{-1} = 3305.6, 2924.8, 2852.4, 1734.6, 1654.0, 1531.9, 1455.4, 1369.3, 1231.2, 1160.0, 1101.8, 734.6, 696.7.

***R*$_f$** (cyclohexane / ethyl acetate 2:1) = 0.60.

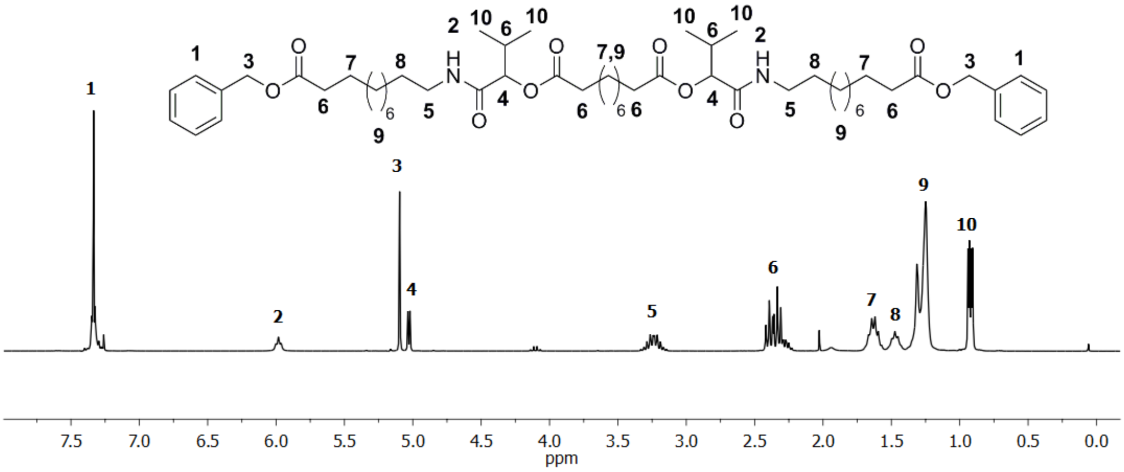

1st deprotection: Synthesis of Dimer LO_{2h}

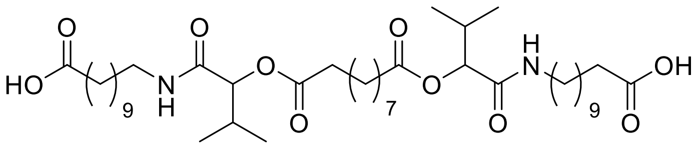

Substance $\mathbf{LO_{2g}}$ (3.08 g, 3.24 mmol, 1.0 eq) was dissolved in 8 mL ethyl acetate and palladium on activated charcoal **19** (300 mg, 10 wt%) was added. The reaction mixture was purged with hydrogen (balloon) and then stirred overnight under hydrogen atmosphere. The heterogeneous catalyst was filtered off and the solvent was evaporated under reduced pressure to obtain product $\mathbf{LO_{2h}}$ without further purification in a yield of 97% (2.41 g, 3.13 mmol) as highly viscous, colourless oil.

^{1}**H NMR** (300 MHz, $CDCl_3$) δ / ppm: 6.03 (t, J = 5.6 Hz, 2H, ^{1}), 5.03 (d, J = 4.5 Hz, 2H, ^{2}), 3.38 – 3.09 (m, 4H, ^{3}), 2.48 – 2.19 (m, 10H, ^{4}), 1.60 (m, 8H, ^{5}), 1.53 – 1.42 (m, 4H, ^{6}), 1.29 (m, 32H, ^{7}), 0.95 (ddd, J = 10.3, 6.9, 3.4 Hz, 12H, ^{8}).

^{13}**C NMR** (75 MHz, CDCl3) δ / ppm: 179.08, 172.72, 169.61, 78.10, 39.33, 34.33, 34.13, 30.60, 29.58, 29.43, 29.32, 29.21, 29.14, 29.06, 26.88, 25.03, 24.80, 18.86, 17.11.

HRMS-FAB-MS of $[C_{42}H_{77}N_2O_{10}]^+$: calculated: 769.5573, found: 769.5573.

IR (ATR platinum diamond): ν /cm^{-1} = 3307.0, 2925.3, 2853.4, 1738.3, 1648.9, 1541.0, 1463.7, 1370.1, 1165.8, 1125.4, 1004.9, 929.0, 722.4.

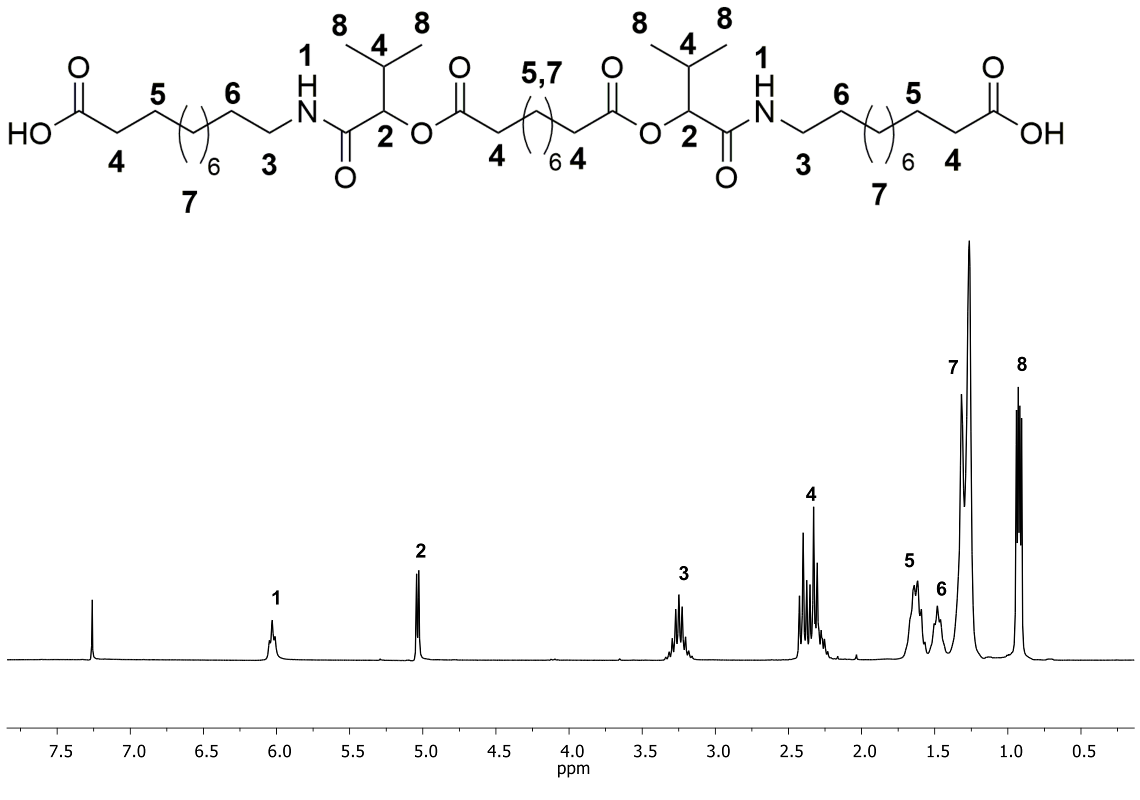

2nd Passerini reaction: Synthesis of Tetramer **LO$_{4g}$**

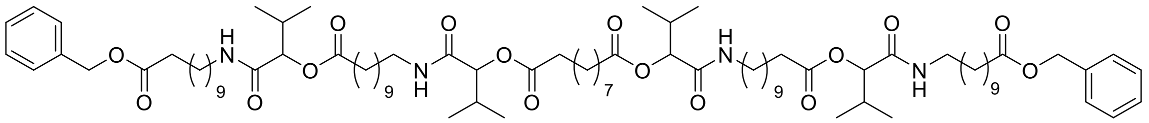

Substance **LO$_{2h}$** (2.34 g, 3.05 mmol, 1.0 eq.) was dissolved in DCM (7.0 mL, 0.5 M). Subsequently, monomer **M1** (2.75 g 9.14 mmol, 3.0 eq.) and isobutyraldehyde **11c** (0.84 mL, 66.0 mg, 9.14 mmol, 3.0 eq.) were added and the reaction mixture was stirred at room temperature for 24 hours. The solvent was removed under reduced pressure and the crude product was purified by column chromatography (cyclohexane / ethyl acetate 4:1 → 1:1) to obtain the desired product **LO$_{2g}$** in a yield of 99% (4.70 g, 3.04 mmol) as a yellowish, highly viscous oil.

^{1}H NMR (300 MHz, CDCl$_3$) δ / ppm: 7.40 – 7.28 (m, 10H, ^{1}), 6.02 (dd, *J* = 13.8, 8.4 Hz, 4H, ^{2}), 5.08 (s, 4H, ^{3}), 5.03 – 4.97 (m, 4H, ^{4}), 3.37 – 3.10 (m, 8H, ^{5}), 2.48 – 2.11 (m, 16H, ^{6}), 1.72 – 1.53 (m, 12H, ^{7}), 1.50 – 1.39 (m, 8H, ^{8}), 1.27 (d, *J* = 16.4 Hz, 56H, ^{9}), 1.05 – 0.70 (m, 24H, ^{10}).

^{13}C NMR (75 MHz, CDCl$_3$) *δ* / ppm: 173.71, 172.60, 172.58, 169.31, 136.16, 128.57, 128.18, 77.99, 77.95, 66.09, 39.19, 34.35, 34.31, 34.26, 30.56, 29.62, 29.46, 29.37, 29.23, 29.13, 29.08, 26.87, 25.03, 24.97, 18.83, 17.04, 17.02.

HRMS-ESI-MS of [$C_{88}H_{146}O_{16}N_4Na$]$^+$: calculated: 1538.0626, found: 1538.0636.

IR (ATR platinum diamond): ν /cm^{-1} = 3305.4, 2924.8, 2853.2, 1736.5, 1653.4, 1532.9, 1462.1, 1369.4, 1232.0, 1161.4, 1003.8, 734.4, 697.4.

***R*$_f$** (cyclohexane / ethyl acetate 1:1) = 0.75.

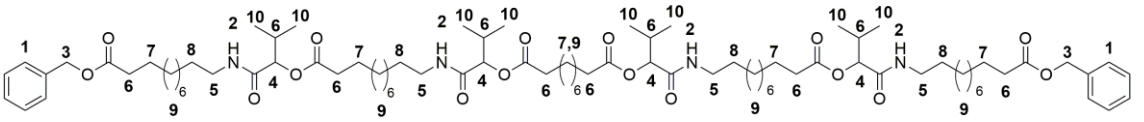

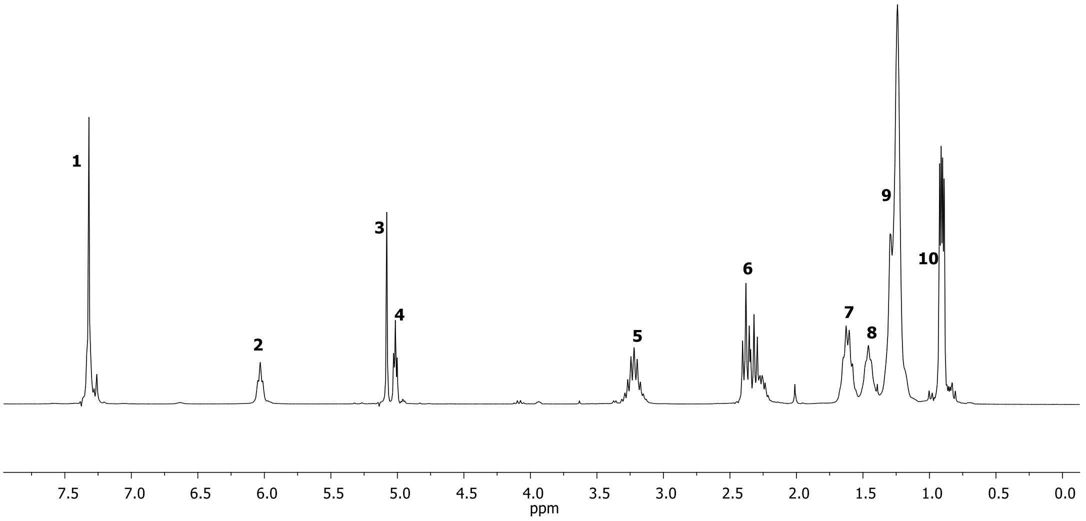

2nd deprotection: Synthesis of Tetramer **LO_{4h}**

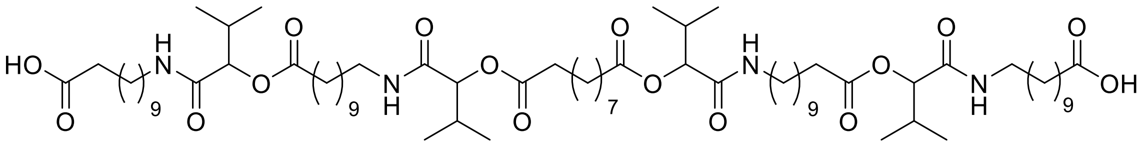

Substance **LO_{4g}** (1.78 g, 1.17 mmol, 1.0 eq) was dissolved in 3.5 mL ethyl acetate and palladium on activated charcoal **19** (178 mg, 10 wt%) was added. The reaction mixture was purged with hydrogen (balloon) and then stirred overnight under hydrogen atmosphere. The heterogeneous catalyst was filtered off and the solvent was evaporated under reduced pressure to obtain product **LO_{4h}** without further purification in a yield of 97% (1.53 g, 1.14 mmol) as highly viscous, colourless oil.

^{1}H NMR (300 MHz, $CDCl_3$) δ / ppm: 6.24 – 5.95 (m, 4H, ^{1}), 4.99 (t, *J* = 4.3 Hz, 4H, ^{2}), 3.37 – 3.01 (m, 8H, ^{3}), 2.48 – 2.12 (m, 16H, ^{4}), 1.72 – 1.51 (m, 12H, ^{5}), 1.49 – 1.39 (m, 8H, ^{6}), 1.25 (m, 56H, ^{7}), 0.89 (dd, *J* = 6.8, 3.5 Hz, 24H, ^{8}).

^{13}C NMR (75 MHz, $CDCl_3$) δ / ppm: 178.21, 172.66, 169.53, 77.96, 77.92, 39.25, 39.22, 34.27, 34.22, 34.07, 30.52, 29.55, 29.50, 29.45, 29.40, 29.35, 29.30, 29.22, 29.18, 29.13, 29.05, 26.83, 25.01, 24.92, 24.78, 18.79, 17.03, 17.00.

HRMS-ESI-MS of $[C_{74}H_{134}N_4O_{16}Na]^+$: calculated: 1357.9687, found: 1357.9690.

IR (ATR platinum diamond): ν /cm^{-1} = 3305.2, 2924.8, 2853.6, 1737.5, 1649.1, 1537.7, 1463.4, 1369.6, 1232.5, 1162.2, 1125.8, 1107.8, 923.7, 721.8, 646.3, 418.0.

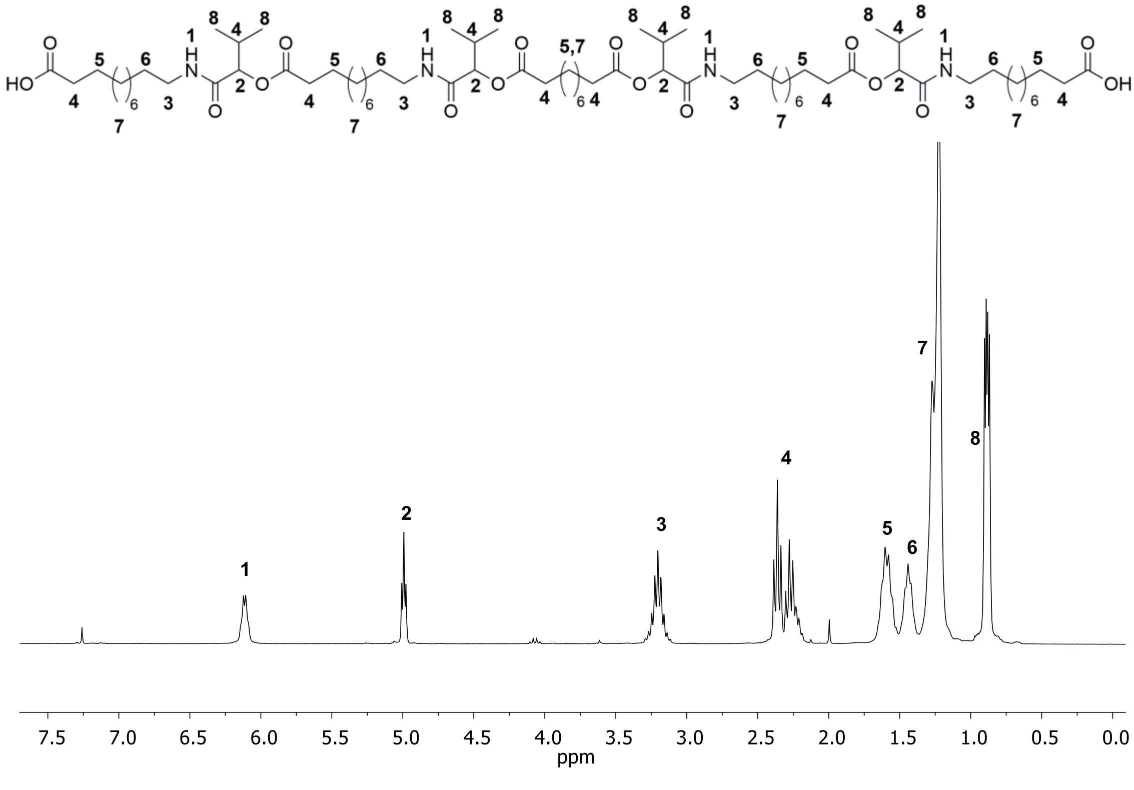

3rd Passerini reaction: Synthesis of Hexamer LO$_{6g}$

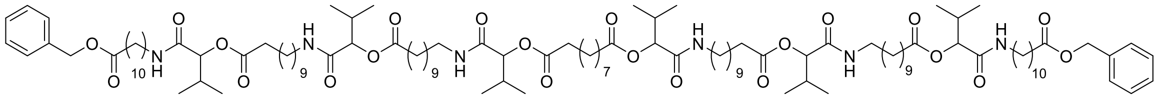

Substance **LO$_{4h}$** (0.96 g, 0.72 mmol, 1.0 eq.) was dissolved in DCM (2.1 mL, 0.3 M). Subsequently, monomer **M1** (0.65 g, 2.15 mmol, 3.0 eq.) and isobutyraldehyde **11c** (0.20 mL, 15.0 mg, 2.15 mmol, 3.0 eq.) were added and the reaction mixture was stirred at room temperature for 48 hours. The solvent was removed under reduced pressure and the crude product was purified by column chromatography (cyclohexane / ethyl acetate 5:1 → 0:1) to obtain the desired product **LO$_{6g}$** in a yield of 95% (1.42 g, 0.68 mmol) as a yellowish, highly viscous oil.

^{1}H NMR (300 MHz, CDCl$_3$) δ / ppm: 7.35 – 7.26 (m, 10H, ^{1}), 6.07 (s, 6H, ^{2}), 5.06 (s, 4H, ^{3}), 4.98 (t, J = 3.9 Hz, 6H, ^{4}), 3.30 – 3.08 (m, 12H, ^{5}), 2.48 – 2.11 (m, 22H, ^{6}), 1.59 (m, 16H, ^{7}), 1.50 – 1.35 (m, 12H, ^{8}), 1.35 – 1.09 (m, 80H, ^{9}), 0.91 (m, 36H, ^{10}).

^{13}C NMR (75 MHz, CDCl$_3$) δ / ppm: 173.64, 172.57, 169.27, 162.93, 136.09, 132.16, 128.76, 128.34, 128.26, 127.87, 127.47, 127.18, 78.48, 77.81, 77.28, 66.01, 65.44, 40.01, 39.63, 39.13, 37.91, 34.28, 34.23, 34.19, 30.46, 29.54, 29.40, 29.31, 29.17, 29.08, 27.84, 27.25, 26.81, 24.96, 24.90, 19.33, 18.84, 18.69, 18.20, 17.55, 17.06, 16.89, 16.40, 16.24.

HRMS-ESI-MS of $[C_{120}H_{204}O_{22}N_6Na]^+$: calculated: 2104.4921, found: 2104.4951.
$[C_{120}H_{204}O_{22}N_6Na_2]^{2+}$: calculated: 1063.7407, found: 1063.7431.

IR (ATR platinum diamond): ν /cm^{-1} = 3306.1, 2925.3, 2853.5, 1737.2, 1652.2, 1533.3, 1462.4, 1369.4, 1232.2, 1160.5, 1003.9, 724.3, 697.2, 411.7.

***R*$_f$** (cyclohexane / ethyl acetate 1:1) = 0.30.

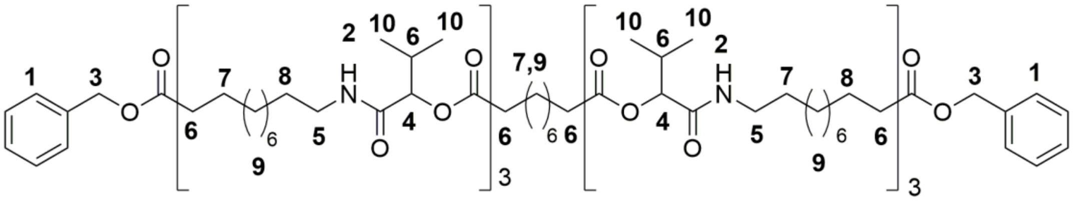
1
3
6
7
8
9
6
5
2
10
6
10
4
3
7,9
6
6
6
10
6
10
2
4
5
7
8
9
6
6
3
1
3

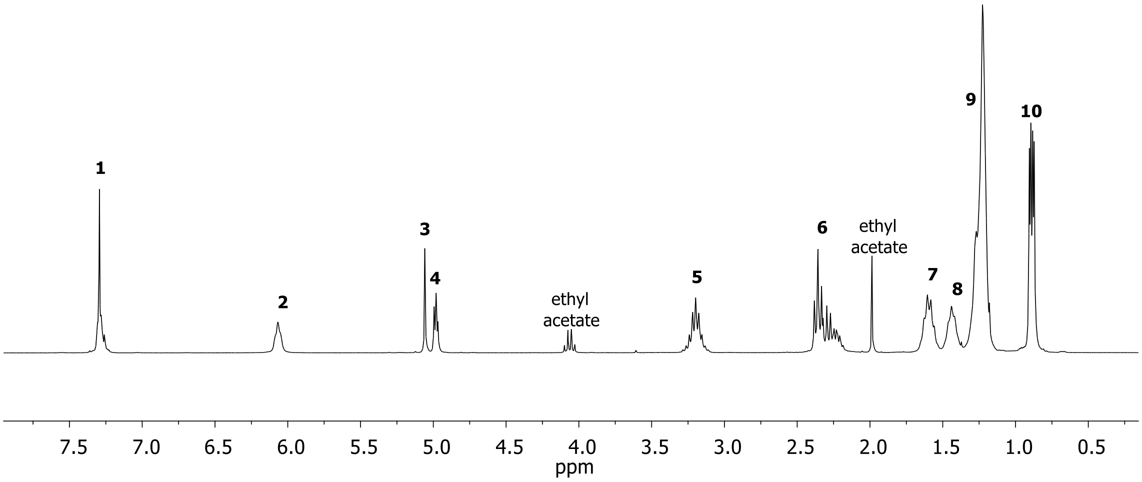
1
2
3
4
ethyl acetate
5
6
ethyl acetate
7
8
9
10
7.5
7.0
6.5
6.0
5.5
5.0
4.5
4.0
3.5
3.0
2.5
2.0
1.5
1.0
0.5
ppm

3rd deprotection: Synthesis of Hexamer LO$_{6h}$

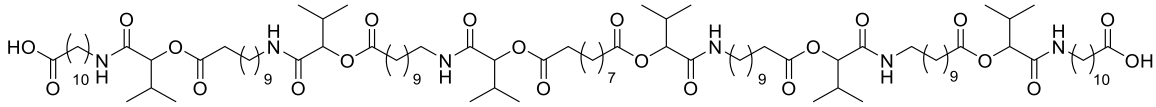

Substance **LO$_{6g}$** (1.17 g, 0.56 mmol, 1.0 eq) was dissolved in 5 mL ethyl acetate and palladium on activated charcoal **19** (117 mg, 10 wt%) was added. The reaction mixture was purged with hydrogen (balloon) and then stirred overnight under hydrogen atmosphere. The heterogeneous catalyst was filtered off and the solvent was evaporated under reduced pressure to obtain product **LO$_{6h}$** without further purification in a yield of 99% (1.08 g, 0.56 mmol) as highly viscous, colourless oil.

^{1}H NMR (400 MHz, CDCl$_3$) δ / ppm: 6.17 (s, 6H, ^{1}), 4.90 (m, 6H, ^{2}), 3.13 (m, 12H, ^{3}), 2.40 – 1.98 (m, 22H, ^{4}), 1.52 (m, 16H, ^{5}), 1.32 (m, 12H, ^{6}), 1.16 (s, 80H, ^{7}), 0.87 – 0.73 (m, 36H, ^{8}).

^{13}C NMR (101 MHz, CDCl$_3$) δ / ppm: 177.46, 172.63, 172.61, 172.58, 171.20, 169.51, 77.80, 60.36, 39.14, 34.12, 34.01, 30.43, 29.40, 29.36, 29.33, 29.26, 29.23, 29.10, 29.03, 28.98, 26.74, 24.89, 24.83, 24.75, 20.98, 19.17, 18.70, 16.92, 15.47, 14.12.

HRMS-ESI-MS of $[C_{106}H_{192}N_6O_{22}Na]^+$: calculated:1924.3982, found: 1924.4089.

$[C_{106}H_{192}N_6O_{22}Na_2]^{2+}$: calculated: 973.6937, found: 973.6936.

IR (ATR platinum diamond): ν /cm^{-1} = 3306.4, 2924.9, 2853.6, 1738.1, 1650.2, 1536.9, 1463.5, 1369.7, 1233.0, 1162.7, 1162.7, 1126.2, 1007.6, 924.2, 721.8, 646.9, 411.6.

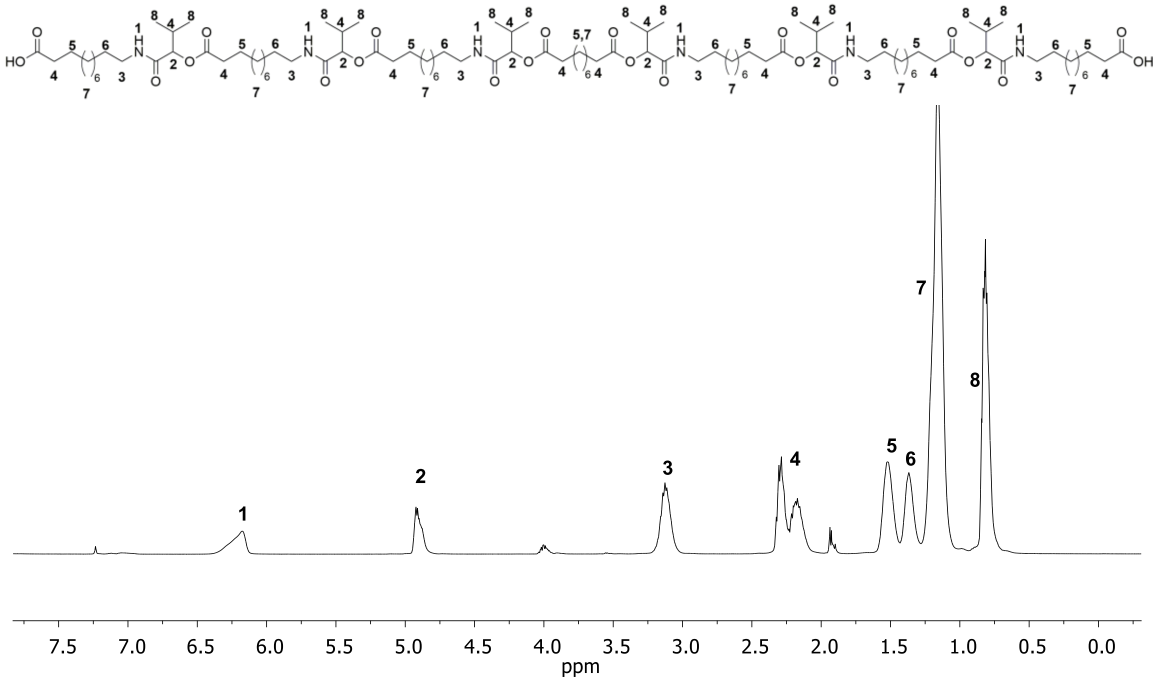

Introduction of the double bond to the oligomeric backbone

Dimer with terminal double bonds: Synthesis of Dimer DO$_2$

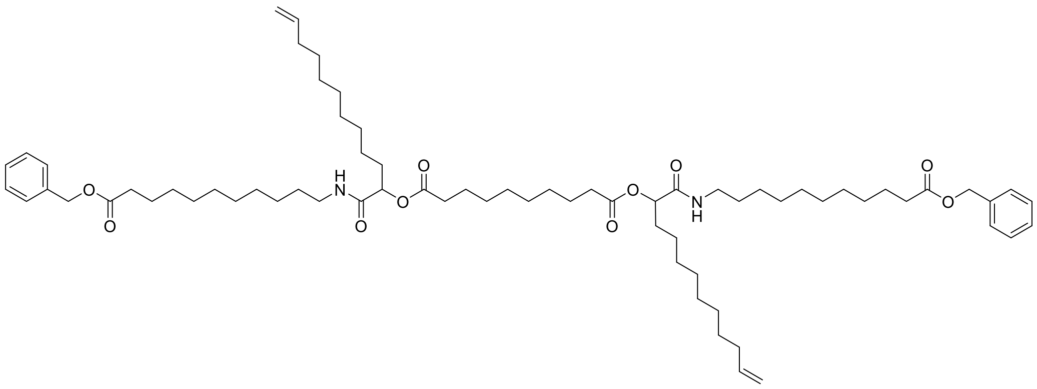

Sebacic acid **10** (500 mg, 2.47 mmol, 1.0 eq.) was dissolved in 2.5 mL DCM. Subsequently, monomer **M1** (2.24 g, 7.42 mmol, 3.0 eq.) and 10-undecenal **11d** (1.50 mL, 1.25 g, 7.42 mmol, 3.0 eq.) were added and the reaction mixture was stirred at room temperature for 24 hours. The solvent was removed under reduced pressure and the crude product was purified by column chromatography (cyclohexane / ethyl acetate 8:1 → 2:1) to obtain the desired product **DO$_2$** in a yield of 89% (2.52 g, 2.20 mmol) as a yellowish, highly viscous oil.

^{1}H NMR (300 MHz, CDCl$_3$) δ / ppm: 7.43 – 7.27 (m, 10H, ^{1}), 6.01 (t, *J* = 5.5 Hz, 2H, ^{2}), 5.79 (ddt, *J* = 16.9, 10.2, 6.7 Hz, 2H, ^{3}), 5.21 – 5.06 (m, 6H, ^{4}), 4.94 (m, 4H, ^{5}), 3.35 – 3.12 (m, 4H, ^{6}), 2.47 – 2.20 (m, 8H, ^{7}), 2.02 (q, *J* = 6.8 Hz, 4H, ^{8}), 1.91 – 1.71 (m, 4H, ^{9}), 1.63 (m, 8H, ^{10}), 1.54 – 1.40 (m, 4H, ^{11}), 1.29 (m, 56H, ^{12}).

^{13}C NMR (75 MHz, CDCl$_3$) *δ* / ppm: 173.74, 172.48, 169.89, 163.24, 139.23, 136.20, 128.62, 128.23, 114.24, 74.03, 66.14, 39.28, 34.39, 34.34, 33.87, 31.99, 29.64, 29.53, 29.43, 29.30, 29.18, 29.15, 28.97, 26.91, 25.01, 24.96, 24.84.

HRMS-ESI-MS of $[C_{70}H_{112}O_{10}N_2Na]^+$: calculated: 1163.8209, found:1163.8230.
$[C_{70}H_{112}O_{10}N_2Na_2]^{2+}$: calculated: 593.4051, found: 593.3827.

IR (ATR platinum diamond): ν /cm^{-1} = 3327.7, 2920.5, 2850.4, 1738.2, 1660.7, 1537.0, 1468.8, 1437.8, 1417.1, 1388.6, 1363.6, 1289.1, 1262.7, 1236.7, 1211.7, 1166.3, 1047.0, 985.3, 908.5, 908.5, 803.6, 720.7, 696.0, 658.9, 577.7, 456.6, 412.1.

***R*$_f$** (cyclohexane / ethyl acetate 2:1) = 0.48.

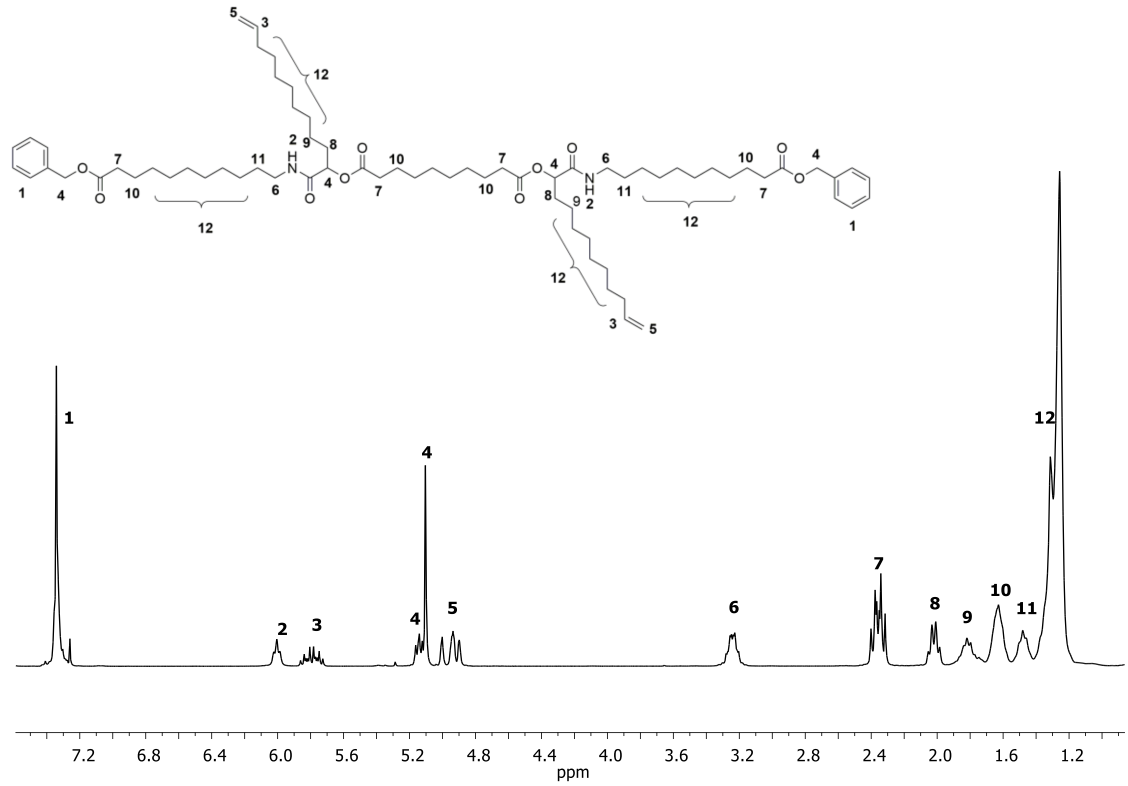
1
2
3
4
4
5
6
7
8
9
10
11
12
7.2
6.8
6.4
6.0
5.6
5.2
4.8
4.4
4.0
3.6
3.2
2.8
2.4
2.0
1.6
1.2
ppm

Tetramer with terminal double bonds and cyclohexyl side chains: Synthesis of Tetramer DO$_{4a}$

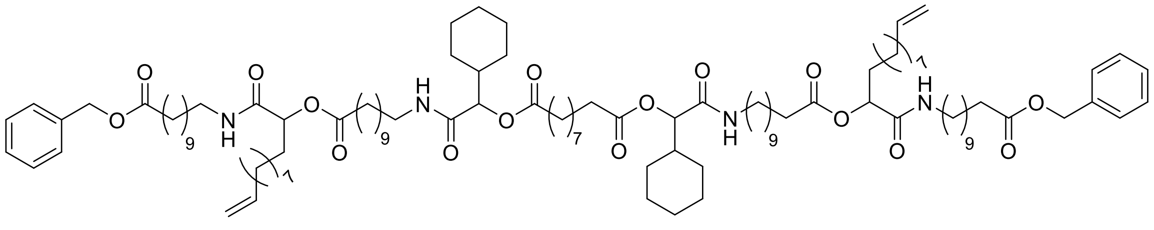

Substance **LO$_{2f}$** (492 mg, 0.58 mmol, 1.0 eq.) was dissolved in 1.2 mL DCM. Subsequently, monomer **M1** (0.52 g 1.74 mmol, 3.0 eq.) and 10-undecenal **11d** (0.35 mL, 29.0 mg, 1.74 mmol, 3.0 eq.) were added and the reaction mixture was stirred at room temperature for 24 hours. The solvent was removed under reduced pressure and the crude product was purified by column chromatography (cyclohexane / ethyl acetate 10:1 → 1:1) to obtain the desired product **DO$_{4a}$** in a yield of 92% (0.95 g, 0.53 mmol) as a yellowish, highly viscous oil.

^{1}H NMR (300 MHz, CDCl$_3$) δ / ppm: 7.32 (s, 10H, ^{1}), 6.03 (m, 4H, ^{2}), 5.77 (ddt, *J* = 13.3, 10.1, 6.6 Hz, 4H, ^{3}), 5.06 (m, 8H, ^{4}), 4.90 (m, 4H, ^{5}), 3.22 (m, 8H, ^{6}), 2.33 (m, 12H, ^{7}), 2.10 – 1.87 (m, 6H, ^{8}), 1.84 – 1.53 (m, 22H, ^{9}), 1.42 (m, 8H, ^{10}), 1.37 – 0.70 (m, 92H, ^{11}).

^{13}C NMR (75 MHz, CDCl$_3$) *δ* / ppm: 173.68, 172.54, 172.50, 169.89, 169.23, 139.16, 136.16, 128.56, 128.16, 114.18, 77.69, 73.94, 66.08, 40.00, 39.22, 39.18, 34.33, 34.25, 33.81, 31.95, 29.58, 29.47, 29.38, 29.24, 29.12, 29.09, 28.92, 27.40, 26.86, 26.11, 26.02, 25.91, 24.97, 24.79.

HRMS-ESI-MS of $[C_{108}H_{178}O_{16}N_4Na]^+$: calculated: 1810.3130, found: 1810.3153.
$[C_{108}H_{178}O_{16}N_4Na_2]^{2+}$: calculated: 916.6511, found: 916.6506.

IR (ATR platinum diamond): ν /cm^{-1} = 3294.9, 2919.6, 2850.4, 1733.2, 1655.2, 1554.0, 1465.5, 1379.4, 1213.8, 1173.1, 1102.5, 988.2, 908.6, 722.5, 695.9.

***R*$_f$** (cyclohexane / ethyl acetate 2:1) = 0.48.

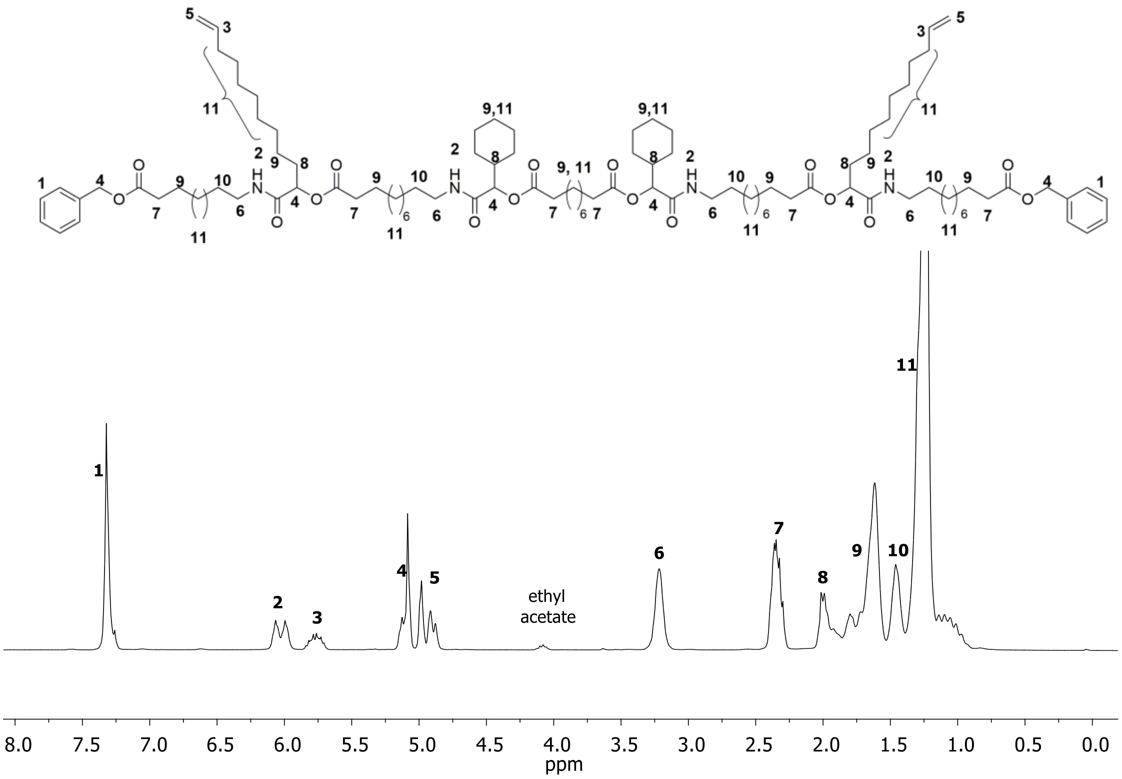
1
2
3
4
5
ethyl
acetate
6
7
8
9
10
11
9,11
8.0
7.5
7.0
6.5
6.0
5.5
5.0
4.5
4.0
3.5
3.0
2.5
2.0
1.5
1.0
0.5
0.0
ppm

Tetramer with terminal double bonds and isopropyl side chains: Synthesis of Tetramer DO_{4b}

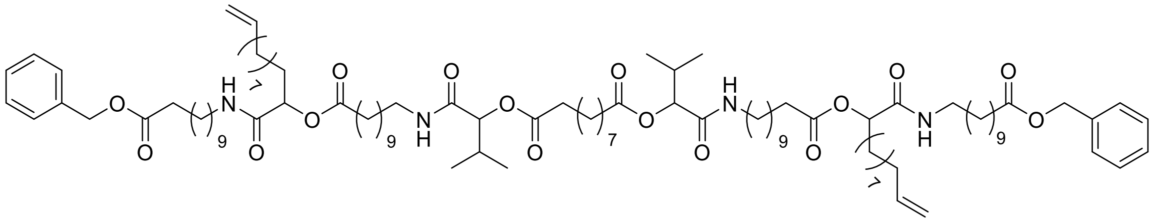

Substance **LO_{2h}** (380 mg, 0.49 mmol, 1.0 eq.) was dissolved in 1.0 mL DCM. Subsequently, monomer **M1** (0.45 g 1.48 mmol, 3.0 eq.) and 10-undecenal **11d** (300 µL, 250 mg, 1.48 mmol, 3.0 eq.) were added and the reaction mixture was stirred at room temperature for 24 hours. The solvent was removed under reduced pressure and the crude product was purified by column chromatography (cyclohexane / ethyl acetate 5:1 → 1:1) to obtain the desired product **DO_{4b}** in a yield of 98% (0.83 g, 0.48 mmol) as a yellowish, highly viscous oil.

^{1}H NMR (300 MHz, $CDCl_3$) δ / ppm: 7.44 – 7.28 (m, 10H, ^{1}), 6.05 (m, 4H, ^{2}), 5.77 (ddt, *J* = 16.9, 10.2, 6.7 Hz, 4H, ^{3}), 5.19 – 5.05 (m, 8H, ^{4}), 5.05 – 4.82 (m, 4H, ^{5}), 3.36 – 3.08 (m, 8H, ^{6}), 2.49 – 2.16 (m, 12H, ^{7}), 2.00 (q, *J* = 6.7 Hz, 4H, ^{8}), 1.88 – 1.72 (m, 4H, ^{9}), 1.62 (m, 12H, ^{10}), 1.51 – 1.39 (m, 8H, ^{11}), 1.27 (m, 80H, ^{12}), 0.96 – 0.82 (m, 12H, ^{13}).

^{13}C NMR (75 MHz, $CDCl_3$) *δ* / ppm: 173.69, 172.56, 172.50, 169.90, 169.30, 139.17, 136.17, 128.57, 128.17, 114.19, 78.01, 73.95, 66.08, 39.21, 34.34, 34.26, 33.82, 31.96, 30.56, 29.63, 29.58, 29.48, 29.39, 29.25, 29.13, 29.09, 28.93, 26.87, 24.97, 24.80, 18.82, 17.06.

HRMS-ESI-MS of $[C_{102}H_{170}O_{16}N_4Na]^+$: calculated: 1730.2504, found: 1730.2545.
$[C_{102}H_{170}O_{16}N_4Na_2]^{2+}$: calculated: 876.6198, found: 876.6189.

IR (ATR platinum diamond): ν /cm^{-1} = 3295.6, 2920.9, 2851.0, 1735.3, 1653.6, 1542.2, 1465.4, 1368.9, 1238.8, 1215.1, 1166.6, 992.6, 909.6, 722.6, 696.7, 417.4.

R_f (cyclohexane / ethyl acetate 2:1) = 0.31.

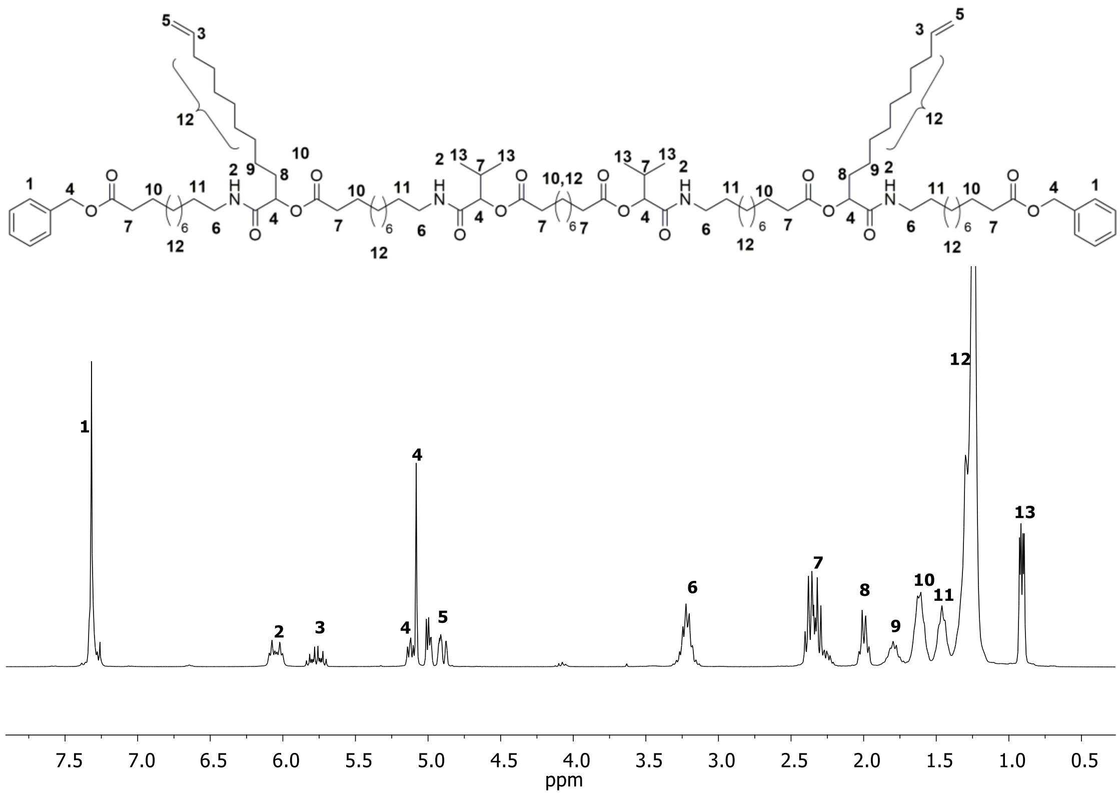
1
2
3
4
4
5
6
7
8
9
10
11
12
13
7.5
7.0
6.5
6.0
5.5
5.0
4.5
4.0
3.5
3.0
2.5
2.0
1.5
1.0
0.5
ppm

Hexamer with terminal double bonds and cyclohexyl side chains: Synthesis of Hexamer **DO$_{6a}$**

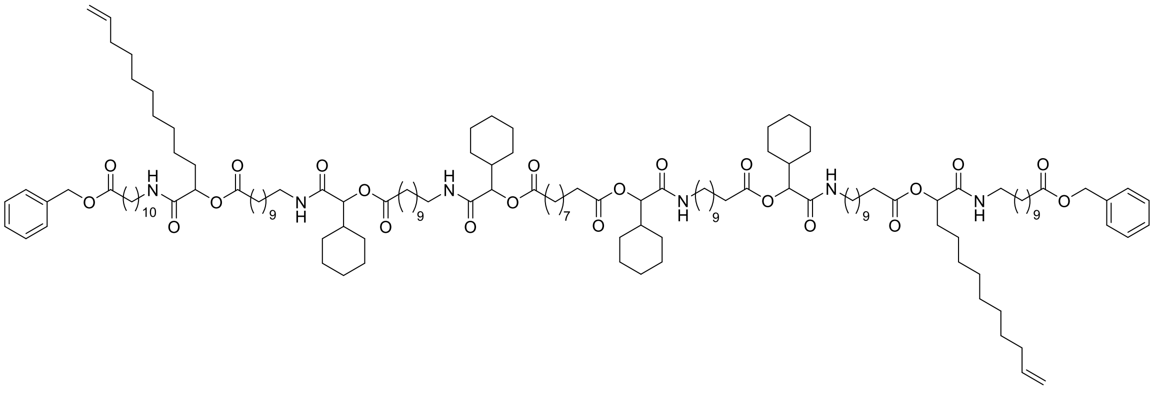

Substance **LO$_{4f}$** (907 mg, 0.61 mmol, 1.0 eq.) was dissolved in 1.8 mL DCM. Subsequently, monomer **M1** (2.24 g 7.42 mmol, 3.0 eq.) and 10-undecenal **11d** (1.50 mL 1.25 g, 7.42 mmol, 3.0 eq.) were added and the reaction mixture was stirred at room temperature for 48 hours. The solvent was removed under reduced pressure and the crude product was purified by column chromatography (cyclohexane / ethyl acetate 8:1 → 2:1) to obtain the desired product **DO$_{6a}$** in a yield of 89% (2.52 g, 2.20 mmol) as a yellowish, highly viscous oil.

^{1}H NMR (300 MHz, CDCl$_3$) δ / ppm: 7.42 – 7.27 (m, 10H, ^{1}), 6.06 (m, 6H, ^{2}), 5.78 (ddt, *J* = 16.9, 10.2, 6.7 Hz, 4H, ^{3}), 5.20 – 5.06 (m, 8H, ^{4}), 5.02 – 4.86 (m, 4H, ^{5}), 3.36 – 3.09 (m, 12H, ^{6}), 2.46 – 2.28 (m, 16H, ^{7}), 2.08 – 1.87 (m, 8H, ^{8}), 1.83 – 1.55 (m, 36H, ^{9}), 1.52 – 1.40 (m, 12H, ^{10}), 1.37 – 0.89 (m, 128H, ^{11}).

^{13}C NMR (75 MHz, CDCl$_3$) *δ* / ppm: 173.70, 172.59, 172.56, 172.51, 169.89, 169.26, 169.24, 139.18, 136.16, 128.57, 128.18, 114.19, 77.69, 77.65, 73.95, 70.64, 66.09, 46.02, 40.02, 39.23, 39.18, 34.35, 34.27, 33.83, 31.96, 29.62, 29.50, 29.40, 29.26, 29.22, 29.14, 29.11, 28.93, 27.78, 27.36, 26.89, 26.12, 26.04, 25.92, 24.98, 24.80.

HRMS-ESI-MS of [$C_{146}H_{244}O_{22}N_6Na]^+$: calculated:2456.8051, found: 2456.8034.
[$C_{146}H_{244}O_{22}N_6Na_2]^{2+}$: calculated: 1239.8972, found: 1239.8995.
[$C_{146}H_{244}O_{22}N_6Na_3]^{3+}$: calculated: 834.2612, found: 834.2596.

IR (ATR platinum diamond): ν /cm^{-1} = 3293.4, 2922.3, 2851.7, 1736.8, 1654.6, 1535.7, 1450.5, 1375.3, 1161.8, 1101.7, 989.3, 908.7, 722.9, 696.8.

***R*$_f$** (cyclohexane / ethyl acetate 2:1) = 0.48.

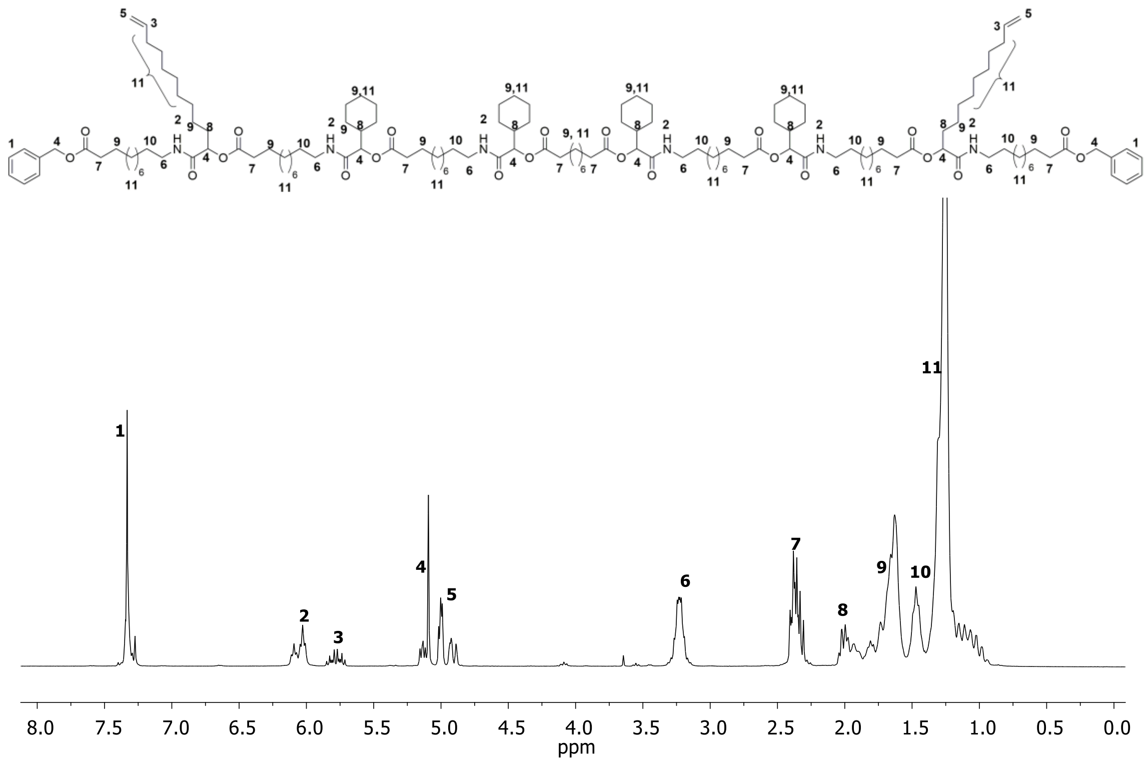
1
2
3
4
5
6
7
8
9
10
11
8.0
7.5
7.0
6.5
6.0
5.5
5.0
4.5
4.0
3.5
3.0
2.5
2.0
1.5
1.0
0.5
0.0
ppm

Hexamer with terminal double bonds and isopropyl side chains: Synthesis of Hexamer DO_{6b}

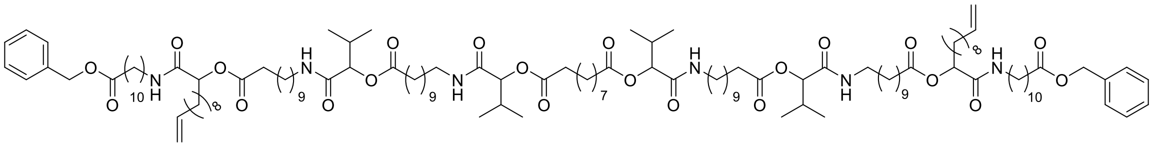

Substance **LO_{4h}** (294 mg, 0.22 mmol, 1.0 eq.) was dissolved in 2.0 mL DCM. Subsequently, monomer **M1** (199 mg 0.66 mmol, 3.0 eq.) and 10-undecenal **11d** (0.13 mL, 0.11 g, 0.66 mmol, 3.0 eq.) were added and the reaction mixture was stirred at room temperature for 48 hours. The solvent was removed under reduced pressure and the crude product was purified by column chromatography (cyclohexane / ethyl acetate 5:1 → 0:1) to obtain the desired product **DO_{6b}** in a yield of 88% (0.44 g, 0.19 mmol) as a yellowish, highly viscous oil.

^{1}H NMR (300 MHz, $CDCl_3$) δ / ppm: 7.43 – 7.23 (m, 10H), 6.16 – 5.91 (m, 6H), 5.76 (ddt, *J* = 16.9, 10.2, 6.7 Hz, 2H), 5.19 – 5.05 (m, 10H), 5.01 – 4.80 (m, 4H), 3.36 – 3.11 (m, 12H), 2.47 – 2.16 (m, 20H), 2.06 – 1.94 (m, 4H), 1.88 – 1.70 (m, 4H), 1.61 (m, 16H), 1.50 – 1.39 (m, 12H), 1.35 – 1.07 (m, 104H), 0.93 (m, 24H).

^{13}C NMR (75 MHz, $CDCl_3$) *δ* / ppm: 173.69, 172.62, 172.58, 172.52, 169.90, 169.33, 156.85, 139.18, 136.19, 128.58, 128.18, 114.20, 101.45, 78.03, 77.99, 73.97, 66.09, 39.21, 34.36, 34.32, 34.28, 33.82, 31.97, 30.57, 29.64, 29.60, 29.49, 29.39, 29.25, 29.15, 29.10, 28.94, 26.88, 25.04, 24.99, 24.81, 18.83, 17.05.

HRMS-ESI-MS of $[C_{134}H_{228}O_{22}N_6H]^+$: calculated: 2274.6979, found: 2274.6714
$[C_{134}H_{228}O_{22}N_6Na_2]^{2+}$: calculated: 1137.8526, found: 1137.7821.

IR (ATR platinum diamond): ν /cm^{-1} = 3292.7, 2922.8, 2851.9, 1736.2, 1655.5, 1536.8, 1464.9, 1370.4, 1239.6, 1166.3, 994.6, 909.4, 722.6, 696.7, 417.8.

***R*$_f$** (cyclohexane / ethyl acetate 3:2) = 0.40.

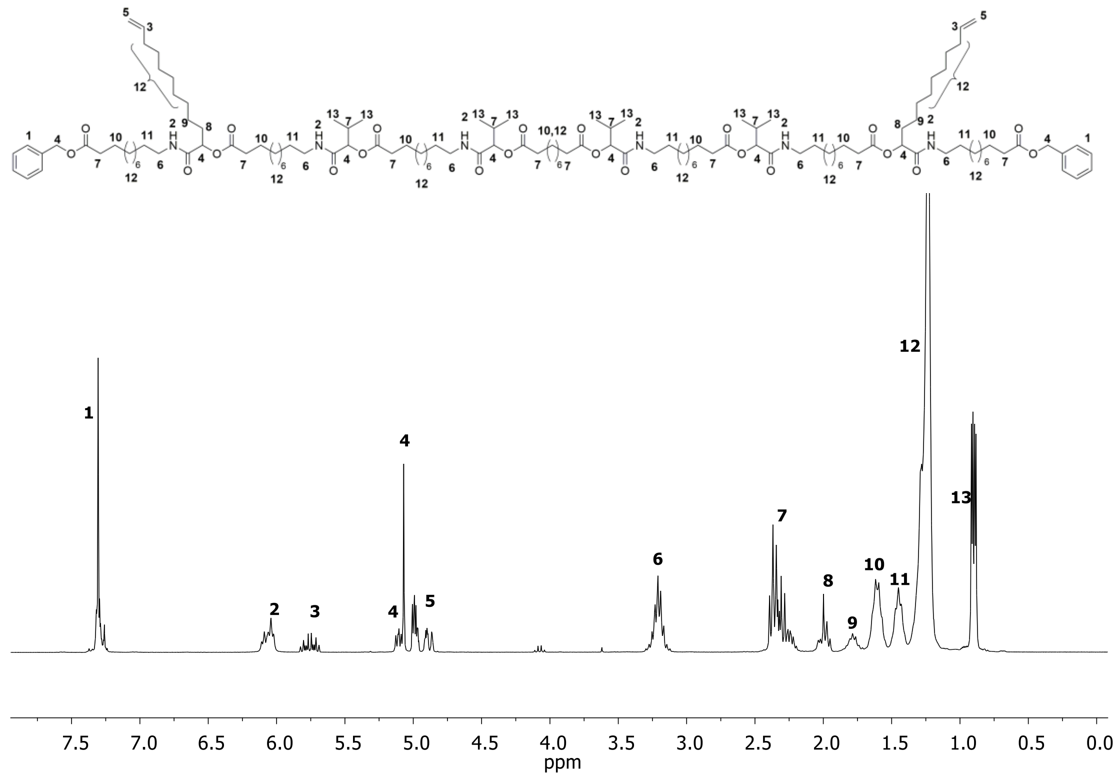
1
2
3
4
4
5
6
7
8
9
10
11
12
13
7.5
7.0
6.5
6.0
5.5
5.0
4.5
4.0
3.5
3.0
2.5
2.0
1.5
1.0
0.5
0.0
ppm

Octamer with terminal double bonds and ethyl side chains: Synthesis of Octamer DO_{8a}*

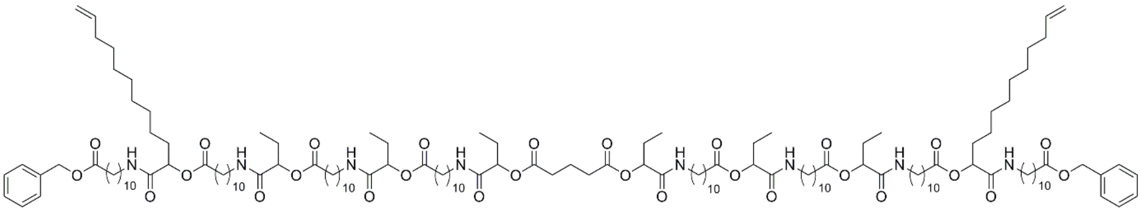

Substance **LO_{6b}** (0.43 g, 0.25 mmol, 1.0 eq.) was dissolved in DCM (1 mL, 0.25 M). Subsequently, 10-undecenal **11d** (0.17 mL, 0.14 g, 0.83 mmol, 3.3 eq.) and the monomer **M1** (0.25 g, 0.81 mmol, 3.2 eq.) were added. The reaction mixture was stirred at room temperature for 48 hours and the solvent was evaporated under reduced pressure. The crude product was purified by column chromatography (hexane / ethyl acetate 1:1 → 1:6) to obtain substance **DO_{8a}** as colourless, highly viscous oil in a yield of 91% (0.60 g, 0.23 mmol).

^{1}H NMR (600 MHz, $CDCl_3$) δ / ppm: 7.38 – 7.27 (m, 10H, CH, aromatic, ^{1}), 6.33 – 6.02 (m, 8H, 8 NH, ^{2}), 5.77 (ddt, J = 16.9, 10.2, 6.7 Hz, 2H, 2 CH=, ^{3}), 5.15 – 5.03 (m, 12H, 2 CH_2, 8 CH, ^{4}), 4.98 – 4.87 (m, 4H, 2 =CH_2, ^{5}), 3.31 – 3.13 (m, 16H, 8 CH_2, ^{6}), 2.53 – 2.45 (m, 4H, 2 CH_2, ^{7}), 2.40 – 2.29 (m, 16H, 8 CH_2, ^{8}), 2.03 – 1.96 (m, 6H, 3 CH_2, ^{9}), 1.93 – 1.72 (m, 16H, 8 CH_2, ^{10}), 1.68 – 1.56 (m, 16H, 8 CH_2, ^{11}), 1.47 (m, 16H, 8 CH_2, ^{12}), 1.29 (m, 120H, 60 CH_2, ^{13}), 0.93 – 0.83 (m, 18H, 6 CH_3, ^{14}).

^{13}C NMR (151 MHz, $CDCl_3$) δ / ppm: 173.7, 172.5, 172.0, 171.8, 169.9, 169.7, 169.5, 169.5, 139.2, 136.2, 128.6, 128.2, 128.2, 114.2, 75.2, 74.9, 74.0, 66.1, 39.4, 39.3, 39.3, 34.4, 34.4, 33.9, 33.0, 32.9, 32.0, 29.6, 29.6, 29.5, 29.4, 29.4, 29.3, 29.3, 29.2, 29.2, 29.1, 29.0, 26.9, 25.2, 25.2, 25.0, 24.8, 20.2, 20.1, 9.2, 9.2, 9.1.

FAB-MS of $[C_{155}H_{265}N_8O_{28}]^+$: calculated: 2686.9, found: 2685.6.

IR (ATR platinum diamond): ν /cm^{-1} = 3304.1, 3077.9, 2922.6, 2851.9, 1737.2, 1653.6, 1534.1, 1456.1, 1374.5, 1230.7, 1156.7, 1100.8, 990.4, 907.7, 722.5, 696.9, 404.7.

R_f (hexane / ethyl acetate 5:11) = 0.58.

---

[*] This synthesis was conducted by Katharina Wetzel during the Master thesis [339]

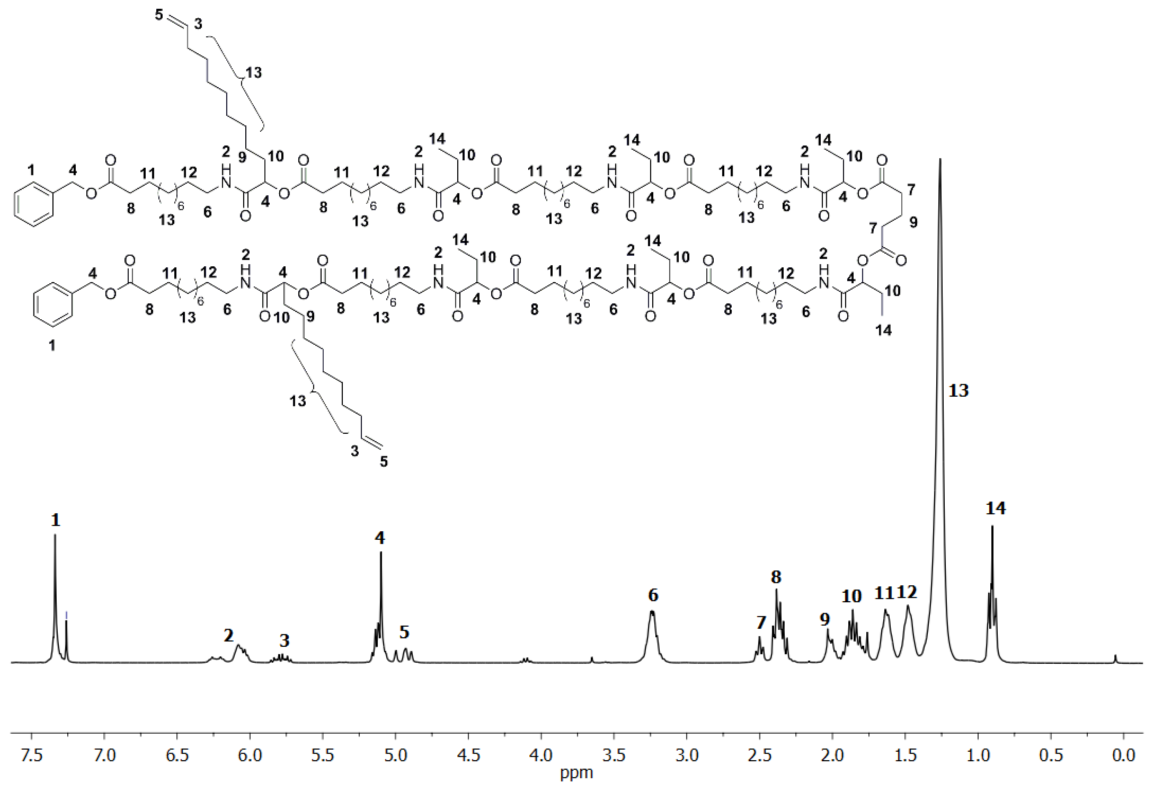
1
2
3
4
5
6
7
8
9
10
11
12
13
14
7.5
7.0
6.5
6.0
5.5
5.0
4.5
4.0
3.5
3.0
2.5
2.0
1.5
1.0
0.5
0.0
ppm

Octamer with terminal double bonds and cyclohexyl side chains: Synthesis of Octamer $\mathbf{DO_{8b}}$*

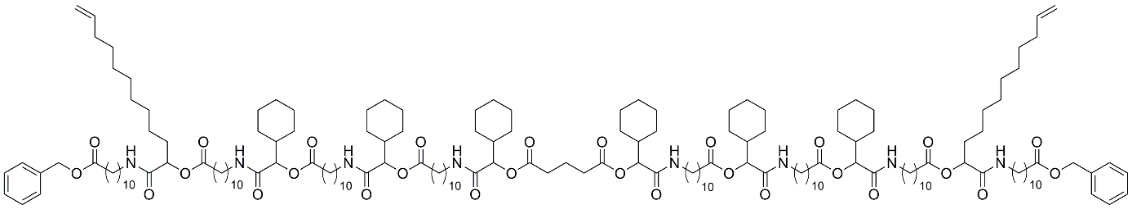

Substance $\mathbf{LO_{6d}}$ (0.31 g, 0.15 mmol, 1.0 eq.) was dissolved in DCM (0.3 mL, 0.5 M). Subsequently, monomer **M1** (0.13 g, 0.44 mmol, 3.0 eq.) and 10-undecenal **11d** (73.0 mg 0.44 mmol, 3.0 eq.) were added and the reaction mixture was stirred at room temperature for 48 hours. The solvent was removed under reduced pressure and the crude product was purified by column chromatography (cyclohexane / ethyl acetate 5:1 → 1:3) to obtain the product $\mathbf{DO_{8b}}$ in a yield of 93% (1.25 g, 0.42 mmol) as lightly yellow, highly viscous oil.

^{1}H NMR (400 MHz, $CDCl_3$) δ / ppm: 7.36 – 7.28 (m, 10H, CH, aromatic, ^{1}), 6.27 – 5.95 (m, 8H, 8 NH, ^{2}), 5.77 (ddt, J = 16.9, 10.2, 6.7 Hz, 2H, 2 CH=, ^{3}), 5.13 (dd, J = 7.1, 4.8 Hz, 2H, =CH_2, ^{4}), 5.09 (s, 4H, 2 CH_2, ^{5}), 5.02 – 4.92 (m, 8H, 8 CH, ^{6}), 4.90 (ddt, J = 10.2, 2.2, 1.1 Hz, 2H, =CH_2, ^{6}), 3.33 – 3.11 (m, 16H, 8 CH_2, ^{7}), 2.53 – 2.44 (m, 4H, 2 CH_2, ^{8}), 2.42 – 2.25 (m, 16H, 8 CH_2, ^{9}), 2.07 – 1.85 (m, 8H, 6 CH, CH_2, ^{10}), 1.85 – 1.54 (m, 50H, 25 CH_2, ^{11}), 1.53 – 1.39 (m, 16H, 8 CH_2, ^{12}), 1.38 – 0.87 (m, 154H, 77 CH_2, ^{13}).

^{13}C NMR (101 MHz, $CDCl_3$) δ / ppm: 173.8, 172.6, 172.5, 172.1, 172.0, 169.9, 169.3, 169.1, 139.2, 136.2, 128.6, 128.2, 128.2, 114.2, 78.1, 78.1, 76.8, 74.0, 66.1, 40.0, 40.0, 39.3, 39.3, 39.2, 34.4, 34.3, 33.9, 33.1, 32.9, 32.0, 29.7, 29.6, 29.5, 29.4, 29.3, 29.3, 29.2, 29.2, 29.1, 29.0, 27.4, 27.4, 26.9, 26.1, 26.1, 26.1, 26.0, 25.1, 25.0, 25.0, 24.8.

FAB-MS of $[C_{179}H_{301}N_8O_{28}]^+$: calculated: 3011.2 found: 3011.1.

IR (ATR platinum diamond): ν /cm^{-1} = 3303.0, 2922.1, 2851.2, 1737.5, 1651.8, 1533.2, 1449.5, 1371.7, 1232.9, 1232.9, 1150.3, 1100.8, 987.8, 907.9, 722.2, 696.3, 580.6, 428.2.

***R*$_f$** (cyclohexane / ethyl acetate 1:1) = 0.67.

---

* This synthesis was conducted by Katharina Wetzel during the Master thesis [339]

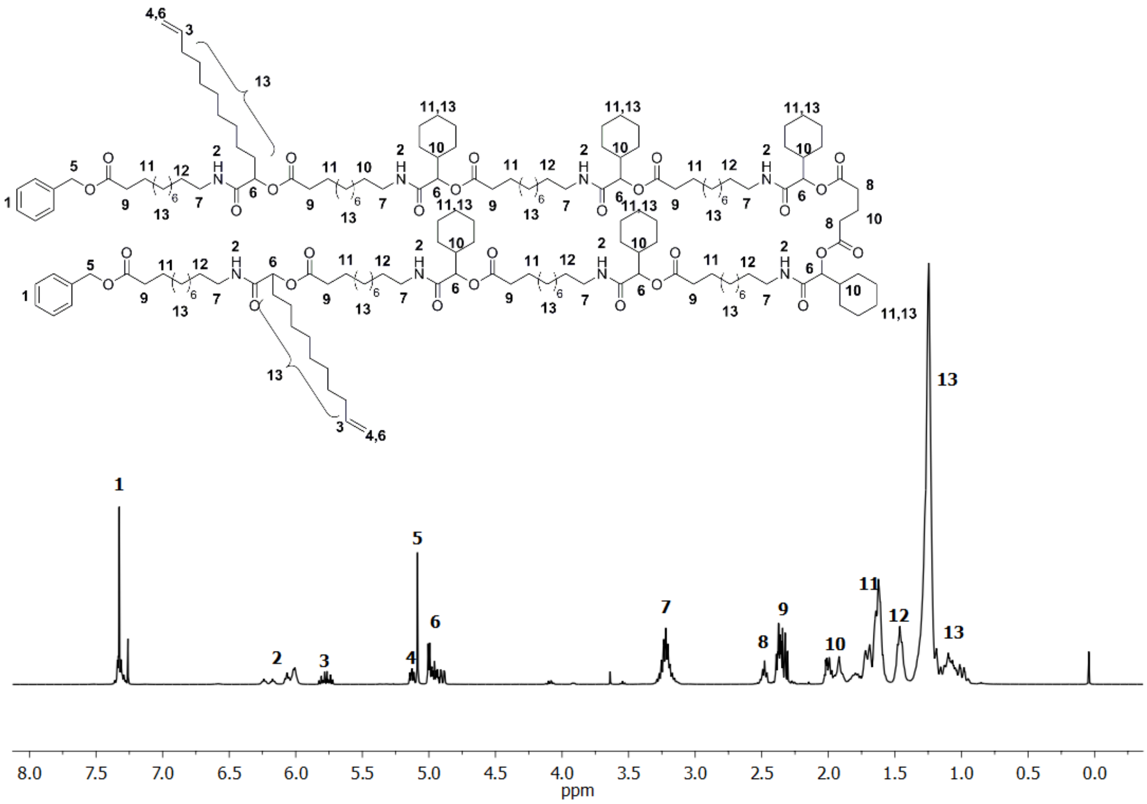
1
2
3
4
5
6
7
8
9
10
11
12
13
8.0
7.5
7.0
6.5
6.0
5.5
5.0
4.5
4.0
3.5
3.0
2.5
2.0
1.5
1.0
0.5
0.0
ppm
4,6
11,13

Octamer with terminal double bonds and cyclohexyl side chains: Synthesis of Octamer **DO_{8c}**

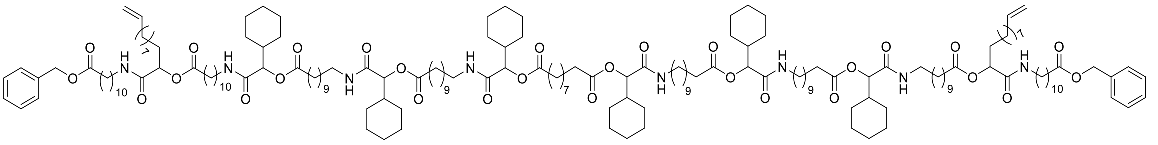

Substance **LO_{6f}** (311 mg, 0.145 mmol, 1.0 eq.) was dissolved in DCM (0.3 mL, 0.5 M). Subsequently, monomer **M1** (131 mg, 0.44 mmol, 3.0 eq.) and 10-undecenal **11d** (73.0 mg, 0.44 mmol, 3.0 eq.) were added and the reaction mixture was stirred at room temperature for 48 hours. The solvent was removed under reduced pressure and the crude product was purified by column chromatography (cyclohexane / ethyl acetate 5:1 → 0:1) to obtain the product **DO_{8c}** in a yield of 93% (415 g, 0.14 mmol) as lightly yellow, highly viscous oil.

^{1}H NMR (300 MHz, $CDCl_3$) δ / ppm: 7.38 – 7.17 (m, 10H, ^{1}), 6.18 – 5.95 (m, 8H, ^{2}), 5.88 – 5.63 (m, 2H, ^{3}), 5.17 – 5.02 (m, 12H, ^{4}), 5.00 – 4.79 (m, 4H, ^{5}), 3.33 – 3.06 (m, 16H, ^{6}), 2.43 – 2.23 (m, 20H, ^{7}), 2.17 – 1.84 (m, 10H, ^{8}), 1.80 – 1.51 (m, 48H, ^{9}), 1.52 – 1.35 (m, 16H, ^{10}), 1.37 – 0.72 (m, 164H, ^{11}).

^{13}C NMR (75 MHz, $CDCl_3$) δ / ppm: 173.64, 172.56, 172.48, 169.87, 169.23, 139.12, 136.13, 128.53, 128.13, 114.15, 101.21, 73.91, 66.04, 39.98, 39.14, 34.27, 33.78, 31.93, 29.58, 29.45, 29.35, 29.22, 29.11, 29.06, 28.89, 27.34, 26.85, 26.08, 26.00, 25.89, 24.98, 24.94, 24.77.

HRMS-ESI-MS of $[C_{184}H_{310}N_8O_{28}Na]^+$: calculated: 3103.2972, found: 3103.2957.
$[C_{184}H_{310}N_8O_{28}Na_2]^{2+}$: calculated: 1563.1432, found: 1563.1469.
$[C_{184}H_{310}N_8O_{28}Na_3]^{3+}$: calculated: 1049.7585, found: 1049.7561.

IR (ATR platinum diamond): ν /cm^{-1} = 3305.5, 2922.9, 2852.2, 1738.0, 1651.8, 1534.8, 1450.3, 1373.1, 1159.6, 1101.5, 989.5, 908.6, 722.7, 696.9, 429.9.

R_f (cyclohexane / ethyl acetate 1:1) = 0.67.

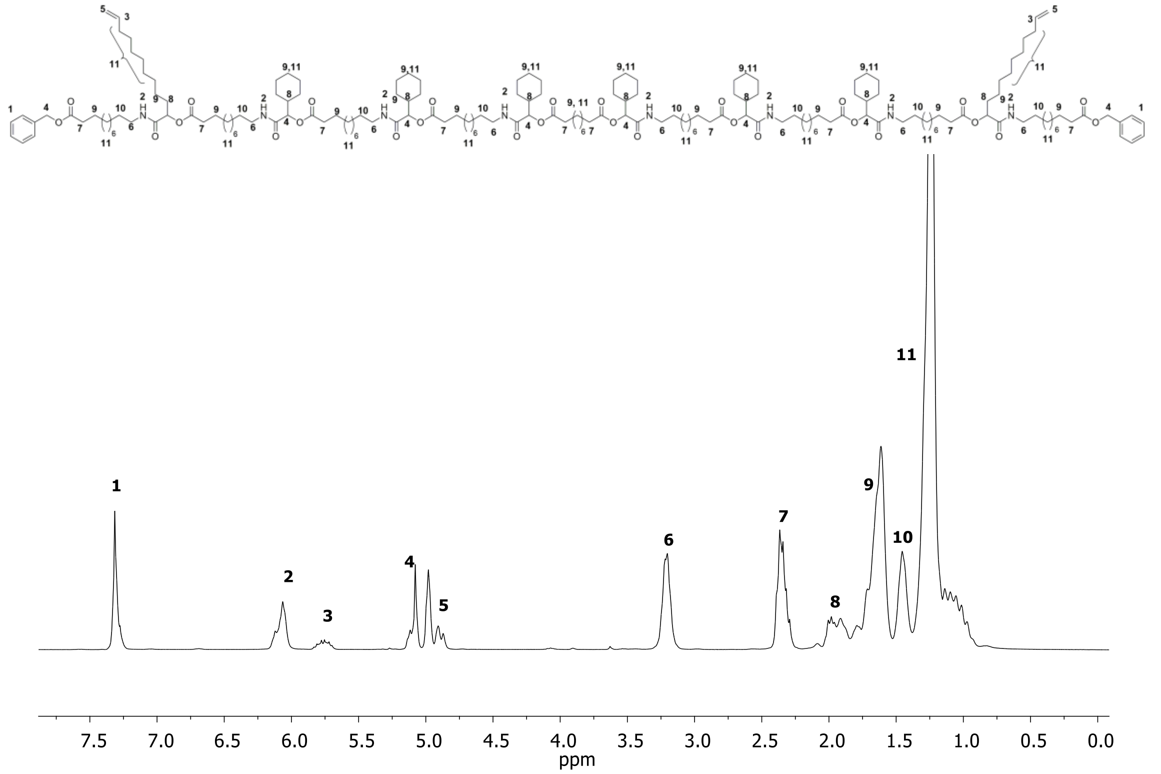
1
2
3
4
5
6
7
8
9
10
11
7.5
7.0
6.5
6.0
5.5
5.0
4.5
4.0
3.5
3.0
2.5
2.0
1.5
1.0
0.5
0.0
ppm

Octamer with terminal double bonds and isopropyl side chains: Synthesis of Octamer **DO$_{8d}$**

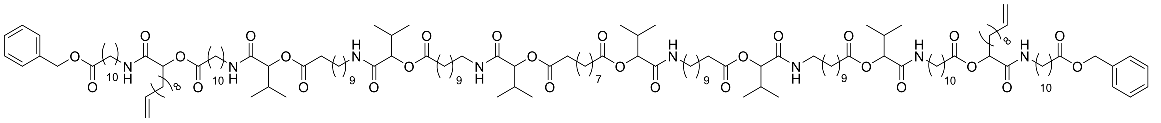

Substance **LO$_{6h}$** (0.17 g, 89 µmol, 1.0 eq.) was dissolved in DCM (0.2 mL, 0.25 M) and 10-undecenal **11d** (54 µL, 45 mg, 0.27 mmol, 3.0 eq.) and monomer **M1** (81 mg, 0.27 mmol, 3.0 eq.) were added. The reaction mixture was stirred at room temperature for 48 hours and the solvent was evaporated under reduced pressure. The crude product was purified by column chromatography (cyclohexane / ethyl acetate 4:1 → 0:1) to obtain substance **DO$_{8d}$** as colourless, highly viscous oil in a yield of 91% (0.23 g, 0.23 mmol).

^{1}H NMR (400 MHz, $CDCl_3$) δ / ppm: 7.38 – 7.27 (m, 10H, ^{1}), 6.14 – 5.97 (m, 8H, ^{2}), 5.76 (ddt, J = 16.9, 10.2, 6.7 Hz, 2H, ^{3}), 5.17 – 5.05 (m, 12H, ^{4}), 5.03 – 4.84 (m, 4H, ^{5}), 3.34 – 3.06 (m, 16H, ^{6}), 2.46 – 2.16 (m, 26H, ^{7}), 2.03 – 1.93 (m, 4H, ^{8}), 1.86 – 1.69 (m, 4H, ^{9}), 1.69 – 1.54 (m, 20H, ^{10}), 1.51 – 1.37 (m, 16H, ^{11}), 1.36 – 1.11 (m, 128H, ^{12}), 1.01 – 0.75 (m, 36H, ^{13}).

^{13}C NMR (101 MHz, $CDCl_3$) δ / ppm: 173.69, 172.62, 172.58, 172.51, 171.16, 169.90, 169.34, 169.31, 139.16, 136.13, 128.55, 128.40, 128.18, 128.16, 114.18, 77.97, 77.93, 77.36, 73.92, 66.07, 60.41, 51.46, 39.21, 39.18, 34.33, 34.32, 34.28, 34.24, 33.80, 31.94, 30.54, 29.60, 29.56, 29.46, 29.37, 29.23, 29.20, 29.13, 29.12, 29.08, 28.91, 26.86, 25.01, 24.96, 24.78, 21.07, 19.26, 18.81, 17.01, 15.48, 14.23.

HRMS-ESI-MS of $[C_{166}H_{286}N_8O_{28}Na_2]^{2+}$: calculated: 1443.0493, found: 1443.0526.
$[C_{166}H_{286}N_8O_{28}Na_3]^{3+}$: calculated: 969.6959, found: 969.6964

IR (ATR platinum diamond): ν /cm^{-1} = 3292.0, 2923.0, 2852.1, 1736.3, 1655.4, 1536.7, 1464.8, 1370.5, 1239.4, 1166.0, 1107.9, 995.2, 909.9, 722.8, 696.8, 419.0.

***R*$_{f}$** (cyclohexane / ethyl acetate 2:3) = 0.42.

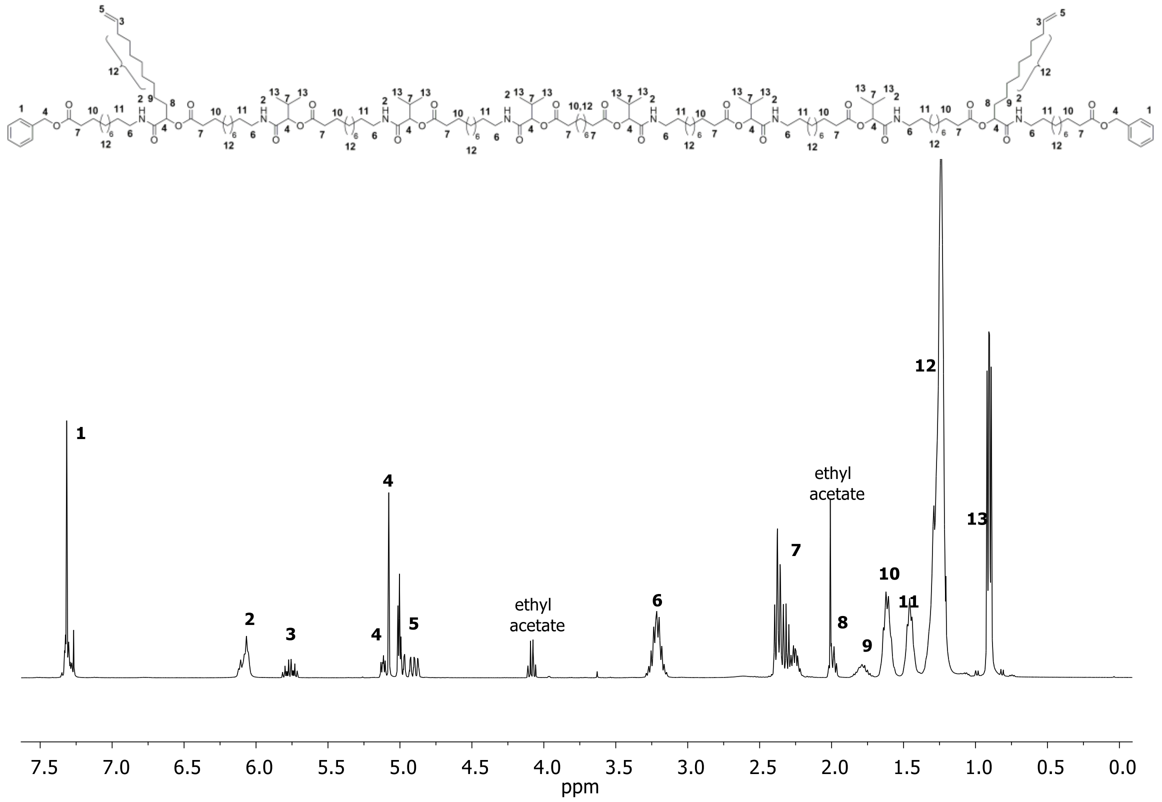
1
2
3
4
4
5
ethyl acetate
6
7
ethyl acetate
8
9
10
11
12
13
7.5
7.0
6.5
6.0
5.5
5.0
4.5
4.0
3.5
3.0
2.5
2.0
1.5
1.0
0.5
0.0
ppm

Decamer with terminal double bonds and cyclohexyl side chains : Synthesis of Decamer DO_{10}

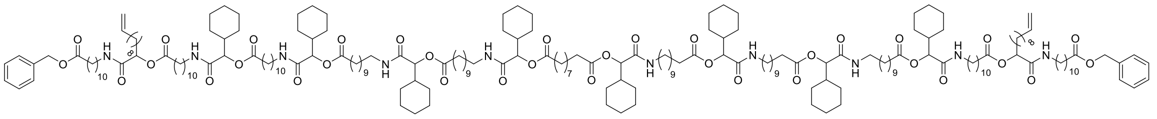

Substance **LO_{8f}** (278 mg, 99 µmol, 1.0 eq.) was dissolved in DCM (0.3 mL, 0.3 M). Subsequently, monomer **M1** (90 mg, 0.30 mmol, 3.0 eq.) and 10-undecenal **11d** (50 mg, 0.30 mmol, 3.0 eq.) were added and the reaction mixture was stirred at room temperature for 48 hours. The solvent was removed under reduced pressure and the crude product was purified by column chromatography (cyclohexane / ethyl acetate 4:1 → 0:1) to obtain the product **DO_{10}** in a yield of 99% (400 g, 99 µmol) as lightly yellow, highly viscous oil.

^{1}H NMR (300 MHz, $CDCl_3$) δ / ppm: 7.39 – 7.27 (m, 10H, ^{1}), 6.16 – 5.97 (m, 10H, ^{2}), 5.77 (m, 2H, ^{3}), 5.16 – 5.06 (m, 14H, ^{4}), 5.03 – 4.84 (m, 4H, ^{5}), 3.32 – 3.11 (m, 20H, ^{6}), 2.47 – 2.24 (m, 24H, ^{7}), 2.09 – 1.76 (m, 12H, ^{8}), 1.75 – 1.53 (m, 60H, ^{9}), 1.52 – 1.39 (m, 20H, ^{10}), 1.37 – 0.69 (m, 200H, ^{11}).

^{13}C NMR (101 MHz, $CDCl_3$) δ / ppm: 177.84, 174.24, 173.69, 172.61, 172.58, 172.51, 169.97, 169.33, 169.31, 161.06, 139.10, 136.06, 128.50, 128.34, 128.13, 128.10, 114.13, 107.80, 107.58, 106.33, 77.60, 77.56, 77.36, 76.00, 73.85, 72.78, 72.01, 68.55, 67.62, 67.54, 67.40, 66.04, 61.01, 60.39, 51.43, 41.63, 39.92, 39.19, 39.14, 37.25, 34.89, 34.28, 34.24, 34.22, 34.18, 33.75, 31.89, 29.65, 29.51, 29.43, 29.33, 29.19, 29.15, 29.08, 29.03, 28.85, 27.79, 27.30, 27.06, 26.81, 26.04, 25.96, 25.84, 24.94, 24.90, 24.87, 24.72, 23.89, 23.81, 23.79, 22.66, 22.42, 22.16, 21.02, 19.05, 14.17, 14.10.

HRMS-ESI-MS of $[C_{222}H_{376}N_{10}O_{34}Na_2]^{2+}$: calculated: 1886.3892, found: 1886.4028.
$[C_{222}H_{376}N_{10}O_{34}Na_3]^{3+}$: calculated: 1265.2559, found: 1265.2576.

IR (ATR platinum diamond): ν /cm^{-1} = 3294.7, 2923.3, 2853.1, 1737.8, 1651.5, 1536.1, 1450.2, 1369.1, 1160.5, 1101.1, 1071.8, 989.0, 925.7, 722.6, 697.4.

R_f (cyclohexane / ethyl acetate 1:1) = 0.58.

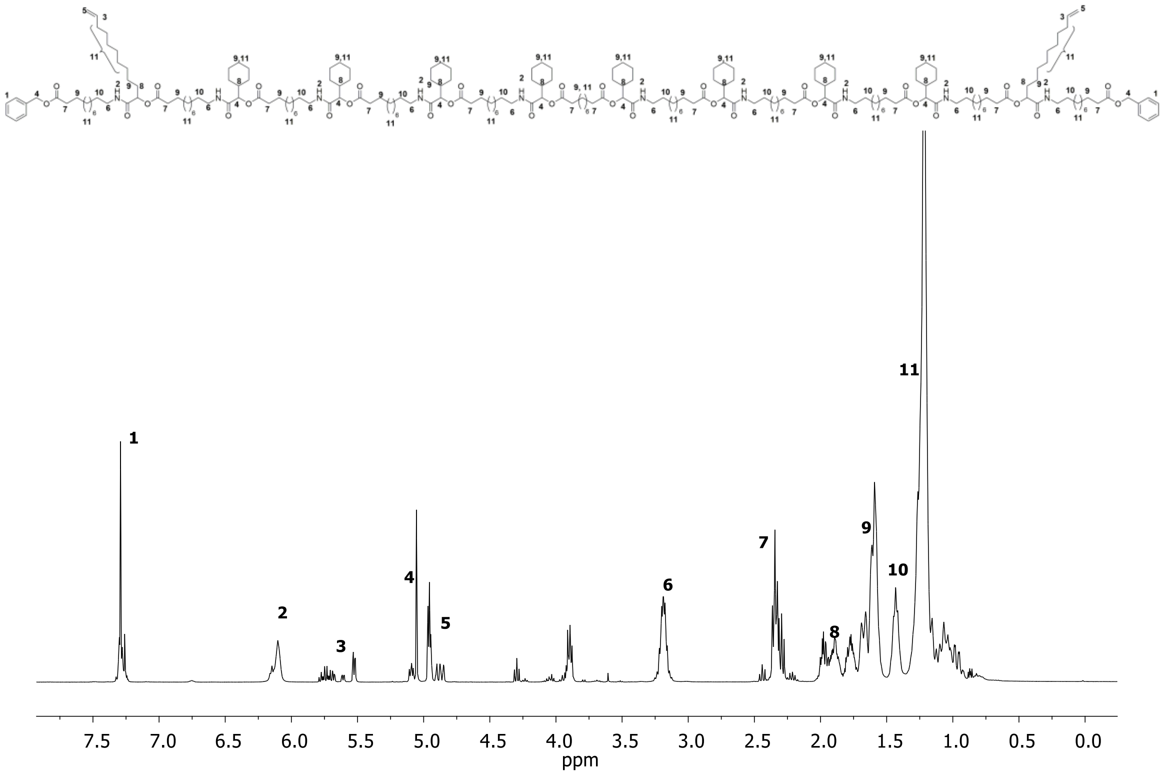
1
2
3
4
5
6
7
8
9
10
11
7.5
7.0
6.5
6.0
5.5
5.0
4.5
4.0
3.5
3.0
2.5
2.0
1.5
1.0
0.5
0.0
ppm

6.3.1.3 Macrocyclisation and Characterisation of the Macrocycles

The different macrocycles were formed *via* ring-closing metathesis of the substances **DO_2**; **$DO_{4a,b}$**; **$DO_{6a,b}$**; **$DO_{8a,b,c,d}$**.

For this purpose, the following optimised synthesis protocol was applied:

The linear oligomer with terminal double bonds (substances **DO_2**; **$DO_{4a,b}$**; **$DO_{6a,b}$**; **$DO_{8a,b,c,d}$**) (0.03 mmol, 1.0 eq.) was dissolved in chloroform (5×10^{-4} M). Subsequently, *p*-benzoquinone **69** (0.3 eq.) and Grubbs 1st generation catalyst **12** (10 mol%), both dissolved in of chloroform (2 mL), were added under argon atmosphere. The reaction mixture was heated to 45 °C and stirred under argon atmosphere. After two, three and four hours of reaction time, another 10 mol% of Grubbs 1st generation catalyst **12**, dissolved in 2 mL of chloroform, were added to the solution. After a reaction time of five hours, the reaction was quenched by addition of ethyl vinyl ether **70**. The solvent was removed under reduced pressure and the crude product (substances **MO_2**; **$MO_{4a,b}$**; **$MO_{6a,b}$**; **$MO_{8a,b,c,d}$**., see below) was analysed by SEC-ESI-MS.

List of the obtained macrocycles

Table S 1. List of the structures of all formed macrocycles.

Substance	Structure
MO$_2$ Dimer	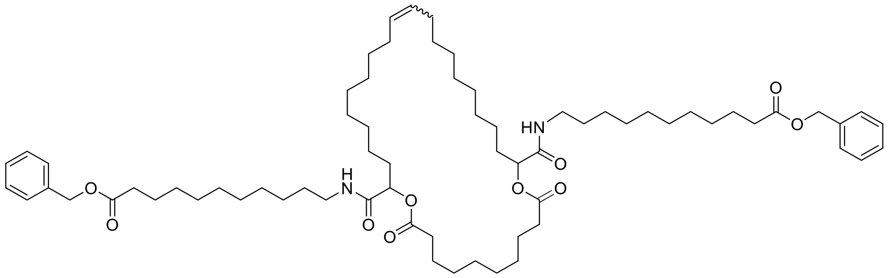
MO$_{4a}$ Tetramer with cyclohexyl side chains	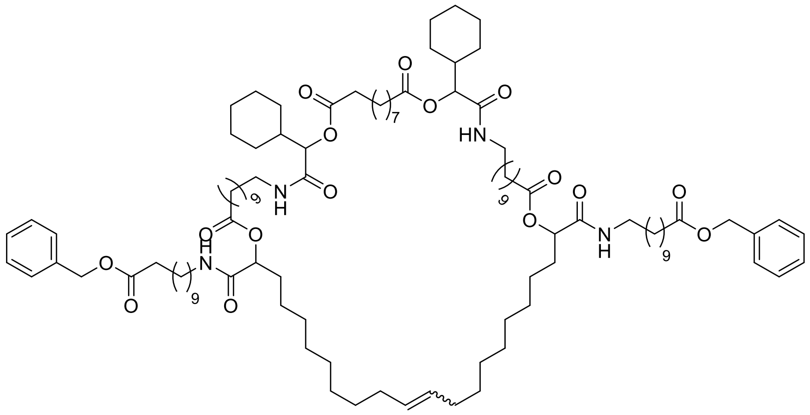
MO$_{4b}$ Tetramer with isopropyl side chains	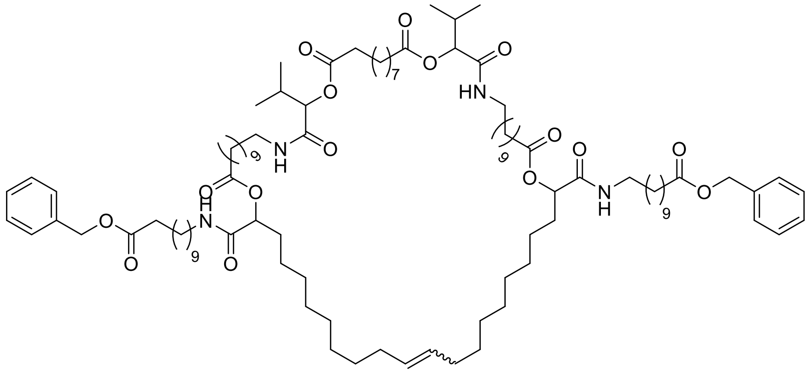

MO$_{6a}$ Hexamer with cyclohexyl side chains	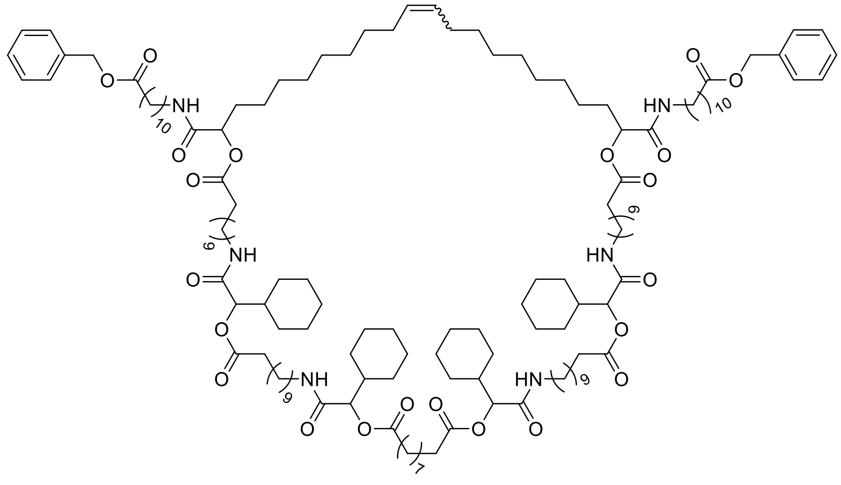
MO$_{6b}$ Hexamer with isopropyl side chains	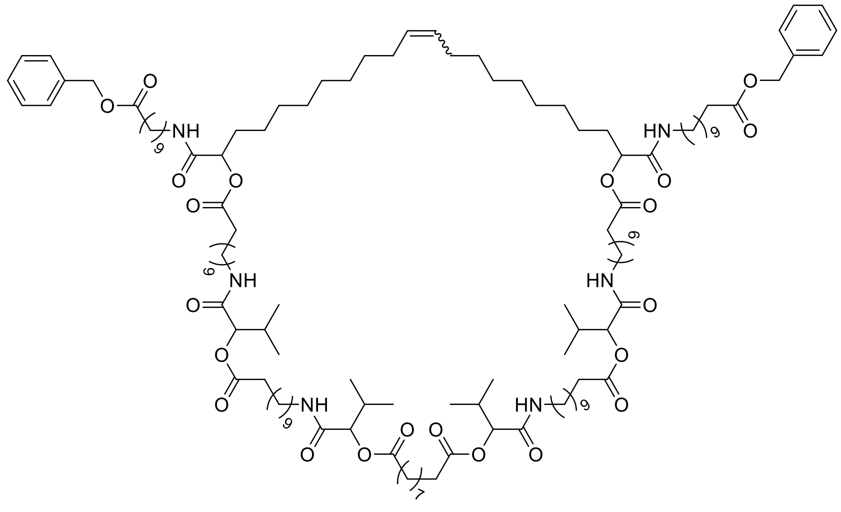
MO$_{8a}$ * Octamer with ethyl side chains (C5 core unit)	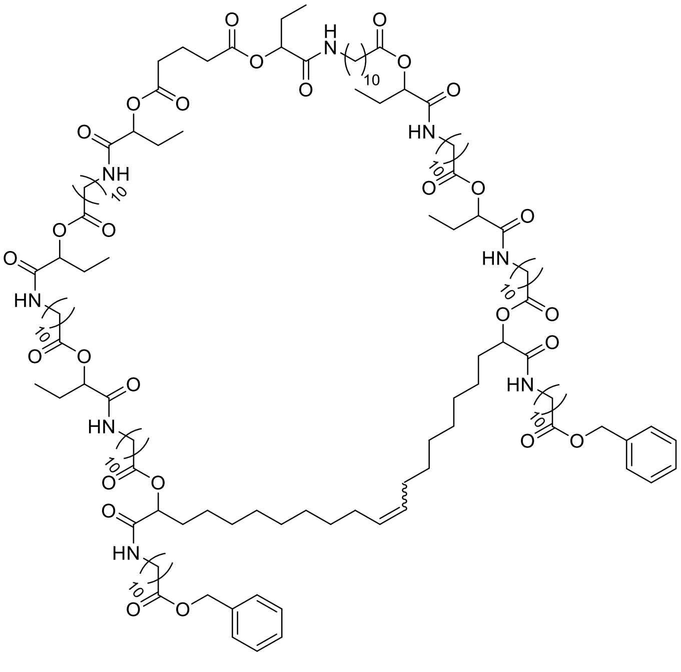

---

[*] This RCM reaction was conducted by Katharina Wetzel during the Master thesis [339]

MO$_{8b}$ [*] Octamer with cyclohexyl side chains (C5 core unit)	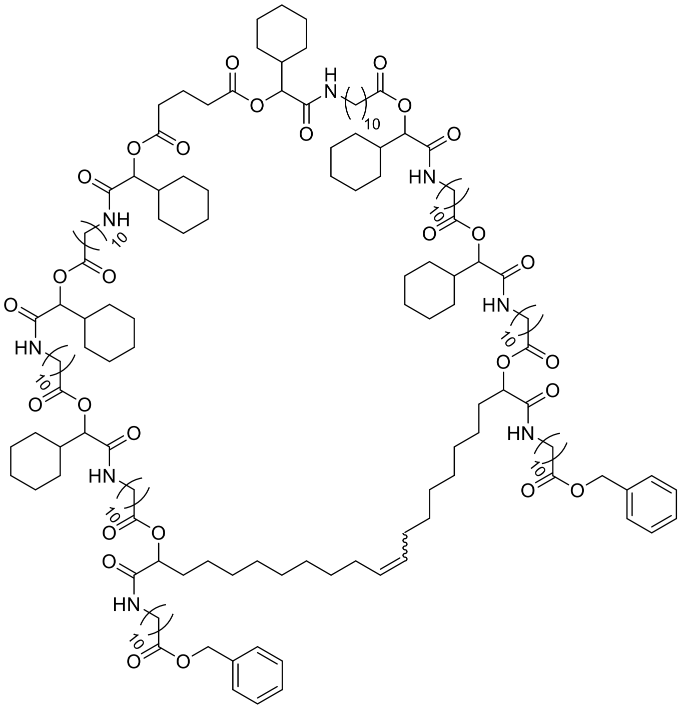
MO$_{8c}$ Octamer with cyclohexyl side chains (C10 core unit)	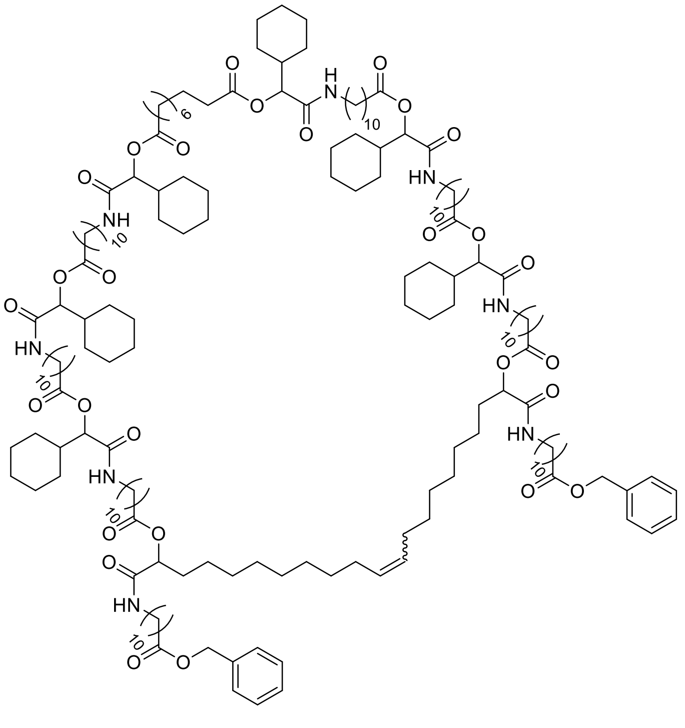

---

[*] This RCM reaction was conducted by Katharina Wetzel during the Master thesis [339]

MO$_{8d}$ Octamer with isopropyl side chains	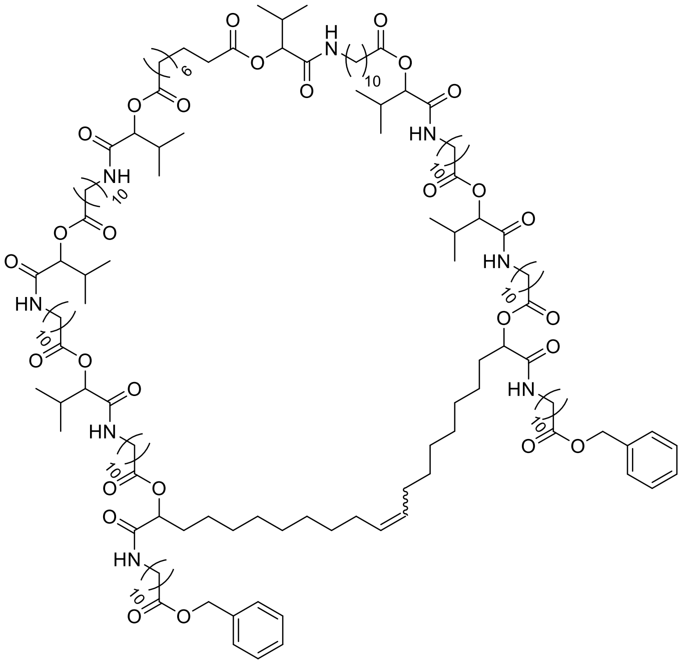
MO$_{10}$ Decamer with cyclohexyl side chains	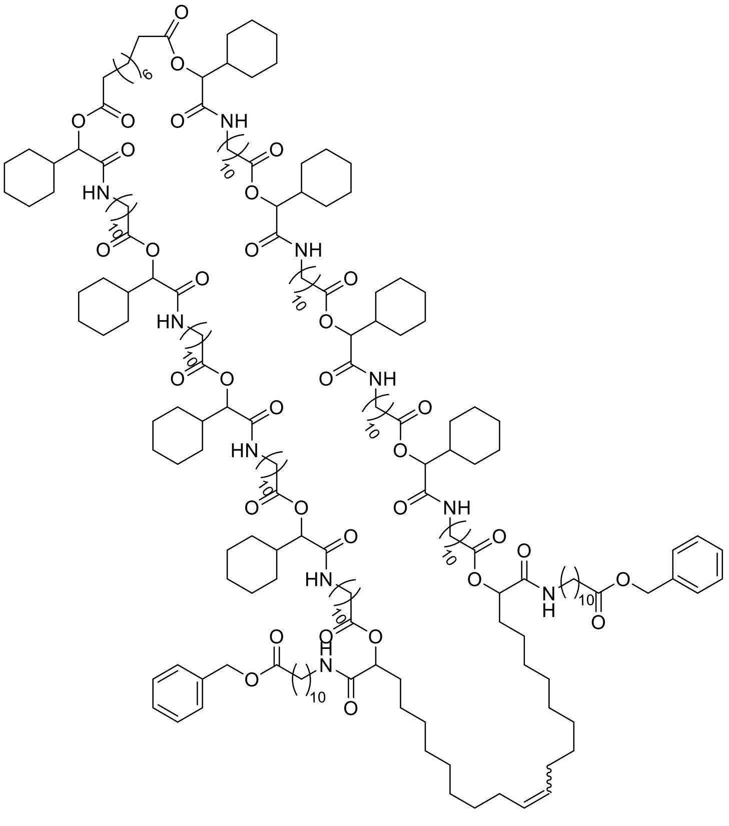

Examples of SEC-ESI-MS analysis of crude macrocycles to identify side products

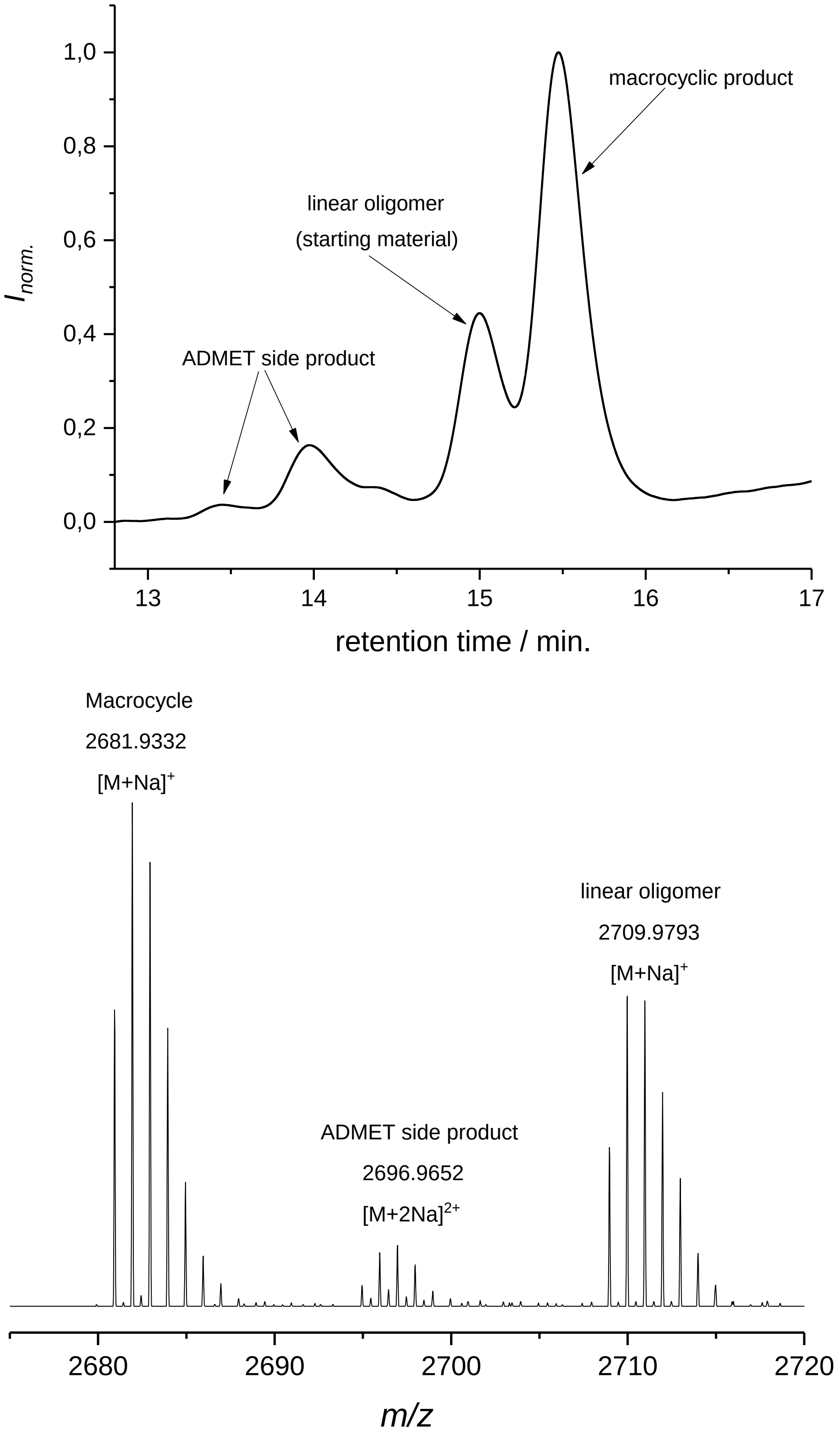

Figure S 1: SEC-ESI-MS results of a crude macrocycle. Top: SEC trace of the cyclic octamer **MO$_{8a}$** *with ethyl side chains, showing different peaks, which were identified with the help of the MS spectrum (bottom).*

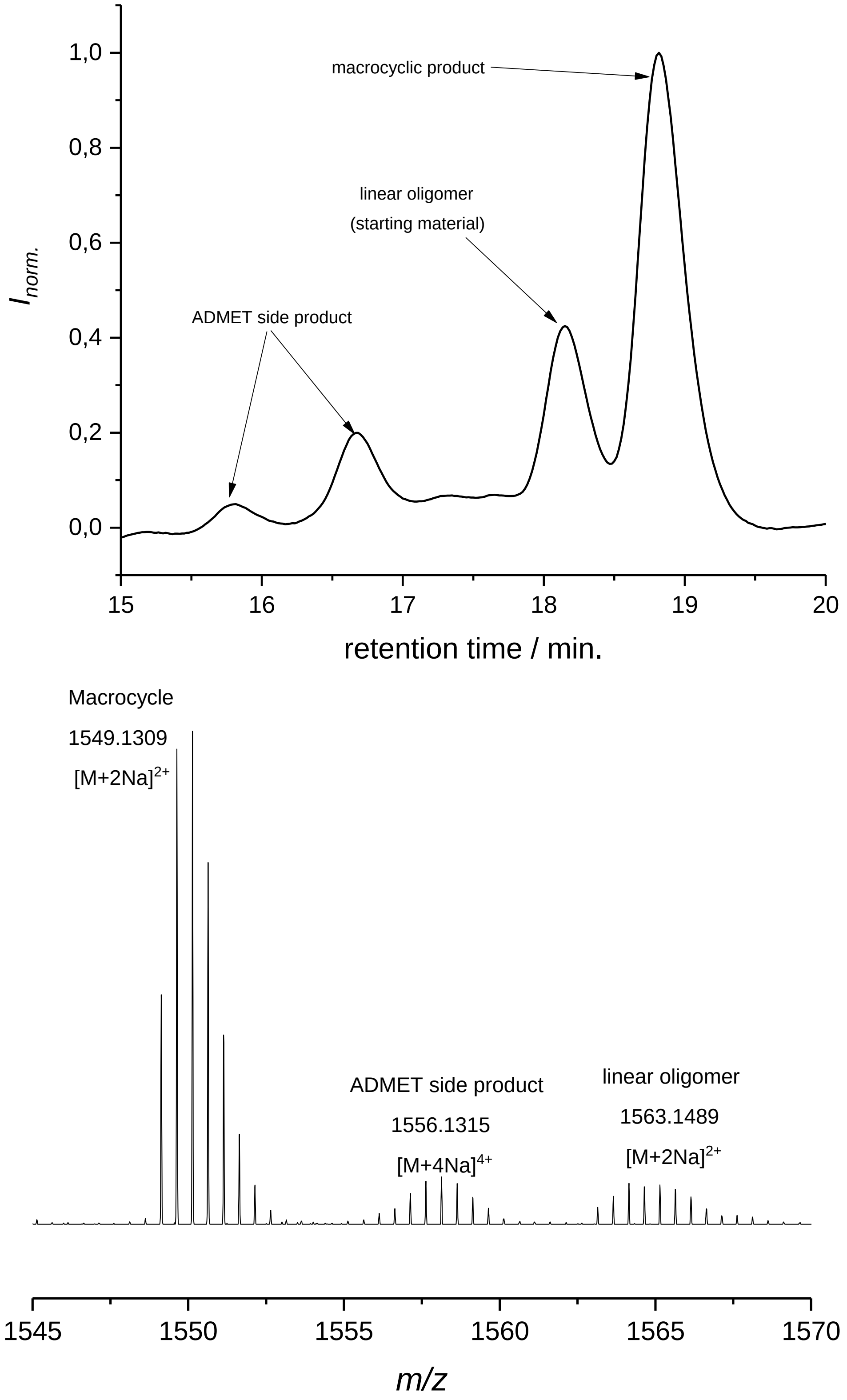

*Figure S 2. SEC-ESI-MS results of a crude macrocycle. Top: SEC trace of the cyclic octamer **MO$_{8b}$** with cyclohexyl side chains, showing different peaks, which were identified with the help of the MS spectrum (bottom).*

Characterization of the macrocycles *via* ESI-MS

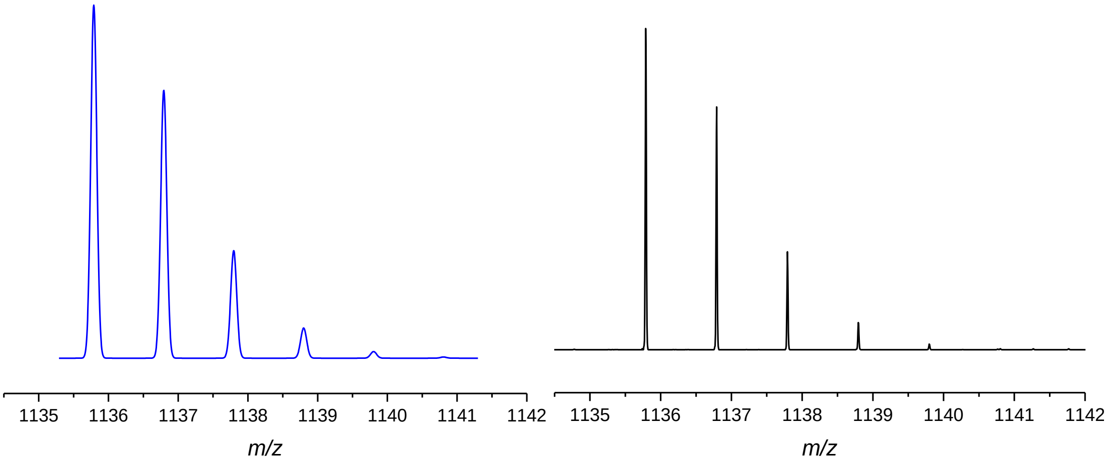

Figure S 3. Characterization of the cyclic dimer ***MO$_2$*** *by ESI-MS. Comparison of the calculated isotopic pattern (blue) with the measured one (black).*

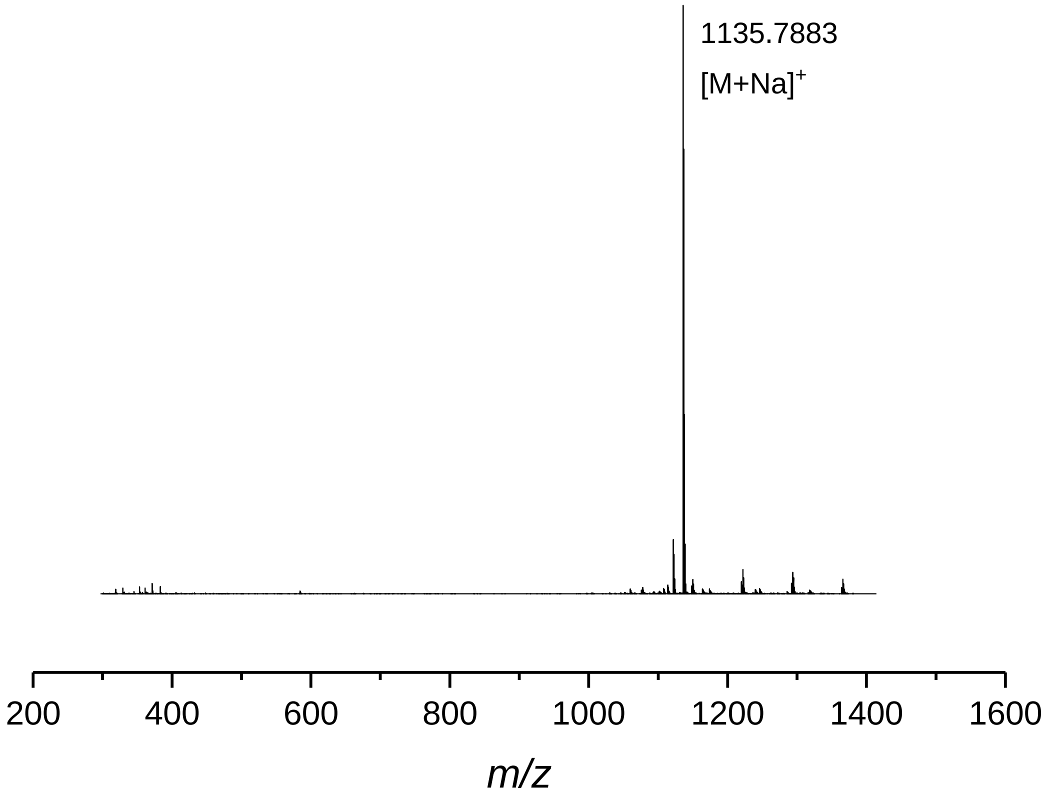

Figure S 4. ESI-MS spectrum of the crude reaction mixture after cyclization. The singly charged sodium cation of the macrocycle ***MO$_2$*** *was observed.*

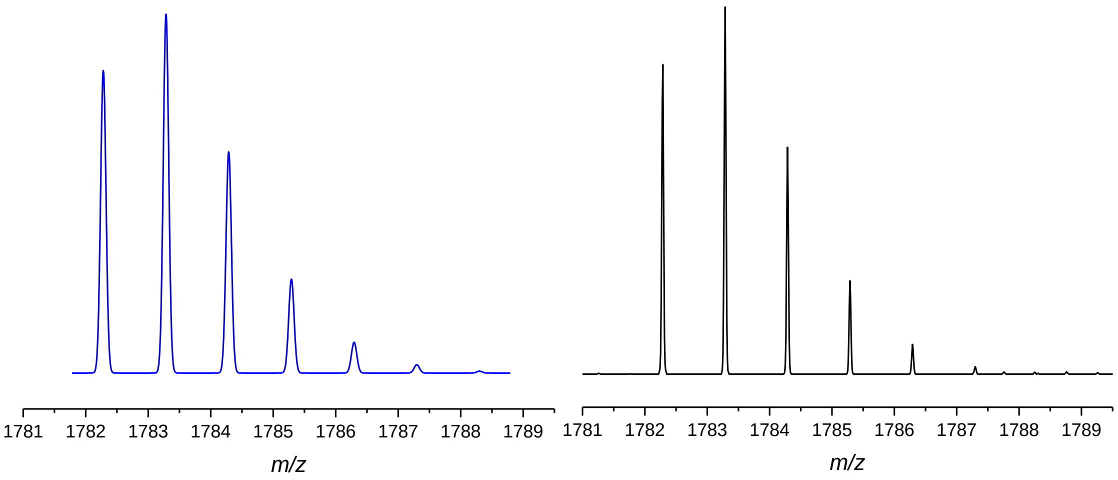

Figure S 5. Characterization of the cyclic tetramer ***MO$_{4a}$*** *with cyclohexyl side chains by ESI-MS. Comparison of the calculated isotopic pattern (blue) with the measured one (black).*

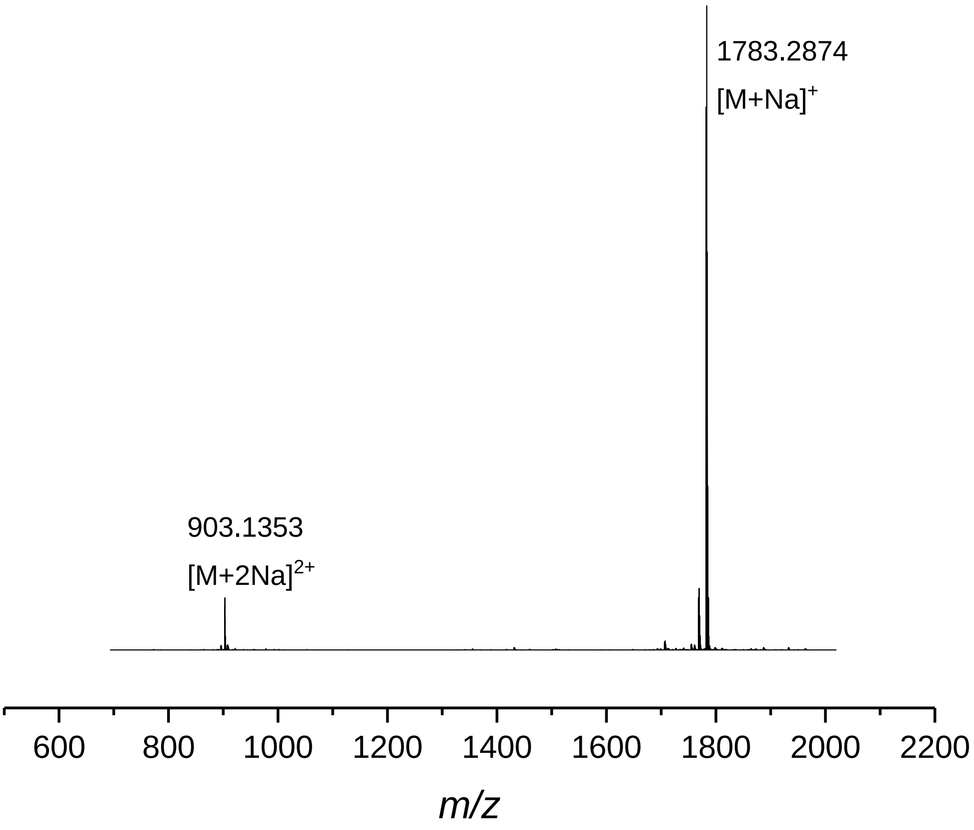

Figure S 6.ESI-MS spectrum of the crude reaction mixture after cyclization. The singly and doubly charged sodium cations of the macrocycle ***MO$_{4a}$*** *were observed.*

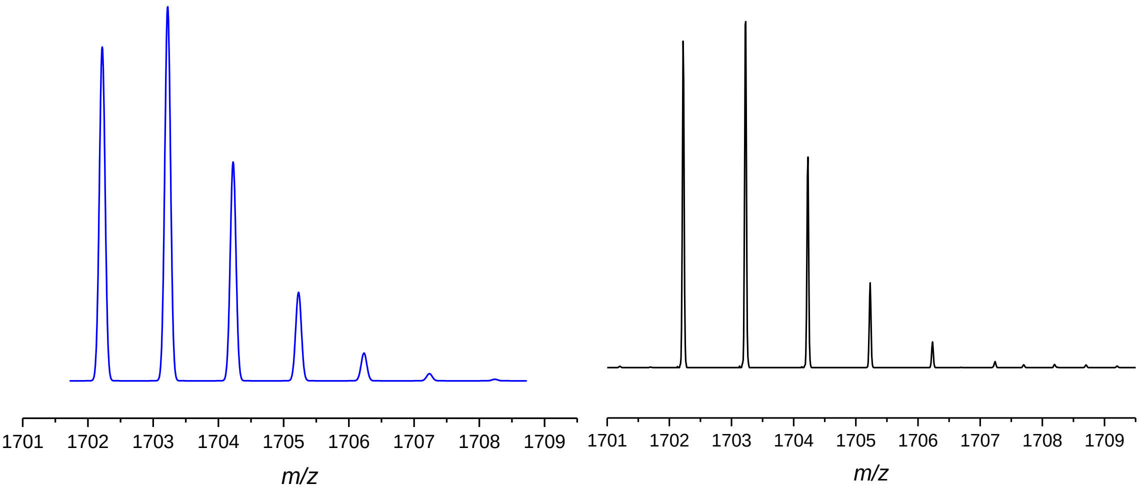

*Figure S 7. Characterization of the cyclic tetramer **MO$_{4b}$** with isopropyl side chains by ESI-MS. Comparison of the calculated isotopic pattern (blue) with the measured one (black).*

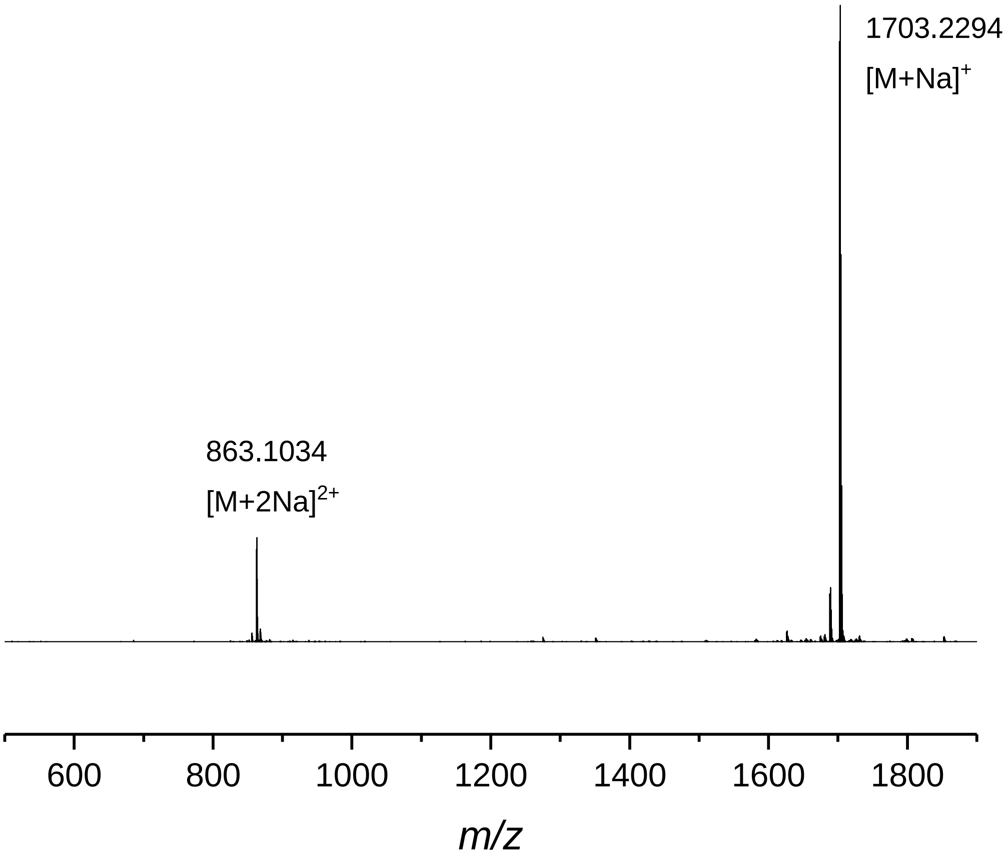

*Figure S 8.ESI-MS spectrum of the crude reaction mixture after cyclization. The singly and doubly charged sodium cations of the macrocycle **MO$_{4b}$** were observed.*

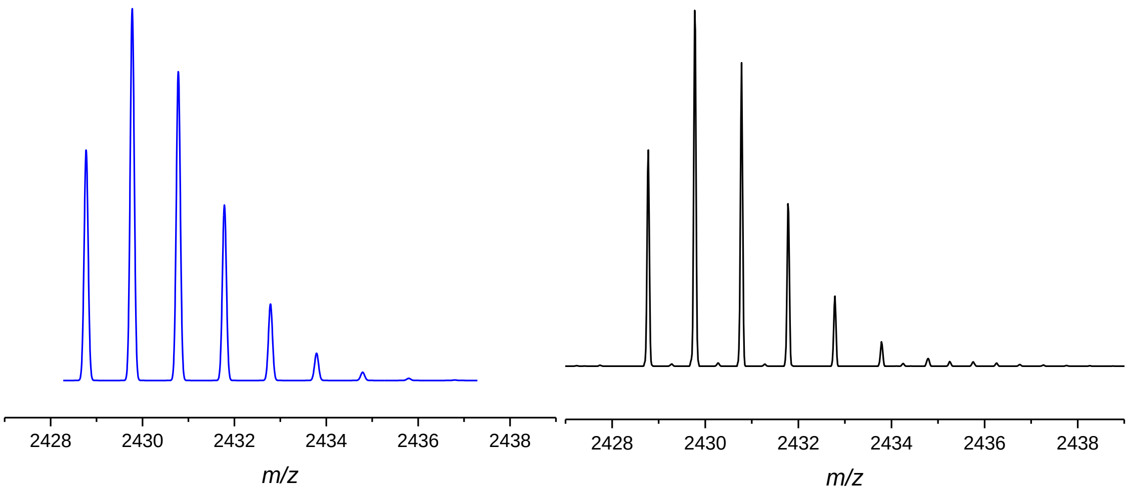

Figure S 9. Characterization of the cyclic hexamer ***MO$_{6a}$*** *with cyclohexyl side chains by ESI-MS. Comparison of the calculated isotopic pattern (blue) with the measured one (black).*

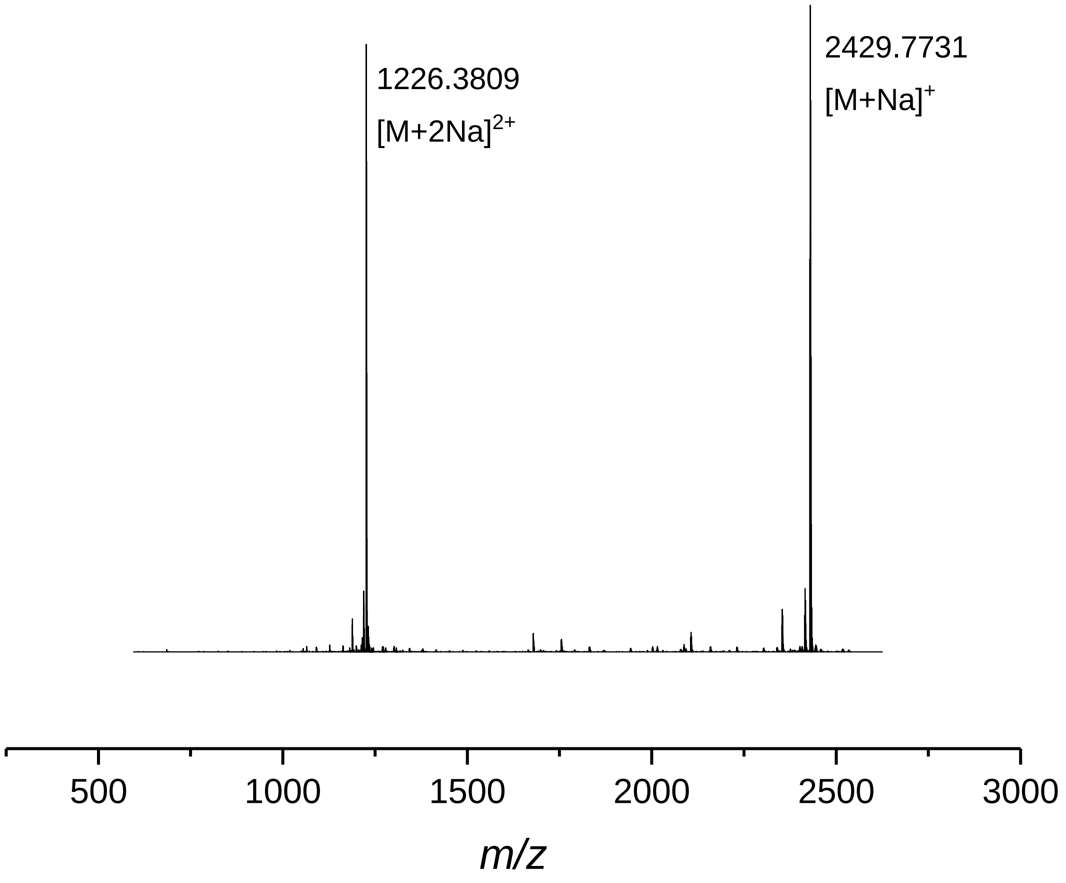

Figure S 10. ESI-MS spectrum of the crude reaction mixture after cyclization. The singly and doubly charged sodium cations of the macrocycle ***MO$_{6a}$*** *were observed.*

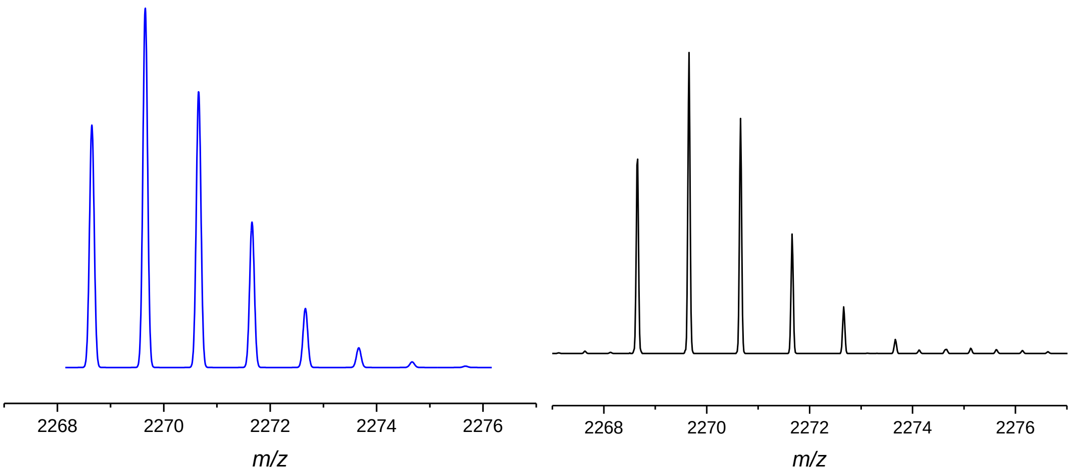

*Figure S 11. Characterization of the cyclic hexamer **MO$_{6b}$** with isopropyl side chains by ESI-MS. Comparison of the calculated isotopic pattern (blue) with the measured one (black).*

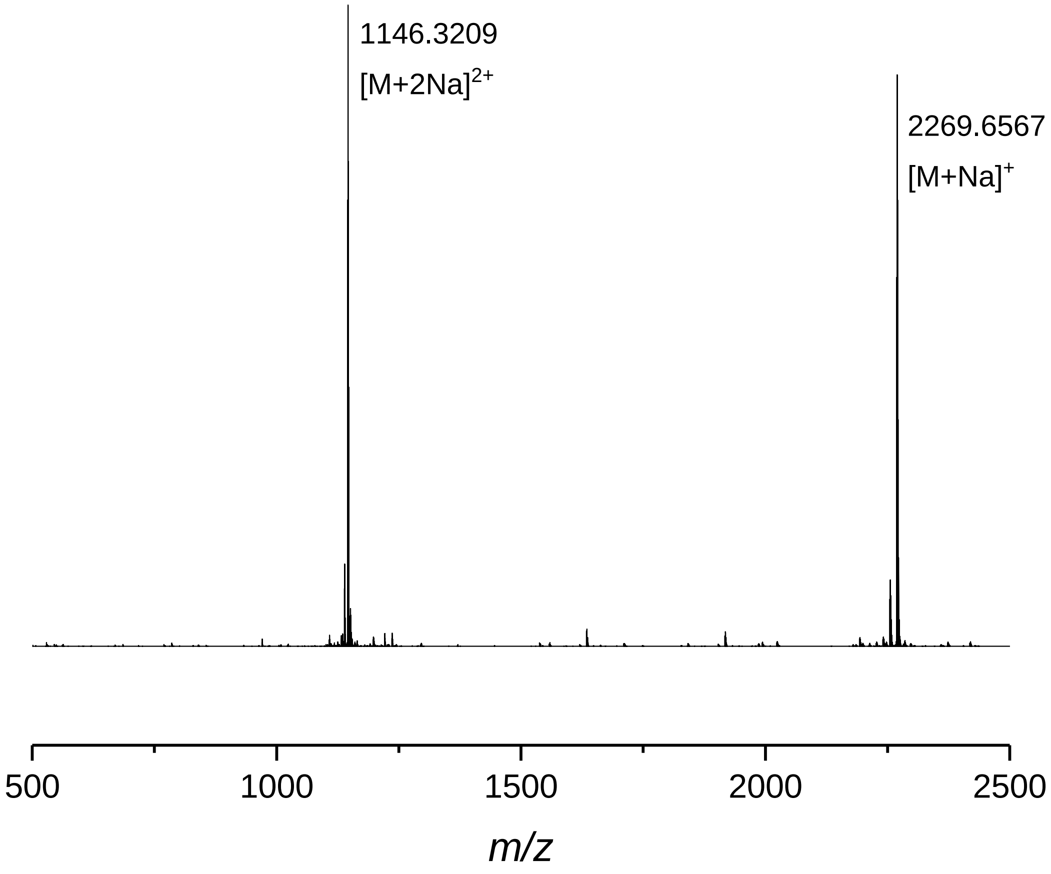

*Figure S 12.ESI-MS spectrum of the crude reaction mixture after cyclization. The singly and doubly charged sodium cations of the macrocycle **MO$_{6b}$** were observed.*

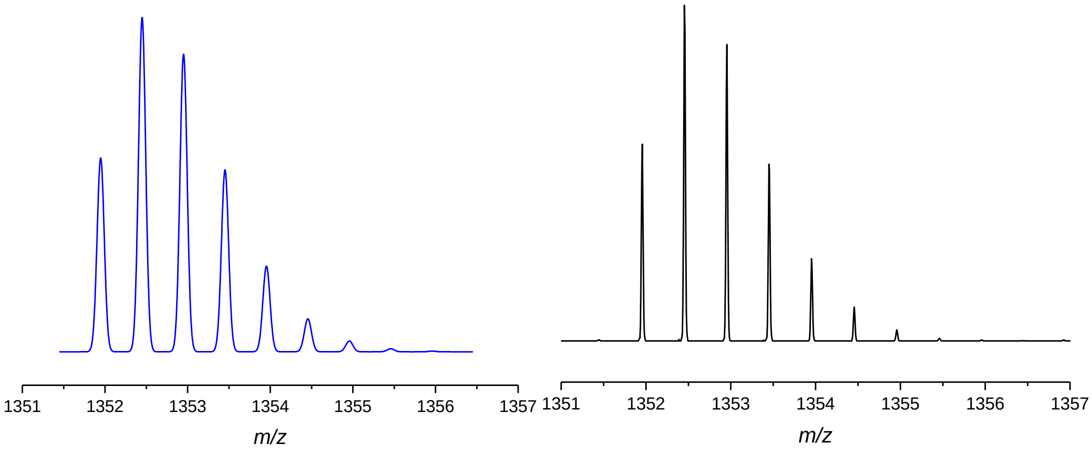

*Figure S 13. Characterization of the cyclic octamer **MO$_{8a}$** with ethyl side chains (C5 core unit) by ESI-MS. Comparison of the calculated isotopic pattern (blue) with the measured one (black).*

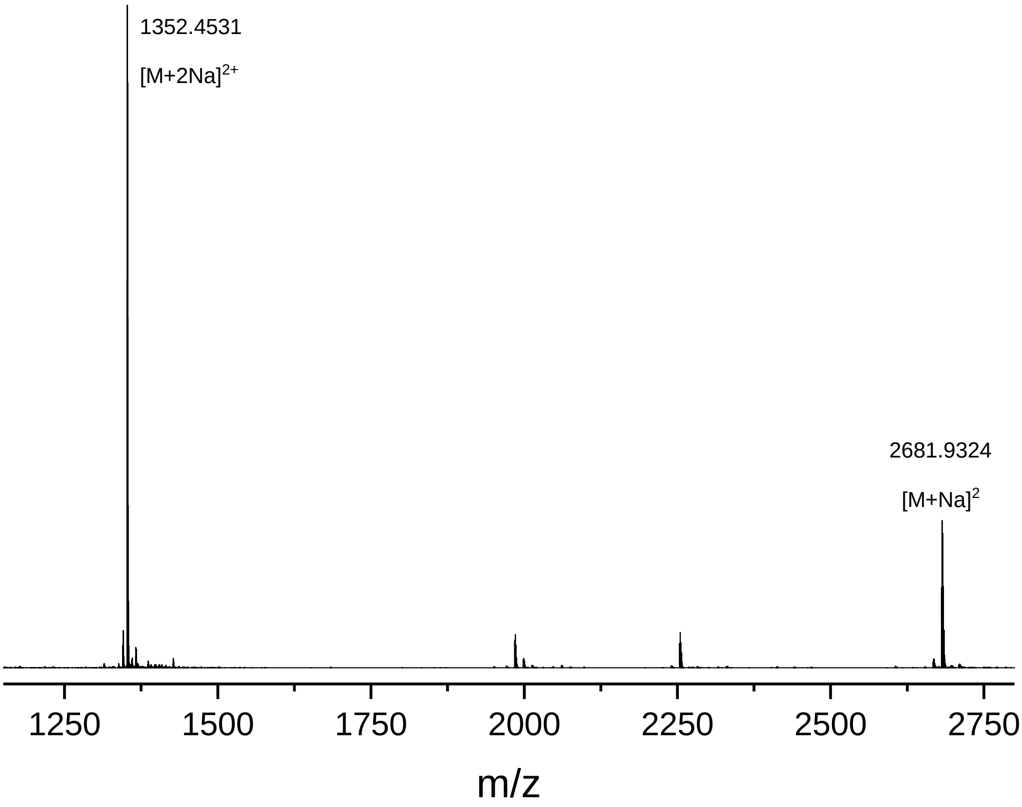

*Figure S 14.ESI-MS spectrum of the crude reaction mixture after cyclization. The singly and doubly charged sodium cations of the macrocycle **MO$_{8a}$** were observed.*

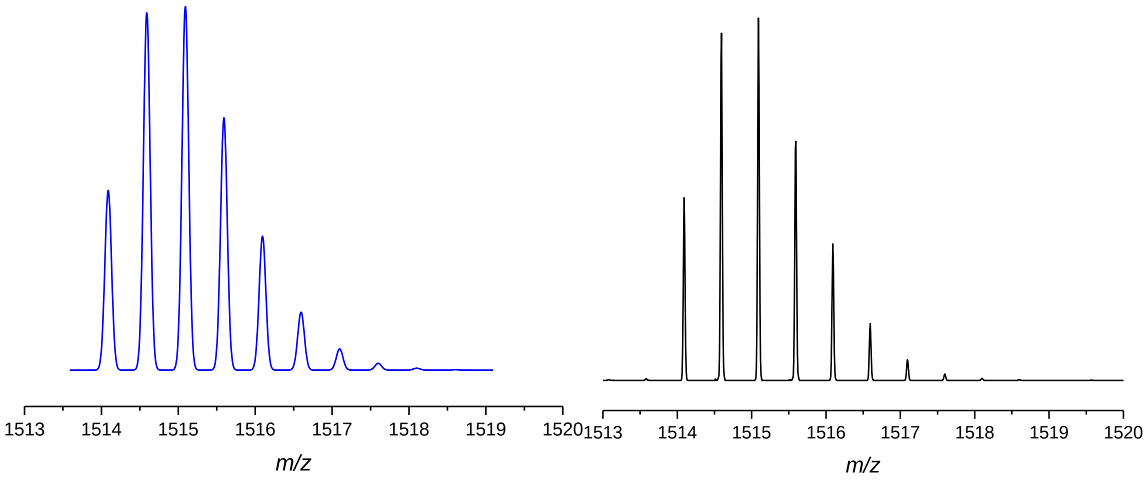

Figure S 15. Characterization of the cyclic octamer ***MO$_{8b}$*** *with cyclohexyl side chains (C5 core unit) by ESI-MS. Comparison of the calculated isotopic pattern (blue) with the measured one (black).*

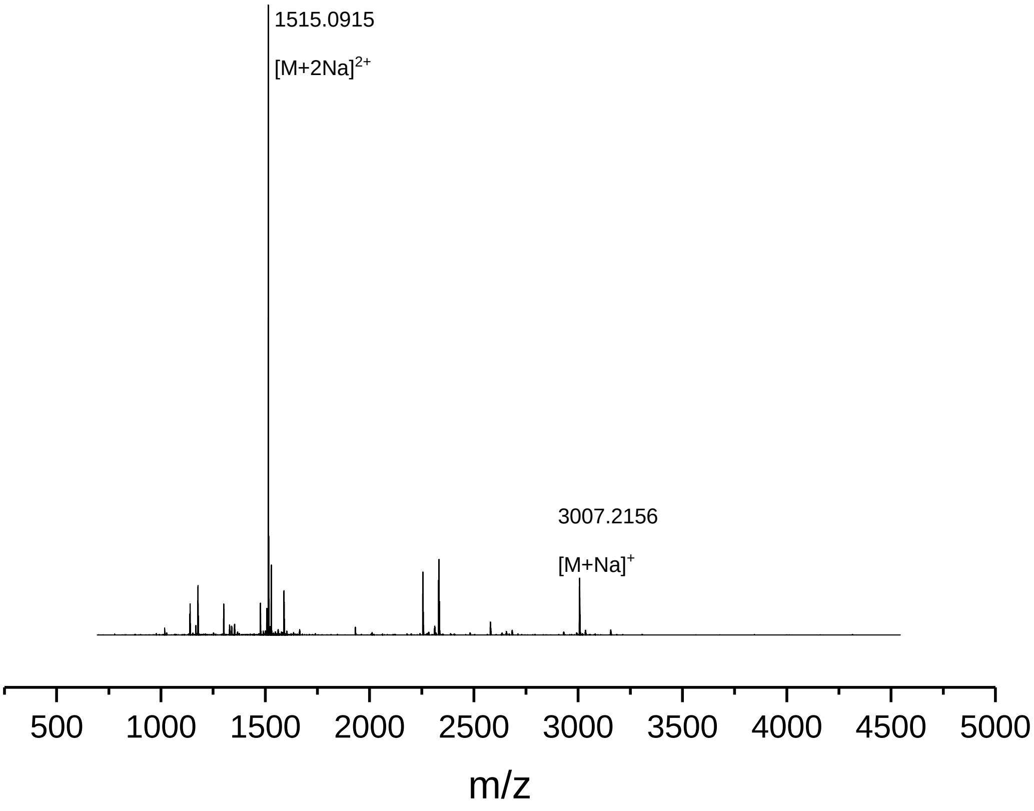

Figure S 16. ESI-MS spectrum of the crude reaction mixture after cyclization. The singly and doubly charged sodium cations of the macrocycle ***MO$_{8b}$*** *were observed.*

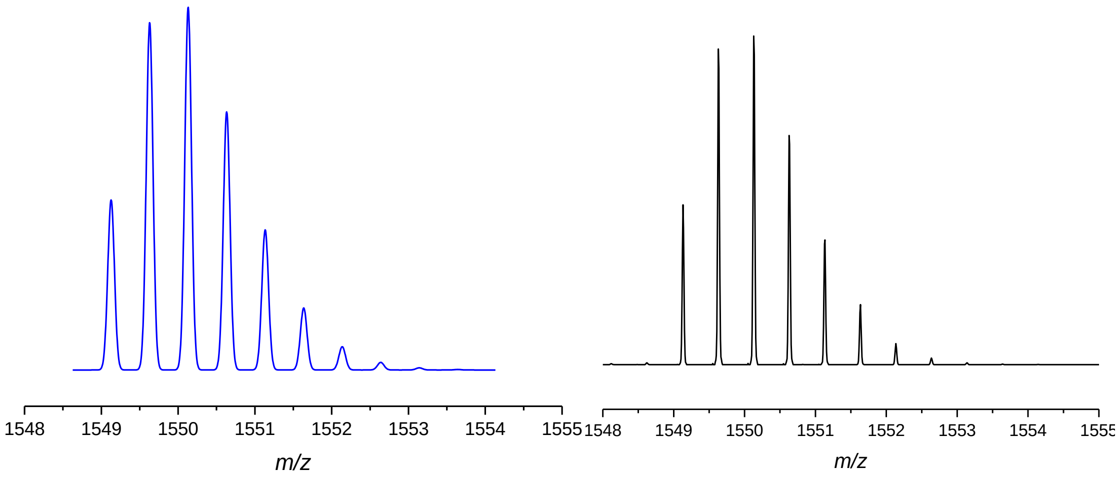

Figure S 17. Characterization of the cyclic octamer ***MO$_{8c}$*** *with cyclohexyl side chains (C10 core unit) by ESI-MS. Comparison of the calculated isotopic pattern (blue) with the measured one (black).*

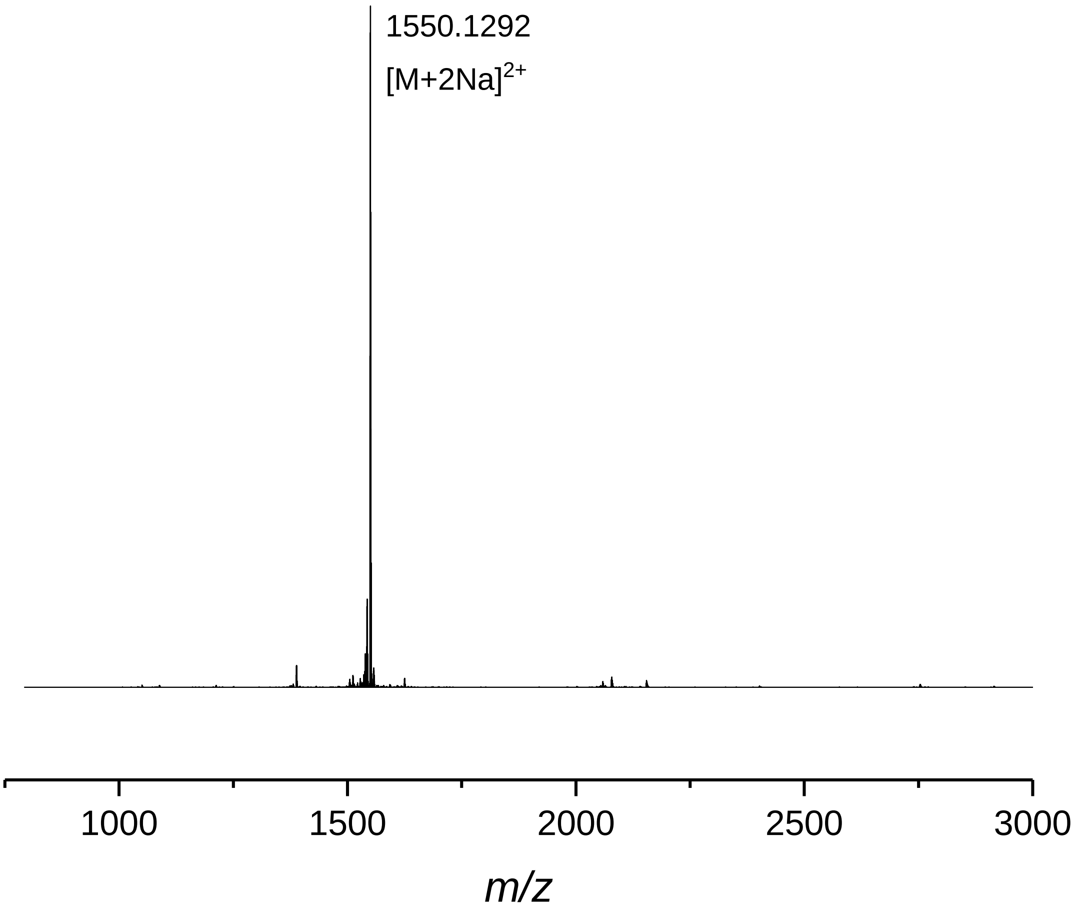

Figure S 18.ESI-MS spectrum of the crude reaction mixture after cyclization. The doubly charged sodium cation of the macrocycle ***MO$_{8c}$*** *was observed.*

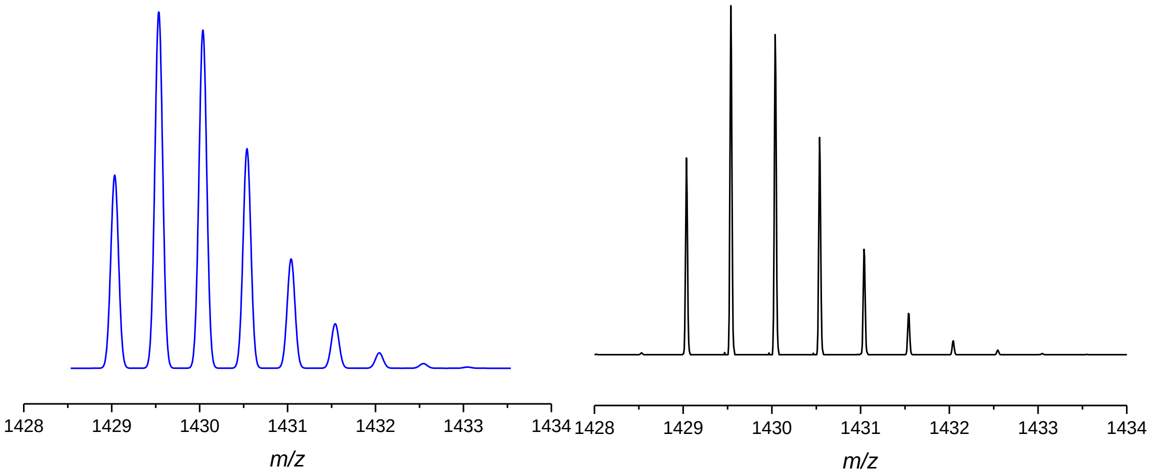

*Figure S 19. Characterization of the cyclic octamer **MO_{8d}** with isopropyl side chains by ESI-MS. Comparison of the calculated isotopic pattern (blue) with the measured one (black).*

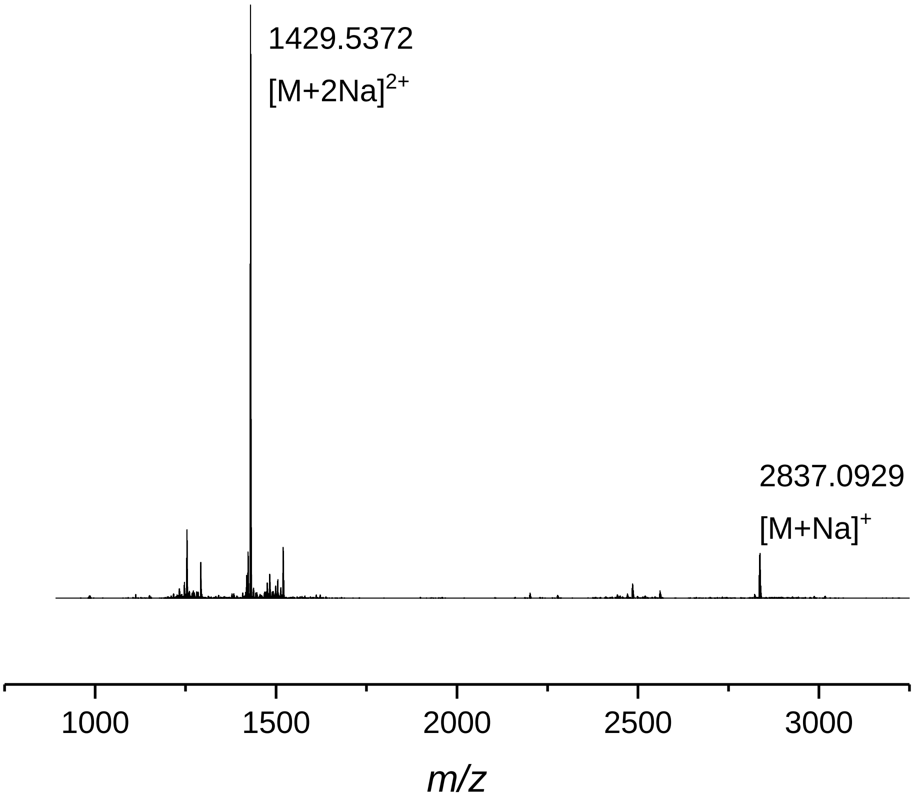

*Figure S 20. ESI-MS spectrum of the crude reaction mixture after cyclization. The singly and doubly charged sodium cations of the macrocycle **MO_{8d}** were observed.*

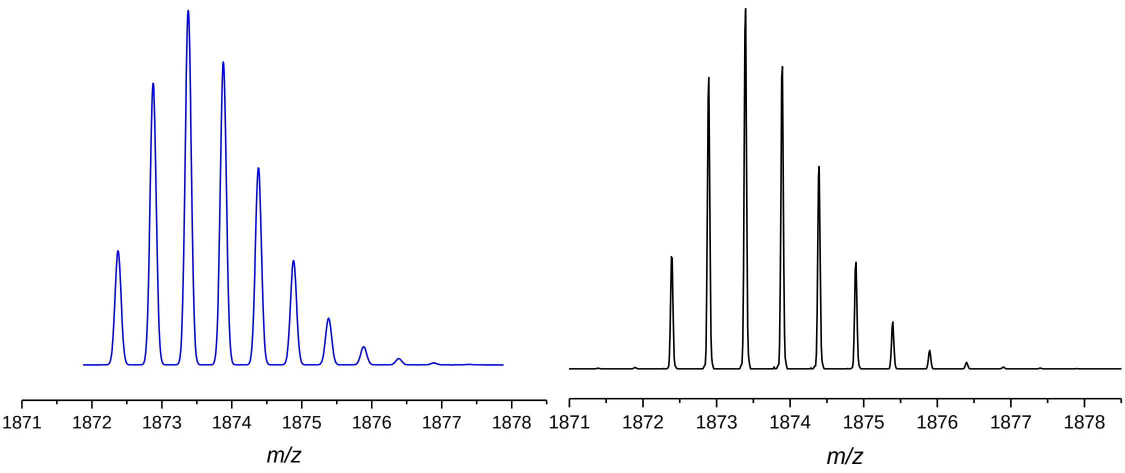

*Figure S 21 Characterization of the cyclic decamer **MO_{10}** with cyclohexyl side chains by ESI-MS. Comparison of the calculated isotopic pattern (blue) with the measured one (black).*

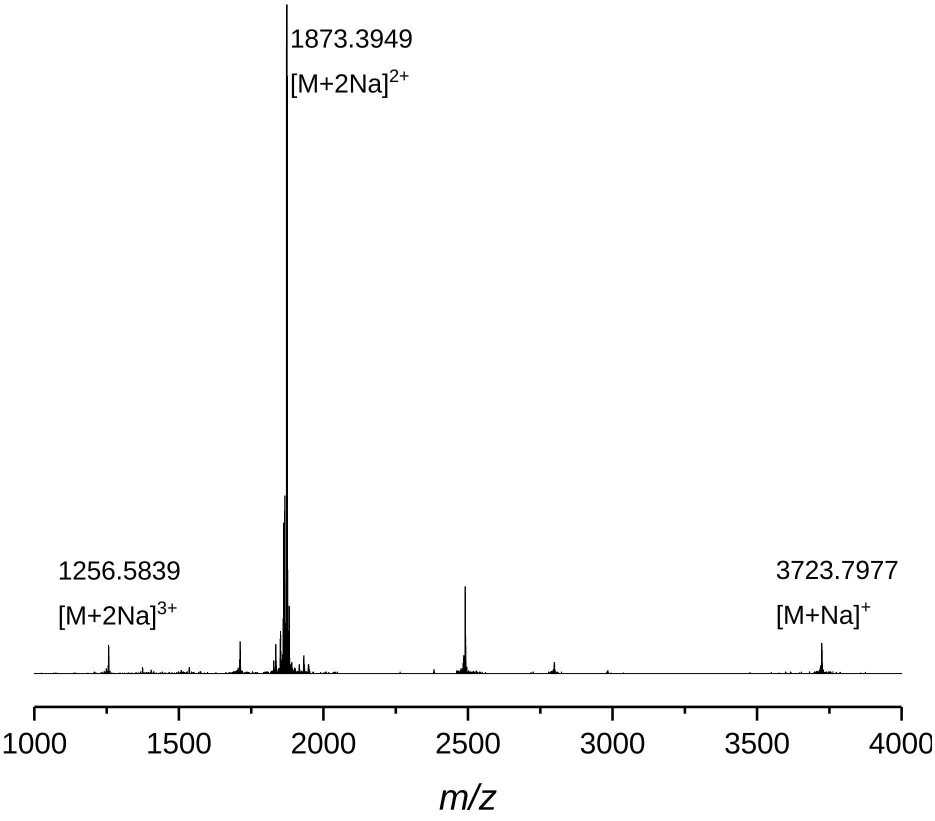

*Figure S 22. ESI-MS spectrum of the crude reaction mixture after cyclization. The singly doubly and triply charged sodium cations of the macrocycle **MO_{10}** were observed.*

SEC Characterization

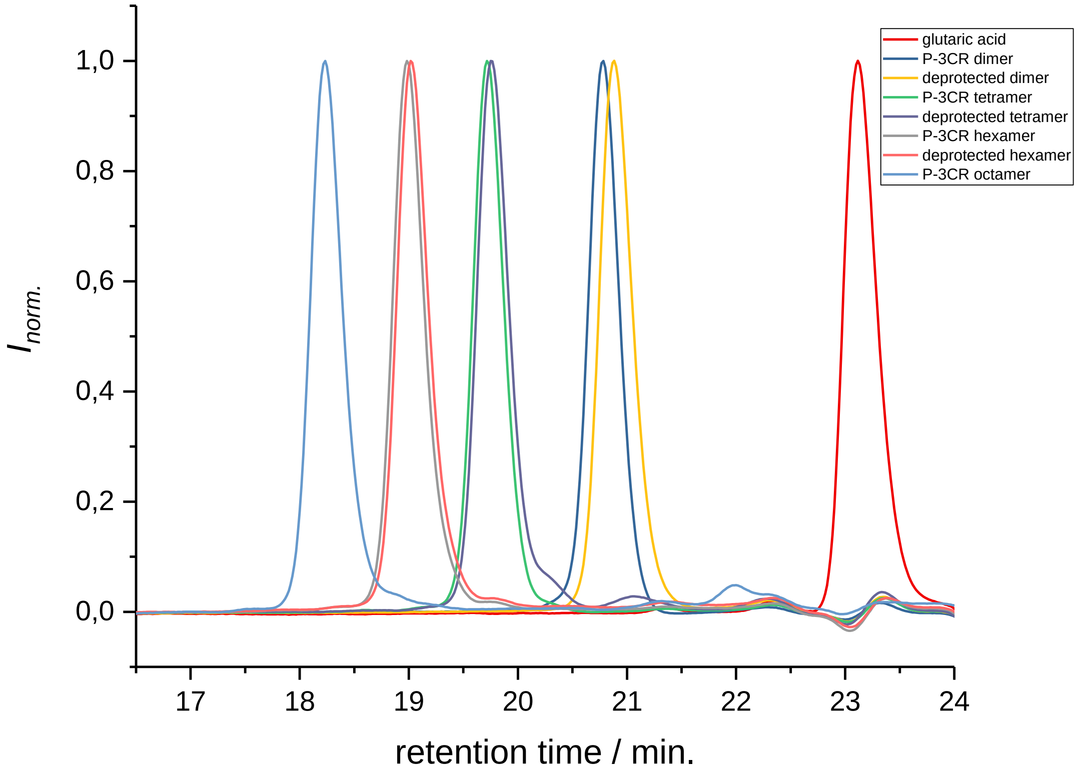

Figure S 23. SEC results of linear oligomers with ethyl side chains and C5 core unit.

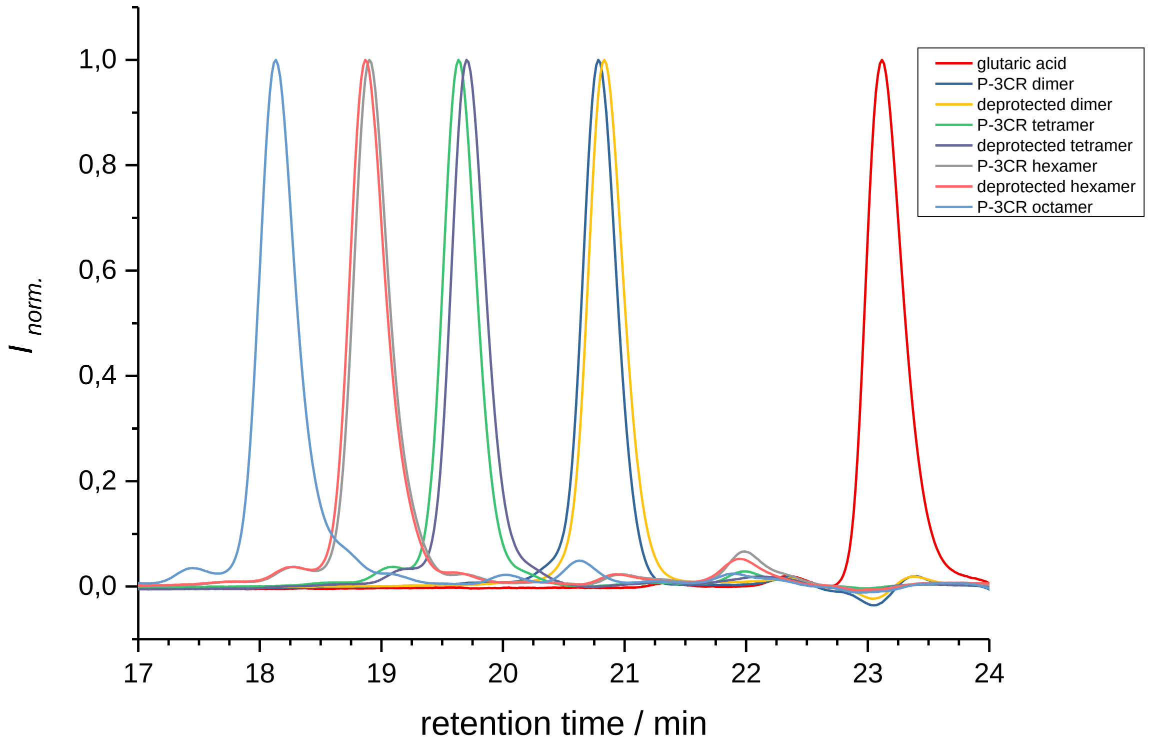

Figure S 24. SEC results of linear oligomers with cyclohexyl side chains and C5 core unit.

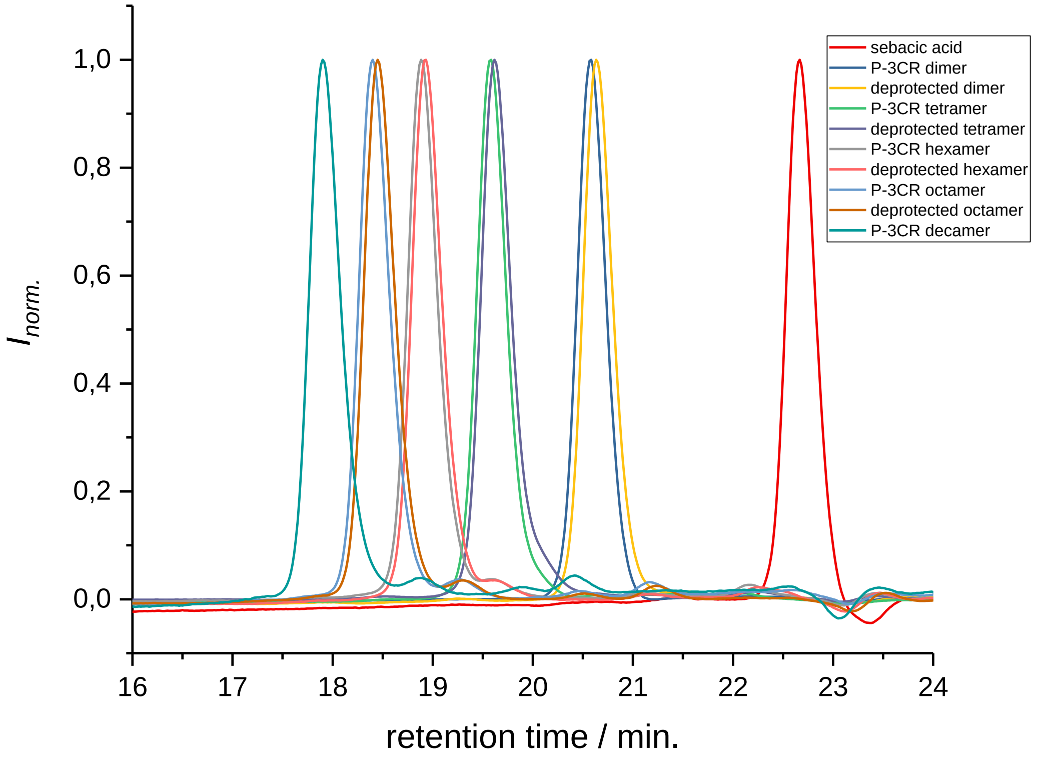

Figure S 25. SEC analysis of linear oligomers with cyclohexyl side chains and C10 core unit.

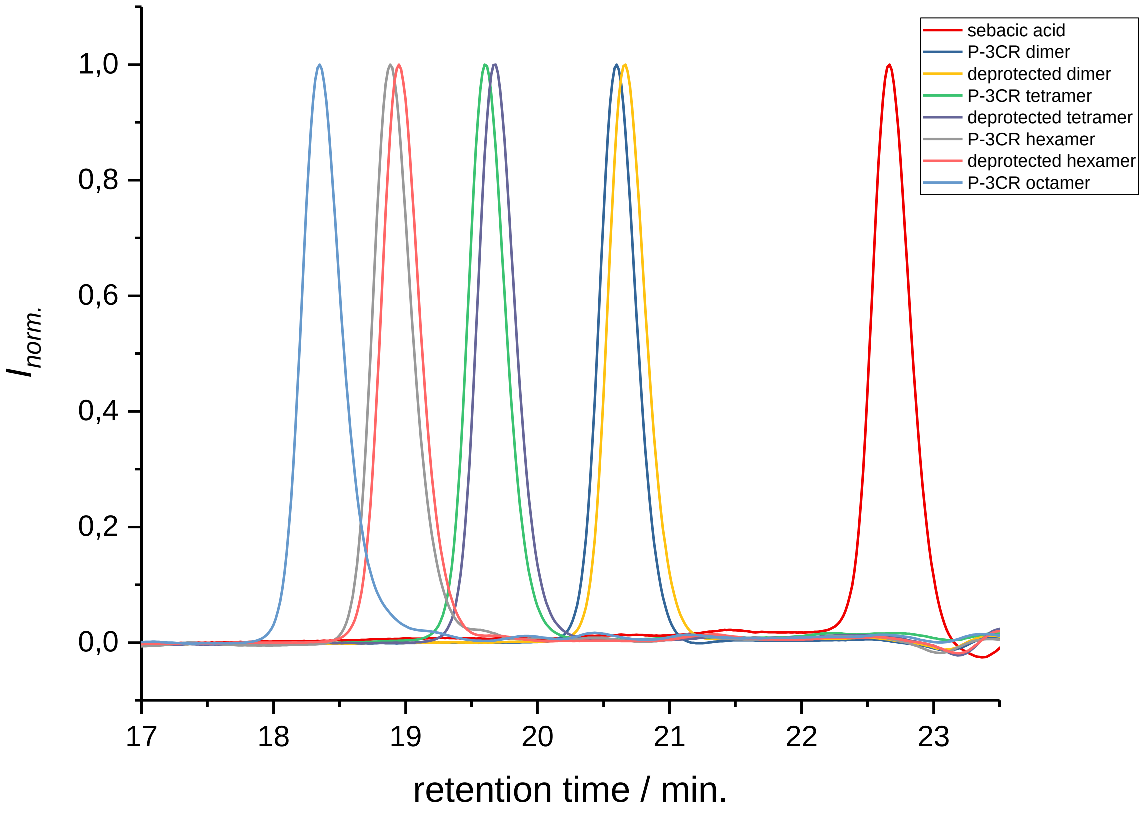

Figure S 26. SEC analysis of linear oligomers with isopropyl side chains and C10 core unit

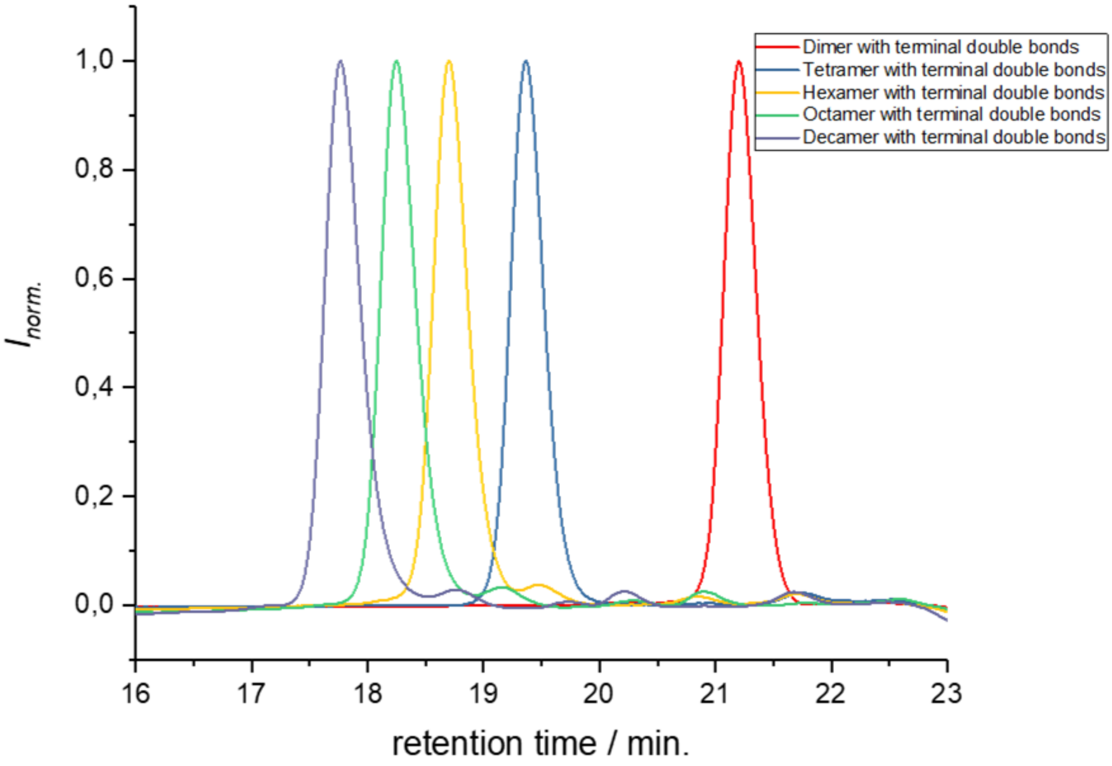

Figure S 27. SEC analysis of linear oligomers with cyclohexyl side chains and terminal double bonds.

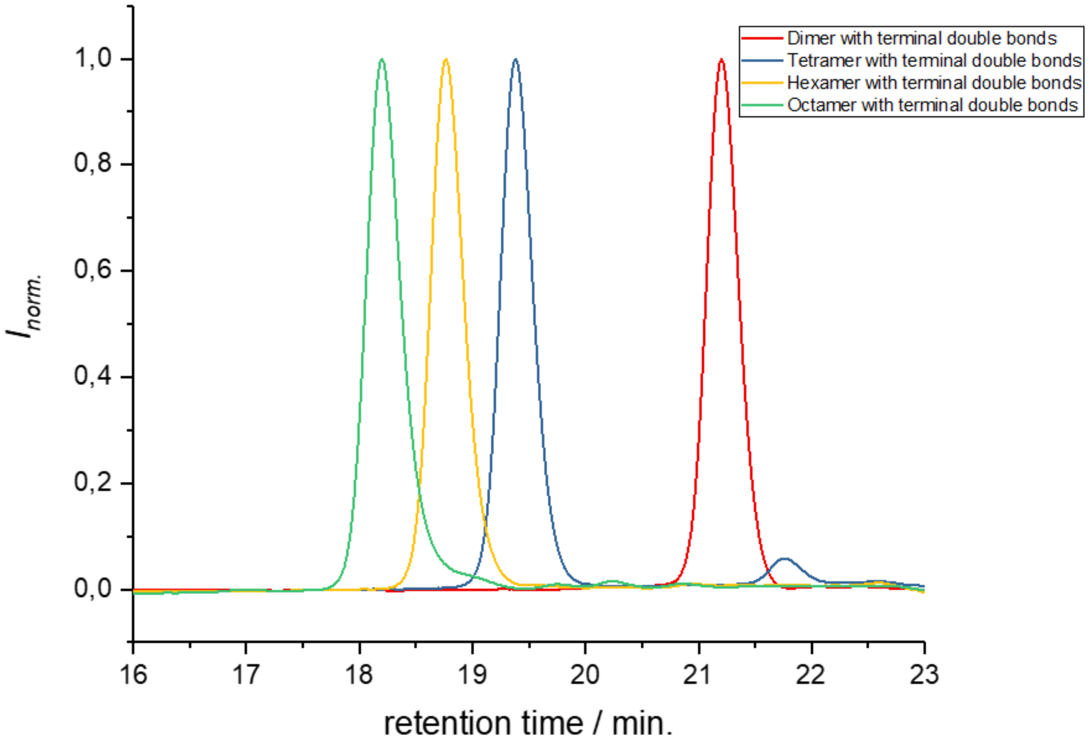

Figure S 28. SEC analysis of linear oligomers with isopropyl side chains and terminal double bonds.

Comparison of the conversion of three macrocyclic octamers with different side chains

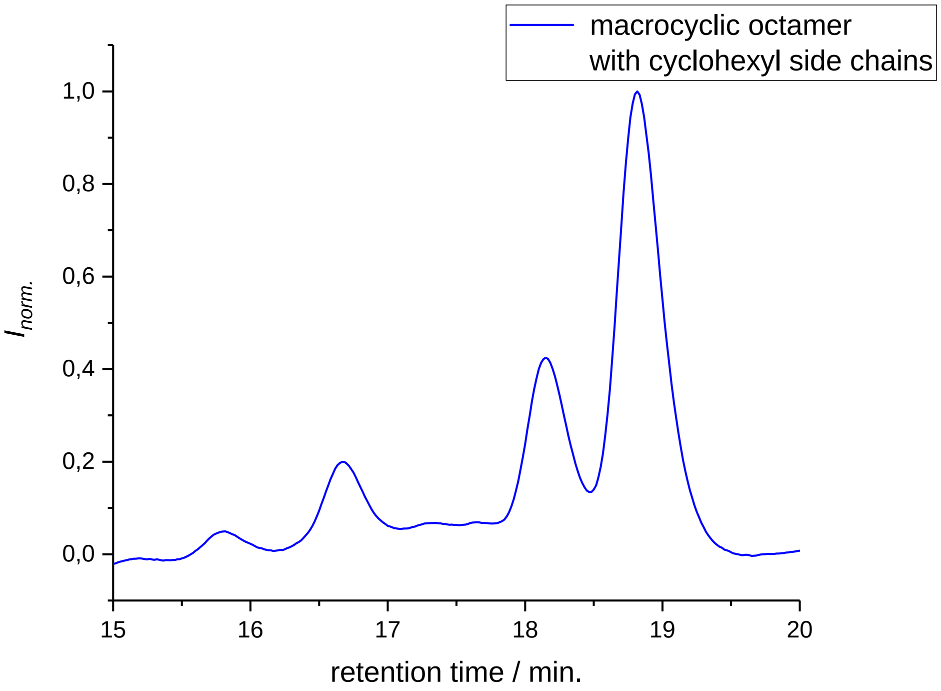

Figure S 29. SEC analysis of crude macrocycle ***MO_{8b}*** *carrying cyclohexyl side chains.*

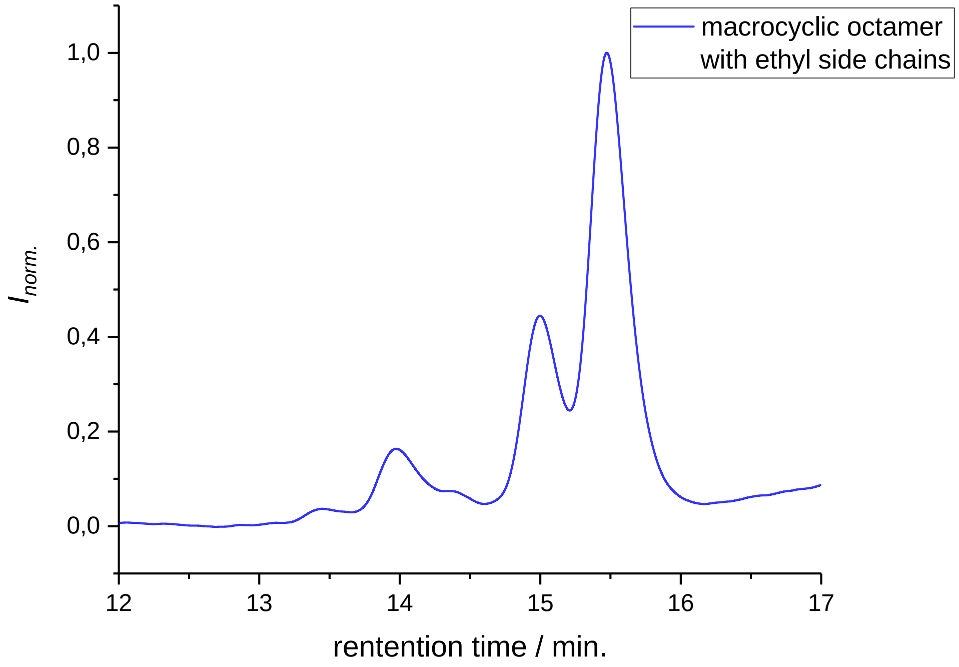

Figure S 30. SEC analysis of crude macrocycle ***MO_{8a}*** *carrying ethyl side chains.*

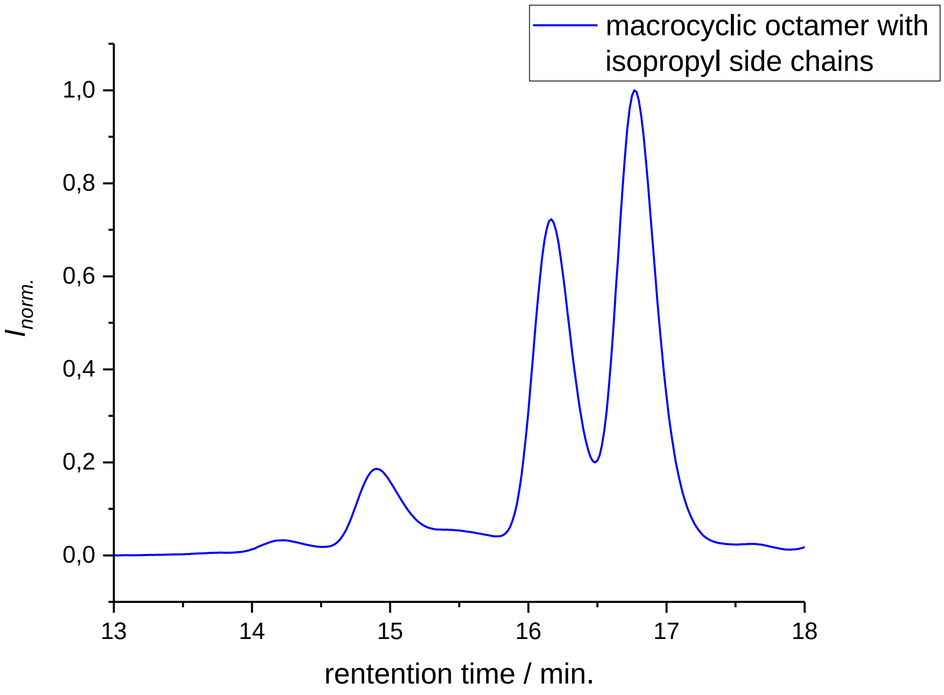

Figure S 31. SEC analysis of crude macrocycle ***MO_{8d}*** *carrying isopropyl side chains*

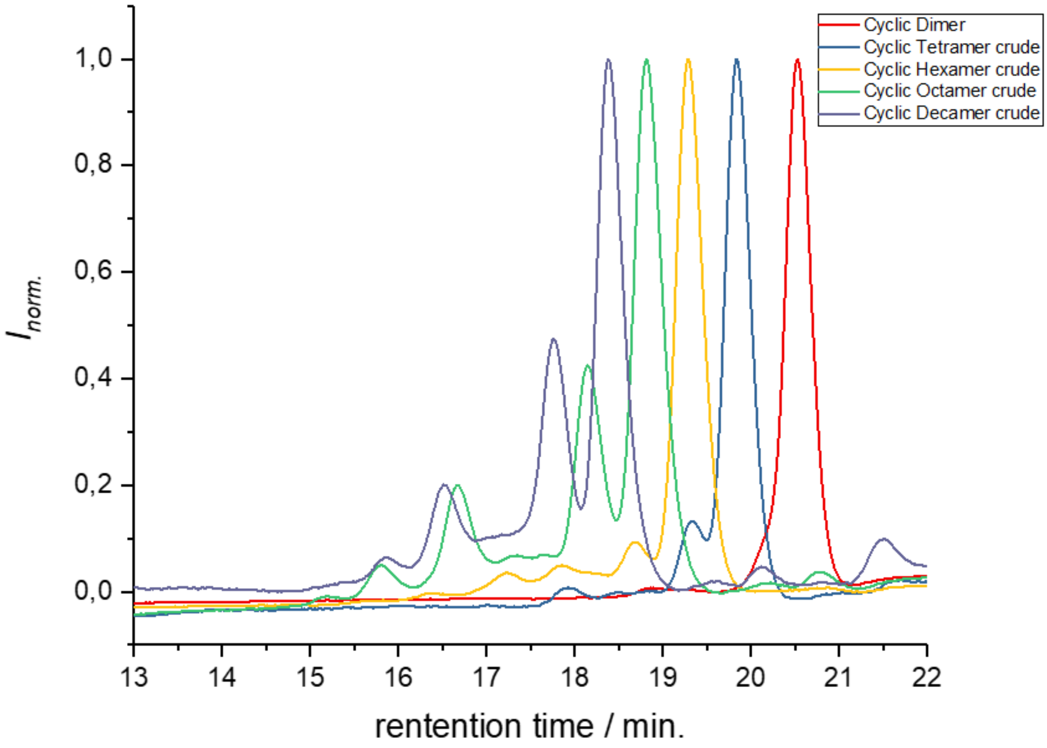

Figure S 32. SEC analysis of crude macrocycles of different size with cyclohexyl side chains.

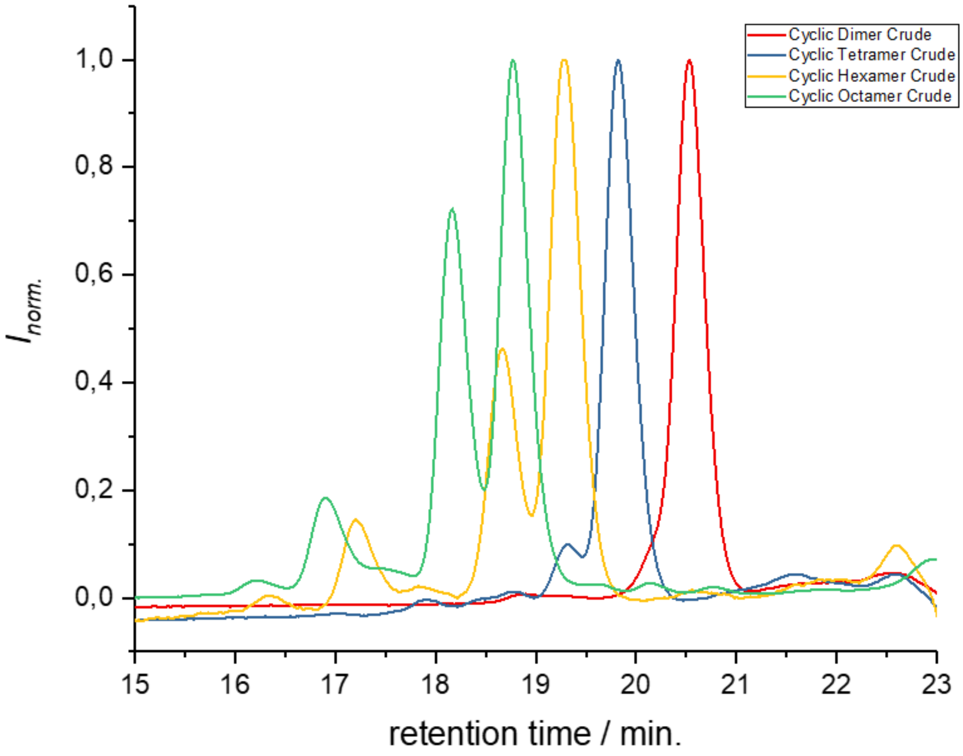

Figure S 33. SEC analysis of crude macrocycles of different size with isopropyl side chains.

6.3.2 Experimental procedures of Chapter 4.1.2

6.3.2.1 Monomer syntheses

Synthesis of monomer M2

Synthesised according to previously reported procedure[400]

Esterification

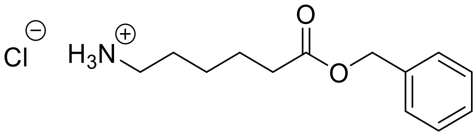

6-Aminohexanoic acid **1b** (1.98 g, 15.0 mmol, 1.00 eq.) was suspended in 10 mL THF and benzyl alcohol **3** (20.3 mL, 20.9 g, 0.19 mol, 12.9 eq.) was added. The suspension was cooled in an ice bath and subsequently thionyl chloride **4** (3.4 mL, 5.53 g, 46.5 mmol, 3.10 eq.) was added dropwise at 0 °C. After addition of the thionyl chloride **4**, the solution was warmed to room temperature and stirred overnight. The yellow solution was then poured into 200 mL diethyl ether and stored in the freezer for one hour. The product was the filtered off and dried under high vacuum. 6-(benzyloxy)-6- oxohexane-1-ammoniumchloride **2b** was obtained as a white solid in a yield of 96% (3.71 g).

^{1}H-NMR (300 MHz, MeOD) δ/ppm: 7.51 – 7.13 (m, 5H, 5 CH aromatic, ^{1}), 5.11 (s, 2H, CH_2, ^{2}), 2.90 (t, J = 7.6 Hz, 2H, CH_2, ^{3}), 2.41 (t, J = 7.3 Hz, 2H, CH_2, ^{4}), 1.84 – 1.54 (m, 4H, CH_2, ^{5}), 1.54 – 1.25 (m, 2H, CH_2, ^{6}).

^{13}C-NMR (75 MHz, MeOD) δ/ppm: 174.8, 137.7, 129.5, 129.2, 67.2, 40.5, 34.6, 28.2, 26.8, 25.4.

HRMS FAB-MS of $[C_{13}H_{20}NO_2]^+$: calculated: 222.1489, found: 222.1489.

IR (ATR platinum diamond): ν /cm^{-1} = 3383.3, 3031.0, 2940.1, 1731.7, 1605.1, 1497.1, 1467.6, 1454.4, 1387.4, 1356.4, 1311.1, 1248.2, 1214.9, 1166.3, 1143.5, 1045.2, 1013.3, 964.0, 937.9, 827.1, 748.1, 695.7, 578.8, 520.4, 474.2.

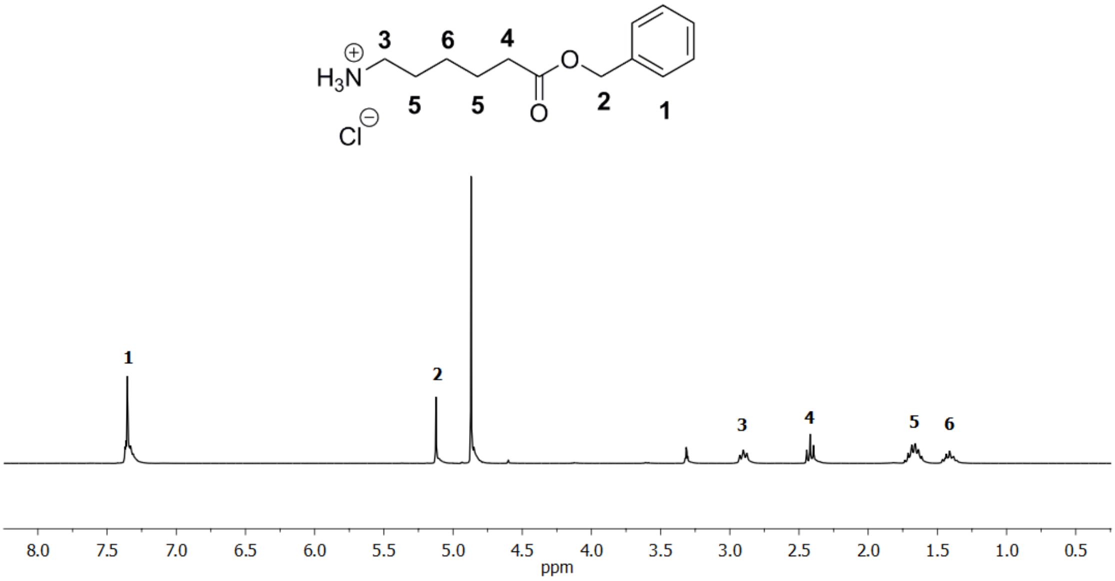
H3N
Cl
O
O
1
2
3
4
5
5
6
8.0
7.5
7.0
6.5
6.0
5.5
5.0
4.5
4.0
3.5
3.0
2.5
2.0
1.5
1.0
0.5
ppm

Synthesised according to previously reported procedure[400]

N-Formylation

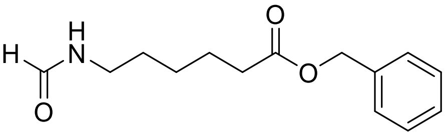

6-(Benzyloxy)-6-oxohexane-1-ammoniumchloride **2b** (3.29 g, 12.7 mmol, 1.00 eq.), was dissolved in trimethyl orthoformate **5** (14.1 mL, 13.6 g, 0.13 mol, 10.1 eq.) and stirred for 24 hours at 100 °C. The excess of trimethyl orthoformate **5** was removed under reduced pressure and the product was purified by column chromatography (hexane/ethyl acetate 3:1 → 0:1), and the yellowish liquid **8b** was obtained in a yield of 73% (2.31 g).

^{1}H-NMR (300 MHz, $CDCl_3$) δ/ppm: 8.13 (s, 1H, formamide, ^{1}), 7.45 – 7.27 (m, 5H, aromatic, ^{2}), 5.59 (s, 1H, NH, ^{3}), 5.11 (s, 2H, CH_2, ^{4}), 3.41 – 3.06 (m, 2H, CH_2, ^{5}), 2.37 (t, *J* = 7.3 Hz, 2H, CH_2, ^{6}), 1.78 – 1.59 (m, 2H, CH_2, ^{7}), 1.59 – 1.44 (m, 2H, CH_2, ^{7}), 1.42 – 1.24 (m, 2H, CH_2, ^{7}).

^{13}C-NMR (75 MHz, $CDCl_3$) δ/ppm: 173.4, 164.7, 161.3, 136.1, 128.6, 128.3, 66.2, 41.5, 37.9, 34.1, 30.9, 29.1, 26.3, 25.9, 24.4, 24.4.

HRMS-FAB-MS of $[C_{14}H_{20}NO_3]^+$: calculated: 250.1438, found: 250.1437.

IR (ATR platinum diamond): ν /cm^{-1} = 3291.8, 3032.8, 2934.5, 2859.8, 1730.0, 1658.2, 1528.3, 1454.5, 1382.6, 1213.2, 1154.0, 1100.2, 1000.9, 736.8, 697.2, 497.6.

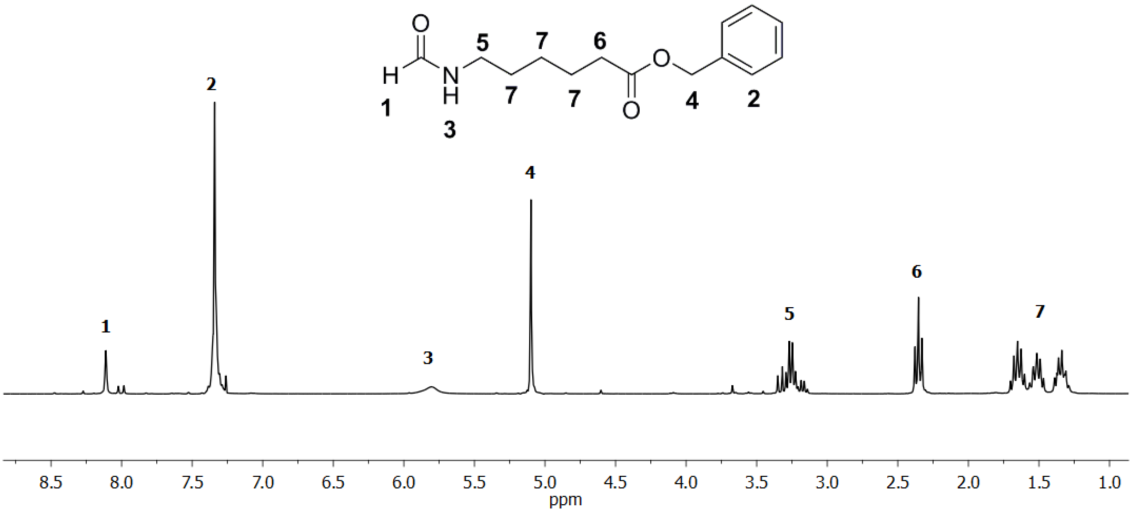

Synthesised according to previously reported procedure[400]

Dehydration

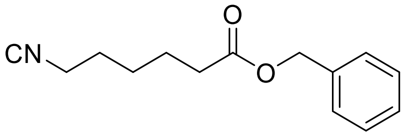

Benzyl-6-formamidohexanoate **8b** (1.70 g, 6.84 mmol, 1.00 eq.) was dissolved in 20 mL DCM (0.34 M), diisopropylamine **7** (2.98 mL, 2.15 g, 21.2 mmol, 3.10 eq.) was added and the reaction mixture was cooled to 0 °C. Subsequently, phosphoryl trichloride **6** (0.83 mL, 1.36 g, 8.89 mmol, 1.30 eq.) was added dropwise and the reaction mixture was then stirred at room temperature for two hours. The reaction was quenched by addition of a 20% solution of sodium carbonate (9.0 mL) at 0 °C. After stirring this mixture for 30 minutes, 20 mL water and 20 mL DCM were added. The aqueous phase was separated and the organic layer was washed with water (3 x 20 mL) and brine (20 mL). The combined organic layers were dried over sodium sulfate and the solvent was evaporated under reduced pressure. The crude product was then purified by column chromatography (hexane/ethyl acetate 9:1 →3:1). The product monomer **M2** was obtained as brown oil in a yield of 74% (1.17 g).

^{1}H-NMR (300 MHz, $CDCl_3$) δ/ppm: 7.50 – 7.29 (m, 5H, 5 CH aromatic, ^{1}), 5.12 (s, 2H, CH_2, ^{2}), 3.47 – 3.27 (m, 2H, CH_2, ^{3}), 2.39 (t, J = 7.4 Hz, 2H, CH_2, ^{4}), 1.80 – 1.58 (m, 4H, CH_2, ^{5}), 1.55 – 1.36 (m, 2H, CH_2, ^{6}).

^{13}C-NMR (75 MHz, $CDCl_3$) δ/ppm: 173.1, 156.1, 136.0, 128.6, 128.3, 66.3, 41.4, 34.0, 28.8, 25.9, 24.1.

HRMS-FAB-MS of $[C_{14}H_{18}NO_2]^+$: calculated: 232.1332, found: 232.1331.

IR (ATR platinum diamond): ν /cm^{-1} = 3023.3, 2943.9, 2863.6, 2146.5, 1730.2, 1496.6, 1454.1, 1382.3, 1351.9, 1257.5, 1152.2, 1093.8, 1001.3, 737.4, 697.6, 578.7, 504.9, 454.9.

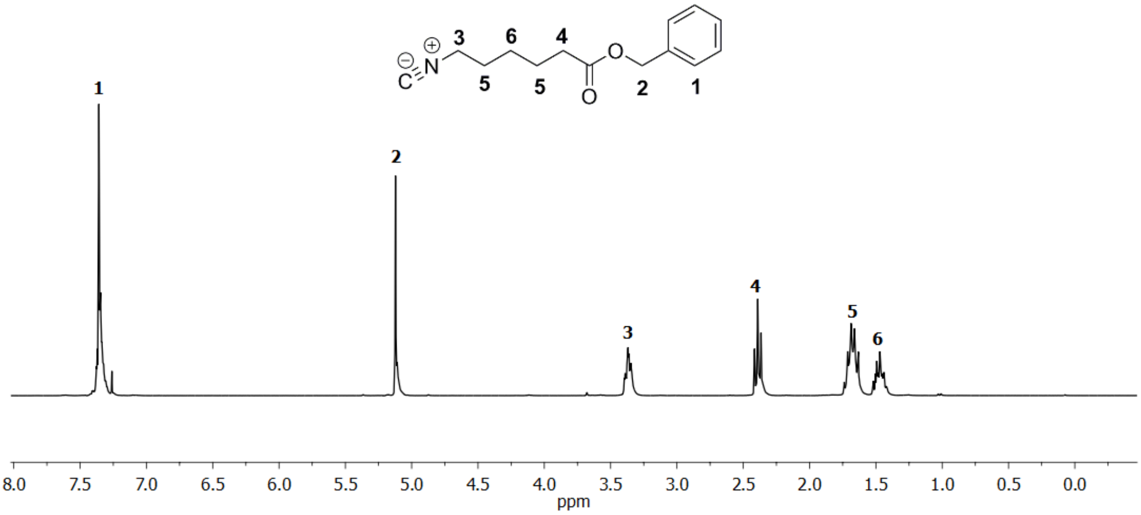

Synthesis of monomer M3*

Esterification

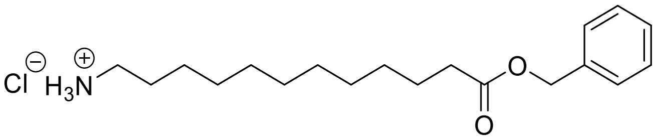

12-aminododecanic acid **1c** (13.2 g, 61.5 mmol, 1.00 eq.) was suspended in THF (16 mL). After the addition of benzyl alcohol **3** (95.4 mL, 99.7 g, 922 mmol, 15.0 eq.), the suspension was cooled with an ice bath to 0 °C and thionyl chloride **4** (17.9 mL, 29.2 g, 246 mmol, 4.00 eq.) was added dropwise. Afterwards, the suspension was stirred at room temperature for 24 hours. Subsequently, 500 mL of diethyl ether were added, and the solution was stored in the freezer for 2 hours. The mixture was filtered and 500 mL of diethyl ether were added to the precipitate. The mixture was stored in the freezer for another 2 hours and the precipitate was filtered off and dried under reduced pressure. A 1:1 mixture of the desired ammonium salt **2c** (14.1 g, 46.1 mmol) and the unreacted starting material was obtained as a white solid in a yield of 75%. The mixture was used without purification.

^{1}H-NMR (300 MHz, CD_3OD) δ/ppm: 7.34 – 7.25 (m, 5H, aromatic, ^{1}), 5.07 (s, 2H, CH_2, ^{2}), 2.87 (t, J = 7.7 Hz, 2H, CH_2, ^{3}), 2.32 (t, J = 7.3 Hz, 2H, CH_2, ^{4}), 1.68 – 1.51 (m, 4H, CH_2, ^{5}), 1.41 – 1.21 (m, 14H, CH_2, ^{6}).

^{13}C-NMR (126 MHz, CD_3OD) δ/ppm: 175.19, 137.71, 129.51, 129.16, 67.07, 40.77, 35.04, 30.49, 30.47, 30.42, 30.29, 30.17, 30.07, 28.54, 27.43, 26.02.

HRMS-FAB-MS of $[C_{19}H_{32}O_2N]^+$ calculated: 306.2433 found: 306.2431.

IR (ATR platinum diamond): ν /cm^{-1} = 3197.3, 3021.6, 2914.0, 2847.6, 1734.6, 1583.4, 1517.9, 1497.2, 1470.5, 1414.7, 1390.8, 1362.3, 1326.9, 1294.8, 1265.3, 1235.9, 1205.0, 1175.5, 1145.4, 1116.4, 1096.6, 1028.3, 1001.7, 960.7, 929.6, 908.7, 858.2, 824.0, 776.1, 726.2, 694.0, 609.2, 575.5, 507.7, 485.3, 460.2, 434.6.

---

[*] Carried out by Philipp Treu in the Vertieferarbeit "Synthesis of a Sequence-Defined Oligomer using AB Monomers" (under the lab-supervision of Katharina Wetzel).

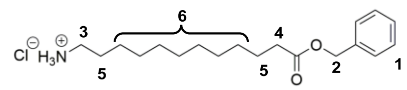
6
3
4
Cl⁻ H₃N⁺
5
5
O
O
2
1

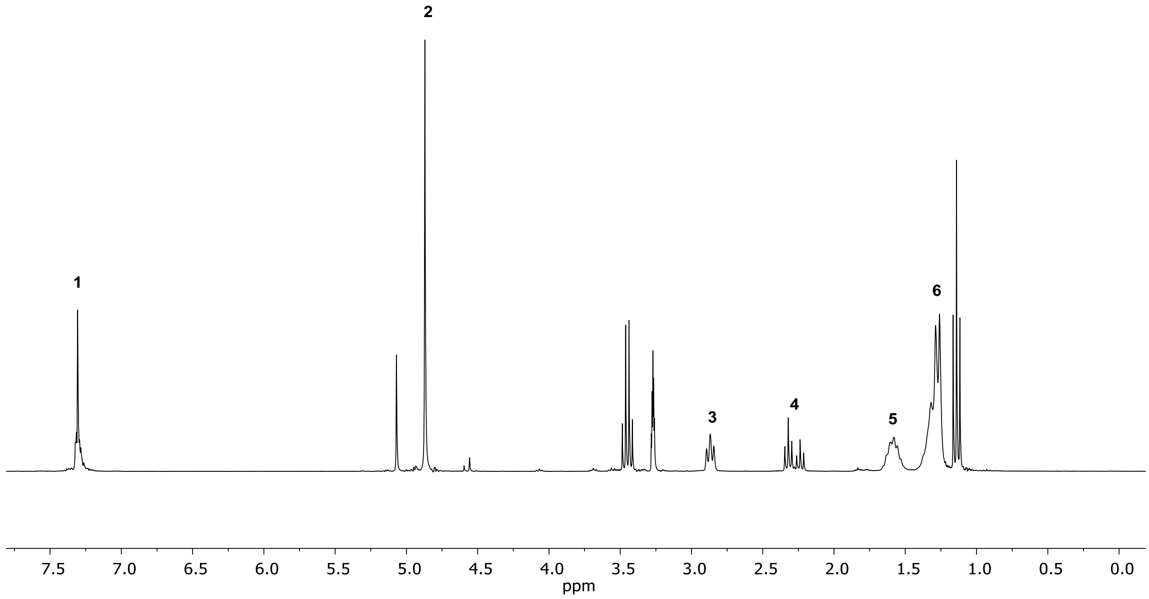
2
1
6
3
4
5
7.5
7.0
6.5
6.0
5.5
5.0
4.5
4.0
3.5
3.0
2.5
2.0
1.5
1.0
0.5
0.0
ppm

N-Formylation

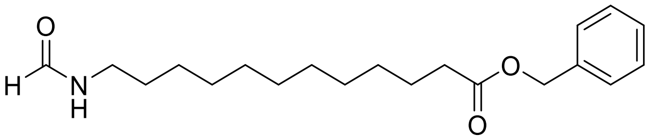

The ammonium salt **2c** (13.5 g, 33.4 mmol, 1.00 eq.) was stirred with trimethyl orthoformate **5** (48.3 mL, 46.8 g, 441 mmol, 11.2 eq.) under reflux at 105 °C overnight. Subsequently, the orthoformate **5** was evaporated under reduced pressure. The crude product **8c** (12.4 g, 37.2 mmol) was obtained as a yellow oil in a quantitative yield and was used without further purification.

^{1}H-NMR (300 MHz, $CDCl_3$) δ/ppm: 8.17 – 7.96 (m, 1H, formamide, ^{1}), 7.41 – 7.21 (m, 5H, aromatic, ^{2}), 5.09 (s, 2H, CH_2, ^{3}), 3.79 – 3.09 (m, 4H,CH_2, ^{4}), 2.38 – 2.30 (m, 2H, CH_2, ^{5}), 1.70 – 1.56 (m, 2H, CH_2, ^{6}), 1.39 – 1.13 (m, 14H, CH_2, ^{7}).

^{13}C-NMR (126 MHz, CD_3OD) δ/ppm: 173.77, 161.34, 136.16, 128.59, 128.21, 128.18, 66.11, 38.24, 34.36, 29.55, 29.50, 29.47, 29.40, 29.25, 29.13, 26.88, 24.98.

HRMS-FAB-MS of $[C_{20}H_{32}O_3N]^+$ calculated: 334.2382 found: 334.2384.

IR (ATR platinum diamond): ν /cm^{-1} = 3284.9, 3198.7, 3033.9, 2914.6, 2848.7, 1734.8, 1654.2, 1548.1, 1518.5, 1497.3, 1470.9, 1416.7, 1381.7, 1326.9, 1289.5, 1262.1, 1233.8, 1202.2, 1158.9, 1097.8, 1073.2, 1027.6, 1001.5, 945.3, 899.3, 869.3, 823.8, 775.7, 749.2, 726.5, 695.6, 608.5, 577.0, 527.3, 488.7, 460.1, 432.7, 407.4.

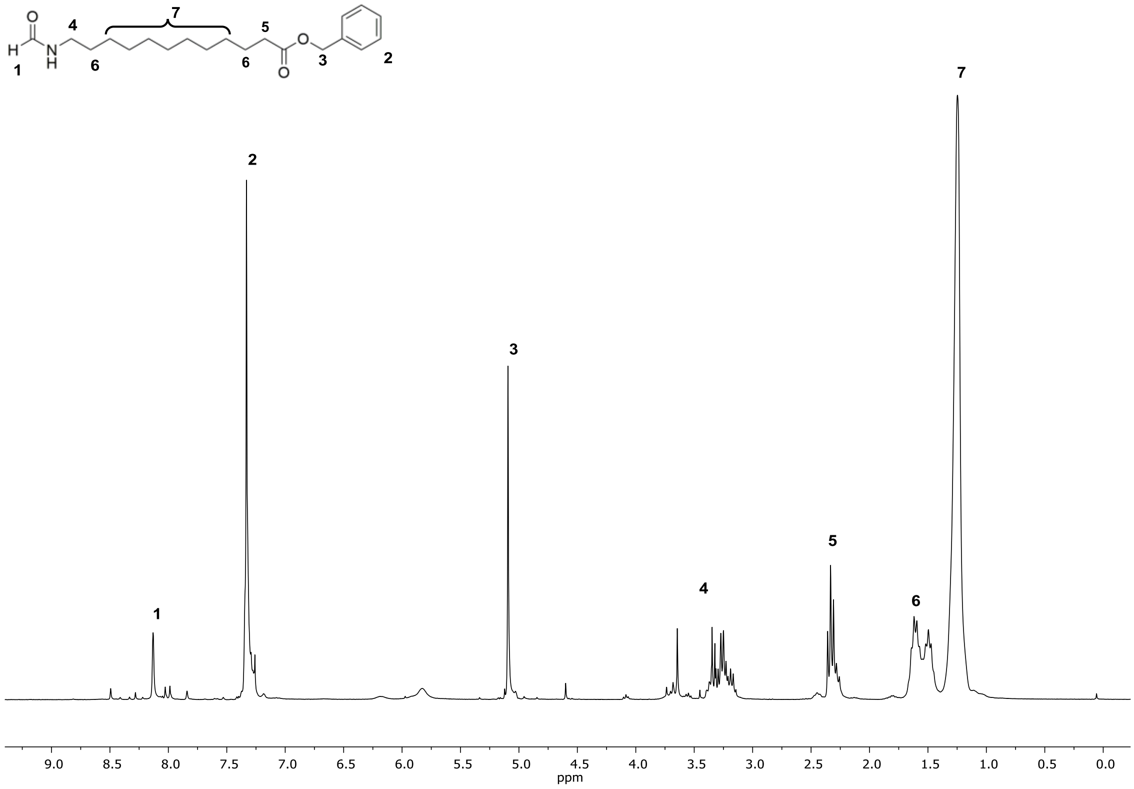

Dehydration

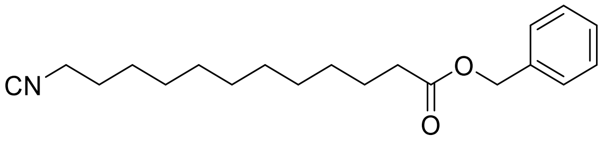

The formamide **8c** (12.4 g, 37.2 mmol, 1.00 eq.) was dissolved in DCM (115 mL) and diisopropylamine **7** (16.2 mL, 11.7 g, 115 mmol, 3.10 eq.) was added. The solution was cooled to 0 °C with an ice bath. Then, phosphoryl trichloride **6** (5.50 mL, 9.30 g, 55.7 mmol, 1.50 eq.) was added dropwise to the reaction mixture. The yellow solution was stirred for two hours at room temperature and was cooled to 0 °C again. The reaction was quenched by the addition of a sodium carbonate solution (20 wt%, 90 mL) and stirred for another 30 minutes at room temperature. DCM (100 mL) and water (100 mL) were added to the mixture and the organic layer was separated. The organic layer was washed with water (2 × 80 mL) and brine (80 mL), dried over sodium sulfate and the solvent was evaporated under reduced pressure. The crude product was purified by column chromatography (cyclohexane/ethyl acetate 12:1 → 4:1). Monomer **M3** (3.73 g, 11.8 mmol) was obtained as a yellow oil in a yield of 32%.

^{1}H-NMR (300 MHz, $CDCl_3$) δ/ppm: 7.41 – 7.30 (m, 5H, aromatic, ^{1}), 5.12 (s, 2H,CH_2 , ^{2}), 3.41 – 3.35 (m, 2H, CH_2, ^{3}), 2.40 – 2.29 (m, 2H, CH_2, ^{4}), 1.70 – 1.60 (m, 4H, CH_2, ^{5}), 1.30 – 1.25 (m, 14H, CH_2, ^{6}).

^{13}C-NMR (101 MHz, $CDCl_3$) δ/ppm: 173.80, 136.23, 128.65, 128.27, 66.17, 41.73, 41.67, 41.61, 34.42, 29.50, 29.45, 29.42, 29.30, 29.20, 28.79, 26.41, 25.03.

HRMS-FAB-MS of $[C_{20}H_{30}O_2N]^+$ calculated: 316.2271 found 316.2272.

IR (ATR platinum diamond): ν /cm^{-1} = 3065.7, 3032.9, 2925.1, 2854.3, 2146.5, 1734.1, 1497.7, 1455.2, 1351.0, 1278.8, 1160.4, 1103.0, 1026.9, 994.8, 735.8, 697.1, 661.7, 554.8, 500.1.

***R*~f~** (cyclohexane / ethyl acetate 5:1) = 0.55.

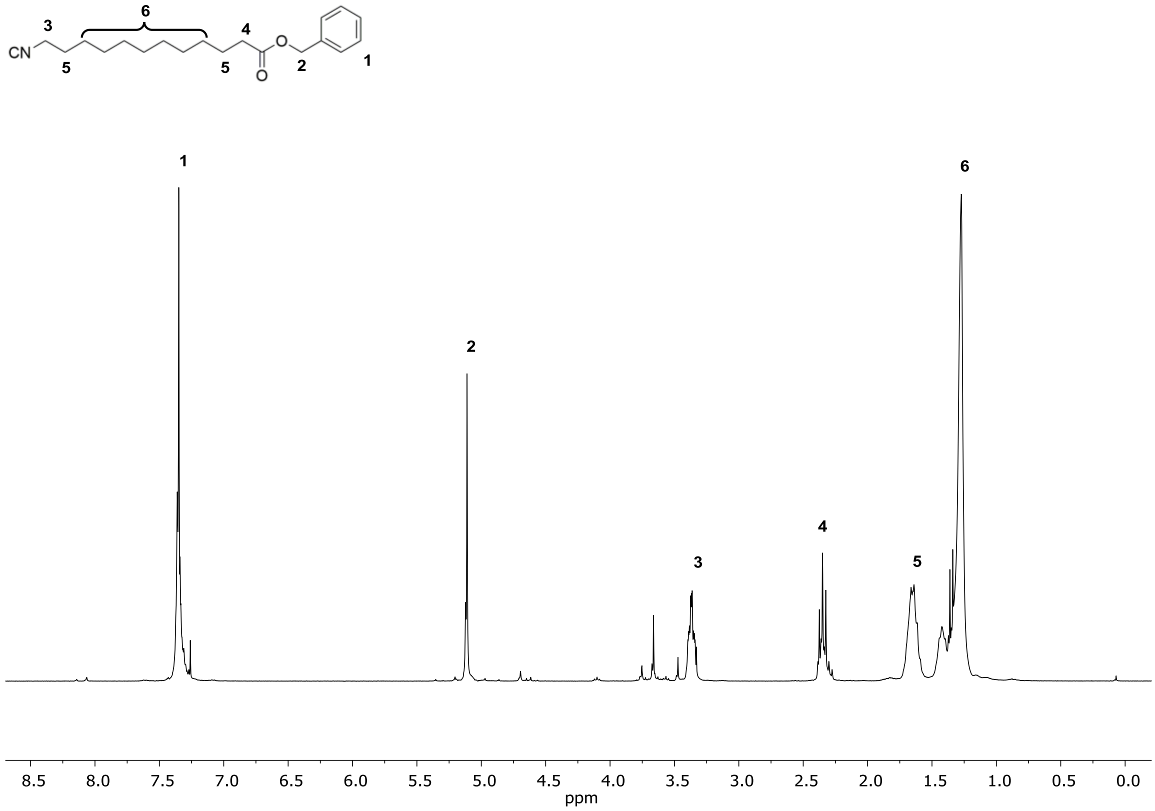

CN
3
5
6
5
4
O
O
2
1
1
2
3
4
5
6
8.5
8.0
7.5
7.0
6.5
6.0
5.5
5.0
4.5
4.0
3.5
3.0
2.5
2.0
1.5
1.0
0.5
0.0
ppm

Evaluation of the reactivity of monomer M3[*]

Passerini reaction

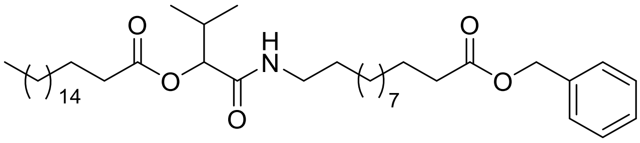

Stearic acid **13** (79.9 mg, 0.28 mmol, 1.00 eq.) were suspended in 0.42 mL DCM. Subsequently, monomer **M3** (132.9 mg, 0.42 mmol, 1.50 eq.) and isobutyraldehyde **11c** (38.0 µL, 30.4 mg, 0.42 mmol, 1.50 eq.) were added. The colourless reaction mixture was stirred at room temperature for 24 hours. Afterwards, the solvent was removed under reduced pressure and the crude product was purified by column chromatography (cyclohexane/ethyl acetate 18:1→10:1) and the pure product **71** was obtained as white solid in a yield of 71% (133.5 mg, 0.20 mmol).

^{1}**H-NMR** (300 MHz, CDCl$_3$) δ/ppm: 7.50 – 7.26 (m, 5H, aromatic, ^{1}), 5.96 – 5.92 (m, 1H, NH, ^{2}), 5.11 (s, 2H, CH$_2$, ^{3}), 5.07 (d, J = 4.2 Hz, 1H, CH, ^{4}), 3.30 – 3.20 (m, 2H, CH$_2$, ^{5}), 2.44 – 2.29 (m, 5H, CH, CH$_2$, ^{6}), 1.69 – 1.61 (m, 4H, CH$_2$, ^{7}), 1.51 – 1.45 (m, 2H, CH$_2$, ^{8}), 1.25 (s, 42H, CH$_2$, ^{9}), 0.96 – 0.85 (m, 9H, CH$_3$, ^{10}).

^{13}**C-NMR** (101 MHz, CDCl$_3$) δ/ppm: 174.6, 173.5, 170.2, 137.0, 129.5, 129.1, 78.8, 67.0, 40.1, 35.3, 32.8, 31.4, 30.6, 30.3, 30.1, 27.8, 26.0, 25.7, 23.6, 19.7.

HRMS-FAB-MS of $[C_{42}H_{74}O_5N]^+$calculated: 672.5567, found: 672.5569.

IR (ATR platinum diamond): ν /cm^{-1} = 3255.6, 3090.6, 2916.6, 2849.6, 1740.8, 1649.7, 1571.8, 1466.6, 1382.6, 1159.7, 994.9, 720.9, 696.7, 416.0.

---

[*] Carried out by Yixuan Jia in the Vertieferarbeit "Synthesis of AB-monomers for sequence-defined macromolecules and evaluation of their reactivity" (under lab-supervision of Katharina Wetzel).

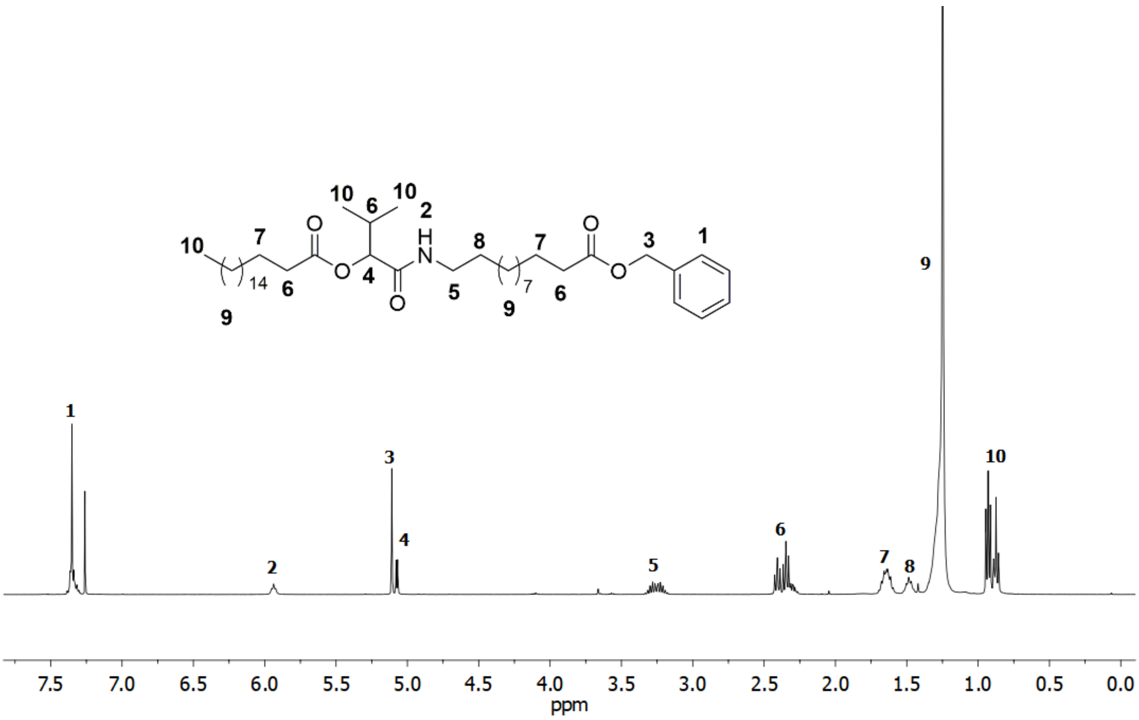
10
6
10
2
7
O
H
N
8
7
O
3
1
10
14
6
O
4
5
9
7
6
O
9
O
9
1
2
3
4
5
6
7
8
10
7.5
7.0
6.5
6.0
5.5
5.0
4.5
4.0
3.5
3.0
2.5
2.0
1.5
1.0
0.5
0.0
ppm

Deprotection

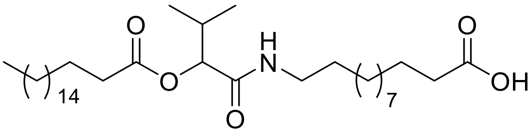

The Passerini product **71** (121 mg, 0.18 mmol, 1.00 eq.) were dissolved in ethyl acetate (0.36 ml) and palladium on activated charcoal **19** (12.1 mg, 10 wt%) was added. The reaction mixture was purged with hydrogen by using a balloon and stirred under hydrogen atmosphere overnight at room temperature. Afterwards the heterogeneous catalyst was filtered off and the solvent was evaporated under reduced pressure. The desired deprotected product **72** (101.50 mg, 0.17 mmol) was obtained as white solid in a yield of 97%.

^{1}**H-NMR** (300 MHz, $CDCl_3$) δ/ppm: 5.99 (t, J = 5.9 Hz, 1H, NH, ^{1}), 5.07 (d, J = 4.4 Hz, 1H, CH, ^{2}), 3.39 – 3.15 (m, 2H, CH_2, ^{3}), 2.43 – 2.31 (m, 5H, CH, CH_2, ^{4}), 1.67 – 1.59 (m, 4H, CH_2, ^{5}), 1.51 – 1.46 (m, 2H, CH_2, ^{6}), 1.26 (s, 42H, CH_2, ^{7}), 0.94 – 0.85 (m, 9H, CH_3, ^{8}).

^{13}**C-NMR** (101 MHz, $CDCl_3$) δ/ppm: 178.0, 171.6, 168.4, 38.2, 33.3, 32.9, 30.9, 29.5, 28.6, 28.4, 28.3, 28.1, 28.0, 25.8, 24.0, 23.7.

HRMS-FAB-MS of $[C_{35}H_{68}O_5N]^+$ calculated: 582.5097, found: 582.5099.

IR (ATR platinum diamond): ν /cm^{-1} = 3299.9, 2915.7, 2848.8, 1737.0, 1698.9, 1654.6, 1562.3, 1467.3, 1168.4, 1107.5, 1010.1, 927.8, 720.7, 682.8, 418.3.

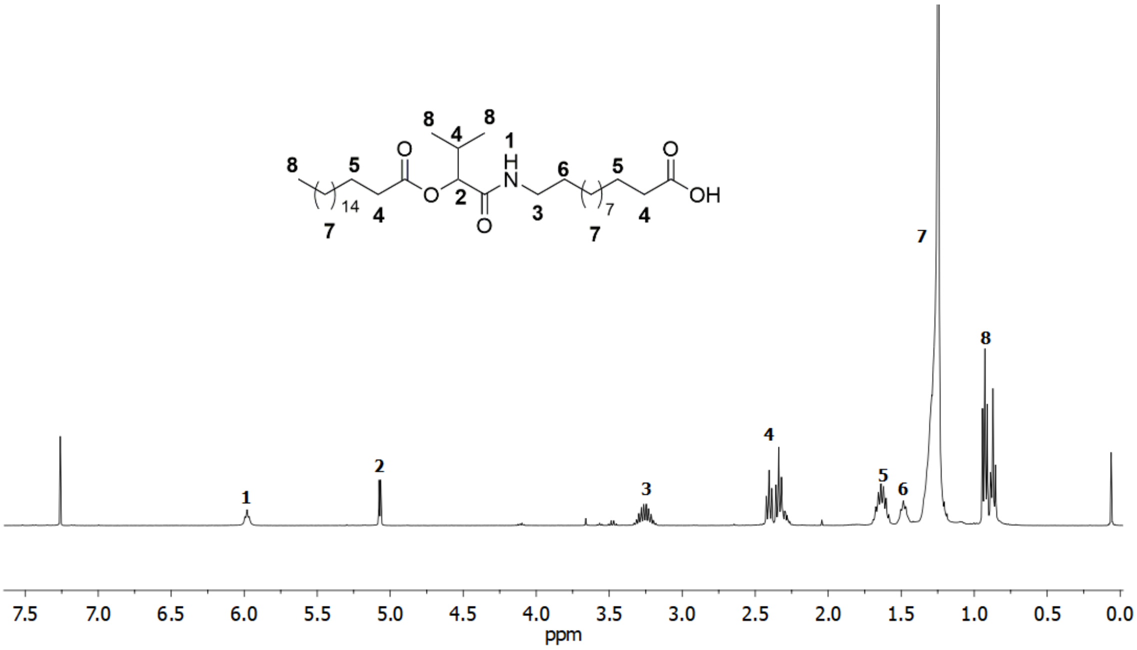

Synthesis of monomer M4

Synthesised according to previously reported procedure[400]

Esterification

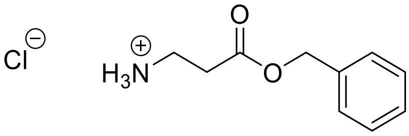

ß-Alanine **1d** (2.06 g, 23.1 mmol, 1.00 eq.) were suspended in 25 mL THF and benzyl alcohol **3** (27.8 mL, 28.9 g, 0.27 mol, 11.50 eq.) were added. The suspension was cooled in an ice bath and subsequently thionyl chloride **4** (5.00 mL, 8.16 g, 68.6 mmol, 2.96 eq.) were added dropwise at 0 °C. After addition of the thionyl chloride **4**, the solution was warmed to room temperature and stirred overnight. The yellow solution was then poured into 230 mL diethyl ether and stored in the freezer for one hour. The product was then filtered off and dried under high vacuum. The pure product **2d** was obtained as a white solid in a yield of 81% (4.05 g).

^{1}H-NMR (300 MHz, MeOD) δ/ppm: 7.55 – 7.14 (m, 5H, 5 CH aromatic, ^{1}), 5.19 (s, 2H, CH_2, ^{2}), 3.22 (t, J = 5.9 Hz, 2H, CH_2, ^{3}), 2.76 (m, 2H, CH_2, ^{4}).

^{13}C-NMR (75 MHz, MeOD) δ/ppm: 171.9, 137.1, 129.6, 129.4, 67.9, 36.4, 32.3.

FAB-MS of $[C_{10}H_{14}NO_2]^+$: calculated: 180.1103, found: 180.1104.

IR (ATR platinum diamond): ν /cm^{-1} = 3243.9, 2795.8, 2038.6, 1709.8, 1597.0, 1494.9, 1452.4, 1404.8, 1362.8, 1324.6, 1222.6, 1135.4, 1103.6, 1056.5, 981.9, 857.8, 801.7, 748.1, 698.8, 585.4, 569.0, 458.1, 409.1.

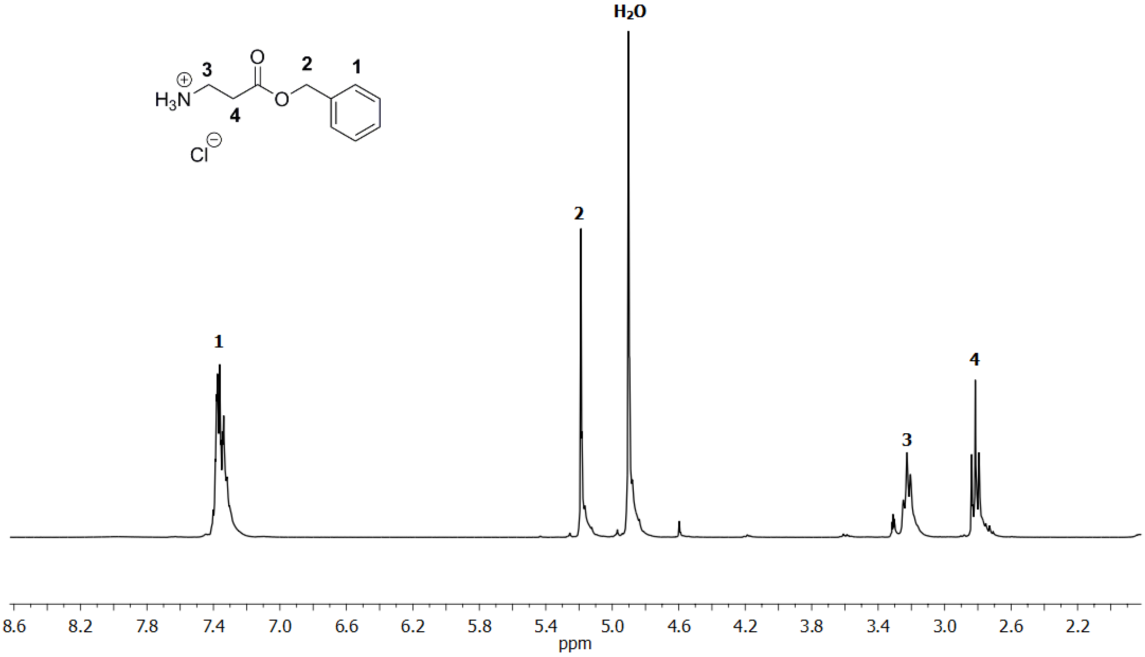

Synthesised according to previously reported procedure[400]

N-Formylation

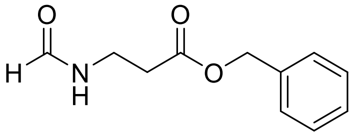

Substance **2d** (4.05 g, 18.7 mmol, 1.00 eq.), was dissolved in 20.4 mL trimethyl orthoformate **5** (19.8 g, 1.87 mol, 10.00 eq.) and stirred for twelve hours at 100 °C. Trimethyl orthoformate **5** was removed under reduced pressure and the product was purified by column chromatography (hexane/ethyl acetate 2:1 → 0:1), and the yellowish liquid **8d** was obtained in a yield of 52% (2.00 g).

^{1}H-NMR (300 MHz, $CDCl_3$) δ/ppm: 8.01 (s, 1H, formamide, ^{1}), 7.46 – 7.16 (m, 5H, aromatic, ^{2}), 6.63 (s, 1H, NH, ^{3}), 5.12 (s, 2H, CH_2, ^{4}), 3.55 - 3.38 (m, 2H, CH_2, ^{5}), 2.69 - 2.46 (m, 2H, CH_2, ^{6}).

^{13}C-NMR (75 MHz, $CDCl_3$) δ/ppm: 173.0, 163.8, 137.5, 129.5, 129.2, 67.4, 34.8.

HRMS-FAB-MS of $[C_{11}H_{14}NO_3]^+$: calculated: 208.0968, found: 208.0967.

IR (ATR platinum diamond): ν /cm^{-1} = 3291.1, 3033.7, 2947.3, 2869.9, 1729.1, 1658.6, 1521.0, 1454.2, 1383.4, 1315.1, 1213.8, 1166.6, 1066.5, 1002.3, 821.1, 738.0, 696.8, 467.5.

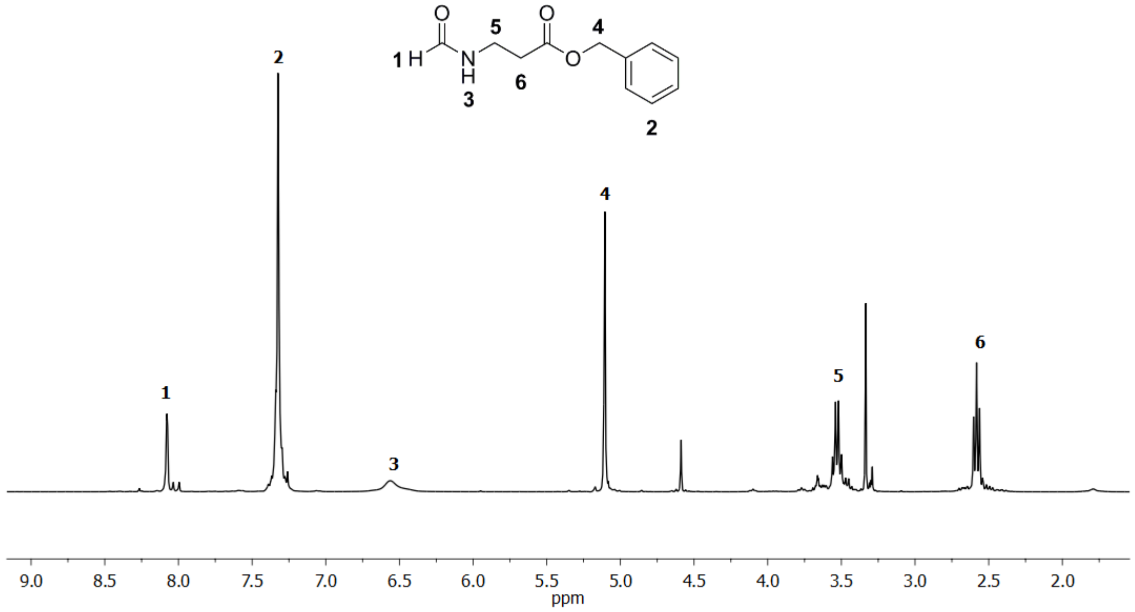

Synthesised according to previously reported procedure[400]

Dehydration

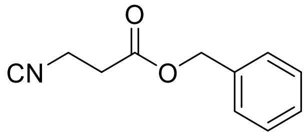

Benzyl 3-formamidopropanoate **8d** (1.06 g, 5.12 mmol, 1.00 eq.) was dissolved in DCM (25 mL, 0.20 M), diisopropylamine **7** (2.33 mL, 1.68 g, 16.6 mmol, 3.24 eq.) was added and the reaction mixture was cooled to 0 °C. Subsequently, phosphoryl trichloride **6** (0.60 mL, 0.98 g, 6.39 mmol, 1.25 eq.) was added dropwise and the reaction mixture was then stirred at room temperature for two hours. The reaction was quenched by addition of a 20% sodium carbonate solution (9.0 mL) at 0 °C. After stirring this mixture for 30 minutes, 20 mL water and 20 mL DCM were added. The aqueous phase was separated and the organic layer was washed with water (3 x 20 mL) and brine (20 mL). The combined organic layers were dried over sodium sulfate and the solvent was evaporated under reduced pressure. The crude product was then purified by column chromatography (hexane/ethyl acetate 5:1 → 2:1). The product monomer **M4** was obtained as brown oil in a yield of 74% (0.72 g).

^{1}H-NMR (300 MHz, $CDCl_3$) δ/ppm: 7.39 (s, 5H, aromatic, ^{1}), 5.18 (s, 2H, CH_2, ^{2}), 3.71 (t, J = 6.8 Hz, 2H, CH_2, ^{3}), 2.78 (t, J = 6.8 Hz, 2H, CH_2, ^{4}).

^{13}C-NMR (126 MHz, $CDCl_3$) δ/ppm: 169.33, 157.59, 135.25, 128.74, 128.64, 128.49, 67.19, 37.17, 34.21.

HRMS-FAB-MS of $[C_{11}H_{10}NO_2]^+$: calculated: 188.0712, found: 188.0710.

IR (ATR platinum diamond): ν /cm^{-1} = 3034.3, 2150.2, 1733.7, 1497.9, 1454.6, 1389.5, 1355.3, 1313.0, 1263.0, 1215.2, 1171.1, 1052.7, 986.8, 956.4, 916.1, 832.3, 738.2, 696.8, 577.6, 482.4.

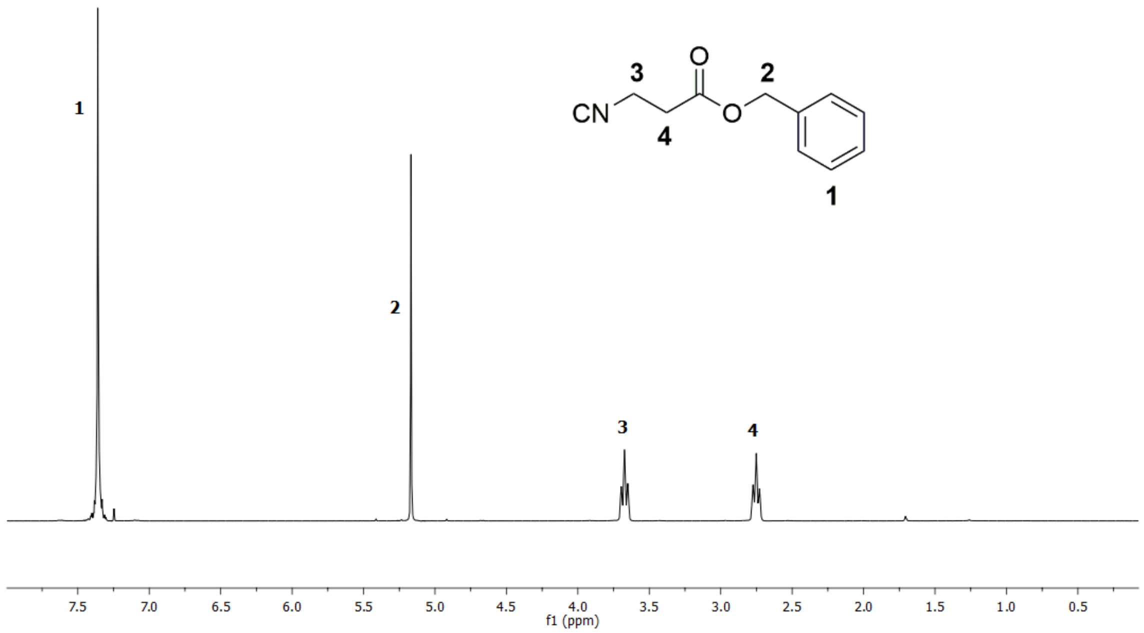
1
2
3
4
CN
O
O
3
4
2
1
7.5
7.0
6.5
6.0
5.5
5.0
4.5
4.0
3.5
3.0
2.5
2.0
1.5
1.0
0.5
f1 (ppm)

Synthesis of monomer M5[*]

Esterification

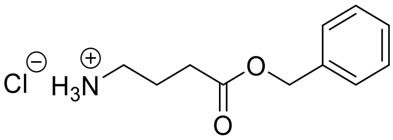

4-aminobutyric acid **1e** (15.0 g, 146 mmol, 1.00 eq.) was suspended in THF (145 mL). After the addition of benzyl alcohol **3** (180 mL, 189 g, 1.75 mol, 12.0 eq.), the suspension was cooled in an ice bath to 0 °C and thionyl chloride **4** (32.0 mL, 52.0 g, 437 mmol, 3.00 eq.) was added dropwise. Afterwards, the suspension was stirred at room temperature for 19 hours. Subsequently, 500 mL diethyl ether were added, and the solution was stored in the freezer for 2 hours. The mixture was filtered, and 500 mL diethyl ether were added to the precipitate and stored in the freezer for another two hours. The precipitate was filtered off and the crude product **2e** (29.8 g, 130 mmol) was obtained as a white solid in a yield of 89%.

^{1}H-NMR (300 MHz, CD_3OD) *δ*/ppm: 7.41 – 7.19 (m, 5H, aromatic, ^{1}), 5.14 (s, 2H, CH_2, ^{2}), 2.99 (t, *J* = 7.7 Hz, 2H, CH_2, ^{3}), 2.59 – 2.44 (m, 2H, CH_2, ^{4}), 2.04 – 1.88 (m, 2H, CH_2, ^{5}).

^{13}C-NMR (101 MHz, CD_3OD) *δ*/ppm: 173.77, 137.44, 129.55, 129.29, 127.98, 67.48, 40.03, 31.68, 23.74.

HRMS-FAB-MS of $[C_{11}H_{15}O_2N]^+$ calculated: 194.1181 found 194.1181.

IR (ATR platinum diamond): ν /cm^{-1} = 3208.2, 2979.1, 2916.7, 2878.8, 2749.1, 2624.9, 2471.5, 2055.6, 1732.0, 1605.7, 1489.9, 1467.1, 1454.7, 1415.8, 1391.6, 1356.2, 1328.6, 1281.4, 1230.7, 1191.1, 1141.4, 1117.7, 1053.9, 1029.2, 987.7, 949.0, 921.8, 857.6, 771.2, 746.6, 696.8, 579.5, 545.5, 480.1.

---

[*] Carried out by Philipp Treu in the Vertieferarbeit "Synthesis of a Sequence-Defined Oligomer using AB Monomers" (under the lab-supervision of Katharina Wetzel).

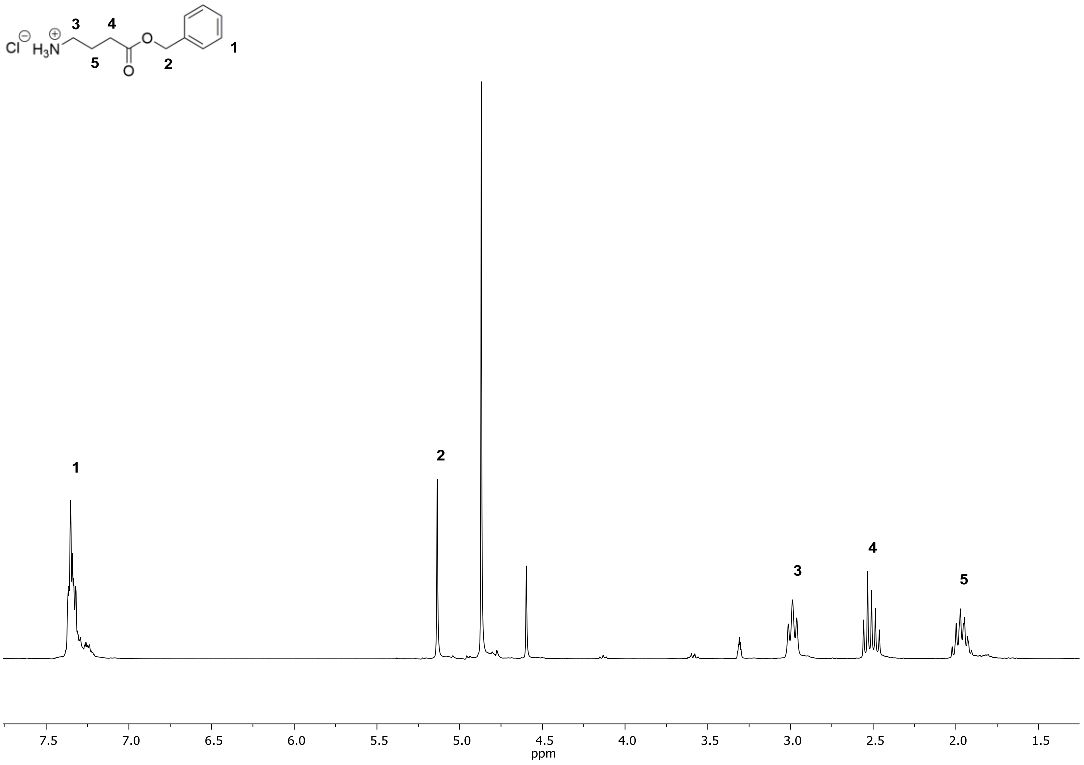
Cl H3N
3
4
5
2
1
1
2
3
4
5
7.5
7.0
6.5
6.0
5.5
5.0
4.5
4.0
3.5
3.0
2.5
2.0
1.5
ppm

N-Formylation

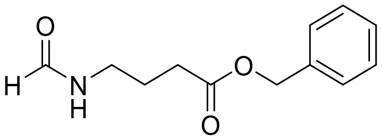

The ammonium salt **2e** (29.75 g, 130 mmol, 1.00 eq.) was stirred with trimethyl orthoformate **5** (168.4 mL, 163.4 g, 1,54 mol, 12.0 eq.) under reflux at 105 °C overnight. Subsequently, the orthoformate **5** was evaporated under reduced pressure. The crude product **8e** (26.01 g, 117.6 mmol) was obtained as a yellow oil in a yield of 91% and was used without further purification.

^{1}H-NMR (300 MHz, $CDCl_3$) δ/ppm: 8.16 – 7.87 (m, 1H, formamide, ^{1}), 7.38 – 7.24 (m, 5H, aromatic, ^{2}), 6.53 (broad s, 1H, NH, ^{3}), 5.09 (s, 2H, CH_2, ^{4}), 3.32 – 3.20 (m, 2H, CH_2, ^{5}), 2.47 – 2.30 (m, 2H, CH_2, ^{6}), 1.91 – 1.74 (m, 2H, CH_2, ^{7}).

^{13}C-NMR (101 MHz, $CDCl_3$) δ/ppm: 172.55, 161.51, 135.48, 128.17, 128.15, 127.82, 65.82, 36.89, 31.06, 24.18.

HRMS-FAB-MS of $[C_{12}H_{16}O_3N]^+$ calculated: 221.1052 found 221.1050.

IR (ATR platinum diamond): ν /cm^{-1} = 3283.1, 3062.2, 3034.5, 2941.6, 2874.6, 2753.5, 1730.2, 1659.4, 1531.2, 1497.9, 1454.0, 1384.5, 1352.7, 1320.7, 1235.3, 1161.4, 1082.5, 1028.1, 972.6, 737.5, 696.7, 578.7, 500.1.

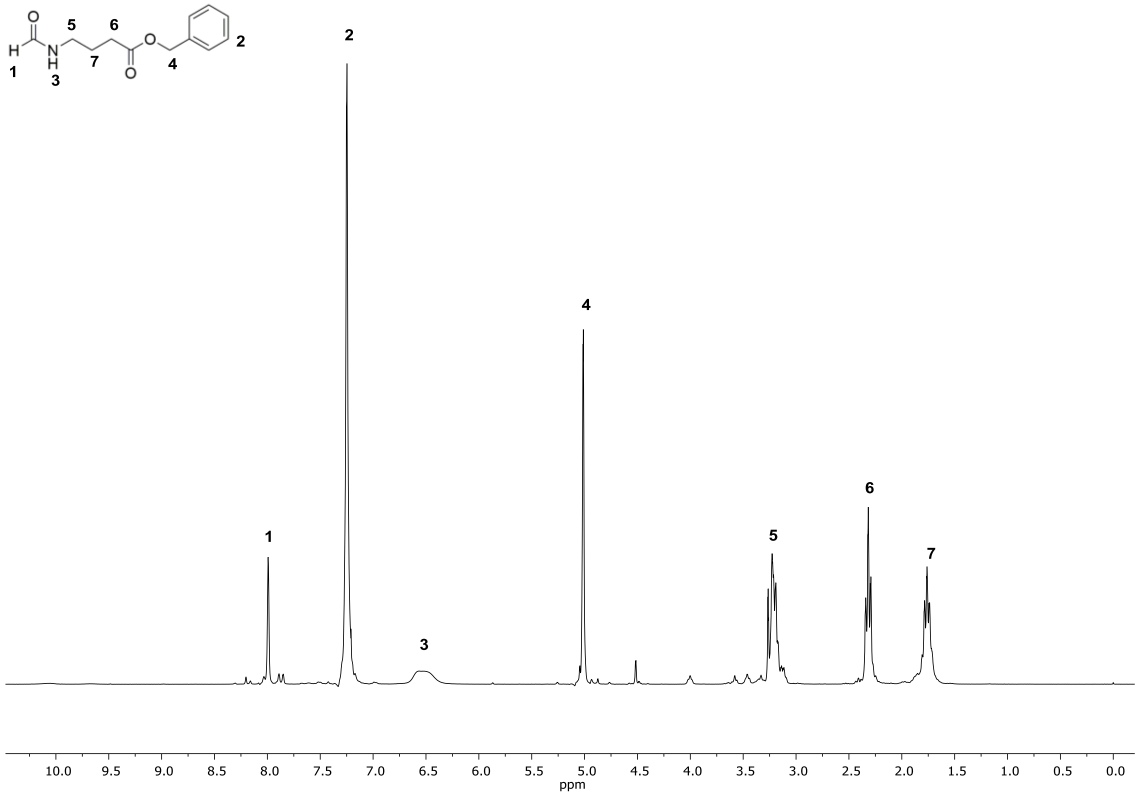

Dehydration

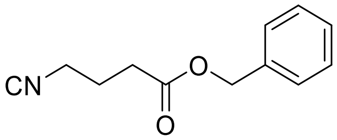

The formamide **8e** (26.0 g, 118 mmol, 1.00 eq.) was dissolved in DCM (400 mL) and diisopropylamine **7** (70.2 mL, 50.5 g, 500 mmol, 4.20 eq.) was added. The solution was cooled to 0 °C with an ice bath. Then, phosphoryl trichloride **6** (15.2 mL, 25.5 g, 166.5 mmol, 1.4 eq.) was added dropwise to the reaction mixture. The yellow solution was stirred for two hours at room temperature and was cooled to 0 °C again. The reaction was quenched by the addition of a 20 wt% sodium carbonate solution (150 mL) and stirred for another 45 minutes at room temperature. 80 mL DCM and 80 mL water were added to the mixture and the organic layer was separated. The organic layer was washed with water (3 × 80 mL) and brine (80 mL), dried over sodium sulfate and the solvent was evaporated under reduced pressure. The crude product was purified by column chromatography (cyclohexane/ethyl acetate 10:1 → 3:1). Monomer **M5** (16.51 g, 81.3 mmol) was obtained as a yellow oil in a yield of 69%.

^{1}H-NMR (300 MHz, $CDCl_3$) δ/ppm: 7.37 – 7.19 (m, 5H, aromatic, ^{1}), 5.07 (s, 2H, CH_2, ^{2}), 3.45 – 3.36 (m, 2H, CH_2, ^{3}), 2.53 – 2.42 (m, 2H, CH_2, ^{4}), 1.99 – 1.89 (m, 2H, CH_2, ^{5}).

^{13}C-NMR (101 MHz, $CDCl_3$) δ/ppm: 171.94, 135.64, 128.63, 128.39, 128.26, 66.57, 40.81, 30.46, 24.29.

HRMS-FAB-MS of $[C_{12}H_{14}O_2N]^+$ calculated: 204.1025 found 204.1024.

IR (ATR platinum diamond): ν /cm^{-1} = 3089.3, 3066.3, 3034.0, 2951.2, 2893.3, 2148.1, 1730.5, 1607.3, 1586.4, 1497.7, 1454.4, 1418.8, 1387.8, 1354.8, 1320.7, 1254.5, 1163.3, 1081.2, 1017.4, 969.7, 901.3, 860.5, 737.9, 697.0, 578.5, 499.9.

***R*$_f$** (cyclohexane / ethyl acetate 3:1) = 0.43.

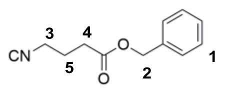
CN
3
4
5
O
O
2
1

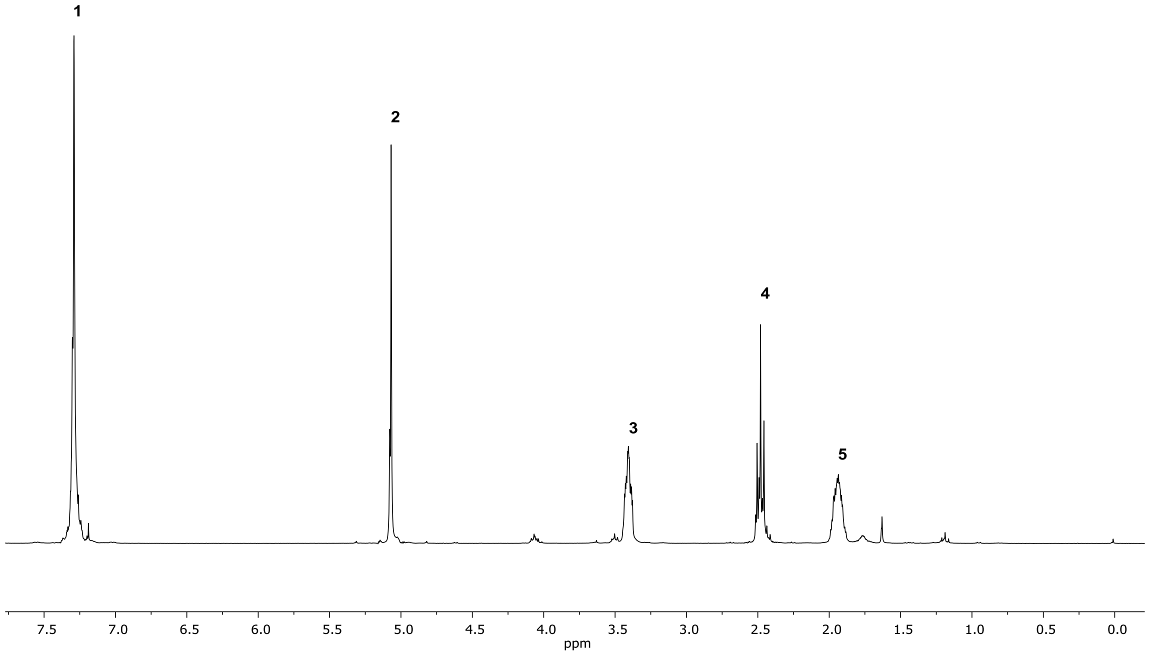
1
2
3
4
5
7.5
7.0
6.5
6.0
5.5
5.0
4.5
4.0
3.5
3.0
2.5
2.0
1.5
1.0
0.5
0.0
ppm

Evaluation of the reactivity of monomer M5*

Passerini reaction

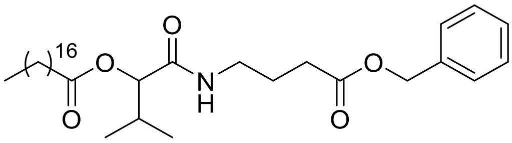

Stearic acid **13** (700 mg, 2.46 mmol, 1.00 eq.) was suspended in DCM (5.0 mL). Subsequently, **monomer M5** (750 mg, 3.69 mmol, 1.50 eq.) and isobutyraldehyde **11c** (0.34 mL, 266 mg, 3.69 mmol, 1.50 eq.) were added. The reaction mixture was stirred for 48 hours at room temperature and the crude product was purified by column chromatography (cyclohexane/ethyl acetate 10:1 → 4:1), resulting in a yield of 94% of the desired Passerini product **73** (1.30 g, 2.32 mmol), which was obtained as a white solid.

^{1}H-NMR (400 MHz, $CDCl_3$) δ/ppm: 7.40 – 7.30 (m, 5H, aromatic, ^{1}), 6.30 (s, 1H, NH, ^{2}), 5.11 (s, 2H, CH_2, ^{3}), 5.07 (d, *J* = 4.2 Hz, 1H, CH, ^{4}), 3.39 – 3.25 (m, 2H, CH_2, ^{5}), 2.48 – 2.37 (m, 2H, CH_2, ^{6}), 2.35 – 2.22 (m, 1H, CH, ^{7}), 1.86 (quint, *J* = 6.9 Hz, 2H, CH_2, ^{8}), 1.73 – 1.58 (m, 2H, CH_2, ^{9}), 1.42 – 1.19 (m, 30H, CH_2, ^{10}), 0.96 – 0.84 (m, 9H, CH_3, ^{11}).

^{13}C-NMR (101 MHz, $CDCl_3$) δ/ppm: 173.45, 172.81, 169.74, 128.74, 128.48, 128.36, 77.83, 66.63, 38.82, 34.41, 32.06, 31.86, 30.66, 29.84, 29.79, 29.74, 29.61, 29.50, 29.41, 29.31, 25.12, 24.45, 22.83, 18.94, 16.99, 14.27.

HRMS-FAB-MS of $[C_{34}H_{58}O_5N]^+$ calculated: 560.4315 found: 560.4314.

IR (ATR platinum diamond): ν /cm^{-1} = 3325.5, 3288.6, 3071.3, 2916.3, 2849.6, 1728.9, 1650.6, 1537.7, 1466.8, 1438.9, 1416.3, 1383.5, 1366.0, 1288.3, 1223.2, 1201.2, 1161.7, 1030.7, 1014.4, 980.8, 930.6, 869.5, 798.1, 744.0, 722.4, 696.5, 575.1, 519.7, 474.6, 443.8.

***R*$_f$** (cyclohexane / ethyl acetate (2:1)) = 0.54.

---

[*] Carried out by Philipp Treu in the Vertieferarbeit “Synthesis of a Sequence-Defined Oligomer using AB Monomers” (under the lab-supervision of Katharina Wetzel).

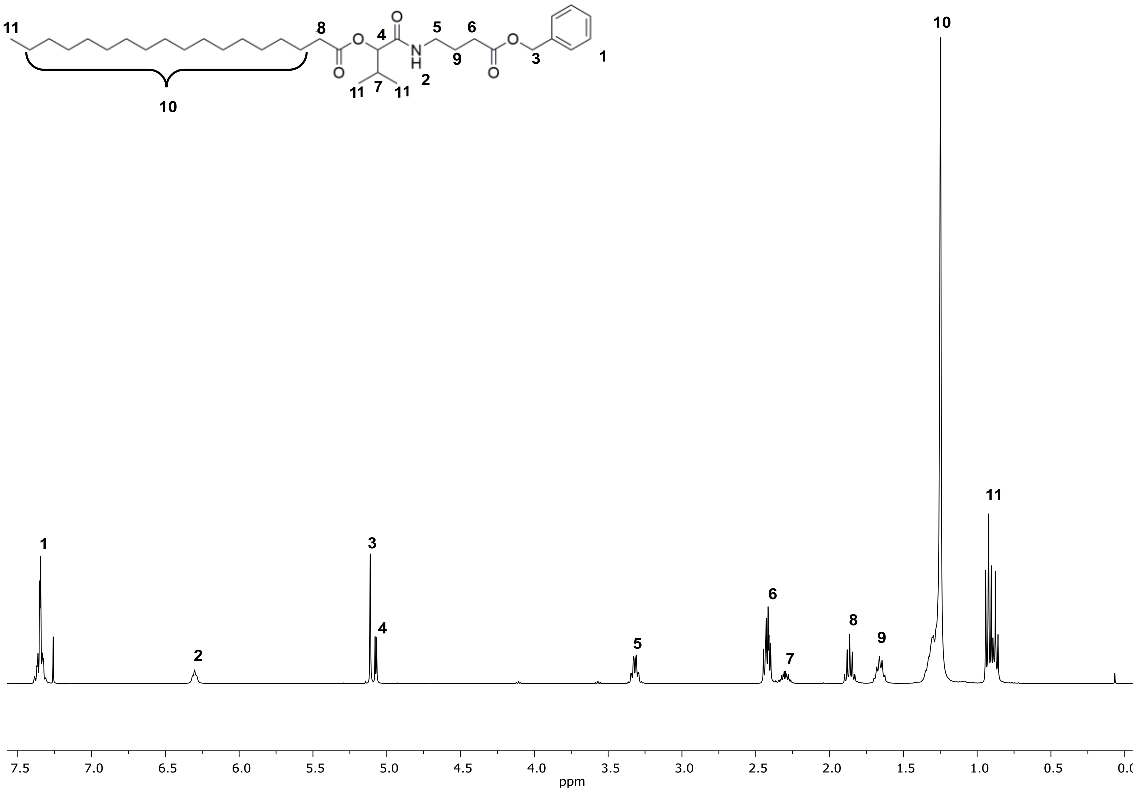
11
8
4
5
6
O
N
H
9
3
1
10
11
7
11
2
10
11
1
3
4
2
5
6
7
8
9
7.5
7.0
6.5
6.0
5.5
5.0
4.5
4.0
3.5
3.0
2.5
2.0
1.5
1.0
0.5
0.0
ppm

Deprotection

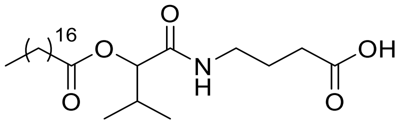

The Passerini product **73** (1.30 g, 2.32 mmol, 1.00 eq.) was dissolved in ethyl acetate (4.70 mL) and palladium on activated charcoal **19** (130 mg, 10 wt%) was added. Subsequently, the reaction mixture was purged with hydrogen using a balloon and stirred under hydrogen atmosphere for 24 hours. Afterwards, the heterogeneous catalyst was filtered off and the solvent was evaporated under reduced pressure. The desired deprotected carboxylic acid **74** (1.03 g, 2.32 mmol) was obtained as a white solid in a yield of 100%.

^{1}H-NMR (300 MHz, CDCl$_3$) δ/ppm: 6.34 (m, 1H, NH, ^{1}), 5.04 (d, *J* = 4.4 Hz, 1H, CH, ^{2}), 3.40 – 3.26 (m, 2H, CH$_2$, ^{3}), 2.49 – 2.33 (m, 2H, CH$_2$, ^{4}), 2.32 – 2.20 (m, 1H, CH, ^{5}), 1.92 – 1.76 (m, 2H, CH$_2$, ^{6}), 1.73 – 1.52 (m, 2H, CH$_2$, ^{7}), 1.49 – 1.05 (m, 30H, CH$_2$, ^{8}), 0.96 – 0.81 (m, 9H, CH$_3$, ^{9}).

^{13}C-NMR (101 MHz, CDCl$_3$) δ/ppm: 177.76, 170.18, 77.91, 38.67, 34.37, 32.03, 31.43, 30.62, 29.81, 29.76, 29.72, 29.58, 29.47, 29.38, 29.27, 25.09, 24.54, 22.80, 18.87, 17.04, 14.22.

HRMS-FAB-MS of $[C_{27}H_{52}O_5N]^+$ calculated: 470.3840 found: 470.3841.

IR (ATR platinum diamond): ν /cm^{-1} = 3284.1, 3100.4, 2916.1, 2849.2, 2233.5, 2161.3, 2076.2, 2030.7, 2019.5, 1988.0, 1967.5, 1742.0, 1698.7, 1652.1, 1569.4, 1466.8, 1439.5, 1406.2, 1380.5, 1345.7, 1287.6, 1253.8, 1219.1, 1160.8, 1137.0, 1094.4, 1066.7, 1012.5, 937.5, 862.7, 811.6, 722.1, 676.7, 491.9, 467.2, 410.7.

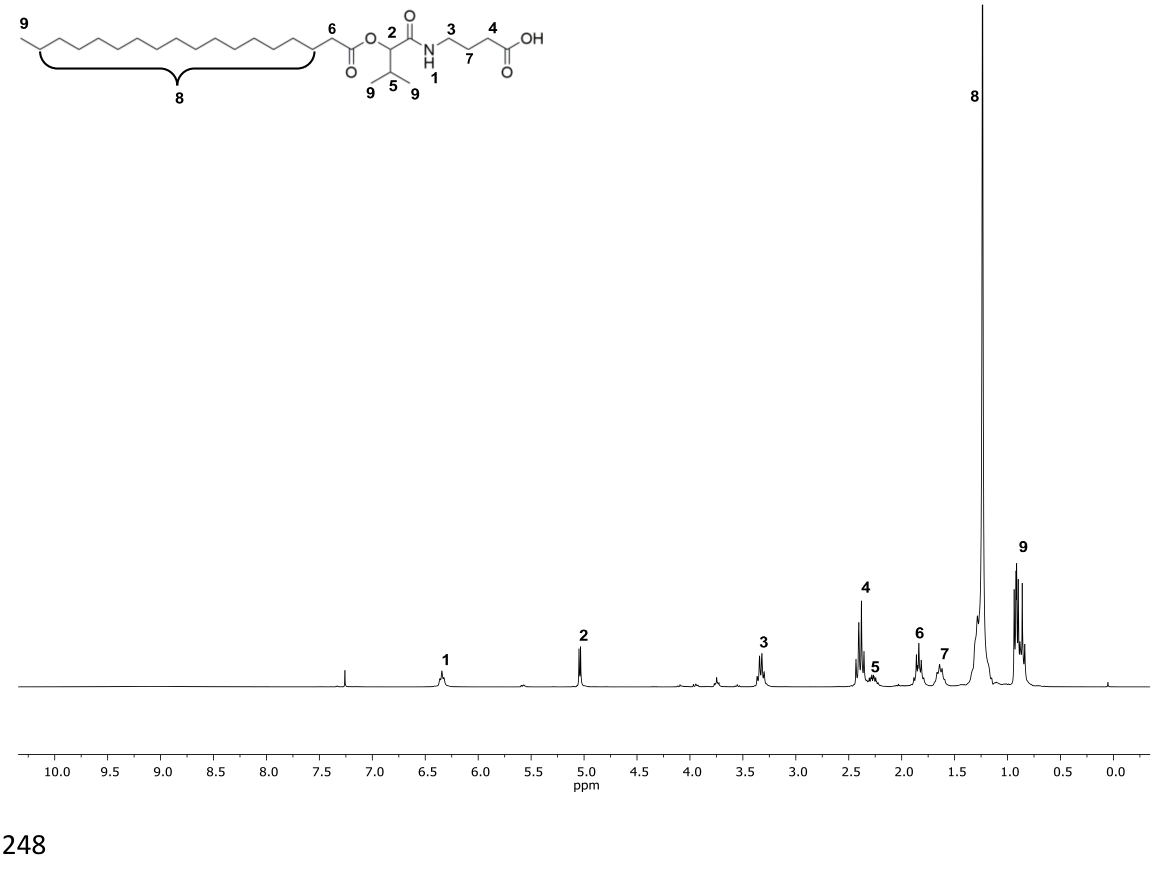

Synthesis of monomer M6[*]

Esterification

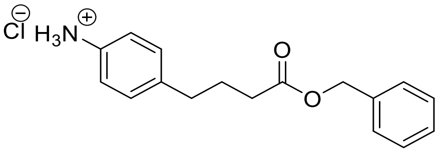

4-(4-aminophenyl)butanoic acid **1f** (1.00 g, 5.58 mmol, 1.00 eq.) was dissolved in THF (5.6 mL) and benzyl alcohol **3** (6.38 mL, 6.64 g, 61.4 mmol, 11.0 eq.) was added. Subsequently, the mixture was cooled to 0 °C and thionyl chloride **4** (1.42 mL, 2.32 g, 19.5 mmol, 3.50 eq.) was added dropwise. Afterwards, the solution was stirred at room temperature for 21 hours. Diethyl ether (10 mL) was added and the solution was stored in the freezer overnight. The white precipitate was filtered off and washed with cold diethyl ether (5 mL). The desired product **2f** (1.34 g, 4.37 mmol) was obtained as a white solid in a yield of 78%.

^{1}H-NMR (300 MHz, CD_3OD) δ/ppm: 7.36 – 7.33 (m, 9H, aromatic, ^{1}), 5.12 (s, 2H, CH_2, ^{2}), 2.69 (t, J = 7.6 Hz, 2H, CH_2, ^{3}), 2.39 (t, J = 7.2 Hz, 2H, CH_2, ^{4}), 1.94 (quint, J = 7.4 Hz, 2H, CH_2, ^{5}).

^{13}C-NMR (75 MHz, CD_3OD) δ/ppm: 207.7, 174.7, 144.4, 137.7, 131.3, 129.6, 129.3, 127.4, 124.1, 67.2, 35.3, 34.2, 27.6.

HRMS-FAB-MS of $[C_{17}H_{20}O_2N]^+$ calculated: 270.2135, found: 270.2137.

IR (ATR platinum diamond): ν /cm^{-1} = 2947.5, 2920.5, 2803.5, 2597.8, 1719.6, 1567.3, 1532.4, 1607.7, 1454.2, 1351.4, 1190.9, 1106.6, 962.6, 905.0, 812.5, 744.6, 607.3, 573.9, 487.4.

---

[*] Carried out by Roman Nickisch in the Vertieferarbeit “Synthesis of Aromatic AB Monomers for the Synthesis of Sequence-Defined Oligomers” (under lab-supervision of Katharina Wetzel).

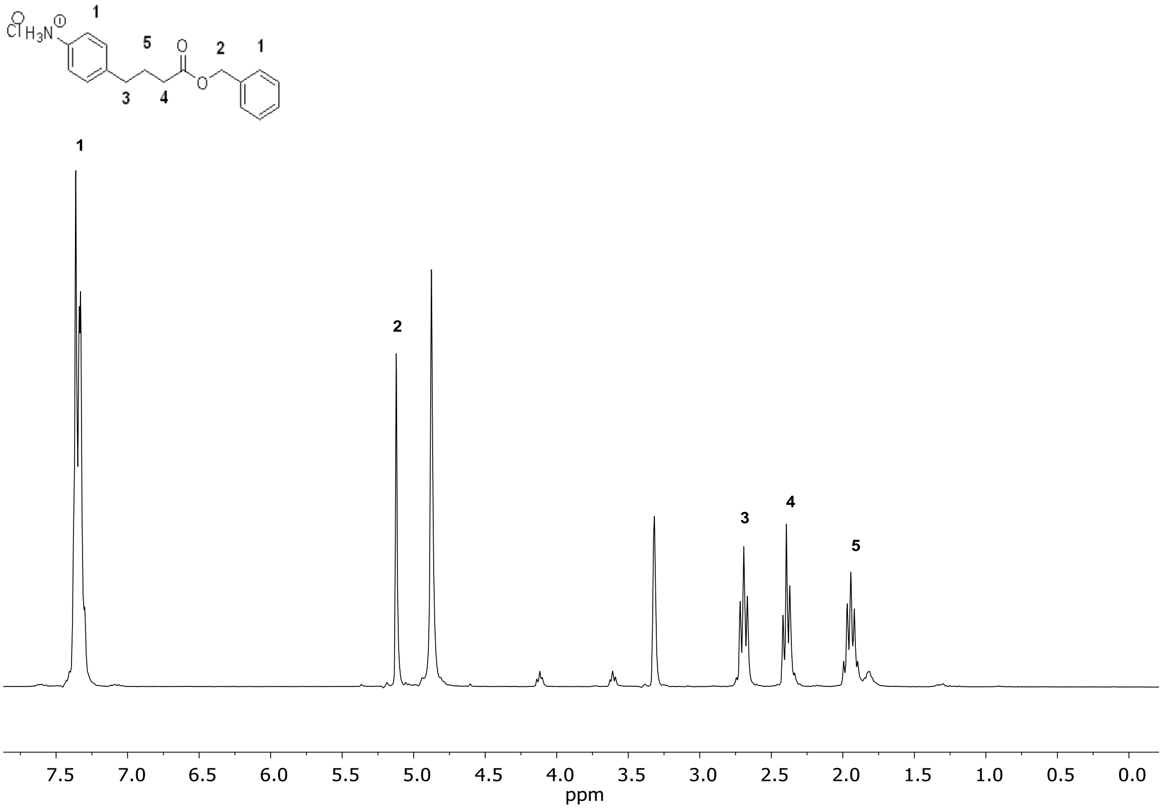
ClH3N⊕
1
5
O
2
1
3
4
O
1
2
3
4
5
7.5
7.0
6.5
6.0
5.5
5.0
4.5
4.0
3.5
3.0
2.5
2.0
1.5
1.0
0.5
0.0
ppm

N-Formylation

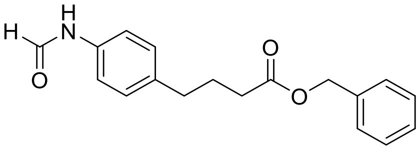

The ammonium salt **2f** (700 mg, 2.29 mmol, 1.00 eq.) was dissolved in trimethyl orthoformate **5** (2.48 mL, 2.43 g, 22.9 mmol, 10.0 eq.) and heated to 100 °C. The reaction was stirred under reflux overnight. Subsequently, the crude product was purified by column chromatography (cyclohexane/ethyl acetate 5:1 → 1:1). The desired *N*-formamide **8f** (492 mg, 1.65 mmol) was obtained as colourless oil in a yield of 72%.

^{1}H-NMR (300 MHz, CD_3OD) δ/ppm: 8.63 – 8.21 (m, 1H, CH, ^{1}), 7.46 – 7.43 (m, 2H, aromatic, ^{2}), 7.35 – 7.29 (m, 5H, aromatic, ^{3}), 7.15 – 7.04 (m, 2H, aromatic, ^{4}), 5.09 (s, 2H, CH_2, ^{5}), 2.57 (t, *J* = 7.6 Hz, 2H, CH_2, ^{6}), 2.35 (t, *J* = 7.3 Hz, 2H, CH_2, ^{7}), 1.89 (quint, *J* = 7.4 Hz, 2H, CH_2, ^{8}).

^{13}C-NMR (75 MHz, CD_3OD) δ/ppm: 174.9, 161.5, 144.0, 139.1, 130.7, 130.0, 129.5, 129.3, 121.2, 119.9, 94.5, 67.2, 35.4, 34.3, 27.8.

HRMS-FAB-MS of $[C_{18}H_{20}O_3N]^+$ calculated: 298.1443, found: 298.1139.

IR (ATR platinum diamond): ν /cm^{-1} = 3307.5, 3274.6, 3164.3, 3062.7, 3031.9, 2937.2, 2865.2, 1729.8, 1674.3, 1608.5, 1518.0, 1454.2, 1411.0, 1299.9, 1254.7, 1139.5, 1001.7, 964.7, 837.2, 736.4, 697.3, 543.0.

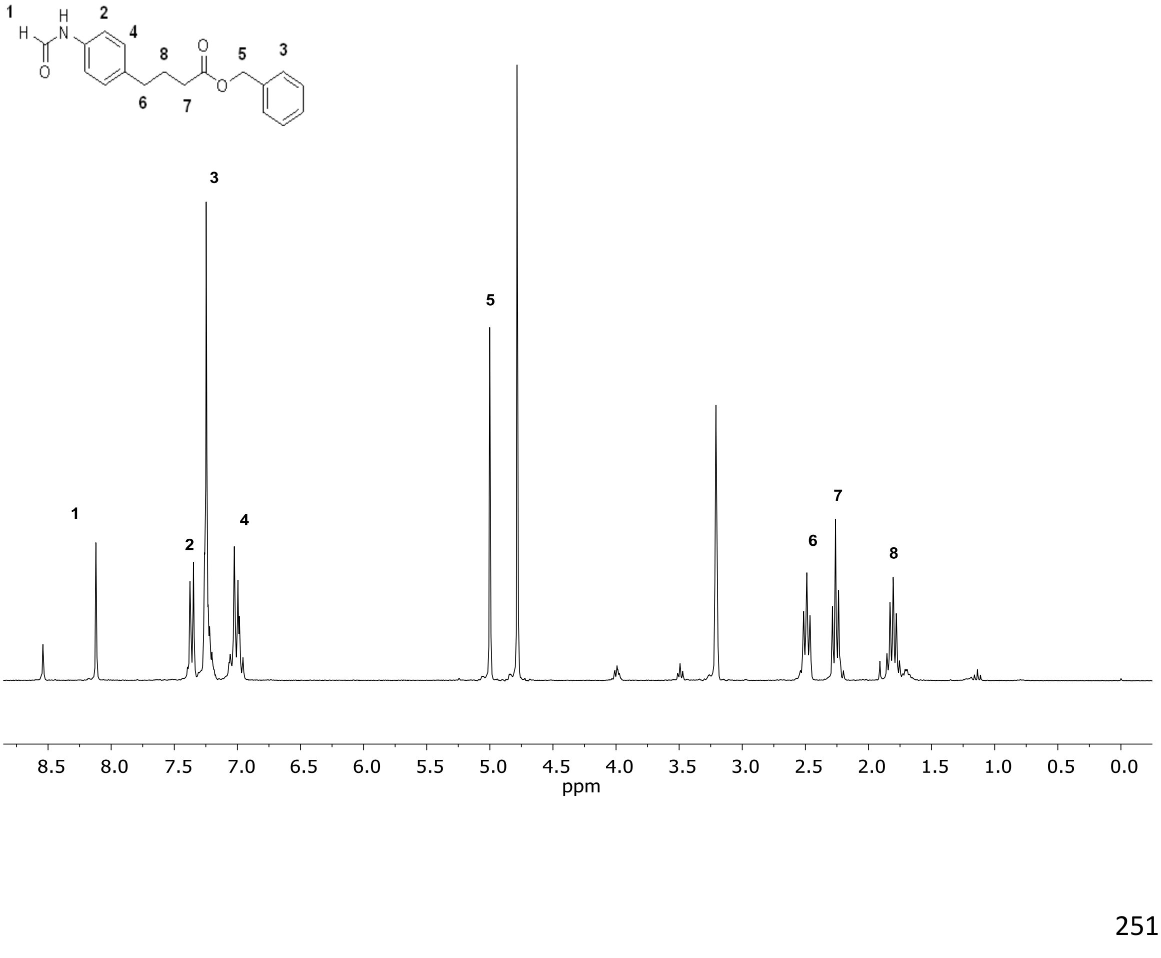

Dehydration

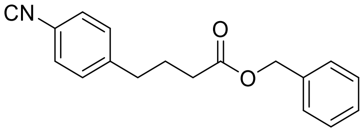

The formamide **8f** (433 mg, 1.46 mmol, 1.00 eq.) was dissolved in DCM (4.60 mL) and diisopropylamine **7** (0.634 mL, 456 mg, 4.51 mmol, 3.10 eq.) was added. The colourless solution was cooled to 0 °C using an ice bath. Then, phosphoryl trichloride **6** (0.173 mL, 290 mg, 1.89 mmol, 1.30 eq.) was added dropwise. The solution was stirred for two hours at room temperature. Subsequently, the yellow reaction mixture was cooled to 0 °C, quenched by addition of a 20 wt% sodium carbonate solution (1.79 mL) and was stirred for another 30 minutes at room temperature. DCM (2 mL) and water (2 mL) were added to the mixture and the organic layer was separated and washed with water (3x 2 mL) and brine (1x 2 mL). The combined organic layers were dried over sodium sulfate and the solvent was evaporated under reduced pressure. The crude product was purified by column chromatography (cyclohexane/ethyl acetate 18:1 → 6:1). The desired isocyanide monomer **M6** (275 mg, 985 µmol) was obtained as green liquid in a yield of 68%.

^{1}H-NMR (300 MHz, CD_3OD) δ/ppm: 7.40 – 7.33 (m, 5H, aromatic, ^{1}), 7.29 – 7.26 (m, 2H, aromatic, ^{2}), 7.17 – 7.14 (m, 2H, aromatic, ^{3}), 5.11 (s, 2H, CH_2, ^{4}), 2.65 (t, *J* = 7.7 Hz, 2H, CH_2, ^{5}), 2.37 (t, *J* = 7.3 Hz, 2H, CH_2, ^{6}), 1.95 (quint, *J* = 7.5 Hz, 2H, CH_2 ,^{7}).

^{13}C-NMR (75 MHz, CD_3OD) δ/ppm: 173.0, 163.5 143.2, 136.0, 129.5, 128.7, 128.4, 128.3, 126.5, 101.2, 66.4, 34.8, 33.5, 26.3.

HRMS-FAB-MS of $[C_{18}H_{18}O_2N]^+$ calculated: 280.1338, found: 280.1336.

IR (ATR platinum diamond): ν /cm^{-1} = 3064.8, 3033.9, 2943.4, 2867.3, 2122.7, 1731.9, 1505.6, 1454.2, 1384.3, 1141.6, 1040.8, 1003.8, 964.7, 845.4, 822.8, 736.4, 697.2, 547.1, 512.2, 483.4.

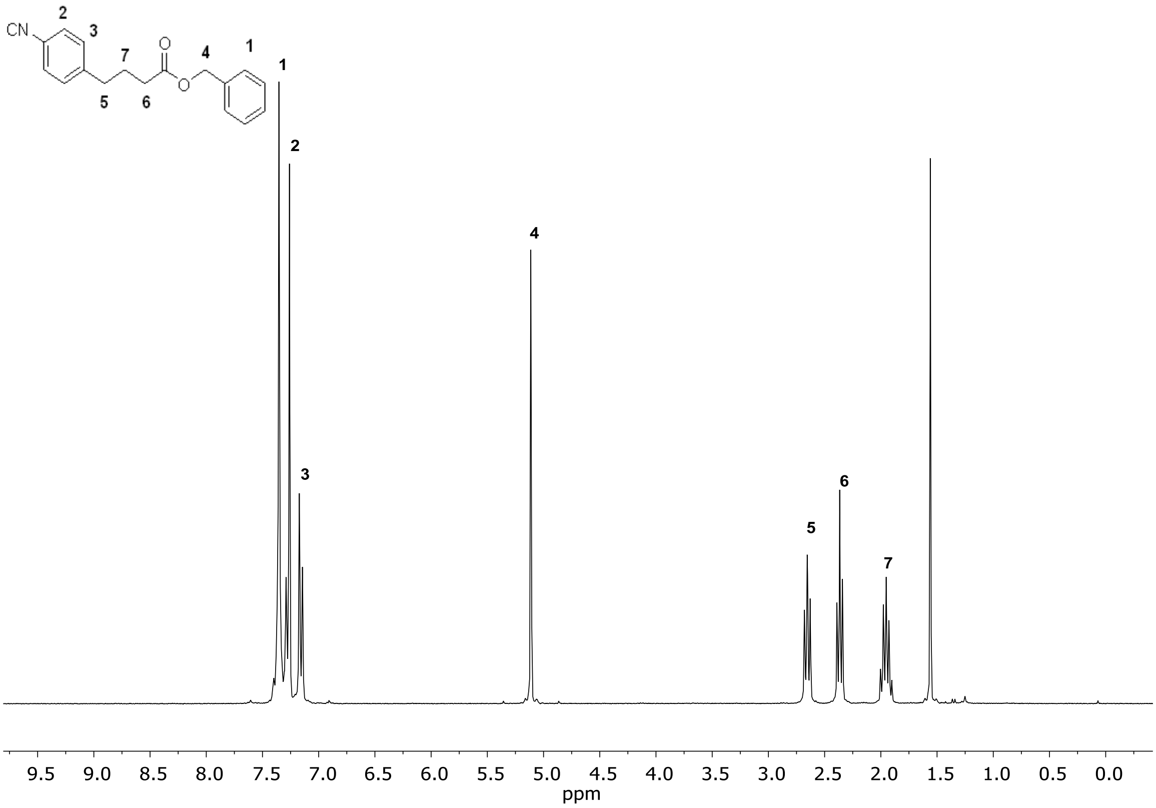
CN
2
3
7
O
4
1
O
5
6
1
2
3
4
5
6
7
9.5
9.0
8.5
8.0
7.5
7.0
6.5
6.0
5.5
5.0
4.5
4.0
3.5
3.0
2.5
2.0
1.5
1.0
0.5
0.0
ppm

Evaluation of the reactivity of monomer M6*

Passerini reaction

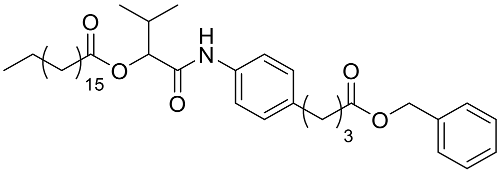

Stearic acid **13** (199 mg, 699 µmol, 1.00eq.) was suspended in DCM (1.75 ml). Subsequently, monomer **M6** (195 mg, 699 µmol, 1.00 eq.) and isobutyraldehyde **11c** (63.8 µL, 50.4 mg, 699 µmol, 1.00 eq.) were added. Then, the reaction mixture was stirred for 24 hours at room temperature. The crude product was purified by column chromatography (cyclohexane/ethyl acetate 15:1 → 10:1) and the desired Passerini product **75** (365 mg, 574 µmol) was obtained as a white solid in a yield of 82%.

^{1}H-NMR (300 MHz, $CDCl_3$) δ/ppm: 7.61 (s, 1H, NH, ^{1}), 7.41 (d, J = 8.4 Hz, 2H, aromatic, ^{2}), 7.38 – 7.31 (m, 5H, aromatic, ^{3}), 7.11 (d, J = 8.4 Hz, 2H, aromatic, ^{4}), 5.19 (d, J = 4.6 Hz, 1H, CH, ^{5}), 5.11 (s, 2H, CH_2, ^{6}), 2.61 (t, J = 7.5 Hz, 2H, CH_2, ^{7}), 2.47 (t, J = 7.5 Hz, 2H, CH_2, ^{8}), 2.42 – 2.34 (m, 3H, CH_2, CH, ^{9}), 1.94 (quint, J = 7.5 Hz, 2H, CH_2, ^{10}), 1.75 – 1.64 (m, 2H, CH_2, ^{11}), 1.42 – 1.17 (m, 28H, CH_2, ^{12}), 1.00 (d, J = 6.8 Hz, 6H, CH_3, ^{13}), 0.88 (t, J = 6.5 Hz, 3H, CH_3, ^{14}).

^{13}C-NMR (75 MHz, $CDCl_3$) δ/ppm: 172.6, 167.6, 163.1, 157.0, 150.8, 136.2, 135.0, 129.2, 128.7, 128.4, 120.4, 101.3, 78.2, 66.3, 34.6, 34.5, 33.7, 32.1, 30.9, 29.8, 29.6, 29.5, 29.4, 29.3, 26.7, 25.2, 24.2, 22.8, 18.9, 17.2, 14.3.

FAB-MS of $[C_{40}H_{62}O_5N]^+$ calculated: 636.5, found: 636.5.

IR (ATR platinum diamond): ν /cm^{-1} = 3311.6, 2955.7, 2916.7, 2850.8, 1723.7, 1672.2, 1598.2, 1532.4, 1468.6, 1458.3, 1415.1, 1386.3, 1357.5, 1316.4, 1260.9, 1238.3, 1213.6, 1184.8, 1172.4, 1145.7, 1108.7, 1030.5, 995.5, 977.0, 929.7, 835.1, 789.8, 775.4, 736.4, 719.9, 697.3, 672.6, 510.1.

---

* Carried out by Roman Nickisch in the Vertieferarbeit "Synthesis of Aromatic AB Monomers for the Synthesis of Sequence-Defined Oligomers" (under lab-supervision of Katharina Wetzel).

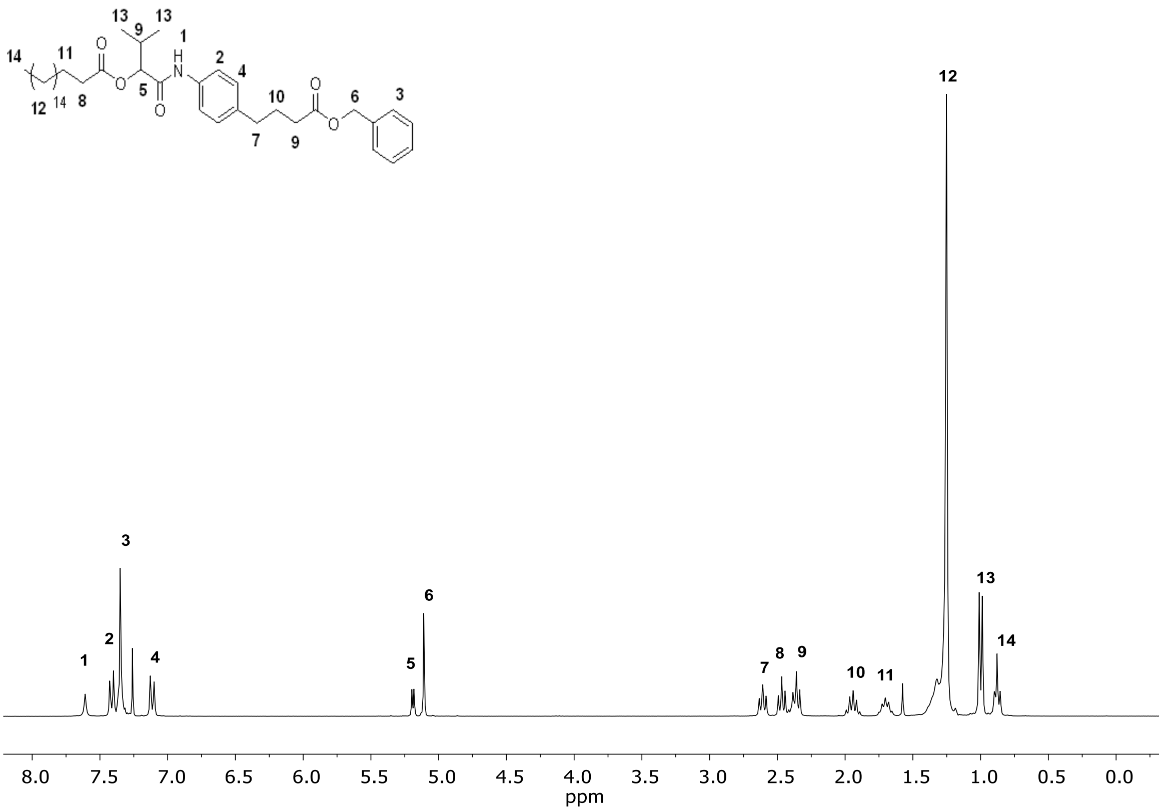
13
9
13
1
14
11
O
H
N
2
4
O
5
O
12
14
8
10
O
6
3
O
7
9
12
3
6
2
1
4
5
13
14
7
8
9
10
11
8.0
7.5
7.0
6.5
6.0
5.5
5.0
4.5
4.0
3.5
3.0
2.5
2.0
1.5
1.0
0.5
0.0
ppm

Deprotection

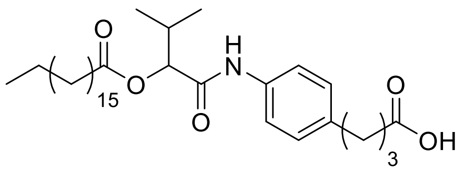

The Passerini product **75** (302 mg, 474 µmol, 1.00 eq.) was dissolved in ethyl acetate (3.20 mL) and palladium on activated charcoal **19** (30.2 mg, 10 wt%) was added. Subsequently, the reaction mixture was purged with hydrogen **XX** using a balloon and stirred under hydrogen atmosphere overnight. Afterwards, the heterogeneous catalyst was filtered off and the solvent was evaporated under reduced pressure. The desired deprotected carboxylic acid **76** (237 mg, 434 µmol) was obtained as a white solid in a yield of 92%.

^{1}H-NMR (300 MHz, $CDCl_3$) δ/ppm: 7.64 (s, 1H, NH, ^{1}), 7.43 (d, *J* = 8.3 Hz, 2H, aromatic, ^{2}), 7.15 (d, *J* = 8.3 Hz, 2H, aromatic, ^{3}), 5.19 (d, *J* = 4.6 Hz, 1H, CH, ^{4}), 2.64 (t, *J* = 7.5 Hz, 2H, CH_2, ^{5}), 2.47 (t, *J* = 7.5 Hz, 2H, CH_2, ^{6}), 2.41 – 2.33 (m, 3H, CH_2, CH, ^{7}), 1.94 (m, 2H, CH_2, ^{8}), 1.70 (t, *J* = 7.2 Hz, 2H, CH_2, ^{9}), 1.40 – 1.17 (m, 28H, CH_2, ^{10}), 1.00 (d, *J* = 6.8 Hz, 6H, CH_3, ^{11}), 0.87 (t, *J* = 6.8 Hz, 3H, CH_3 ^{12}).

^{13}C-NMR (75 MHz, $CDCl_3$) δ/ppm: 179.2, 172.8, 167.7, 138.0, 135.0, 129.1, 120.5, 78.2, 34.5, 34.4, 33.3, 32.0, 30.9, 29.8, 29.7, 29.6, 29.5, 29.4, 29.3, 26.4, 25.2, 22.8, 18.9, 17.3, 14.2.

FAB-MS of $[C_{33}H_{56}O_5N]^+$ calculated: 546.4, found: 546.4.

IR (ATR platinum diamond): ν /cm^{-1} = 3336.3, 2953.7, 2910.7, 2848.8, 1744.2, 1699.0, 1672.2, 1596.1, 1522.1, 1468.6, 1413.1, 1382.2, 1310.2, 1248.5, 1213.6, 1153.9, 1104.5, 1038.7, 1014.0, 923.5, 837.2, 794.0, 722.0, 672.6, 569.8, 516.3.

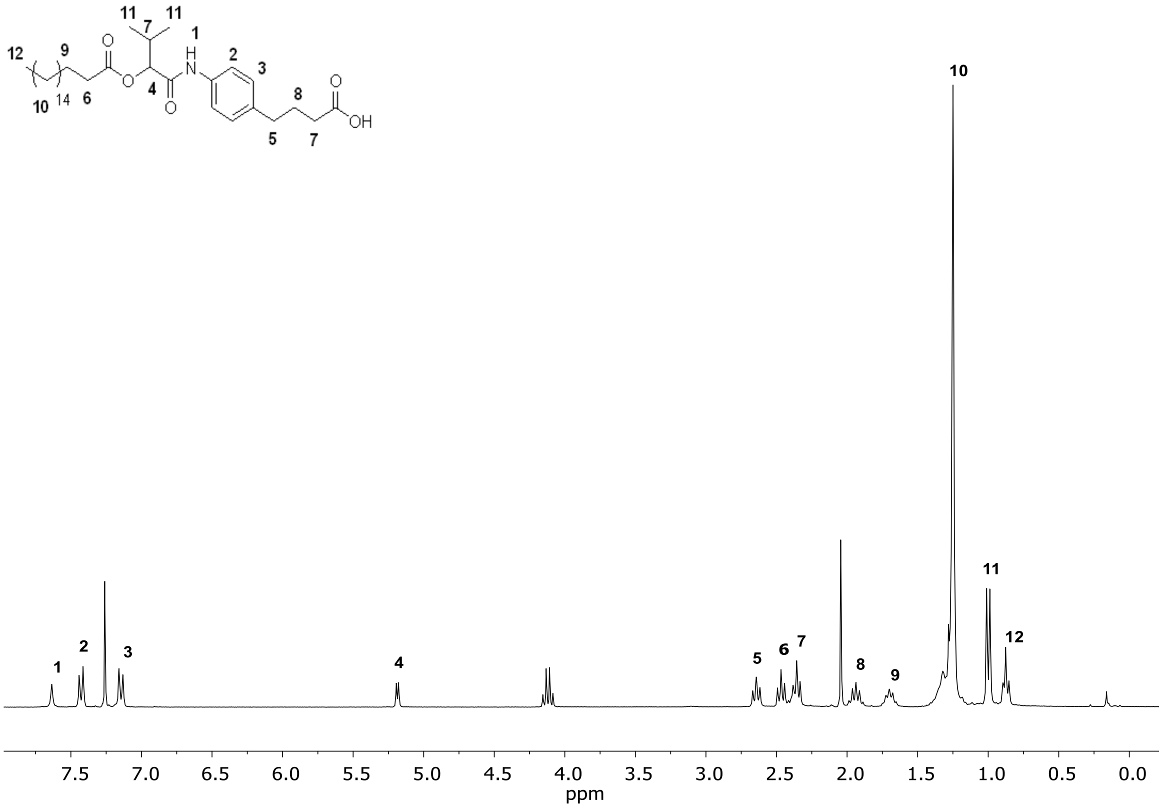
11
7
11
1
12
9
O
H
N
2
3
O
4
O
10
14
6
O
8
O
OH
5
7
10
11
12
1
2
3
4
5
6
7
8
9
7.5
7.0
6.5
6.0
5.5
5.0
4.5
4.0
3.5
3.0
2.5
2.0
1.5
1.0
0.5
0.0
ppm

Synthesis of monomer M7[*]

Esterification

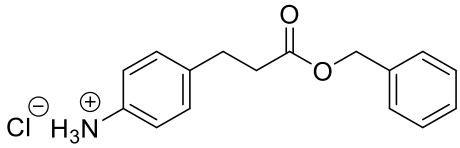

3-(4-Aminophenyl) propanoic acid **1g** (12.61 g, 75 mmol, 1.00 eq.) was suspended in THF (75 mL). After the addition of benzyl alcohol **3** (85.4 mL, 89.2 g, 825 mmol, 11.0 eq.), the suspension was cooled with an ice bath to 0 °C and thionyl chloride **4** (19.2 mL, 31.2 g, 263 mmol, 3.50 eq.) was added dropwise. Afterwards, the suspension was stirred at room temperature for 15 hours. Subsequently, 500 mL diethyl ether were added, and the solution was stored in the freezer for 2 hours. The mixture was filtered, and 500 mL diethyl ether were added to the precipitate and stored in the freezer for another 2 hours. The precipitate was filtered off and the crude product **2g** (20.3 g, 69.6 mmol) was obtained as a white solid in a yield of 93%.

^{1}H-NMR (300 MHz, CD_3OD) δ/ppm: 7.36 – 7.25 (m, 9H, aromatic, ^{1}), 5.07 (s, 2H, CH_2, ^{2}), 2.97 (t, J = 7.4 Hz, 2H, CH_2, ^{3}), 2.69 (t, J = 7.4 Hz, 2H, CH_2, ^{4}).

^{13}C-NMR (500 MHz, CD_3OD) δ/ppm: 173.88, 143.36, 137.48, 131.21, 129.92, 129.51, 129.26, 129.21, 124.12, 67.28, 36.33, 31.24.

HRMS-FAB-MS of $[C_{16}H_{18}O_2N]^+$ calculated: 256.1338 found: 256.1337.

IR (ATR platinum diamond): ν /cm^{-1} = 2914.7, 2837.1, 2601.3, 1963.0, 1738.3, 1620.9, 1580.7, 1566.6, 1527.8, 1508.2, 1453.0, 1379.0, 1345.4, 1305.8, 1277.7, 1258.4, 1212.3, 1193.0, 1147.1, 1109.4, 1081.0, 1043.2, 1025.1, 990.9, 953.0, 933.0, 912.9, 834.5, 812.6, 757.7, 732.1, 695.0, 641.8, 573.3, 546.4, 499.1, 481.6, 461.1.

---

[*] Carried out by Philipp Treu in the Vertieferarbeit “Synthesis of a Sequence-Defined Oligomer using AB Monomers” (under the lab-supervision of Katharina Wetzel).

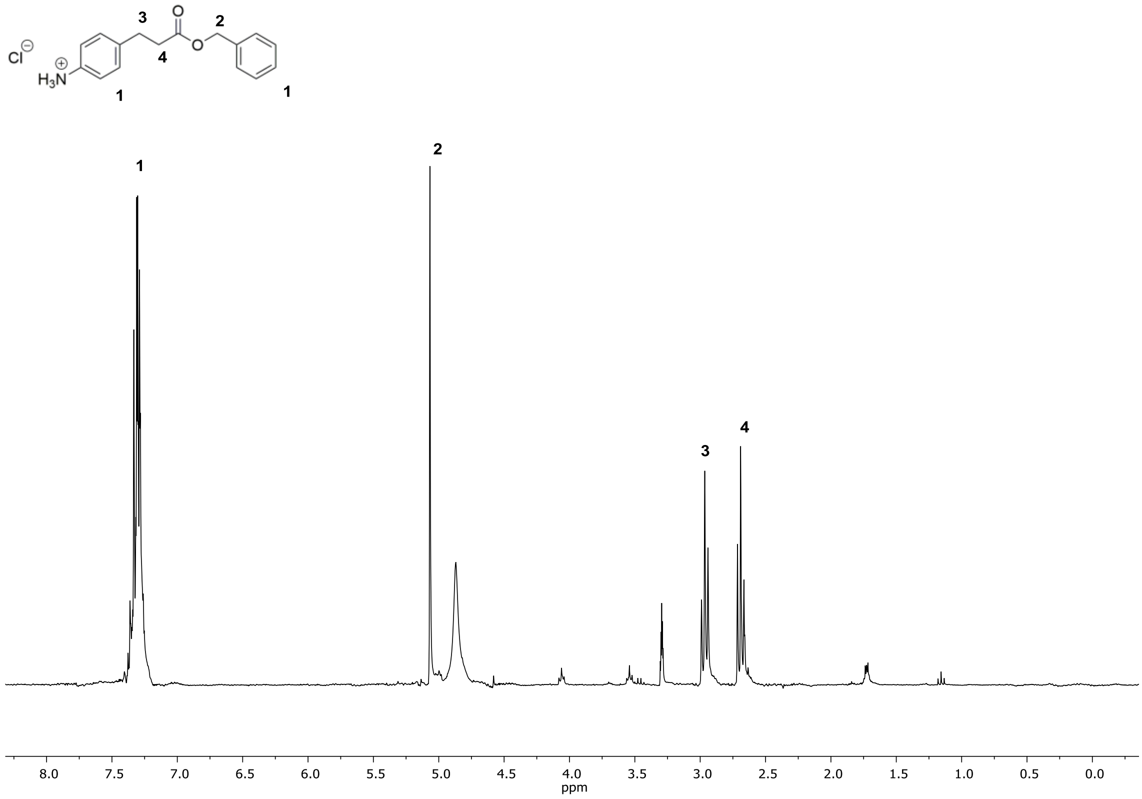
Cl⊖
H3N⊕
3
4
2
O
O
1
1
1
2
3
4
8.0
7.5
7.0
6.5
6.0
5.5
5.0
4.5
4.0
ppm
3.5
3.0
2.5
2.0
1.5
1.0
0.5
0.0

N-Formylation

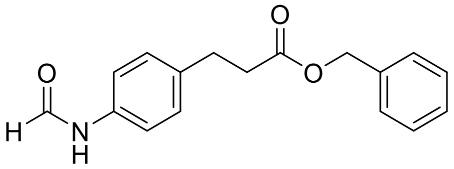

The ammonium salt **2g** (20.3 g, 69.6 mmol, 1.00 eq.) was stirred with trimethyl orthoformate **5** (78.0 mL, 75.7 g, 716 mmol, 10.2 eq.) under reflux at 105 °C overnight. Subsequently, the orthoformate **5** was evaporated under reduced pressure. The crude product **8g** (19.5 g, 68.9 mmol) was obtained as a yellow oil in a yield of 99% and was used without further purification.

^{1}H-NMR (300 MHz, $CDCl_3$) δ/ppm: 8.66 – 8.56 (m, 0.5H, formamide, ^{1}), 8.33 – 8.01 (m, 0.5H, formamide, ^{1}), 7.45 – 6.95 (m, 9H, aromatic,^{2}), 5.08 (s, 2H, CH_2, ^{3}), 2.96 – 2.86 (m, 2H, CH_2, ^{4}), 2.68 – 2.57 (m, 2H, CH_2, ^{5}).

^{13}C-NMR (101 MHz, $CDCl_3$) δ/ppm: 172.76, 163.05, 159.29, 137.43, 136.78, 135.86, 135.37, 135.15, 120.21, 119.12, 66.38, 35.97, 30.36.

HRMS-FAB-MS of $[C_{17}H_{18}O_3N]^+$ calculated: 284.1287 found: 284.1288.

IR (ATR platinum diamond): ν /cm^{-1} = 3306.5, 3200.4, 3113.5, 3033.0, 2944.7, 2867.0, 2775.0, 1897.5, 1728.7, 1682.1, 1603.0, 1518.5, 1454.1, 1412.0, 1381.9, 1352.7, 1291.4, 1256.5, 1147.4, 1109.0, 1025.9, 984.9, 908.4, 823.7, 735.6, 696.1, 578.9, 536.1, 454.8, 411.1.

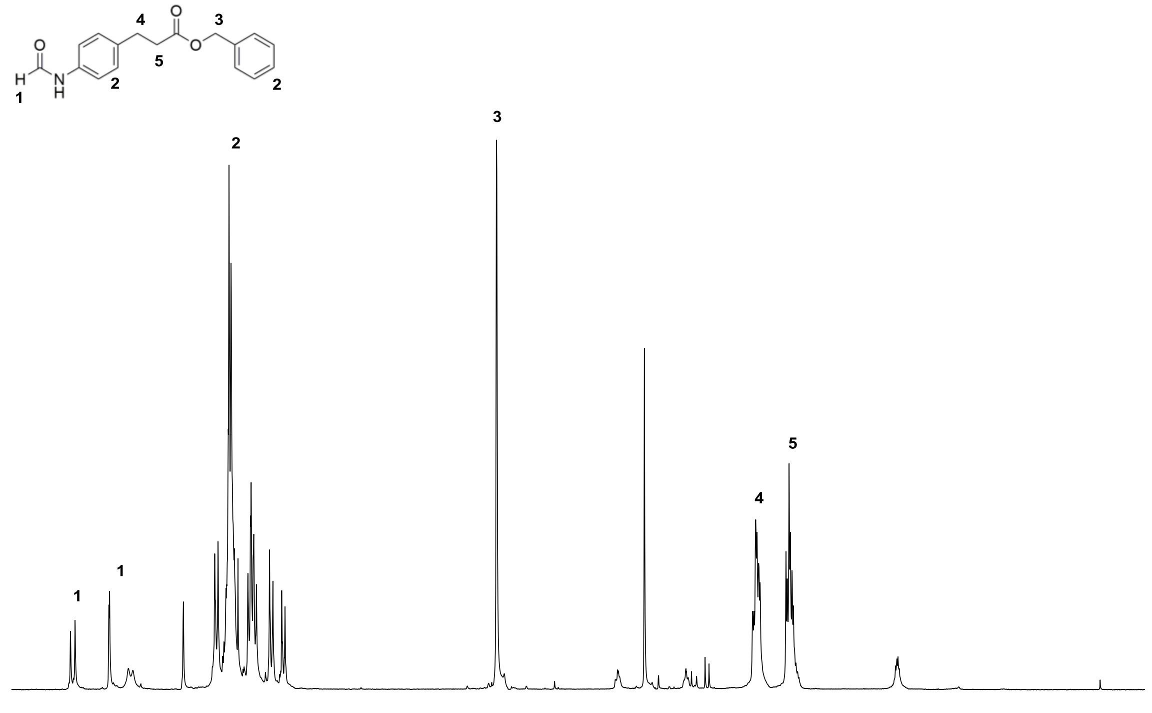

Dehydration

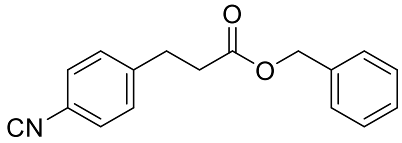

The formamide **8g** (19.5 g, 68.9 mmol, 1.00 eq.) was dissolved in DCM (210 mL) and diisopropylamine **7** (30.0 mL, 21.6 g, 213 mmol, 3.10 eq.) was added. The solution was cooled to 0 °C with an ice bath. Then, phosphoryl trichloride **6** (8.90 mL, 14.9 g, 89.6 mmol, 1.30 eq.) was added dropwise to the reaction mixture. The yellow solution was stirred for two hours at room temperature and was cooled to 0 °C again. The reaction was quenched by the addition of a 20 wt% solution of sodium carbonate (150 mL) and stirred for another 30 minutes at room temperature. DCM (150 mL) and water (150 mL) were added to the mixture and the organic layer was separated. The organic layer was washed with water (3 × 150 mL) and brine (150 mL), dried over sodium sulfate and the solvent was evaporated under reduced pressure. The crude product was purified by column chromatography (cyclohexane/ ethyl acetate 10:1 → 3:1). Monomer **M7** (10.10 g, 38.1 mmol) was obtained as a green oil in a yield of 55%.

^{1}H-NMR (300 MHz, $CDCl_3$) δ/ppm: 7.31 – 7.08 (m, 9H, aromatic, ^{1}), 5.03 (s, 2H, CH_2, ^{2}), 2.91 (t, J = 7.5 Hz, 2H, CH_2, ^{3}), 2.60 (t, J = 7.5 Hz, 2H, CH_2, ^{4}).

^{13}C-NMR (126 MHz, $CDCl_3$) δ/ppm: 172.11, 142.12, 135.72, 129.38, 128.58, 128.35, 128.31, 126.45, 66.43, 35.34, 30.53.

HRMS-FAB-MS of $[C_{17}H_{16}O_2N]^+$ calculated: 266.1181 found: 266.1182.

IR (ATR platinum diamond): ν /cm^{-1} = 3065.5, 3034.5, 2949.3, 2122.9, 1730.9, 1606.7, 1505.6, 1454.4, 1418.7, 1382.8, 1353.3, 1289.5, 1150.6, 1105.3, 1019.7, 976.3, 909.9, 827.5, 736.0, 696.6, 578.6, 533.9, 512.6, 484.2, 461.6.

***R*f** (cyclohexane/ethyl acetate 4:1) = 0.56.

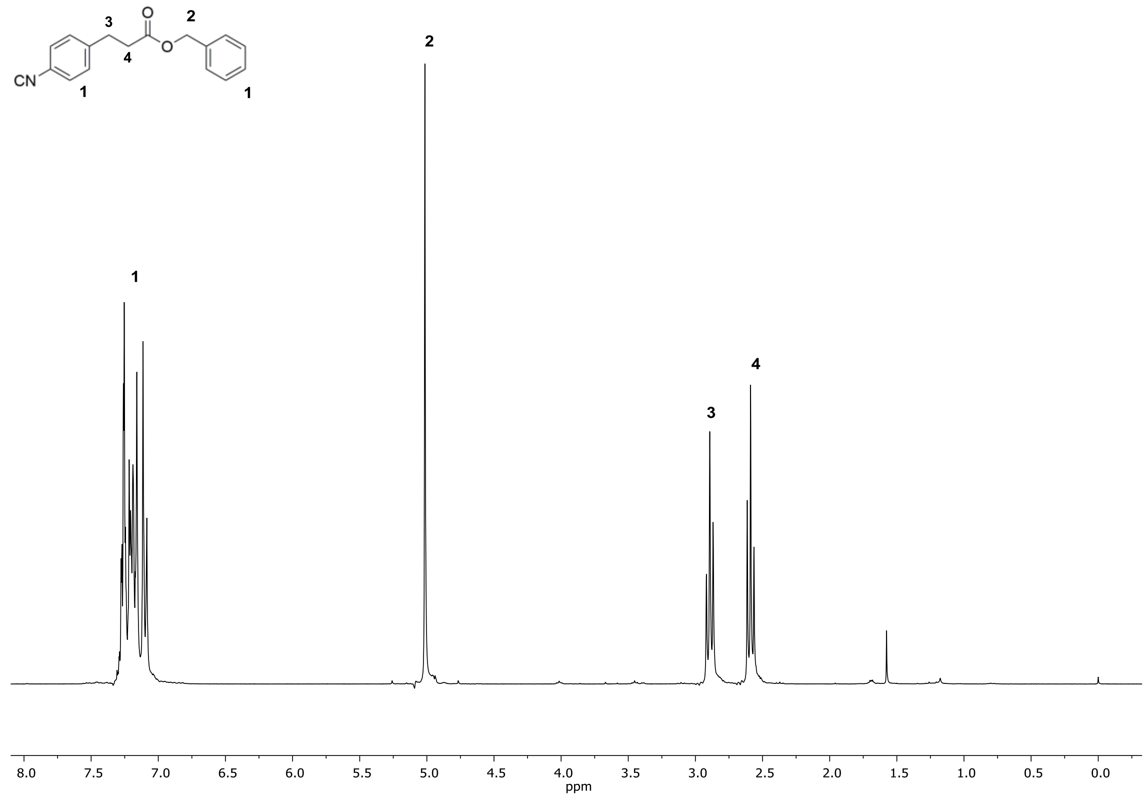
3
2
4
CN
1
1
2
1
4
3
8.0
7.5
7.0
6.5
6.0
5.5
5.0
4.5
4.0
ppm
3.5
3.0
2.5
2.0
1.5
1.0
0.5
0.0

Evaluation of the reactivity of monomer M7[*]

Passerini reaction

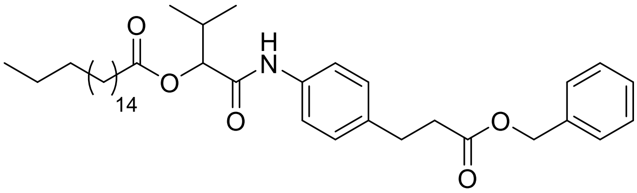

Stearic acid **13** (0.21 g, 0.74 mmol, 1.00 eq.) was suspended in 1.10 mL DCM. Subsequently, monomer **M7** (0.29 g, 1.11 mmol, 1.50 eq.) and isobutyraldehyde **11c** (100 µL, 80.0 mg, 1.11 mmol, 1.50 eq.) were added. The yellow reaction mixture was stirred at room temperature for 24 hours. Afterwards the solvent was removed under reduced pressure and the crude product was purified by column chromatography (cyclohexane/ethyl acetate 15:1→8:1) to obtain the desired Passerini product **77** as white solid in a yield of 48% of (0.22 g, 0.36 mmol). At the same time the monomer **M7** from the other fraction was partially recovered (0.066 g, 0.34 eq.) and can be reused.

^{1}H-NMR (300 MHz, $CDCl_3$) δ/ppm: 7.73 (s, 1H, NH, ^{1}), 7.42 (d, J = 8.4 Hz, 2H, aromatic, ^{2}), 7.36 – 7.28 (m, 5H, aromatic, ^{3}), 7.14 (d, J = 8.4 Hz, 2H, aromatic, ^{4}), 5.17 (d, J = 4.7 Hz, 1H, CH, ^{5}), 5.10 (s, 2H, CH_2, ^{6}), 2.93 (t, J = 7.7 Hz, 2H, CH_2, ^{7}), 2.65 (t, J = 7.7 Hz, 2H, CH_2, ^{8}), 2.47 (t, J = 7.5 Hz, 2H, CH_2, ^{9}), 1.72 – 1.63 (m, 2H, CH_2, ^{10}), 1.26 (m, 28H, CH_2, ^{11}), 1.00 (d, J = 6.9 Hz, 6H, CH_3, ^{12}), 0.94 – 0.79 (m, 3H, CH_3, ^{13}).

^{13}C-NMR (101 MHz, $CDCl_3$) δ/ppm: 173.5, 168.5, 137.8, 136.8, 136.1, 129.4, 121.2, 78.9, 67.22, 36.8, 35.2, 32.8, 31.7, 31.3, 30.6, 30.3, 30.1, 26.0, 23.6, 19.7, 18.1, 15.1.

HRMS-FAB-MS of $[C_{39}H_{60}O_5N]^+$calculated: 622.4471, found: 622.4470.

IR (ATR platinum diamond): ν /cm^{-1} = 2916.9, 2848.6, 1738.2, 1671.6, 1535.3, 1516.7, 1470.8, 1414.0, 1388.5, 1295.8, 1252.1, 1166.3, 1019.4, 850.0, 803.9, 734.5, 719.1, 577.4, 534.1.

---

[*] Carried out by Yixuan Jia in the Vertieferarbeit "Synthesis of AB-monomers for sequence-defined macromolecules and evaluation of their reactivity" (under lab-supervision of Katharina Wetzel).

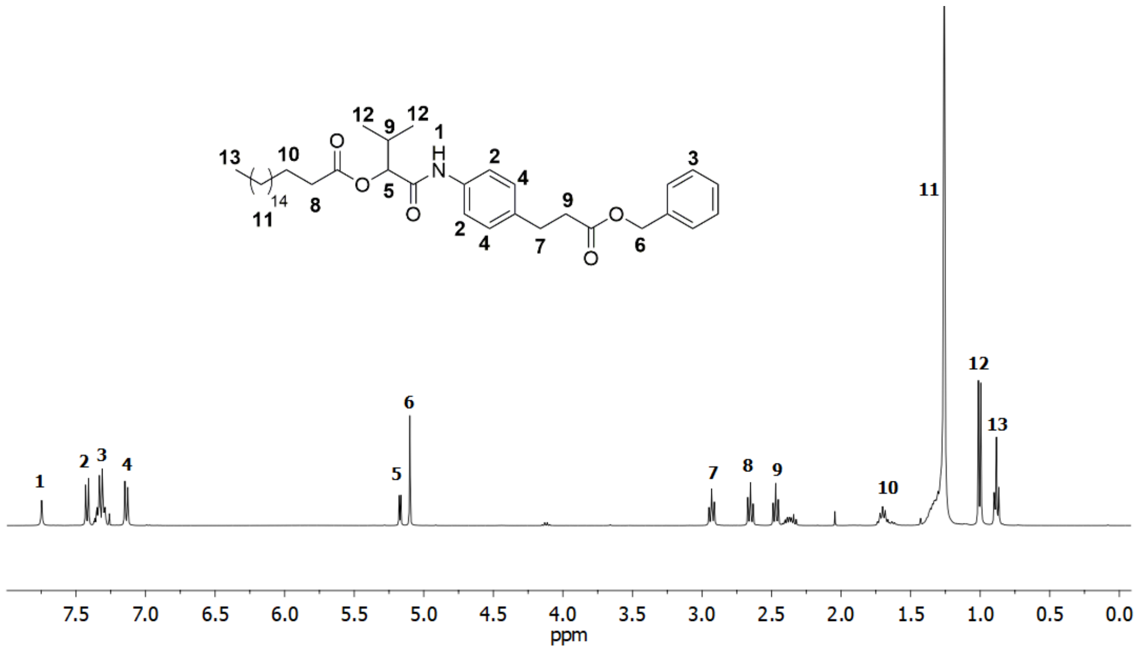
13
10
14
11
8
O
O
12
9
12
1
H
N
5
O
2
4
2
4
9
7
O
O
6
3
11
12
13
1
2
3
4
5
6
7
8
9
10
7.5
7.0
6.5
6.0
5.5
5.0
4.5
4.0
3.5
3.0
2.5
2.0
1.5
1.0
0.5
0.0
ppm

Deprotection

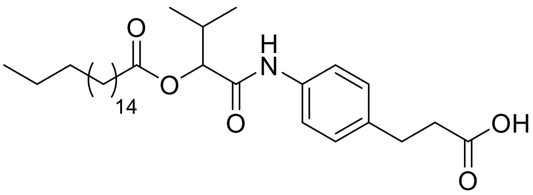

The Passerini product **77** (110 mg, 0.18 mmol, 1.00 eq.) were dissolved in ethyl acetate (0.36 ml, 0.50 M) and palladium on activated charcoal **19** (11.0 mg, 10 wt%) was added. The reaction mixture was purged with hydrogen by using a balloon and stirred under hydrogen atmosphere overnight at room temperature. Afterwards the heterogeneous catalyst was filtered off and the solvent was evaporated under reduced pressure. The desired deprotected product **78** (85.1 mg, 0.16 mmol) was obtained as white solid in a yield of 90%.

^{1}**H-NMR** (300 MHz, $CDCl_3$) δ/ppm: 7.74 (s, 1H, NH, ^{1}), 7.36 (d, *J* = 8.4 Hz, 2H, aromatic, ^{2}), 7.09 (d, *J* = 8.4 Hz, 2H, aromatic, ^{3}), 5.09 (d, *J* = 4.8 Hz, 1H, CH, ^{4}), 2.84 (t, *J* = 7.6 Hz, 2H, CH_2, ^{5}), 2.57 (t, *J* = 7.6 Hz, 2H, CH_2, ^{6}), 2.39 (t, *J* = 7.5 Hz, 2H, CH_2, ^{7}), 1.64 – 1.57 (m, 2H, CH_2, ^{8}), 1.18 (m, 28H, CH_2, ^{9}), 0.93 (d, *J* = 6.8 Hz, 6H, CH_3, ^{10}), 0.85 – 0.76 (m, 3H, CH_3, ^{11}).

^{13}C-NMR (101 MHz, $CDCl_3$) δ/ppm: 177.5, 171.8, 166.7, 135.7, 134.2, 128.1, 127.8, 119.4, 78.9, 67.2, 34.6, 33.1, 29.8, 28.7, 28.3, 28.1, 24.0, 23.7, 21.9, 21.7.

HRMS-FAB-MS of $[C_{32}H_{54}O_5N]^+$calculated: 532.4002, found: 532.4003.

IR (ATR platinum diamond): ν /cm^{-1} = 2917.2, 2848.8, 1737.2, 1708.9, 1667.6, 1603.6, 1530.9, 1469.8, 1414.3, 1297.1, 1255.2, 1169.5, 1018.7, 948.0, 829.3, 808.9, 719.6, 662.9, 547.7, 511.9, 416.9.

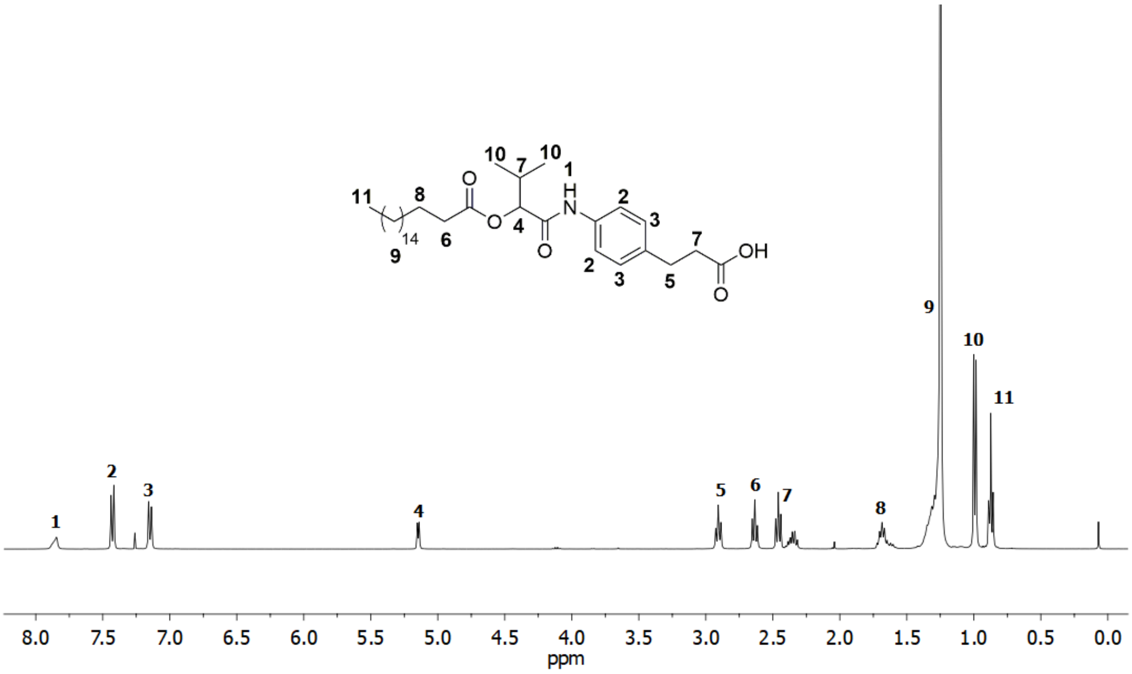

Synthesis of monomer M8[*]

Esterification

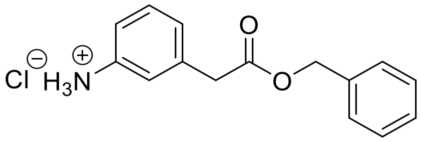

3-aminophenylacetic acid **1h** (10.0 g, 66.4 mmol, 1.00 eq.) was suspended in THF (70 mL). After the addition of benzyl alcohol **3** (75.6 mL, 79.0 g, 731 mmol, 11.0 eq.), the suspension was cooled in an ice bath to 0 °C and thionyl chloride **4** (17.0 mL, 28.0 g, 235 mmol, 3.54 eq.) was added dropwise. Afterwards the suspension was stirred at room temperature for 20 hours. Subsequently, 500 mL diethyl ether were added, and the solution was stored in the freezer for two hours. The precipitate was filtered off and the crude product **2h** (10.4 g, 37.4 mmol) was obtained as a slightly brown solid in a yield of 56%.

^{1}H-NMR (300 MHz, CD_3OD) δ/ppm: 7.54 – 7.14 (m, 9H, aromatic, ^{1}), 5.08 (s, 2H, CH_2, ^{2}), 3.76 (s, 2H, CH_2, ^{3}).

^{13}C-NMR (101 MHz, CD_3OD) δ/ppm: 173.06, 142.63, 138.28, 131.98, 131.33, 131.29, 129.54, 129.32, 129.18, 128.24, 127.97, 125.17, 122.76, 65.17, 41.00.

HRMS-FAB-MS of $[C_{15}H_{16}O_2N]^+$ calculated: 242.1181 found: 242.1181.

IR (ATR platinum diamond): ν /cm^{-1} = 3031.5, 2964.2, 2900.3, 2714.5, 2629.1, 2546.8, 2236.5, 1904.7, 1722.3, 1603.3, 1571.4, 1492.9, 1455.8, 1420.5, 1377.8, 1335.7, 1300.4, 1250.5, 1213.4, 1190.5, 1166.9, 1150.1, 1108.4, 1064.1, 1030.7, 992.5, 972.6, 947.5, 907.7, 794.3, 761.1, 741.5, 717.6, 694.4, 683.9, 600.0, 576.9, 530.9, 519.6, 484.9, 443.3.

---

[*] Carried out by Philipp Treu in the Vertieferarbeit "Synthesis of a Sequence-Defined Oligomer using AB Monomers" (under the lab-supervision of Katharina Wetzel).

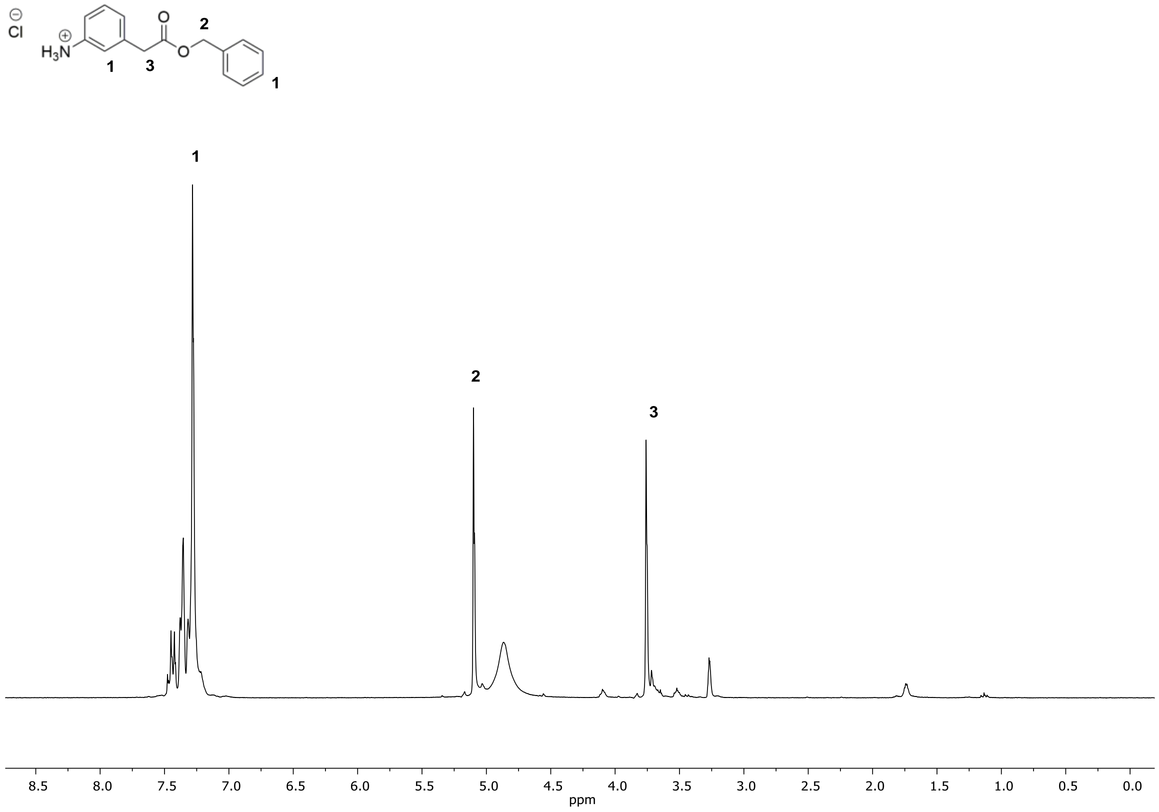
Cl
H$_3$N
O
O
1
3
2
1
1
2
3
8.5
8.0
7.5
7.0
6.5
6.0
5.5
5.0
4.5
4.0
3.5
3.0
2.5
2.0
1.5
1.0
0.5
0.0
ppm

N-Formylation

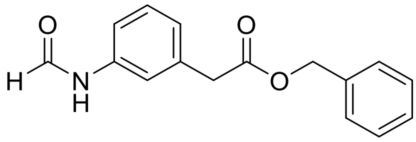

The ammonium salt **2h** (10.3 g, 37.0 mmol, 1.00 eq.) was stirred with trimethyl orthoformate **5** (40.5 mL, 39.3 g, 370 mmol, 10.0 eq.) under reflux at 105 °C overnight. Subsequently, the orthoformate **5** was evaporated under reduced pressure. The crude product **8h** (9.96 g, 37.0 mmol) was obtained as a yellow oil in quantitative yield and was used without further purification.

^{1}H-NMR (300 MHz, CDCl$_3$) δ/ppm: 8.56 (d, J = 11.4 Hz, 0.5H, formamide, ^{1}), 8.18 (s, 0.5H, formamide, ^{1}), 7.70 – 6.72 (m, 9H, aromatic, ^{2}), 5.06 (s, 2H, CH$_2$, ^{3}), 3.57 (s, 2H, CH$_2$, ^{4}).

^{13}C-NMR (101 MHz, CDCl$_3$) δ/ppm: 171.46, 162.82, 135.80, 135.70, 134.84, 129.34, 128.63, 128.34, 128.25, 126.20, 122.51, 120.85, 66.79.

HRMS-FAB-MS of [C$_{16}$H$_{16}$O$_3$N]$^+$ calculated: 270.1130 found: 270.1132.

IR (ATR platinum diamond): ν /cm^{-1} = 3318.4, 3146.2, 3031.9, 2944.3, 2891.9, 1729.4, 1688.6, 1644.5, 1595.2, 1546.7, 1491.5, 1441.6, 1376.7, 1262.6, 1211.7, 1144.6, 999.8, 894.2, 785.8, 735.8, 694.8, 580.7, 499.2.

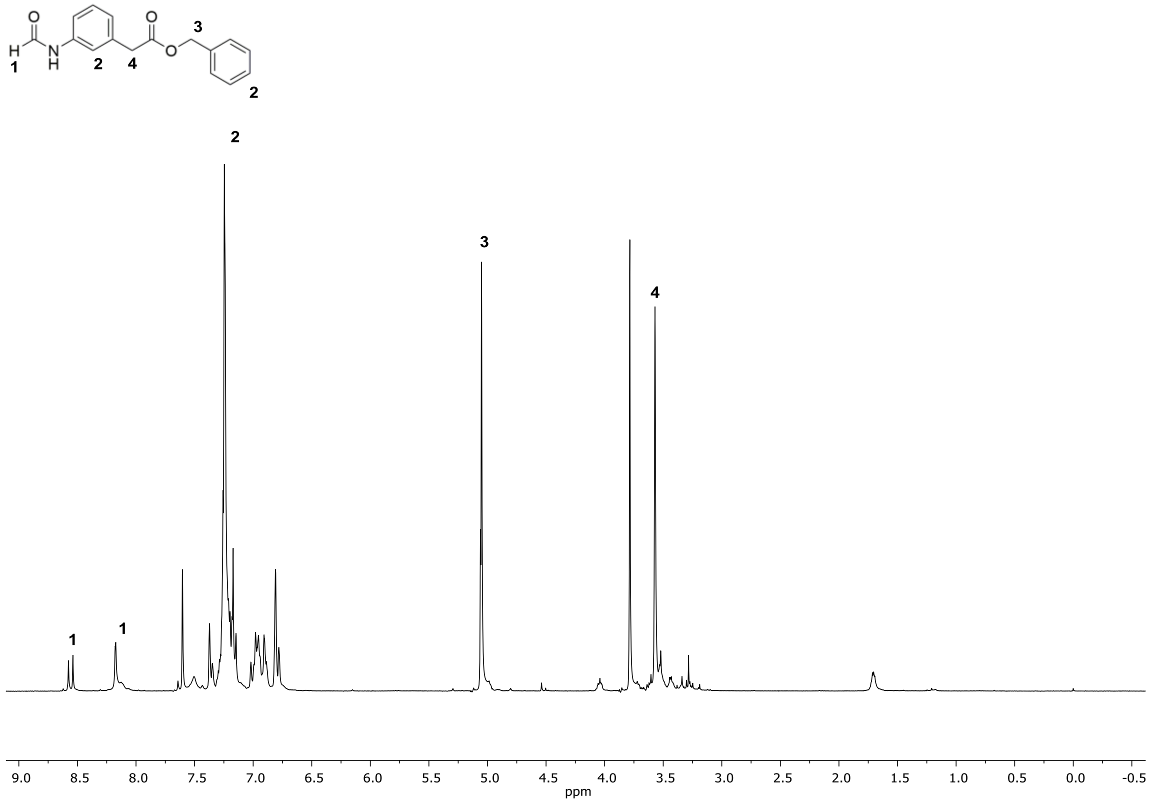

Dehydration

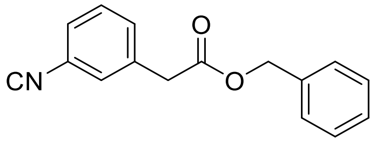

The formamide **8h** (10.7 g, 39.7 mmol, 1.00 eq.) was dissolved in DCM (120 mL) and diisopropylamine **7** (14.1 mL, 19.5 g, 139 mmol, 3.50 eq.) was added. The solution was cooled to 0 °C in an ice bath. Then, phosphoryl trichloride **6** (5.10 mL, 8.60 g, 51.6 mmol, 1.30 eq.) was added dropwise to the reaction mixture. The yellow solution was stirred for two hours at room temperature and was afterwards cooled to 0 °C again. The reaction was quenched by the addition of a 20 wt% sodium carbonate solution (100 mL) and stirred for another 30 minutes at room temperature. 100 mL DCM and 100 mL water were added to the mixture and the organic layer was separated. The organic layer was washed with water (3 × 100 mL) and brine (100 mL), dried over sodium sulfate and the solvent was evaporated under reduced pressure. The crude product was purified by column chromatography (cyclohexane/ethyl acetate 10:1 → 3:1). Monomer **M8** (3.90 g, 15.6 mmol) was obtained as a green oil in a yield of 39%.

^{1}H-NMR (300 MHz, $CDCl_3$) δ/ppm: 7.36 – 7.07 (m, 9H, aromatic, ^{1}), 5.06 (s, 2H, CH_2, ^{2}), 3.58 (s, 2H, CH_2, ^{3}).

^{13}C-NMR (101 MHz, $CDCl_3$) δ/ppm: 170.42, 135.67, 135.51, 130.53, 129.64, 128.69, 128.52, 128.35, 127.33, 125.23, 67.06, 40.65.

HRMS-FAB-MS of $[C_{16}H_{14}O_2N]^+$ calculated: 252.1025 found: 252.1024.

IR (ATR platinum diamond): ν /cm^{-1} = 3058.5, 3029.1, 2973.7, 2944.7, 2917.8, 2889.7, 2128.6, 1959.6, 1724.0, 1601.4, 1586.2, 1485.9, 1453.2, 1423.1, 1377.2, 1338.3, 1289.7, 1236.0, 1219.2, 1191.0, 1179.1, 1153.3, 1080.8, 1029.2, 1002.8, 970.0, 940.8, 907.5, 878.9, 829.9, 796.6, 760.8, 740.2, 712.8, 696.4, 681.2, 601.5, 579.3, 553.1, 499.2, 473.7, 449.1.

***R*$_f$** (cyclohexane / ethyl acetate (4:1)) = 0.47.

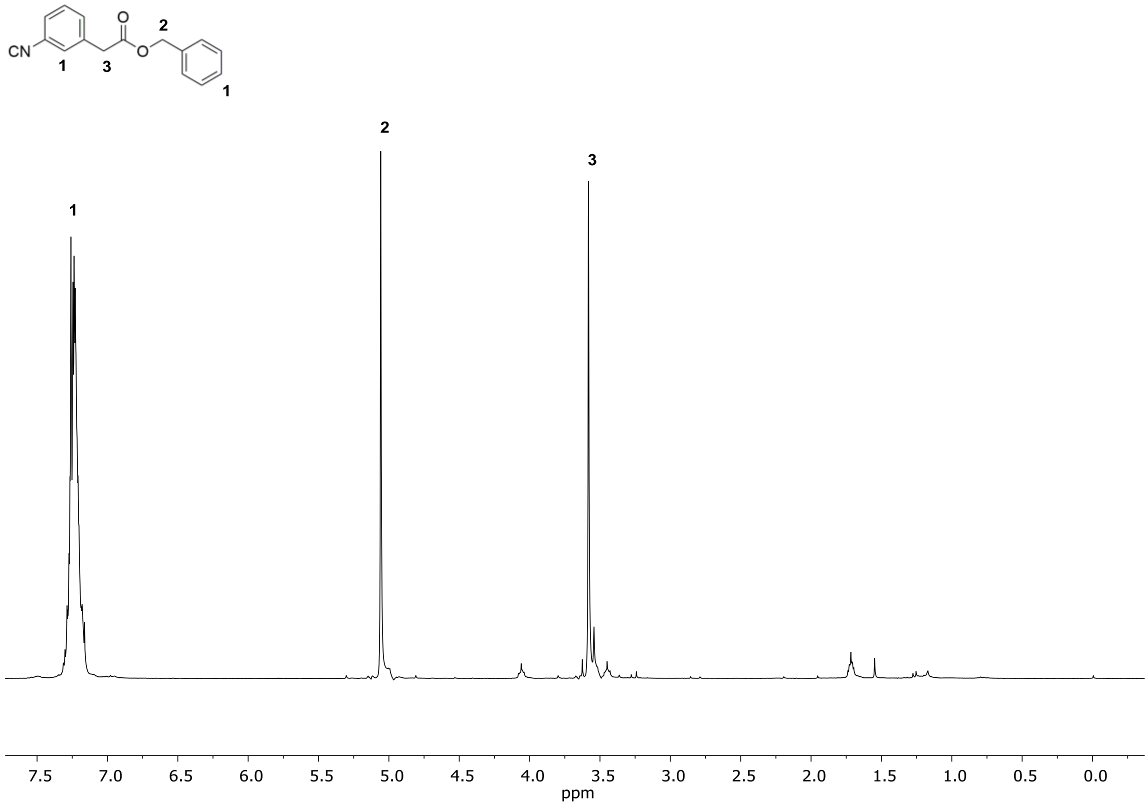
CN
O
2
1
3
1
1
2
3
7.5
7.0
6.5
6.0
5.5
5.0
4.5
4.0
3.5
3.0
2.5
2.0
1.5
1.0
0.5
0.0
ppm

Synthesis of monomer M9 *

Esterification

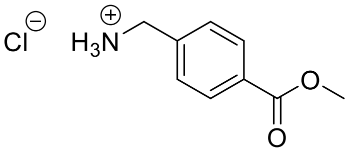

Methanol (74 mL) was added to 4-(aminomethyl)benzoic acid **1i** (5.64 g, 37.0 mmol, 1.00 eq.). Then, the suspension was cooled in an ice bath to 0 °C and thionyl chloride **4** (9.53 mL, 15.5 g, 131 mmol, 3.50 eq.) was added dropwise. Afterwards, the solution was stirred at room temperature for 26 hours. Subsequently, diethyl ether (150 mL) was added and the solution was stored in the freezer overnight. The white precipitate was filtered off and washed with diethyl ether (*ca.* 10 mL). The mother liquor was stored in the freezer once again and the precipitate was filtered off and washed with diethyl ether (*ca.* 10 mL). The desired product **14** (7.10 g, 32.5 mmol) was obtained as a white solid in a yield of 88%.

^{1}H-NMR (300 MHz, CD_3OD) δ/ppm: 8.08 (d, J = 8.4 Hz, 2H, aromatic, ^{1}), 7.56 (d, J = 8.1 Hz, 2H, aromatic, ^{2}), 4.19 (s, 3H, CH_3, ^{3}), 3.91 (s, 2H, CH_2, ^{4}).

^{13}C-NMR (75 MHz, CD_3OD) δ/ppm: 158.3, 139.5, 134.2, 131.2, 130.1, 52.8, 43.9.

HRMS-FAB-MS of $[C_9H_{12}O_2N]^+$ calculated: 166.0863, found: 166.0863.

IR (ATR platinum diamond): ν /cm^{-1} = 3007.7, 2959.9, 2877.6, 2752.1, 2686.2, 2573.2, 1719.6, 1596.1, 1577.6, 1476.8, 1464.5, 1435.7, 1380.2, 1281.4, 1188.9, 1110.7, 1075.8, 1024.3, 960.6, 878.3, 863.9, 835.1, 787.8, 763.1, 701.4, 623.2, 530.7, 475.1.

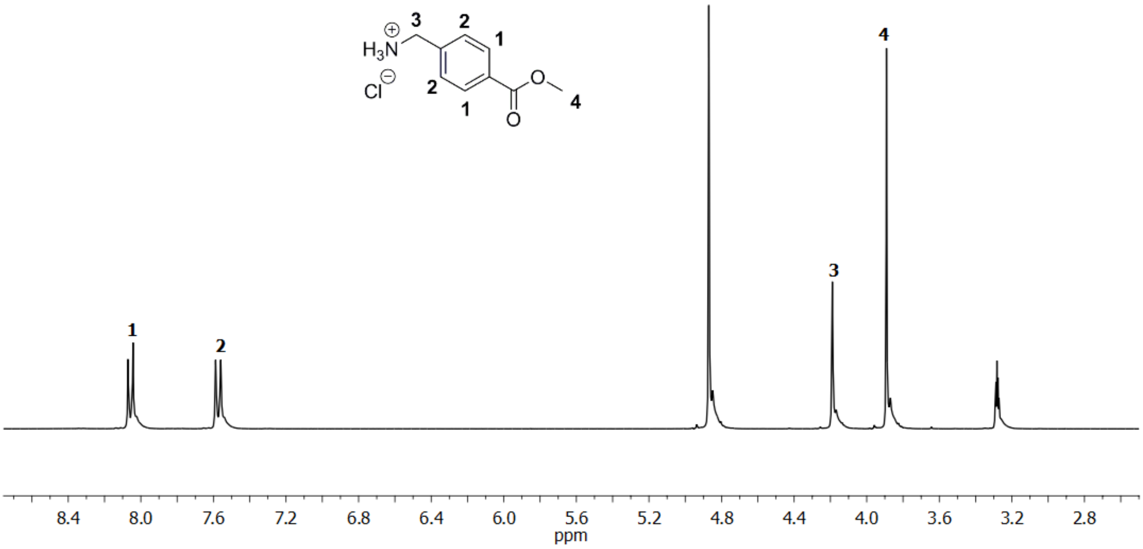

---

[*] Synthesis optimisation was done by Katharina Wetzel. Scale-up was carried out by Roman Nickisch in the Vertieferarbeit "Synthesis of Aromatic AB Monomers for the Synthesis of Sequence-Defined Oligomers" (under lab-supervision of Katharina Wetzel).

N-Formylation

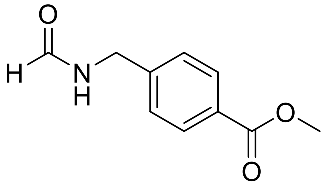

The ammonium salt **14** (7.02 g, 34.8 mmol, 1.00 eq.) was stirred with trimethyl orthoformate **5** (37.7 ml, 36.9 g, 348 mmol, 10.0 eq.) under reflux at 100 °C overnight. Subsequently, the excess of orthoformate **5** was evaporated under reduced pressure to obtain needle-like white crystals. The crude product **15** (6.28 g, 32.5 mmol) was obtained in a yield of 93% and was used without further purification.

^{1}H-NMR (300 MHz, CD_3OD) δ/ppm: 8.25 – 8.18 (m, 1H, CH, ^{1}), 8.07 – 7.90 (d, J = 8.4 Hz, 2H, aromatic, ^{2}), 7.49 – 7.32 (d, J = 8.1 Hz, 2H, aromatic, ^{3}), (4.47 (s, 2H, CH_2, ^{4}), 3.89 (s, 3H, CH_3, ^{5}).

^{13}C-NMR (75 MHz, CD_3OD) δ/ppm: 163.78, 145.08, 130.76, 130.26, 128.77, 128.51, 52.58, 42.27.

HRMS-EI-MS of $[C_{10}H_{11}O_3N]^+$ calculated: 193.0733, found: 193.0736.

IR (ATR platinum diamond): ν /cm^{-1} = 3268.4, 3198.5, 3044.2, 3019.5, 2959.9, 2885.9, 2859.1, 2766.5, 1719.6, 1653.7, 1629.1, 1610.5, 1538.6, 1456.3, 1448.0, 1429.5, 1413.1, 1392.5, 1347.2, 1330.8, 1310.2, 1275.3, 1236.2, 1217.7, 1193.0, 1174.5, 1100.4, 1018.2, 952.3, 843.3, 765.2, 750.8, 724.0, 701.4, 514.2, 489.5.

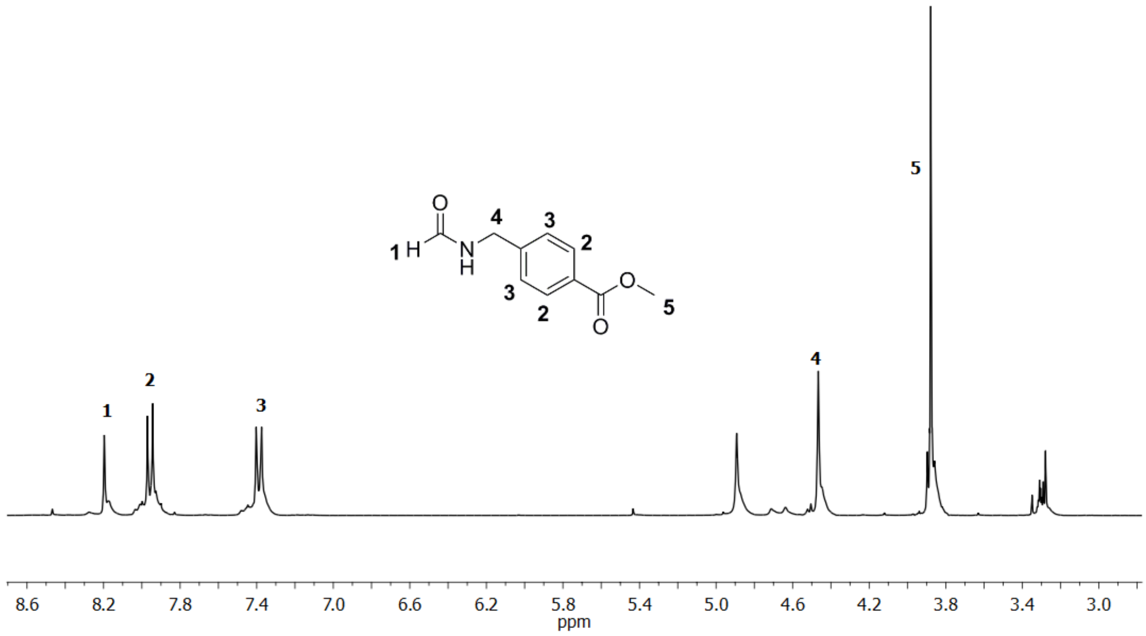

Transesterification

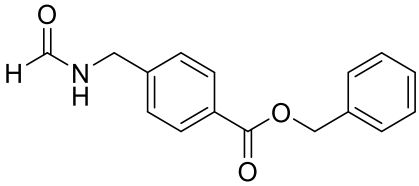

The methyl ester **15** (6.17 g, 31.9 mmol, 1.00 eq.) was dissolved in benzyl alcohol **3** (13.3 mL, 13.8 g, 128 mmol, 4.00 eq.) and DBU **17** (971 mg, 6.38 mmol, 20 mol%) was added. Subsequently, the colourless solution was heated to 150 °C and stirred for 22 hours. Then, the brown solution was purified by column chromatography (cyclohexane/ethyl acetate 7:1 → 0:1). The benzyl ester **16** (3.74 g, 13.9 mmol) was obtained as a yellowish solid in a yield of 44%.

^{1}H-NMR (300 MHz, CD_3OD) δ/ppm: 8.16 – 8.12 (m, 1H, CH, ^{1}), 8.00 – 7.98 (m, 2H, aromatic, ^{2}), 7.44 – 7.28 (m, 7H, aromatic, ^{3}), 5.33 (m, 2H, CH_2, ^{4}), 4.46 (m, 2H, CH_2, ^{5}).

^{13}C-NMR (75 MHz, CD_3OD) δ/ppm: 163.8, 130.89, 129.6, 129.2, 128.6, 115.5, 107.1, 94.8, 92.3, 67.8, 42.3, 33.0.

HRMS-FAB-MS of $[C_{16}H_{16}O_3N]^+$ calculated: 270.1130, found: 270.1132.

IR (ATR platinum diamond): ν /cm^{-1} = 3266.3, 3031.9, 2955.7, 2887.9, 1715.4, 1649.6, 1627.0, 1612.6, 1530.3, 1495.4, 1448.0, 1417.2, 1384.3, 1365.8, 1267.0, 1224.8, 1176.5, 1094.3, 1010.2, 940.0, 915.3, 849.5, 822.8, 754.9, 693.2, 625.3, 596.5, 512.2.

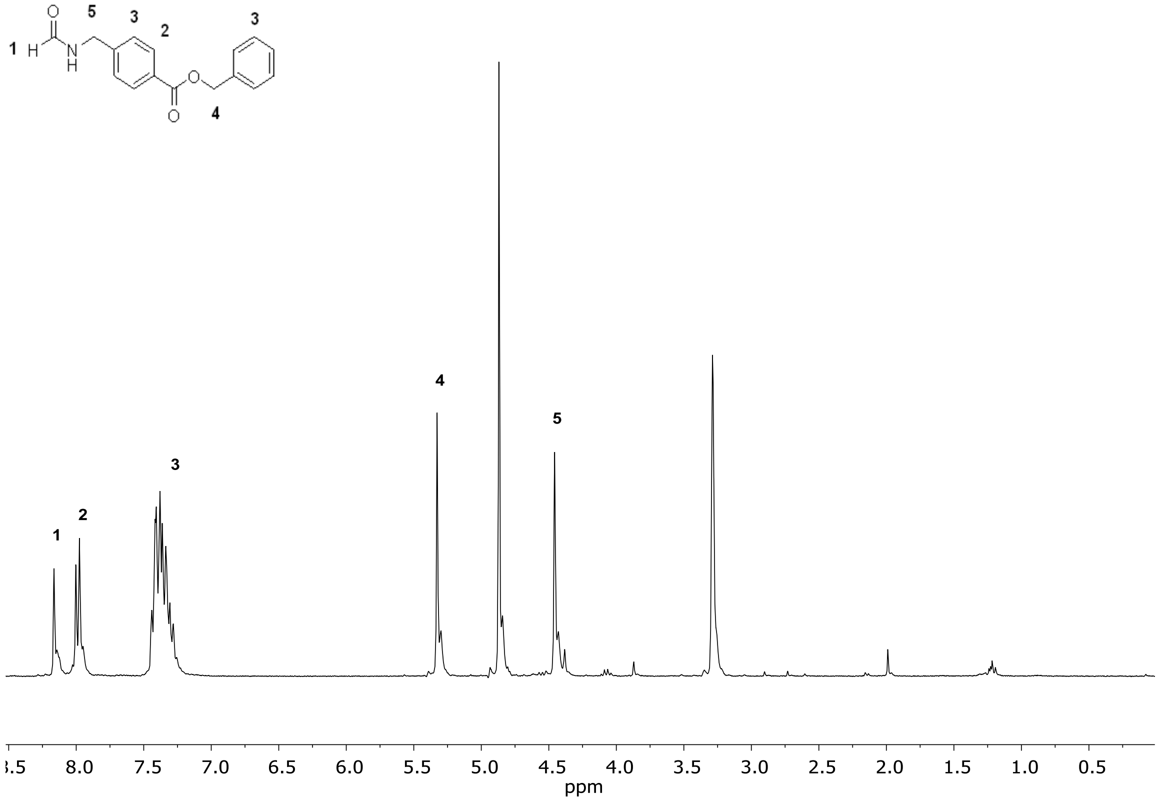

Dehydration

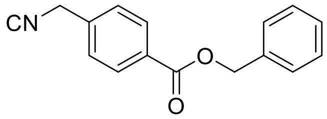

The formamide **16** (3.74 g, 13.9 mmol, 1.00 eq.) was dissolved in DCM (47 mL) and diisopropylamine **7** (6.06 mL, 4.36 g, 43.1 mmol, 3.10 eq.) was added. The slightly yellow solution was cooled to 0 °C using an ice bath. Then, phosphoryl trichloride **6** (1.65 mL, 2.78 g, 18.1 mmol, 1.30 eq.) was added dropwise to the reaction mixture. The reaction mixture was stirred for two hours at room temperature and was cooled to 0 °C again. The reaction was quenched by the addition of a 20 wt% solution of sodium carbonate (17 mL) and stirred for another 30 minutes at room temperature. 15 mL DCM and 15 mL water were added to the mixture and the organic layer was separated. The aqueous phase was extracted with DCM (10 mL). The combined organic layers were washed with water (2x 35 mL) and brine (20 mL), dried over sodium sulfate and the solvent was evaporated under reduced pressure. The crude product was purified by column chromatography (cyclohexane/ethyl acetate 12:1 → 0:1). The isocyanide monomer **M9** (2.66 g, 10.6 mmol) was obtained as an amber solid in a yield of 76%.

^{1}H-NMR (300 MHz, CD_3OD) δ/ppm: 8.06 (d, J = 8.4 Hz, 2H, aromatic, ^{1}), 7.50 – 7.31 (m, 7H, aromatic, ^{2}), 5.34 (s, 2H, CH_2, ^{3}), 4.84 (s, 2H, CH_2, ^{4}).

^{13}C-NMR (75 MHz, CD_3OD) δ/ppm: 165.8, 163.0, 158.8, 150.7, 137.2, 135.9, 130.4, 128.7, 128.3, 126.6, 67.0, 45.3.

HRMS-FAB-MS of $[C_{16}H_{14}O_2N]^+$ calculated: 252.1025, found: 252.1026.

IR (ATR platinum diamond): ν /cm^{-1} = 3052.4, 2935.8, 2149.4, 1713.4, 1612.6, 1495.4, 1456.3, 1427.4, 1417.2, 1380.2, 1320.5, 1273.2, 1178.6, 1104.5, 1016.1, 977.0, 950.3, 915.3, 839.2, 828.9, 734.3, 699.3, 602.7, 508.1, 479.3, 452.5.

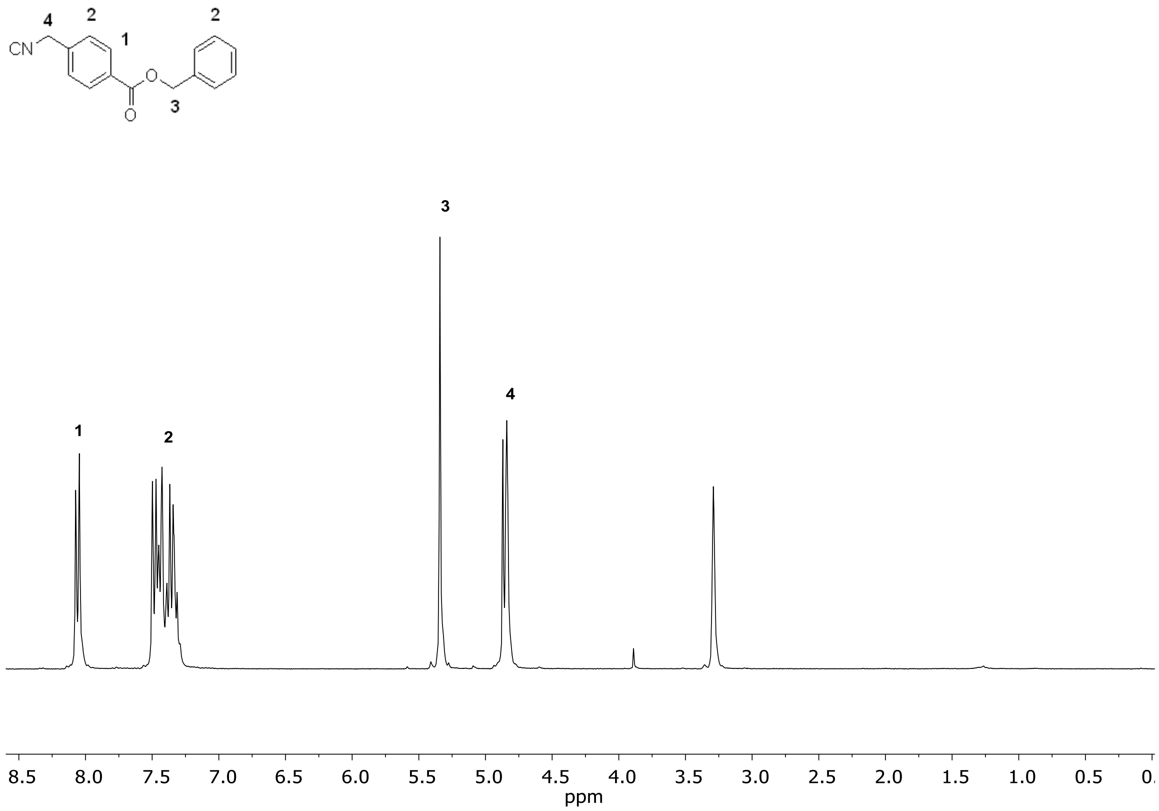
4
2
1
2
CN
O
O
3
3
4
1
2
8.5
8.0
7.5
7.0
6.5
6.0
5.5
5.0
4.5
4.0
3.5
3.0
2.5
2.0
1.5
1.0
0.5
0.
ppm

Evaluation of the reactivity of monomer M9*

Passerini reaction

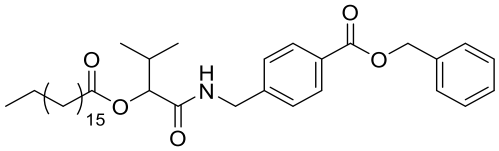

Stearic acid **13** (75.5 mg, 265 µmol, 1.00 eq.) was suspended in DCM (1.15 ml). Subsequently, monomer **M9** (100 mg, 398 µmol, 1.50 eq.) and isobutyraldehyde **11c** (36.0 µL, 28.7 mg, 398 µmol, 1.50 eq.) were added. The reaction mixture was stirred for 48 hours at room temperature, the solvent was evaporated under reduced pressure and the crude product was purified by column chromatography (cyclohexane/ethyl acetate 17:1 → 2:1). The Passerini product **79** (107.6 mg, 177 mmol) was obtained as a white solid in a yield of 45%.

^{1}H-NMR (300 MHz, $CDCl_3$) *δ*/ppm: 8.04 (d, *J* = 8.2 Hz, 2H, aromatic, ^{1}), 7.47 – 7.29 (m, 7H, aromatic, ^{2}), 6.29 (t, *J* = 5.7 Hz, 1H, NH, ^{3}), 5.36 (s, 2H, CH_2, ^{4}), 5.13 (d, *J* = 4.4 Hz, 1H, CH, ^{5}), 4.62 – 4.45 (m, 2H, CH_2, ^{6}), 2.41 – 2.28 (m, 3H, CH_2, CH, ^{7}), 1.69 – 1.57 (m, 2H, CH_2, ^{8}), 1.36 – 1.16 (m, 28H, CH_2, ^{9}), 0.95(dd, *J* = 6.8 Hz, *J* = 3.8 Hz, 6H, CH_3, ^{10}), 0.88 (t, *J* = 6.6 Hz, 3H, CH_3, ^{11}).

^{13}C-NMR (75 MHz, $CDCl_3$) *δ*/ppm: 172.8, 169.7, 157.1, 143.4, 138.6, 130.3, 128.8, 128.4, 128.3, 127.6, 66.9, 42.9, 39.9, 34.4, 32.1, 30.8, 29.8, 29.7, 29.6, 29.5, 29.4, 29.3, 25.2, 22.8, 18.9, 17.2, 14.3.

HRMS-FAB-MS of $[C_{38}H_{58}O_5N]^+$ calculated: 608.4310, found: 608.4308.

IR (ATR platinum diamond): ν/cm-1 = 3280.7, 2914.6, 2848.8, 1719.6, 1655.8, 1552.95, 1468.6, 1376.1, 1269.1, 1234.1, 1174.5, 1098.4, 1020.2, 756.9, 717.9, 695.2.

---

[*] Carried out by Roman Nickisch in the Vertieferarbeit “Synthesis of Aromatic AB Monomers for the Synthesis of Sequence-Defined Oligomers” (under lab-supervision of Katharina Wetzel).

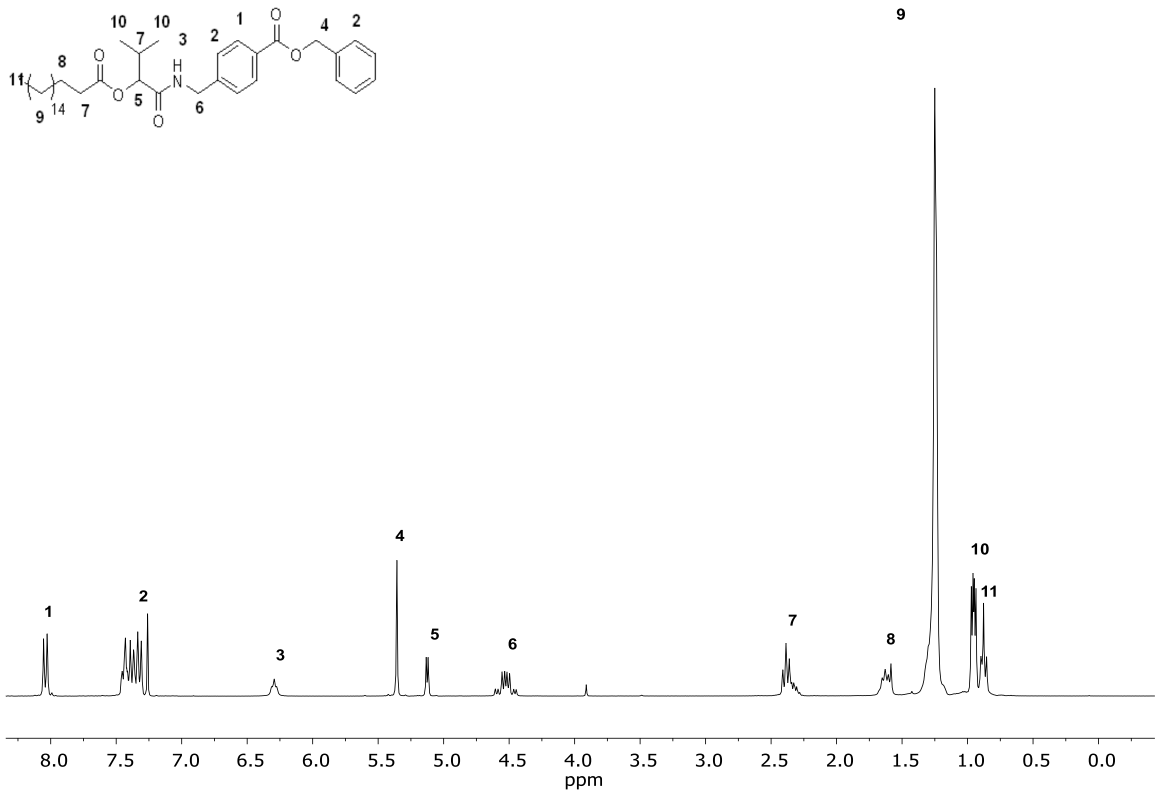

10
7
10
3
2
1
4
2
8
11
9
14
7
5
6
9
4
10
11
1
2
3
5
6
7
8
8.0
7.5
7.0
6.5
6.0
5.5
5.0
4.5
4.0
3.5
3.0
2.5
2.0
1.5
1.0
0.5
0.0
ppm

Deprotection

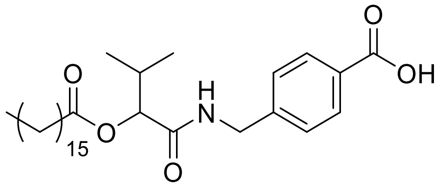

The Passerini product **79** (81.0 mg, 133 µmol, 1.00 eq.) was dissolved in ethyl acetate (2.2 ml) and palladium on activated charcoal **19** (8.10 mg, 10 wt%) was added. Subsequently, the reaction mixture was purged with hydrogen using a balloon and stirred under hydrogen atmosphere for three hours. Afterwards, the heterogeneous catalyst was filtered off and the solvent was evaporated under reduced pressure. The desired deprotected carboxylic acid **80** (34.9 mg, 67.4 µmol) was obtained as a white solid in a yield of 51%.

^{1}H-NMR (300 MHz, $CDCl_3$) *δ*/ppm: 8.05 (d, *J* = 8.0 Hz, 2H, aromatic, ^{1}), 7.35 (d, *J* = 8.1 Hz, 2H, aromatic, ^{2}), 6.42 (t, *J* = 5.9 Hz, 1H, NH, ^{3}), 5.13 (d, *J* = 4.5 Hz, 1H, CH, ^{4}), 4.62 – 4.47 (m, 2H, CH_2, ^{5}), 2.42 – 2.27 (m, 3H, CH_2, CH, ^{6}), 1.71 – 1.56 (m, 2H, CH_2, ^{7}), 1.37 – 1.15 (m, 28H, CH_2, ^{8}), 0.96 (dd, *J* = 6.6 Hz, *J* = 2.8 Hz, 6H, CH_3, ^{9}), 0.87 (t, *J* = 6.3 Hz, 3H CH_3, ^{10}).

^{13}C-NMR (75 MHz, $CDCl_3$) *δ*/ppm: 173.0, 171.1, 163.2, 144.1, 130.8, 128.8, 127.7, 78.1, 43.0, 34.4, 32.1, 30.8, 29.8, 29.7, 29.6, 29.5, 29.4, 29.3, 25.1, 22.8, 18.9, 17.2, 14.2.

HRMS-FAB-MS of $[C_{31}H_{52}O_5N]^+$ calculated: 518.3845, found: 518.3848.

IR (ATR platinum diamond): ν $^{/cm^{-1}}$ = 3280.7, 2914.6, 2848.8, 1734.0, 1690.8, 1655.8, 1612.6, 1553.0, 1468.6, 1431.6, 1378.1, 1348.5, 1293.8, 1236.2, 1172.4, 1110.7, 1005.8, 929.7, 763.1, 719.9, 697.3, 547.1.

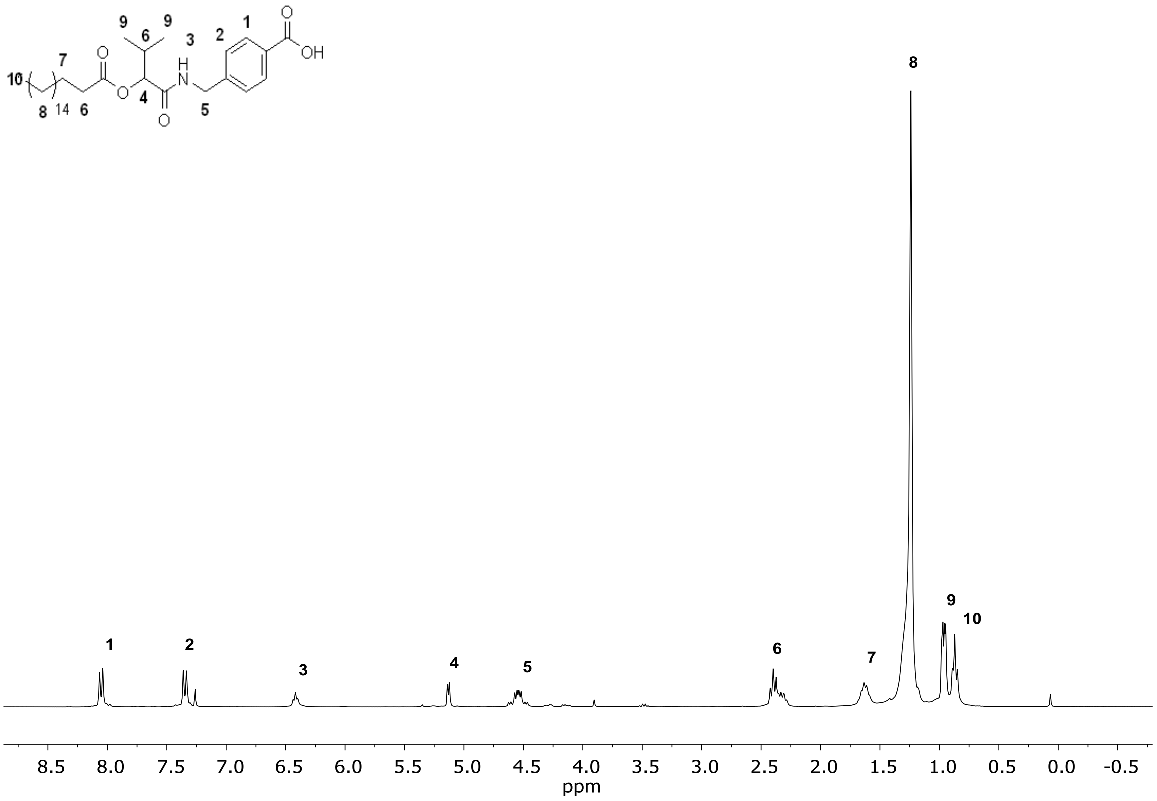

9
9
6
3
2
1
O
OH
7
O
H
N
10
O
4
8
14
6
O
5
8
9
10
1
2
3
4
5
6
7
8.5
8.0
7.5
7.0
6.5
6.0
5.5
5.0
4.5
4.0
3.5
3.0
2.5
2.0
1.5
1.0
0.5
0.0
-0.5
ppm

6.3.2.2 Oligomer synthesis

6.3.2.2.1 Backbone variation

1st Passerini reaction

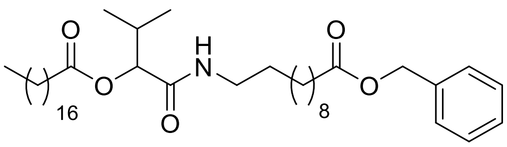

Stearic acid **13** (1.50 g, 5.27 mmol, 1.00 eq.) was suspended in DCM (5.3 mL, 1. M). Subsequently, isobutyraldehyde **11c** (0.73 mL, 0.57 g, 7.91 mmol, 1.50 eq.) and monomer **M1** (2.38 g, 7.91 mmol, 1.50 eq.) were added and the reaction mixture was stirred at room temperature for 24 hours. The solvent was removed under reduced pressure and the crude product was purified by column chromatography (cyclohexane / ethyl acetate 15:1 → 11:1) to obtain the desired product **18** in a yield of 98% (3.40 g, 5.17 mmol) as a white solid.

^{1}H NMR (300 MHz, CDCl$_3$) δ / ppm: 7.41 – 7.28 (m, 5H, ^{1}), 6.00 – 5.90 (m, 1H, ^{2}), 5.11 (s, *J* = 5.4 Hz, 2H, ^{3}), 5.07 (d, *J* = 4.4 Hz, 1H, ^{4}), 3.36 – 3.15 (m, 2H, ^{5}), 2.48 – 2.24 (m, 5H, ^{6}), 1.72 – 1.53 (m, 4H, ^{7}), 1.53 – 1.42 (m, 2H, ^{8}), 1.40 – 1.17 (m, 40H, ^{9}), 1.01 – 0.79 (m, 9H, ^{10}).

^{13}C NMR (101 MHz, CDCl$_3$) δ / ppm: 173.78, 172.66, 169.37, 136.25, 128.65, 128.27, 78.00, 66.17, 39.26, 34.43, 32.05, 30.63, 29.82, 29.78, 29.73, 29.70, 29.59, 29.55, 29.48, 29.46, 29.39, 29.32, 29.29, 29.22, 26.96, 25.17, 25.05, 22.81, 18.91, 17.04, 14.25.

HRMS-FAB-MS of $[C_{41}H_{72}N_1O_5]^+$: calculated: 658.5405 found: 658.5404.

IR (ATR platinum diamond): ν / cm^{-1} = 3286.3, 3091.2, 2916.3, 2848.8, 1737.5, 1649.5, 1551.1, 1498.2, 1469.7, 1416.1, 1379.3, 1294.7, 1272.0, 1254.6, 1233.1, 1212.7, 1157.0, 1108.5, 1031.8, 1013.1, 986.7, 927.3, 721.6, 693.6, 578.5, 521.2, 474.1, 414.3.

***R*$_f$** : (cyclohexane / ethyl acetate 5:1) = 0.41.

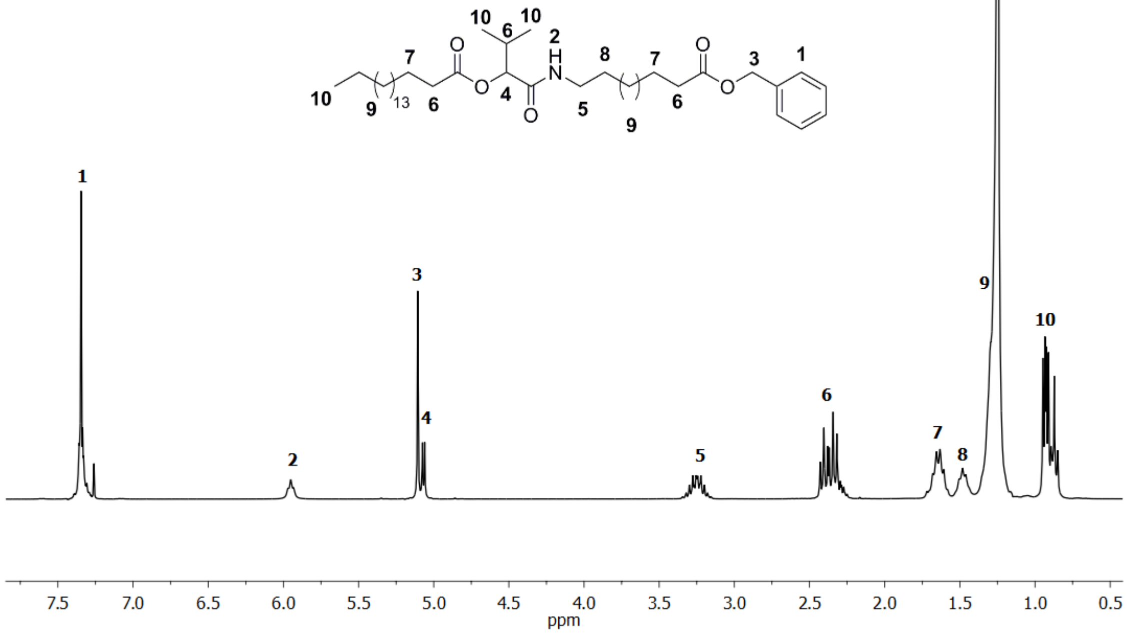
10
6
10
2
H
N
O
O
O
O
O
O
7
8
7
3
1
10
9
13
6
4
5
9
6
1
2
3
4
5
6
7
8
9
10
7.5
7.0
6.5
6.0
5.5
5.0
4.5
4.0
3.5
3.0
2.5
2.0
1.5
1.0
0.5
ppm

1st deprotection

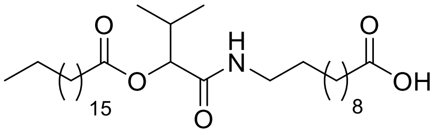

Substance **18** (2.10 g, 3.19 mmol, 1.00 eq.) was dissolved in ethyl acetate (6.4 mL, 0.5 M). Subsequently, palladium on activated charcoal **19** (0.21 g, 10 wt%.) was suspended in the solution. The reaction mixture was purged with hydrogen (2 balloons) and stirred under hydrogen atmosphere overnight. The heterogeneous catalyst was filtered off and the solvent was evaporated under reduced pressure to obtain the desired product **20** in a yield of 87% (1.57 g, 2.77 mmol) as a white solid.

^{1}H NMR (300 MHz, $CDCl_3$) δ / ppm: 6.11 – 5.89 (m, 1H, ^{1}), 5.06 (d, *J* = 4.4 Hz, 1H, ^{2}), 3.40 – 3.14 (m, 2H, ^{3}), 2.45 – 2.23 (m, 5H, ^{4}), 1.70 – 1.54 (m, 4H, ^{5}), 1.52 – 1.37 (m, 2H, ^{6}), 1.24 (s, 40H, ^{7}), 0.97 – 0.73 (m, 9H, ^{8}).

^{13}C NMR (101 MHz, $CDCl_3$) δ / ppm: 179.36, 172.72, 169.54, 132.72, 78.01, 39.30, 34.44, 34.12, 32.05, 30.62, 29.82, 29.78, 29.73, 29.64, 29.59, 29.48, 29.39, 29.28, 29.25, 29.11, 27.50, 27.10, 26.92, 25.17, 24.79, 22.81, 18.89, 17.04, 14.24.

HRMS-FAB-MS of $[C_{34}H_{66}N_1O_5]^+$: calculated: 568.4936 found: 568.4935.

IR (ATR platinum diamond): ν / cm^{-1} = 3288.8, 2913.5, 2849.4, 2341.8, 1736.2, 1701.5, 1653.4, 1561.1, 1470.5, 1431.5, 1410.1, 1373.7, 1349.8, 1326.2, 1271.2, 1253.1, 1234.7, 1215.2, 1199.7, 1098.2, 1023.5, 920.6, 716.4, 682.7, 534.2, 454.0, 410.8.

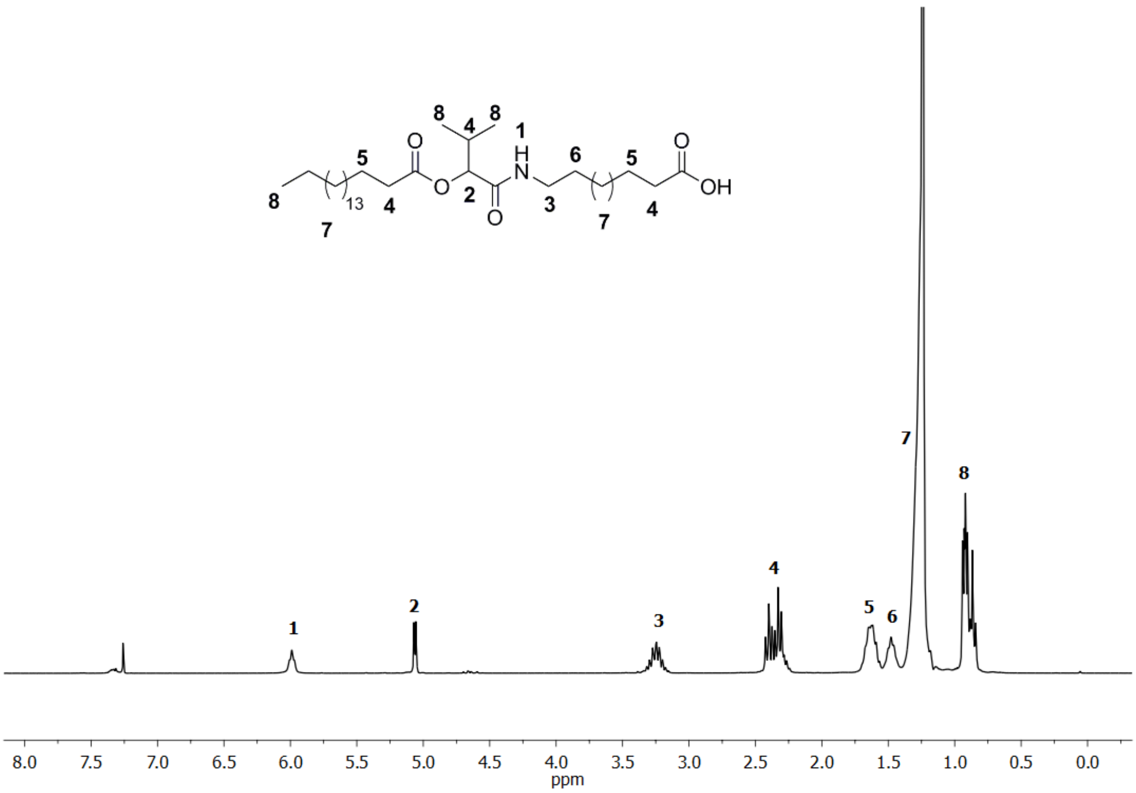
8
4
8
1
H
N
6
5
O
5
O
O
OH
8
13
4
2
O
3
7
4
7
1
2
3
4
5
6
7
8
8.0
7.5
7.0
6.5
6.0
5.5
5.0
4.5
4.0
3.5
3.0
2.5
2.0
1.5
1.0
0.5
0.0
ppm

2nd Passerini reaction

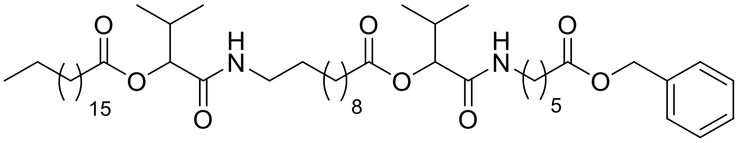

Substance **20** (1.49 g, 2.62 mmol, 1.0 eq.) was dissolved in DCM (5.2 mL, 0.5 M). Subsequently, isobutyraldehyde **11c** (0.36 mL, 0.28 g, 3.93 mmol, 1.5 eq.) and monomer **M2** (0.91 g, 3.93 mmol, 1.5 eq.) were added and the reaction mixture was stirred at room temperature for 24 hours. The solvent was removed under reduced pressure and the crude product was purified by column chromatography (cyclohexane / ethyl acetate 10:1 → 0:1) to obtain the desired product **22** in a yield of 98% (2.24 g, 2.57 mmol) as a white solid.

^{1}H NMR (300 MHz, CDCl$_3$) δ / ppm: 7.39 – 7.19 (m, 5H, ^{1}), 6.08 – 5.90 (m, 2H, ^{2}), 5.09 (s, 2H, ^{3}), 5.06 – 5.01 (m, 2H, ^{4}), 3.33 – 3.09 (m, 4H, ^{5}), 2.44 – 2.18 (m, 8H, ^{6}), 1.72 – 1.40 (m, 6H, ^{7}), 1.39 – 1.29 (m, 4H, ^{8}), 1.28 – 1.03 (m, 42H, ^{9}), 1.01 – 0.61 (m, 15H, ^{10}).

^{13}C NMR (101 MHz, CDCl$_3$) δ / ppm: 173.40, 172.65, 169.42, 169.37, 136.09, 128.64, 128.30, 128.26, 77.97, 66.23, 39.21, 38.94, 34.39, 34.34, 34.12, 32.00, 30.60, 29.77, 29.67, 29.54, 29.50, 29.42, 29.32, 29.24, 29.19, 26.90, 26.35, 25.12, 25.06, 24.49, 22.77, 18.86, 17.03, 14.20.

HRMS-ESI-MS of [M+H]$^+$ [C$_{52}$H$_{91}$N$_2$O$_8$]$^+$: calculated: 871.6770 found: 871.6764.

IR (ATR platinum diamond): ν / cm^{-1} = 3277.4, 3091.4, 2916.4, 2849.9, 1739.2, 1650.7, 1562.7, 1467.6, 1371.6, 1271.5, 1253.6, 1233.8, 1214.1, 1160.5, 1101.8, 995.9, 924.3, 721.0, 697.0.

***R*$_f$** : (cyclohexane / ethyl acetate 2:3) = 0.55.

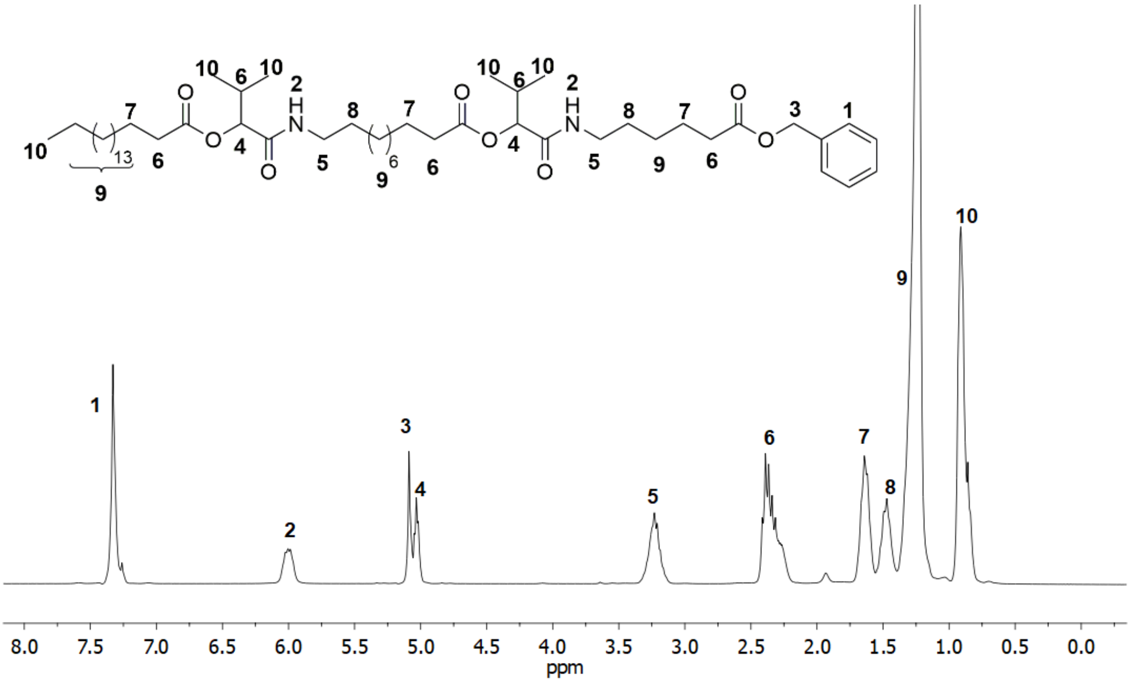

2nd deprotection

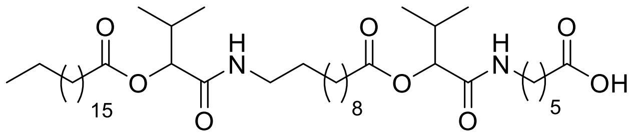

Substance **22** (2.08 g, 2.41 mmol, 1.00 eq.) was dissolved in ethyl acetate (5.0 mL, 0.5 M). Subsequently, palladium on activated charcoal **19** (0.20 g, 10 wt%.) was suspended in the solution. The reaction mixture was purged with hydrogen (2 balloons) and stirred under hydrogen atmosphere overnight. The heterogeneous catalyst was filtered off and the solvent was evaporated under reduced pressure to obtain the desired product **27** in a yield of 93% (1.74 g, 2.23 mmol) as a white solid.

^{1}H NMR (300 MHz, CDCl$_3$) δ / ppm: 6.26 – 6.03 (m, 2H, ^{1}), 5.07 – 5.01 (m, 2H, ^{2}), 3.34 – 3.14 (m, 4H, ^{3}), 2.36 (dt, J = 15.2, 7.0 Hz, 8H, ^{4}), 1.76 – 1.63 (m, 6H, ^{5}), 1.64 – 1.41 (m, 4H, ^{6}), 1.24 (s, 42H, ^{7}), 0.99 – 0.72 (m, 15H, ^{8}).

^{13}C NMR (101 MHz, CDCl$_3$) δ / ppm: 177.69, 172.75, 172.73, 169.63, 77.97, 39.30, 39.00, 34.38, 34.33, 33.84, 32.00, 30.58, 29.77, 29.73, 29.68, 29.60, 29.54, 29.50, 29.43, 29.34, 29.28, 29.23, 29.20, 26.87, 26.32, 25.11, 25.07, 24.37, 22.76, 18.84, 17.05, 17.03, 14.19..

HRMS-ESI-MS of $[C_{49}H_{85}N_2O_{10}]^+$: calculated: 781.6300 found: 781.6297.

IR (ATR platinum diamond): ν / cm^{-1} = 3258.9, 3091.2, 2916.9, 2850.0, 1742.1, 1650.4, 1544.7, 1466.8, 1415.8, 1370.8, 1271.8, 1233.7, 1213.8, 1191.0, 1160.8, 1103.4, 1011.4, 927.6, 720.9, 414.4.

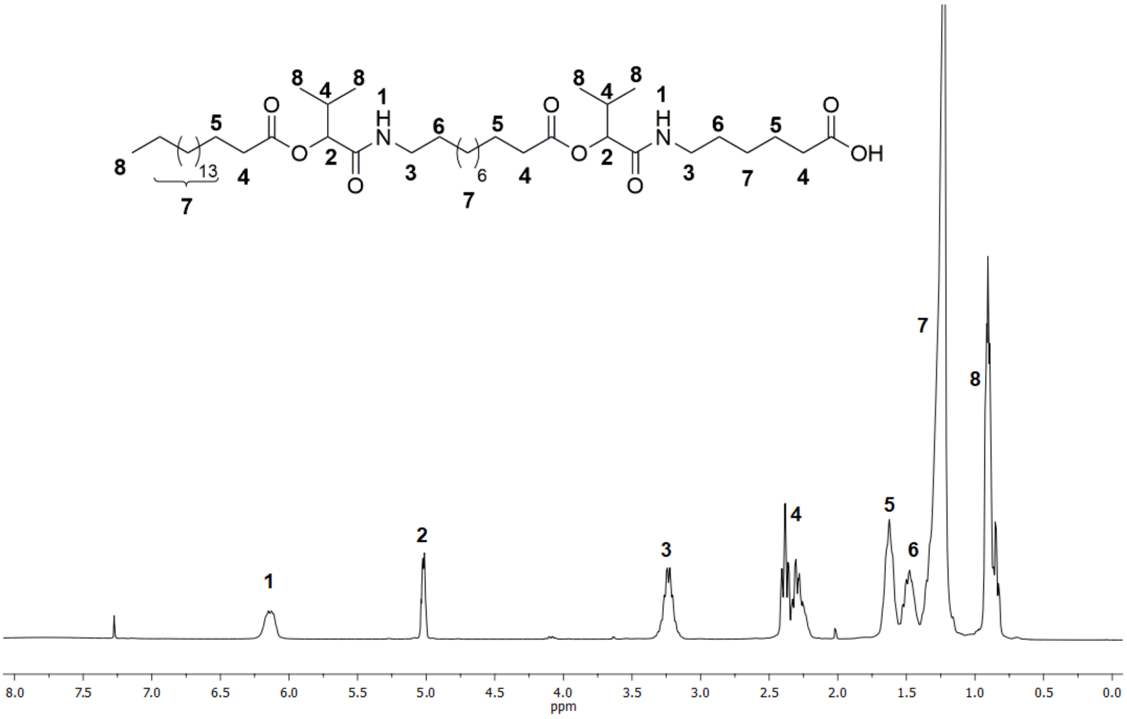

3rd Passerini reaction

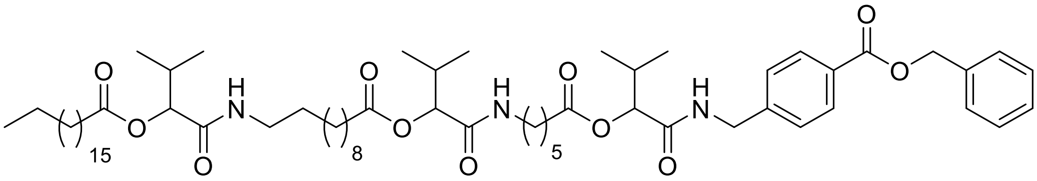

Substance **27** (1.47 g, 1.89 mmol, 1.00 eq.) was dissolved in DCM (5.4 mL, 0.3 M). Subsequently, isobutyraldehyde **11c** (0.26 mL, 0.20 g, 2.83 mmol, 1.50 eq.) and monomer **M9** (0.71 g, 2.83 mmol, 1.50 eq.) were added and the reaction mixture was stirred at room temperature for 48 hours. The solvent was removed under reduced pressure and the crude product was purified by column chromatography (cyclohexane / ethyl acetate 7:1 → 0:1) to obtain the desired product **23** in a yield of 99% (2.24 g, 1.88 mmol) as a yellowish oil.

^{1}H NMR (300 MHz, CDCl$_3$) δ / ppm: 8.03 (d, J = 8.2 Hz, 2H, ^{1}), 7.48 – 7.29 (m, 7H, ^{2}), 6.49 (s, 1H, ^{3}), 5.99 (m, 2H, ^{4}), 5.35 (s, 2H, ^{5}), 5.12 – 4.96 (m, 3H, ^{6}), 4.65 – 4.43 (m, 2H, ^{7}), 3.38 – 3.17 (m, 4H, ^{8}), 2.48 – 2.18 (m, 9H, ^{9}), 1.77 – 1.57 (m, 6H, ^{10}), 1.63 – 1.38 (m, 11.2 Hz, 4H, ^{11}), 1.25 (s, 42H, ^{12}), 1.00 – 0.77 (m, 21H, ^{13}).

^{13}C NMR (101 MHz, CDCl$_3$) δ / ppm: 172.76, 172.70, 172.60, 169.69, 169.54, 169.42, 166.23, 143.65, 136.05, 129.60, 129.38, 128.93, 128.51, 128.07, 127.82, 127.37, 77.92, 66.82, 39.24, 34.34, 32.01, 30.66, 30.55, 29.78, 29.25, 28.19, 27.32, 26.17, 25.14, 24.41, 22.78, 21.14, 18.92, 18.32, 14.14.

HRMS-ESI-MS [M+H]$^+$of [$C_{65}H_{105}N_3O_{11}$]: calculated: 1104.7822 found: 1104.7820.

IR (ATR platinum diamond): ν / cm^{-1} = 3274.4, 3090.9, 2918.7, 2850.9, 1741.7, 1650.4, 1612.8, 1533.3, 1465.8, 1416.5, 1371.2, 1270.1, 1161.4, 1102.1, 1018.0, 747.6, 721.6, 696.8, 525.4, 411.0.

***R*$_f$** : (cyclohexane / ethyl acetate 1:1) = 0.58.

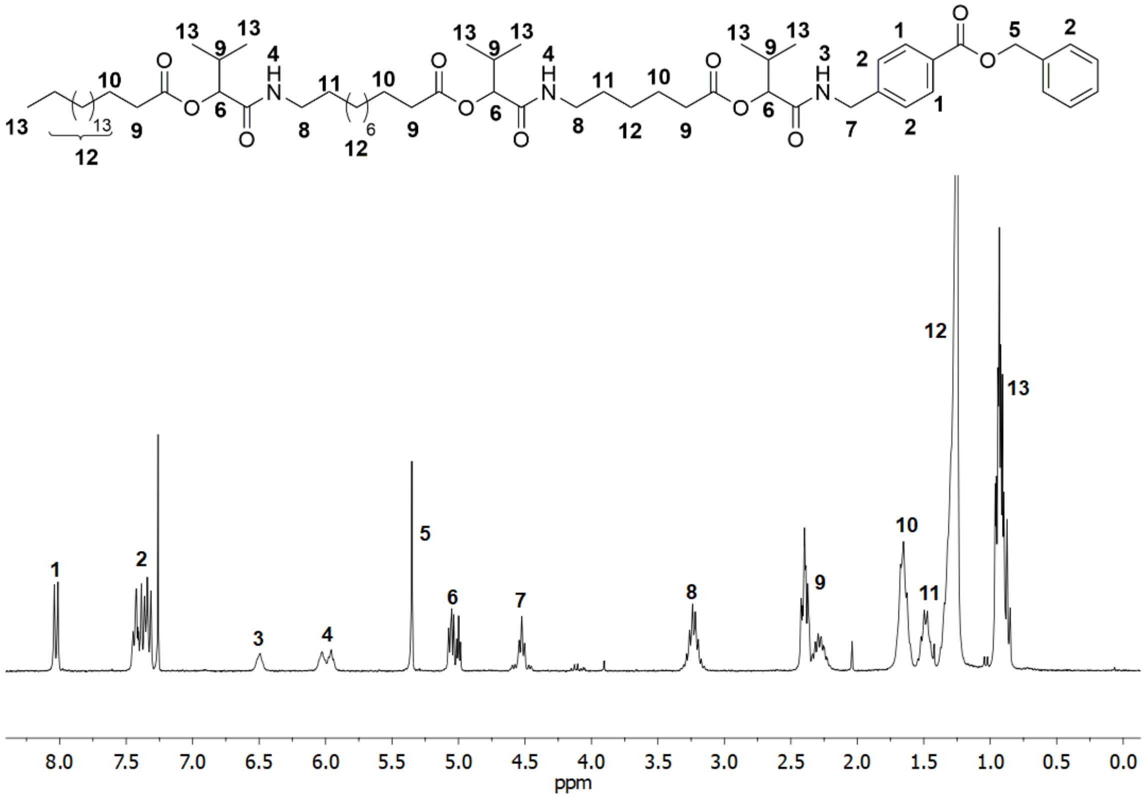
1
2
3
4
5
6
7
8
9
10
11
12
13
8.0
7.5
7.0
6.5
6.0
5.5
5.0
4.5
4.0
3.5
3.0
2.5
2.0
1.5
1.0
0.5
0.0
ppm

3rd deprotection

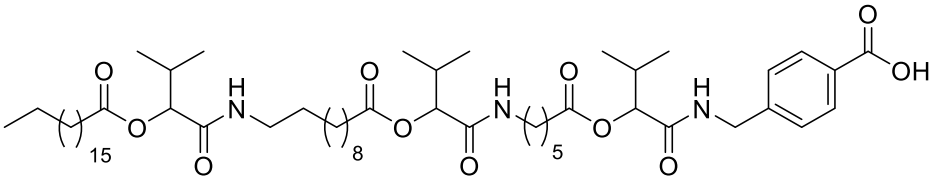

Substance **23** (2.07 g, 1.87 mmol, 1.00 eq.) was dissolved in ethyl acetate (3.80 mL, 0.5 M). Subsequently, palladium on activated charcoal **19** (0.21 g, 10 wt%.) was suspended in the solution. The reaction mixture was purged with hydrogen (3 balloons) and stirred under hydrogen atmosphere overnight. The heterogeneous catalyst was filtered off and the solvent was evaporated under reduced pressure to obtain the desired product **28** in a yield of 81% (1.53 g, 1.51 mmol) as a white solid.

^{1}H NMR (400 MHz, $CDCl_3$) δ / ppm: 8.04 – 7.92 (m, 2H, ^{1}), 7.36 – 7.28 (m, 2H, ^{2}), 6.79 (s, 1H, ^{3}), 6.20 (s, 2H, ^{4}), 5.04 (d, *J* = 1.6 Hz, 1H, ^{5}), 5.00 – 4.94 (m, 2H, ^{6}), 4.60 – 4.40 (m, 2H, ^{7}), 3.21 (dd, *J* = 14.4, 7.3 Hz, 4H, ^{8}), 2.36 (dd, *J* = 14.4, 8.1 Hz, 9H, ^{9}), 1.70 – 1.54 (m, 6H, ^{10}), 1.47 (d, *J* = 6.3 Hz, 4H, ^{11}), 1.23 (s, 42H, ^{12}), 1.05 – 0.70 (m, 21H, ^{13}).

^{13}C NMR (101 MHz, $CDCl_3$) δ / ppm: 172.94, 172.78, 169.82, 169.76, 169.68, 143.97, 130.55, 129.02, 127.60, 78.24, 78.05, 77.97, 77.36, 42.90, 39.31, 38.84, 34.40, 34.33, 34.00, 32.01, 30.70, 30.60, 29.78, 29.74, 29.69, 29.61, 29.56, 29.49, 29.45, 29.41, 29.36, 29.25, 29.21, 29.18, 26.88, 26.14, 25.12, 25.05, 24.39, 22.78, 18.87, 17.29, 17.12, 17.03, 14.22.

HRMS-ESI-MS $[M+H]^+$ of $[C_{58}H_{99}N_3O_{11}]$: calculated: 1014.7352 found: 1014.7343.

IR (ATR platinum diamond): ν / cm^{-1} = 3276.6, 3091.0, 2917.1, 2850.2, 1740.2, 1692.1, 1651.0, 1613.2, 1547.0, 1466.4, 1433.1, 1370.1, 1317.1, 1294.0, 1234.1, 1164.4, 1017.0, 929.3, 854.2, 762.1, 720.9, 548.8, 414.9.

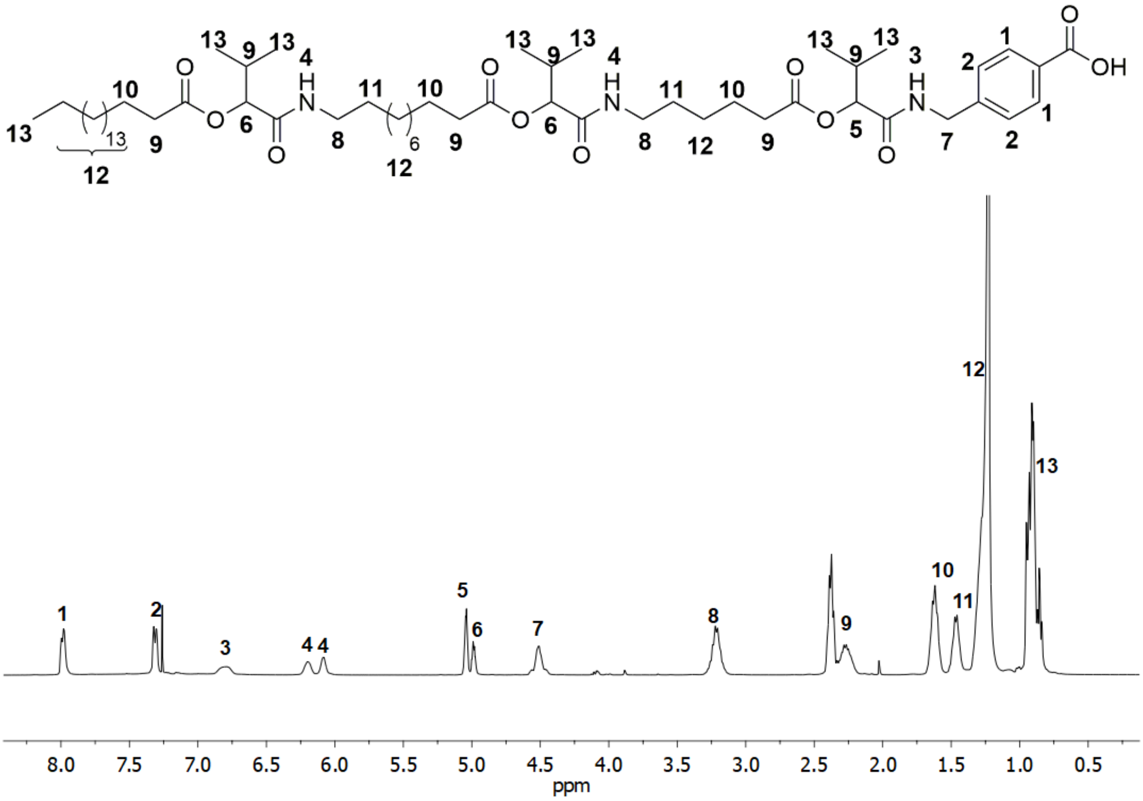
13
9
13
4
O
10
H
N
11
10
O
6
9
12
6
O
8
12
9
13
12
5
3
7
2
1
OH
8.0
7.5
7.0
6.5
6.0
5.5
5.0
4.5
4.0
3.5
3.0
2.5
2.0
1.5
1.0
0.5
ppm

4th Passerini reaction

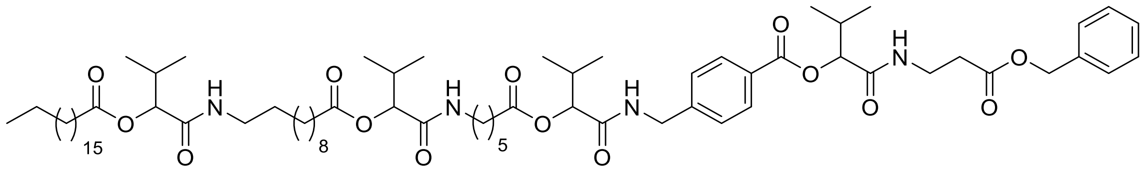

Substance **28** (1.35 g, 1.35 mmol, 1.00 eq.) was dissolved in DCM (2.70 mL, 0.5 M). Subsequently, isobutyraldehyde **11c** (0.18 mL, 0.14 g, 2.00 mmol, 1.50 eq.) and monomer **M4** (0.38 g, 2.00 mmol, 1.50 eq.) were added and the reaction mixture was stirred at room temperature for 48 hours. The solvent was removed under reduced pressure and the crude product was purified by column chromatography (cyclohexane / ethyl acetate 3:1 → 1:3) to obtain the desired product **25** in a yield of 92% (1.57 g, 1.23 mmol) as a yellowish oil.

^{1}H NMR (400 MHz, $CDCl_3$) δ / ppm: 8.00 (d, J = 8.1 Hz, 2H, ^{1}), 7.39 – 7.22 (m, 7H, ^{2}), 6.79 – 6.64 (m, 2H, ^{3}), 6.04 (dt, J = 11.1, 4.7 Hz, 2H, ^{4}), 5.26 – 4.92 (m, 4H, ^{5}), 4.62 – 4.42 (m, 2H, ^{6}), 3.62 – 3.41 (m, 2H, ^{7}), 3.32 – 3.09 (m, 5H, ^{8}), 2.68 – 2.18 (m, 11H, ^{9}), 1.70 – 1.57 (m, 6H, ^{10}), 1.54 – 1.38 (m, 4H, ^{11}), 1.36 – 1.15 (m, 42H, ^{12}), 1.03 – 0.72 (m, 28H, ^{13}).

^{13}C NMR (101 MHz, $CDCl_3$) δ / ppm: 172.77, 172.68, 172.62, 172.27, 169.74, 169.70, 169.51, 169.45, 169.39, 165.26, 144.30, 135.59, 130.24, 128.67, 128.53, 128.45, 128.28, 127.76, 127.73, 78.61, 78.16, 77.99, 77.94, 66.59, 42.82, 39.21, 38.72, 34.69, 34.38, 34.32, 34.02, 33.92, 31.99, 30.84, 30.71, 30.58, 29.76, 29.72, 29.67, 29.65, 29.54, 29.49, 29.43, 29.41, 29.34, 29.26, 29.23, 29.18, 26.89, 26.12, 25.11, 25.05, 24.38, 24.32, 22.76, 18.95, 18.85, 17.26, 17.05, 17.01, 14.27, 14.20.

HRMS-ESI-MS $[M+H]^+$ of $[C_{73}H_{118}N_4O_{14}]$: calculated: 1275.8717 found: 1275.8743.

IR (ATR platinum diamond): ν / cm^{-1} = 3289.2, 3090.0, 2918.5, 2850.8, 1738.0, 1650.8, 1533.3, 1465.8, 1416.6, 1369.9, 1254.6, 1162.5, 1101.8, 1017.8, 927.8, 747.1, 721.0, 697.5, 410.2.

R_f : (cyclohexane / ethyl acetate 1:3) = 0.48.

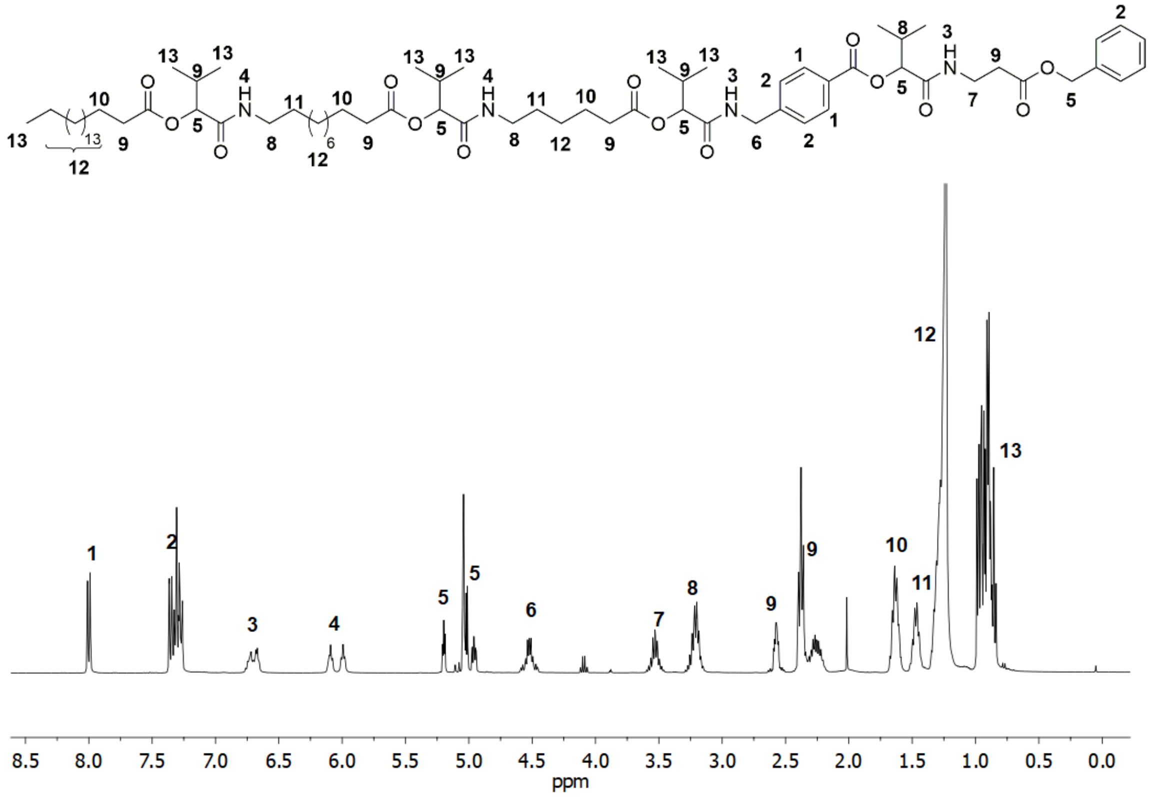
1
2
3
4
5
5
6
7
8
9
9
10
11
12
13
8.5
8.0
7.5
7.0
6.5
6.0
5.5
5.0
4.5
4.0
3.5
3.0
2.5
2.0
1.5
1.0
0.5
0.0
ppm

4th deprotection

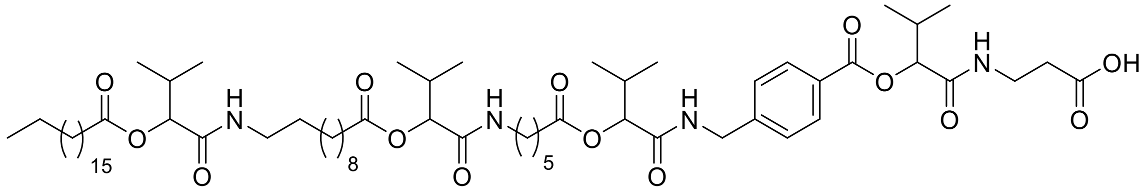

Substance **24** (1.49 g, 1.16 mmol, 1.00 eq.) was dissolved in ethyl acetate (5.0 mL, 0.25 M). Subsequently, palladium on activated charcoal **19** (0.15 g, 10 wt%.) was suspended in the solution. The reaction mixture was purged with hydrogen (3 balloons) and stirred under hydrogen atmosphere overnight. The heterogeneous catalyst was filtered off and the solvent was evaporated under reduced pressure to obtain the desired product **29** in a yield of 99% (1.41 g, 1.16 mmol) as a highly viscous oil.

^{1}H NMR (300 MHz, CDCl$_3$) δ / ppm: 8.00 (d, J = 8.1 Hz, 2H, ^{1}), 7.35 (t, J = 7.6 Hz, 2H, ^{2}), 7.12 – 6.83 (m, 2H, ^{3}), 6.38 – 5.95 (m, 2H, ^{4}), 5.32 – 5.16 (m, 1H, ^{5}), 5.13 – 4.89 (m, 3H, ^{6}), 4.61 – 4.32 (m, 2H, ^{7}), 3.57 – 3.40 (m, 2H, ^{8}), 3.31 – 3.05 (m, 4H, ^{9}), 2.59 – 2.13 (m, 12H, ^{10}), 1.62 (d, J = 6.7 Hz, 6H, ^{11}), 1.46 (s, 4H, ^{12}), 1.28 (d, J = 26.4 Hz, 42H, ^{13}), 1.14 – 0.79 (m, 27H, ^{14}).

^{13}C NMR (101 MHz, CDCl$_3$) δ / ppm: 174.60, 172.91, 172.74, 170.02, 169.97, 169.64, 165.26, 144.22, 130.22, 128.45, 127.67, 107.71, 106.44, 103.88, 100.08, 78.46, 78.35, 77.91, 68.03, 67.74, 67.51, 67.42, 67.10, 66.10, 42.83, 41.17, 39.27, 38.86, 34.52, 34.38, 34.30, 33.94, 33.56, 32.36, 32.00, 30.92, 30.59, 29.78, 29.73, 29.68, 29.60, 29.55, 29.49, 29.44, 29.41, 29.35, 29.26, 29.24, 29.22, 29.18, 28.94, 26.88, 26.08, 25.68, 25.11, 25.04, 24.29, 23.92, 23.48, 22.77, 18.99, 18.86, 17.39, 17.30, 17.06, 17.01, 14.22.

HRMS-ESI-MS [M+H]$^+$ of [C$_{66}$H$_{112}$N$_4$O$_{14}$]: calculated: 1185.8248 found: 1185.8254.

IR (ATR platinum diamond): ν / cm^{-1} = 3271.1, 3090.3, 2918.3576, 3.7671, 1741.1, 1650.3, 1537.7, 1465.8, 1416.5, 1370.0, 1254.2, 1162.1, 1102.0, 994.5, 926.7, 720.1.

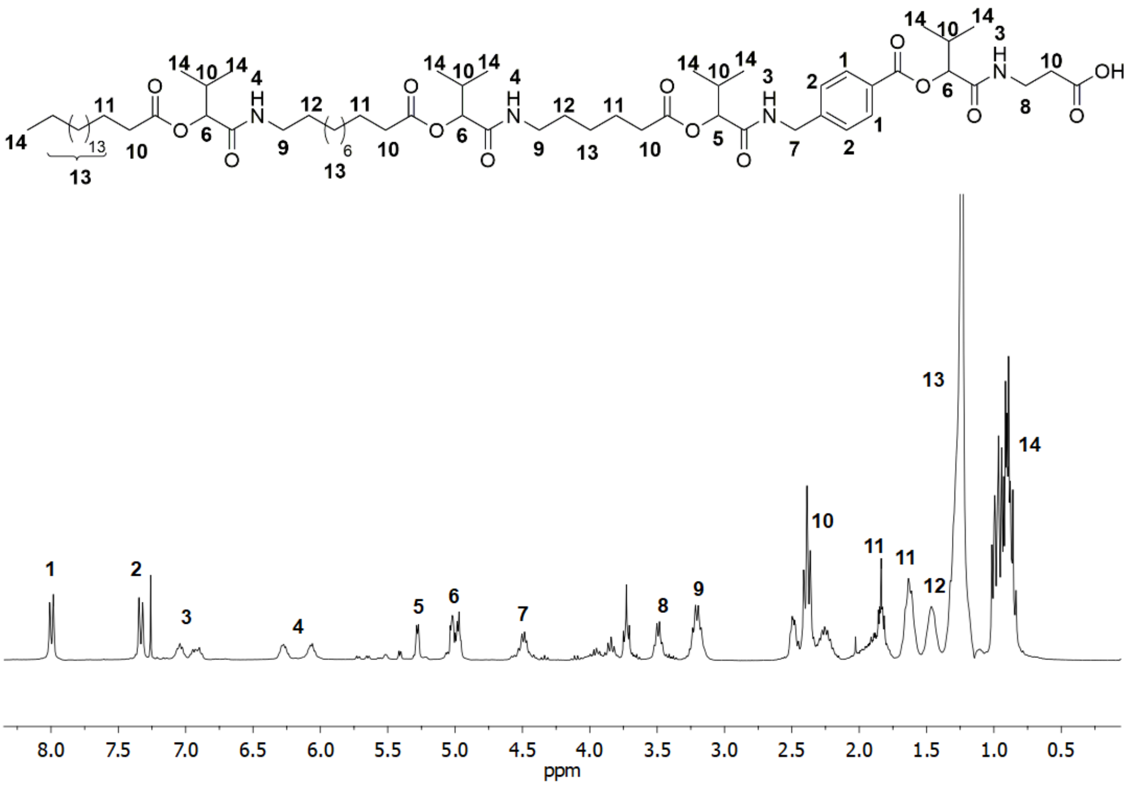
1
2
3
4
5
6
7
8
9
10
11
11
12
13
14
8.0
7.5
7.0
6.5
6.0
5.5
5.0
4.5
4.0
3.5
3.0
2.5
2.0
1.5
1.0
0.5
ppm
OH

5th Passerini reaction

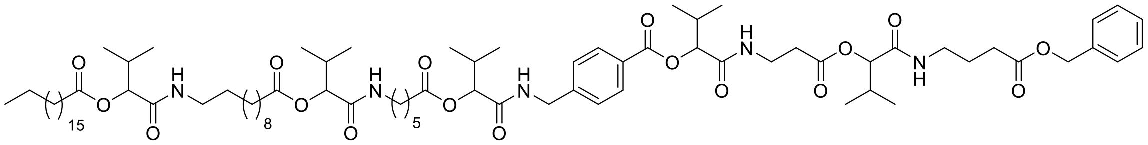

Substance **29** (1.39 g, 1.18 mmol, 1.00 eq.) was dissolved in DCM (4.0 mL, 0.3 M). Subsequently, isobutyraldehyde **11c** (164 µL, 129 mg, 1.80 mmol, 1.50 eq.) and monomer **M5** (366 mg, 1.80 mmol, 1.50 eq.) were added and the reaction mixture was stirred at room temperature for 48 hours. The solvent was removed under reduced pressure and the crude product was purified by column chromatography (cyclohexane / ethyl acetate 2:1 → 1:4) to obtain the desired product **29** in a yield of 82% (1.40 g, 0.96 mmol) as a highly viscous oil.

^{1}H NMR (400 MHz, $CDCl_3$) δ / ppm: 8.06 – 7.94 (m, 2H, ^{1}), 7.34 (d, *J* = 7.9 Hz, 7H, ^{2}), 7.08 – 6.59 (m, 3H, ^{3}), 6.21 – 5.91 (m, 2H, ^{4}), 5.27 – 4.73 (m, 5H, ^{5}), 4.67 – 4.33 (m, 2H, ^{6}), 3.79 – 3.40 (m, 4H, ^{7}), 3.36 – 3.02 (m, 4H, ^{8}), 2.75 – 1.72 (m, 15H, ^{9}), 1.64 (d, *J* = 6.2 Hz, 8H, ^{10}), 1.48 (d, *J* = 6.7 Hz, 4H, ^{11}), 1.39 – 1.15 (m, 42H, ^{12}), 1.09 – 0.74 (m, 33H, ^{13}).

^{13}C NMR (101 MHz, $CDCl_3$) δ / ppm: 173.71, 172.83, 172.72, 171.65, 169.79, 169.74, 169.56, 169.44, 169.34, 165.53, 165.29, 144.28, 135.80, 130.30, 130.23, 128.71, 128.43, 128.27, 127.76, 127.67, 78.96, 78.63, 78.21, 77.97, 77.36, 66.65, 66.61, 58.52, 42.87, 39.25, 38.79, 34.58, 34.42, 34.36, 34.20, 34.02, 32.03, 31.83, 30.88, 30.74, 30.62, 29.80, 29.76, 29.71, 29.68, 29.57, 29.53, 29.46, 29.38, 29.30, 29.26, 29.22, 26.92, 26.18, 25.15, 25.09, 24.49, 24.41, 24.17, 22.80, 19.01, 18.89, 18.54, 17.34, 17.11, 17.03, 16.93, 16.85, 14.24.

HRMS-ESI-MS $[M+H]^+$of $[C_{82}H_{133}N_5O_{17}]$: calculated: 1460.9769 found: 1460.9792.

IR (ATR platinum diamond): ν / cm^{-1} = 3304.1, 2963.7, 2924.6, 2853.7, 1735.9, 1654.0, 1533.2, 1463.7, 1417.2, 1369.8, 1246.5, 1162.6, 1099.1, 1018.2, 745.9, 697.5, 638.4.

***R*$_f$** : (cyclohexane / ethyl acetate 1:4) = 0.52.

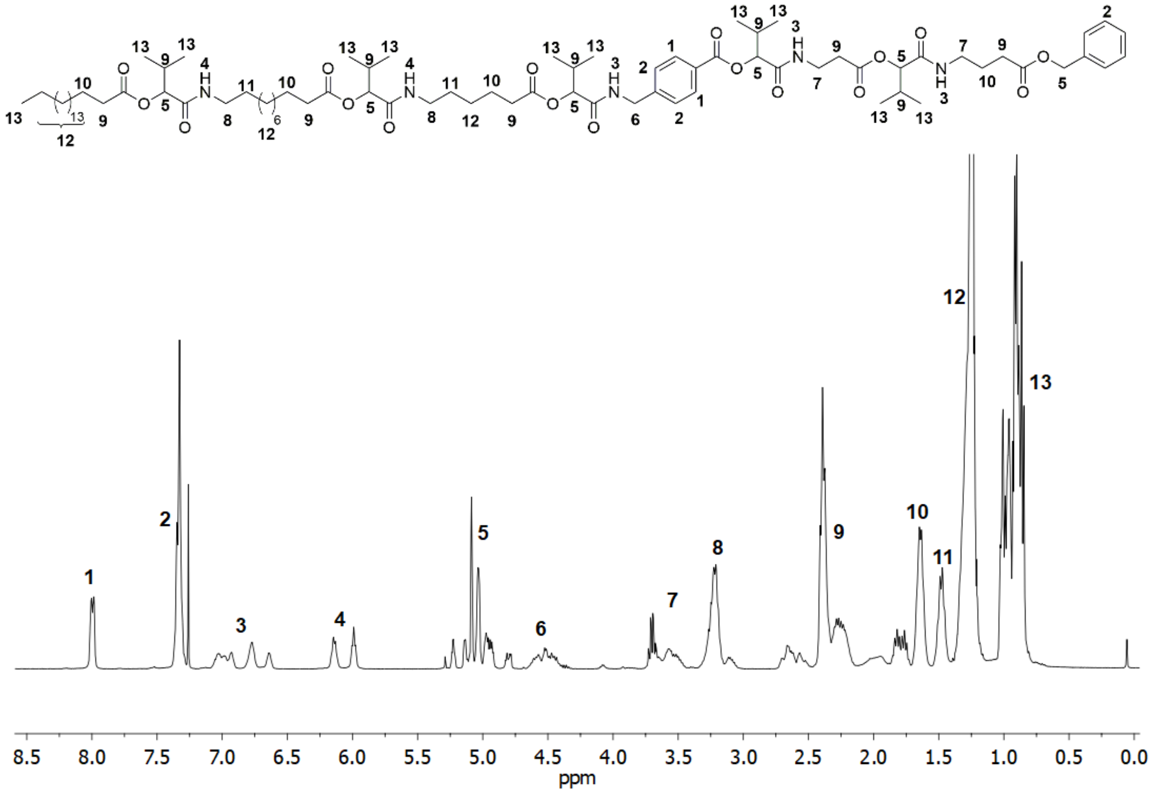
1
2
3
4
5
6
7
8
9
10
11
12
13
8.5
8.0
7.5
7.0
6.5
6.0
5.5
5.0
4.5
4.0
3.5
3.0
2.5
2.0
1.5
1.0
0.5
0.0
ppm

5th deprotection

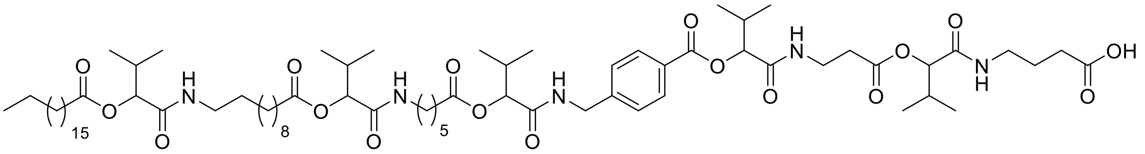

Substance **25** (1.33 g, 0.91 mmol, 1.00 eq.) was dissolved in THF (6.0 mL, 0.15 M). Subsequently, palladium on activated charcoal **19** (0.13 g, 10 wt%.) was suspended in the solution. The reaction mixture was purged with hydrogen (3 balloons) and stirred under hydrogen atmosphere overnight. The heterogeneous catalyst was filtered off and the solvent was evaporated under reduced pressure to obtain the desired product **30** in a yield of 97% (1.21 g, 0.88 mmol) as a highly viscous oil.

^{1}H NMR (400 MHz, CDCl$_3$) δ / ppm: 7.94 (t, J = 7.1 Hz, 2H, ^{1}), 7.30 (d, J = 7.7 Hz, 2H, ^{2}), 7.23 – 6.90 (m, 3H, ^{3}), 6.08 (d, J = 71.6 Hz, 2H, ^{4}), 5.22 – 4.74 (m, 5H, ^{5}), 4.64 – 4.32 (m, 2H, ^{6}), 3.63 – 3.41 (m, 2H, ^{7}), 3.30 – 3.00 (m, 6H, ^{8}), 2.97 – 2.74 (m, 2H, ^{9}), 2.59 – 2.09 (m, 13H, ^{10}), 1.87 – 1.67 (m, 2H, ^{11}), 1.65 – 1.52 (m, 6H, ^{12}), 1.43 (d, J = 6.1 Hz, 4H, ^{13}), 1.22 (d, J = 17.6 Hz, 42H, ^{14}), 1.05 – 0.62 (m, 15H, ^{15}).

^{13}C NMR (101 MHz, CDCl$_3$) δ / ppm: 176.54, 176.38, 172.91, 172.74, 171.41, 170.66, 170.32, 169.88, 169.75, 169.54, 165.60, 165.41, 144.44, 130.28, 130.24, 128.39, 127.76, 127.65, 78.83, 78.73, 78.26, 77.93, 42.87, 39.86, 39.62, 39.26, 38.80, 35.05, 34.40, 34.34, 34.01, 33.95, 33.72, 32.16, 32.01, 30.90, 30.70, 30.61, 30.52, 29.79, 29.74, 29.69, 29.64, 29.56, 29.51, 29.45, 29.43, 29.36, 29.28, 29.25, 29.20, 29.11, 26.90, 26.11, 25.13, 25.06, 24.36, 23.36, 23.02, 22.78, 18.94, 18.87, 17.34, 17.25, 17.07, 17.02, 16.83, 16.71, 16.68, 14.23.

HRMS-ESI-MS [M+H]$^+$ of [$C_{75}H_{127}N_5O_{17}$]: calculated: 1370.9300 found: 1370.9318.

IR (ATR platinum diamond): ν / cm^{-1} = 3296.6, 3089.9, 2963.3, 2920.5, 2851.4, 1737.3, 1650.6, 1537.0, 1465.2, 1416.6, 1369.9, 1245.3, 1162.7, 1101.7, 1017.9, 928.0, 720.1, 639.6, 409.3.

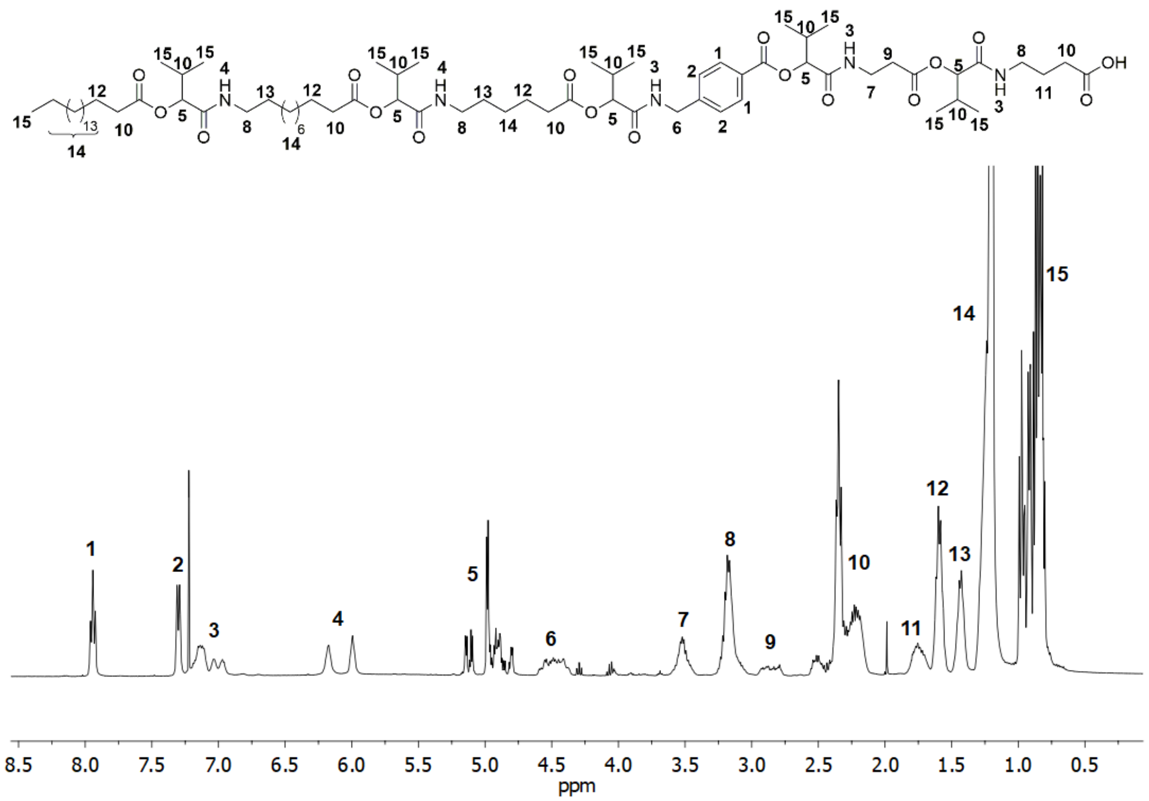
1
2
3
4
5
6
7
8
9
10
11
12
13
14
15
8.5
8.0
7.5
7.0
6.5
6.0
5.5
5.0
4.5
4.0
3.5
3.0
2.5
2.0
1.5
1.0
0.5
ppm
OH

6th Passerini reaction

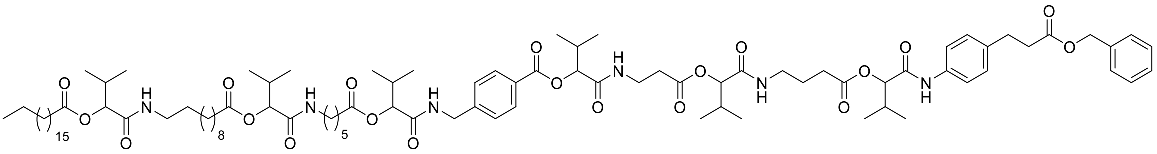

Substance **30** (1.14 g, 0.83 mmol, 1.00 eq.) was dissolved in DCM (5.0 mL, 0.15 M). Subsequently, isobutyraldehyde **11c** (230 µL, 180 mg, 2.50 mmol, 1.50 eq.) and monomer **M7** (0.66 g, 2.50 mmol, 1.50 eq.) were added and the reaction mixture was stirred at room temperature for 48 hours. The solvent was removed under reduced pressure and the crude product was purified by column chromatography (cyclohexane / ethyl acetate 3:2 → 1:2) to obtain the desired product **26** in a yield of 85% (1.27 g, 0.74 mmol) as a yellowish solid.

^{1}H NMR (400 MHz, $CDCl_3$) δ / ppm: 9.10 – 5.80 (m, 19H, ^{1}), 5.29 – 4.25 (m, 12H, ^{2}), 3.38 – 2.83 (m, 8H, ^{3}), 2.80 – 2.08 (m, 18H, ^{4}), 1.82 – 1.56 (m, 8H, ^{5}), 1.47 (s, 4H, ^{6}), 1.26 (s, 42H, ^{7}), 1.09 – 0.60 (m, 39H, ^{8}).

^{13}C NMR (101 MHz, $CDCl_3$) δ / ppm: 172.78, 172.71, 169.93, 169.59, 169.45, 136.05, 135.93, 130.25, 130.17, 128.78, 128.64, 128.29, 127.58, 120.93, 120.81, 120.22, 79.10, 78.25, 77.94, 77.48, 77.16, 76.84, 66.38, 39.23, 38.73, 36.05, 34.39, 34.34, 34.01, 32.00, 30.88, 30.67, 30.60, 30.47, 29.77, 29.73, 29.68, 29.66, 29.55, 29.50, 29.44, 29.35, 29.28, 29.24, 29.19, 26.90, 26.10, 25.12, 25.06, 24.39, 22.77, 18.97, 18.87, 17.32, 17.16, 17.08, 17.01, 14.22.

HRMS-ESI-MS $[M+H]^+$of $[C_{96}H_{150}N_6O_{20}]$: calculated: 1708.0978 found: 1708.0978.

IR (ATR platinum diamond): ν / cm^{-1} = 3308.4, 2964.1, 2925.0, 2853.7, 1736.5, 1655.9, 1611.3, 1530.9, 1464.0, 1415.6, 1369.9, 1245.6, 1158.8, 1126.5, 1105.2, 1018.0, 833.5, 746.8, 697.6, 648.0.

***R*$_f$** : (cyclohexane / ethyl acetate 1:4) = 0.37.

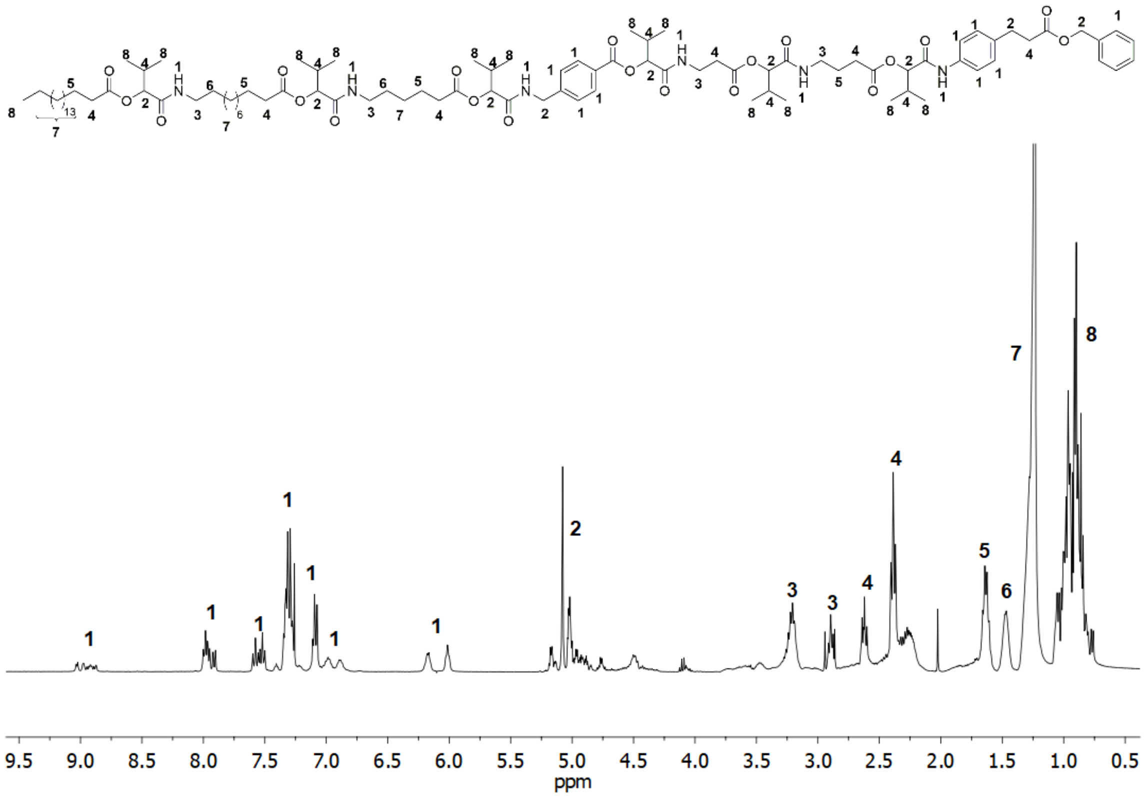
1
1
1
1
1
1
1
2
3
3
4
4
5
6
7
8
9.5
9.0
8.5
8.0
7.5
7.0
6.5
6.0
5.5
5.0
4.5
4.0
3.5
3.0
2.5
2.0
1.5
1.0
0.5
ppm

6th deprotection

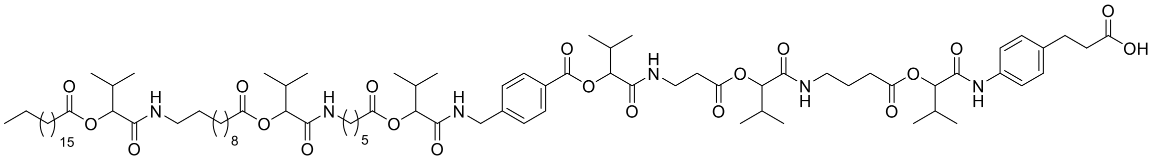

Substance **26** (1.15 g, 0.67 mmol, 1.00 eq.) was dissolved in THF (5.0 mL, 0.15 M). Subsequently, palladium on activated charcoal **19** (0.11 g, 10 wt%.) was suspended in the solution. The reaction mixture was purged with hydrogen (3 balloons) and stirred under hydrogen atmosphere overnight. The heterogeneous catalyst was filtered off and the solvent was evaporated under reduced pressure to obtain the desired product **31** in a yield of 99% (1.07 g, 0.66 mmol) as a highly viscous oil.

^{1}H NMR (500 MHz, $CDCl_3$) δ / ppm: 9.03 – 5.96 (m, 14H, ^{1}), 5.25 – 4.41 (m, 10H, ^{2}), 4.10 – 2.68 (m, 8H, ^{3}), 2.66 – 1.70 (m, 18H, ^{4}), 1.69 – 1.53 (m, 8H, ^{5}), 1.53 – 1.40 (m, 4H, ^{6}), 1.39 – 1.14 (m, 42H, ^{7}), 1.08 – 0.73 (m, 39H, ^{8}).

^{13}C NMR (126 MHz, $CDCl_3$) δ / ppm: 202.62, 175.37, 173.24, 172.96, 172.78, 170.28, 170.21, 170.14, 170.09, 169.80, 169.59, 168.34, 144.38, 135.91, 130.27, 130.24, 130.17, 130.12, 128.79, 128.73, 128.69, 127.77, 127.60, 121.07, 121.04, 120.96, 120.46, 107.73, 106.47, 103.91, 100.10, 78.98, 78.85, 78.74, 78.68, 78.59, 78.51, 78.30, 78.27, 78.02, 77.97, 77.41, 77.16, 76.91, 68.66, 68.06, 67.76, 67.54, 67.44, 67.13, 67.06, 66.13, 42.87, 41.19, 39.29, 38.87, 38.82, 38.21, 35.61, 34.92, 34.79, 34.41, 34.34, 34.16, 33.99, 33.96, 32.55, 32.39, 32.38, 32.02, 31.19, 30.87, 30.75, 30.71, 30.61, 30.50, 30.33, 29.79, 29.77, 29.75, 29.70, 29.64, 29.60, 29.56, 29.52, 29.45, 29.43, 29.37, 29.29, 29.25, 29.20, 29.11, 29.07, 29.01, 27.91, 26.90, 26.17, 26.11, 26.05, 25.70, 25.13, 25.06, 24.91, 24.35, 23.93, 23.91, 23.54, 23.50, 23.42, 22.79, 22.76, 22.28, 18.97, 18.90, 18.87, 17.64, 17.48, 17.40, 17.34, 17.28, 17.18, 17.11, 17.04, 16.91, 16.61, 16.58, 14.23.

HRMS-ESI-MS $[M+H]^+$of $[C_{89}H_{144}N_6O_{20}]$: calculated: 1618.0508 found: 1618.0494.

IR (ATR platinum diamond): ν / cm^{-1} = 3312.2, 2963.9, 2924.7, 2854.0, 1733.1, 1655.7, 1611.9, 1533.8, 1463.7, 1415.7, 1370.0, 1246.4, 1164.3, 1106.0, 1018.0, 923.1, 837.1, 635.2, 410.5.

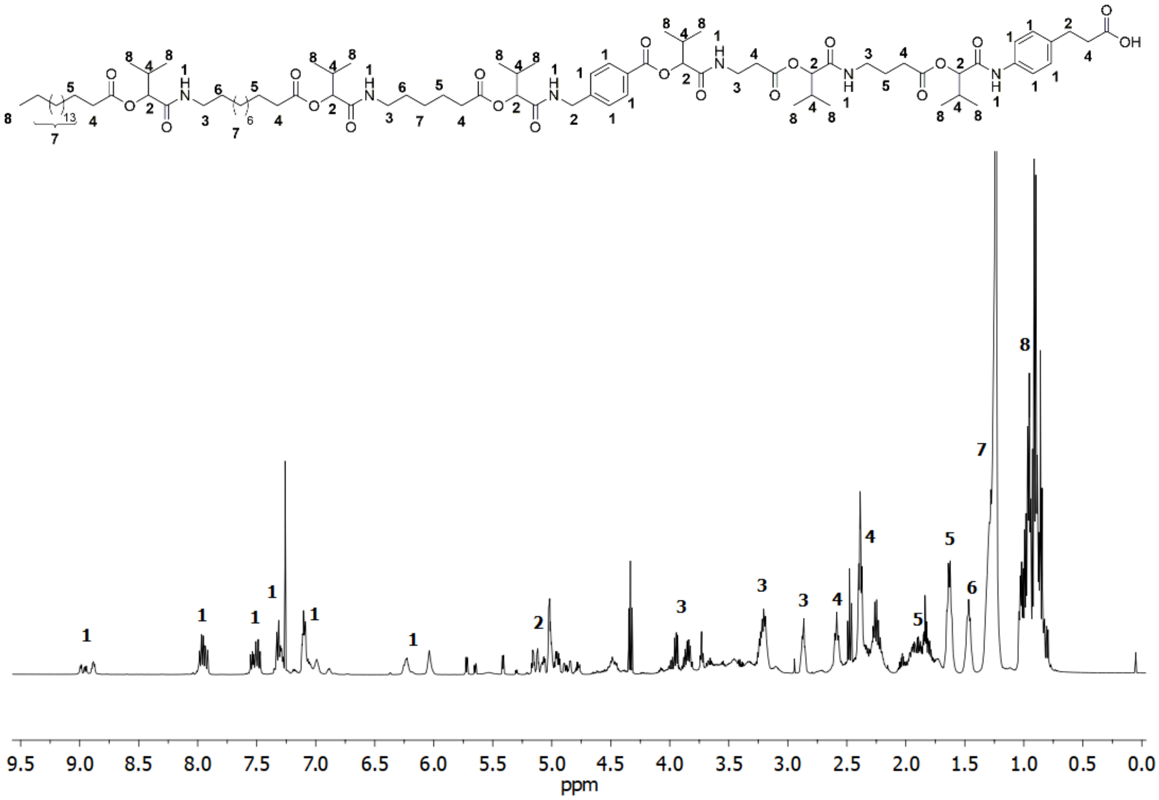
1
1
1
1
1
1
2
3
3
3
4
4
5
5
6
7
8
9.5
9.0
8.5
8.0
7.5
7.0
6.5
6.0
5.5
5.0
4.5
4.0
3.5
3.0
2.5
2.0
1.5
1.0
0.5
0.0
ppm
OH
O
N
H
13
6

7th Passerini reaction

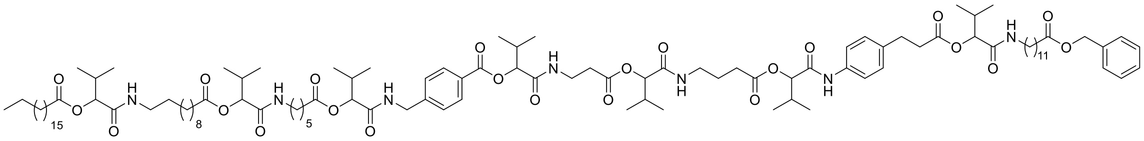

Substance **31** (0.98 g, 0.61 mmol, 1.00 eq.) was dissolved in DCM (2.0 mL, 0.3 M). Subsequently, isobutyraldehyde **11c** (79.0 µL, 131 mg, 1.82 mmol, 3.00 eq.) and monomer **M3** (0.57 g, 1.82 mmol, 3.00 eq.) were added and the reaction mixture was stirred at room temperature for 48 hours. The solvent was removed under reduced pressure and the crude product was purified by column chromatography (cyclohexane / ethyl acetate 3:1 → 1:5, with 5% of triethyl amine) to obtain the desired product **32** in a yield of 92% (1.12 g, 0.56 mmol) as a highly viscous oil.

^{1}H NMR (400 MHz, CDCl$_3$) δ / ppm: 9.17 – 5.74 (m, 20H, ^{1}), 5.27 – 4.35 (m, 13H, ^{2}), 3.75 – 2.65 (m, 10H, ^{3}), 2.65 – 2.07 (m, 21H, ^{4}), 1.92 – 1.53 (m, 10H, ^{5}), 1.53 – 1.36 (m, 6H, ^{6}), 1.35 – 1.12 (m, 56H, ^{7}), 1.11 – 0.66 (m, 45H, ^{8}).

^{13}C NMR (101 MHz, CDCl$_3$) δ / ppm: 173.81, 172.70, 171.77, 169.95, 169.59, 169.44, 169.21, 136.16, 130.19, 128.59, 128.50, 128.22, 128.20, 120.98, 78.23, 77.92, 77.36, 66.12, 60.47, 39.21, 35.68, 34.38, 34.36, 34.31, 33.98, 31.98, 30.86, 30.68, 30.58, 30.31, 29.75, 29.71, 29.66, 29.63, 29.53, 29.48, 29.46, 29.41, 29.33, 29.29, 29.26, 29.21, 29.17, 26.88, 25.10, 25.03, 25.00, 22.75, 21.12, 18.95, 18.88, 18.85, 18.79, 17.31, 17.07, 17.00, 14.26, 14.19.

HRMS-ESI-MS [M+H]$^+$ of [$C_{113}H_{181}N_7O_{23}$]: calculated: 2005.3282 found: 2005.3289.

IR (ATR platinum diamond): ν / cm^{-1} = 3301.4, 2963.7, 2924.9, 2853.8, 1737.3, 1654.8, 1611.7, 1531.4, 1463.8, 1415.8, 1369.9, 1244.9, 1159.2, 1126.1, 1106.0, 1003.4, 834.1, 697.4, 636.1, 412.4.

***R*$_f$** : (cyclohexane / ethyl acetate 1:4, with 4% triethyl amine) = 0.45.

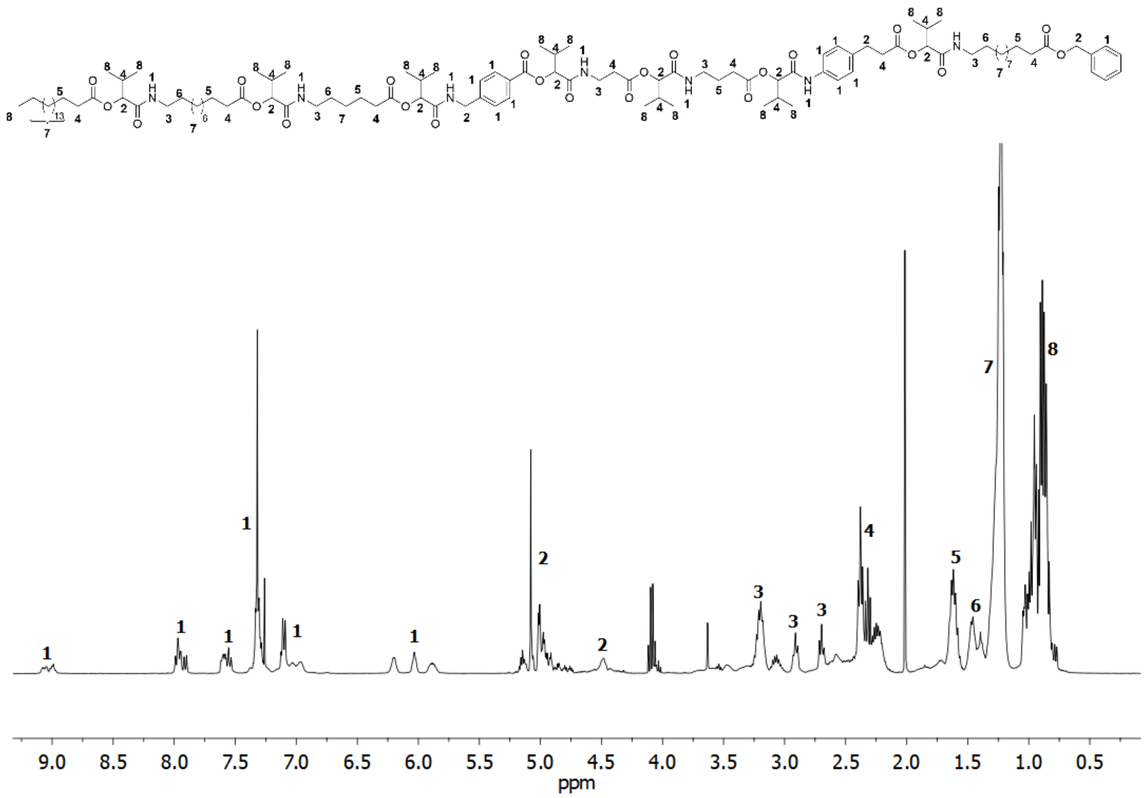
1
1
1
1
1
1
2
2
3
3
3
4
5
6
7
8
9.0
8.5
8.0
7.5
7.0
6.5
6.0
5.5
5.0
4.5
4.0
3.5
3.0
2.5
2.0
1.5
1.0
0.5
ppm

7th deprotection

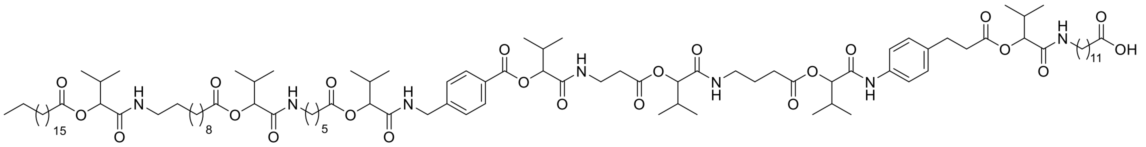

Substance **32** (0.99 g, 0.49 mmol, 1.00 eq.) was dissolved in THF (2.5 mL, 0.2 M). Subsequently, palladium on activated charcoal **19** (99 mg, 10 wt%.) was suspended in the solution. The reaction mixture was purged with hydrogen (4 balloons) and stirred under hydrogen atmosphere overnight. The heterogeneous catalyst was filtered off and the solvent was evaporated under reduced pressure to obtain the desired product **21** in a yield of 81% (760 mg, 0.39 mmol) as a highly viscous oil.

^{1}H NMR (400 MHz, $CDCl_3$) δ / ppm: 9.16 – 5.82 (m, 15H, ^{1}), 5.74 – 3.75 (m, 11H, ^{2}), 3.29 – 2.54 (m, 10H, ^{3}), 2.39 – 1.86 (m, 21H, ^{4}), 1.84 – 1.50 (m, 10H, ^{5}), 1.49 – 1.33 (m, 6H, ^{6}), 1.20 (s, 56H, ^{7}), 1.04 – 0.67 (m, 45H, ^{8}).

^{13}C NMR (101 MHz, $CDCl_3$) δ / ppm: 176.55, 172.89, 172.73, 171.78, 170.01, 169.70, 169.53, 169.33, 130.09, 130.00, 128.55, 128.46, 127.52, 120.97, 107.88, 107.62, 106.37, 78.48, 78.19, 77.88, 68.61, 67.67, 67.60, 67.44, 42.77, 39.19, 38.72, 35.61, 34.30, 34.23, 33.95, 32.31, 31.92, 30.79, 30.52, 30.25, 29.70, 29.65, 29.61, 29.54, 29.50, 29.47, 29.43, 29.36, 29.28, 29.20, 29.16, 29.11, 29.00, 27.83, 26.82, 26.74, 26.08, 25.03, 24.97, 24.81, 24.26, 23.93, 23.84, 23.83, 22.69, 22.18, 18.83, 18.78, 18.73, 17.26, 17.04, 16.96, 14.14.

HRMS-ESI-MS $[M+H]^+$of $[C_{106}H_{175}N_7O_{23}]$: calculated: 1915.2812 found: 1915.2852.

IR (ATR platinum diamond): ν / cm^{-1} = 3335.9, 2928.1, 1727.7, 1659.9, 1537.5, 1460.2, 1369.7, 1240.9, 1175.8, 1066.1, 1034.7, 990.8, 924.1, 850.1, 534.5, 410.3.

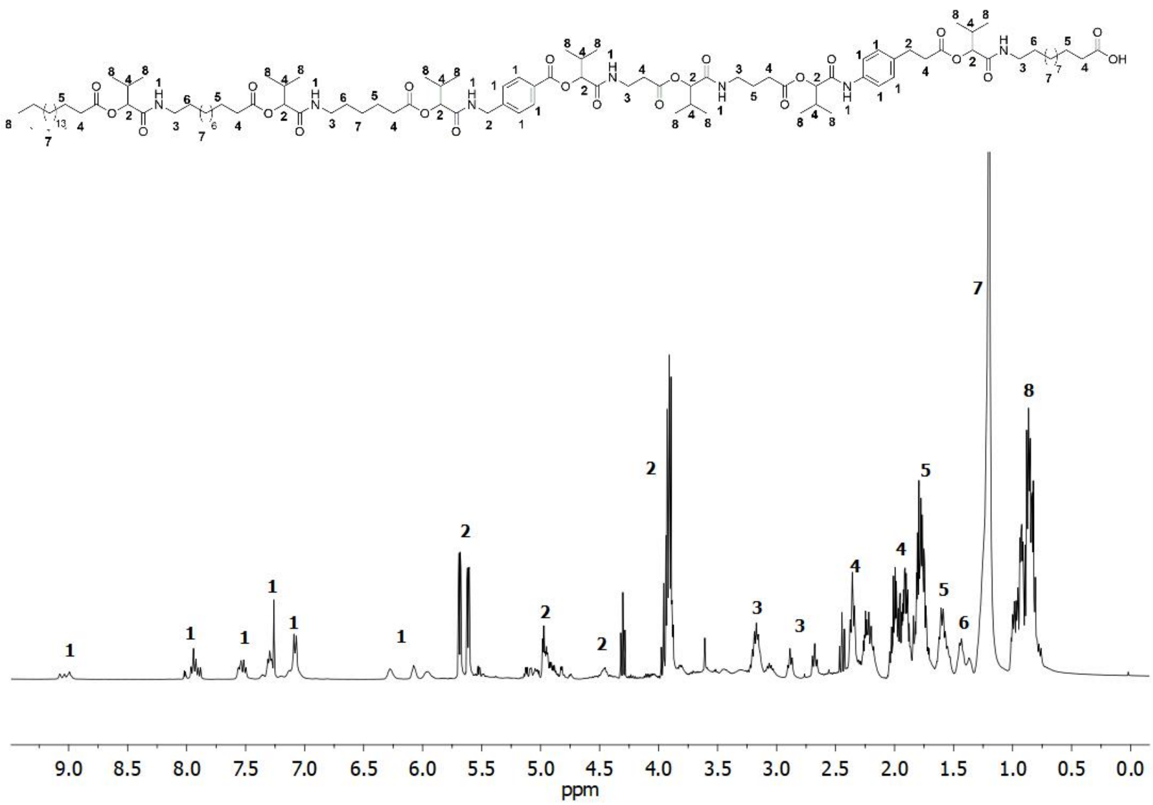
1
1
1
1
1
1
2
2
2
2
3
3
4
4
5
5
6
7
8
9.0
8.5
8.0
7.5
7.0
6.5
6.0
5.5
5.0
4.5
4.0
3.5
3.0
2.5
2.0
1.5
1.0
0.5
0.0
ppm

6.3.2.2.2 Dual sequence-definition

1st Passerini reaction

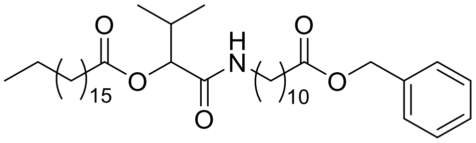

Stearic acid **13** (1.50 g, 5.27 mmol, 1.00 eq.) was suspended in DCM (5.3 mL, 1. M). Subsequently, isobutyraldehyde **11c** (0.73 mL, 0.57 g, 7.91 mmol, 1.50 eq.) and monomer **M1** (2.38 g, 7.91 mmol, 1.50 eq.) were added and the reaction mixture was stirred at room temperature for 24 hours. The solvent was removed under reduced pressure and the crude product was purified by column chromatography (cyclohexane / ethyl acetate 15:1 → 11:1) to obtain the desired product **33** in a yield of 98% (3.40 g, 5.17 mmol) as a white solid.

^{1}H NMR (400 MHz, CDCl$_3$) δ / ppm: 7.40 – 7.28 (m, 5H, ^{1}), 5.96 (t, J = 5.5 Hz, 1H, ^{2}), 5.10 (s, 2H, ^{3}), 5.06 (d, J = 4.4 Hz, 1H, ^{4}), 3.34 – 3.15 (m, 2H, ^{5}), 2.46 – 2.23 (m, 5H, ^{6}), 1.74 – 1.56 (m, 4H, ^{7}), 1.54 – 1.40 (m, 2H, ^{8}), 1.25 (s, 40H, ^{9}), 0.99 – 0.79 (m, 9H, ^{10}).

^{13}C NMR (101 MHz, CDCl$_3$) δ / ppm: 173.77, 172.65, 169.38, 136.22, 128.64, 128.26, 77.97, 66.16, 39.25, 34.42, 32.03, 30.62, 29.81, 29.78, 29.77, 29.76, 29.71, 29.68, 29.58, 29.54, 29.47, 29.44, 29.38, 29.31, 29.27, 29.20, 26.94, 25.15, 25.04, 22.80, 18.89, 17.03, 14.24.

HRMS-ESI-MS [M+H]$^+$ of [$C_{41}H_{71}NO_5$]: calculated: 658.5405 found: 658.5391.

IR (ATR platinum diamond): ν / cm^{-1} = 3286.0, 2916.0, 2848.6, 1737.5, 1649.3, 1550.4, 1498.2, 1469.6, 1415.9, 1378.9, 1294.7, 1272.1, 1254.6, 1212.7, 1157.5, 1108.5, 1031.7, 1013.0, 986.5, 927.3, 722.0, 693.6, 578.8, 473.8.

***R*f** : (cyclohexane / ethyl acetate 5:1) = 0.42.

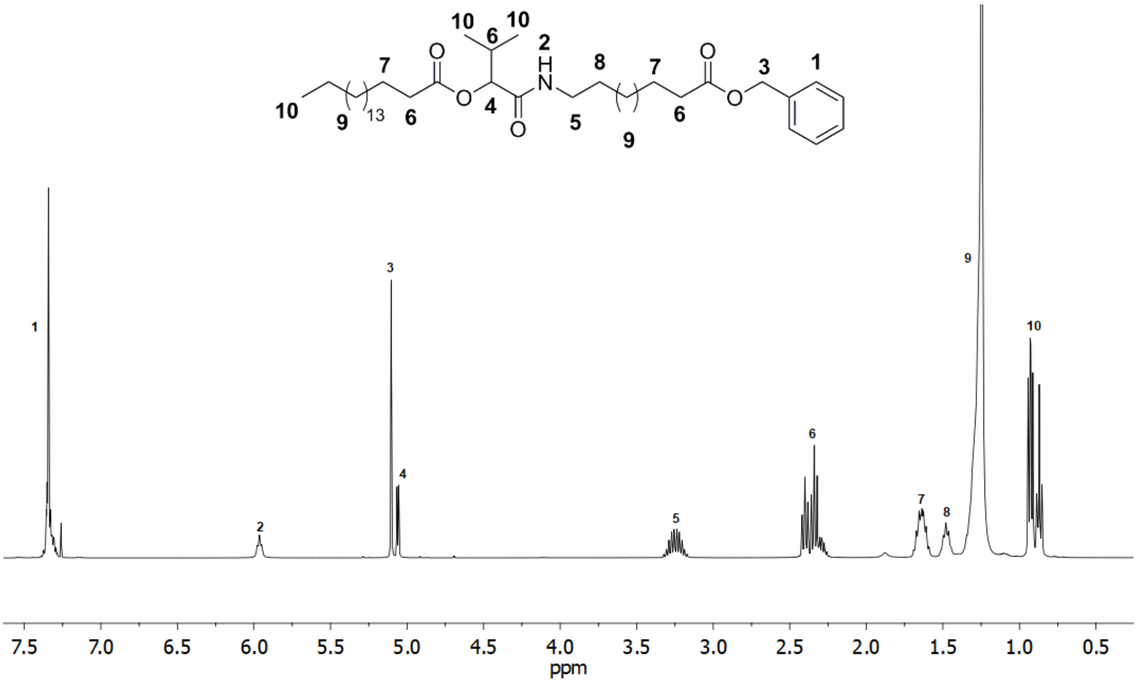
10
6
10
2
7
8
7
3
1
10
9
13
6
4
5
9
6
1
2
3
4
5
6
7
8
9
10
7.5
7.0
6.5
6.0
5.5
5.0
4.5
4.0
3.5
3.0
2.5
2.0
1.5
1.0
0.5
ppm

1st deprotection

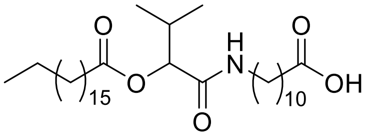

Substance **33** (3.31 g, 5.03 mmol, 1.0 eq.) was dissolved in THF (17 mL, 0.3 M). Subsequently, palladium on activated charcoal **19** (0.33 g, 10 wt%.) was suspended in the solution. The reaction mixture was purged with hydrogen (3 balloons) and stirred under hydrogen atmosphere overnight. The heterogeneous catalyst was filtered off and the solvent was evaporated under reduced pressure to obtain the desired product **34** in a yield of 99% (2.68 g, 4.98 mmol) as a white solid.

^{1}H NMR (400 MHz, CDCl$_3$) δ / ppm: 5.99 (t, *J* = 5.1 Hz, 1H, ^{1}), 5.06 (d, *J* = 4.4 Hz, 1H, ^{2}), 3.40 – 3.14 (m, 2H, ^{3}), 2.45 – 2.23 (m, 5H, ^{4}), 1.70 – 1.54 (m, 4H, ^{5}), 1.52 – 1.37 (m, 2H, ^{6}), 1.24 (s, 40H, ^{7}), 0.97 – 0.73 (m, 9H, ^{8}).

^{13}C NMR (101 MHz, CDCl$_3$) δ / ppm: 179.08, 172.74, 169.58, 128.27, 108.06, 107.73, 106.46, 77.98, 68.65, 67.80, 67.77, 67.55, 39.30, 34.42, 34.08, 32.04, 30.61, 29.81, 29.77, 29.72, 29.61, 29.58, 29.48, 29.38, 29.36, 29.27, 29.23, 29.09, 27.92, 26.90, 25.15, 24.79, 24.03, 23.94, 23.92, 22.81, 22.30, 18.89, 17.03, 14.24.

HRMS-ESI-MS [M+H]$^{+}$ of [$C_{34}H_{65}NO_5$]: calculated: 568.4936 found: 568.4922.

IR (ATR platinum diamond): ν / cm^{-1} = 3287.3, 2916.4, 2848.9, 1744.5, 1704.0, 1651.1, 1551.1, 1468.7, 1435.6, 1378.0, 1294.9, 1272.2, 1253.7, 1233.6, 1214.4, 1190.8, 1159.5, 1108.4, 1069.6, 1035.5, 991.7, 928.2, 722.1, 685.6.

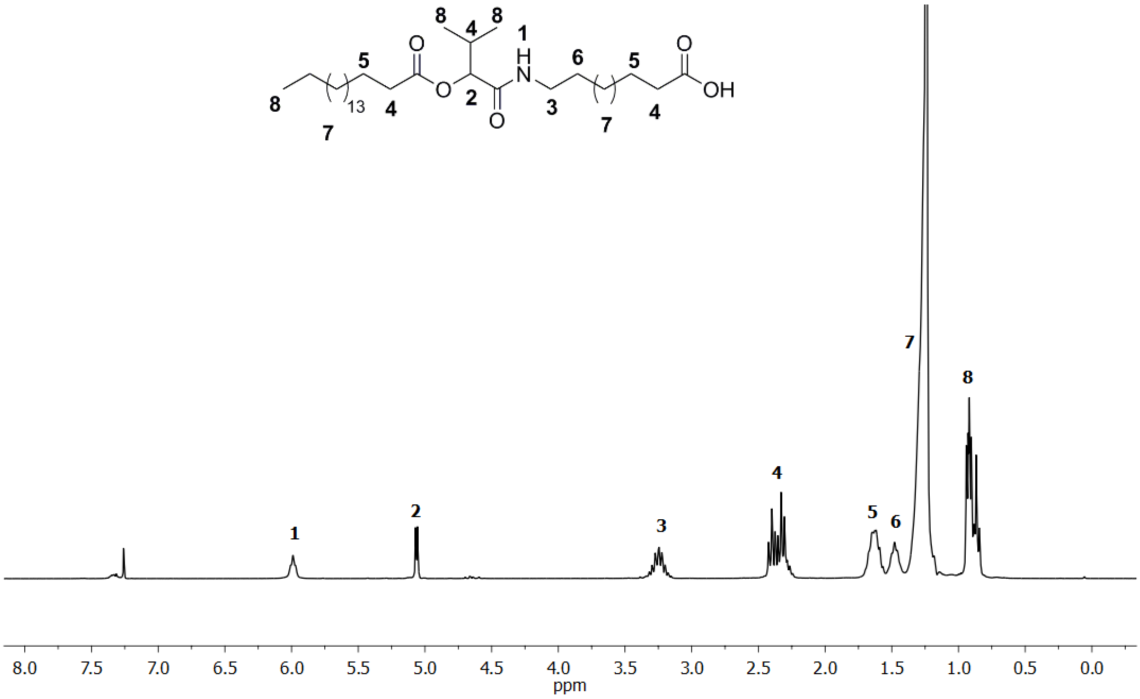

2nd Passerini reaction

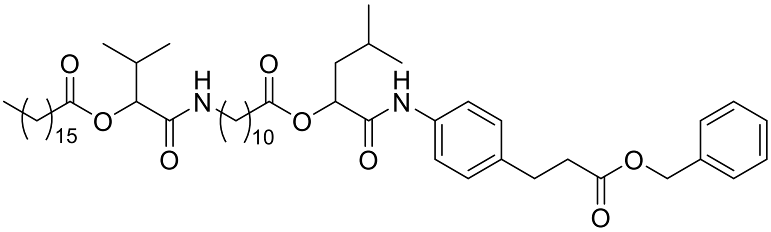

Substance **34** (3.25 g, 6.03 mmol, 1.00 eq.) was dissolved in DCM (12 mL, 0.5 M). Subsequently, isovaleraldehyde **11e** (0.97 mL, 0.78 g, 9.04 mmol, 1.50 eq.) and monomer **M7** (2.40 g, 9.04 mmol, 1.50 eq.) were added and the reaction mixture was stirred at room temperature for 24 hours. The solvent was removed under reduced pressure and the crude product was purified by column chromatography (cyclohexane / ethyl acetate 15:1 → 2:1) and a second time using another gradient (cyclohexane / ethyl acetate 20:1 → 2:1, with 5% of triethyl amine) to obtain the desired product **35** in a yield of 65% (3.50 g, 3.93 mmol) as a highly viscous oil.

^{1}H NMR (400 MHz, CDCl$_3$) δ / ppm: 7.89 (s, 1H, ^{1}), 7.50 – 7.04 (m, 9H, ^{2}), 6.02 (s, 1H, ^{3}), 5.36 – 5.24 (m, 1H, ^{4}), 5.08 (s, 2H, ^{5}), 5.05 (d, *J* = 4.4 Hz, 1H, ^{6}), 3.33 – 3.15 (m, 2H, ^{7}), 2.91 (t, *J* = 7.6 Hz, 2H, ^{8}), 2.68 – 2.56 (m, 2H, ^{9}), 2.45 – 2.22 (m, 6H, ^{10}), 1.91 – 1.59 (m, 6H, ^{11}), 1.47 – 1.41 (m, 2H, ^{12}), 1.39 – 1.14 (m, 40H, ^{13}), 1.02 – 0.78 (m, 15H, ^{14}).

^{13}C NMR (101 MHz, CDCl$_3$) δ / ppm: 172.86, 172.70, 172.68, 169.41, 168.44, 136.87, 135.90, 135.47, 128.93, 128.80, 128.61, 128.30, 120.51, 120.26, 119.87, 77.95, 77.48, 77.16, 76.84, 72.89, 66.37, 40.79, 39.21, 35.98, 34.37, 34.33, 32.26, 31.99, 30.58, 30.42, 29.77, 29.73, 29.67, 29.62, 29.54, 29.46, 29.43, 29.37, 29.34, 29.22, 29.13, 26.88, 25.11, 24.97, 24.62, 23.53, 23.16, 22.76, 21.91, 18.86, 17.01, 14.21.

HRMS-ESI-MS [M+H]$^+$ of [$C_{56}H_{90}N_2O_8$]: calculated: 919.6770 found: 919.6747.

IR (ATR platinum diamond): ν / cm^{-1} = 3275.3, 2917.5, 2849.8, 1740.5, 1674.9386, 2.4158, 1606.5, 1537.2, 1466.9, 1414.7, 1370.0, 1306.2205, 1251.2, 1213.5, 1159.8, 1069.5, 828.4, 723.4, 697.5, 536.1.

***R*$_f$** : (cyclohexane / ethyl acetate 2:1) = 0.45.

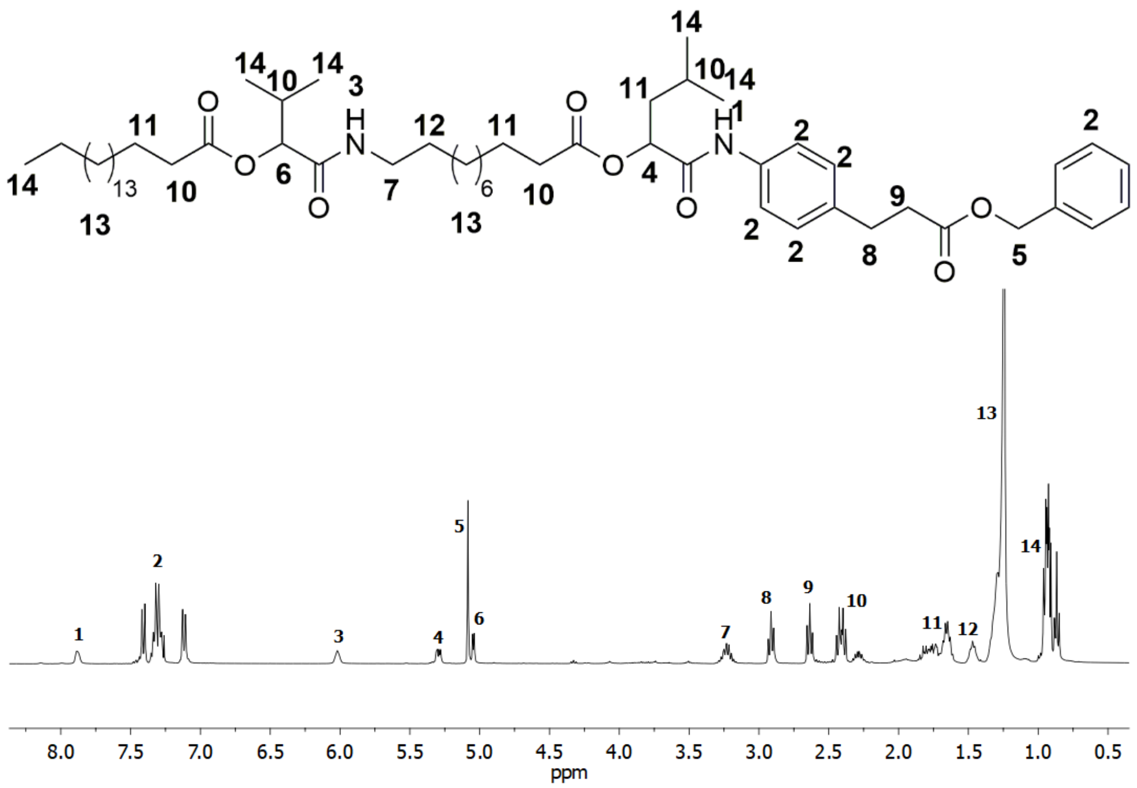
14
10
14
3
O
11
H
N
12
11
O
11
14
10
14
H
1
2
2
14
13
13
10
O
6
O
7
6
13
10
O
4
O
9
O
2
2
8
O
5
2
2
1
2
3
4
5
6
7
8
9
10
11
12
13
14
8.0
7.5
7.0
6.5
6.0
5.5
5.0
4.5
4.0
3.5
3.0
2.5
2.0
1.5
1.0
0.5
ppm

2nd deprotection

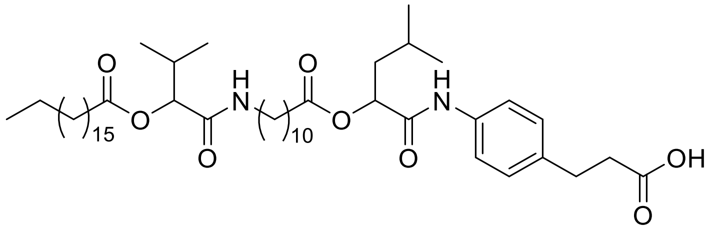

Substance **35** (2.83 g, 3.09 mmol, 1.00 eq.) was dissolved in THF (10.0 mL, 0.3 M). Subsequently, palladium on activated charcoal **19** (0.28 g, 10 wt%.) was suspended in the solution. The reaction mixture was purged with hydrogen (4 balloons) and stirred under hydrogen atmosphere overnight. The heterogeneous catalyst was filtered off and the solvent was evaporated under reduced pressure to obtain the desired product **36** in a yield of 99% (2.45 g, 3.05 mmol) as a highly viscous oil.

^{1}H NMR (400 MHz, $CDCl_3$) δ / ppm: 7.91 (s, 1H, ^{1}), 7.42 (d, *J* = 8.4 Hz, 2H, ^{2}), 7.14 (d, *J* = 8.4 Hz, 2H, ^{2}), 6.04 (t, *J* = 4.7 Hz, 1H, ^{3}), 5.31 – 5.28 (m, 1H, ^{4}), 5.08 – 4.99 (m, 1H, ^{5}), 3.37 – 3.14 (m, 2H, ^{6}), 2.90 (t, *J* = 7.6 Hz, 2H, ^{7}), 2.62 (t, *J* = 7.6 Hz, 2H, ^{8}), 2.49 – 2.21 (m, 6H, ^{9}), 2.11 – 1.57 (m, 6H, ^{10}), 1.53 – 1.40 (m, 2H, ^{11}), 1.38 – 1.04 (m, 40H, ^{12}), 1.02 – 0.77 (m, 15H, ^{13}).

^{13}C NMR (101 MHz, $CDCl_3$) δ / ppm: 177.35, 173.00, 172.79, 172.77, 169.66, 168.53, 136.89, 135.49, 128.96, 120.33, 107.72, 106.45, 77.96, 77.48, 77.16, 76.84, 72.95, 67.76, 67.54, 40.79, 39.32, 35.64, 34.40, 34.36, 32.02, 30.59, 30.19, 29.80, 29.76, 29.71, 29.59, 29.57, 29.46, 29.37, 29.26, 29.14, 26.88, 25.13, 25.01, 24.64, 23.93, 23.18, 22.79, 21.93, 18.87, 17.03, 14.24.

HRMS-ESI-MS $[M+H]^+$ of [$C_{49}H_{84}N_2O_8$]: calculated: 829.6300 found: 829.6279.

IR (ATR platinum diamond): ν / cm^{-1} = 3277.4, 2917.5, 2849.8, 1742.7, 1673.5, 1652.7, 1607.0, 1538.5, 1465.0, 1415.2, 1369.6, 1309.1, 1252.1, 1162.3, 1111.9, 1066.9, 1035.2, 991.5, 926.3, 834.8, 721.9, 677.9, 531.1.

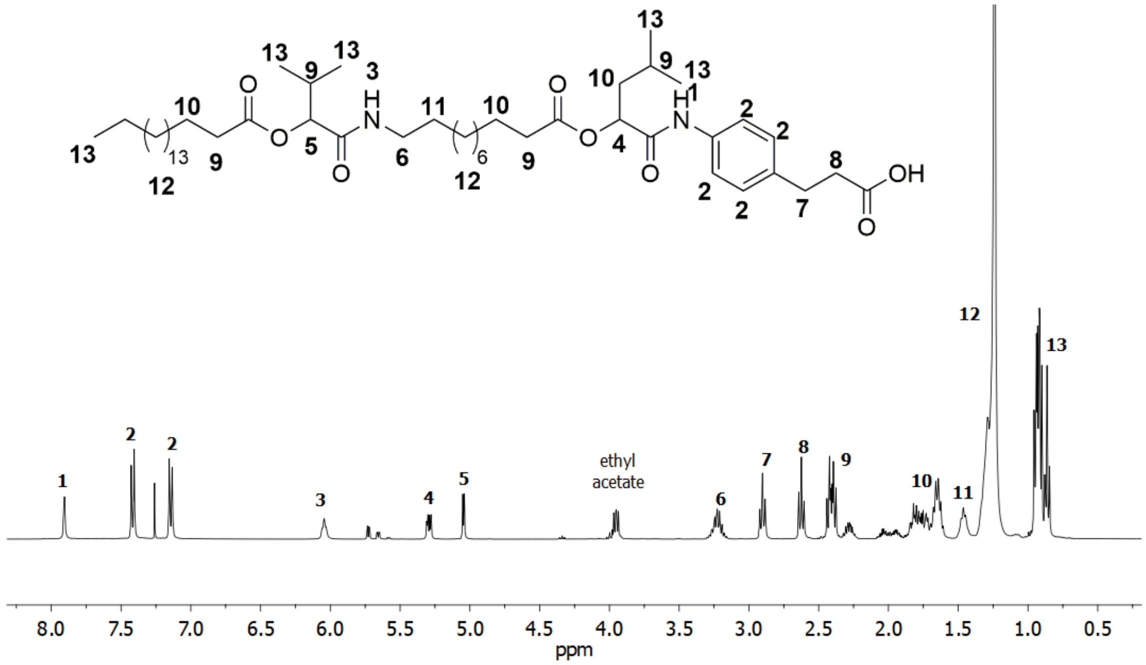
13
10
13
12
9
13
9
13
3
H
N
O
O
5
O
11
10
6
12
6
9
O
O
10
13
9
13
1
H
N
4
O
2
2
2
2
8
7
OH
O
1
2
2
3
4
5
ethyl
acetate
6
7
8
9
10
11
12
13
8.0
7.5
7.0
6.5
6.0
5.5
5.0
4.5
4.0
3.5
3.0
2.5
2.0
1.5
1.0
0.5
ppm

3rd Passerini reaction

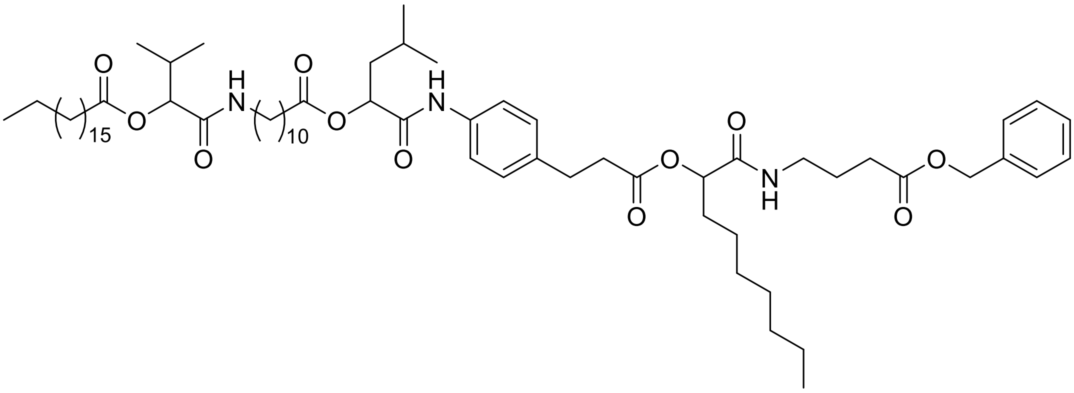

Substance **36** (3.36 g, 4.1 mmol, 1.00 eq.) was dissolved in DCM (8.2 mL, 0.5 M). Subsequently, octanal **11f** (0.98 mL, 0.80 g, 6.30 mmol, 1.50 eq.) and monomer **M4** (1.28 g, 6.3 mmol, 1.50 eq.) were added and the reaction mixture was stirred at room temperature for 48 hours. The solvent was removed under reduced pressure and the crude product was purified by column chromatography (cyclohexane / ethyl acetate 15:1 → 2:1, with 5% triethyl amine) to obtain the desired product **37** in a yield of 47% (2.24 g, 1.93 mmol) as a highly viscous oil.

^{1}H NMR (300 MHz, CDCl$_3$) δ / ppm: 8.05 (s, 1H, ^{1}), 7.54 – 7.05 (m, 9H, ^{2}), 6.22 – 5.90 (m, 2H, ^{3}), 5.29 – 5-25 (m, 1H, ^{4}), 5.15 – 5.06 (s, 2H, ^{5}), 5.03 (d, *J* = 4.3 Hz, 2H, ^{6}), 3.38 – 3.05 (m, 2H, ^{7}), 3.06 – 2.90 (m, 2H, ^{8}), 2.75 – 2.61 (m, 2H, ^{9}), 2.50 – 2.15 (m, 8H, ^{10}), 2.02 – 1.55 (m, 10H, ^{11}), 1.54 – 1.37 (m, 2H, ^{12}), 1.36 – 1.04 (m, 50H, ^{13}), 1.01 – 0.66 (m, 20H, ^{14}).

^{13}C NMR (101 MHz, CDCl$_3$) δ / ppm: 173.58, 172.90, 172.68, 172.66, 171.64, 170.04, 169.38, 168.60, 136.41, 135.78, 135.71, 128.78, 128.64, 128.36, 128.18, 120.42, 77.90, 74.08, 72.81, 66.94, 66.51, 40.75, 39.18, 38.65, 35.57, 34.33, 34.24, 32.34, 31.95, 31.77, 31.66, 30.54, 30.21, 29.73, 29.69, 29.64, 29.59, 29.50, 29.42, 29.40, 29.35, 29.31, 29.19, 29.10, 29.08, 26.85, 25.07, 24.91, 24.82, 24.58, 24.33, 23.51, 23.13, 22.73, 22.64, 21.84, 18.83, 16.98, 14.18, 14.14.

HRMS-ESI-MS [M+H]$^+$ of [$C_{69}H_{113}N_3O_{11}$]: calculated: 1160.8448 found: 1160.8435.

IR (ATR platinum diamond): ν/ cm^{-1} = 3293.8, 2921.9, 2852.4, 1738.6, 1653.7, 1608.5, 1533.4, 1464.9, 1414.8, 1370.0, 1243.4, 1160.9, 1067.5, 1001.6732, 829.1, 722.3, 697.0, 528.5.

***R*$_f$** : (cyclohexane / ethyl acetate 7:3, with 5% triethyl amine) = 0.38.

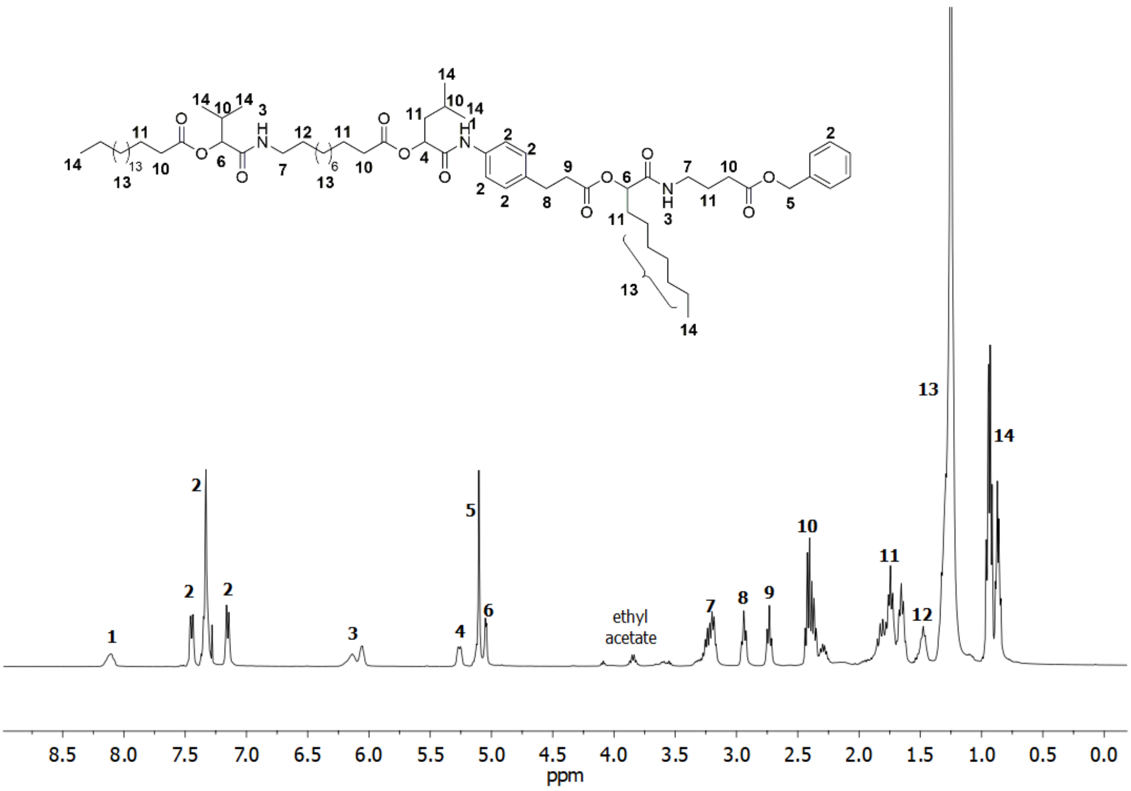
1
2
2
2
3
4
5
6
ethyl
acetate
7
8
9
10
11
12
13
14
8.5
8.0
7.5
7.0
6.5
6.0
5.5
5.0
4.5
4.0
3.5
3.0
2.5
2.0
1.5
1.0
0.5
0.0
ppm

3rd deprotection

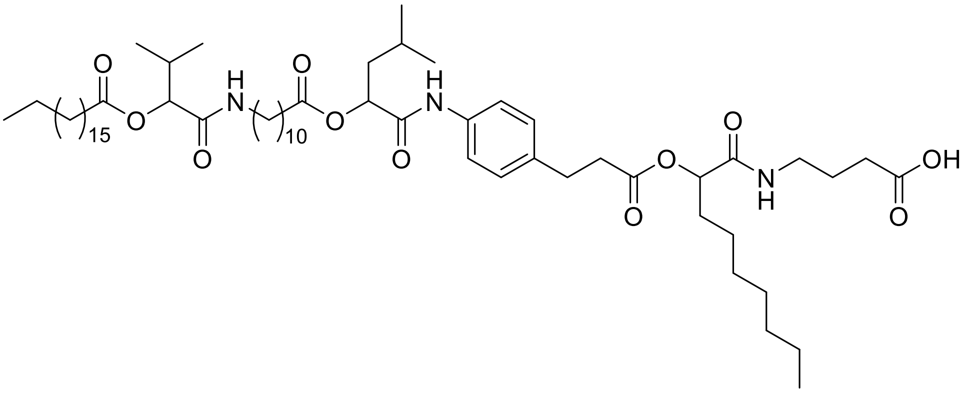

Substance **37** (2.20 g, 2.02 mmol, 1.00 eq.) was dissolved in THF (10 mL, 0.2 M). Subsequently, palladium on activated charcoal **19** (0.23 g, 10 wt%.) was suspended in the solution. The reaction mixture was purged with hydrogen (4 balloons) and stirred under hydrogen atmosphere overnight. The heterogeneous catalyst was filtered off and the solvent was evaporated under reduced pressure to obtain the desired product **38** in a yield of 99% (2.08 g, 2.00 mmol) as a highly viscous oil.

^{1}H NMR (300 MHz, CDCl$_3$) δ / ppm: 8.15 (s, 1H, ^{1}), 7.50 – 7.00 (m, 4H, ^{2}), 6.26 – 5.99 (m, 2H, ^{3}), 5.28 – 5.20 (m, 1H, ^{4}), 5.13 – 4.96 (m, 2H, ^{5}), 3.32 – 3.04 (m, 2H, ^{6}), 2.92 (t, J = 7.1 Hz, 2H, ^{7}), 2.72 (t, J = 7.2 Hz, 2H, ^{8}), 2.59 – 2.14 (m, 8H, ^{9}), 2.12 – 1.52 (m, 10H, ^{10}), 1.51 – 1.37 (m, 2H, ^{11}), 1.22 (s, 50H, ^{12}), 1.00 – 0.71 (m, 20H, ^{13}).

^{13}C NMR (101 MHz, CDCl$_3$) δ / ppm: 176.43, 173.39, 172.75, 171.79, 170.49, 169.69, 168.80, 136.53, 135.73, 128.82, 120.64, 107.68, 106.42, 77.89, 74.13, 72.90, 67.73, 67.50, 40.74, 39.28, 38.65, 35.48, 34.37, 34.30, 31.98, 31.94, 31.80, 31.31, 30.58, 30.19, 29.76, 29.72, 29.67, 29.59, 29.54, 29.42, 29.34, 29.22, 29.17, 29.11, 29.09, 26.83, 25.10, 24.91, 24.89, 24.61, 24.37, 23.90, 23.17, 22.76, 22.67, 21.82, 18.85, 16.99, 14.20, 14.16.

HRMS-ESI-MS [M+H]$^+$ of [$C_{62}H_{107}N_3O_{11}$]: calculated: 1070.7978 found: 1070.7958.

IR (ATR platinum diamond): ν/ cm^{-1} = 3314.0, 2923.6, 2853.7, 1738.5, 1657.5, 1609.1, 1536.9, 1462.9, 1415.0, 1369.6, 1241.5, 1166.9, 1121.6, 1067.4905, 1036.0, 992.3, 928.4, 833.7, 721.5, 531.3, 411.6.

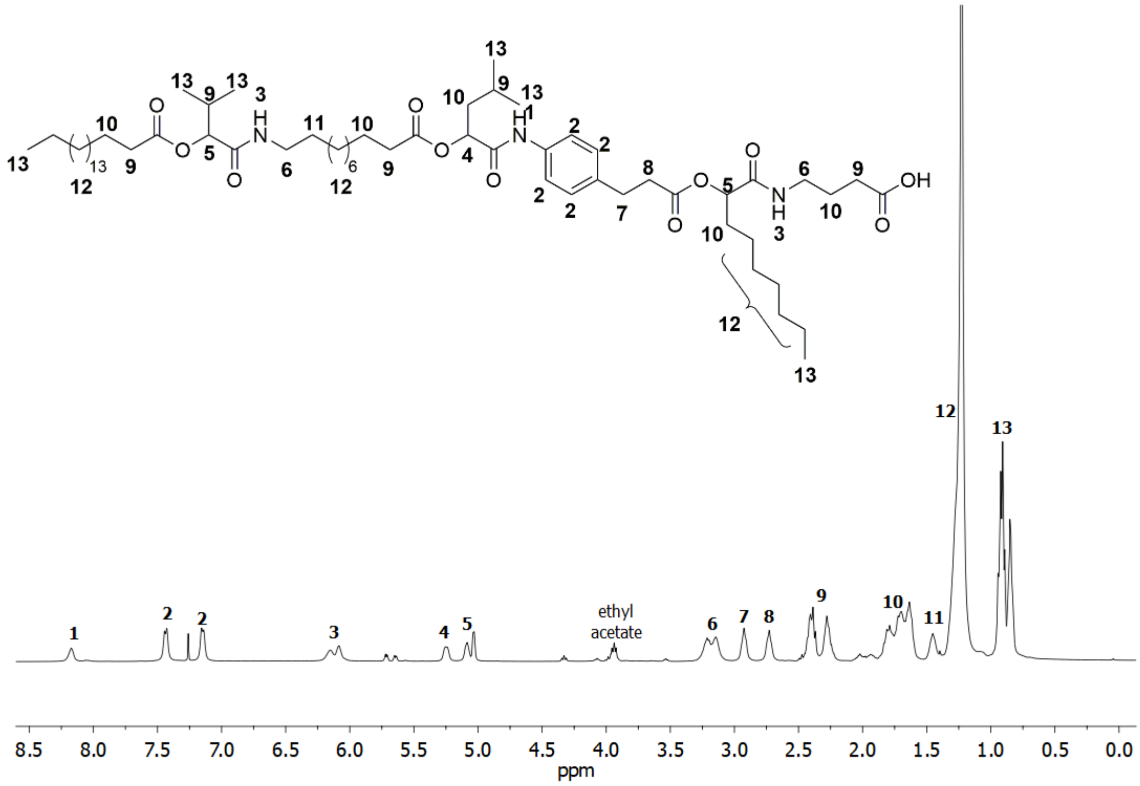
1
2
2
3
4
5
ethyl acetate
6
7
8
9
10
11
12
13
8.5
8.0
7.5
7.0
6.5
6.0
5.5
5.0
4.5
4.0
3.5
3.0
2.5
2.0
1.5
1.0
0.5
0.0
ppm

4th Passerini reaction

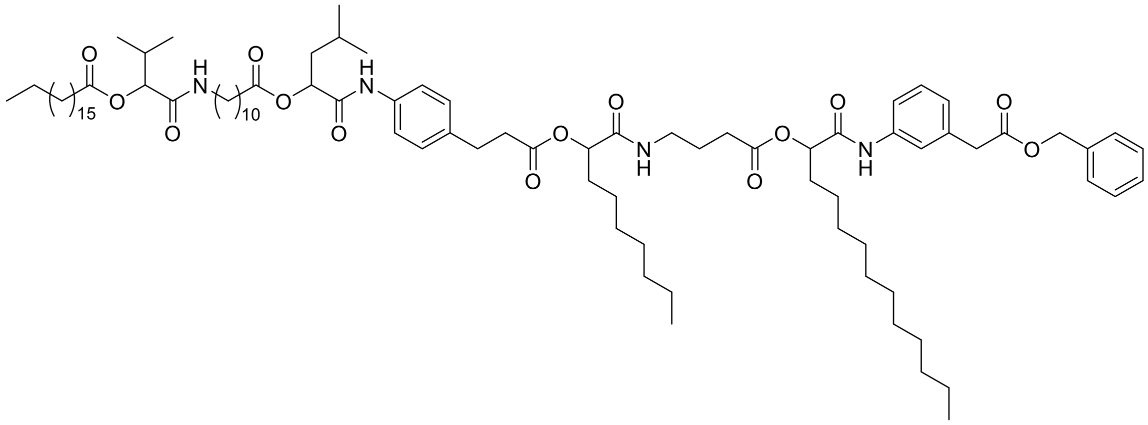

Substance **38** (2.13 g, 2.00 mmol, 1.00 eq.) was dissolved in DCM (4.0 mL, 0.5 M). Subsequently, dodecanal **11g** (0.67 mL, 0.55 g, 3.00 mmol, 1.50 eq.) and monomer **M8** (0.75 g, 3.00 mmol, 1.50 eq.) were added and the reaction mixture was stirred at room temperature for 48 hours. The solvent was removed under reduced pressure and the crude product was purified by column chromatography (cyclohexane / ethyl acetate 12:1 → 1:1, with 5% of triethyl amine) to obtain the desired product **39** in a quantitative yield (2.96 g, 2.00 mmol) as a yellow highly viscous oil.

^{1}H NMR (400 MHz, $CDCl_3$) δ / ppm: 8.83 – 6.65 (m, 1H, ^{1}), 8.03 (s, 1H, ^{2}), 7.69 – 6.91 (m, 13H, ^{3}), 6.03 (s, 2H, ^{4}), 5.24 (m, 2H, ^{5}),5.11 – 5.06 (s, 2H, ^{6}), 5.05 – 5.03 (m, 2H, ^{7}), 3.71 – 3.44 (m, 2H, ^{8}), 3.39 – 2.99 (m, 4H, ^{9}), 3.24 – 2.84 (m, 2H, ^{10}), 2.83 – 2.63 (m, 2H, ^{10}), 2.55 – 2.15 (m, 8H, ^{11}), 2.13 – 1.53 (m, 12H, ^{12}), 1.56 – 1.38 (m, 2H, ^{13}), 1.24 (s, 68H, ^{14}), 1.01 – 0.65 (m, 21H, ^{15}).

^{13}C NMR (101 MHz, $CDCl_3$) δ / ppm: 173.02, 172.71, 172.57, 171.78, 171.71, 171.36, 170.71, 169.44, 168.81, 168.66, 138.00, 137.94, 136.37, 135.82, 134.51, 128.98, 128.92, 128.83, 128.58, 128.26, 128.18, 125.38, 121.64, 120.42, 120.37, 119.49, 77.94, 74.51, 74.26, 72.87, 66.70, 41.25, 40.74, 39.22, 37.91, 35.52, 34.37, 34.29, 32.15, 31.98, 31.89, 31.79, 30.95, 30.58, 30.21, 30.13, 29.75, 29.70, 29.66, 29.61, 29.53, 29.41, 29.33, 29.22, 29.12, 26.87, 25.10, 24.95, 24.61, 23.14, 22.75, 22.66, 21.84, 18.85, 17.01, 14.20, 14.16.

HRMS-ESI-MS $[M+H]^+$ of $[C_{90}H_{144}N_4O_{14}]$: calculated: 1506.0752 found: 1506.0745.

IR (ATR platinum diamond): ν/ cm^{-1} = 3306.6, 2923.0, 2853.2, 1738.8, 1659.8, 1610.9, 1536.8, 1493.2, 1444.1, 1415.0, 1371.6, 1240.1, 1149.2889, 1002.3, 828.3, 775.6, 722.5, 695.5, 492.6.

***R*$_f$** : (cyclohexane / ethyl acetate 7: 5) = 0.58.

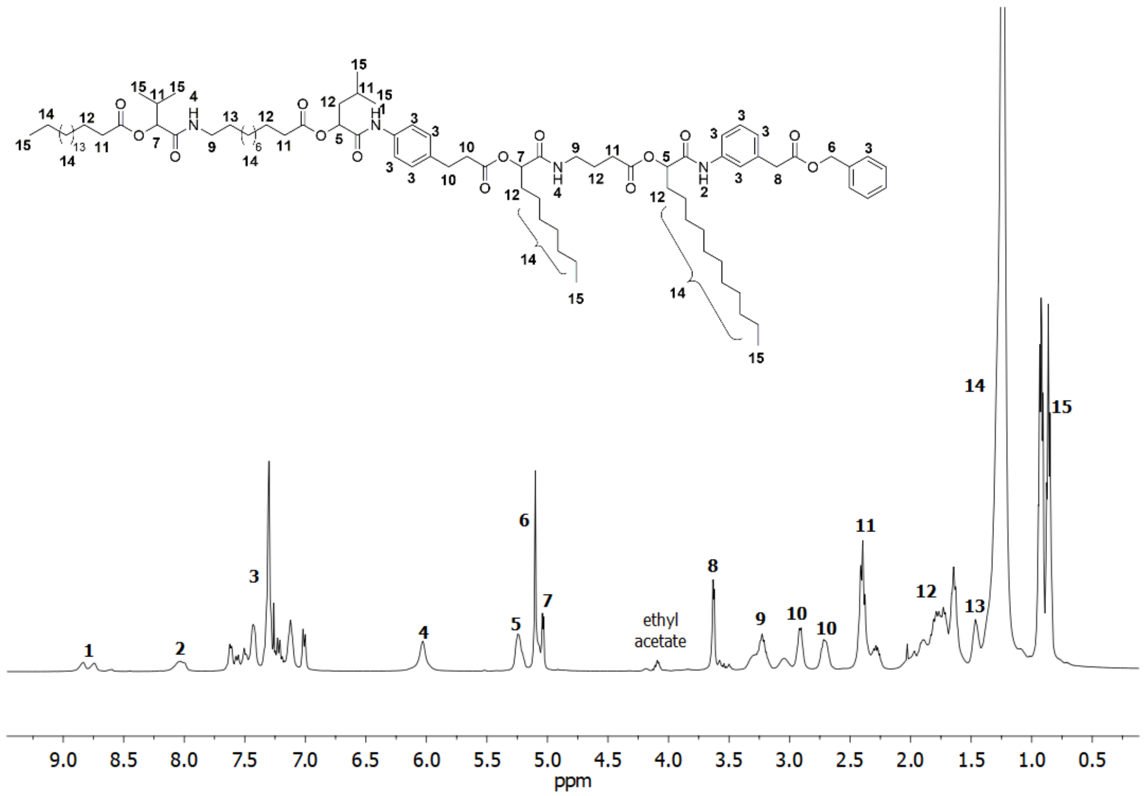
1
2
3
4
5
6
7
ethyl acetate
8
9
10
10
11
12
13
14
15
9.0
8.5
8.0
7.5
7.0
6.5
6.0
5.5
5.0
4.5
4.0
3.5
3.0
2.5
2.0
1.5
1.0
0.5
ppm

4th deprotection

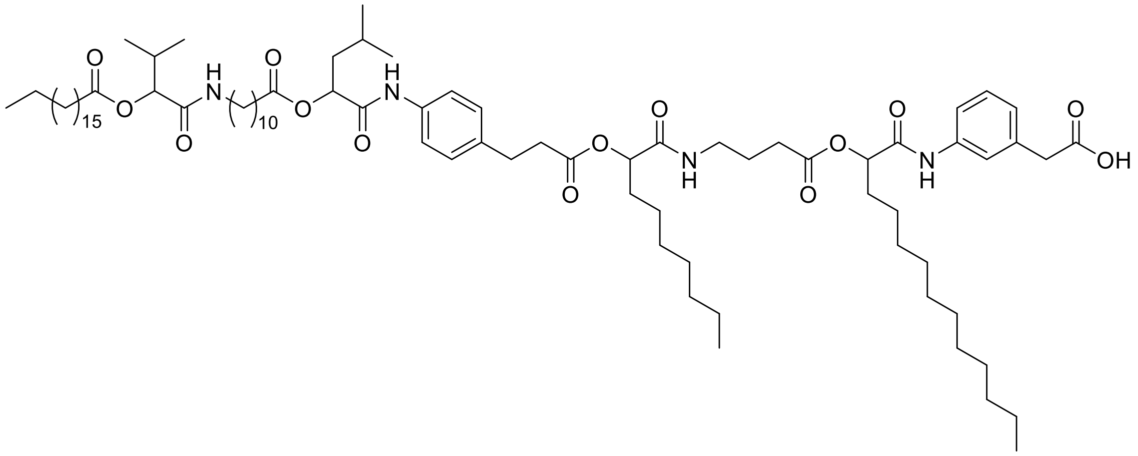

Substance **39** (2.16 g, 1.46 mmol, 1.00 eq.) was dissolved in THF (10.0 mL, 0.15 M). Subsequently, palladium on activated charcoal **19** (0.22 g, 10 wt%.) was suspended in the solution. The reaction mixture was purged with hydrogen (3 balloons) and stirred under hydrogen atmosphere overnight. The heterogeneous catalyst was filtered off and the solvent was evaporated under reduced pressure to obtain the desired product **40** in a yield of 99% (2.01 g, 1.44 mmol) as a highly viscous oil.

^{1}H NMR (500 MHz, $CDCl_3$) δ / ppm: 8.98 – 8.67 (m, 1H, ^{1}), 8.23 – 8.02 (m, 1H, ^{2}), 7.68 – 6.95 (m, 8H, ^{3}), 6.27 – 5.98 (m, 2H, ^{4}), 5.33 – 5.10 (m, 2H, ^{5}), 5.10 – 4.90 (m, 2H, ^{6}), 3.63 – 3.44 (m, 2H, ^{7}), 3.37 – 3.12 (m, 4H, ^{8}), 3.12 – 2.59 (m, 4H, ^{9}), 2.43 – 2.15 (m, 8H, ^{10}), 2.00 – 1.53 (m, 12H, ^{11}), 1.51 – 1.32 (m, 2H, ^{12}), 1.40 – 1.02 (m, 68H, ^{13}), 0.98 – 0.69 (m, 21H, ^{14}).

^{13}C NMR (126 MHz, $CDCl_3$) δ / ppm: 174.70, 173.35, 173.30, 172.80, 172.78, 172.74, 172.03, 172.00, 171.36, 170.91, 170.86, 170.81, 170.77, 169.66, 169.02, 169.00, 168.85, 168.82, 137.96, 137.88, 136.49, 136.44, 135.76, 135.72, 134.54, 134.52, 129.03, 129.01, 128.82, 128.80, 125.57, 125.53, 121.59, 121.55, 120.55, 120.51, 119.63, 119.57, 107.70, 106.44, 77.97, 77.96, 74.61, 74.57, 74.28, 72.95, 68.67, 67.74, 67.52, 60.53, 41.01, 40.72, 39.29, 38.02, 37.90, 35.52, 35.47, 34.38, 34.29, 32.14, 32.12, 32.06, 32.00, 31.99, 31.91, 31.81, 31.81, 31.00, 30.92, 30.60, 30.21, 30.14, 29.78, 29.76, 29.73, 29.72, 29.70, 29.69, 29.64, 29.61, 29.58, 29.55, 29.44, 29.35, 29.24, 29.19, 29.13, 27.90, 26.85, 26.06, 26.03, 25.15, 25.11, 24.99, 24.94, 24.86, 24.63, 23.91, 23.89, 23.15, 22.77, 22.68, 22.25, 21.84, 21.13, 18.85, 17.02, 14.27, 14.21, 14.17.

HRMS-ESI-MS $[M+H]^+$ of $[C_{83}H_{138}N_4O_{14}]$: calculated: 1416.0282 found: 1416.0226.

IR (ATR platinum diamond): ν/ cm^{-1} =3304.0, 2922.9, 2853.1, 1739.3, 1659.3, 1611.9, 1537.8, 1493.0, 1444.5, 1415.0, 1370.4, 1240.8, 1153.3, 829.1, 775.9, 720.7, 531.2, 444.4.

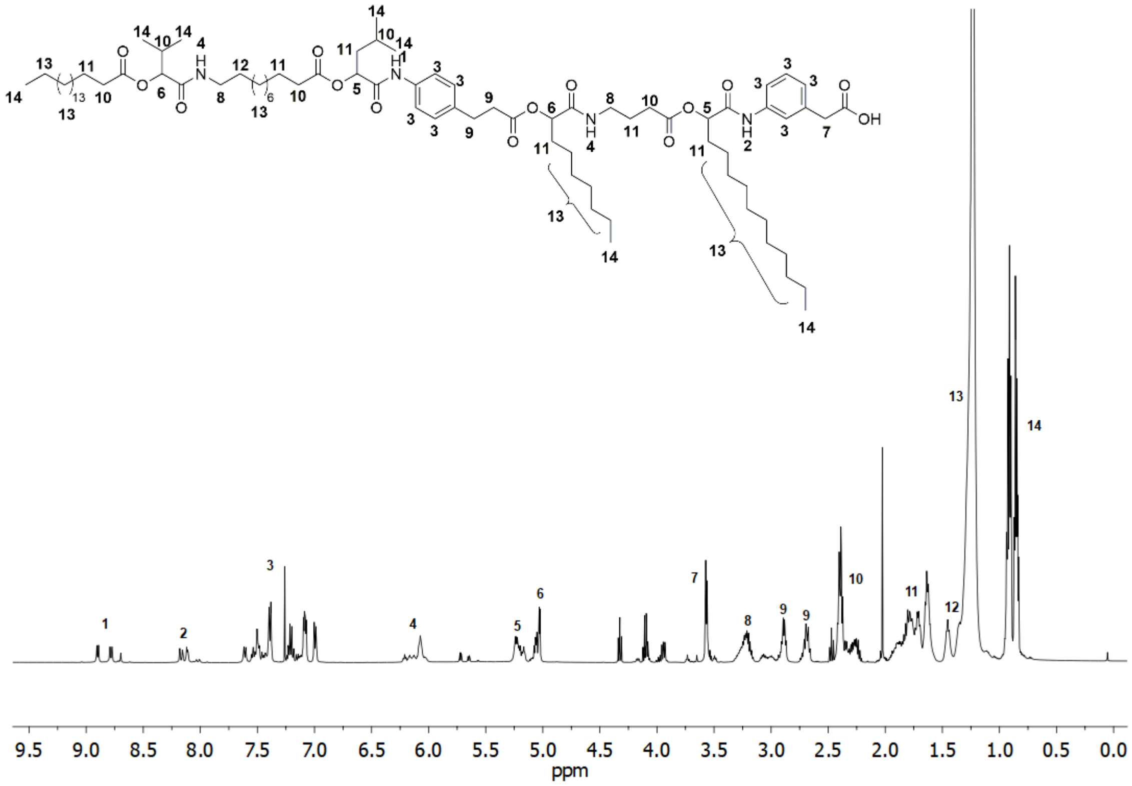
OH
1
2
3
4
5
6
7
8
9
10
11
12
13
14
9.5
9.0
8.5
8.0
7.5
7.0
6.5
6.0
5.5
5.0
4.5
4.0
3.5
3.0
2.5
2.0
1.5
1.0
0.5
0.0
ppm

5th Passerini reaction

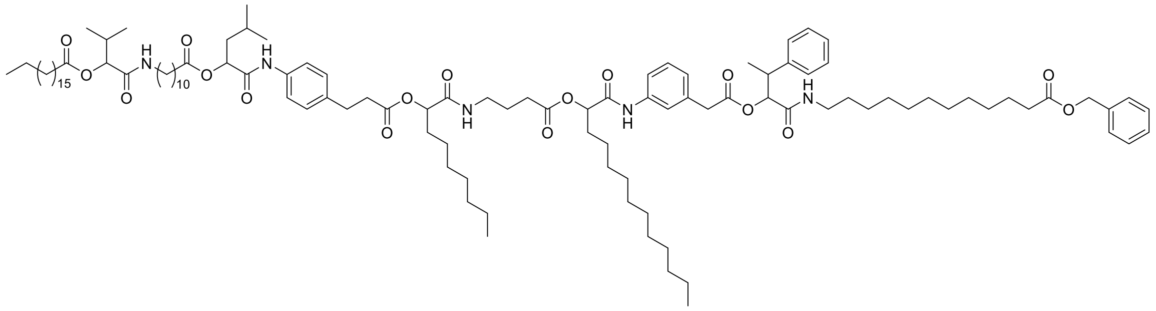

Substance **40** (1.92 g, 1.38 mmol, 1.00 eq.) was dissolved in DCM (4.0 mL, 0.35 M). Subsequently, 2-phenylpropanal (0.28 mL, 0.28 g, 2.10 mmol, 1.50 eq.) and monomer **M3** (0.66 g, 2.10 mmol, 1.50 eq.) were added and the reaction mixture was stirred at room temperature for 48 hours. The solvent was removed under reduced pressure and the crude product was purified by column chromatography (cyclohexane / ethyl acetate 12:1 → 1:1, with 5% of triethyl amine) to obtain the desired product **41** in a yield of 81% (2.05 g, 1.12 mmol) as a white solid.

^{1}H NMR (300 MHz, $CDCl_3$) δ / ppm: 9.14 – 8.88 (m, 1H, ^{1}), 8.23 – 7.98 (m, 1H, ^{2}), 7.80 – 6.82 (m, 18H, ^{3}), 6.17 – 5.94 (m, 3H, ^{4}), 5.35 – 5.14 (m, 3H, ^{5}), 5.12 – 5.05 (m, 2H, ^{6}), 5.03 (m, 2H, ^{7}), 3.74 – 3.47 (m, 3H, ^{8}), 3.44 – 3.10 (m, 6H, ^{9}), 3.08 – 2.60 (m, 4H, ^{10}), 2.51 – 2.17 (m, 10H, ^{11}), 2.04 – 1.53 (m, 14H, ^{12}), 1.45 (m, 4H, ^{13}), 1.40 – 1.00 (m, 82H, ^{14}), 0.99 – 0.71 (m, 24H, ^{15}).

^{13}C NMR (126 MHz, $CDCl_3$) δ / ppm: 173.79, 172.70, 172.68, 172.51, 171.78, 169.51, 169.45, 169.03, 168.71, 168.68, 141.54, 136.29, 136.15, 135.88, 134.05, 128.79, 128.64, 128.58, 128.39, 128.28, 128.24, 128.21, 128.18, 127.90, 127.84, 126.97, 126.93, 120.39, 119.61, 78.05, 77.95, 77.94, 74.26, 72.86, 66.12, 51.50, 45.87, 41.65, 41.63, 41.59, 41.48, 41.16, 40.73, 39.21, 39.07, 35.51, 35.43, 34.39, 34.35, 34.27, 34.17, 32.14, 32.06, 31.97, 31.95, 31.89, 31.79, 31.78, 30.75, 30.57, 30.23, 30.12, 29.74, 29.72, 29.70, 29.69, 29.66, 29.65, 29.60, 29.56, 29.52, 29.41, 29.32, 29.27, 29.24, 29.21, 29.20, 29.15, 29.12, 26.91, 26.86, 26.77, 26.69, 26.66, 25.32, 25.18, 25.14, 25.09, 25.02, 24.99, 24.94, 24.62, 23.15, 22.74, 22.65, 21.83, 18.84, 17.56, 17.01, 14.74, 14.18, 14.14, 13.22, 8.63.

HRMS-ESI-MS $[M+H]^+$ of $[C_{112}H_{177}N_5O_{17}]$: calculated: 1865.3212 found: 1865.3248.

IR (ATR platinum diamond): ν / cm^{-1} = 3295.8, 2923.7, 2852.7, 1739.7, 1659.5, 1610.7, 1536.5, 1493.9, 1448.5, 1415.5, 1372.2, 1238.2, 1152.2, 1046.7, 827.9, 722.2, 698.7, 536.2.

R_f : (cyclohexane / ethyl acetate 5:3) = 0.53.

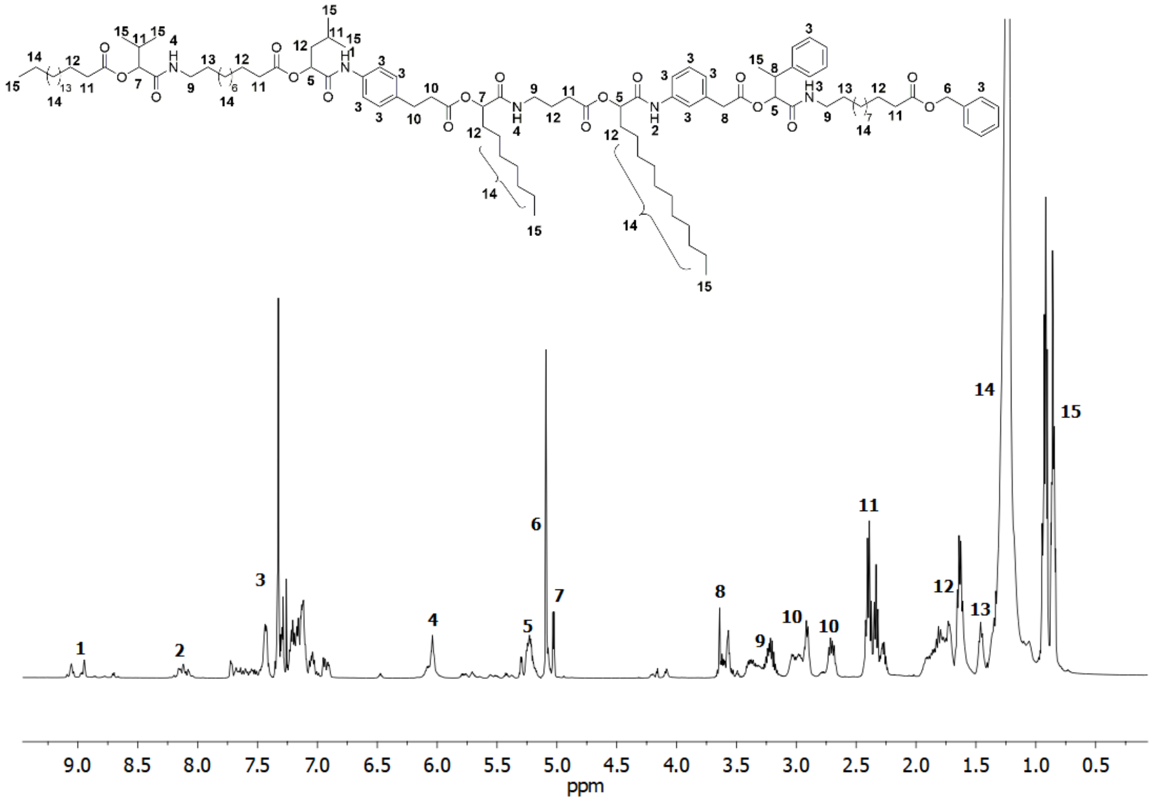
1
2
3
4
5
6
7
8
9
10
10
11
12
13
14
15
9.0
8.5
8.0
7.5
7.0
6.5
6.0
5.5
5.0
4.5
4.0
3.5
3.0
2.5
2.0
1.5
1.0
0.5
ppm

6.3.2.2.3 Tandem ESI-MS fragmentation of tetramer **39**

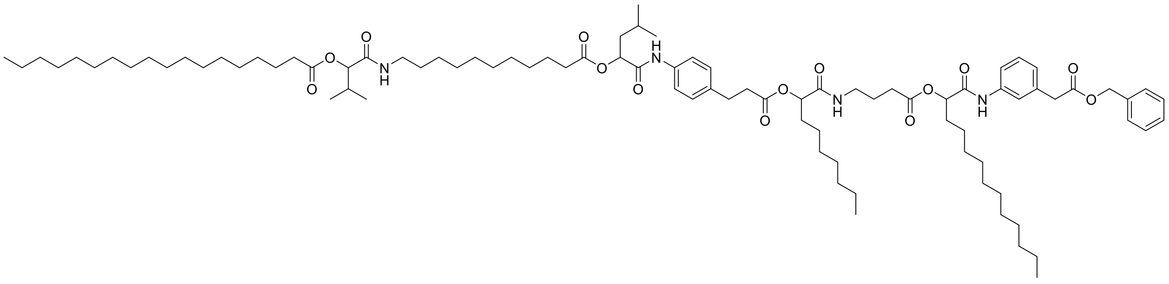

*Figure S 34. Molecular structure of tetramer **39** that was used for sequential read-out by tandem mass spectrometry.*

*Table S 2. ESI-MS fragments of tetramer **39** obtained by tandem ESI-MS read-out.*

Fragment	**$m/z_{calc.}$**	**m/z_{found}**	**Δ [mmu]**
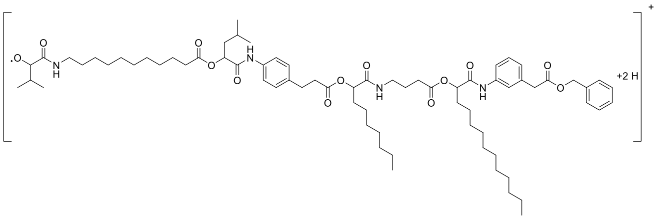	1239.8137	1239.8114	2.26
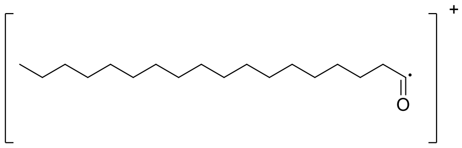	267.2688	267.2677	1.05
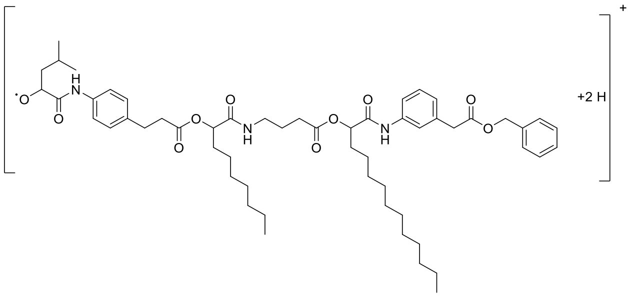	956.5989	956.5972	1.76
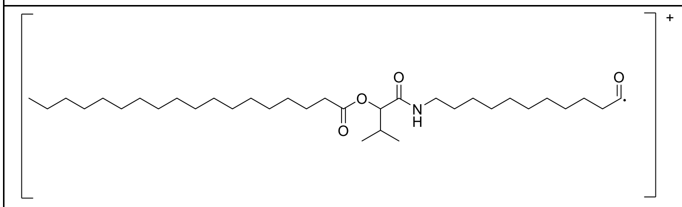	550.4835	550.4822	1.34

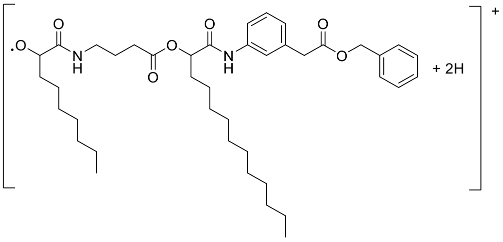	695.4624	695.4615	0.94
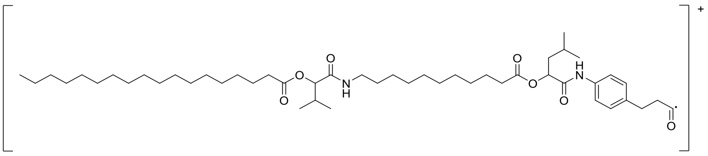	811.6200	811.61751	2.49
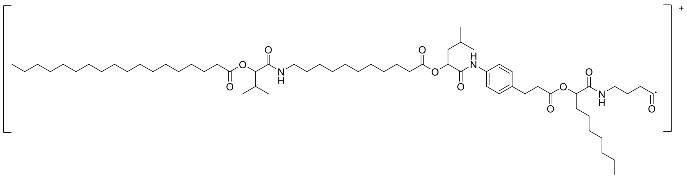	1052.7878	1052.7850	2.82

6.3.3 Experimental Procedures Chapter 4.2

6.3.3.1 Linker molecule synthesis:

Synthesis of diene-isocyanide, L1

Synthesised according to previously reported procedure.[401]

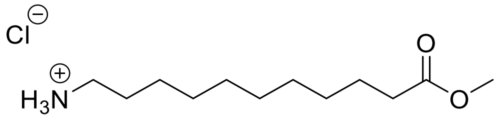

15.0 g of 11-Aminoundecanoic acid **1a** (74.5 mmol, 1.0 eq.) was suspended in 150 mL methanol and the suspension was cooled in an ice bath to 0°C. Subsequently, 18.9 mL of thionyl chloride **4** (31,0 g, 0.26 mol, 3.5 eq.) was added dropwise. After addition of the thionyl chloride **4**, the solution was not cooled anymore and the reaction was stirred at room temperature overnight. The yellowish solution was then poured into 500 mL of cold diethyl ether and stored in the freezer for one hour. The product was filtered off and dried under high vacuum. 11-Methoxy-11-oxoundecan-1-ammonium chloride **42** was obtained as a white powder in a yield of 99% (18.6 g). The crude product was used without further purification.

^{1}H-NMR: (300 MHz, CD_3OD) δ /ppm: 3.62 (s, 3H, $OC\underline{H}_3$, ^{1}), 2.91 (t, J = 7.0 Hz, 2H, $C\underline{H}_2NH_3^+$, ^{2}), 2.34 – 2.20 (t, J = 7.4 Hz, 2H, $C\underline{H}_2COOCH_3$, ^{3}), 1.75 – 1.47 (m, 4H, $C\underline{H}_2CH_2COOCH_3$, $C\underline{H}_2CH_2NH_3^+$, ^{4}), 1.45 – 1.15 (m, 12H, CH_2, ^{5}).

^{13}C NMR (101 MHz, CD_3OD) δ /ppm: 175.98, 51.95, 40.79, 34.78, 30.39, 30.37, 30.29, 30.15, 30.13, 28.55, 27.42, 25.99.

HRMS (EI) m/z: $[M\text{-}H]^+$ calculated for $[C_{12}H_{26}NO_2^+]$: 215.1885, found: 215.1885.

HRMS (EI) m/z: $[M]^+$ calculated for $[C_{12}H_{26}NO_2^+]$: 216.1964, found: 215.1964.

IR (ATR platinum diamond): ν /cm^{-1} = 2919.6, 2849.0, 1722.7, 1609.3, 1561.6, 1510.5, 1468.4, 1444.0, 1419.7, 1375.8, 1361.1, 1334.4, 1306.4, 1277.0, 1245.3, 1210.8, 1174.4, 1114.6, 1097.5, 1042.5, 1001.3, 970.9, 938.3, 885.8, 791.9, 741.7, 723.4, 702.5, 593.8, 504.1, 450.0, 425.6.

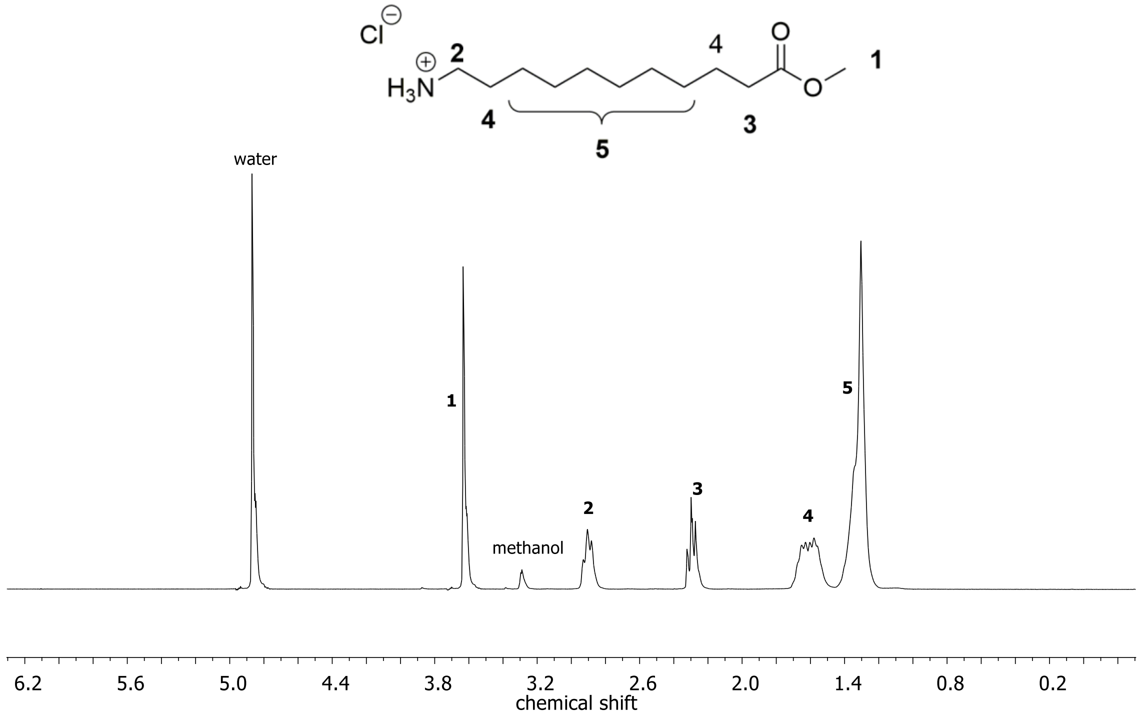
Cl
H3N
2
4
4
5
3
1
O
O
water
1
methanol
2
3
4
5
6.2
5.6
5.0
4.4
3.8
3.2
2.6
2.0
1.4
0.8
0.2
chemical shift

Methyl 11-formamidoundecanoate

Synthesised according to previously reported procedure.[401]

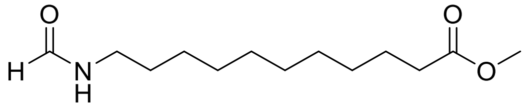

18.8 g of 11-methoxy-11-oxoundecan-1-aminium chloride **42** (74.9 mmol, 1.0 eq.) was dissolved in 81 mL of trimethyl orthoformate **5** (78.5 g, 0.74 mol, 10.0 eq.), heated to 100 °C and stirred under reflux for 12 hours. The solvent was evaporated under reduced pressure and 15.6 g (0.64 mol) of the product was obtained as a white solid in a yield of 98%. The crude product **43** was used without further purification.

^{1}H-NMR: (300 MHz, CDCl$_3$) *δ* /ppm: 8.19 – 7.87 (m, 1H, $\underline{H}$CO, ^{1}), 6.37 – 5.88 (m, 1H, N$\underline{H}$, ^{2}), 3.61 (s, 3H, OC$\underline{H}_3$, ^{3}), 3.38 – 3.01 (m, 2H, C$\underline{H}_2$, ^{4}), 2.24 (t, *J* = 7.5 Hz, 2H, C$\underline{H}_2$, ^{5}), 1.69 – 1.36 (m, 4H, C$\underline{H}_2$, ^{6}), 1.22 (s, 12H, C$\underline{H}_2$, ^{7}).

^{13}C NMR (101 MHz, CDCl$_3$) *δ* /ppm: 174.32, 155.78, 155.70, 155.62, 51.48, 41.69, 41.61, 41.52, 34.12, 29.32, 29.22, 29.14, 28.71, 26.35, 24.97.

HRMS (EI) m/z: [M]$^+$ calculated for [$C_{13}H_{25}NO_3^+$]: 243.1834, found: 243.1835.

IR (ATR platinum diamond): *ν* /cm^{-1} = 3260.2, 2915.9, 2849.2, 1734.8, 1682.9, 1638.4, 1536.6, 1463.7, 1435.9, 1379.1, 1334.7, 1301.2, 1268.8, 1226.8, 1204.6, 1169.6, 1113.3, 1058.1, 1001.9, 980.3, 905.0, 883.3, 738.2, 721.3, 518.8, 449.3.

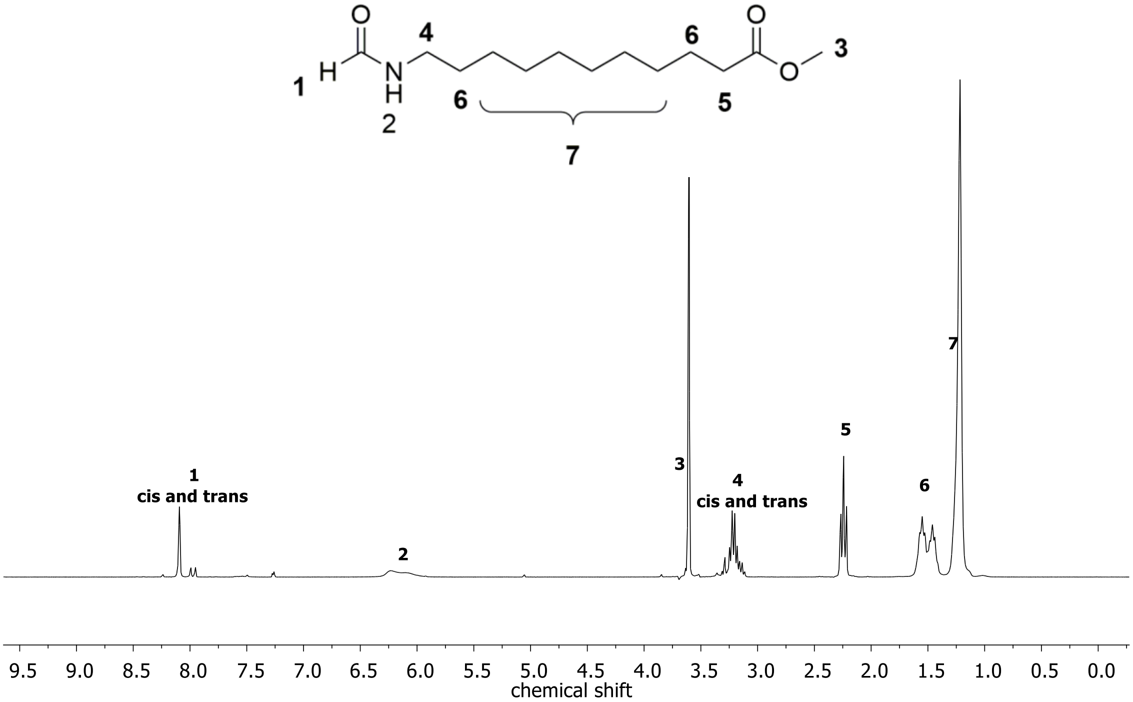

Methyl 11-isocyanoundecanoate

Synthesised according to previously reported procedure.[401]

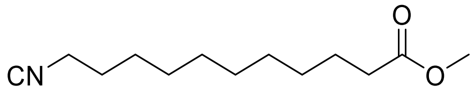

12.8 g of Methyl 11-formamidoundecanoate **43** was dissolved in 180 mL DCM and 22.3 mL of diisopropyl amine **7** (16.1 g, 0.16 mol, 3.0 eq.) was added to the solution. The mixture was then cooled with an ice bath to 0 °C and 6.3 mL of phosphoryl trichloride **6** (10.5 g, 68.8 mmol, 1.3 eq.) was added dropwise. After the addition, the ice bath was removed and the solution was allowed to warm up and was stirred for two hours at room temperature. The reaction was then quenched by addition of sodium carbonate solution (75 mL, 20%) at 0 °C. The mixture was stirred for another 30 minutes at room temperature and subsequently, 80 mL of DCM and 80 mL of water were added. The phases were separated and the organic layer was washed with water (3 times 80 mL) and brine (80 mL). The combined organic layers were dried over sodium sulfate, the solvent was evaporated under reduced pressure and the crude product was purified by column chromatography (hexane:ethyl acetate 19:1 → 10:1). The product **44** was obtained as a yellowish liquid in a yield of 70% (8.4 g, 37.1 mmol)

^{1}H-NMR: (400 MHz, $CDCl_3$) *δ* /ppm: 3.65 (s, 3H, $OC\underline{H}_3$ ^{1}), 3.44 – 3.26 (m, 2H, $C\underline{H}_2$, ^{2}), 2.29 (t, *J* = 7.5 Hz, 2H, $C\underline{H}_2$, ^{3}), 1.77 – 1.56 (m, 4H, $C\underline{H}_2$, ^{4}), 1.48 – 1.18 (m, 12H, $C\underline{H}_2$, ^{5}).

^{13}C NMR (75 MHz, $CDCl_3$) δ /ppm: 174.32, 155.70, 51.48, 41.69, 41.61, 41.52, 34.12, 29.32, 29.22, 29.14, 28.71, 26.35, 24.97.

HRMS (EI) m/z $[M]^+$ calculated for $[C_{13}H_{23}NO_2^+]$: 225.1729, found: 225.1729.

IR (ATR platinum diamond): *ν* /cm^{-1} = 2925.9, 2855.1, 2146.5 (isocyanide), 1735.6, 1435.9, 1353.1, 1194.8, 1170.0, 1104.5, 1010.8, 849.3, 722.4, 428.2.

***R*$_f$** (hexane / ethyl acetate (5:1)) = 0.51.

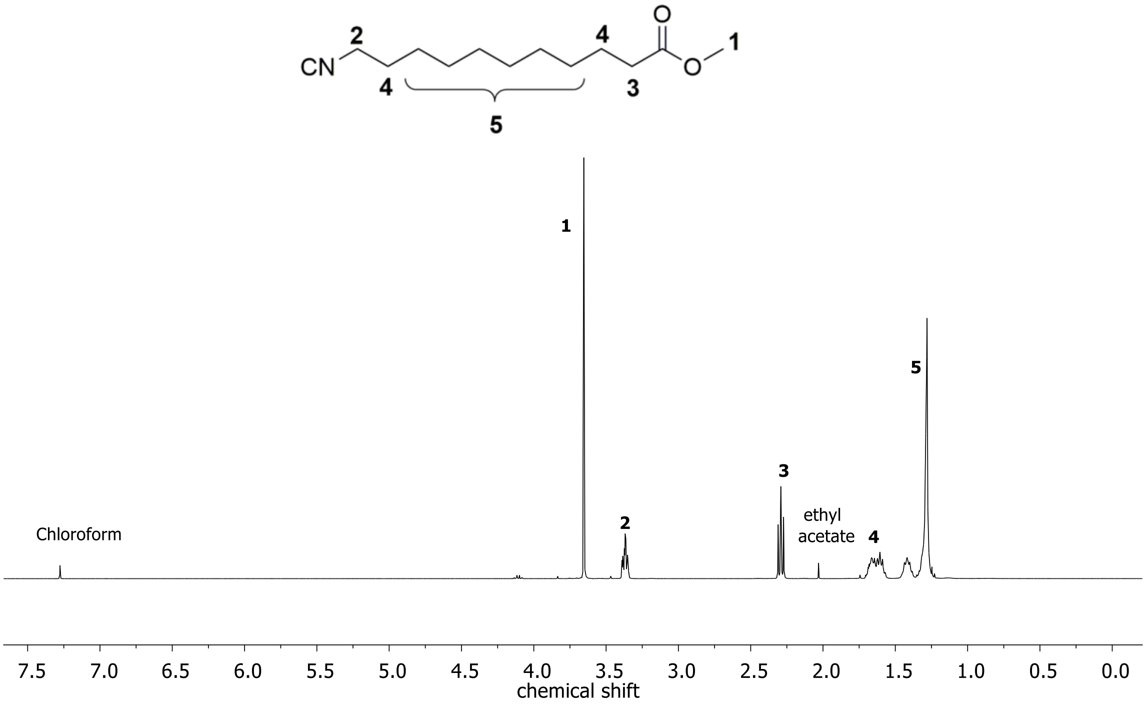
2
4
CN
4
5
4
3
O
O
1
1
5
3
2
Chloroform
ethyl acetate
4
7.5
7.0
6.5
6.0
5.5
5.0
4.5
4.0
3.5
3.0
2.5
2.0
1.5
1.0
0.5
0.0
chemical shift

(2*E*,4*E*)-hexa-2,4-diene-1-yl 11-isocyanoundecanoate

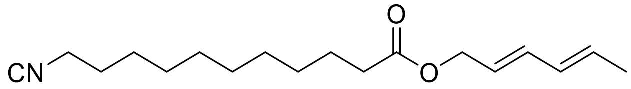

To a mixture of 8.3 g of methyl 11-isocyanoundecanoate **44** (36.3 mmol, 1.0 eq.) and 7.2 g of sorbic alcohol **45** (73.3 mmol, 2.0 eq.), 25.5 mg of TBD **46** (1.8 mmol, 5.0 mol%) was added as a catalyst and the reaction mixture was heated to 60 °C under a reduced pressure of 175 mbar at the rotavapor for 1 hour. Subsequently, the pressure was further decreased to 6 mbar and the temperature was decreased to 50 °C for another two and a half hours. Methanol was distilled off during the reaction. The crude product was purified by column chromatography (hexane:ethyl acetate 19:1→15:1) and **L1** was obtained as a slightly yellow liquid in a yield of 95% (10.1 g, 34.6 mmol).

^{1}H-NMR: (400 MHz, $CDCl_3$) δ /ppm: 6.28 – 6.15 (m, 1H, HC=C, ^{1}), 6.08 – 5.97 (m, 1H, HC=C, ^{2}), 5.79 – 5.65 (m, 1H, HC=C, ^{3}), 5.65 – 5.53 (m, 1H, HC=C, ^{4}), 4.54 (d, *J* = 6.6 Hz, 2H, COOCH_2, ^{5}), 3.40 – 3.30 (m, 2H, CH_2, ^{6}), 2.28 (t, *J* = 7.5 Hz, 2H, CH_2, ^{7}), 1.74 (d, *J* = 6.7 Hz, 3H, CH_3, ^{8}), 1.69 – 1.53 (m, 4H, CH_2, ^{9}), 1.46 – 1.19 (m, 12H, CH_2, ^{10}).

^{13}C NMR (75 MHz, $CDCl_3$) δ /ppm: 173.57, 134.77, 131.15, 130.51, 123.91, 64.75, 41.66, 41.58, 41.49, 34.33, 29.30, 29.20, 29.13, 29.11, 28.70, 26.33, 24.94, 18.15.

HRMS (EI) m/z $[M]^{+\cdot}$ calculated for $[C_{18}H_{29}NO_2^{+}]$: 292,2198, found: 292.2198.

IR (ATR platinum diamond): *v* /cm^{-1} = 2926.4, 2855.1, 2146.4 (isocyanide), 1732.0, 1661.7, 1453.4, 1377.6, 1350.9, 1231.0, 1163.5, 1104.2, 988.0, 924.7, 722.8, 506.3.

***R*$_f$** (hexane / ethyl acetate (5:1)) = 0.66.

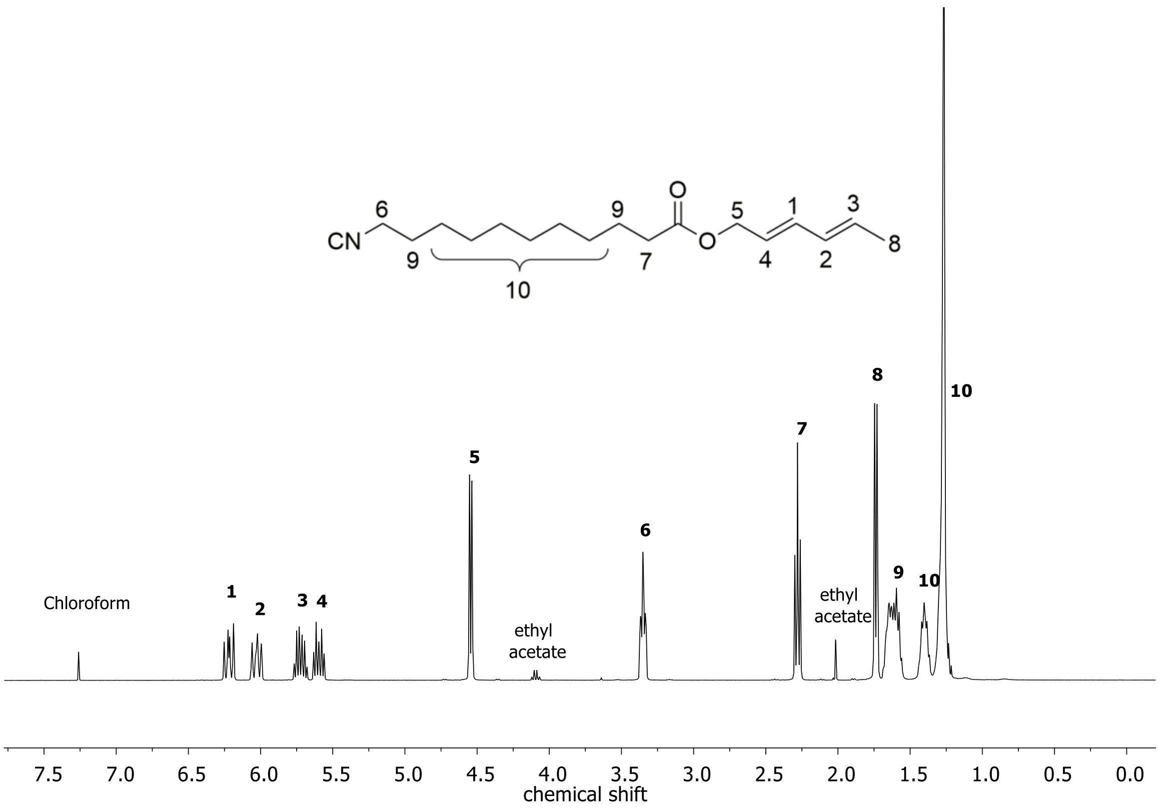
CN
6
9
10
9
7
O
O
5
4
1
2
3
8
Chloroform
1
2
3 4
5
ethyl acetate
6
7
ethyl acetate
8
9
10
10
7.5
7.0
6.5
6.0
5.5
5.0
4.5
4.0
3.5
3.0
2.5
2.0
1.5
1.0
0.5
0.0
chemical shift

Synthesis of 1,2,4-triazoline-3,5-dione hexanoic acid (TAD-COOH), L2:*

Synthesis of ethyl phenyl hydrazine-1,2-dicarboxylate

Synthesised according to previously reported procedure.[304]

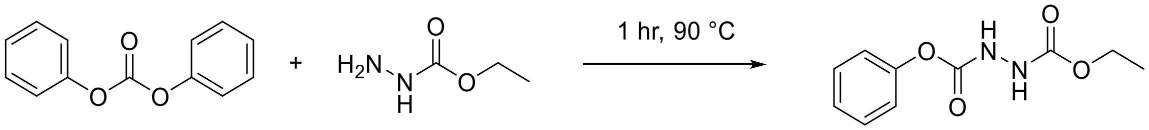

Diphenyl carbonate **50** (60.02 g, 0.280 mol, 1.0 equiv.) and ethyl carbazate **51** (58.37 g, 0.560 mol, 2.0 equiv.) were heated and stirred in bulk at 90 °C for 1 hour. The reaction was then precipitated into water (1.5 L) resulting in an emulsion. The precipitation was stirred fast for several hours and a white solid formed. The precipitation was filtered off and the precipitate was dried overnight under vacuum at 40 °C, resulting in a white, crystalline solid **48**. Yield = 40.21 g, 64%.

^{1}H NMR: (300 MHz, DMSO-*d$_6$*) *δ*/ppm: 9.67 (s, 1H, PhOC=ONH, ^{1}), 9.24 (s, 1H, NHC=OOCH$_2$CH$_3$, ^{2}), 7.46-7.35 (m, 2H, Ph, ^{4}), 7.30-7.21 (m, 1H, Ph, ^{5}), 7.14-7.08 (m, 2H, Ph, ^{6}), 4.07 (q, 2H, *J* = 7.09, 7.09, CH$_2$CH$_3$, ^{7}), 1.19 (t, 3H, *J* = 7.08, CH$_2$CH$_3$, ^{8}).

^{13}C NMR (APT, 100 MHz, DMSO-*d$_6$*) *δ*/ppm: 156.43, 154.86, 150.61, 129.48, 125.39, 121.47, 60.70, 14.52.

HRMS (ESI) *m/z*: [M + H]$^+$ for [$C_{10}H_{13}N_2O_4^+$]; calculated: 225.08698, found: 225.0872.

IR (ATR platinum diamond): *v* /cm^{-1} = 3225, 1742, 1699, 1519,1489, 1224, 1189, 1160, 1094, 1045, 907, 792, 723, 688.

---

[*] The synthesis of Linker molecule L2 was performed by cooperation partner Joshua Holloway at Gent University

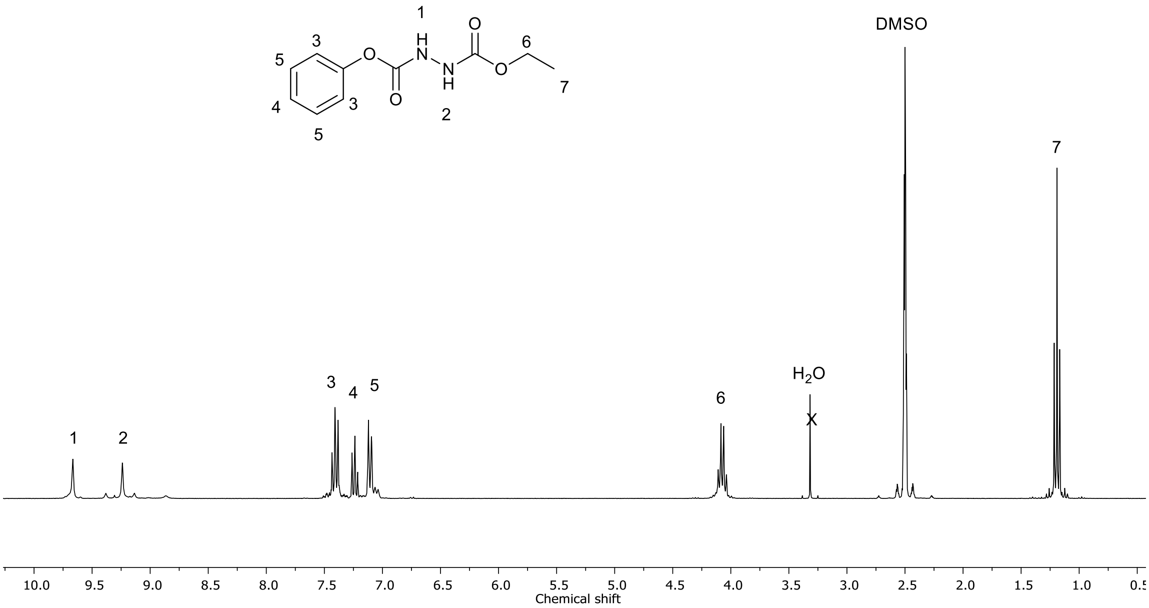
1
2
3
4
5
6
7
H
N
O
DMSO
H_2O
X
10.0
9.5
9.0
8.5
8.0
7.5
7.0
6.5
6.0
5.5
5.0
4.5
4.0
3.5
3.0
2.5
2.0
1.5
1.0
0.5
Chemical shift

Synthesis of hexanoic acid semicarbazide

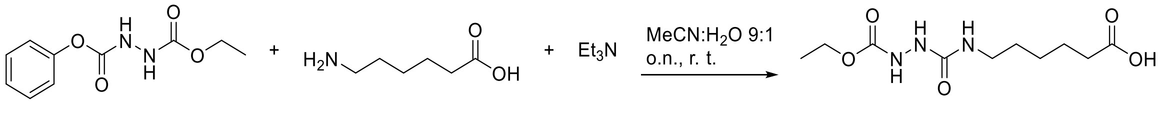

Aminocaproic acid **1b** (5.854 g, 44.6 mmol, 1.0 equiv.) and ethyl phenyl hydrazine dicarboxylate **48** (10.0 g, 44.6 mmol, 1.0 equiv.) were dissolved in a 9:1 solution of acetonitrile:H_2O (150 mL). Triethylamine **81** (12.4 mL, 89.2 mmol, 2.0 equiv.) was added and the reaction was stirred for at least 24 hours at room temperature. The acetonitrile was then removed *in vacuo* and then the residual water phase was diluted further with water (400 mL) and extracted three times with ethyl acetate to remove the phenol by-product from the reaction. The aqueous phase was then acidified to pH 1 with HCl in water (36%) before removal of the water *in vacuo*. Water (20 mL) was then added and the product was stirred vigorously at room temperature overnight to extract any residual, unreacted aminocaproic acid **1b**. The reaction mixture was then filtered and the white precipitate **49** dried overnight under vacuum at 40 °C. Yield =7.40 g, 64%.

^{1}H NMR (300 MHz, DMSO-*d₆*) *δ*/ppm: 11.96 (s, 1H, $COO\underline{H}$, ^{1}), 8.70 (s, 1H, $OC{=}ON\underline{H}$, ^{2}), 7.61 (s, 1H, $HNN\underline{H}C{=}ONH$, ^{3}), 6.29 (s, 1H, $HNNHC{=}ON\underline{H}$, ^{4}), 4.02 (q, 2H, *J* = 7.08, 7.09, $HNC{=}ONHC\underline{H_2}$ ^{5}), 2.97 (q, 2H, *J* = 6.61, 6.65, $CH_3C\underline{H_2}O$, ^{6}), 2.18 (t, 2H, *J* = 7.38, $C\underline{H_2}COOH$, ^{7}), 1.48 (p, 2H, *J* = 7.40, 7.40, $NHC{=}ONHCH_2C\underline{H_2}$ ^{8}), 1.41-1.31 (m, 2H, $C\underline{H_2}CH_2COOH$, ^{9}), 1.28-1.20 (m, 2H, $(CH_2)_2C\underline{H_2}(CH_2)_2$, ^{10}), 1.17 (t, 3H, *J* = 7.09, $C\underline{H_3}$, ^{11}).

^{13}C NMR (APT, 100 MHz, DMSO-*d₆*) *δ*/ppm: 174.44, 158.22, 156.89, 60.30, 38.96, 33.64, 29.58, 25.81, 24.25, 14.54.

HRMS (ESI) *m/z*: $[M + H]^+$ for $[C_{10}H_{20}N_3O_5^+]$; calculated: 262.1403, found: 262.1396.

IR (ATR platinum diamond): *v* /cm^{-1} = 3283, 2939, 1728, 1711, 1662, 1560, 1531, 1474, 1365, 1272, 1229, 1201, 1056, 898, 738, 648.

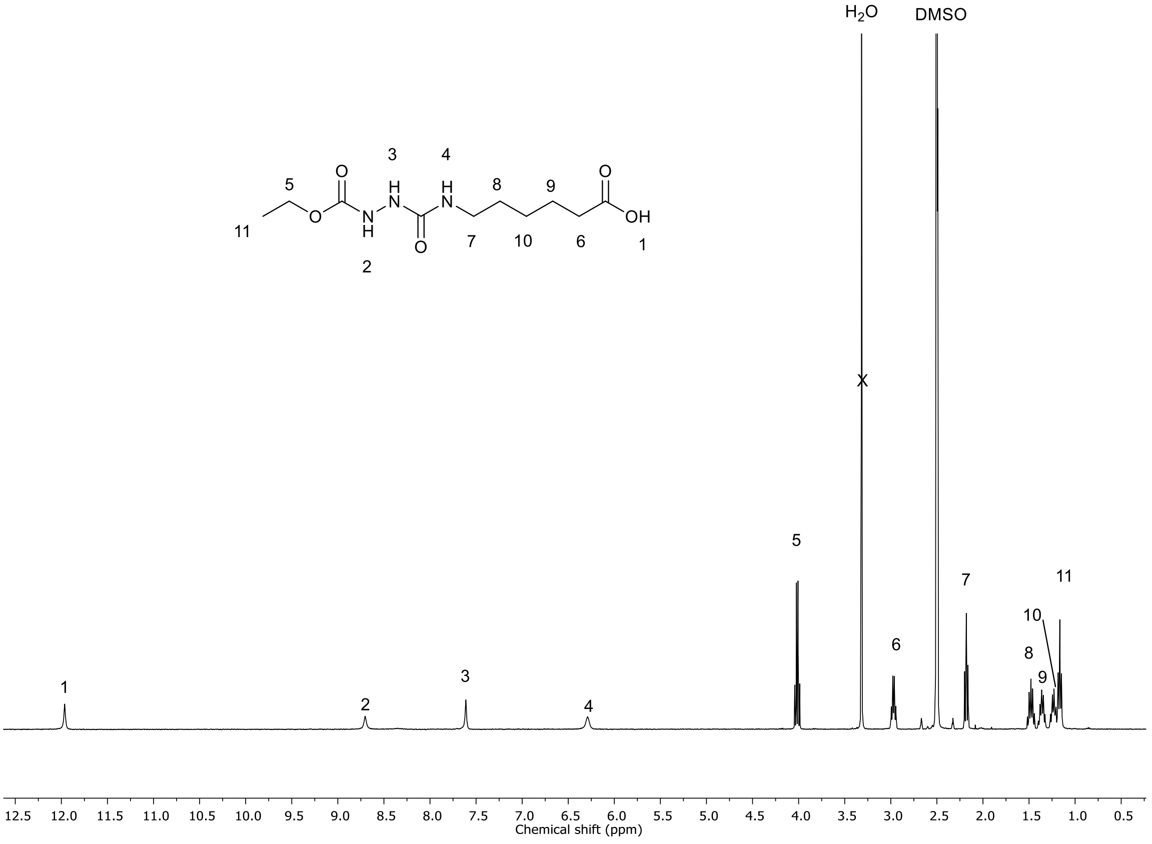
H2O
DMSO
3
4
5
O
H
N
N
H
H
N
8
9
O
OH
11
O
2
O
7
10
6
1
X
5
7
11
10
6
8
9
1
3
2
4
12.5
12.0
11.5
11.0
10.5
10.0
9.5
9.0
8.5
8.0
7.5
7.0
6.5
6.0
5.5
5.0
4.5
4.0
3.5
3.0
2.5
2.0
1.5
1.0
0.5
Chemical shift (ppm)

Ring closure of semicarbazide: Hexanoic acid urazole formation

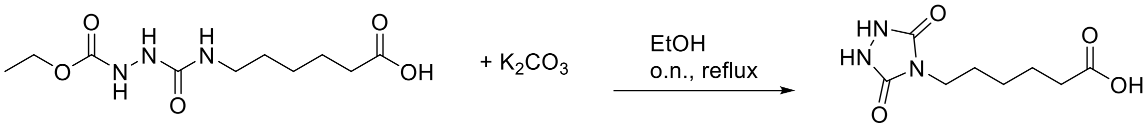

The semicarbazide **49** (6.05 g, 23.2 mmol, 1.0 equiv.) was solubilised in ethanol (100 mL). K_2CO_3 (12.7 g, 91.9 mmol, 4.0 equiv.) was added and the reaction was stirred at reflux overnight. The reaction was then cooled to room temperature, filtered and the filtrate was evaporated *in vacuo* to complete dryness. The resulting solid was then solubilised in a minimum volume of 1,4-dioxane and then acidified at room temperature to pH = 1 with HCl in 1,4-dioxane. The precipitate was then filtered off and the solvent was then removed *in vacuo*, yielding a white, crystalline solid **47**. Yield = 3.304 g, 67%.

^{1}H NMR (400 MHz, DMSO-*d$_6$*) δ/ppm: 11.99 (s, 1H, COO$\underline{H}$, ^{1}), 10.02 (s, 2H, $\underline{H}$N-N$\underline{H}$, ^{2}), 3.39-3.30 (m, 2H, UrC$\underline{H_2}$, ^{3}), 2.18 (t, 2H, *J* = 7.33, C$\underline{H_2}$COOH, ^{4}), 1.50 (h, 4H, *J* = 6.07, 8.87, 7.47, $CH_2C\underline{H_2}CH_2C\underline{H_2}CH_2$, ^{5}), 1.28-1.18 (m, 2H, $(CH_2)_2C\underline{H_2}(CH_2)_2$, ^{6}).

^{13}C NMR (100 MHz, DMSO-*d$_6$*) δ/ppm: 174.38, 155.06, 37.75, 33.49, 27.27, 25.59, 24.02.

HRMS (ESI) *m/z*: $[M + H]^+$ for $[C_8H_{14}N_3O_4^+]$; calculated: 216.0984, found: 216.0981.

IR (ATR platinum diamond): ν /cm^{-1} = 3166, 2931, 1668, 1474, 1415, 1348, 1225, 1190, 1116, 1030, 895, 849, 791, 767, 735, 639, 617.

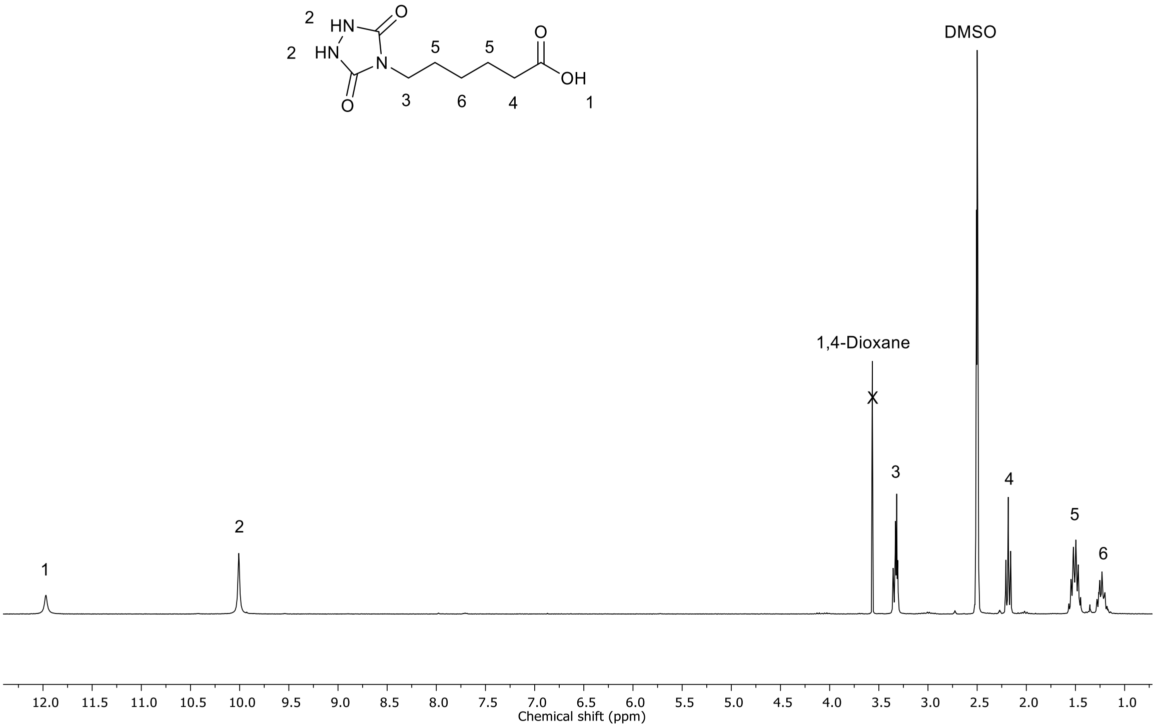

Oxidation of urazole to corresponding 1,2,4-triazoline-3,5-dione

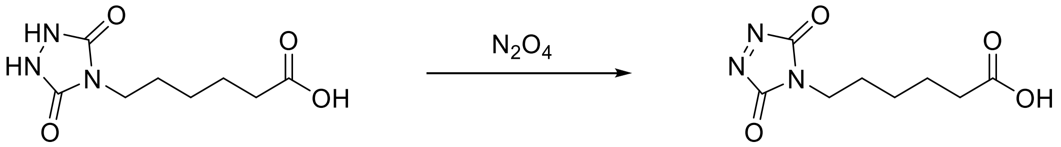

The urazole carboxylic acid **47** (0.920 g, 4.27 mmol, 1.0 equiv.) was suspended in anhydrous ethyl acetate (100 mL). $MgSO_4$ (5.15 g, 42.8 mmol, 10 equiv.) was added. The reaction mixture was flushed for approximately 5 minutes with N_2O_4 gas, during which the white suspension became vividly pink in colour. The reaction mixture was then filtered and the solvent from the filtrate was removed *in vacuo*. The isolated TAD moiety **L2** was used stored under inert atmosphere at -20 °C because of the inherent high reactivity and instability of TAD compounds. ^1H NMR was used to determine the disappearance of the urazole proton resonances, to verify quantitative conversion, but the yield was not quantified.

^{1}H NMR (300 MHz, DMSO-*d₆*) δ/ppm: 3.46 (t, 2H, J = 7.09, TADC$\underline{H_2}$, ^{1}), 2.18 (t, 2H, J = 7.34, C$\underline{H_2}$COOH, ^{2}), 1.64-1.43 (m, 4H, $CH_2C\underline{H_2}CH_2C\underline{H_2}CH_2$, ^{3}), 1.34-1.22 (m, 2H, $(CH_2)_2C\underline{H_2}(CH_2)_2$, ^{4}).

^{13}C NMR (100 MHz, DMSO-*d₆*) δ/ppm: 174.34, 160.15, 40.50, 33.42, 26.39, 25.38, 23.89.

HRMS (ESI) *m/z*: $[M + H]^+$ for $[C_8H_{12}N_3O_4^+]$; calculated: 214.0822, found: 214.1879.

HRMS (ESI) *m/z*: $[M + Na]^+$ for $[C_8H_{11}N_3O_4]$; calculated: 236.0642, found: 236.1720.

IR (ATR platinum diamond): ν /cm^{-1} = 2934, 2357, 1742, 1698, 1525, 1393, 1336, 1270, 1212, 1176, 1137, 946, 853, 728, 677.

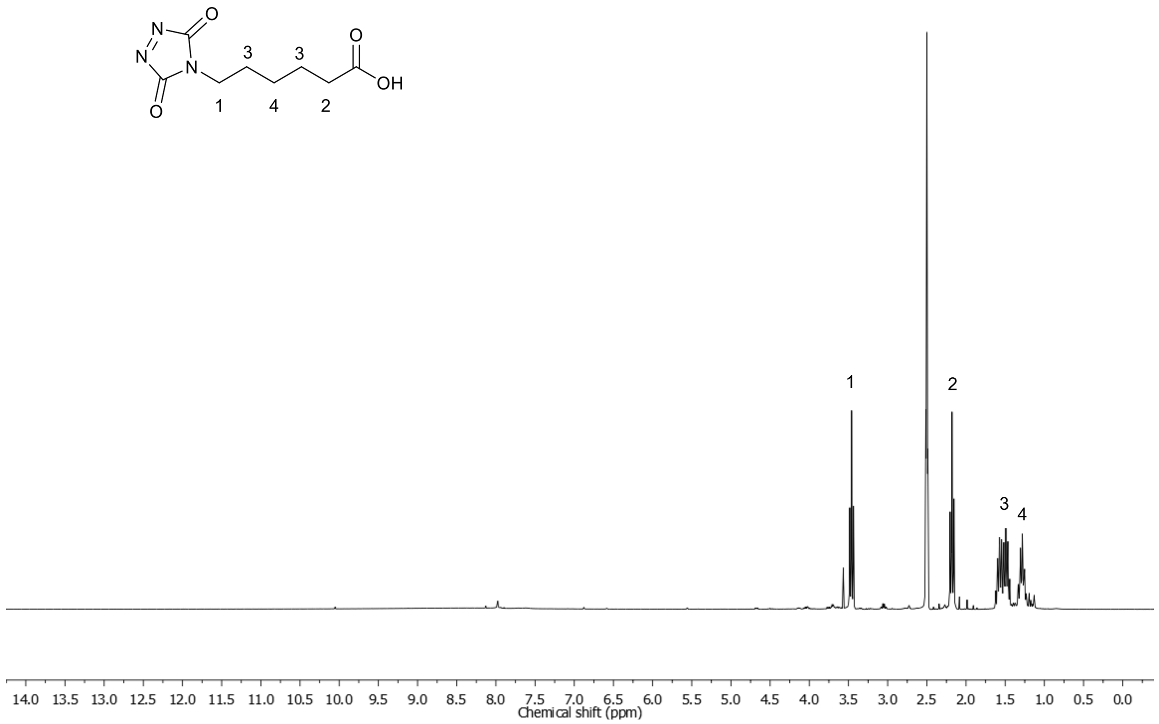

6.3.3.2 Solid-phase synthesis of sequence-defined oligomer[*]

Loading of the 2-chlorotrityl chloride resin

Loading of the resin was achieved *via* an adapted version of a previously reported approach. [23]

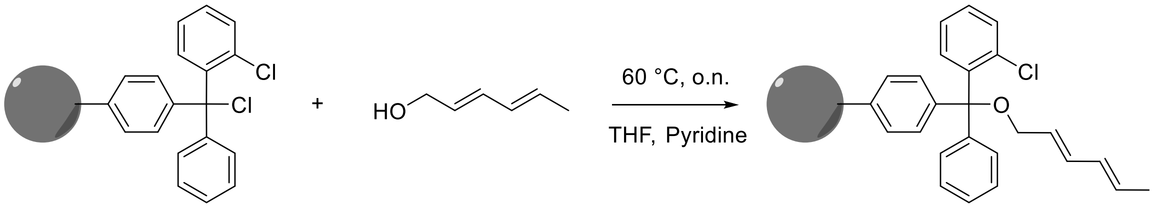

2-Chlorotrityl chloride resin (100-200 mesh, 1.6 mmol/g)(1.5 g, 1.0 equiv.) and sorbic alcohol **45** (0.355 g, 1.5 equiv.) were dissolved in THF (15 mL) and pyridine **82** (0.58 mL, 3.0 equiv.) under N_2 atmosphere and shaken vigorously at 60 °C overnight. The reaction was then filtered and shaken 3 times for 10 minutes with a 17:2:1 solution of DCM:MeOH:DIPEA (3 × 30 mL) to cap any unreacted sites, filtering after each 10 minute shake. The resin **54** was washed with DMF (3 × 30 mL), DCM (3 × 30 mL) and Et_2O (3 × 30 mL), dried under vacuum at room temperature for 4 hours, and then used directly for the first reaction step (*vide infra*).

Solid-phase synthesis protocol

The synthesis was carried out *via* a two-step, iterative protocol. The protocol was repeated for up to 12 cycles, yielding a sequence-defined dodecamer. In addition to the dodecamer synthesised, a monomer **62**, dimer **63**, trimer **64** and nonamer **65** were also synthesised to allow full characterisation of the three components of the ABC sequence.

Step 1: TAD-COOH addition

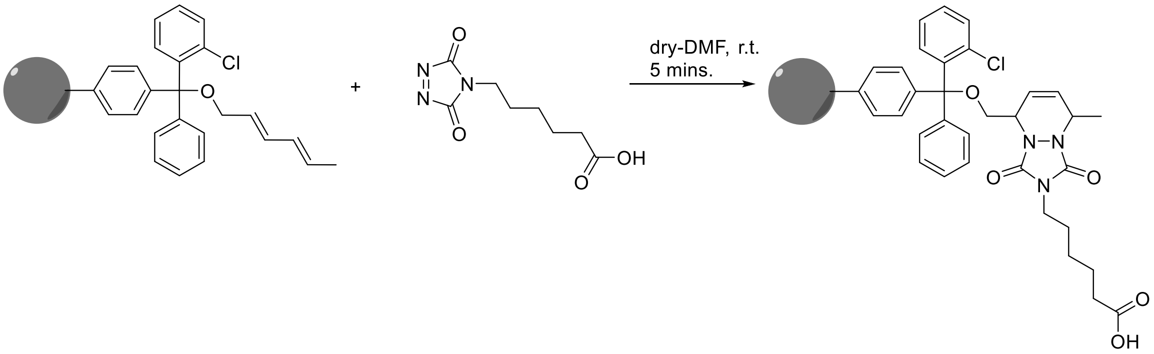

The diene functionalised resin **54** (50.0 mg, 1.0 equiv.) was swollen for at least 10 min. in anhydrous DMF (500 µL). This was then filtered off. TAD-COOH **L2** (34 mg, 2.0 equiv.) solubilised in anhydrous DMF (500 µL) was added and the reaction was shaken vigorously at room temperature for 5 minutes. The reaction was then filtered and the resin subsequently washed with DMF (×4), $CHCl_3$ (×4), MeOH (×4) and Et_2O (×4). The reaction was analysed by LC-MS (see

---

[*] The solid phase synthesis was performed by cooperation partner Joshua Holloway at Gent University.

Figure S1). To do this, 2 mg of the reaction resin was removed and suspended for 5 minutes in a 1% TFA solution (in DCM). This was then filtered, concentrated by evaporation and then diluted with acetonitrile.

Step 2: P-3CR

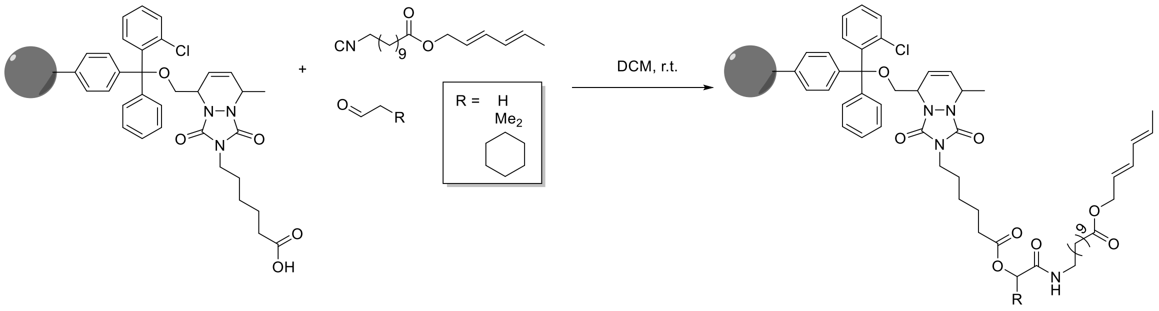

The resin from step 1 was swollen for at least 10 minutes in DCM (500 µL). Then, the diene isocyanide linker molecule **L1** (0.350 g, 15 equiv.) and propanal **11a**, isobutyraldehyde **11c** or cyclohexanal **11b** (20 equiv.) were added. The reaction was shaken vigorously at room temperature for 30 minutes. After the 4th, 7th and 9th cycles, the reaction time was increased by a further 30 minutes as the reaction was slower as the chains lengthened (see IR monitoring results). The reaction was then filtered and the resin subsequently washed with DMF (×4), $CHCl_3$ (×4), MeOH (×4) and Et_2O (×4). A 2 mg sample was again prepared for LC-MS analysis after each cycle as described above up until the 8th cycle when the molecular weight of the oligomer was beyond the measurable limits of the instrument, thus thereafter no intermediate analysis *via* LC-MS or HRMS was done.

This iterative, two-step protocol was repeated up to 12 times and was then capped as described below, resulting in a sequence-defined dodecamer. Yield = 14.4 mg, overall yield = 5%.

Diene capping with Phenyl TAD 66

A separate monomer **62**, dimer **63**, trimer **64** and dodecamer **65** were synthesised and capped with phenyl TAD **66** (synthesised according to previously reported work)[402] to prevent further reaction of the conjugated double bond and to prevent partial hydrolysis of the conjugated ester bond during the mild cleavage conditions. The capping was done by first swelling the resin for at least 10 mins in anhydrous DMF (500 µL). This was then filtered off. Afterwards, phenyl-TAD (PhTAD **66**) (5.0 equiv.) was dissolved in anhydrous DMF (500 µl) and added to the resin. The reaction was shaken vigorously at room temperature for 5 minutes. The reaction was then filtered, and the resin subsequently washed with DMF (×4), $CHCl_3$ (×4), MeOH (×4) and Et_2O (×4). The oligomer was cleaved entirely from the resin by suspension for 5 minutes in a 1% TFA solution **61** (in DCM). This was then filtered and concentrated by evaporation. The resulting colourless-yellow film was dried under vacuum at room temperature for several hours.

LC-MS analysis of sequence-defined oligomers synthesised on solid-phase:

1st TAD-COOH Diels-Alder addition to the solid-phase resin:

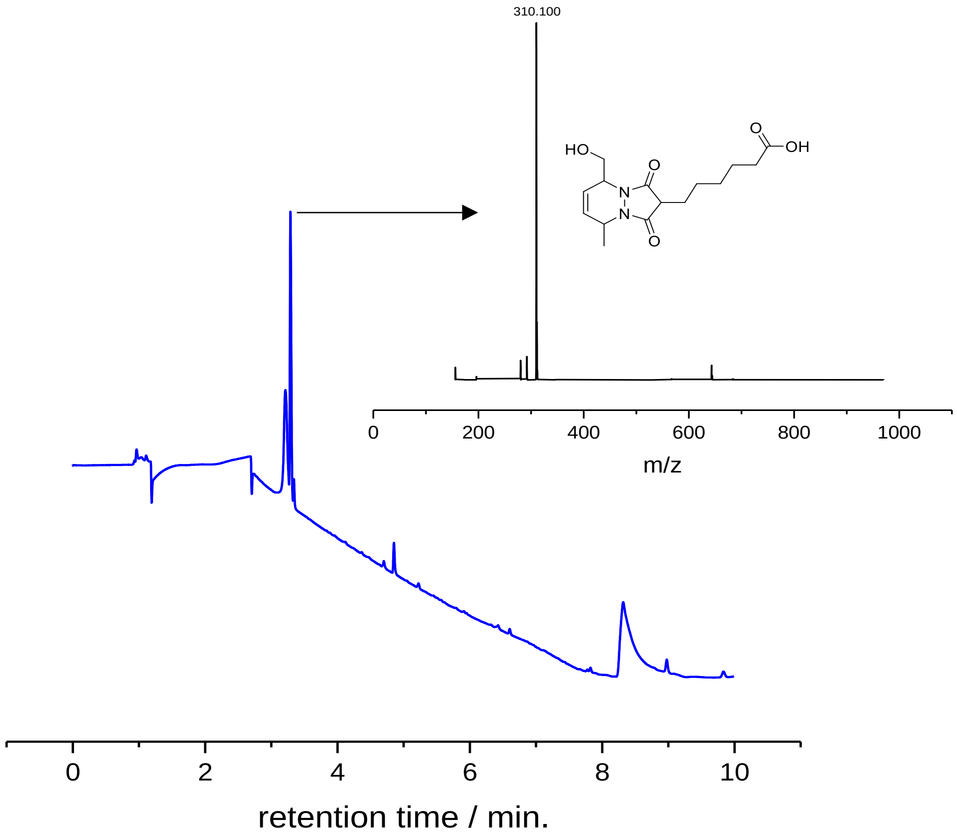

Figure S 35. LC-MS chromatogram (λ = 214 nm) of the adduct formed when TAD-COOH reacted with the diene-functionalised resin.

1st solid-phase P-3CR:

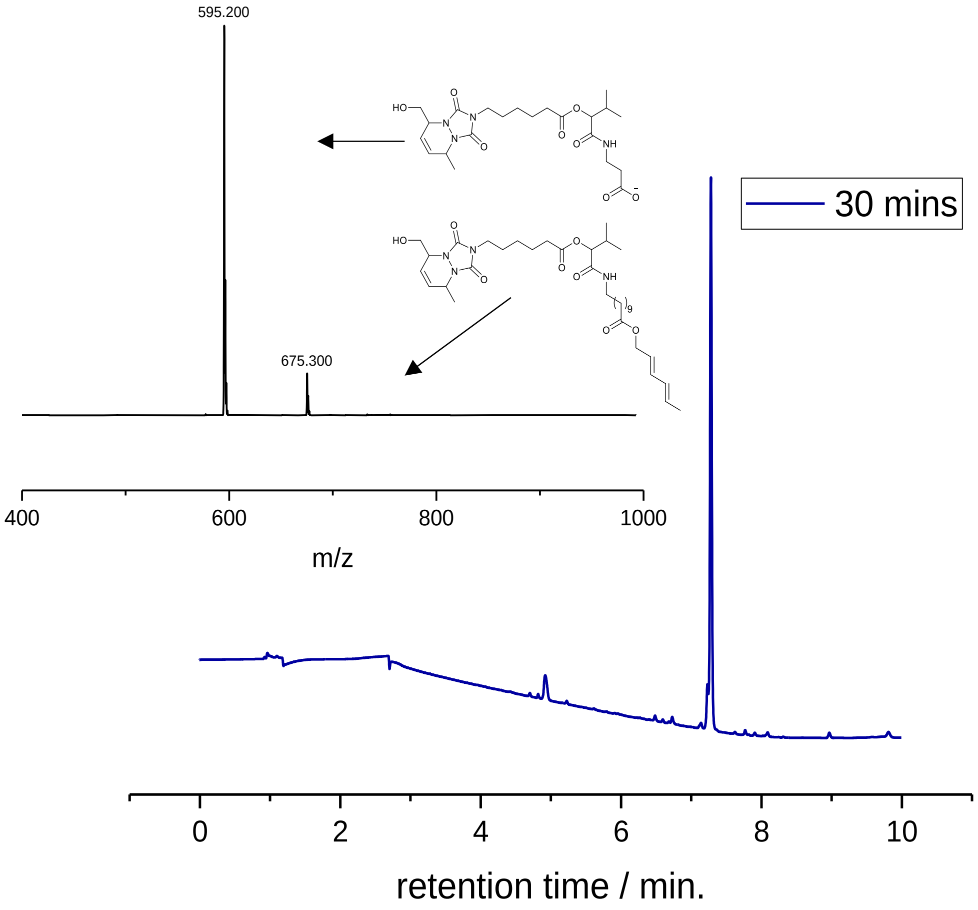

Figure S 36. LC-MS chromatogram (λ = 214 nm) of the 1st P-3CR on the solid-phase. The reaction is observed to be already complete after 30 minutes, with the only two peaks at 4.9 and 7.3 minutes both corresponding to the desired product. The ionisation of the molecule during LC-MS accounts for the fragmentation pattern observed in the MS spectrum.

Stacked LC-MS chromatograms showing the second up to the eighth iterative reaction cycle:

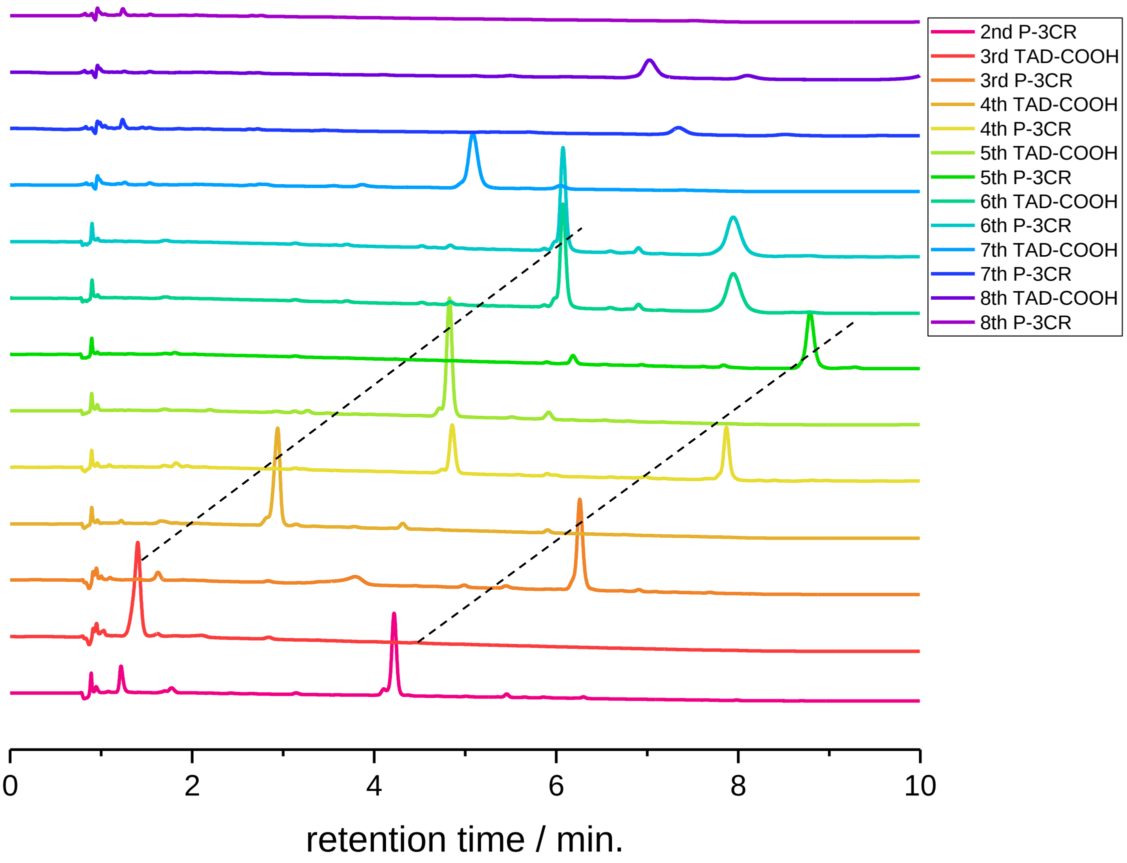

Figure S 37. LC-MS chromatograms (λ = 214 nm). A clear shift in the retention time between the carboxylic acid terminated chain and diene terminated chain can be seen. By following the same step in the cycle, one can also see a shift in retention time as the molecular weight increases. It should be noted that this does not continue in a liner fashion because from the 2nd to the 5th cycle, the solvent gradient (from acetonitrile to water) was 75-100%, and from the 6th to the 8th cycle it was 90-100%. The LC-MS gives little information after the 7th TAD-COOH addition.

HRMS results of the solid-phase synthesised sequence-defined oligomers:

PhTAD capped monomer, dimer, trimer, nonamer and dodecamer:

Sample name	m/z exp.	formula	m/z theo.	Δ m/z
Monomer 62	872.4503	$[C_{44}H_{63}N_7O_{10}Na]^+$	872.4529	0.0026
Monomer 62	850.4689	$[C_{44}H_{63}N_7O_{10}H]^+$	850.4709	0.0020
Dimer 63	1429.8302	$[C_{73}H_{109}N_6O_7NH_4]^+$	1429.8341	0.0038
Trimer 64	2051.1721	$[C_{106}H_{161}N_{15}O_{24}Na]^+$	2051.1731	0.0010
Trimer 64	1037.0803	$[C_{106}H_{161}N_{15}O_{24}Na_2]^{2+}$	1037.0812	0.0009
Trimer 64	2029.1907	$[C_{106}H_{161}N_{15}O_{24}H]^+$	2029.1912	0.0005
Trimer 64	1015.0980	$[C_{106}H_{161}N_{15}O_{24}H_2]^{2+}$	1015.0992	0.0012
Nonamer 65	2704.6421	$[C_{282}H_{448}N_{36}O_{64}Na_2]^{2+}$	2704.6346	0.0075
Nonamer 65	1810.7606	$[C_{282}H_{448}N_{36}O_{64}Na_3]^{3+}$	1810.7528	0.0078
Nonamer 65	1363.8164	$[C_{282}H_{448}N_{36}O_{64}Na_4]^{4+}$	1363.8119	0.0045
Nonamer 65	1095.6492	$[C_{282}H_{448}N_{36}O_{64}Na_5]^{5+}$	1095.6475	0.0017
Nonamer 65	2682.6045	$[C_{282}H_{448}N_{36}O_{64}H_2]^{2+}$	2682.6527	0.0482
Dodecamer	3669.7145	$[C_{382}H_{599}N_{51}O_{87}Na_2]^{2+}$	3669.6900	0.0245
Dodecamer 52	2454.1257	$[C_{382}H_{599}N_{51}O_{87}Na_3]^{3+}$	2454.1231	0.0026
Dodecamer 52	1846.3446	$[C_{382}H_{599}N_{51}O_{87}Na_4]^{4+}$	1846.3396	0.0050
Dodecamer 52	1481.6702	$[C_{382}H_{599}N_{51}O_{87}Na_5]^{5+}$	1481.6695	0.0007
Dodecamer 52	1238.5566	$[C_{382}H_{599}N_{51}O_{87}Na_6]^{6+}$	1238.5561	0.0005
Dodecamer 52	1064.9032	$[C_{382}H_{599}N_{51}O_{87}Na_7]^{7+}$	1064.9037	0.0005
Dodecamer 52	2432.1402	$[C_{382}H_{599}N_{51}O_{87}H_3]^{3+}$	2432.1411	0.0009
Dodecamer 52	1824.3595	$[C_{382}H_{599}N_{51}O_{87}H_4]^{4+}$	1824.1411	0.0018
Dodecamer 52	1459.6874	$[C_{382}H_{599}N_{51}O_{87}H_5]^{5+}$	1459.6876	0.0004
Dodecamer 52	1216.5735	$[C_{382}H_{599}N_{51}O_{87}H_6]^{6+}$	1216.5742	0.0007
Dodecamer 52	1043.0632	$[C_{382}H_{599}N_{51}O_{87}H_7]^{7+}$	1042.9218	0.1414

Nonamer 65 isotopic pattern and SEC-ESI-MS results (solid-phase, before optimisation):

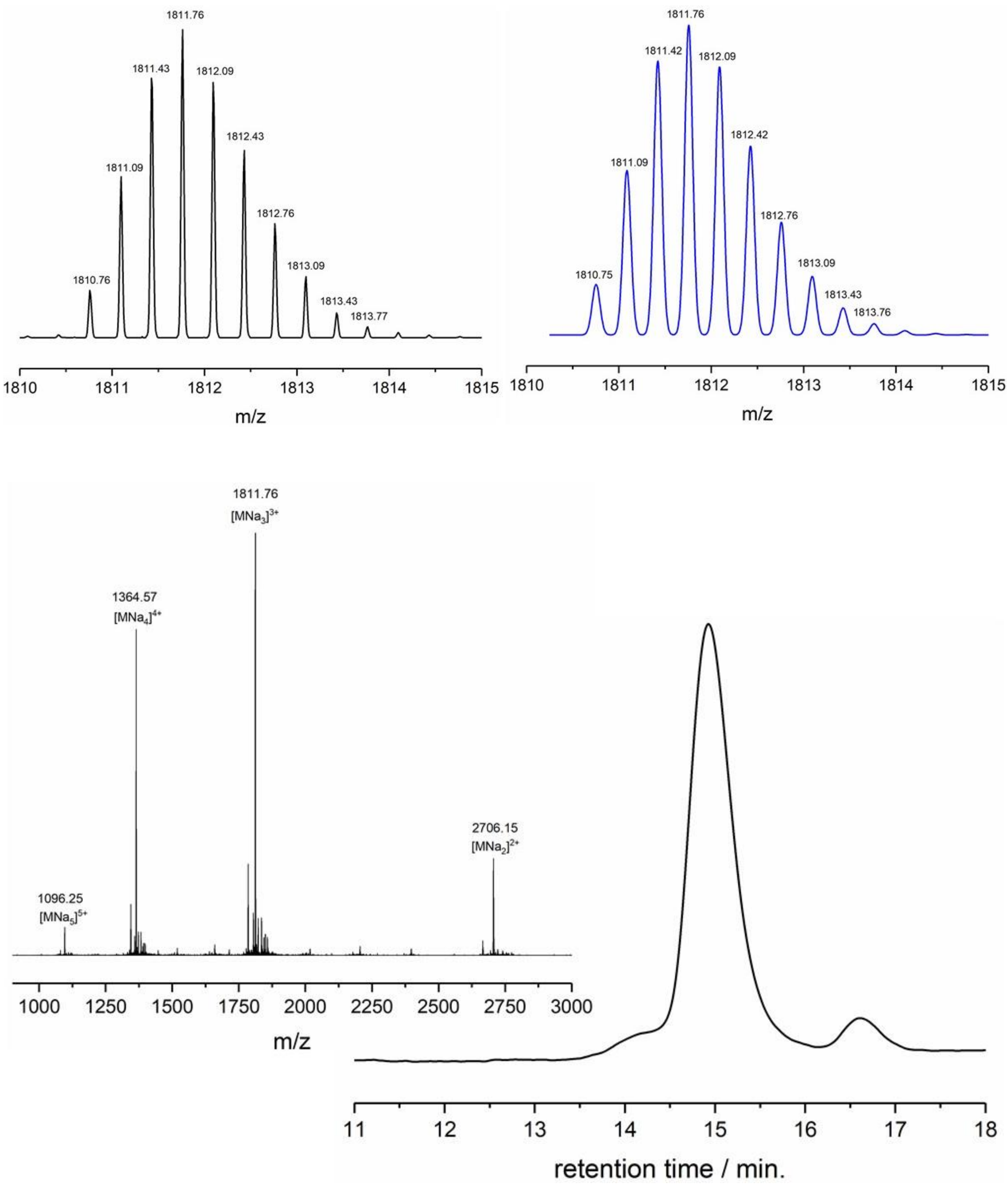

*Figure S 38. SEC-ESI-MS chromatogram and corresponding mass spectrum as well as isotopic pattern at 14.90 min retention time of the nonamer **65** synthesised on solid phase.*

Dodecamer 52 isotopic pattern and SEC-ESI-MS results (solid phase, before optimisation):

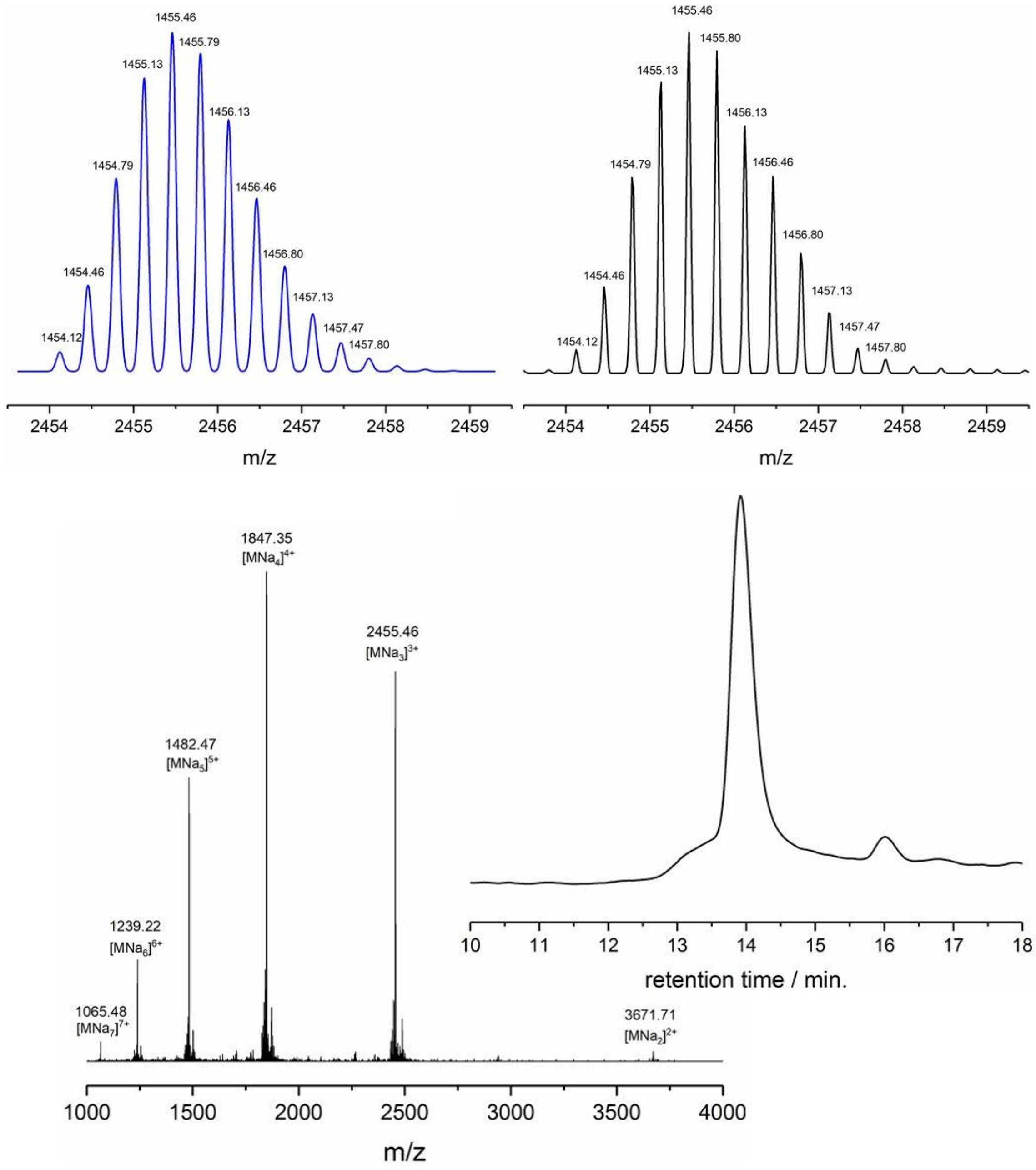

*Figure S 39. SEC-ESI-MS chromatogram and corresponding mass spectrum as well as isotopic pattern at 13.91 min retention time of the dodecamer **52** synthesised on solid phase.*

HRMS results of growing oligomer (solid phase, 2nd-9th cycle):

Sample name	m/z exp.	formula	m/z theo.	Δ m/z
2nd TAD COOH addition	888.5066	$[C_{44}H_{70}N_7O_{12}]^+$	888.5070	0.0004
2nd P-3CR	1237.7671	$[C_{65}H_{105}N_8O_{15}]^+$	1237.7694	0.0023
3rd TAD COOH addition	1450.8398	$[C_{73}H_{116}N_{11}O_{19}]^+$	1450.8444	0.0046
3rd TAD COOH addition	1467.8684	$[C_{73}H_{115}N_{11}O_{19}NH_4]^+$	1467.8709	0.0025
3rd P-3CR	1854.1453	$[C_{98}H_{157}N_{12}O_{22}]^+$	1854.1530	0.0023
4th TAD COOH addition	2084.2503	$[C_{106}H_{167}N_{15}O_{26}NH_4]^+$	2084.2545	0.0042
4th P-3CR	2447.5242	$[C_{128}H_{204}N_{16}O_{29}NH_4]^+$	2447.5318	0.0076
5th TAD COOH addition	2665.5801	$[C_{136}H_{215}N_{19}O_{33}Na]^+$	2665.5622	0.0179
5th P-3CR	3014.8362	$[C_{157}H_{250}N_{20}O_{36}Na]^+$	3014.8239	0.0123
6th TAD COOH addition	3227.9143	$[C_{165}H_{261}N_{23}O_{40}Na]^+$	3227.8880	0.0263
6th TAD COOH addition	1625.4449	$[C_{165}H_{261}N_{23}O_{40}Na_2]^{2+}$	1625.4440	0.0009
6th TAD COOH addition	1091.2903	$[C_{165}H_{261}N_{23}O_{40}Na_3]^{3+}$	1091.2924	0.0021
6th P-3CR	1827.1003	$[C_{190}H_{302}N_{24}O_{43}Na_2]^{2+}$	1827.0984	0.0019
6th P-3CR	1225.7278	$[C_{190}H_{302}N_{24}O_{43}Na_3]^{3+}$	1225.7286	0.0008
7th TAD COOH addition	3844.3025	$[C_{198}H_{313}N_{27}O_{47}Na]^+$	3844.2716	0.0309
7th TAD COOH addition	1933.6581	$[C_{198}H_{313}N_{27}O_{47}Na_2]^{2+}$	1933.6358	0.0223
7th TAD COOH addition	1296.7524	$[C_{198}H_{313}N_{27}O_{47}Na_3]^{3+}$	1296.7536	0.0012
7th P-3CR	2115.2764	$[C_{220}H_{350}N_{28}O_{50}Na_2]^{2+}$	2115.2745	0.0019
8th TAD COOH addition	2221.8201	$[C_{228}H_{361}N_{31}O_{54}Na_2]^{2+}$	2221.8120	0.0081
8th P-3CR	2396.4470	$[C_{249}H_{396}N_{32}O_{57}Na_2]^{2+}$	2396.4428	0.0042
8th P-3CR	1605.2920	$[C_{249}H_{396}N_{32}O_{57}Na_3]^{3+}$	1605.2916	0.0004
9th P-3CR	2704.6414	$[C_{282}H_{448}N_{36}O_{64}Na_2]^{2+}$	2704.6346	0.0068
9th P-3CR	1810.7607	$[C_{282}H_{448}N_{36}O_{64}Na_3]^{3+}$	1810.7518	0.0089
9th P-3CR	1363.8149	$[C_{282}H_{448}N_{36}O_{64}Na_4]^{4+}$	1363.8119	0.0030
9th P-3CR	1095.6473	$[C_{282}H_{448}N_{36}O_{64}Na_5]^{5+}$	1095.6474	0.0001

NMR spectra of solid-phase synthesised sequence-defined oligomers:

*PhTAD capped monomer **62**:*

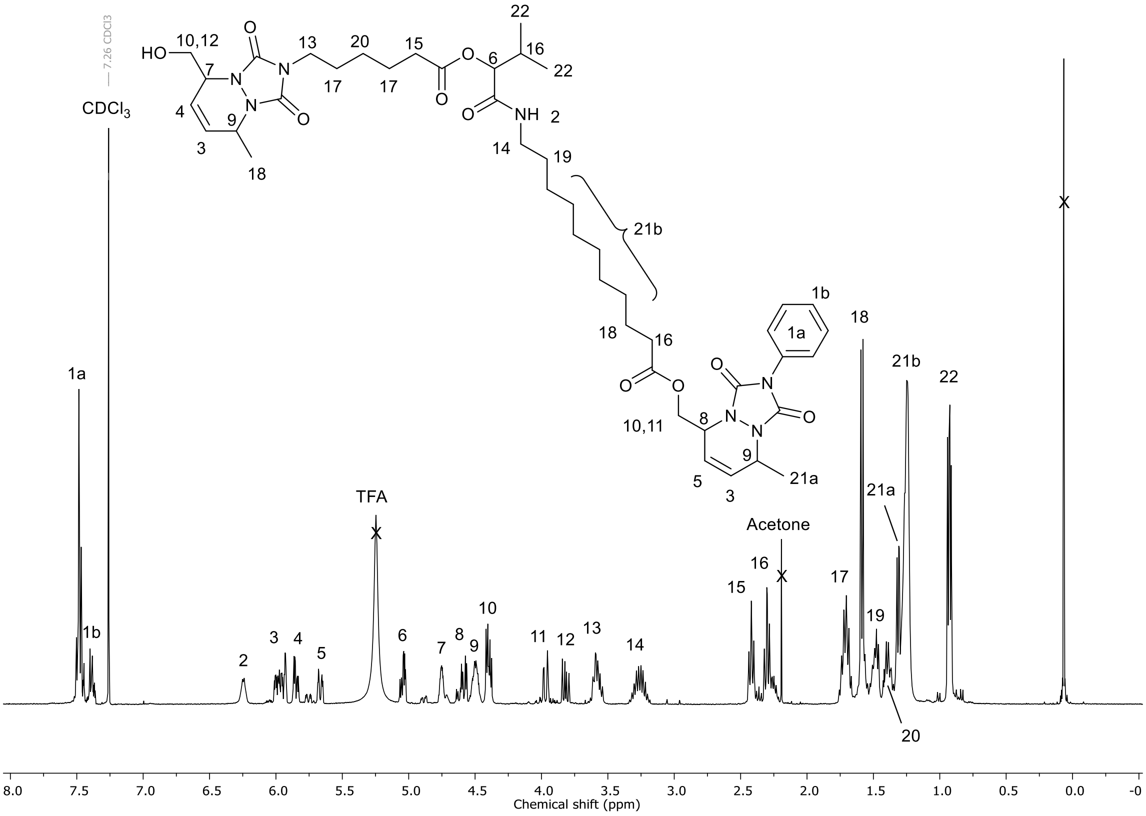

^{1}**H NMR** (300 MHz, CDCl$_3$) δ /ppm: 7.58-7.44 (m, 4H, ^{1a}), 7.43-7.35 (m, 1H, ^{1b}), 6.24 (s, 1H, ^{2}), 6.02-5.92 (m, 2H, ^{3}), 5.88-5.82 (m, 1H, ^{4}), 5.70-5.64 (m, 1H, ^{5}), 5.03 (dd, 1H, J = 1.65, 4.76, ^{6}), 4.75 (s, 1H, ^{7}), 4.66-4.55 (m, 1H, ^{8}), 4.49 (s, 2H, ^{9}), 4.40 (dd, 2H, J = 5.13, 11.60, ^{10}), 3.94 (d, 1H, J = 9.94, ^{11}), 3.82 (dd, 1H, J = 7.51, 12.39, ^{12}), 3.65-3.53 (m, 2H, ^{13}), 3.41-3.13 (m, 2H, ^{14}), 2.42 (t, 2H, J = 7.45, ^{15}), 2.33-2.21 (m, 3H, ^{16}), 1.78-1.65 (m, 4H, ^{17}), 1.59 (d, 5H, J = 6.59, ^{18}), 1.53-1.45 (m, 2H, ^{19}), 1.45-1.35 (m, 2H, ^{20}), 1.35-1.16 (m, 14H, ^{21a,b}), 0.93 (dd, 5H, J = 4.21, 6.77, ^{22}).

^{13}**C NMR** (APT, 100MHz, CDCl3) δ /ppm: 173.80, 172.47, 170.90, 158.85, 158.44, 155.67, 1525.60, 151.56, 131.02, 129.89, 29.34, 129.06, 128.58, 126.00, 121.17, 120.90, 77.96, 65.77, 64.90, 62.70, 59.11, 53.14, 51.33, 49.65, 39.81, 39.34, 34.12, 33.93, 30.71, 29.49, 29.40, 29.17, 27.53, 26.87, 26.00, 24.78, 24.31, 19.69, 18.79, 17.95, 1711.

HRMS (ESI)

m/z exp.	formula	m/z theo.	Δ m/z
872.4503	$[C_{44}H_{63}N_7O_{10}Na]^+$	872.4529	0.0026
850.4689	$[C_{44}H_{63}N_7O_{10}H]^+$	850.4709	0.0020

*PhTAD capped dimer **63**:*

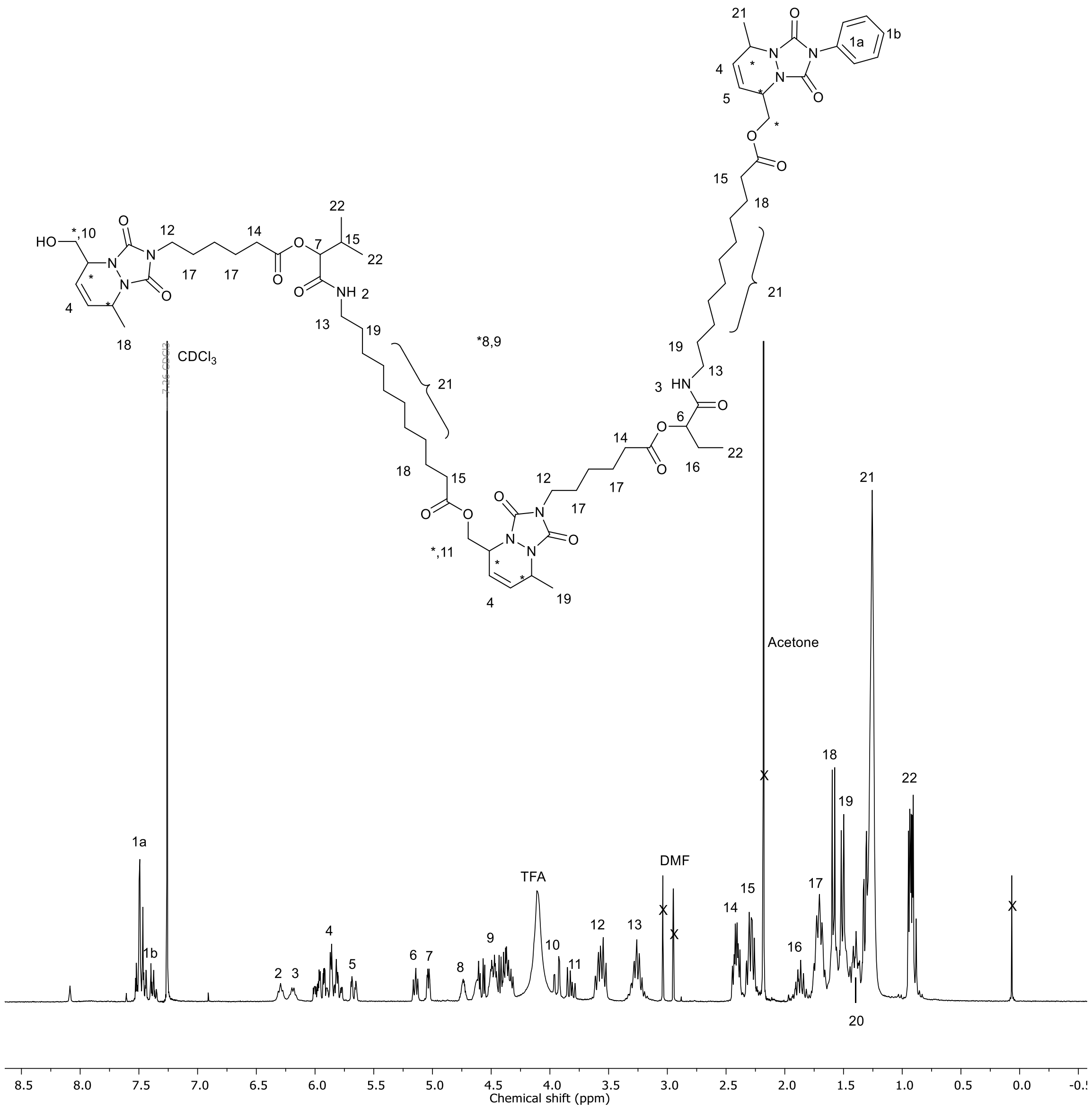

^{1}H NMR (300 MHz, CDCl$_3$) δ /ppm: 7.56-7.44 (m, 4H, ^{1a}), 7.42-7.33 (m, 1H, ^{1b}), 6.30 (t, 1H, J = 5.90, 5.63, ^{2}), 6.19 (d, 2H, J = 5.59, ^{3}), 6.04-5.75 (m, 5H, ^{4}), 5.71-5.64 (m, 1H, ^{5}), 5.14 (dd, 1H, J = 5.02, 6.47, ^{6}), 5.03 (dd, 1H, J = 1.69, 4.69, ^{7}), 4.78-4.29 (m, 10H, ^{8,9}), 3.94 (dd, 1H, J = 2.33, 12.40, ^{10}), 3.82 (ddd, 1H, J = 0.70, 7.27, 12.37, ^{11}), 3.63-3.50 (m, 4H, ^{12}), 3.36-3.17 (m, 4H, ^{13}), 2.47-2.36 (m, 4H, ^{14}), 2.29 (ddd, 5H, J = 5.03, 6.99, 8.18, ^{15}), 1.95-1.80 (m, 2H, ^{16}), 1.70 (p, 8H, J = 7.11, 6.94, ^{17}), 1.59 (d, 7H, J = 6.59, ^{18}), 1.55-1.46 (m, 7H, ^{19}), 1.46-1.36 (m, 4H, ^{20}), 1.36-1.11 (m, 27H, ^{21}), 0.99-0.87 (m, 9H, ^{22}).

^{13}C NMR (APT, 100MHz, CDCl3) δ /ppm: 173.64, 173.56, 170.61, 170.21, 129.96, 129.29, 129.00, 128.41, 125.88, 121.53, 121.11, 121.05, 78.07, 74.83, 65.11, 62.74, 62.68, 59.35, 59.30, 53.16, 52.93, 51.31, 51.08, 49.65, 39.63, 39.26, 38.99, 34.13, 34.10, 31.08, 30.70, 29.57, 29.46, 29.34, 29.30, 29.23, 29.20, 27.67, 27.57, 26.94, 26.94, 26.11, 26.06, 25.25, 24.81, 24.39, 19.64, 19.51, 18.85, 17.96, 17.94, 17.14.

HRMS (ESI)

m/z exp.	formula	m/z theo.	Δ m/z
1429.8302	$[C_{73}H_{109}N_6O_7NH_4]^+$	1429.8341	0.0038

*PhTAD capped trimer **64**:*

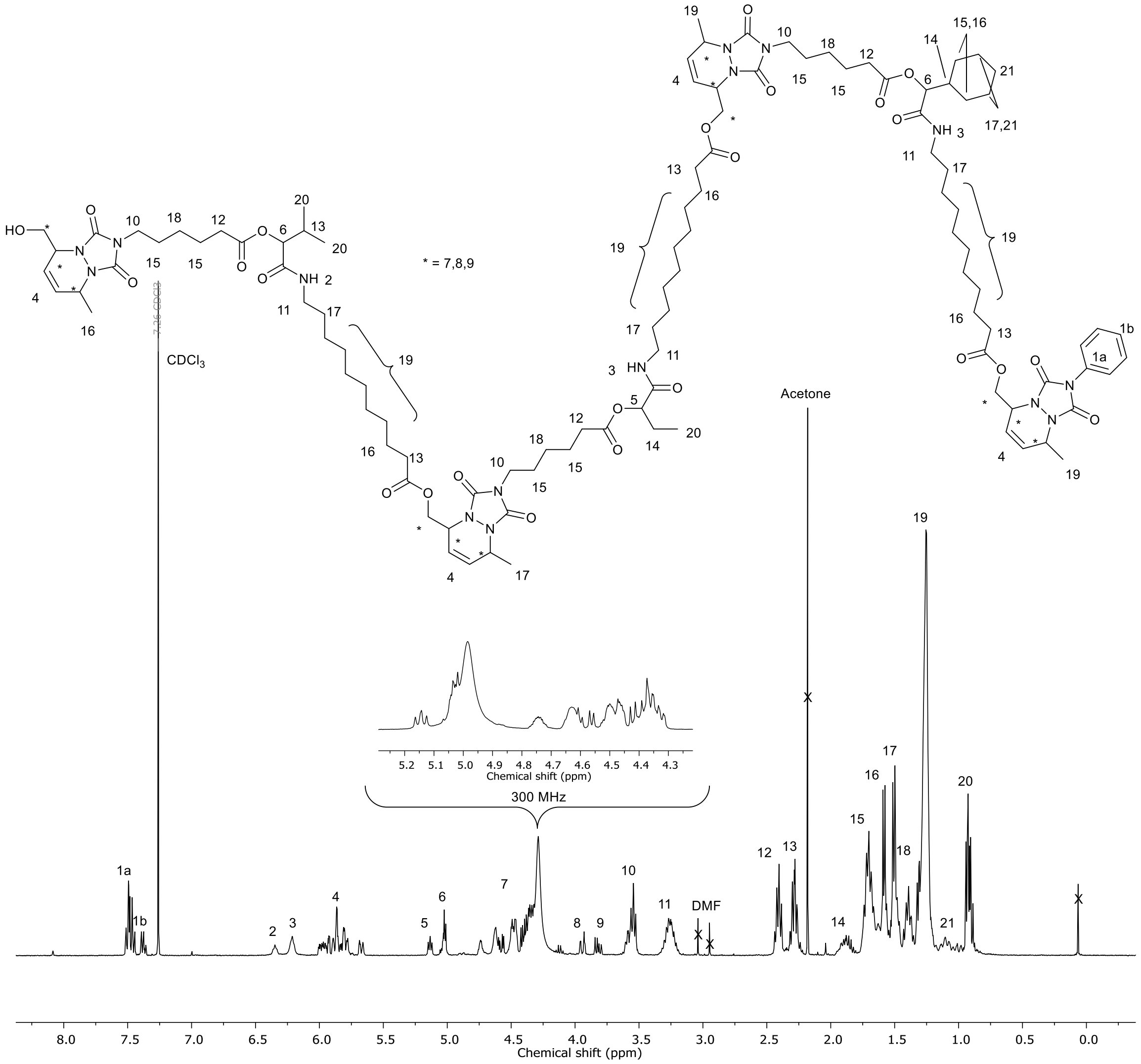

^{1}H NMR (400 MHz, CDCl$_3$) δ /ppm: 7.54-7.43 (m, 4H, ^{1a}), 7.41-7.34 (m, 1H, ^{1b}), 6.35 (s, 1H, ^{2}), 6.21 (s, 2H, ^{3}), 6.03-5.61 (m, 8H, ^{4}), 5.18-5.09 (m, 1H, ^{5}), 5.09-4.99 (m, 1H, ^{6}), 4.77-4.17 (m, 14H, ^{7}), 3.93 (dd, 1H, J = 2.31, 9.76, 2.05, ^{8}), 3.84 (dd, 1H, J = 6.80, 4.88, 7.32, ^{9}), 3.64-3.49 (m, 6H, ^{10}), 3.38-3.16 (m, 6H, ^{11}), 2.40 (t, 6H, ^{12}), 2.37-2.22 (m, 7H, ^{13}), 1.99-1.81 (m, 3H, ^{14}), 1.80-1.65 (m, 14H, ^{15}), 1.58 (d, 11H, J = 6.59, ^{16}), 1.51 (d, 11H, J = 6.59, ^{17}), 1.43-1.34 (m, 6H, ^{18}), 1.34-1.17 (m, 42H, ^{19}), 1.14-1.00 (m, 4H, ^{21}), 1.00-0.78 (m, 9H, ^{20}).

^{13}C NMR (APT, 100MHz, CDCl3) δ /ppm: 173.59, 172.39, 170.88, 170.45, 170.42, 158.83, 158.41, 152.75, 129.93, 129.87, 129.29, 129.02, 128.45, 125.91, 121.42, 121.06, 121.00, 78.02, 77.64, 74.77, 65.02, 62.75, 62.68, 59.26, 59.22, 53.15, 52.92, 51.31, 51.09, 39.70, 39.67, 39.27, 39.02, 34.12, 34.10, 34.04, 33.99, 30.70, 29.84, 29.54, 29.47, 29.45, 29.43, 29.35, 29.33, 29.31, 29.27, 29.22, 29.19, 27.67, 26.92, 26.13, 26.09, 26.04, 24.80, 24.40, 24.37, 19.65, 19.50, 18.83.

HRMS (ESI)

Sample name	m/z exp.	formula	m/z theo.	Δ m/z
Trimer	2051.1721	$[C_{106}H_{161}N_{15}O_{24}Na]^+$	2051.1731	0.0010
Trimer	1037.0803	$[C_{106}H_{161}N_{15}O_{24}Na_2]^{2+}$	1037.0812	0.0009
Trimer	2029.1907	$[C_{106}H_{161}N_{15}O_{24}H]^+$	2029.1912	0.0005
Trimer	1015.0980	$[C_{106}H_{161}N_{15}O_{24}H_2]^{2+}$	1015.0992	0.0012

*PhTAD capped dodecamer **52**:*

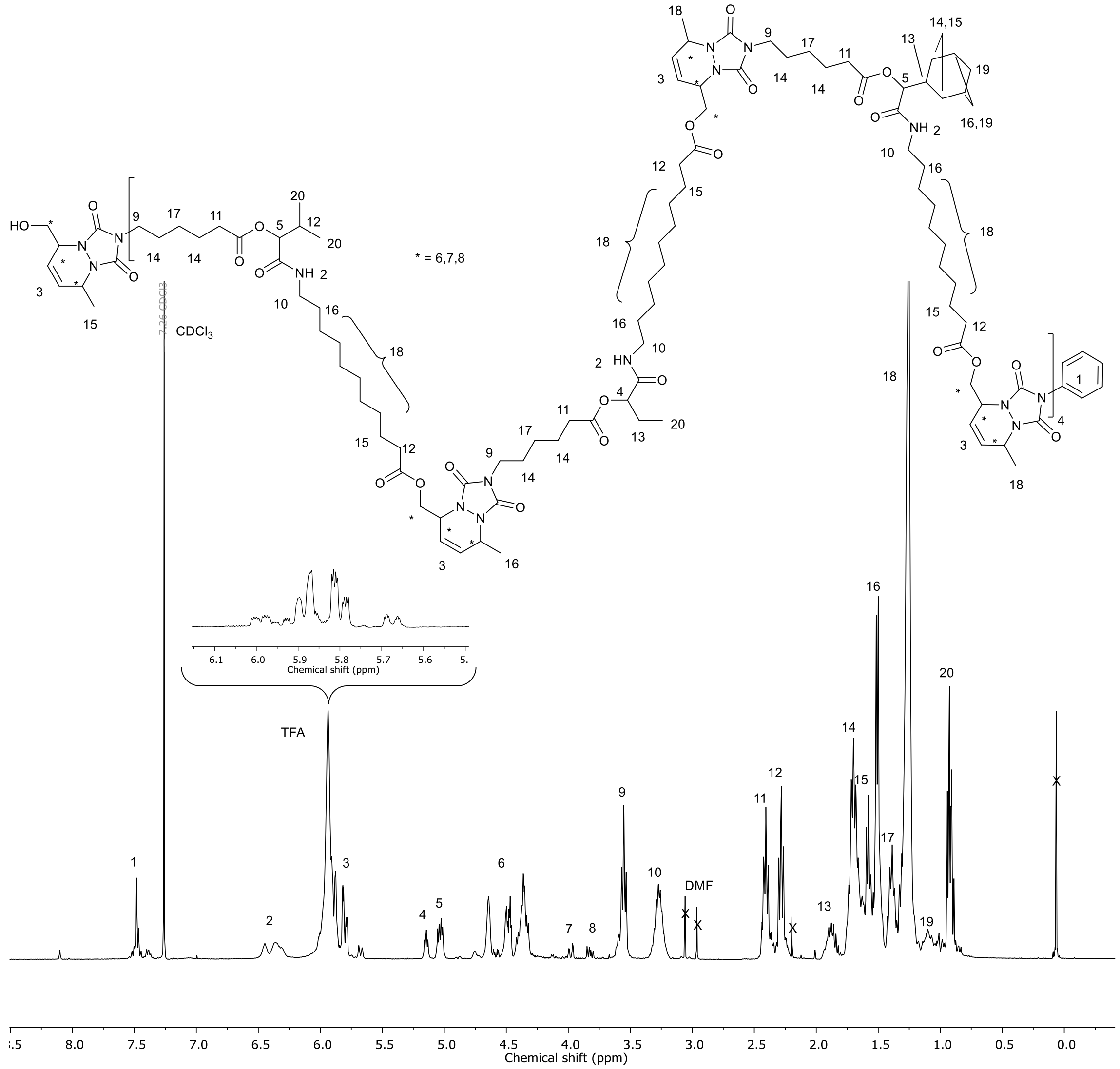

^{1}H NMR (400 MHz, $CDCl_3$) *δ* /ppm: 7.55-7.35 (m, 5H, ^{1}), 6.50-6.27 (m, 12H, ^{2}), 6.07-5.63 (s, 26H, ^{3}), 5.18-5.10 (m, 4H, ^{4}), 5.08-4.98 (m, 8H, ^{5}), 4.80-4.24 (m, 50H, ^{6}), 3.97 (dd, 1H, *J* = 2.06, 10.44, 1.76, ^{7}), 3.85 (dd, 1H, *J* = 7.23, 4.57, 7.73, ^{8}), 3.55 (t, 24H, *J* = 7.26 ^{9}), 3.34-3.18 (m, 24H, ^{10}), 2.48-2.33 (m, 24H, ^{11}), 2.33-1.21 (m, 25H, ^{12}), 1.97-1.78 (m, 12H, ^{13}), 1.78-1.61 (m, 56H, ^{14}), 1.58 (t, 35H, *J* = 6.90, ^{15}), 1.51 (d, 44H, *J* = 6.47, ^{16}), 1.45-1.35 (m, 24H, ^{17}), 1.35-1.17 (m, 168H, ^{18}), 1.16-0.97 (m, 16H, ^{19}), 0.96-0.82 (m, 36H, ^{20}).

^{13}C NMR (APT, 100MHz, CDCl3) *δ* /ppm: 173.73, 172.49, 172.29, 171.45, 171.07, 171.00, 158.93, 158.52, 153.82, 152.70, 129.87, 129.76, 129.34, 129.07, 128.61, 126.01, 121.13, 120.93, 116.35, 113.51, 77.84, 74.67, 64.85, 62.77, 53.14, 52.92, 51.08, 40.12, 39.85, 39.09, 34.09, 33.96, 30.72, 29.54, 29.45, 29.42, 29.33, 29.25, 29.21, 27.63, 27.50, 26.90, 26.09, 26.05, 26.02, 25.90, 25.26, 24.79, 24.34, 19.70, 19.55, 18.79, 17.08.

IR (ATR platinum diamond): *v* /cm^{-1} = 3355, 2930, 2856, 1740, 1692, 1555 1461, 1427, 1372 1209, 1154, 891, 805, 780, 766, 693, 646.

HRMS (ESI)

Sample name	m/z exp.	formula	m/z theo.	Δ m/z
Dodecamer	3669.7145	$[C_{382}H_{599}N_{51}O_{87}Na_2]^{2+}$	3669.6900	0.0245
Dodecamer	2454.1257	$[C_{382}H_{599}N_{51}O_{87}Na_3]^{3+}$	2454.1231	0.0026
Dodecamer	1846.3446	$[C_{382}H_{599}N_{51}O_{87}Na_4]^{4+}$	1846.3396	0.0050
Dodecamer	1481.6702	$[C_{382}H_{599}N_{51}O_{87}Na_5]^{5+}$	1481.6695	0.0007
Dodecamer	1238.5566	$[C_{382}H_{599}N_{51}O_{87}Na_6]^{6+}$	1238.5561	0.0005
Dodecamer	1064.9032	$[C_{382}H_{599}N_{51}O_{87}Na_7]^{7+}$	1064.9037	0.0005
Dodecamer	2432.1402	$[C_{382}H_{599}N_{51}O_{87}H_3]^{3+}$	2432.1411	0.0009
Dodecamer	1824.3595	$[C_{382}H_{599}N_{51}O_{87}H_4]^{4+}$	1824.1411	0.0018
Dodecamer	1459.6874	$[C_{382}H_{599}N_{51}O_{87}H_5]^{5+}$	1459.6876	0.0004
Dodecamer	1216.5735	$[C_{382}H_{599}N_{51}O_{87}H_6]^{6+}$	1216.5742	0.0007
Dodecamer	1043.0632	$[C_{382}H_{599}N_{51}O_{87}H_7]^{7+}$	1042.9218	0.1414

6.3.3.3 Solution-phase synthesis of sequence-defined oligomer:

1st Passerini reaction

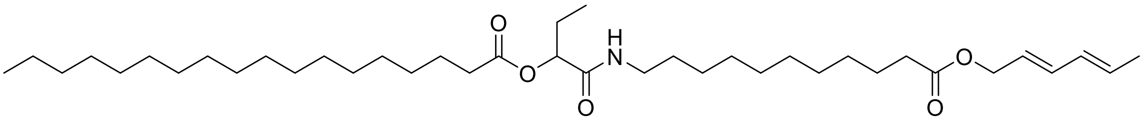

0.20 g of Stearic acid **13** (0.70 mmol, 1.0 eq.) was dissolved in 2.0 mL DCM (DCM) (0.35 M). 100 µL Propanal **11a** (82.0 mg, 1.40 mmol, 2.0 eq.) and 0.31 g of linker molecule **L1** (1.05 mmol, 1.5 eq.) were added and the mixture was stirred at room temperature for 12 hours. Subsequently, the solvent was removed under reduced pressure and the crude product was purified by column chromatography (hexane/ethyl acetate 15:1 → ethyl acetate) to afford product **55** as a white solid in a yield of 97% (433 mg, 0.68 mmol). Furthermore, the excess of the monomer was recovered (67 mg, 0.23 eq.) and could be reused.

^{1}H NMR (400 MHz, CDCl$_3$) *δ* /ppm: 6.28 – 6.19 (m, 1H, ^{1}), 6.11 – 5.96 (m, 2H, ^{1}), 5.80 – 5.68 (m, 1H, ^{1}), 5.68 – 5.53 (m, 1H, ^{1}), 5.15 (dd, *J* = 6.6, 4.9 Hz, 1H, ^{2}), 4.57 (d, *J* = 6.6 Hz, 2H, ^{3}), 3.36 – 3.15 (m, 2H, ^{4}), 2.39 (t, *J* = 7.5 Hz, 2H, ^{5}), 2.30 (t, *J* = 7.6 Hz, 2H, ^{5}), 2.01 – 1.81 (m, 2H, ^{6}), 1.81 – 1.72 (m, 3H, ^{7}), 1.72 – 1.55 (m, 6H, ^{8}), 1.54 – 1.17 (m, 40H, ^{9}), 1.00 – 0.75 (m, 6H, ^{10}).

^{13}C NMR (101MHz, CDCl3) *δ* /ppm: 172.59, 169.81, 77.36, 74.94, 39.34, 34.50, 32.07, 29.84, 29.80, 29.75, 29.61, 29.51, 29.42, 29.36, 29.29, 26.97, 25.22, 25.15, 22.84, 18.26, 14.26, 9.14.

ESI-MS:

m/z exp.	formula	m/z theo.	Δ m/z
656.5205	$[C_{39}H_{71}NO_5Na]^+$	656.5224	0.0019
634.5405	$[C_{39}H_{71}NO_5H]^+$	634.5392	0.0013

IR (ATR platinum diamond): *ν* /cm^{-1} = 3255.6, 3090.6, 2916.9, 2849.8, 1733.2, 1653.1, 1549.0, 1466.4, 1380.3, 1292.6, 1270.4, 1254.7, 1240.4, 1210.1, 1188.6, 1160.3, 1105.0, 987.4, 923.2, 721.5, 699.2, 511.4, 440.2, 396.0.

***R*$_f$**: (hexane / ethyl acetate (4:1)) = 0.56.

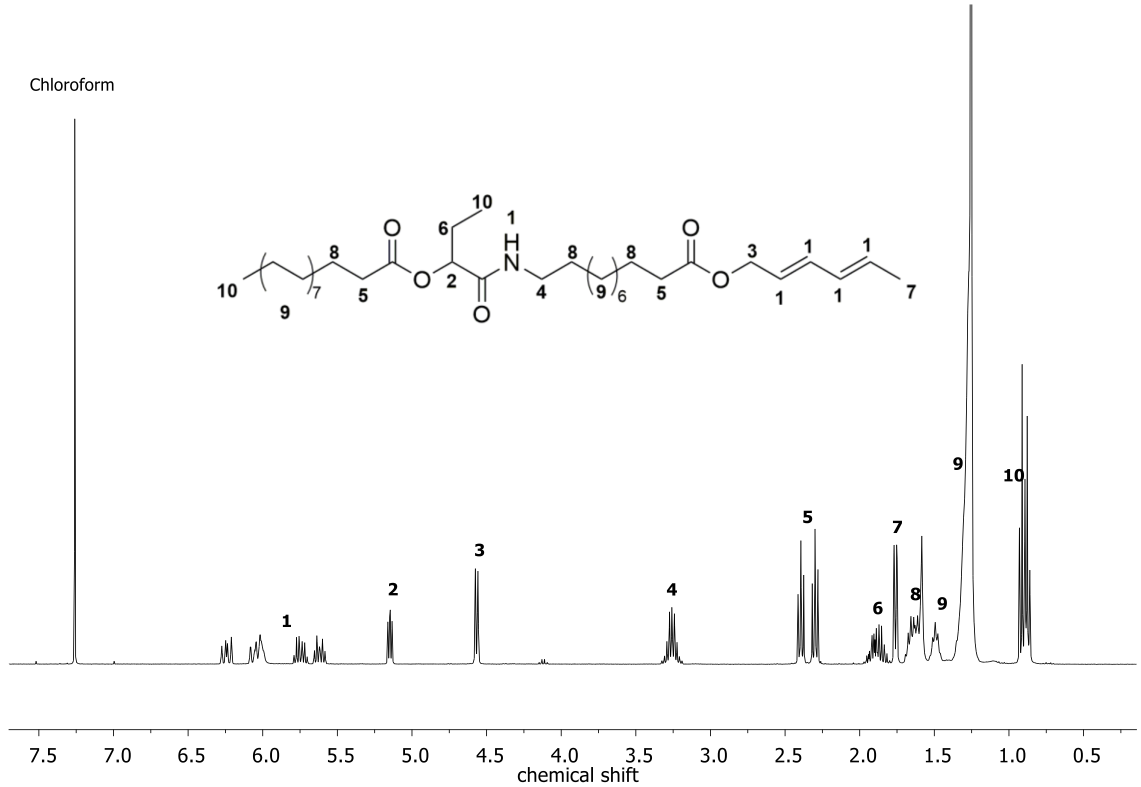
Chloroform
10
9
7
8
5
6
1
2
3
4
7.5
7.0
6.5
6.0
5.5
5.0
4.5
4.0
3.5
3.0
2.5
2.0
1.5
1.0
0.5
chemical shift

1st TAD-Diels Alder reaction

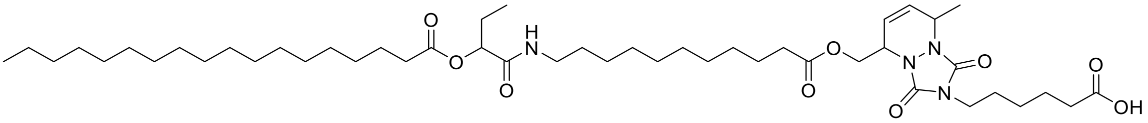

0.402 g of **55** (0.634 mmol, 1.0 eq.) was dissolved in 3 mL dry ethyl acetate and 0.150 g of linker molecule **L2** (0.697 mmol, dissolved in 1 mL dry ethyl acetate) was added dropwise to the solution, until it stayed pink, indicating that **55** was fully converted. 20 µL of 2,3-dimethylbut-2-ene (17 mg, 0.20 mmol) was added to the reaction mixture in order to quench the excess of the TAD compound **L2**. The solvent was evaporated under reduced pressure and the crude product **56** was used without further purification or analysis.

2nd Passerini reaction

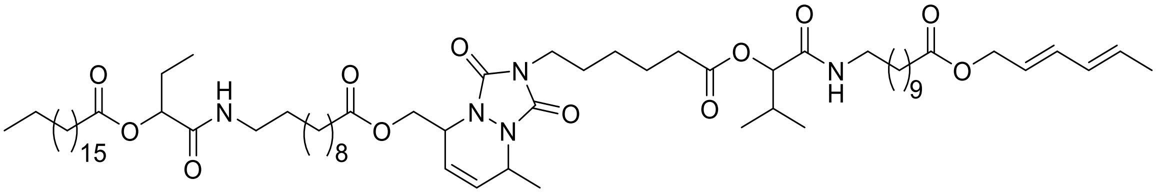

0.516 g of **56** (0.609 mmol, 1.0 eq.) was dissolved in 3 mL DCM. Subsequently, 0.11 mL of isobutyraldehyde **11c** (87 g, 1.218 mmol, 2.0 eq.) and 0.266 g of **L1** (0.914 mmol, 1.5 eq.) were added. The reaction was stirred for 12 hours at room temperature and the crude product was purified by column chromatography (hexane:ethyl acetate 10:1→1:2). Product **83** was obtained as a yellowish, highly viscous oil in a yield of 88% (648 mg, 0.535 mmol, overall yield over two reaction steps).

^{1}H NMR (500 MHz, $CDCl_3$) δ /ppm: 6.46 – 5.43 (m, 8H, ^{1}), 5.19 – 5.09 (m, 1H, ^{2}), 5.06 – 4.94 (m, 1H, ^{3}), 4.60 (s, 1H, ^{4}), 4.55 (d, *J* = 6.6 Hz, 2H, ^{5}), 4.50 – 4.43 (m, 1H, ^{6}), 4.34 (m, 2H, ^{7}), 3.59 – 3.48 (m, 2H, ^{8}), 3.33 – 3.14 (m, 4H, ^{9}), 2.47 – 2.34 (m, 4H, ^{10}), 2.34 – 2.20 (m, 5H, ^{11}), 1.88 (m, 2H, ^{12}), 1.65 (m, 14H, ^{13}), 1.50 (d, *J* = 6.4 Hz, 6H, ^{14}), 1.43 – 0.97 (m, 54H, ^{15}), 0.96 – 0.81 (m, 12H, ^{16}).

^{13}C NMR (126 MHz, $CDCl_3$) δ /ppm: 173.77, 173.45, 172.58, 172.32, 169.78, 169.34, 153.97, 153.93, 152.78, 152.76, 134.90, 131.32, 130.56, 129.95, 129.93, 123.95, 121.18, 121.17, 78.09, 74.88, 68.09, 64.88, 62.70, 52.91, 52.89, 51.07, 51.04, 39.31, 39.20, 38.92, 34.45, 34.21, 34.12, 34.08, 32.04, 30.67, 29.81, 29.79, 29.77, 29.72, 29.70, 29.58, 29.48, 29.39, 29.35, 29.33, 29.25, 29.23, 27.70, 26.98, 26.94, 26.17, 25.72, 25.20, 25.11, 25.05, 24.99, 24.80, 24.49, 22.81, 19.44, 19.42, 19.30, 18.90, 18.26, 17.08, 15.51, 14.25, 9.13.

ESI-MS:

m/z exp.	formula	m/z theo.	Δ m/z
1232.8729	$[C_{69}H_{119}N_5O_{12}Na]^+$	1232.8747	0.0018
627.4334	$[C_{69}H_{119}N_5O_{12}Na_2]^{2+}$	627.9320	0.49
426.2844	$[C_{69}H_{119}N_5O_{12}Na_3]^{3+}$	426.2844	0.00
1210.8928	$[C_{69}H_{119}N_5O_{12}H]^+$	1210.8928	0.00
605.4518	$[C_{69}H_{119}N_5O_{12}H_2]^{2+}$	605.9500	0.49

IR (ATR platinum diamond): *v* /cm^{-1} = 3306.1, 2918.1, 2850.7, 1738.9, 1705.0, 1652.0, 1534.5, 1455.0, 1421.5, 1376.8, 1235.2, 1161.7, 1111.7, 988.9, 765.6, 721.7, 413.1.

***R*$_f$**: (hexane / ethyl acetate (1:1)) = 0.42.

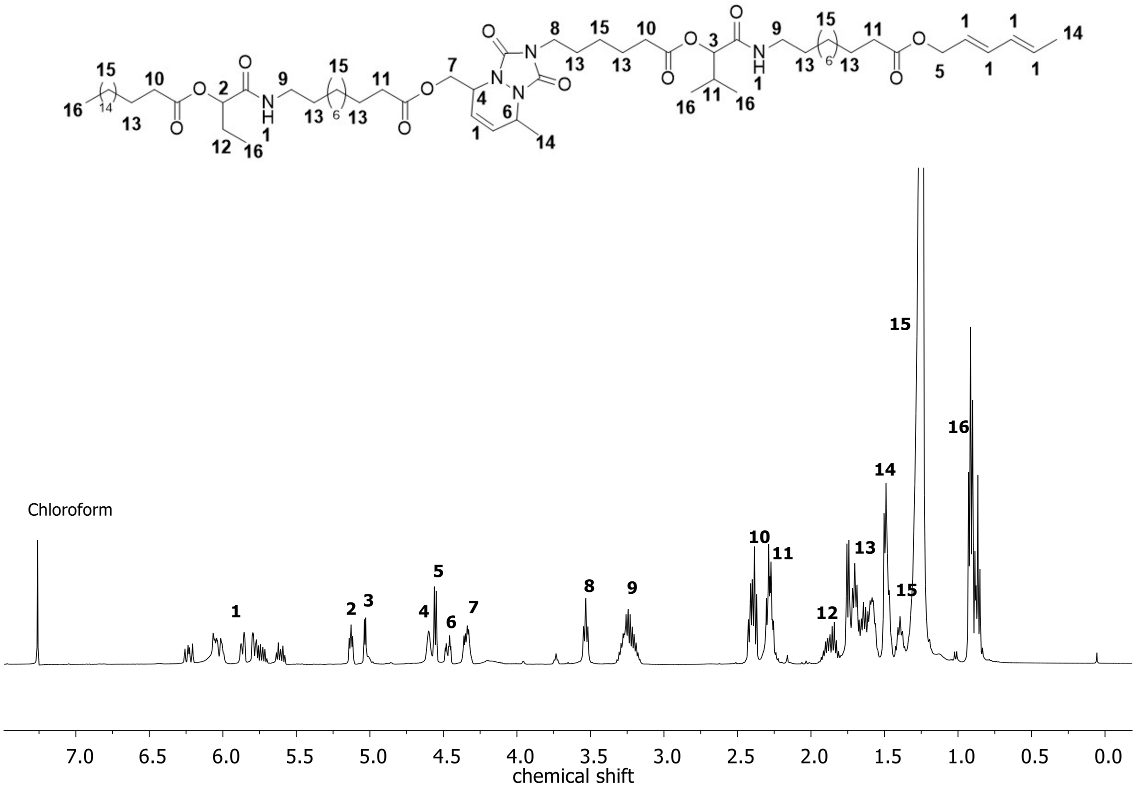

2nd TAD-Diels Alder reaction

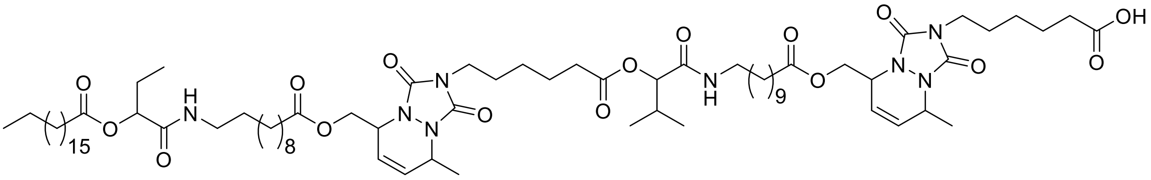

0.568 g of **83** (0.469 mmol, 1.0 eq.) was dissolved in 3 mL dry ethyl acetate and 0.110 g of linker molecule **L2** (0.516 mmol, 1.1 eq., dissolved in 1 mL dry ethyl acetate) was added dropwise to the solution, until it stayed pink, indicating that **83** was fully converted. 20 µL of 2,3-dimethylbut-2-ene (17 mg, 0.20 mmol) was added to the reaction mixture in order to quench the excess of the TAD compound **L2**. The solvent was evaporated under reduced pressure and the crude product **84** was used without further purification or analysis.

3rd Passerini reaction

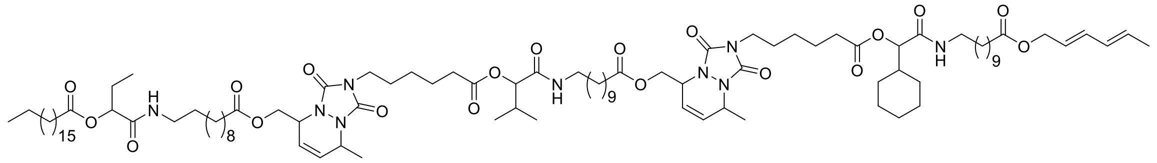

0.647 g of **84** (0.454 mmol, 1.0 eq.) was dissolved in 3 mL DCM. Subsequently, 0.11 mL of cyclohexanal **11b** (0.102 g, 0.908 mmol, 2.0 eq.) and 0.198 g of **L1** (0.681 mmol, 1.5 eq.) were added. The reaction was stirred for 12 hours at room temperature and the crude product was purified by column chromatography (hexane:ethyl acetate 5:1→1:3). Product **85** was obtained as a yellowish, highly viscous oil in a yield of 73% (591 mg, 0.323 mmol, overall yield over two reaction steps).

^{1}H NMR (500 MHz, CDCl$_3$) *δ* /ppm: 6.28 – 5.55 (m, 11H, ^{1}), 5.14 – 5.09 (m, 1H, ^{2}), 5.02 (m, 2H, ^{3}), 4.60 (s, 2H, ^{4}), 4.55 (d, *J* = 6.6 Hz, 2H, ^{5}), 4.51 – 4.41 (m, 2H, ^{6}), 4.441 – 4.29 (m, 4H, ^{7}), 3.53 (t, *J* = 7.2 Hz, 4H, ^{8}), 3.32 – 3.15 (m, 6H, ^{9}), 2.45 – 2.34 (m, 6H, ^{10}), 2.33 – 2.23 (m, 7H, ^{11}), 1.98 – 1.80 (m, 3H, ^{12}), 1.78 – 1.55 (m, 22H, ^{13}), 1.49 (d, *J* = 6.5 Hz, 9H, ^{14}), 1.42 – 0.98 (m, 78H, ^{15}), 0.95 – 0.79 (m, 12H, ^{16}).

^{13}C NMR (126 MHz, CDCl$_3$) δ /ppm: 173.77, 173.45, 172.59, 172.35, 172.31, 169.78, 169.36, 169.29, 153.95, 153.91, 152.79, 152.77, 134.90, 131.32, 130.56, 129.92, 123.95, 121.19, 78.09, 77.80, 74.88, 68.10, 64.88, 62.70, 52.92, 51.05, 51.02, 40.12, 39.31, 38.93, 34.45, 34.12, 34.08, 32.04, 30.67, 29.81, 29.79, 29.77, 29.72, 29.70, 29.58, 29.48, 29.39, 29.36, 29.33, 29.25, 29.23, 27.71, 27.40, 26.98, 26.94, 26.18, 26.10, 25.99, 25.73, 25.20, 25.11, 25.06, 24.80, 24.66, 24.49, 24.47, 22.81, 19.42, 18.90, 18.27, 17.10, 14.25, 9.13.

ESI-MS:

m/z exp.	formula	m/z theo.	Δ m/z
1849.2576	$[C_{102}H_{171}N_9O_{19}Na]^+$	1849.2583	0.00070
936.1214	$[C_{102}H_{171}N_9O_{19}Na_2]^{2+}$	936.1238	0.0024
1827.2785	$[C_{102}H_{171}N_9O_{19}H]^+$	1827.2764	0.0021
914.1408	$[C_{102}H_{171}N_9O_{19}H_2]^{2+}$	914.1418	0.0010

IR (ATR platinum diamond): ν /cm^{-1} = 3309.2, 2923.6, 2852.8, 1736.9, 1703.5, 1533.2, 1453.3, 1421.6, 1376.0, 1236.1, 1158.1, 1114.2, 989.1, 765.6, 721.9.

***R*$_f$**: (hexane / ethyl acetate (1:2)) = 0.28.

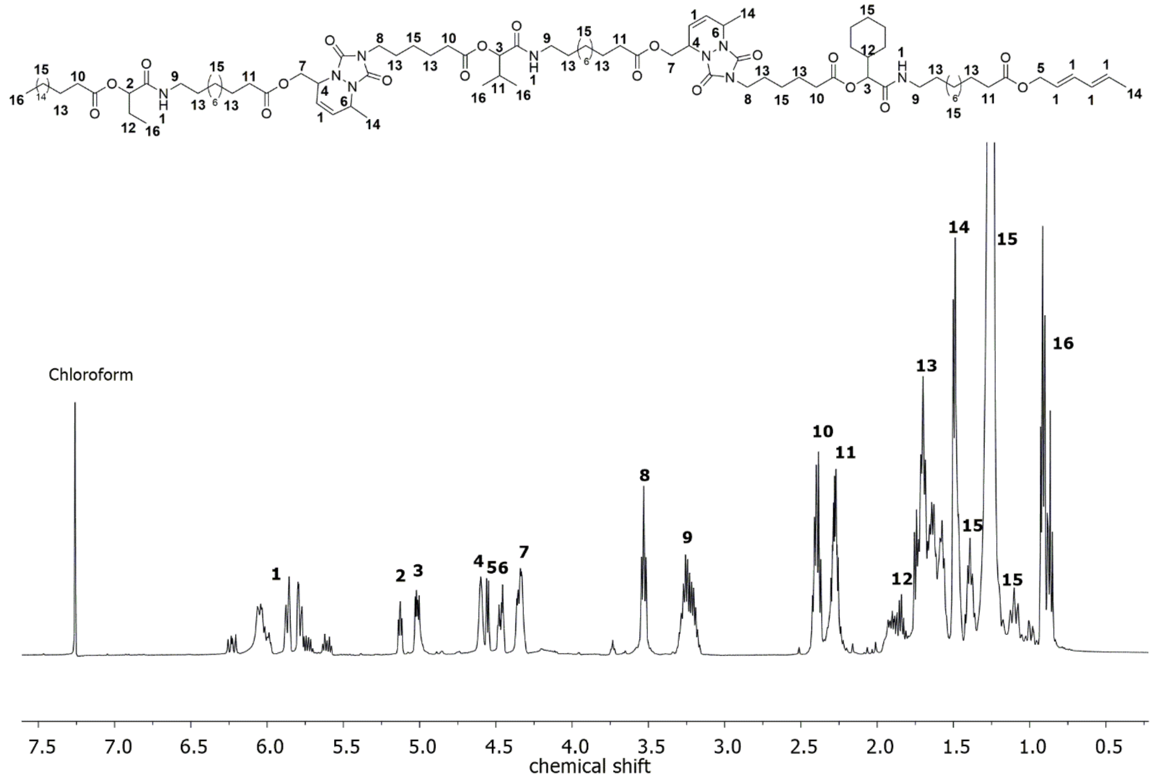

3rd TAD-Diels Alder reaction

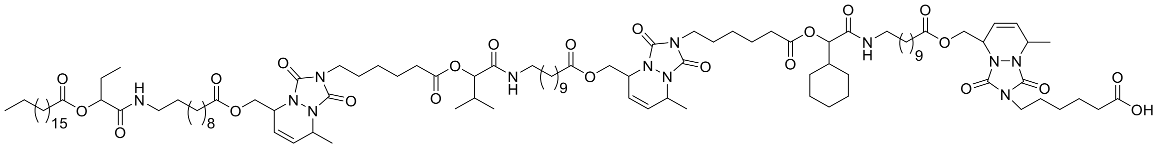

0.545 g of **85** (0.298 mmol, 1.0 eq.) was dissolved in 3 mL dry ethyl acetate and 73 mg of linker molecule **L2** (0.343 mmol, 1.1 eq., dissolved in 2 mL dry ethyl acetate) was added dropwise to the solution, until it stayed pink, indicating that **85** was fully converted. 20 µL of 2,3-dimethylbut-2-ene (17 mg, 0.20 mmol) was added to the reaction mixture in order to quench the excess of the TAD compound **L2**. The solvent was evaporated under reduced pressure and the crude product **86** was used without further purification or analysis.

4th Passerini reaction

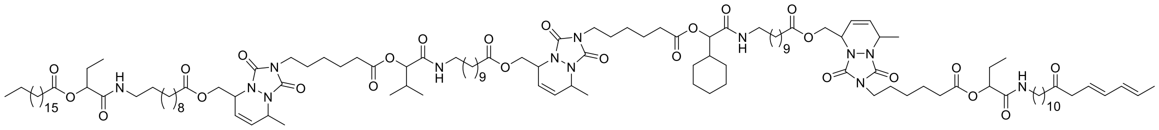

0.571 g of **86** (0.282 mmol, 1.0 eq.) was dissolved in 2 mL DCM. Subsequently, 0.11 mL of propanal **11a** (0.098 g, 1.69 mmol, 6.0 eq.) and 0.370 g of **L1** (0.681 mmol, 4.5 eq.) were added. The reaction was stirred for 18 hours at room temperature and the crude product was purified by column chromatography (hexane:ethyl acetate 2:1→1:6). Product **87** was obtained as a yellowish, highly viscous oil in a yield of 82% (472 mg, 0.231 mmol, overall yield over two reaction steps).

^{1}H NMR (500 MHz, CDCl$_3$) *δ* /ppm: 6.35 – 5.51 (m, 14H, ^{1}), 5.18 – 5.06 (m, 2H, ^{2}), 5.06 – 4.95 (m, 2H, ^{3}), 4.60 (s, 3H, ^{4}), 4.55 (d, *J* = 6.6 Hz, 2H, ^{5}), 4.51 – 4.43 (m, 3H, ^{6}), 4.39 – 4.29 (m, 6H, ^{7}), 3.58 – 3.44 (m, 6H, ^{8}), 3.32 – 3.14 (m, 8H, ^{9}), 2.48 – 2.35 (m, 8H, ^{10}), 2.34 – 2.19 (m, 9, ^{11}), 1.98 – 1.80 (m, 5H, ^{12}), 1.79 – 1.53 (m, 30H, ^{13}), 1.49 (d, *J* = 6.6 Hz, 12H, ^{14}), 1.42 – 0.95 (m, 92H, ^{15}), 0.94 – 0.83 (m, 15H, ^{16}).

^{13}C NMR (126 MHz, CDCl$_3$) δ /ppm: 173.78, 173.46, 172.59, 172.35, 172.18, 169.78, 169.70, 169.36, 169.30, 153.95, 153.91, 152.79, 134.90, 131.32, 130.56, 129.92, 123.95, 121.19, 78.10, 77.80, 74.98, 74.88, 68.09, 64.88, 62.70, 52.92, 51.05, 51.02, 40.12, 39.35, 39.31, 38.93, 34.45, 34.12, 34.08, 32.04, 30.67, 29.81, 29.79, 29.77, 29.72, 29.70, 29.58, 29.48, 29.39, 29.36, 29.33, 29.23, 27.71, 27.42, 26.98, 26.96, 26.94, 26.17, 26.13, 26.10, 25.99, 25.73, 25.20, 25.11, 25.05, 24.80, 24.49, 24.47, 24.43, 22.81, 19.42, 18.90, 18.27, 17.10, 14.25, 9.13, 9.12.

ESI-MS:

m/z exp.	formula	m/z theo.	Δ m/z
2411.5938	$[C_{131}H_{217}N_{13}O_{26}Na]^{+}$	2411.5950	0.00012
1217.2901	$[C_{131}H_{217}N_{13}O_{26}Na_2]^{2+}$	1217.2921	0.0020
819.0242	$[C_{131}H_{217}N_{13}O_{26}Na_3]^{3+}$	819.1911	0.16
2389.6139	$[C_{131}H_{217}N_{13}O_{26}H]^{+}$	2389.6131	0.00080
1195.3119	$[C_{131}H_{217}N_{13}O_{26}H_2]^{2+}$	1195.3102	0.0017
797.0047	$[C_{131}H_{217}N_{13}O_{26}H_3]^{3+}$	797.2092	0.20

IR (ATR platinum diamond): ν /cm^{-1} = 3306.6, 2924.1, 1853.1, 1736.9, 1702.6, 1533.6, 1453.6, 1421.6, 1376.7, 1237.0, 1157.8, 1114.9, 989.2, 765.7, 722.3.

***R*$_f$**: (hexane / ethyl acetate (1:6)) = 0.68.

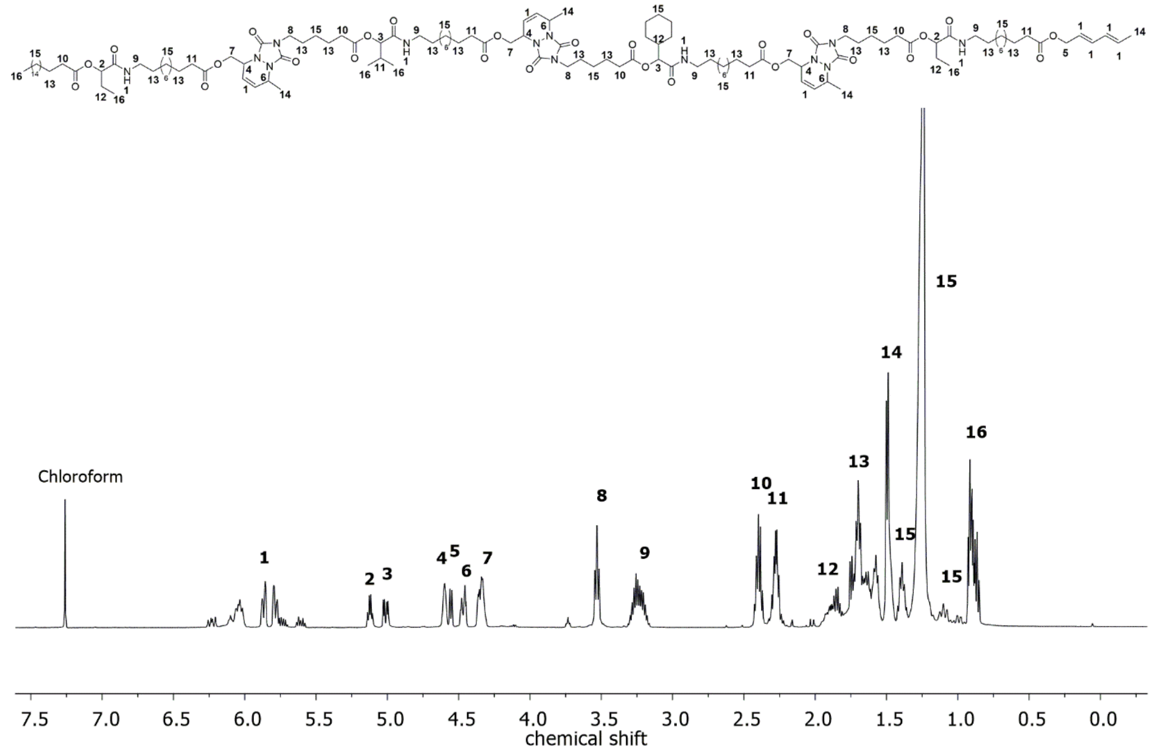

4th TAD-Diels Alder reaction

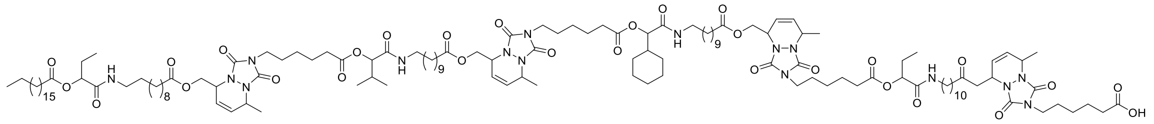

0.419 g of **87** (0.175 mmol, 1.0 eq.) was dissolved in 3 mL dry ethyl acetate and 43 mg of linker molecule **L2** (0.202 mmol, 1.1 eq. dissolved in 2 mL dry ethyl acetate) was added dropwise to the solution, until it stayed pink, indicating that **87** was fully converted. 20 µL of 2,3-dimethylbut-2-ene (17 mg, 0.20 mmol) was added to the reaction mixture in order to quench the excess of the TAD compound **L2**. The solvent was evaporated under reduced pressure and the crude product **88** was used without further purification or analysis.

5th Passerini reaction

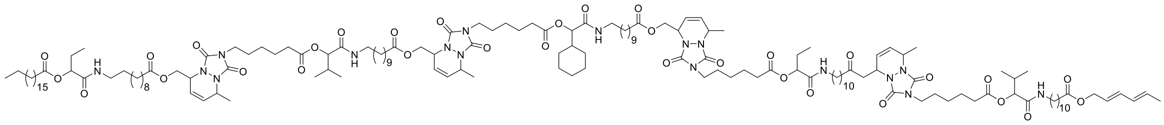

0.455 g of **88** (0.175 mmol, 1.0 eq.) was dissolved in 2 mL DCM. Subsequently, 0.095 mL of isobutyraldehyde **11c** (0.075 g, 1.05 mmol, 6.0 eq.) and 0.229 g of **L1** (0.787 mmol, 4.5 eq.) were added. The reaction was stirred for 24 hours at room temperature and the crude product was purified by column chromatography (hexane:ethyl acetate 3:2→EtOAc). Product **89** was obtained as a yellowish, highly viscous oil in a yield of 94% (486 mg, 0.164 mmol, overall yield over two reaction steps).

^{1}H NMR (500 MHz, $CDCl_3$) *δ* /ppm: 6.33 – 5.53 (m, 17H,^{1}), 5.17 – 5.08 (m, 2H, ^{2}), 5.06 – 4.97 (m, 3H, ^{3}), 4.60 (s, 4H, ^{4}), 4.56 (d, *J* = 6.6 Hz, 2H, ^{5}), 4.51 – 4.41 (m, 4H, ^{6}), 4.40 – 4.29 (m, 8H, ^{7}), 3.60 – 3.46 (m, 8H, ^{8}), 3.36 – 3.13 (m, 10H, ^{9}), 2.45 – 2.34 (m, 10H, ^{10}), 2.32 – 2.19 (m, 12H, ^{11}), 1.98 – 1.83 (m, 5H, ^{12}), 1.80 – 1.53 (m, 38H, ^{13}), 1.50 (d, *J* = 6.5 Hz, 15H, ^{14}), 1.42 – 0.97 (m, 106H, ^{15}), 0..95 – 0.80 (m, 21H, ^{16}).

^{13}C NMR (126 MHz, $CDCl_3$) δ /ppm: 173.78, 173.46, 172.59, 172.35, 172.21, 169.78, 169.72, 169.36, 169.31, 153.95, 153.92, 152.80, 134.90, 131.32, 130.56, 129.92, 123.96, 121.20, 78.10, 77.81, 74.98, 74.88, 68.10, 64.89, 62.71, 52.93, 51.05, 51.03, 40.12, 39.36, 39.32, 38.93, 34.46, 34.13, 34.09, 32.05, 30.68, 29.82, 29.80, 29.78, 29.73, 29.71, 29.59, 29.49, 29.39, 29.36, 29.34, 29.24, 27.71, 27.43, 26.99, 26.97, 26.95, 26.18, 26.15, 26.10, 26.00, 25.73, 25.23, 25.20, 25.12, 25.06, 24.81, 24.49, 24.44, 22.82, 19.42, 18.91, 18.27, 17.11, 14.26, 9.14.

ESI-MS:

m/z exp.	formula	m/z theo.	Δ m/z
2987.9553	$[C_{161}H_{265}N_{17}O_{33}Na]^{+}$	2987.9473	0.00080
1505.4646	$[C_{161}H_{265}N_{17}O_{33}Na_2]^{2+}$	1505.4683	0.0037
1011.3071	$[C_{161}H_{265}N_{17}O_{33}Na_3]^{3+}$	1011.3086	0.0015
2965.9715	$[C_{161}H_{265}N_{17}O_{33}H]^{+}$	2965.9654	0.0061
1483.4880	$[C_{161}H_{265}N_{17}O_{33}H_2]^{2+}$	1483.4863	0.0017
989.3254	$[C_{161}H_{265}N_{17}O_{33}H_3]^{3+}$	989.3266	0.0012

IR (ATR platinum diamond): ν /cm^{-1} = 3337.5, 2924.7, 2853.4, 1736.8, 1702.1, 1533.1, 1453.8, 1421.8, 1376.0, 1237.2, 1157.7, 1115.7, 990.1, 765.5, 722.3, 537.0.

***R*$_f$**: (ethyl acetate) = 0.50.

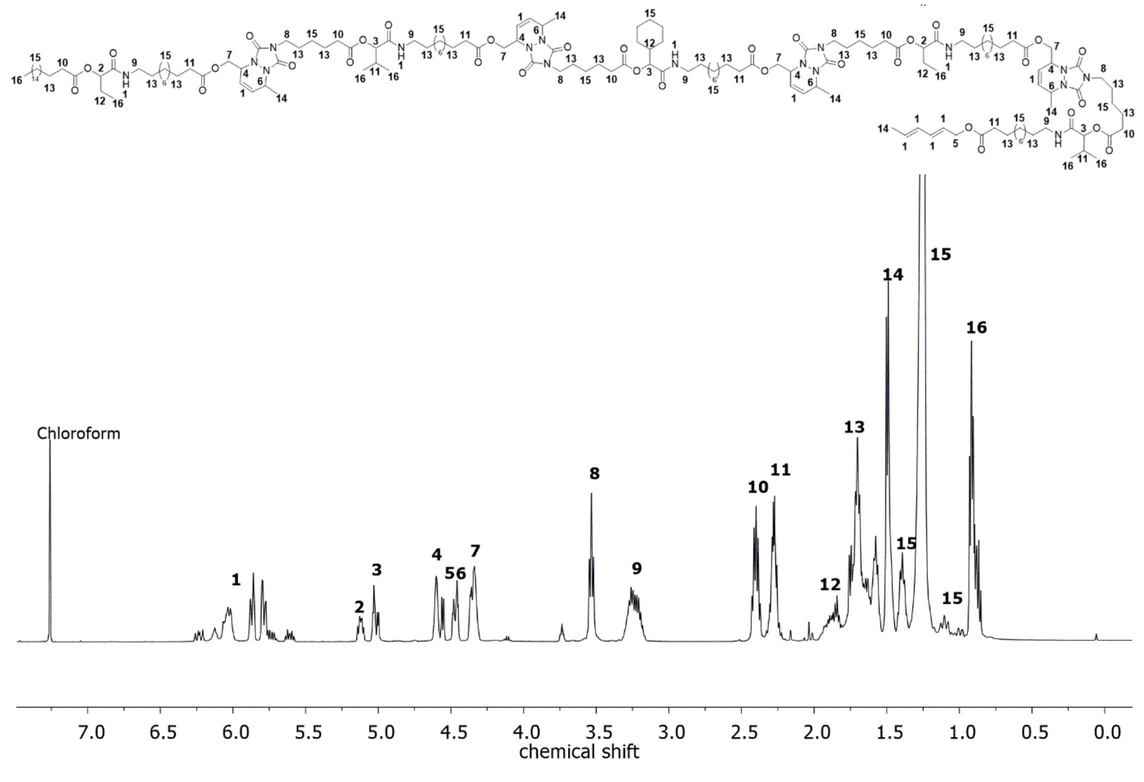

5th TAD-Diels Alder reaction

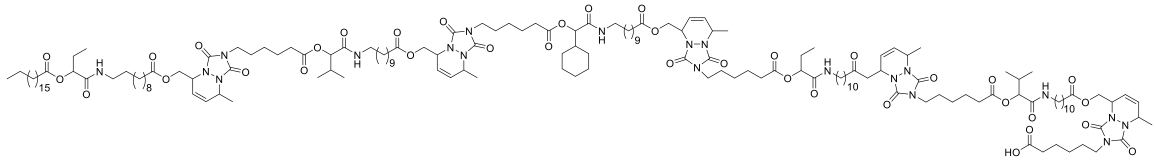

0.471 g of **89** (0.159 mmol, 1.0 eq.) was dissolved in 3 mL dry ethyl acetate and 39 mg of linker molecule **L2** (0.343 mmol, 1.1 eq. dissolved in 2 mL dry ethyl acetate) was added dropwise to the solution, until it stayed pink, indicating that **89** was fully converted. 20 µL of 2,3-dimethylbut-2-ene (17 mg, 0.20 mmol) was added to the reaction mixture in order to quench the excess of the TAD compound **L2**. The solvent was evaporated under reduced pressure and the crude product **90** was used without further purification or analysis.

6th Passerini reaction

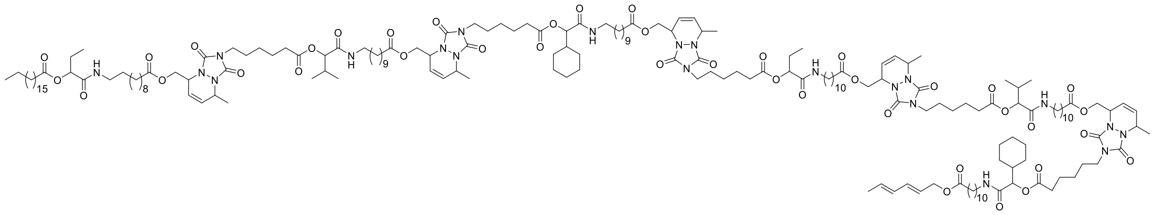

0.505 g of **90** (0.159 mmol, 1.0 eq.) was dissolved in 2 mL DCM. Subsequently, 0.12 mL of cyclohexanal **11b** (0.107 g, 0.954 mmol, 6.0 eq.) and 0.209 g of **L1** (0.702 mmol, 4.5 eq.) were added. The reaction was stirred for 24 hours at room temperature and the crude product was purified by column chromatography (hexane:ethyl acetate 2:1→EtOAc). Product **91** was obtained as a yellowish, highly viscous oil in a yield of 70% (400 mg, 0.112 mmol, overall yield over two reaction steps).

^{1}H NMR (500 MHz, $CDCl_3$) δ /ppm: 6.29 – 5.50 (m, 20H, ^{1}), 5.11 – 4.99 (m, 2H, ^{2}), 4.99 – 4.90 (m, 4H, ^{3}), 4.54 (s, 5H, ^{4}), 4.50 (d, J = 6.6 Hz, 2H, ^{5}), 4.45 – 4.35 (m, 5H, ^{6}), 4.33 – 4.24 (m, 10H, ^{7}), 3.55 – 3.39 (m, 10H, ^{8}), 3.28 – 3.08 (m, 12H, ^{9}), 2.41 – 2.30 (m, 12H, ^{10}), 2.28 – 2.12 (m, 14H, ^{11}), 1.94 – 1.75 (m, 6H, ^{12}), 1.73 – 1.46 (m, 46H, ^{13}), 1.44 (d, J = 6.5 Hz, 18H, ^{14}), 1.41 – 0.90 (m, 130H, ^{15}), 0.89 – 0.72 (m, 21H, ^{16}).

^{13}C NMR (126 MHz, $CDCl_3$) δ /ppm: 173.47, 172.60, 172.36, 169.80, 169.38, 169.32, 153.92, 153.89, 152.80, 134.91, 131.33, 130.57, 129.92, 123.96, 121.20, 78.10, 77.81, 77.41, 77.16, 76.91, 74.98, 74.88, 68.10, 64.89, 62.71, 52.93, 51.03, 40.12, 39.32, 38.94, 34.46, 34.13, 34.09, 32.05, 30.68, 29.82, 29.78, 29.73, 29.59, 29.49, 29.40, 29.37, 29.34, 29.24, 27.72, 27.43, 26.99, 26.97, 26.95, 26.18, 26.15, 26.10, 26.00, 25.73, 25.23, 25.20, 25.12, 25.06, 24.81, 24.49, 24.48, 24.44, 22.82, 19.43, 18.91, 18.28, 17.11, 14.26, 9.14.

ESI-MS:

m/z exp.	formula	m/z theo.	Δ m/z
3604.3611	$[C_{194}H_{317}N_{21}O_{40}Na]^+$	3604.3309	0.0291
1813.6621	$[C_{194}H_{317}N_{21}O_{40}Na_2]^{2+}$	1813.6601	0.0020
1216.7808	$[C_{194}H_{317}N_{21}O_{40}Na_3]^{3+}$	1216.7698	0.011
3582.3633	$[C_{194}H_{317}N_{21}O_{40}H]^+$	3582.3490	0.014
1791.6817	$[C_{194}H_{317}N_{21}O_{40}H_2]^{2+}$	1791.6781	0.0036
1194.7871	$[C_{194}H_{317}N_{21}O_{40}H_3]^{3+}$	1194.7878	0.0007

IR (ATR platinum diamond): *ν* /cm^{-1} = 3325.9, 2924.7, 2853.3, 1736.9, 1701.7, 1534.3, 1453.5, 1421.7, 1376.3, 1237.1, 1157.7, 1115.7, 765.4, 722.2, 537.1.

***R*$_f$**: (ethyl acetate) = 0.68.

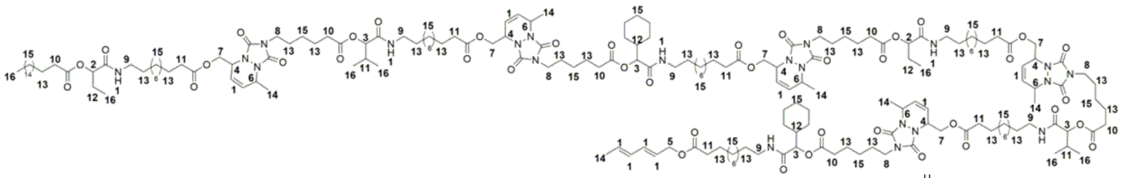

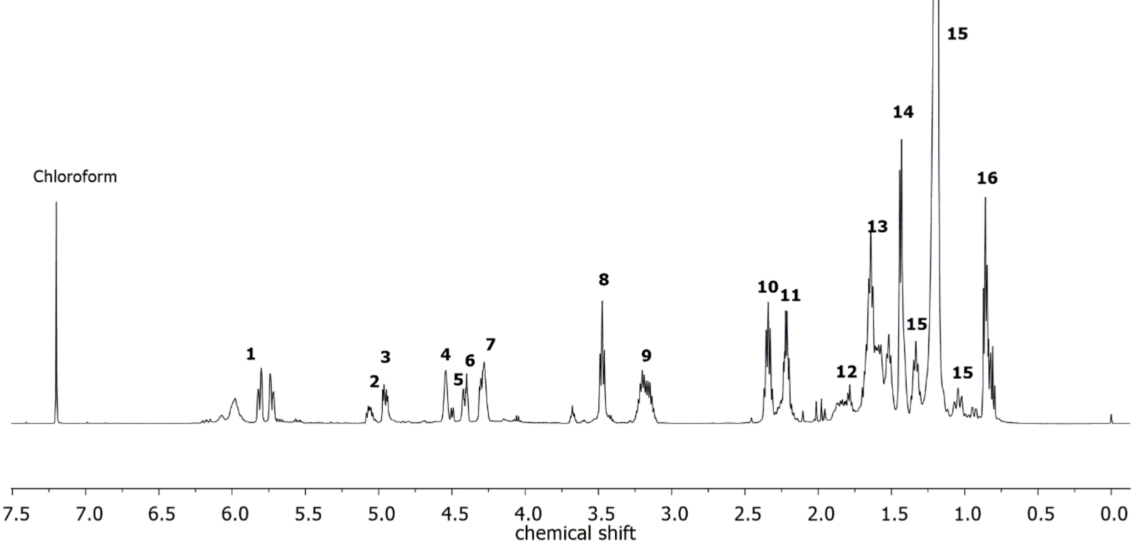

6th TAD-Diels Alder reaction

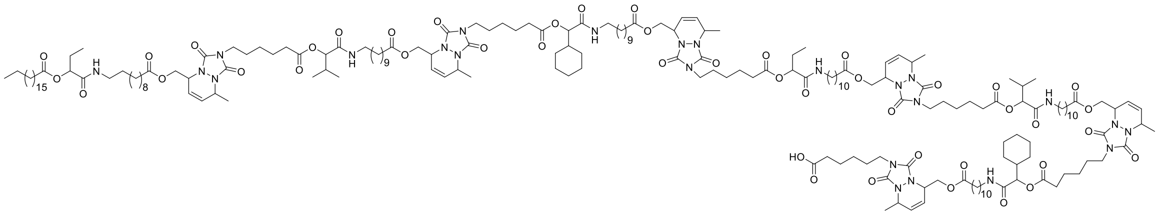

0.360 g of **91** (0.100 mmol, 1.0 eq.) was dissolved in 3 mL dry ethyl acetate and 25 mg of linker molecule **L2** (0.115 mmol, 1.15 eq. dissolved in 2 mL dry ethyl acetate) was added dropwise to the solution, until it stayed pink, indicating that **91** was fully converted. 20 µL of 2,3-dimethylbut-2-ene (17 mg, 0.20 mmol) was added to the reaction mixture in order to quench the excess of the TAD compound **L2**. The solvent was evaporated under reduced pressure and the crude product **92** was used without further purification or analysis.

7th Passerini reaction

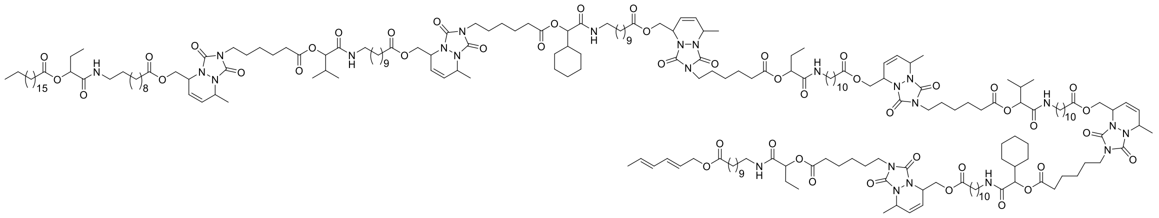

0.379 g of **92** (0.10 mmol, 1.0 eq.) was dissolved in 2 mL DCM. Subsequently, 43 µL of propanal **11a** (0.035 g, 0.60 mmol, 6.0 eq.) and 0.131 g of **L1** (0.45 mmol, 4.5 eq.) were added. The reaction was stirred for 24 hours at room temperature and the crude product was purified by column chromatography (hexane:ethyl acetate 1:2→EtOAc). Product **93** was obtained as a yellowish, highly viscous oil in a yield of 75% (277 mg, 0.067 mmol, overall yield over two reaction steps).

^{1}H-NMR: (500 MHz, $CDCl_3$) *δ* /ppm: 6.28 – 5.51 (m, 23H, ^{1}), 5.17 – 5.08 (m, 3H, ^{2}), 5.07 – 4.97 (m, 4H, ^{3}), 4.60 (s, 6H, ^{4}), 4.56 (d, *J* = 6.6 Hz, 2H, ^{5}), 4.51 – 4.43 (m, 6H, ^{6}), 4.40 – 4.29 (m, 12H, ^{7}), 3.64 – 3.46 (m, 12H, ^{8}), 3.36 – 3.11 (m, 14H, ^{9}), 2.49 – 2.36 (m, 14H, ^{10}), 2.33 – 2.19 (m, 16H, ^{11}), 1.97 – 1.81 (m, 8H, ^{12}), 1.80 – 1.55 (m, 54H, ^{13}), 1.50 (d, *J* = 6.5 Hz, 21H, ^{14}), 1.43 – 0.95 (m, 144H, ^{15}), 0.94 – 0.74 (m, 24H, ^{16}).

^{13}C NMR (126 MHz, $CDCl_3$) δ /ppm: 173.79, 173.47, 172.60, 172.36, 172.22, 172.19, 169.79, 169.73, 169.37, 169.32, 153.93, 153.89, 152.82, 152.80, 134.91, 131.33, 130.57, 129.92, 123.96, 121.20, 78.10, 77.81, 74.98, 74.88, 68.10, 64.89, 62.71, 52.93, 51.03, 51.00, 40.12, 39.36, 39.31, 38.93, 34.46, 34.13, 34.09, 32.05, 30.67, 29.90, 29.82, 29.78, 29.73, 29.59, 29.49, 29.39, 29.36, 29.34, 29.24, 27.72, 27.43, 26.99, 26.96, 26.18, 26.14, 26.10, 26.00, 25.73, 25.22, 25.20, 25.12, 25.06, 24.81, 24.49, 24.48, 24.44, 22.82, 19.42, 18.91, 18.27, 17.11, 14.26, 9.14.

ESI-MS:

m/z exp.	formula	m/z theo.	Δ m/z
2094.8369	$[C_{223}H_{363}N_{25}O_{47}Na_2]^{2+}$	2094.8284	0.0085
1404.2249	$[C_{223}H_{363}N_{25}O_{47}Na_3]^{3+}$	1404.2153	0.0096
1058.9108	$[C_{223}H_{363}N_{25}O_{47}Na_4]^{4+}$	1058.9088	0.0020
4144.7088	$[C_{223}H_{363}N_{25}O_{47}H]^{+}$	4144.6856	0.014
2072.8495	$[C_{223}H_{363}N_{25}O_{47}H_2]^{2+}$	2072.8464	0.0232
1382.2363	$[C_{223}H_{363}N_{25}O_{47}H_3]^{3+}$	1382.2334	0.0029
1036.9266	$[C_{223}H_{363}N_{25}O_{47}H_4]^{4+}$	1036.9269	0.0003

IR (ATR platinum diamond): *v* /cm^{-1} = 3336.0, 2924.9, 2853.6, 1736.9, 1701.1, 1534.2, 1453.7, 1422.0, 1377.1, 1237.4, 1115.8, 989.9, 765.5, 722.2, 637.6, 538.2.

***R*$_f$**: (ethyl acetate) = 0.37.

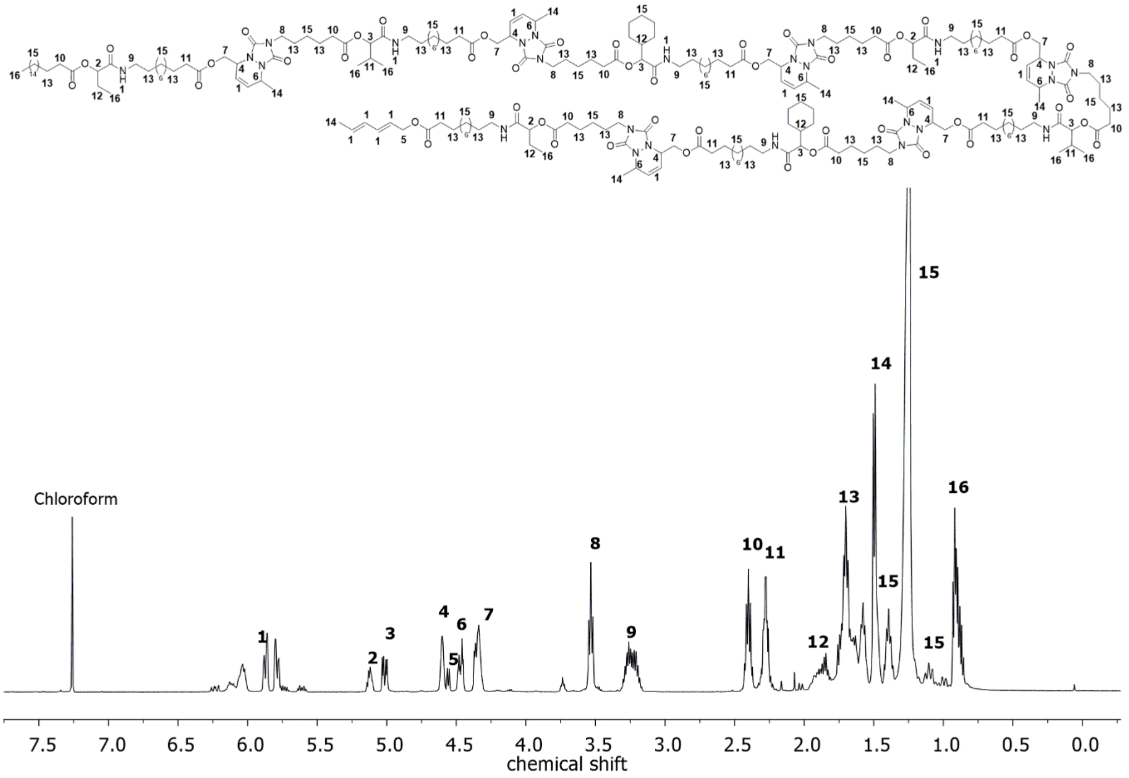

7th TAD-Diels Alder reaction

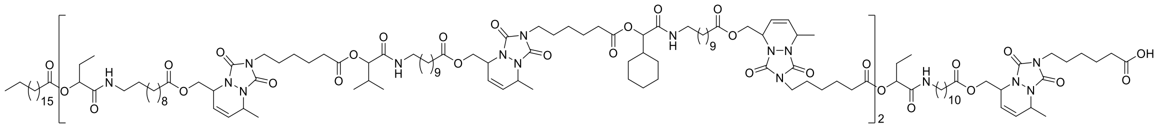

0.236 g of **93** (0.056 mmol, 1.0 eq.) was dissolved in 3 mL dry ethyl acetate and 14 mg of linker molecule **L2** (0.066 mmol, 1.15 eq. dissolved in 2 mL dry ethyl acetate) was added dropwise to the solution, until it stayed pink, indicating that **93** was fully converted. 20 µL of 2,3-dimethylbut-2-ene (17 mg, 0.20 mmol) was added to the reaction mixture in order to quench the excess of the TAD compound **L2**. The solvent was evaporated under reduced pressure and the crude product **94** was used without further purification or analysis.

8th Passerini reaction

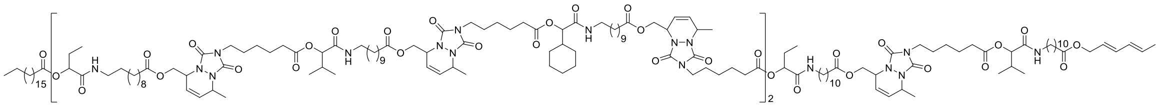

0.249 g of **94** (0.057 mmol, 1.0 eq.) was dissolved in 2 mL DCM. Subsequently, 31 µL of isobutyraldehyde **11c** (25 mg, 0.342 mmol, 6.0 eq.) and 0.075 g of **L1** (0.260 mmol, 4.5 eq.) were added. The reaction was stirred for 24 hours at room temperature and the crude product was purified by column chromatography (hexane:ethyl acetate 1:2→EtOAc+6% MeOH). Product **95** was obtained as a yellowish, highly viscous oil in a yield of 94% (253 mg, 0.053 mmol, overall yield over two reaction steps).

^{1}H NMR (500 MHz, CDCl$_3$) *δ* /ppm 6.30 – 5.52 (m, 26H, ^{1}), 5.15 – 5.07 (m, 3H, ^{2}), 5.04 – 4.94 (m, 5H, ^{3}), 4.59 (s, 7H, ^{4}), 4.55 (d, *J* = 6.6 Hz, 2H, ^{5}), 4.49 – 4.43 (m, 7H, 6), 4.39 – 4.29 (m, 14H, ^{7}), 3.58 – 3.48 (m, 14H, ^{8}), 3.33 – 3.13 (m, 16H, ^{9}), 2.47 – 2.35 (m, 16H, ^{10}), 2.33 – 2.20 (m, 19H, ^{11}), 1.99 – 1.79 (m, 8H, ^{12}), 1.77 – 1.53 (m, 62H, ^{13}), 1.49 (d, *J* = 6.6 Hz, 24H, ^{14}), 1.45 – 0.94 (m, 158H, ^{15}), 0.94 – 0.80 (m, 30H, ^{16}).

^{13}C NMR (126 MHz, CDCl$_3$) δ /ppm: 173.73, 173.42, 172.57, 172.32, 172.19, 169.78, 169.72, 169.35, 169.30, 153.94, 153.91, 152.82, 152.81, 134.86, 131.25, 130.60, 129.93, 124.00, 121.24, 78.14, 77.84, 77.73, 75.01, 74.91, 64.85, 62.72, 52.96, 51.04, 51.02, 40.14, 39.36, 39.33, 38.94, 34.46, 34.14, 34.09, 32.04, 30.68, 29.80, 29.79, 29.73, 29.58, 29.48, 29.38, 29.35, 29.33, 29.24, 27.70, 27.48, 26.98, 26.96, 26.19, 26.15, 26.11, 26.01, 25.23, 25.20, 25.12, 25.06, 24.82, 24.50, 24.48, 24.45, 22.80, 19.41, 18.89, 18.22, 17.13, 14.23, 9.13.

ESI-MS:

m/z exp.	formula	m/z theo.	Δ m/z
2383.0051	$[C_{253}H_{411}N_{29}O_{54}Na_2]^{2+}$	2383.0045	0.0006
1596.3312	$[C_{253}H_{411}N_{29}O_{54}Na_3]^{3+}$	1596.3328	0.0016
1202.9986	$[C_{253}H_{411}N_{29}O_{54}Na_4]^{4+}$	1202.9969	0.0017
2361.0244	$[C_{253}H_{411}N_{29}O_{54}H_2]^{2+}$	2361.0226	0.0018
1574.3540	$[C_{253}H_{411}N_{29}O_{54}H_3]^{3+}$	1574.3508	0.0032
1181.2661	$[C_{253}H_{411}N_{29}O_{54}H_4]^{4+}$	1181.0149	0.2512

IR (ATR platinum diamond): *ν* /cm^{-1} = 3337.4, 2925.3, 2853.6, 1736.9, 1700.8, 1534.2, 1453.8, 1422.0, 1376.9, 1237.4, 1157.6, 1116.2, 765.5, 722.2, 537.2.

***R*f**: (ethyl acetate) = 0.125.

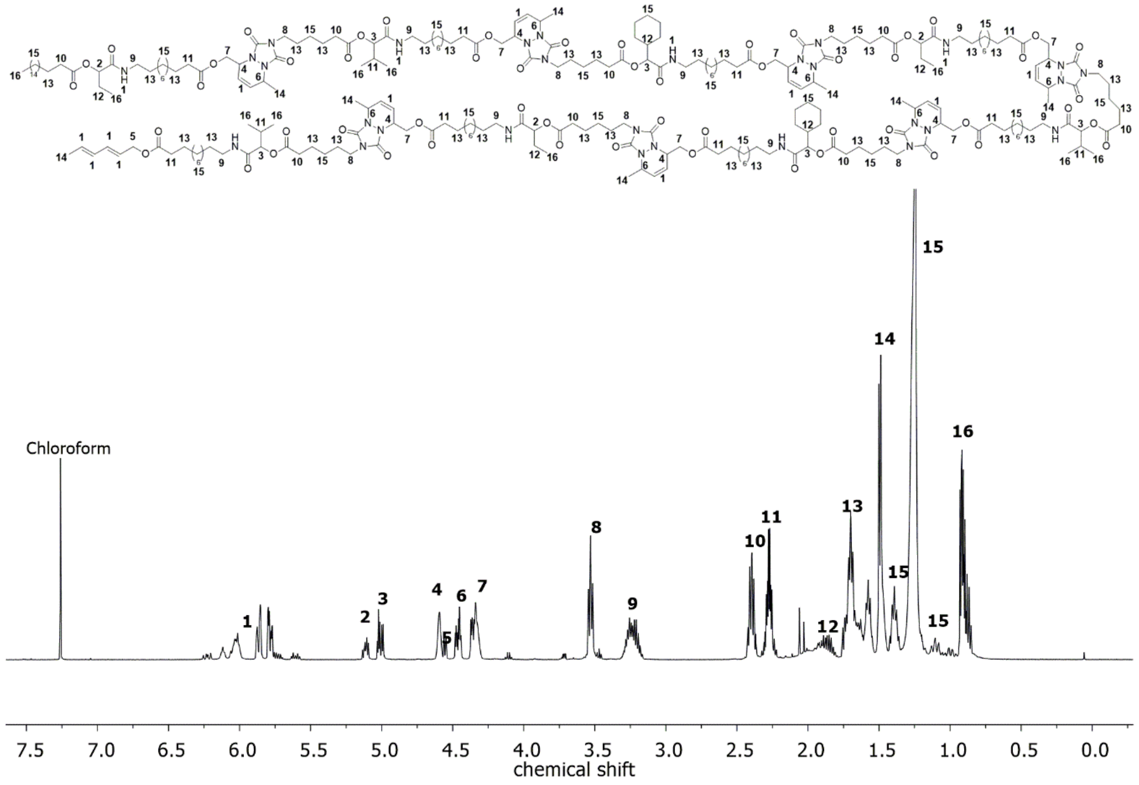

8th TAD-Diels Alder reaction

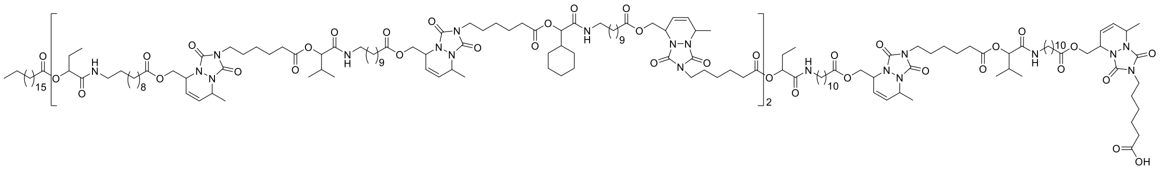

0.202 g of **95** (0.043 mmol, 1.0 eq.) was dissolved in 3 mL dry ethyl acetate and 11 mg of linker molecule **L2** (0.049 mmol, 1.15 eq. dissolved in 2 mL dry ethyl acetate) was added dropwise to the solution, until it stayed pink, indicating that **95** was fully converted. 20 µL of 2,3-dimethylbut-2-ene (17 mg, 0.20 mmol) was added to the reaction mixture in order to quench the excess of the TAD compound **L2**. The solvent was evaporated under reduced pressure and the crude product **96** was used without further purification or analysis.

9th Passerini reaction

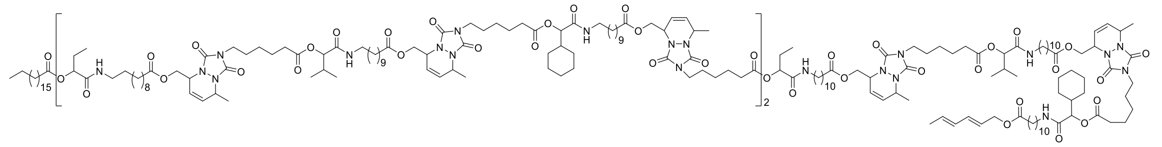

0.211 g of **96** (0.043 mmol, 1.0 eq.) was dissolved in 2 mL DCM. Subsequently, 0.32 µL of cyclohexanal **11b** (29 mg, 0.257 mmol, 6.0 eq.) and 0.56 g of **L1** (0.193 mmol, 4.5 eq.) were added. The reaction was stirred for 24 hours at room temperature and the crude product was purified by column chromatography (hexane : ethyl acetate 1:2.5→EtOAc+10% MeOH). Product **53** was obtained as a yellowish, highly viscous oil in a yield of 78% (179 mg, 0.0335 mmol, overall yield over two reaction steps).

^{1}H NMR (500 MHz, $CDCl_3$) δ /ppm: 6.27 – 5.53 (m, 29H, ^{1}), 5.14 – 5.06 (m, 3H, ^{2}), 5.03 – 4.95 (m, 6H, ^{3}), 4.59 (s, 8H, ^{4}), 4.55 (d, J = 6.6 Hz, 2H, ^{5}), 4.48 – 4.41 (m, 8H, ^{6}), 4.38 – 4.27 (m, 16H, ^{7}), 3.59 – 3.45 (m, 16H, ^{8}), 3.30 – 3.13 (m, 18H, ^{9}), 2.46 – 2.34 (m, 18H, ^{10}), 2.32 – 2.18 (m, 21H, ^{11}), 1.97 – 1.78 (m, 9H, ^{12}), 1.77 – 1.52 (m, 70H, ^{13}), 1.49 (d, J = 6.6 Hz, 27H, ^{14}), 1.42 – 0.94 (m, 182H, ^{15}), 0.94 – 0.76 (m, 30H, ^{16}).

^{13}C NMR (126 MHz, $CDCl_3$) δ /ppm: 173.40, 172.55, 172.31, 172.18, 169.75, 169.69, 169.33, 169.27, 153.91, 153.88, 152.78, 152.77, 134.85, 131.25, 130.56, 129.90, 123.96, 121.20, 78.09, 77.79, 74.97, 74.87, 64.83, 62.69, 52.93, 52.91, 51.02, 50.99, 40.11, 39.33, 39.29, 38.91, 34.43, 34.11, 34.06, 32.01, 30.65, 29.78, 29.73, 29.71, 29.55, 29.45, 29.35, 29.32, 29.31, 29.21, 27.68, 27.43, 26.96, 26.93, 26.16, 26.12, 26.08, 25.98, 25.20, 25.18, 25.09, 25.03, 24.78, 24.47, 24.45, 24.42, 22.78, 19.39, 18.87, 18.22, 17.10, 14.21, 9.11.

ESI-MS:

m/z exp.	formula	m/z theo.	Δ m/z
2691.2043	$[C_{286}H_{463}N_{33}O_{61}Na_2]^{2+}$	2691.1963	0.0080
1801.7965	$[C_{286}H_{463}N_{33}O_{61}Na_3]^{3+}$	1801.7940	0.0025
1357.0934	$[C_{286}H_{463}N_{33}O_{61}Na_4]^{4+}$	1357.0928	0.0006
2669.2178	$[C_{286}H_{463}N_{33}O_{61}H_2]^{2+}$	2669.2144	0.0034
1779.8157	$[C_{286}H_{463}N_{33}O_{61}H_3]^{3+}$	1779.8120	0.0037
1335.1125	$[C_{286}H_{463}N_{33}O_{61}H_4]^{4+}$	1335.1108	0.0017
1068.2902	$[C_{286}H_{463}N_{33}O_{61}H_5]^{5+}$	1068.2901	0.0001

IR (ATR platinum diamond): ν /cm^{-1} = 3336.7, 2925.2, 2853.6, 1737.1, 1700.5, 1533.9, 1453.6, 1422.0, 1377.3, 1237.0, 1157.5, 1116.1, 765.5, 722.3, 5371, 423.1.

***R*$_f$**: (ethyl acetate) = 0.19.

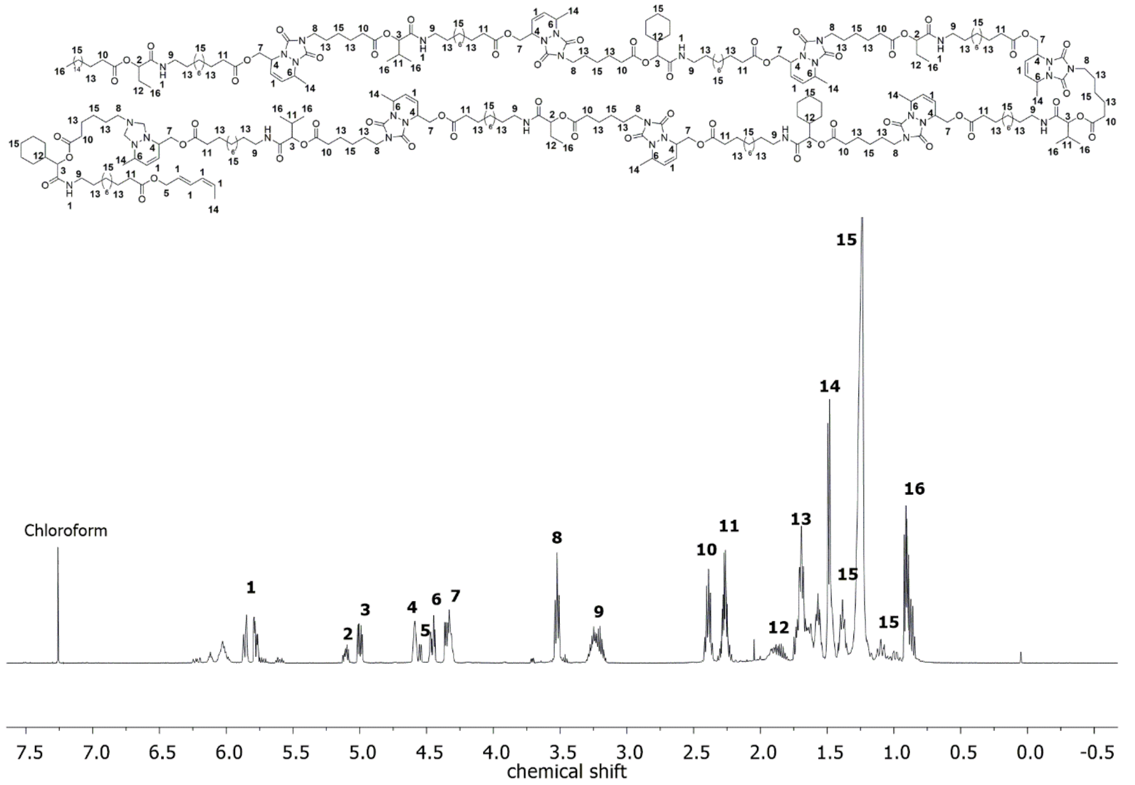

SEC-ESI-MS analysis of the sequence-defined nonamer 53 synthesised in solution

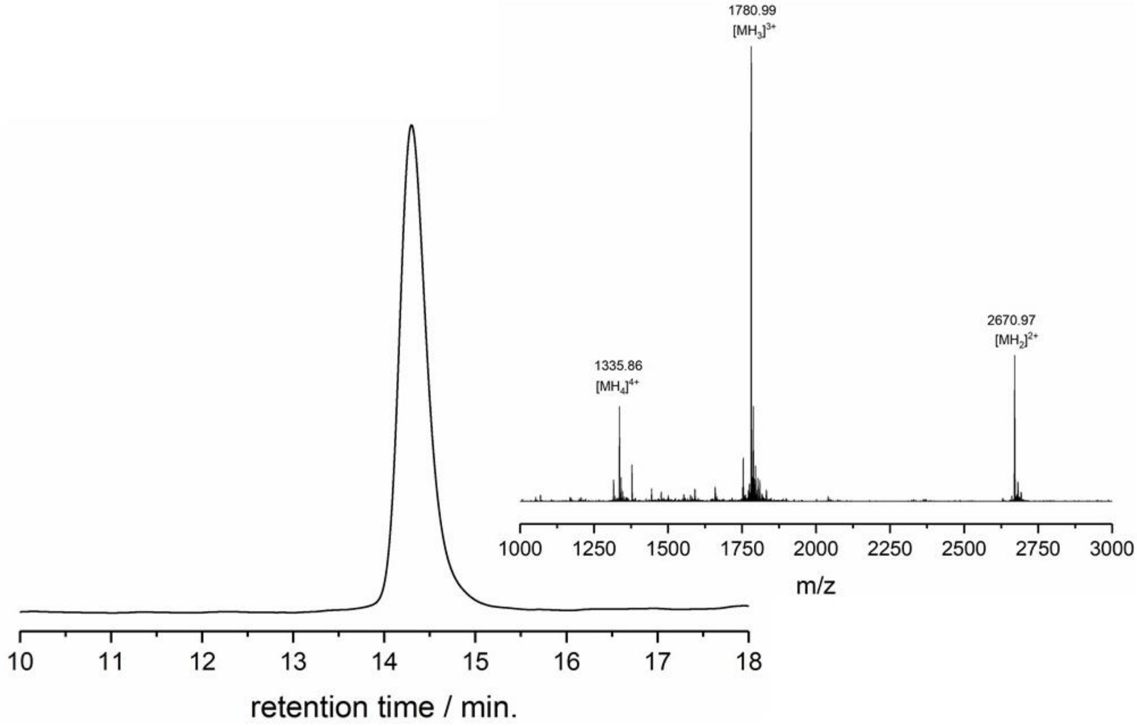

Figure S 40. SEC chromatogrm of the sequence-defined nonamer ***53*** *prepared in solution and the corresponding ESI-MS spectrum at a retention time of 14.30 minutes. The doubly- (2670.97 m/z), triply- (1780.99 m/z) and quadruply (1335.86 m/z) charged cations were clearly observed.*

Analysis of isotope pattern of sequence-defined nonamer 53 (solution phase):

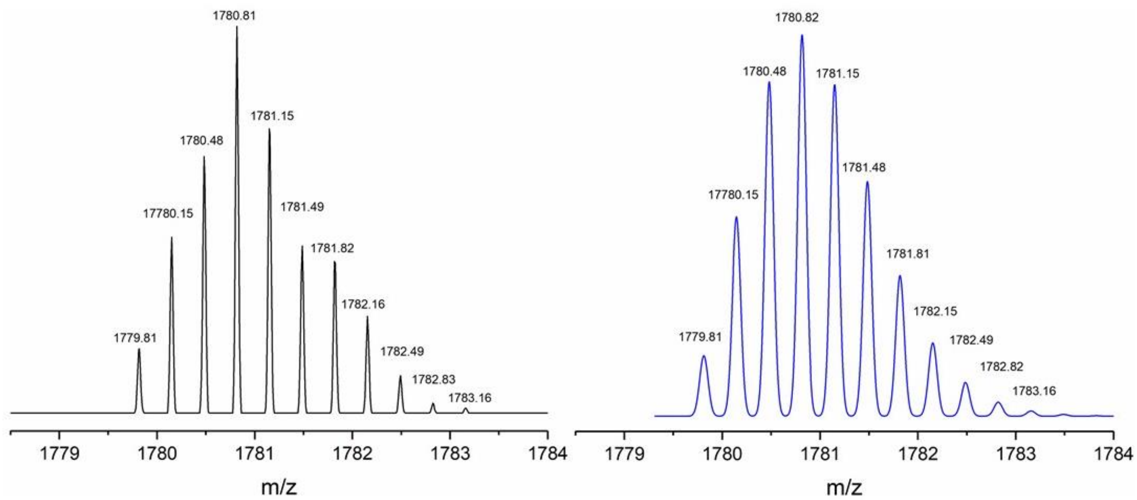

Figure S 41. Left (black): The measured ESI-MS spectrum is shown. Right (blue): The isotope pattern was theoretically calculated with the program mMass. The measured isotope pattern is in very good agreement with the theoretical one for the assumed chemical formula.

Coupling of the nonamer to a symmetric 18-mer 59 using bis-TAD 58

43.5 mg of **53** (0.0081 mmol, 1.0 eq.) were dissolved in 4 mL dry ethyl acetate and 1.33 mg of the bis-TAD compound **58** (0.0037 mmol, 0.45 eq.) were dissolved in 1.3 mL dry ethyl acetate. The bis-TAD solution was added dropwise to the solution of **53** and the reaction mixture was stirred for three hours at room temperature. Subsequently, another 0.29 mg of bis-TAD compound **58** (0.1 eq) was dissolved in 1 mL of dry ethyl acetate and added slowly over 45 minutes to the reaction mixture. The reaction was stirred for half an hour at room temperature and again 0.1 eq. of bis-TAD 58 were added dropwise over 30 minutes. The solvent was evaporated to obtain the desired 18-mer **59**.

ESI-MS:

m/z exp.	**formula**	**m/z theo.**	**Δ m/z**
3701.3316	$[C_{589}H_{936}N_{72}O_{126}Na_3]^{3+}$	3701.2908	0.0708
2781.7322	$[C_{589}H_{936}N_{72}O_{126}Na_4]^{4+}$	2781.7154	0.0168
2229.9799	$[C_{589}H_{936}N_{72}O_{126}Na_5]^{5+}$	2229.9702	0.0097
1862.1526	$[C_{589}H_{936}N_{72}O_{126}Na_6]^{6+}$	1862.1400	0.0126
1599.4105	$[C_{589}H_{936}N_{72}O_{126}Na_7]^{7+}$	1599.4042	0.0063
1402.4830	$[C_{589}H_{936}N_{72}O_{126}Na_8]^{8+}$	1402.3523	0.1307
3679.3341	$[C_{589}H_{936}N_{72}O_{126}H_3]^{3+}$	3679.3089	0.0252
2759.7340	$[C_{589}H_{936}N_{72}O_{126}H_4]^{4+}$	2759.7335	0.0005
2207.9874	$[C_{589}H_{936}N_{72}O_{126}H_5]^{5+}$	2207.9882	0.0004
1840.1585	$[C_{589}H_{936}N_{72}O_{126}H_6]^{6+}$	1840.1581	0.0003
1577.4240	$[C_{589}H_{936}N_{72}O_{126}H_7]^{7+}$	1577.4222	0.0018
1380.3687	$[C_{589}H_{936}N_{72}O_{126}H_8]^{8+}$	1380.3704	0.0017

IR (ATR platinum diamond): ν /cm^{-1} = 3335.3, 2925.0, 2853.4, 1737.0, 1699.9, 1534.1, 1453.7, 1421.6, 1377.8, 1238.3, 1157.5, 1105.0, 765.3, 722.3, 537.6, 421.1.

Kinetic evaluation of the P-3CR *via* online IR:

Online IR Investigation of the reaction kinetics of the first P-3CR using 3 different aldehydes

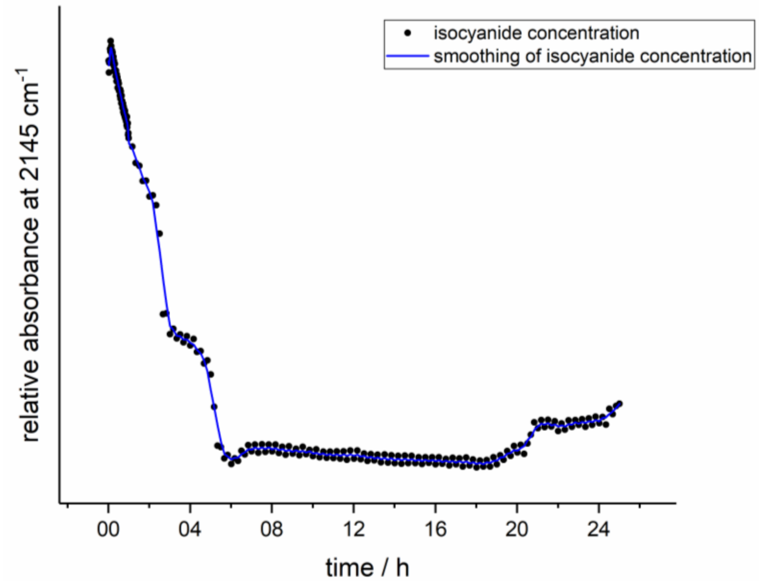

*Figure S 42. Online IR analysis of the P-3CR with stearic acid **13**, linker molecule **L1** and isobutyraldehyde **11c** depicting the decrease of the isocyanide peak at 2145.33 cm-1 with time. Reaching the plateau indicates full conversion, since **L1** was used in excess. The reaction is complete after 6h00min.*

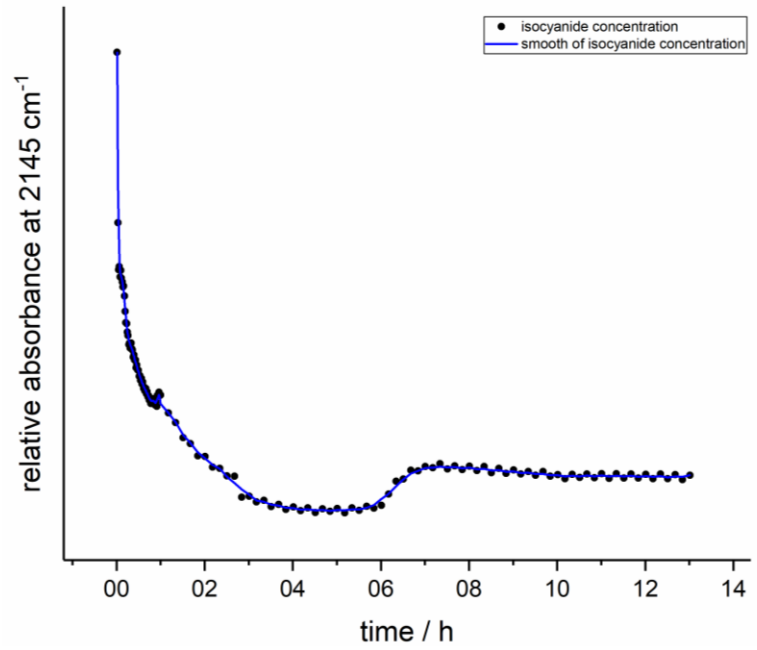

*Figure S 43. Online IR analysis of the P-3CR with stearic acid **13**, linker molecule **L1** and cyclohexylaldehyde **11b** depicting the decrease of the isocyanide peak at 2145.33 cm-1 with time. Reaching the plateau indicates full conversion, since **L1** was used in excess. The reaction is complete after 4h30min.*

Kinetic evaluation of the P-3CR after the fifth reaction cycle

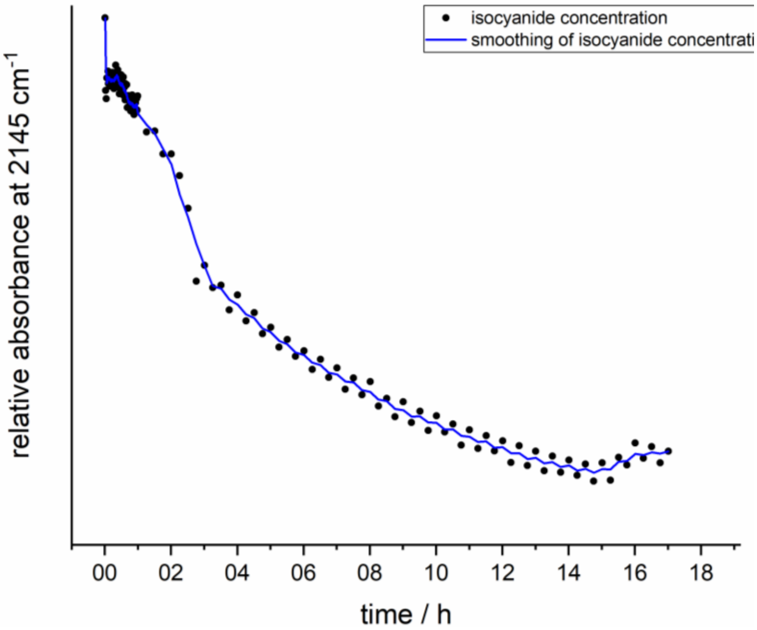

*Figure S 44. Online IR analysis of the P-3CR during the fifth reaction cycle depicting the decrease of isocyanide peak at 2145.33 cm-1 with time. Reaching the plateau indicates full conversion, since **L1** was used in excess. The reaction is complete after 14h45min.*

7 Abbreviations

ADMET	acyclic diene metathesis polymerisation
ATRA	atom transfer radical additions
ATRP	Atom transfer radical polymerisation
CuAAC	Copper-catalysed azide-alkyne cycloaddition
CM	Cross-metathesis
Đ	Dispersity
Da	Dalton
DABCO-Br	Tetrameric 1,4-diazabicyclo[2.2.2]octane bromide
DCC	*N,N'*-Dicyclohexylcarbodiimide
DCM	Dichloromethane
DEAD	Diethyl azodicarboxylate
DFT	Density functional theory
DIC	Diisopropylamine
DLS	Dynamic light scattering
DMF	Dimethylformamide
DMSO	Dimethyl sulfoxide
DMT	Dimethoxy trityl
DNA	Deoxyribonucleic acid

DO_x	Linear oligomer with x repeating units functionalised with terminal double bond
DP	Degree of polymerisation
ESI-MS	Electrospray ionization – mass spectrometry
et al.	et alii
EWG	Electron withdrawing groups
FAB	Fast atom bombardement
Fmoc	9-fluorenyl methoxy carbonyl
FSPE	Fluorous solid phase extraction
FT-IR	Fourier transformed infrared spectroscopy
h	Hour
HBTU	2-(1*H*-benzotriazol-1-yl)-1,1,3,3-tetramethyluronium hexafluorophosphate
HOBt	Hydroxybenzotriazole
HPLC	High-performance liquid chromatography
HRMS	High resolution mass spectrometry
IBX	2-iodoxybenzoic acid
i.e.	id est
IEG	Iterative exponential growth
IMCR	Isocyanide-based multicomponent reaction
IUPAC	International union of pure and applied chemistry
IR	infrared
kDa	Kilo Dalton
LC-MS	Liquid chromatography-mass spectrometry
LO_x	Linear oligomer with x repeating units
m/z	Mass-to-charge ratio
MAA	Methacrylic acid
MALDI	Matrix-assisted laser desorption/ionization
MCR	Multicomponent reactions
MeOH (MeOD)	(deuterated) Methanol
M_n	number average of the molar mass
MO_x	Macrocyclic oligomer with x repeating units
MS	Mass spectrometry
M_w	weight average of the molar mass

Hz	Hertz
min	Minute
NBS	*N*-bromosuccinimide
NICAL	Nitrile imine carboxylic acid ligation
NMP	Nitroxide-mediated radical polymerisation
NMR	Nuclear magnetic resonance spectroscopy
o-MBA	*o*-Methylbenzaldehyde
P-3CR	Passerini three-component reaction
PDI	Polydispersity index
PEG	Poly(ethylene glycol)
PhTAD	Phenyl-TAD
ppm	Parts per million
PyBOP	Benzotriazol-1-yl-oxytripyrrolidino phosphonium hexafluorophosphate
QR	Quick Response
RAFT	Reversible addition-fragmentation chain transfer
RCM	Ring-closing metathesis
RDRP	Reversible-deactivation radical polymerisation
RNA	Ribonucleic acid
ROM	Ring-opening metathesis
ROMP	Ring-opening metathesis polymerisation
S_EAr	Electrophilic aromatic substitution
SEC	Size exclusion chromatography
SM	Self-metathesis
S_N2	Concerted nucleophilic substitution (bimolecular mechanism)
SPPS	Solid-phase peptide synthesis
SUMI	Single unit monomer insertions
TAD	1,2,4-triazoline-3,5-dione
TAD-COOH	Acid-functionalised TAD (Linker **L2**)
TBDMS	Tert-Butyldimethylsilylgruppe
TClCA	Trichloroisocyanuric acid
TEMPO	(2,2,6,6-tetramethylpiperidin-1-yl)oxyl
TFA	Trifluoroacetic acid
T_g	Glass transition temperature

THF	Tetrahydrofuran
TLC	Thin layer chromatography
ToF	Time of flight
TOM	triisopropylsilyl oxy methyl
U-4CR	Ugi four-component reaction
UV	Ultraviolet
UV-Vis	Ultraviolet–visible spectroscopy

8 List of figures and schemes

8.1.1 Figures

Figure 1. Classification and definitions of polymers exhibiting different levels of control. 4

Figure 2. Three examples of commonly utilised resins used as solid support in SPPS. The chloromethyl resin, the 2-chlorotrityl chloride resin and the Rink amide resin are depicted.[52-54] 7

Figure 3. Comparison of the structure of naturally occurring peptides and non-natural peptoids.[18] 9

Figure 4. Structure of an oligonucleotide synthesised by applying the phosphoramidite approach. This example contains the four nucleobases: adenine, cytosine, thymine, and guanine.[92-93] 11

Figure 5. Orthogonal protecting group strategy for the solid phase oligonucleotide synthesis commonly applied in the phosphoramidite approach.[93-94, 100] 12

Figure 6. (a.) Phosphoramidite based monomers "0" and "1" to encode the macromolecules and the thymine containing nucleotide that formed the primer sequence facilitating the subsequent analysis. (b.) iterative approach on a solid support consisting of four steps: (i) Dimethoxy trityl (DMT) deprotection, (ii) coupling step, (iii) oxidation, (iv) capping. The final product is obtained by (v) cleavage from the solid support. Reprinted with permission from A. A. Ouahabi et al., ACS Macro Lett. **2015**, 4, 1077-1080. Copyright © 2015 American Chemical Society.[22] 17

Figure 7. Illustration of the mechanism for encoding and decoding of a QR code works: the QR code as established by Du Prez and colleagues: the QR code was first translated into a bit string which was then transferred to a pentadecimal numerical system. The long sequence was divided into small fragments of defined sizes and marked with an index to reassign the order of the fragments later on. The index is marked in purple. Encoding was done automatically by a Chemcoder. The read-out was done by tandem MS and the results were automatically reconverted by the Chemreader resulting in the original QR code. The figure is reprinted from a publication of Martens et al., which is licensed under a Creative Commons Attribution licence.[40] 21

Figure 8. Read-out of the sequence of a pentamer using MALDI tandem MS/MS. Different characteristic fragmentation patterns were found (marked in blue and purple). The figure is reprinted from a publication of Martens et al., which is licensed under a Creative Commons Attribution licence.[40] 22

Figure 9. Structure of a sequence-defined decamer obtained by the monomer approach bearing ten different side chains.[34] 32

Figure 10. Left: Fluorous solid phase extraction: the fluorous-tagged substrate is purified by using a column packed with silica gel equipped with perfluorinated alkyl chains. By using different solvents, the mixture is separated into a fluorophobic and a fluorophilic fraction. Right: the polymer is synthesised on a soluble polymer support in solution and can be purified by precipitation in another solvent, in which the impurities are soluble. Separation is achieved by simple filtration. Reprinted with permission from S. C. Solleder, et al., Macromol. Rapid Commun. **2017**, 38, 1600711. Copyright © 2017 John Wiley and Sons.[36] 35

Figure 11. The mesomeric resonance structures of isocyanides include a zwitterionic configuration as well as a carbene like structure 42

Figure 12. Examples of two naturally occurring isocyanides.[217-218] 43

Figure 13. Some commonly applied oxidation reagents that are used for the oxidation of urazole to form TAD: NBS: N-bromosuccinimide; DABCO-Br: tetrameric 1,4-diazabicyclo[2.2.2]octane-bromine; TClCA: trichloroisocyanuric acid 56

Figure 14. Selection of the most important commercially available catalysts for olefin metathesis. 68

Figure 15. Example of a fully assinged NMR spectrum of a symmetric hexamer carrying isopropyl side chains. 71

Figure 16. Structures and the results of the SEC analysis of the linear protected and deprotected oligomers (**LO**$_{2,4,6,8}$) carrying isopropyl side chains. The structures and respective SEC traces are assigned by the same colour code. The SEC traces clearly verify the uniform size distribution of the obtained products. 72

Figure 17. SEC characterisation of the final linear precursors **DO**$_{2,4,6,8}$ carrying cyclohexyl side chains. All the oligomers are end-functionalised with terminal double bonds, allowing for subsequent macrocyclisation. 73

Figure 18. ^{1}H NMR comparison of a **LO**$_4$ (**A**) and a **MO**$_4$ (**B**) carrying isopropyl side chains. In the first ^{1}H NMR spectrum, the signals of the terminal double bonds are clearly observed, whereas in the spectrum on the bottom, these signals disappear completely and the signal of the newly formed internal double bond appears, indicating full conversion towards **MO**$_4$. 75

Figure 19. SEC-ESI-MS analysis of a crude macrocyclic octamer **MO**$_8$ with cyclohexyl side chains. Left: SEC trace with assignment of the respective peaks. The peaks could be assigned with the help of the mass spectrum, which is shown on the right. 76

Figure 20. Left: SEC analysis results of the crude macrocyclic products with cyclohexyl side chains and sebacic acid **10** as core unit, revealing the influence of the size of the oligomer on the conversion towards the macrocycle. For the decamer **MO**$_{10}$, a detailed description of the obtained products is depicted exemplary. The different species were identified by SEC-ESI-MS analysis. Right: SEC-ESI-MS analysis of the macrocyclic decamer **MO**$_{10}$ bearing cyclohexyl side chains. The single, double and triple charged sodium cations are clearly observed. The expanded region (panel A) shows the apparent isotopic pattern (black) which was found to be in good agreement with the calculated one (blue, panel B), obtained by the program mMass. 77

Figure 21. Left: Dependence of the oligomer size on the conversion towards the desired macrocycle. The mean values and standard deviation of the conversions for **MO$_{2,4,6,8,10}$** are displayed; the line is only drawn to guide the eye. **MO$_2$** and **MO$_{10}$** do not have a standard deviation since they were not synthesised with different side chains. Right: Comparison of the conversion towards the macrocycles **MO$_8$** carrying different side chains, namely cyclohexyl and isopropyl by SEC analysis. The conversion is 57 and 49% for **MO$_8$** carrying cyclohexyl and isopropyl side chains, respectively. The peaks were identified by SEC-ESI-MS to be **MO$_8$**, **LO$_8$**, and the two ADMET side products (**LO$_8$**)$_2$ and (**MO$_8$**)$_3$, from higher to lower retention time. 78

Figure 22. SEC comparison of a crude macrocyclic octamer with three different narrow PMMA standards, that are commonly used for SEC calibration. In the crude product, four different species are detectable, which can be identified by SEC-ESI-MS analysis. 79

Figure 23. Left: library of the AB-type monomers **M1** – **M9** that were synthesised from the corresponding amino acid in three steps; (*) in case of **M9**, the synthesis is performed via a four-step procedure. By variation of the monomers, different backbone moieties can be introduced to the macromolecules. Right: library of commercially available aldehydes applied to introduce different side chains to the oligomers... 83

Figure 24. Example of the evolution in the proton NMR spectrum during the monomer synthesis. The three spectra show the intermediates **2b** and **8b** (blue: esterification; green: N-formylation) and the final product **M2** (red: dehydration). 85

Figure 25. Example of the evolution in the NMR spectra during the monomer synthesis. The spectra of the three intermediates (purple: methyl ester, turquoise: N-formamide, green: benzyl ester) as well as of the final product **M9** (red) are depicted. 87

Figure 26. Top: the molecule structure of the growing oligomers after each P-3CR up to the heptamer stage, where the monomers were inserted step by step in the following order: **M1**, **M2**, **M9**, **M4**, **M5**, **M7**, and **M3**. Bottom: the SEC results after each P-3CR are verifying the purity of the products. For the assignment of the oligomers, refer to the colour code. 90

Figure 27. Mass spectrum of the backbone-defined hexamer **26**: the singly charged sodium ion was found to be the main peak, indicating high purity of the product. The measured isotopic pattern (black) can be compared with the calculated one obtained by mMass (blue), revealing that they are in good agreement. 91

Figure 28. Top: the molecule structure of stearic acid **13** and the growing oligomers **33** - **41** after each P-3CR and deprotection up to the pentamer stage, where the monomers were inserted step by step in the following order: **M1**, **M7**, **M4**, **M8**, and **M3**. Isobutyraldehyde **11c**, isovaleraldehyde, octanal, dodecanal and 2-phenylpropanal **11h** were used to introduce different side chains. Bottom: the SEC results after each P-3CR and deprotection step are verifying the purity of the products. For the assignment of the oligomers, refer to the colour code. 94

Figure 29. Mass spectrum of the backbone-defined deprotected tetramer: the protonated ion and the singly charged sodium ion was found in the spectrum, indicating the high purity of the product. The measured isotopic pattern (black) can be compared with the calculated one obtained by mMass (blue), revealing that they are in very good agreement. 95

Figure 30. Fragmentation of the dual sequence-defined tetramer **39** by tandem mass spectrometry revealing the expected fragmentation pattern. In the spectrum, the α-fragmentation from both ends of the oligomer is depicted. By recombining the fragments, the initial structure of the tetramer can be retraced. A detailed list of all fragments is depicted in the experimental section (Chapter 6.3.2.2.3, Table S 2) 98

Figure 31. IR spectrum of the final linker molecule **L1** showing a characteristic isocyanide band at 2145 cm^{-1}...105

Figure 32. Left: Example of an online IR measurement during a P-3CR highlighting the isocyanide absorption band at 2145 cm^{-1}. Right: By zooming in, the decrease of the absorbance of the isocyanide peak is clearly observed. 109

Figure 33. Online IR analysis of the P-3CR with stearic acid **13**, linker molecule **L1** and propanal **11a** depicting the absorbance decrease of the isocyanide band at 2145.33 cm^{-1} with time. Reaching the plateau indicates full conversion, since **L1** was used in excess. The reaction is complete after 5h20min. 110

Figure 34. Top: structure of the $[ABC]_3$ sequence-defined nonamer **53** with three different side chains. Bottom left: SEC analysis of the obtained products from the optimised iterative synthesis cycle. The SEC results show the successful prevention of the side reaction and verify the high purity of the products. Bottom right: SEC-ESI-MS analysis of the nonamer showing the chromatogram and the corresponding mass spectrum at a retention time of 14 min 30 s. The assigned mass peaks correspond to the nonamer mass plus two, three and four protons. 113

Figure 35. Proton NMR spectrum of the sequence-defined nonamer **53** synthesised in solution exhibiting an $[ABC]_3$ structure recorded in $CDCl_3$ at 500 MHz. 114

Figure 36. SEC analysis of the symmetric coupled dimer **60**. The SEC trace is clearly visualising that the product was obtained in high purity. 116

Figure 37. Top: SEC-ESI-MS analysis of the bis-TAD coupled 18mer **59**. The mass spectrum corresponds to the retention time of the main peak at a retention time of 13.4 min. The three to eight-fold charged protonated 18-mer ions are clearly observed. Bottom: Comparison of the measured (black) with the calculated isotopic pattern (blue), which are in very good agreement clearly proving the structure of the 18-mer. 117

Figure 38. a) LC-MS chromatograms at λ=214 nm of phenyl-TAD capped monomer **62**, dimer **63** and trimer **64**, demonstrating excellent conversion and purity. The monomer was processed at a solvent gradient of 0 → 100% acetonitrile → water, the dimer **63** and trimer **64** were processed at a 75 → 100% gradient on account of their decreased polarity. The reduced gradient results in a lower retention time for the molecule. b) LC-MS chromatograms at λ=214 nm of the TAD molecule (**L2**) addition step. The increased polarity resulting from the carboxylic acid end-group made the TAD addition step much easier to analyse by LC-MS than the P-3CR step. By following the same step in the cycle, one can see a shift in retention time as the molecular weight increases. It should be noted that the shift in retention time does not continue in a liner fashion because the solvent gradient was changed from 75-100% to 90-100% after the 6th cycle. (See Figure S3 for LC-MS chromatograms of each step in the cycle). 119

Figure 39. Left: Evolution of the solid phase synthesised oligomer from trimer **64** through to nonamer **65** and dodecamer **52** before optimisation. In the chromatogram of the nonamer **65**, and even more in the one of the dodecamer **52**, a minor high molecular weight side-product is observed (left of the main peak), while a dead chain from the trimer level of the synthesis (right of the main peak) is also present. Right: SEC analysis of the solid phase synthesised oligomers after optimisation, depicting the 3.5 mer **67**, 6.5 mer **68** and nonamer **65**. The P-3CR polymerisation side product was significantly reduced following the successful application of the optimisation conditions. 122

8.1.2 Schemes

Scheme 1. Two-step iterative cycle of the SPPS, developed by Merrifield. [16, 51] 7

Scheme 2. Two-step iterative cycle for the preparation of peptoid using the submonomer approach which was reported by Zuckermann and co-workers in 1992.[73] 10

Scheme 3. Protecting group–free solid-phase synthesis exploiting the nucleophilic substitution of cyanuric chloride. With each reaction, the reactivity decreases, making elevated temperatures necessary and thereby avoiding protecting groups.[21] 15

Scheme 4. Iterative two-step synthesis protocol for the formation of sequence-defined macromolecules based on thiolactone chemistry.[23] 20

Scheme 5. In the approach from Johnson an enantiopure AB-monomer bearing an epoxy group and a TBDMS protected alkyne functionality is devided into two parts, one is deprotected, the other one is ring-opened, whereby a side chain can be introduced. Chain elongation is performed by recombining the two parts and repeating the iterative procedure until the desired product is obtained.[147] 24

Scheme 6. Photochemical approach towards sequence-defined macromolecules using bidirectional growth strategies reported by Barner-Kowollik et al. The light-induced chain extension is achieved by switching between NICAL and Diels-Alder reactions while irradiating with distinct wavelengths.[24] 26

Scheme 7. Synthesis of sequence-defined oligomers by switching between photochemistry and multicomponent reactions. The combination of the two different methods was achieved by the design and synthesis of two AB-type linker molecules, that carried a reactive functional group for both of the reactions.[154] 26

Scheme 8. Stepwise iterative approach using the P-3CR and subsequent thiol-ene addition.[27] 30

Scheme 9. AB-monomer approach using the P-3CR and a subsequent deprotection step in a two-step iterative cycle.[34] 31

Scheme 10. Synthetic procedure for the synthesis of sequence-defined macromolecules as candidates for data storage materials offering a high data storage capacity owed to the combination of two powerful MCRs. Reprinted with permission from A. C. Boukis, M. A. Meier, Eur. Polym. J. 2018, 104, 32-38. Copyright © 2018 Elsevier.[38] 33

Scheme 11. (a) Template initiator which is used in the template-assisted living radical polymerisation process. (b) the selective radical addition of MMA monomers by the amine-functionalised and by a crown ether-functionalised template is depicted. The interaction with the template is based on ionic recognition.[181] 37

Scheme 12 The synthesis of a rotaxane-based molecular machine is depicted. It incorporates a strand with amino acid building blocks **(2)**, and a macrocycle with one reactive site for attaching the reactive arm **(3)**. The terminal blocking group **(5)** prevents the threaded macrocycle from coming off the strand before all amino acids have been collected. Reprinted with permission from B. Lewandowski et al., Science 2013, 339, 189-193. Copyright © 2013 The American Association for the Advancement of Science.[32] 38

Scheme 13. MCRs are differentiated into three main types: In type I, all reactions are reversible, type II reactions have an irreversible last reaction step and in type III reactions, all reaction steps are irreversible,[187] with **A**, **B**: starting material; **C**, **D**, **E**, **O**: intermediates and **P**: product. 40

Scheme 14. Examples of historically important MCRs in chronological order.[191, 194-197] 41

Scheme 15. Different routed towards isocyanides in chronological order.[214, 220-221, 225] 44

Scheme 16. Reaction equations of the two important IMCRs: The P-3CR and the U-4CR.[227-229] 45

Scheme 17. Commonly accepted mechanism of the U-4CR, first introduced by Ivar Ugi in 1961. First, the imine is formed, which is then activated by protonation. The isocyanide is introduced via α-addition and the α-acylaminoamide product is formed upon Mumm rearrangement.[187, 228-229] 46

Scheme 18. Proposed mechanism of the P-3CR which was later supported by kinetic investigations by Ugi and Baker.[227, 232-233] It starts with activation of the aldehyde by hydrogen bonds, which allows for subsequent α-addition to form a cyclic transition state. The product is formed via final rearrangement. .. 47

Scheme 19. Proposed mechanism of the P-3CR by Maeda et al. involving two carboxylic acids. The mechanism was developed based on quantum mechanical calculations in the gas phase.[237] DFT calculations supported the postulated mechanism later.[238] 48

Scheme 20. Different variants of the P-3CR, replacing the acid or the aldehyde component by other functional groups which demonstrates the versatility of the reaction. 50

Scheme 21. Three different ways of P-3CR polymerisation, using different combinations of bifunctional components leading to different polymeric scaffolds. 52

Scheme 22. Oxidation of the urazole precursor leads to the corresponding TAD compound. 53

Scheme 23. The different rate coefficients (L mol^{-1} s^{-1}) in the Diels-Alder reaction with cyclopentadiene at room temperature in toluene. Three different aza-dienophiles are compared, namely cis- and trans-DEAD and phenyl TAD.[291] 54

Scheme 24. Two synthetic routes towards the urozole precursor. Thiele developed the first urazole synthesis by reacting biurea with aniline hydrochloride. The more efficient and modern pathway was later reported by Zinner and Deucker.[284, 292] 55

Scheme 25. The oxidation of urazole to the corresponding TAD compound can either be achieved by halogens or by dinitrogen tetroxide. 56

Scheme 26. The four general thermal TAD-based reactions: Diels-Alder reaction, Alder-Ene reaction, [2+2] cycloaddition and electrophilic aromatic substitution (S$_E$Ar). 57

Scheme 27. The equimolar Diels-Alder reaction of styrene and TAD demonstrates the extraordinary reactivity of TAD as it yields a 1:2 adduct via a reactive intermediate. 58

Scheme 28. General reaction scheme of olefin metathesis.[374] 65

Scheme 29. Reaction mechanism of olefin metathesis, which was proposed by Yves Chauvin.[379] 66

Scheme 30. The three different types of olefin metathesis: Ring-opening metathesis (type A), ring-closing metathesis (type B) and self- or cross-metathesis (type C)[381] 67

Scheme 31. Three-step synthesis of the AB-monomer **M1** bearing an isocyanide and a benzyl ester protected acid. 69

Scheme 32. General reaction scheme for the synthesis of sequence-defined linear precursors, which served as starting material for the synthesis of uniform macrocycles. The linear oligomers are formed in a two-step iterative cycle consisting of the P-3CR and a deprotection step. Cyclisation is performed via RCM after introduction of two terminal olefin functionalities. 70

Scheme 33. Two-step iterative reaction cycle for the synthesis of dual-sequence-defined macromolecules, which allows to control the backbone as well as the side chain at the same time. 82

Scheme 34. Three-step synthesis procedure for the synthesis of monomer **M2** consisting of the esterification, the N-formylation and a final dehydration step. The synthesis procedure was applied in the synthesis of monomers **M1** – **M8**. 84

Scheme 35. Four-step synthesis procedure for the synthesis of monomer **M9**, including the esterification with methanol to form the methyl ester and a transesterification as an additional third step. 86

Scheme 36. Synthesis of linker molecule **L1** containing an isocyanide and a diene moiety. In a first step, an esterification with methanol is carried out, followed by an N-formylation and the dehydration to form the isocyanide. The targeted compound **L1** is obtained via transesterification using sorbic alcohol. 104

Scheme 37. Synthesis of the linker molecule **L2** containing a TAD moiety as well as a carboxylic acid. 106

Scheme 38. Two-step iterative reaction cycle consisting of the P-3CR and the TAD Diels-Alder reaction, which was employed to synthesise sequence-defined macromolecules on solid phase and in solution. Box top left:

different side chains that were introduced to achieve sequence-definition, box top right: two different starting points for solid (resin) and solution phase (stearic acid **13**), respectively. 107

Scheme 39. The P-3CRs that were performed, employing the three aldehydes propanal **11a**, isobutyraldehyde **11c**, and cyclohexane carboxaldehyde **11b**, and screened by online IR in order to optimise the reaction conditions for further reactions. 108

Scheme 40. TAD Diels- Alder reaction using the linker molecule **L2**. In the first reaction cycle, ethyl side chains were introduced to the molecule via a P-3CR. 110

Scheme 41. Side reaction that occurred between the excess of TAD-COOH molecule **L2,** and the diene isocyanide linker molecule **L1,** leading to an undesired Passerini polymerisation with present aldehydes. SEC traces of the obtained P-3CR polymerisation products. The solution phase synthesis enabled successful identification of the side reaction allowing for further optimisation. 111

Scheme 42. Coupling of two sequence-defined nonamers **53** using bis-TAD **58** as a method for increasing the molecular weight of sequence-defined macromolecules. 114

8.1.3 Tables

Table 1. summary of the results of each reaction step during the synthesis of a linear precursor bearing terminal double bonds which is functionalised with cyclohexyl side chains. 74

Table 2. Summary of the results of the monomer syntheses of monomers **M1 – M9** with all their intermediates. 87

Table 3. Summary of the backbone-defined oligomer synthesis. 92

Table 4. Summary of the results obtained in the synthesis of dual sequence-defined macromolecules. The applied monomer and aldehyde component, as well as the yields, applied purification strategy and the calculated and found masses are given. 96

Table 5. Overview of the isolated yields and the exact masses obtained after each synthetic step in the synthesis of linker molecule **L1**. 103

Table 6. Summary of the results obtained after each synthetic step in the synthesis of the linker molecule **L2**. 105

Table 7. Condition screening for the coupling reaction of two monomers using bis-TAD. 115

Table 8. Direct comparison of the two synthesis techniques (i.e. solid phase and solution phase chemistries). 123

8.1.4 Figures and Tables of the experimental section

Figure S 1: SEC-ESI-MS results of a crude macrocycle. Top: SEC trace of the cyclic octamer **MO$_{8a}$** with ethyl side chains, showing different peaks, which were identified with the help of the MS spectrum (bottom). 207

Figure S 2. SEC-ESI-MS results of a crude macrocycle. Top: SEC trace of the cyclic octamer **MO$_{8b}$** with cyclohexyl side chains, showing different peaks, which were identified with the help of the MS spectrum (bottom). 208

Figure S 3. Characterization of the cyclic dimer **MO$_2$** by ESI-MS. Comparison of the calculated isotopic pattern (blue) with the measured one (black). 209

Figure S 4. ESI-MS spectrum of the crude reaction mixture after cyclization. The singly charged sodium cation of the macrocycle **MO$_2$** was observed. 209

Figure S 5. Characterization of the cyclic tetramer **MO$_{4a}$** with cyclohexyl side chains by ESI-MS. Comparison of the calculated isotopic pattern (blue) with the measured one (black). 210

Figure S 6.ESI-MS spectrum of the crude reaction mixture after cyclization. The singly and doubly charged sodium cations of the macrocycle **MO$_{4a}$** were observed. 210

Figure S 7. Characterization of the cyclic tetramer **MO$_{4b}$** with isopropyl side chains by ESI-MS. Comparison of the calculated isotopic pattern (blue) with the measured one (black). 211

Figure S 8.ESI-MS spectrum of the crude reaction mixture after cyclization. The singly and doubly charged sodium cations of the macrocycle **MO$_{4b}$** were observed. 211

Figure S 9. Characterization of the cyclic hexamer **MO$_{6a}$** with cyclohexyl side chains by ESI-MS. Comparison of the calculated isotopic pattern (blue) with the measured one (black). 212

Figure S 10. ESI-MS spectrum of the crude reaction mixture after cyclization. The singly and doubly charged sodium cations of the macrocycle **MO$_{6a}$** were observed. 212

Figure S 11. Characterization of the cyclic hexamer **MO$_{6b}$** with isopropyl side chains by ESI-MS. Comparison of the calculated isotopic pattern (blue) with the measured one (black). 213

Figure S 12.ESI-MS spectrum of the crude reaction mixture after cyclization. The singly and doubly charged sodium cations of the macrocycle **MO$_{6b}$** were observed. 213

Figure S 13. Characterization of the cyclic octamer **MO$_{8a}$** with ethyl side chains (C5 core unit) by ESI-MS. Comparison of the calculated isotopic pattern (blue) with the measured one (black). 214

Figure S 14.ESI-MS spectrum of the crude reaction mixture after cyclization. The singly and doubly charged sodium cations of the macrocycle **MO$_{8a}$** were observed. 214

Figure S 15. Characterization of the cyclic octamer **MO$_{8b}$** with cyclohexyl side chains (C5 core unit) by ESI-MS. Comparison of the calculated isotopic pattern (blue) with the measured one (black). 215

Figure S 16. ESI-MS spectrum of the crude reaction mixture after cyclization. The singly and doubly charged sodium cations of the macrocycle **MO$_{8b}$** were observed. 215

Figure S 17. Characterization of the cyclic octamer **MO$_{8c}$** with cyclohexyl side chains (C10 core unit) by ESI-MS. Comparison of the calculated isotopic pattern (blue) with the measured one (black). 216

Figure S 18.ESI-MS spectrum of the crude reaction mixture after cyclization. The doubly charged sodium cation of the macrocycle **MO$_{8c}$** was observed. 216

Figure S 19. Characterization of the cyclic octamer **MO$_{8d}$** with isopropyl side chains by ESI-MS. Comparison of the calculated isotopic pattern (blue) with the measured one (black). 217

Figure S 20. ESI-MS spectrum of the crude reaction mixture after cyclization. The singly and doubly charged sodium cations of the macrocycle **MO$_{8d}$** were observed. 217

Figure S 21 Characterization of the cyclic decamer **MO$_{10}$** with cyclohexyl side chains by ESI-MS. Comparison of the calculated isotopic pattern (blue) with the measured one (black). 218

Figure S 22. ESI-MS spectrum of the crude reaction mixture after cyclization. The singly doubly and triply charged sodium cations of the macrocycle **MO$_{10}$** were observed........218

Figure S 23. SEC results of linear oligomers with ethyl side chains and C5 core unit. 219

Figure S 24. SEC results of linear oligomers with cyclohexyl side chains and C5 core unit. 219

Figure S 25. SEC analysis of linear oligomers with cyclohexyl side chains and C10 core unit. 220

Figure S 26. SEC analysis of linear oligomers with isopropyl side chains and C10 core unit 220

Figure S 27. SEC analysis of linear oligomers with cyclohexyl side chains and terminal double bonds. 221

Figure S 28. SEC analysis of linear oligomers with isopropyl side chains and terminal double bonds. 221

Figure S 29. SEC analysis of crude macrocycle **MO$_{8b}$** carrying cyclohexyl side chains. 222

Figure S 30. SEC analysis of crude macrocycle **MO$_{8a}$** carrying ethyl side chains. 222

Figure S 31. SEC analysis of crude macrocycle **MO$_{8d}$** carrying isopropyl side chains. 223

Figure S 32. SEC analysis of crude macrocycles of different size with cyclohexyl side chains. 223

Figure S 33. SEC analysis of crude macrocycles of different size with isopropyl side chains. 224

Figure S 34. Molecular structure of tetramer **39** that was used for sequential read-out by tandem mass spectrometry. 323

Figure S 35. LC-MS chromatogram (λ = 214 nm) of the adduct formed when TAD-COOH reacted with the diene-functionalised resin. 341

Figure S 36. LC-MS chromatogram (λ = 214 nm) of the 1st P-3CR on the solid-phase. The reaction is observed to be already complete after 30 minutes, with the only two peaks at 4.9 and 7.3 minutes both corresponding to the desired product. The ionisation of the molecule during LC-MS accounts for the fragmentation pattern observed in the MS spectrum. 342

Figure S 37. LC-MS chromatograms (λ = 214 nm). A clear shift in the retention time between the carboxylic acid terminated chain and diene terminated chain can be seen. By following the same step in the cycle, one can also see a shift in retention time as the molecular weight increases. It should be noted that this does not continue in a liner fashion because from the 2nd to the 5th cycle, the solvent gradient (from acetonitrile to water) was 75-100%, and from the 6th to the 8th cycle it was 90-100%. The LC-MS gives little information after the 7th TAD-COOH addition. 343

Figure S 38. SEC-ESI-MS chromatogram and corresponding mass spectrum as well as isotopic pattern at 14.90 min retention time of the nonamer **65** synthesised on solid phase. 345

Figure S 39. SEC-ESI-MS chromatogram and corresponding mass spectrum as well as isotopic pattern at 13.91 min retention time of the dodecamer **52** synthesised on solid phase. 346

Figure S 40. SEC chromatogrm of the sequence-defined nonamer **53** prepared in solution and the corresponding ESI-MS spectrum at a retention time of 14.30 minutes. The doubly- (2670.97 m/z), triply- (1780.99 m/z) and quadruply (1335.86 m/z) charged cations were clearly observed. 381

Figure S 41. Left (black): The measured ESI-MS spectrum is shown. Right (blue): The isotope pattern was theoretically calculated with the program mMass. The measured isotope pattern is in very good agreement with the theoretical one for the assumed chemical formula. 382

Figure S 42. Online IR analysis of the P-3CR with stearic acid **13**, linker molecule **L1** and isobutyraldehyde **11c** depicting the decrease of the isocyanide peak at 2145.33 cm-1 with time. Reaching the plateau indicates full conversion, since **L1** was used in excess. The reaction is complete after 6h00min. 384

Figure S 43. Online IR analysis of the P-3CR with stearic acid **13**, linker molecule **L1** and cyclohexylaldehyde **11b** depicting the decrease of the isocyanide peak at 2145.33 cm-1 with time. Reaching the plateau indicates full conversion, since **L1** was used in excess. The reaction is complete after 4h30min. 384

Figure S 44. Online IR analysis of the P-3CR during the fifth reaction cycle depicting the decrease of isocyanide peak at 2145.33 cm-1 with time. Reaching the plateau indicates full conversion, since **L1** was used in excess. The reaction is complete after 14h45min. 385

Table S 1. List of the structures of all formed macrocycles. 203

Table S 2. ESI-MS fragments of tetramer **39** obtained by tandem ESI-MS read-out. 323

9 Appendix

9.1 Publications

[8] *^{1}H PFG-NMR Diffusion Study on a Sequence-Defined Macromolecule: Confirming Monodispersity*, X. Guo,‡ K. S. Wetzel,‡ S. C. Solleder, S. Spann, M. A. R. Meier, M. Wilhelm, B. Luy, G. Guthausen,* *Macromol. Chem. Phys.* **2019**, *220*, 1900155.

[7] *Monodisperse, Sequence-Defined Macromolecules as Tool to Evaluate the Limits of Ring-Closing Metathesis*, K. S. Wetzel, M. A. R. Meier,* *Polym. Chem*., **2019**, *10*, 2716-2722.

[6] *Direct Comparison of Solution and Solid Phase Synthesis of Sequence-Defined Macromolecules*, J. O. Holloway,‡ K. S. Wetzel,‡ S. Martens, F. E. Du Prez,* M. A. R. Meier,* *Polym. Chem.*, **2019**, *10*, 3859-3867.

[5] *A Combined Photochemical and Multicomponent Reaction Approach to Precision Oligomers*, W. Konrad, F. R. Bloesser, K. S. Wetzel, A. C. Boukis, M. A. R. Meier,* C. Barner-Kowollik,* *Chem. Eur. J.*, **2018**, *24*, 3413-3419.

[4] *An Update on Isocyanide-Based Multicomponent Reactions in Polymer Science*, A. Llevot, A. C. Boukis, S. Oelmann, K. S. Wetzel, M. A. R. Meier, In: B. Tang, R. Hu (eds) *Polymer Synthesis Based on Triple-bond Building Blocks. Topics in Current Chemistry Collections*. Springer, Cham, **2017**, 127-155.

[3] *Recent Progress in the Design of Monodisperse, Sequence-Defined Macromolecules*, S. C. Solleder, R. V. Schneider, K. S. Wetzel, A. C. Boukis, M. A. R. Meier,* *Macromol. Rapid Commun.* **2017**, *38,* 1600711.

[2] *A Scalable and High-Yield Strategy for the Synthesis of Sequence-Defined Macromolecules*, S. C. Solleder, D. Zengel, K. S. Wetzel, M. A. R. Meier,* *Angew. Chem. Int. Ed.* ***2016**, 55, 1204-1207.*

[1] *Dual Side Chain Control in the Synthesis of Novel Sequence-Defined Oligomers through the Ugi Four-Component Reaction*, S. C. Solleder, K. S. Wetzel, M. A. R. Meier,* *Polym. Chem*. **2015**, *6*, 3201-3204.

***** Corresponding author.

‡ These authors contributed equally to the work.

9.2 Conference contributions

[5] *Dual Sequence-control via the Passerini 3-Component Reactions*, Poster at the European Polymer Federation (EPF) Conference, June 9th – 14th, 2019, Heraklion (Crete), Greece.

[4] *Combining "Click" Chemistry and the Passerini 3-Component Reaction to obtain Sequence-defined Macromolecules*, Poster at the Meeting of the GDCh-Division together with SFB 1176, September 24th – 27th, 2018, Karlsruhe, Germany **(Poster Prize)**.

[3] *Monodisperse, Sequence-defined Macrocycles via Passerini 3-Component Reactions*, Poster at Bordeaux Polymer Conference (BPC), May 28th – 31th, 2018, Bordeaux, France **(Poster Prize)**.

[2] *Monodisperse, Sequence-defined Macrocycles via Multicomponent Reactions*, Poster at the Macromolecular Colloquium Freiburg, February 21st – 23rd, 2018, Freiburg, Germany.

[1] *Synthesis of Monodisperse, Sequence-defined Macrocycles*, Poster at the European Polymer Federation (EPF) Conference, July 2nd – 7th, 2017, Lyon, France.

10 Bibliography

[1] N. Badi, J.-F. Lutz, *Chem. Soc. Rev.* **2009**, *38*, 3383-3390.

[2] F. Crick, L. Barnett, S. Brenner, R. J. Watts-Tobin, **1961**.

[3] F. H. Crick, *J. Mol. Biol.* **1968**, *38*, 367-379.

[4] E. Fischer, *Berichte der deutschen chemischen Gesellschaft* **1894**, *27*, 3479-3483.

[5] J. D. Watson, F. H. Crick, *Nature* **1953**, *171*, 737-738.

[6] H. Staudinger, *Berichte der deutschen chemischen Gesellschaft (A and B Series)* **1926**, *59*, 3019-3043.

[7] M. Miyamoto, M. Sawamoto, T. Higashimura, *Macromolecules* **1984**, *17*, 265-268.

[8] K. Ziegler, *Angew. Chem.* **1936**, *49*, 499-502.

[9] M. Szwarc, M. Levy, R. Milkovich, *J. Am. Chem. Soc.* **1956**, *78*, 2656-2657.

[10] M. SZWARC, *Nature* **1956**, *178*, 1168.

[11] M. Kato, M. Kamigaito, M. Sawamoto, T. Higashimura, *Macromolecules* **1995**, *28*, 1721-1723.

[12] J.-S. Wang, K. Matyjaszewski, *J. Am. Chem. Soc.* **1995**, *117*, 5614-5615.

[13] G. Moad, E. Rizzardo, *Macromolecules* **1995**, *28*, 8722-8728.

[14] J. Chiefari, Y. Chong, F. Ercole, J. Krstina, J. Jeffery, T. P. Le, R. T. Mayadunne, G. F. Meijs, C. L. Moad, G. Moad, *Macromolecules* **1998**, *31*, 5559-5562.

[15] J.-F. Lutz, *Polym. Chem.* **2010**, *1*, 55-62.

[16] R. B. Merrifield, *J. Am. Chem. Soc.* **1963**, *85*, 2149-2154.

[17] R. B. Merrifield, *Angew. Chem. Int. Ed.* **1985**, *24*, 799-810.

[18] R. J. Simon, R. S. Kania, R. N. Zuckermann, V. D. Huebner, D. A. Jewell, S. Banville, S. Ng, L. Wang, S. Rosenberg, C. K. Marlowe, *Proceedings of the National Academy of Sciences* **1992**, *89*, 9367-9371.

[19] H. Herzner, T. Reipen, M. Schultz, H. Kunz, *Chem. Rev.* **2000**, *100*, 4495-4538.

[20] S. L. Beaucage, R. P. Iyer, *Tetrahedron* **1992**, *48*, 2223-2311.

[21] J. W. Grate, K. F. Mo, M. D. Daily, *Angew. Chem. Int. Ed.* **2016**, *55*, 3925-3930.

[22] A. Al Ouahabi, M. Kotera, L. Charles, J.-F. o. Lutz, *ACS Macro Lett.* **2015**, *4*, 1077-1080.

[23] S. Martens, J. Van den Begin, A. Madder, F. E. Du Prez, P. Espeel, *J. Am. Chem. Soc.* **2016**, *138*, 14182-14185.

[24] W. Konrad, C. Fengler, S. Putwa, C. Barner-Kowollik, *Angew. Chem. Int. Ed.* **2019**, *58*, 7133-7137.

[25] J. Barnes, D. Ehrlich, A. Gao, F. Leibfarth, Y. Jiang, E. Zhou, T. Jamison, J. Johnson, Chem, **2015**.

[26] X. Tong, B.-h. Guo, Y. Huang, *Chem. Commun.* **2011**, *47*, 1455-1457.

[27] S. C. Solleder, M. A. Meier, *Angew. Chem. Int. Ed.* **2014**, *53*, 711-714.

[28] J. J. Haven, J. A. De Neve, T. Junkers, *ACS Macro Lett.* **2017**, *6*, 743-747.

[29] S. Ida, T. Terashima, M. Ouchi, M. Sawamoto, *J. Am. Chem. Soc.* **2009**, *131*, 10808-10809.

[30] S. Ida, M. Ouchi, M. Sawamoto, *Macromol. Rapid Commun.* **2011**, *32*, 209-214.

[31] G. De Bo, S. Kuschel, D. A. Leigh, B. Lewandowski, M. Papmeyer, J. W. Ward, *J. Am. Chem. Soc.* **2014**, *136*, 5811-5814.

[32] B. Lewandowski, G. De Bo, J. W. Ward, M. Papmeyer, S. Kuschel, M. J. Aldegunde, P. M. Gramlich, D. Heckmann, S. M. Goldup, D. M. D'Souza, *Science* **2013**, *339*, 189-193.

[33] S. C. Solleder, K. S. Wetzel, M. A. Meier, *Polym. Chem.* **2015**, *6*, 3201-3204.

[34] S. C. Solleder, D. Zengel, K. S. Wetzel, M. A. Meier, *Angew. Chem. Int. Ed.* **2016**, *55*, 1204-1207.

[35] S. C. Solleder, S. Martens, P. Espeel, F. Du Prez, M. A. R. Meier, *Chem. Eur. J.* **2017**, *23*, 13906-13909.

[36] S. C. Solleder, R. V. Schneider, K. S. Wetzel, A. C. Boukis, M. A. Meier, *Macromol. Rapid Commun.* **2017**, *38*.

[37] M. Blawat, K. Gaedke, I. Huetter, X.-M. Chen, B. Turczyk, S. Inverso, B. W. Pruitt, G. M. Church, *Procedia Computer Science* **2016**, *80*, 1011-1022.

[38] A. C. Boukis, M. A. Meier, *Eur. Polym. J.* **2018**, *104*, 32-38.

[39] J.-F. Lutz, M. Ouchi, D. R. Liu, M. Sawamoto, *Science* **2013**, *341*.

[40] S. Martens, A. Landuyt, P. Espeel, B. Devreese, P. Dawyndt, F. Du Prez, *Nat. Commun.* **2018**, *9*, 4451.

[41] M. A. R. Meier, C. Barner-Kowollik, *Adv. Mater.* **2019**, *31*, 1806027.

[42] J.-F. Lutz, T. Y. Meyer, M. Ouchi, M. Sawamoto, *Sequence-controlled polymers: synthesis, self-assembly, and properties*, ACS Publications, **2014**.

[43] J.-F. Lutz, *ACS Macro Lett.* **2014**, *3*, 1020-1023.

[44] X.-X. Deng, L. Li, Z.-L. Li, A. Lv, F.-S. Du, Z.-C. Li, *ACS Macro Lett.* **2012**, *1*, 1300-1303.

[45] R. F. Stepto, *Pure Appl. Chem.* **2009**, *81*, 351-353.

[46] D. Moatsou, R. K. O'Reilly, *Chem* **2019**, *5*, 487-490.

[47] S. J. Rowan, C. Barner-Kowollik, B. Klumperman, P. Gaspard, R. B. Grubbs, M. A. Hillmyer, L. R. Hutchings, M. K. Mahanthappa, D. Moatsou, R. K. O'Reilly, ACS Publications, **2015**.

[48] T. Lodge, S. Rowan, ACS Publications, **2014**.

[49] A. D. Jenkins, P. Kratochvíl, R. F. T. Stepto, U. W. Suter, in *Pure Appl. Chem., Vol. 68*, **1996**, p. 2287.

[50] R. B. Merrifield, J. M. Stewart, N. Jernberg, *Anal. Chem.* **1966**, *38*, 1905-1914.

[51] M. Amblard, J.-A. Fehrentz, J. Martinez, G. Subra, *Mol. Biotechnol.* **2006**, *33*, 239-254.

[52] S.-S. Wang, *J. Am. Chem. Soc.* **1973**, *95*, 1328-1333.

[53] H. Rink, *Tetrahedron Lett.* **1987**, *28*, 3787-3790.

[54] R. N. Zuckermann, *Peptide Science* **2011**, *96*, 545-555.

[55] L. A. Carpino, G. Y. Han, *The Journal of organic chemistry* **1972**, *37*, 3404-3409.

[56] T. Shioiri, K. Ninomiya, S. Yamada, *J. Am. Chem. Soc.* **1972**, *94*, 6203-6205.

[57] T. Wieland, C. Birr, F. Flor, *Angew. Chem.* **1971**, *83*, 333-334.

[58] J. C. Sheehan, G. P. Hess, *J. Am. Chem. Soc.* **1955**, *77*, 1067-1068.

[59] J. Coste, D. Le-Nguyen, B. Castro, *Tetrahedron Lett.* **1990**, *31*, 205-208.

[60] V. Dourtoglou, J.-C. Ziegler, B. Gross, *Tetrahedron Lett.* **1978**, *19*, 1269-1272.

[61] R. Merrifield, in *Hypotensive Peptides*, Springer, **1966**, pp. 1-13.

[62] R. P. Cheng, S. H. Gellman, W. F. DeGrado, *Chem. Rev.* **2001**, *101*, 3219-3232.

[63] B. Marglin, R. Merrifield, *J. Am. Chem. Soc.* **1966**, *88*, 5051-5052.

[64] B. Gutte, R. Merrifield, *J. Biol. Chem.* **1971**, *246*, 1922-1941.

[65] E. Saxon, C. R. Bertozzi, *Science* **2000**, *287*, 2007-2010.

[66] B. L. Nilsson, L. L. Kiessling, R. T. Raines, *Org. Lett.* **2000**, *2*, 1939-1941.

[67] P. E. Dawson, S. B. Kent, *Annu. Rev. Biochem* **2000**, *69*, 923-960.

[68] M. Baca, T. W. Muir, M. Schnoelzer, S. B. Kent, *J. Am. Chem. Soc.* **1995**, *117*, 1881-1887.

[69] S.-Y. Chen, S. Cressman, F. Mao, H. Shao, D. W. Low, H. S. Beilan, E. N. Cagle, M. Carnevali, V. Gueriguian, P. J. Keogh, *Chem. Biol.* **2005**, *12*, 371-383.

[70] C. W. Wu, T. J. Sanborn, K. Huang, R. N. Zuckermann, A. E. Barron, *J. Am. Chem. Soc.* **2001**, *123*, 6778-6784.

[71] J. Seo, A. E. Barron, R. N. Zuckermann, *Org. Lett.* **2010**, *12*, 492-495.

[72] A. M. Rosales, R. A. Segalman, R. N. Zuckermann, *Soft Matter* **2013**, *9*, 8400-8414.

[73] R. N. Zuckermann, J. M. Kerr, S. B. Kent, W. H. Moos, *J. Am. Chem. Soc.* **1992**, *114*, 10646-10647.

[74] J. E. Murphy, T. Uno, J. D. Hamer, F. E. Cohen, V. Dwarki, R. N. Zuckermann, *Proceedings of the National Academy of Sciences* **1998**, *95*, 1517-1522.

[75] A. S. Culf, R. J. Ouellette, *Molecules* **2010**, *15*, 5282-5335.

[76] T. Uno, E. Beausoleil, R. A. Goldsmith, B. H. Levine, R. N. Zuckermann, *Tetrahedron Lett.* **1999**, *40*, 1475-1478.

[77] P. Armand, K. Kirshenbaum, R. A. Goldsmith, S. Farr-Jones, A. E. Barron, K. T. Truong, K. A. Dill, D. F. Mierke, F. E. Cohen, R. N. Zuckermann, *Proceedings of the National Academy of Sciences* **1998**, *95*, 4309-4314.

[78] K. Kirshenbaum, A. E. Barron, R. A. Goldsmith, P. Armand, E. K. Bradley, K. T. Truong, K. A. Dill, F. E. Cohen, R. N. Zuckermann, *Proceedings of the National Academy of Sciences* **1998**, *95*, 4303-4308.

[79] K. Huang, C. W. Wu, T. J. Sanborn, J. A. Patch, K. Kirshenbaum, R. N. Zuckermann, A. E. Barron, I. Radhakrishnan, *J. Am. Chem. Soc.* **2006**, *128*, 1733-1738.

[80] C. W. Wu, K. Kirshenbaum, T. J. Sanborn, J. A. Patch, K. Huang, K. A. Dill, R. N. Zuckermann, A. E. Barron, *J. Am. Chem. Soc.* **2003**, *125*, 13525-13530.

[81] B. C. Gorske, B. L. Bastian, G. D. Geske, H. E. Blackwell, *J. Am. Chem. Soc.* **2007**, *129*, 8928-8929.

[82] B. C. Gorske, J. R. Stringer, B. L. Bastian, S. A. Fowler, H. E. Blackwell, *J. Am. Chem. Soc.* **2009**, *131*, 16555-16567.

[83] J. R. Stringer, J. A. Crapster, I. A. Guzei, H. E. Blackwell, *J. Am. Chem. Soc.* **2011**, *133*, 15559-15567.

[84] K. T. Nam, S. A. Shelby, P. H. Choi, A. B. Marciel, R. Chen, L. Tan, T. K. Chu, R. A. Mesch, B.-C. Lee, M. D. Connolly, *Nature materials* **2010**, *9*, 454.

[85] R. L. Letsinger, V. Mahadevan, *J. Am. Chem. Soc.* **1965**, *87*, 3526-3527.

[86] M. H. Caruthers, *Science* **1985**, *230*, 281-285.

[87] N. Usman, R. T. Pon, K. K. Ogilvie, *Tetrahedron Lett.* **1985**, *26*, 4567-4570.

[88] N. Usman, K. Ogilvie, M. Jiang, R. Cedergren, *J. Am. Chem. Soc.* **1987**, *109*, 7845-7854.

[89] C. McCollum, A. Andrus, *Tetrahedron Lett.* **1991**, *32*, 4069-4072.

[90] J. Katzhendler, S. Cohen, E. Rahamim, M. Weisz, I. Ringel, J. Deutsch, *Tetrahedron* **1989**, *45*, 2777-2792.

[91] S. Beaucage, M. H. Caruthers, *Tetrahedron Lett.* **1981**, *22*, 1859-1862.

[92] V. T. Ravikumar, T. K. Wyrzykiewicz, D. L. Cole, *Tetrahedron* **1994**, *50*, 9255-9266.

[93] W. S. Marshall, R. J. Kaiser, *Curr. Opin. Chem. Biol.* **2004**, *8*, 222-229.

[94] S. Pitsch, P. A. Weiss, L. Jenny, A. Stutz, X. Wu, *Helv. Chim. Acta* **2001**, *84*, 3773-3795.

[95] D. Caine, J.-H. Fuhrhop, G. Penzlin, *J. Am. Chem. Soc.* **1994**, *116*, 12137-12137.

[96] H. Cramer, R. Rhea, J. Okicki, K. Yirava, R. Silverman, *Nucleosides, Nucleotides and Nucleic Acids* **2003**, *22*, 1733-1736.

[97] L. McBride, M. Caruthers, *Tetrahedron Lett.* **1983**, *24*, 245-248.

[98] N. Sinha, J. Biernat, J. McManus, H. Köster, *Nucleic Acids Res.* **1984**, *12*, 4539-4557.

[99] S. P. Adams, K. S. Kavka, E. J. Wykes, S. B. Holder, G. R. Galluppi, *J. Am. Chem. Soc.* **1983**, *105*, 661-663.

[100] C. B. Reese, *Organic & biomolecular chemistry* **2005**, *3*, 3851-3868.

[101] G. M. Church, Y. Gao, S. Kosuri, *Science* **2012**, *337*, 1628-1628.

[102] V. Zhirnov, R. M. Zadegan, G. S. Sandhu, G. M. Church, W. L. Hughes, *Nature materials* **2016**, *15*, 366.

[103] N. Goldman, P. Bertone, S. Chen, C. Dessimoz, E. M. LeProust, B. Sipos, E. Birney, *Nature* **2013**, *494*, 77.

[104] R. N. Grass, R. Heckel, M. Puddu, D. Paunescu, W. J. Stark, *Angew. Chem. Int. Ed.* **2015**, *54*, 2552-2555.

[105] J. Bornholt, R. Lopez, D. M. Carmean, L. Ceze, G. Seelig, K. Strauss, *ACM SIGARCH Computer Architecture News* **2016**, *44*, 637-649.

[106] Y. Erlich, D. Zielinski, *Science* **2017**, *355*, 950-954.

[107] Z. Wan, Y. Li, S. Bo, M. Gao, X. Wang, K. Zeng, X. Tao, X. Li, Z. Yang, Z.-X. Jiang, *Organic & biomolecular chemistry* **2016**, *14*, 7912-7919.

[108] T. G. Edwardson, K. M. Carneiro, C. J. Serpell, H. F. Sleiman, *Angew. Chem. Int. Ed.* **2014**, *53*, 4567-4571.

[109] R. Häner, F. Garo, D. Wenger, V. L. Malinovskii, *J. Am. Chem. Soc.* **2010**, *132*, 7466-7471.

[110] R. Noir, M. Kotera, B. Pons, J.-S. Remy, J.-P. Behr, *J. Am. Chem. Soc.* **2008**, *130*, 13500-13505.

[111] M. Dubber, J. M. Fréchet, *Bioconjugate Chem.* **2003**, *14*, 239-246.

[112] C. J. Serpell, T. G. Edwardson, P. Chidchob, K. M. Carneiro, H. F. Sleiman, *J. Am. Chem. Soc.* **2014**, *136*, 15767-15774.

[113] D. de Rochambeau, M. Barłóg, T. G. Edwardson, J. J. Fakhoury, R. S. Stein, H. S. Bazzi, H. F. Sleiman, *Polym. Chem.* **2016**, *7*, 4998-5003.

[114] A. Al Ouahabi, L. Charles, J.-F. o. Lutz, *J. Am. Chem. Soc.* **2015**, *137*, 5629-5635.

[115] L. Charles, C. Laure, J. F. Lutz, R. K. Roy, *Rapid Commun. Mass Spectrom.* **2016**, *30*, 22-28.

[116] A. Al Ouahabi, J.-A. Amalian, L. Charles, J.-F. Lutz, *Nat. Commun.* **2017**, *8*, 967.

[117] H. Mutlu, J. F. Lutz, *Angew. Chem. Int. Ed.* **2014**, *53*, 13010-13019.

[118] J.-A. Amalian, A. Al Ouahabi, G. Cavallo, N. F. König, S. Poyer, J.-F. Lutz, L. Charles, *J. Mass Spectrom.* **2017**, *52*, 788-798.

[119] G. Cavallo, A. Al Ouahabi, L. Oswald, L. Charles, J.-F. Lutz, *J. Am. Chem. Soc.* **2016**, *138*, 9417-9420.

[120] U. S. Gunay, B. E. Petit, D. Karamessini, A. Al Ouahabi, J.-A. Amalian, C. Chendo, M. Bouquey, D. Gigmes, L. Charles, J.-F. Lutz, *Chem* **2016**, *1*, 114-126.

[121] J.-A. Amalian, S. Poyer, B. E. Petit, S. Telitel, V. Monnier, D. Karamessini, D. Gigmes, J.-F. Lutz, L. Charles, *Int. J. Mass spectrom.* **2017**, *421*, 271-278.

[122] D. Karamessini, S. Poyer, L. Charles, J. F. Lutz, *Macromol. Rapid Commun.* **2017**, *38*, 1700426.

[123] D. Karamessini, T. Simon-Yarza, S. Poyer, E. Konishcheva, L. Charles, D. Letourneur, J. F. Lutz, *Angew. Chem. Int. Ed.* **2018**, *57*, 10574-10578.

[124] R. K. Roy, A. Meszynska, C. Laure, L. Charles, C. Verchin, J.-F. Lutz, *Nat. Commun.* **2015**, *6*, 7237.

[125] L. Charles, C. Laure, J.-F. o. Lutz, R. K. Roy, *Macromolecules* **2015**, *48*, 4319-4328.

[126] L. Charles, G. Cavallo, V. Monnier, L. Oswald, R. Szweda, J.-F. Lutz, *J. Am. Soc. Mass. Spectrom.* **2017**, *28*, 1149-1159.

[127] A. Burel, C. Carapito, J.-F. o. Lutz, L. Charles, *Macromolecules* **2017**, *50*, 8290-8296.

[128] R. Szweda, M. Tschopp, O. Felix, G. Decher, J. F. Lutz, *Angew. Chem.* **2018**, *130*, 16043-16047.

[129] P. Espeel, L. L. Carrette, K. Bury, S. Capenberghs, J. C. Martins, F. E. Du Prez, A. Madder, *Angew. Chem. Int. Ed.* **2013**, *52*, 13261-13264.

[130] J. O. Holloway, S. Aksakal, F. E. Du Prez, C. R. Becer, *Macromol. Rapid Commun.* **2017**, *38*, 1700500.

[131] S. Celasun, F. E. Du Prez, H. G. Börner, *Macromol. Rapid Commun.* **2017**, *38*, 1700688.

[132] S. Celasun, D. Remmler, T. Schwaar, M. G. Weller, F. Du Prez, H. G. Börner, *Angew. Chem. Int. Ed.* **2019**, *58*, 1960-1964.

[133] K. B. Sharpless, H. Kolb, M. Finn, *Angew Chem Int Ed* **2001**, *40*, 2004-2021.

[134] N. Zydziak, F. Feist, B. Huber, J. O. Mueller, C. Barner-Kowollik, *Chem. Commun.* **2015**, *51*, 1799-1802.

[135] K. Takizawa, H. Nulwala, J. Hu, K. Yoshinaga, C. J. Hawker, *J. Polym. Sci., Part A: Polym. Chem.* **2008**, *46*, 5977-5990.

[136] J. Vandenbergh, G. Reekmans, P. Adriaensens, T. Junkers, *Chemical Science* **2015**, *6*, 5753-5761.

[137] J. Vandenbergh, G. Reekmans, P. Adriaensens, T. Junkers, *Chem. Commun.* **2013**, *49*, 10358-10360.

[138] S. Binauld, D. Damiron, L. A. Connal, C. J. Hawker, E. Drockenmuller, *Macromol. Rapid Commun.* **2011**, *32*, 147-168.

[139] O. I. Paynter, D. J. Simmonds, M. C. Whiting, *J. Chem. Soc., Chem. Commun.* **1982**, 1165-1166.

[140] I. Bidd, M. C. Whiting, *J. Chem. Soc., Chem. Commun.* **1985**, 543-544.

[141] K. Takizawa, C. Tang, C. J. Hawker, *J. Am. Chem. Soc.* **2008**, *130*, 1718-1726.

[142] F. A. Loiseau, K. K. Hii, A. M. Hill, *The Journal of organic chemistry* **2004**, *69*, 639-647.

[143] A. C. French, A. L. Thompson, B. G. Davis, *Angew. Chem.* **2009**, *121*, 1274-1278.

[144] C. J. Burns, L. D. Field, K. Hashimoto, B. J. Petteys, D. D. Ridley, K. S. Sandanayake, *Synth. Commun.* **1999**, *29*, 2337-2347.

[145] F. M. Veronese, G. Pasut, *Drug Discovery Today* **2005**, *10*, 1451-1458.

[146] F. A. Leibfarth, J. A. Johnson, T. F. Jamison, *Proceedings of the National Academy of Sciences* **2015**, *112*, 10617-10622.

[147] J. C. Barnes, D. J. Ehrlich, A. X. Gao, F. A. Leibfarth, Y. Jiang, E. Zhou, T. F. Jamison, J. A. Johnson, *Nature chemistry* **2015**, *7*, 810-815.

[148] E. M. Keegstra, J. W. Zwikker, M. R. Roest, L. W. Jenneskens, *The Journal of organic chemistry* **1992**, *57*, 6678-6680.

[149] D. Niculescu-Duvaz, J. Getaz, C. J. Springer, *Bioconjugate Chem.* **2008**, *19*, 973-981.

[150] S. A. Ahmed, M. Tanaka, *The Journal of organic chemistry* **2006**, *71*, 9884-9886.

[151] Y. Li, X. Qiu, Z.-X. Jiang, *Organic Process Research & Development* **2015**, *19*, 800-805.

[152] H. Zhang, X. Li, Q. Shi, Y. Li, G. Xia, L. Chen, Z. Yang, Z. X. Jiang, *Angew. Chem. Int. Ed.* **2015**, *54*, 3763-3767.

[153] N. Zydziak, W. Konrad, F. Feist, S. Afonin, S. Weidner, C. Barner-Kowollik, *Nat. Commun.* **2016**, *7*, 13672.

[154] W. Konrad, F. R. Bloesser, K. S. Wetzel, A. C. Boukis, M. A. Meier, C. Barner-Kowollik, *Chemistry–A European Journal* **2018**, *24*, 3413-3419.

[155] B. Quiclet-Sire, G. Revol, S. Z. Zard, *Tetrahedron* **2010**, *66*, 6656-6666.

[156] S. Houshyar, D. J. Keddie, G. Moad, R. J. Mulder, S. Saubern, J. Tsanaktsidis, *Polym. Chem.* **2012**, *3*, 1879-1889.

[157] K. Satoh, S. Ozawa, M. Mizutani, K. Nagai, M. Kamigaito, *Nat. Commun.* **2010**, *1*, 6.

[158] D. Oh, M. Ouchi, T. Nakanishi, H. Ono, M. Sawamoto, *ACS Macro Lett.* **2016**, *5*, 745-749.

[159] J. Xu, S. Shanmugam, C. Fu, K.-F. Aguey-Zinsou, C. Boyer, *J. Am. Chem. Soc.* **2016**, *138*, 3094-3106.

[160] G. Székely, M. Schaepertoens, P. R. Gaffney, A. G. Livingston, *Polym. Chem.* **2014**, *5*, 694-697.

[161] G. Székely, M. Schaepertoens, P. R. J. Gaffney, A. G. Livingston, *Chem. Eur. J.* **2014**, *20*, 10038-10051.

[162] Y. Hibi, M. Ouchi, M. Sawamoto, *Nat. Commun.* **2016**, *7*.

[163] J. O. Holloway, K. S. Wetzel, S. Martens, F. E. Du Prez, M. A. R. Meier, *Polym. Chem.* **2019**, *10*, 3859-3867.

[164] A. C. Boukis, K. Reiter, M. Frölich, D. Hofheinz, M. A. Meier, *Nat. Commun.* **2018**, *9*, 1439.

[165] M. Frölich, M. A. Meier, *Nachrichten aus der Chemie* **2019**, *67*, 45-46.

[166] W. Zhang, D. P. Curran, *Tetrahedron* **2006**, *62*, 11837.

[167] H. Jian, J. M. Tour, *The Journal of organic chemistry* **2005**, *70*, 3396-3424.

[168] M. Porel, C. A. Alabi, *J. Am. Chem. Soc.* **2014**, *136*, 13162-13165.

[169] Y. Li, Q. Guo, X. Li, H. Zhang, F. Yu, W. Yu, G. Xia, M. Fu, Z. Yang, Z.-X. Jiang, *Tetrahedron Lett.* **2014**, *55*, 2110-2113.

[170] T. J. Dickerson, N. N. Reed, K. D. Janda, *Chem. Rev.* **2002**, *102*, 3325-3344.

[171] T. T. Trinh, L. Oswald, D. Chan-Seng, L. Charles, J. F. Lutz, *Chemistry–A European Journal* **2015**, *21*, 11961-11965.

[172] M. Landa, M. Kotera, J.-S. Remy, N. Badi, *Eur. Polym. J.* **2016**, *84*, 338-344.

[173] D. M. Rosenbaum, D. R. Liu, *J. Am. Chem. Soc.* **2003**, *125*, 13924-13925.

[174] M. L. McKee, P. J. Milnes, J. Bath, E. Stulz, A. J. Turberfield, R. K. O'Reilly, *Angew. Chem. Int. Ed.* **2010**, *49*, 7948-7951.

[175] R. E. Kleiner, Y. Brudno, M. E. Birnbaum, D. R. Liu, *J. Am. Chem. Soc.* **2008**, *130*, 4646-4659.

[176] Z. J. Gartner, D. R. Liu, *J. Am. Chem. Soc.* **2001**, *123*, 6961-6963.

[177] X. Li, D. R. Liu, *Angew. Chem. Int. Ed.* **2004**, *43*, 4848-4870.

[178] R. Naylor, P. Gilham, *Biochemistry* **1966**, *5*, 2722-2728.

[179] C. Böhler, P. E. Nielsen, L. E. Orgel, *Nature* **1995**, *376*, 578.

[180] J. Niu, R. Hili, D. R. Liu, *Nature Chemistry* **2013**, *5*, 282.

[181] S. Ida, M. Ouchi, M. Sawamoto, *J. Am. Chem. Soc.* **2010**, *132*, 14748-14750.

[182] Y. Hibi, M. Ouchi, M. Sawamoto, *Angew. Chem. Int. Ed.* **2011**, *50*, 7434-7437.

[183] C. O. Dietrich-Buchecker, J. Sauvage, J. Kintzinger, *Tetrahedron Lett.* **1983**, *24*, 5095-5098.

[184] P. L. Anelli, N. Spencer, J. F. Stoddart, *J. Am. Chem. Soc.* **1991**, *113*, 5131-5133.

[185] N. Koumura, E. M. Geertsema, M. B. van Gelder, A. Meetsma, B. L. Feringa, *J. Am. Chem. Soc.* **2002**, *124*, 5037-5051.

[186] J. Sauvage, S. J. F. Stoddart, B. Feringa, *Swedish Academy of Sciences, Stockholm* **2016**.

[187] A. Dömling, I. Ugi, *Angew. Chem. Int. Ed.* **2000**, *39*, 3168-3210.

[188] A. Dömling, *Chem. Rev.* **2006**, *106*, 17-89.

[189] K. S. W. J. O. Holloway, S. Martens, F. E. Du Prez, M. A. R. Meier, *submitted*.

[190] P. Wender, S. Handy, D. Wright, **1997**.

[191] A. Strecker, *Justus Liebigs Annalen der Chemie* **1850**, *75*, 27-45.

[192] J. Wang, X. Liu, X. Feng, *Chem. Rev.* **2011**, *111*, 6947-6983.

[193] S. J. Zuend, M. P. Coughlin, M. P. Lalonde, E. N. Jacobsen, *Nature* **2009**, *461*, 968.

[194] A. Hantzsch, *Justus Liebigs Annalen der Chemie* **1882**, *215*, 1-82.

[195] A. Hantzsch, *Berichte der deutschen chemischen Gesellschaft* **1890**, *23*, 1474-1476.

[196] P. Biginelli, *Berichte der deutschen chemischen Gesellschaft* **1891**, *24*, 1317-1319.

[197] C. Mannich, W. Krösche, *Arch. Pharm.* **1912**, *250*, 647-667.

[198] A. Castro, *Nature* **1967**, *213*, 903.

[199] A. Fürstner, *Angew. Chem. Int. Ed.* **2003**, *42*, 3582-3603.

[200] J. S. Sandhu, *ARKIVOC: Online Journal of Organic Chemistry* **2012**.

[201] G. C. Rovnyak, K. S. Atwal, A. Hedberg, S. D. Kimball, S. Moreland, J. Z. Gougoutas, B. C. O'Reilly, J. Schwartz, M. F. Malley, *J. Med. Chem.* **1992**, *35*, 3254-3263.

[202] R. Robinson, *Journal of the Chemical Society, Transactions* **1917**, *111*, 762-768.

[203] O. Geis, H. G. Schmalz, *Angew. Chem. Int. Ed.* **1998**, *37*, 911-914.

[204] P. Pauson, I. Khand, *Ann. N.Y. Acad. Sci.* **1977**, *295*, 2-14.

[205] P. L. Pauson, *Tetrahedron* **1985**, *41*, 5855-5860.

[206] B. Cornils, W. A. Herrmann, M. Rasch, *Angewandte Chemie International Edition in English* **1994**, *33*, 2144-2163.

[207] N. Chatani, M. Oshita, M. Tobisu, Y. Ishii, S. Murai, *J. Am. Chem. Soc.* **2003**, *125*, 7812-7813.

[208] S. Marcaccini, T. Torroba, *Org. Prep. Proced. Int.* **1993**, *25*, 141-208.

[209] R. Schröder, U. Schöllkopf, E. Blume, I. Hoppe, *Justus Liebigs Annalen der Chemie* **1975**, *1975*, 533-546.

[210] A. M. VANLEUSEN, J. Wildeman, O. Oldenziel, *J. Org. Chem.* **1977**, *42*, 1153-1159.

[211] D. van Leusen, A. M. van Leusen, *Synthesis* **1991**, *1991*, 531-532.

[212] T. J. Deming, B. M. Novak, *J. Am. Chem. Soc.* **1992**, *114*, 7926-7927.

[213] F. Millich, *Chem. Rev.* **1972**, *72*, 101-113.

[214] W. Lieke, *Justus Liebigs Annalen der Chemie* **1859**, *112*, 316-321.

[215] M. S. Edenborough, R. B. Herbert, *Natural product reports* **1988**, *5*, 229-245.

[216] P. J. Scheuer, *Acc. Chem. Res.* **1992**, *25*, 433-439.

[217] W. Rothe, *Pharmazie* **1950**, *5*, 190.

[218] H. Miyaoka, H. Shida, N. Yamada, H. Mitome, Y. Yamada, *Tetrahedron Lett.* **2002**, *43*, 2227-2230.

[219] A. Gautier, *Justus Liebigs Annalen der Chemie* **1868**, *146*, 119-124.

[220] A. W. Hofmann, *Justus Liebigs Annalen der Chemie* **1867**, *144*, 114-120.

[221] I. Ugi, R. Meyr, *Angew. Chem.* **1958**, *70*, 702-703.

[222] I. Ugi, U. Fetzer, U. Eholzer, H. Knupfer, K. Offermann, *Angew. Chem.* **1965**, *77*, 492-504.

[223] H. Eckert, B. Forster, *Angewandte Chemie International Edition in English* **1987**, *26*, 894-895.

[224] I. Ugi, *Agnew. Chem. Int. Ed. Engl* **1977**, *16*, 259-260.

[225] C. G. Neochoritis, T. Zarganes-Tzitzikas, S. Stotani, A. Dömling, E. Herdtweck, K. Khoury, A. Dömling, *ACS combinatorial science* **2015**, *17*, 493-499.

[226] C. G. Neochoritis, S. Stotani, B. Mishra, A. Dömling, *Org. Lett.* **2015**, *17*, 2002-2005.

[227] M. Passerini, L. Simone, *Gazz. Chim. Ital* **1921**, *51*, 126-129.

[228] I. Ugi, R. Meyr, C. Steinbruckner, *Angew Chem* **1959**, *71*, 373-388.

[229] I. Ugi, C. Steinbrückner, *Angew. Chem.* **1960**, *72*, 267-268.

[230] N. Chéron, R. Ramozzi, L. E. Kaïm, L. Grimaud, P. Fleurat-Lessard, *The Journal of organic chemistry* **2012**, *77*, 1361-1366.

[231] J. Zhu, H. Bienaymé, *Multicomponent reactions*, John Wiley & Sons, **2006**.

[232] I. Ugi, R. Meyr, *Chem. Ber.* **1961**, *94*, 2229-2233.

[233] R. H. Baker, D. Stanonis, *J. Am. Chem. Soc.* **1951**, *73*, 699-702.

[234] I. Hagedorn, U. Eholzer, *Chem. Ber.* **1965**, *98*, 936-940.

[235] M. C. Pirrung, K. D. Sarma, *J. Am. Chem. Soc.* **2004**, *126*, 444-445.

[236] I. Ugi, *Angewandte Chemie International Edition in English* **1962**, *1*, 8-21.

[237] S. Maeda, S. Komagawa, M. Uchiyama, K. Morokuma, *Angew. Chem. Int. Ed.* **2011**, *50*, 644-649.

[238] R. Ramozzi, K. Morokuma, *The Journal of organic chemistry* **2015**, *80*, 5652-5657.

[239] U. Fetzer, I. Ugi, *Justus Liebigs Annalen der Chemie* **1962**, *659*, 184-189.

[240] X.-h. Cai, H. Guo, B. Xie, *International Journal of Chemistry* **2011**, *3*, 216.

[241] H. Yanai, T. Oguchi, T. Taguchi, *The Journal of organic chemistry* **2009**, *74*, 3927-3929.

[242] L. Lyu, H. Xie, H. Mu, Q. He, Z. Bian, J. Wang, *Organic Chemistry Frontiers* **2015**, *2*, 815-818.

[243] L. El Kaim, M. Gizolme, L. Grimaud, *Org. Lett.* **2006**, *8*, 5021-5023.

[244] E. Martinand-Lurin, A. Dos Santos, L. El Kaim, L. Grimaud, P. Retailleau, *Chem. Commun.* **2014**, *50*, 2214-2217.

[245] J. E. Semple, T. D. Owens, K. Nguyen, O. E. Levy, *Org. Lett.* **2000**, *2*, 2769-2772.

[246] T. Soeta, Y. Kojima, Y. Ukaji, K. Inomata, *Tetrahedron Lett.* **2011**, *52*, 2557-2559.

[247] T. Ngouansavanh, J. Zhu, *Angew. Chem. Int. Ed.* **2006**, *45*, 3495-3497.

[248] T. Nixey, C. Hulme, *Tetrahedron Lett.* **2002**, *43*, 6833-6835.

[249] T. Yue, M. X. Wang, D. X. Wang, J. Zhu, *Angew. Chem. Int. Ed.* **2008**, *47*, 9454-9457.

[250] U. Kusebauch, B. Beck, K. Messer, E. Herdtweck, A. Dömling, *Org. Lett.* **2003**, *5*, 4021-4024.

[251] H. Bock, I. Ugi, *Journal für Praktische Chemie/Chemiker-Zeitung* **1997**, *339*, 385-389.

[252] R. Frey, S. G. Galbraith, S. Guelfi, C. Lamberth, M. Zeller, *Synlett* **2003**, *2003*, 1536-1538.

[253] L. Banfi, G. Guanti, R. Riva, *Chem. Commun.* **2000**, 985-986.

[254] I. Ugi, K. Rosendahl, *Chem. Ber.* **1961**, *94*, 2233-2238.

[255] R. Neidlein, *Zeitschrift für Naturforschung B* **1964**, *19*, 1159-1160.

[256] O. Kreye, B. Westermann, L. A. Wessjohann, *Synlett* **2007**, *2007*, 3188-3192.

[257] C. B. Gilley, M. J. Buller, Y. Kobayashi, *Org. Lett.* **2007**, *9*, 3631-3634.

[258] C. B. Gilley, Y. Kobayashi, *The Journal of organic chemistry* **2008**, *73*, 4198-4204.

[259] T. Lindhorst, H. Bock, I. Ugi, *Tetrahedron* **1999**, *55*, 7411-7420.

[260] O. Kreye, C. Trefzger, A. Sehlinger, M. A. Meier, *Macromol. Chem. Phys.* **2014**, *215*, 2207-2220.

[261] M. Passerini, *Gazz. Chim. Ital* **1923**, *53*, 331-333.

[262] L.-J. Zhang, X.-X. Deng, F.-S. Du, Z.-C. Li, *Macromolecules* **2013**, *46*, 9554-9562.

[263] N. Kolb, M. A. Meier, *Eur. Polym. J.* **2013**, *49*, 843-852.

[264] R. Kakuchi, P. Theato, *ACS Macro Lett.* **2014**, *3*, 329-332.

[265] C. Zhu, B. Yang, Y. Zhao, C. Fu, L. Tao, Y. Wei, *Polym. Chem.* **2013**, *4*, 5395-5400.

[266] M. Rubinshtein, C. R. James, J. L. Young, Y. J. Ma, Y. Kobayashi, N. C. Gianneschi, J. Yang, *Org. Lett.* **2010**, *12*, 3560-3563.

[267] O. Kreye, T. Tóth, M. A. Meier, *J. Am. Chem. Soc.* **2011**, *133*, 1790-1792.

[268] O. Kreye, O. Türünç, A. Sehlinger, J. Rackwitz, M. A. Meier, *Chemistry–A European Journal* **2012**, *18*, 5767-5776.

[269] L. M. de Espinosa, M. A. Meier, *Chem. Commun.* **2011**, *47*, 1908-1910.

[270] A. Sehlinger, L. M. de Espinosa, M. A. Meier, *Macromol. Chem. Phys.* **2013**, *214*, 2821-2828.

[271] A. Sehlinger, O. Kreye, M. A. Meier, *Macromolecules* **2013**, *46*, 6031-6037.

[272] A. Sehlinger, K. Ochsenreither, N. Bartnick, M. A. Meier, *Eur. Polym. J.* **2015**, *65*, 313-324.

[273] G.-m. Wu, W.-l. Sun, Z.-q. Shen, *Chin. J. Polym. Sci.* **2009**, *27*, 293-296.

[274] H. Wu, C. Fu, Y. Zhao, B. Yang, Y. Wei, Z. Wang, L. Tao, *ACS Macro Lett.* **2015**, *4*, 1189-1193.

[275] A. Sehlinger, P.-K. Dannecker, O. Kreye, M. A. Meier, *Macromolecules* **2014**, *47*, 2774-2783.

[276] Y.-Z. Wang, X.-X. Deng, L. Li, Z.-L. Li, F.-S. Du, Z.-C. Li, *Polym. Chem.* **2013**, *4*, 444-448.

[277] A. Sehlinger, R. Schneider, M. A. Meier, *Eur. Polym. J.* **2014**, *50*, 150-157.

[278] A. Lv, X.-X. Deng, L. Li, Z.-L. Li, Y.-Z. Wang, F.-S. Du, Z.-C. Li, *Polym. Chem.* **2013**, *4*, 3659-3662.

[279] S. Oelmann, S. Solleder, M. Meier, *Polym. Chem.* **2016**, *7*, 1857-1860.

[280] A. C. Boukis, A. Llevot, M. A. Meier, *Macromol. Rapid Commun.* **2016**, *37*, 643-649.

[281] S. Martens, J. O. Holloway, F. E. Du Prez, *Macromol. Rapid Commun.* **2017**, *38*, 1700469.

[282] K. De Bruycker, S. Billiet, H. A. Houck, S. Chattopadhyay, J. M. Winne, F. E. Du Prez, *Chem. Rev.* **2016**, *116*, 3919-3974.

[283] S. Billiet, K. De Bruycker, F. Driessen, H. Goossens, V. Van Speybroeck, J. M. Winne, F. E. Du Prez, *Nature Chemistry* **2014**, *6*, 815.

[284] J. Thiele, O. Stange, *Justus Liebigs Annalen der Chemie* **1894**, *283*, 1-46.

[285] A. Pinner, *Berichte der deutschen chemischen Gesellschaft* **1887**, *20*, 2358-2360.

[286] R. Stollé, *Berichte der deutschen chemischen Gesellschaft* **1912**, *45*, 273-289.

[287] J. E. Herweh, R. M. Fantazier, *Tetrahedron Lett.* **1973**, *14*, 2101-2104.

[288] R. Cookson, S. Gilani, I. Stevens, *Tetrahedron Lett.* **1962**, *3*, 615-618.

[289] J. Sauer, B. Schröder, *Chem. Ber.* **1967**, *100*, 678-684.

[290] R. Cookson, S. Gilani, I. Stevens, *Journal of the Chemical Society C: Organic* **1967**, 1905-1909.

[291] V. D. Kiselev, D. A. Kornilov, I. I. Lekomtseva, A. I. Konovalov, *Int. J. Chem. Kinet.* **2015**, *47*, 289-301.

[292] G. Zinner, W. Deucker, *Arch. Pharm.* **1961**, *294*, 370-372.

[293] R. Cookson, S. Gupte, I. Stevens, *Synth* **1971**, *51*, 121-127.

[294] G. W. Breton, M. Turlington, *Tetrahedron Lett.* **2014**, *55*, 4661-4663.

[295] S. Ogawa, S. Ooki, M. Morohashi, K. Yamagata, T. Higashi, *Rapid Commun. Mass Spectrom.* **2013**, *27*, 2453-2460.

[296] K. Shimada, T. Oe, T. Mizuguchi, *Analyst* **1991**, *116*, 1393-1397.

[297] T. Little, J. Meara, F. Ruan, M. Nguyen, M. Qabar, *Synth. Commun.* **2002**, *32*, 1741-1749.

[298] T. Curtius, *Berichte der deutschen chemischen Gesellschaft* **1890**, *23*, 3023-3033.

[299] T. Curtius, *Journal für Praktische Chemie* **1894**, *50*, 275-294.

[300] T. Curtius, K. Heidenreich, *Berichte der deutschen chemischen Gesellschaft* **1894**, *27*, 773-774.

[301] J. M. Gardlik, L. A. Paquette, *Tetrahedron Lett.* **1979**, *20*, 3597-3600.

[302] L. A. Paquette, R. F. Doehner Jr, *The Journal of organic chemistry* **1980**, *45*, 5105-5113.

[303] S. Mallakpour, Z. Rafiee, *Synth. Commun.* **2007**, *37*, 1927-1934.

[304] L. Vlaminck, B. Van de Voorde, F. E. Du Prez, *Green Chemistry* **2017**, *19*, 5659-5664.

[305] U. Seidel, J. Hellman, D. Schollmeyer, C. Hilger, R. Stadler, *Supramol. Sci.* **1995**, *2*, 45-50.

[306] G. Read, N. R. Richardson, *J. Chem. Soc., Perkin Trans. 1* **1996**, 167-174.

[307] M. Furdik, S. Mikulase, M. Livar, S. Priehrad, *Chem. Zvesti* **1967**, *21*, 427-442.

[308] J. Stickler, W. Pirkle, *The Journal of organic chemistry* **1966**, *31*, 3444-3445.

[309] M. Thiemann, E. Scheibler, K. W. Wiegand, *Ullmann's encyclopedia of industrial chemistry* **2000**.

[310] S. E. Mallakpour, *J. Chem. Educ.* **1992**, *69*, 238.

[311] M. A. Zolfigol, M. H. Zebarjadian, G. Chehardoli, S. E. Mallakpour, M. Shamsipur, *Tetrahedron* **2001**, *57*, 1627-1629.

[312] G. Chehardoli, M. A. Zolfigol, E. Ghaemi, E. Madrakian, K. Niknam, S. Mallakpour, *J. Heterocycl. Chem.* **2012**, *49*, 596-599.

[313] M. A. Zolfigol, E. Ghaemi, E. Madrakian, K. Niknam, *J. Chin. Chem. Soc.* **2008**, *55*, 704-711.

[314] M. A. Zolfigol, G. Chehardoli, E. Ghaemi, E. Madrakian, R. Zare, T. Azadbakht, K. Niknam, S. Mallakpour, *Monatshefte für Chemie-Chemical Monthly* **2008**, *139*, 261-265.

[315] H. Wamhoff, K. Wald, *Org. Prep. Proced. Int.* **1975**, *7*, 251-253.

[316] H. Bock, G. Rudolph, E. Baltin, *Chem. Ber.* **1965**, *98*, 2054-2055.

[317] L. Xiao, Y. Chen, K. Zhang, *Macromolecules* **2016**, *49*, 4452-4461.

[318] S. Vandewalle, S. Billiet, F. Driessen, F. E. Du Prez, *ACS Macro Lett.* **2016**, *5*, 766-771.

[319] M. A. Zolfigol, E. Madrakian, E. Ghaemi, S. Mallakpour, *Synlett* **2002**, *2002*, 1633-1636.

[320] J. M. Ravasco, H. Faustino, A. Trindade, P. M. Gois, *Chemistry–A European Journal* **2019**, *25*, 43-59.

[321] V. D. Kiselev, D. A. Kornilov, A. I. Konovalov, *Int. J. Chem. Kinet.* **2017**, *49*, 562-575.

[322] D. A. Singleton, C. Hang, *J. Am. Chem. Soc.* **1999**, *121*, 11885-11893.

[323] W. Adam, O. De Lucchi, *Tetrahedron Lett.* **1981**, *22*, 929-932.

[324] M. J. Dewar, S. Olivella, J. J. Stewart, *J. Am. Chem. Soc.* **1986**, *108*, 5771-5779.

[325] A. G. Leach, K. Houk, *Chem. Commun.* **2002**, 1243-1255.

[326] A. V. Pocius, J. T. Yardley, *J. Am. Chem. Soc.* **1973**, *95*, 721-725.

[327] A. V. Pocius, J. T. Yardley, *The Journal of Chemical Physics* **1974**, *61*, 2779-2792.

[328] D. Kjell, R. Sheridan, *Journal of photochemistry* **1985**, *28*, 205-214.

[329] H. Wamhoff, K. Wald, *Chem. Ber.* **1977**, *110*, 1699-1715.

[330] W. H. Pirkle, J. Stickler, *J. Am. Chem. Soc.* **1970**, *92*, 7497-7499.

[331] N. D. Epiotis, R. Yates, *The Journal of organic chemistry* **1974**, *39*, 3150-3153.

[332] S. Inagaki, Y. Hirabayashi, *Chem. Lett.* **1978**, *7*, 135-138.

[333] D. P. Kjell, R. S. Sheridan, *J. Am. Chem. Soc.* **1984**, *106*, 5368-5370.

[334] C. Barner-Kowollik, F. E. Du Prez, P. Espeel, C. J. Hawker, T. Junkers, H. Schlaad, W. Van Camp, *Angew. Chem. Int. Ed.* **2011**, *50*, 60-62.

[335] H. Ban, J. Gavrilyuk, C. F. Barbas III, *J. Am. Chem. Soc.* **2010**, *132*, 1523-1525.

[336] H. Ban, M. Nagano, J. Gavrilyuk, W. Hakamata, T. Inokuma, C. F. Barbas III, *Bioconjugate Chem.* **2013**, *24*, 520-532.

[337] S. C. Solleder, M. A. R. Meier, *Angew. Chem. Int. Ed.* **2014**, *53*, 711-714.

[338] K. S. Wetzel, M. A. R. Meier, *Polym. Chem.* **2019**, *10*, 2716-2722.

[339] K. S. Wetzel, Master's thesis, KIT (Karlsruhe), **2016**.

[340] B. A. Laurent, S. M. Grayson, *Chem. Soc. Rev.* **2009**, *38*, 2202-2213.

[341] Y. Tezuka, H. Oike, *J. Am. Chem. Soc.* **2001**, *123*, 11570-11576.

[342] K. Endo, in *New Frontiers in Polymer Synthesis*, Springer, **2008**, pp. 121-183.

[343] X. Lv, X. Zheng, Z. Yang, Z.-X. Jiang, *Organic & biomolecular chemistry* **2018**, *16*, 8537-8545.

[344] H. Jacobson, W. H. Stockmayer, *The Journal of Chemical Physics* **1950**, *18*, 1600-1606.

[345] L. Rique-Lurbet, M. Schappacher, A. Deffieux, *Macromolecules* **1994**, *27*, 6318-6324.

[346] L. Wang, M. O. Vysotsky, A. Bogdan, M. Bolte, V. Böhmer, *Science* **2004**, *304*, 1312-1314.

[347] Y. Tezuka, F. Ohashi, *Macromol. Rapid Commun.* **2005**, *26*, 608-612.

[348] D. Geiser, H. Höcker, *Macromolecules* **1980**, *13*, 653-656.

[349] G. Hild, A. Kohler, P. Rempp, *Eur. Polym. J.* **1980**, *16*, 525-527.

[350] J. Roovers, P. Toporowski, *Macromolecules* **1983**, *16*, 843-849.

[351] R. H. Grubbs, S. J. Miller, G. C. Fu, *Acc. Chem. Res.* **1995**, *28*, 446-452.

[352] A. Deiters, S. F. Martin, *Chem. Rev.* **2004**, *104*, 2199-2238.

[353] C. Heinis, *Nat. Chem. Biol.* **2014**, *10*, 696.

[354] S. Armstrong, *Chem. Soc., Perkin Trans* **1998**, *1*, 371.

[355] I. Nakamura, Y. Yamamoto, *Chem. Rev.* **2004**, *104*, 2127-2198.

[356] J. N. Lambert, J. P. Mitchell, K. D. Roberts, *J. Chem. Soc., Perkin Trans. 1* **2001**, 471-484.

[357] S. A. Kates, N. A. Solé, C. R. Johnson, D. Hudson, G. Barany, F. Albericio, *Tetrahedron Lett.* **1993**, *34*, 1549-1552.

[358] J. J. Storhoff, C. A. Mirkin, *Chem. Rev.* **1999**, *99*, 1849-1862.

[359] M. Göritz, R. Krämer, *J. Am. Chem. Soc.* **2005**, *127*, 18016-18017.

[360] E. M. Driggers, S. P. Hale, J. Lee, N. K. Terrett, *Nature Reviews Drug Discovery* **2008**, *7*, 608.

[361] J. Shi, D. E. Bergstrom, *Angewandte Chemie International Edition in English* **1997**, *36*, 111-113.

[362] L. Zhang, A. J. Stephens, A. L. Nussbaumer, J.-F. Lemonnier, P. Jurček, I. J. Vitorica-Yrezabal, D. A. Leigh, *Nature Chemistry* **2018**, *10*, 1083.

[363] R. D. Adams, M. Huang, W. Huang, J. A. Queisser, *J. Am. Chem. Soc.* **1996**, *118*, 9442-9443.

[364] B. A. Laurent, S. M. Grayson, *J. Am. Chem. Soc.* **2006**, *128*, 4238-4239.

[365] M. Mayor, C. Didschies, *Angew. Chem. Int. Ed.* **2003**, *42*, 3176-3179.

[366] D. V. Kondratuk, L. M. Perdigão, A. M. Esmail, J. N. O'shea, P. H. Beton, H. L. Anderson, *Nature Chemistry* **2015**, *7*, 317.

[367] E. Wasserman, *J. Am. Chem. Soc.* **1960**, *82*, 4433-4434.

[368] G. Gil-Ramírez, D. A. Leigh, A. J. Stephens, *Angew. Chem.* **2015**, *127*, 6208-6249.

[369] M. R. Shah, S. Duda, B. Müller, A. Godt, A. Malik, *J. Am. Chem. Soc.* **2003**, *125*, 5408-5414.

[370] S. Duda, A. Godt, *Eur. J. Org. Chem.* **2003**, *2003*, 3412-3420.

[371] A. Godt, *Eur. J. Org. Chem.* **2004**, *2004*, 1639-1654.

[372] M. Porel, D. N. Thornlow, N. N. Phan, C. A. Alabi, *Nature Chemistry* **2016**, *8*, 590.

[373] T. M. Trnka, R. H. Grubbs, *Acc. Chem. Res.* **2001**, *34*, 18-29.

[374] D. Astruc, *New J. Chem.* **2005**, *29*, 42-56.

[375] Y. Chauvin, *Angew. Chem. Int. Ed.* **2006**, *45*, 3740-3747.

[376] R. R. Schrock, *Angew. Chem. Int. Ed.* **2006**, *45*, 3748-3759.

[377] R. H. Grubbs, *Angew. Chem. Int. Ed.* **2006**, *45*, 3760-3765.

[378] K. J. Ivin, J. C. Mol, *Olefin metathesis and metathesis polymerization*, Elsevier, **1997**.

[379] J. Herisson, Y. Chauvin, *Makromolekulare Chemie* **1971**, *141*, 161-&.

[380] Y. Chauvin, D. Commereuc, D. Cruypelinck, *Die Makromolekulare Chemie: Macromolecular Chemistry and Physics* **1976**, *177*, 2637-2646.

[381] R. H. Grubbs, S. Chang, *Tetrahedron* **1998**, *54*, 4413-4450.

[382] P. Schwab, M. France, J. Ziller, R. Grubbs, *Angewandte Chemie. International edition in English* **1995**, *34*, 2039-2041.

[383] P. Schwab, R. H. Grubbs, J. W. Ziller, *J. Am. Chem. Soc.* **1996**, *118*, 100-110.

[384] R. R. Schrock, J. S. Murdzek, G. C. Bazan, J. Robbins, M. DiMare, M. O'Regan, *J. Am. Chem. Soc.* **1990**, *112*, 3875-3886.

[385] G. Bazan, E. Khosravi, R. R. Schrock, W. Feast, V. Gibson, M. O'Regan, J. Thomas, W. Davis, *J. Am. Chem. Soc.* **1990**, *112*, 8378-8387.

[386] G. C. Bazan, J. H. Oskam, H. N. Cho, L. Y. Park, R. R. Schrock, *J. Am. Chem. Soc.* **1991**, *113*, 6899-6907.

[387] Y. Schrodi, R. L. Pederson, *Aldrichimica Acta* **2007**, *40*, 45-52.

[388] J. A. Berrocal, S. Albano, L. Mandolini, S. Di Stefano, *Eur. J. Org. Chem.* **2015**, *2015*, 7504-7510.

[389] G. C. Vougioukalakis, R. H. Grubbs, *Chem. Rev.* **2010**, *110*, 1746-1787.

[390] P. A. Fokou, M. A. R. Meier, *J. Am. Chem. Soc.* **2009**, *131*, 1664-1665.

[391] P. A. Fokou, M. A. R. Meier, *Macromol. Rapid Commun.* **2010**, *31*, 368-373.

[392] M. Frölich, Master's thesis, KIT (Karlsruhe Institute of Technology) **2017**.

[393] A. C. Boukis, K. Reiter, M. Frölich, D. Hofheinz, M. A. R. Meier, *Nat. Commun.* **2018**, *9*, 1439.

[394] A. C. Boukis, M. A. R. Meier, *Eur. Polym. J.* **2018**, *104*, 32-38.

[395] C. E. Shannon, *The Bell System Technical Journal* **1948**, *27*, 379-423.

[396] W. Konrad, F. R. Bloesser, K. S. Wetzel, A. C. Boukis, M. A. R. Meier, C. Barner-Kowollik, *Chem. Eur. J.* **2018**, *24*, 3413-3419.

[397] X. Elduque, A. Sánchez, K. Sharma, E. Pedroso, A. Grandas, *Bioconjugate Chem.* **2013**, *24*, 832-839.

[398] J. O. Holloway, C. Mertens, F. E. Du Prez, N. Badi, *Macromol. Rapid Commun.* **2019**, *40*, 1800685.

[399] P. Espeel, L. L. G. Carrette, K. Bury, S. Capenberghs, J. C. Martins, F. E. Du Prez, A. Madder, *Angew. Chem. Int. Ed.* **2013**, *52*, 13261-13264.

[400] S. C. Solleder, PhD Thesis thesis, KIT (Karlsruhe), **2016**.

[401] S. Oelmann, M. Meier, *RSC Advances* **2017**, *7*, 45195-45199.

[402] O. Türünç, S. Billiet, K. De Bruycker, S. Ouardad, J. Winne, F. E. Du Prez, *Eur. Polym. J.* **2015**, *65*, 286-297.